Universitat Politècnica de València

Departamento de Comunicaciones

Ph. D. Thesis

Architecture and Communication Protocol to Monitor and Control Water Quality and Irrigation in Agricultural Environments

---

Author:

Laura García García

Supervised by

Jaime Lloret Mauri

Pascal Lorenz

Valencia, June 2021

Abstract

The introduction of technological solutions in agriculture allows reducing the use of resources and increasing the production of the crops. Furthermore, the quality of the water for irrigation can be monitored to ensure the safety of the produce for human consumption. However, the remote location of most fields presents a problem for providing wireless coverage to the sensing nodes and actuators deployed on the fields and the irrigation water canals. The work presented in this thesis addresses the problem of enabling wireless communication among the electronic devices deployed for water quality and field monitoring through a heterogeneous communication protocol and architecture. The first part of the dissertation introduces Precision Agriculture (PA) systems and the importance of water quality and field monitoring. In addition, the technologies that enable wireless communication in PA systems and the use of alternative solutions such as Internet of Underground Things (IoUT) and Unmanned Aerial Vehicles (UAV) are introduced as well. Then, an in-depth analysis on the state of the art regarding the sensors for water, field and meteorology monitoring and the most utilized wireless technologies in PA is performed. Furthermore, the current trends and challenges for Internet of Things (IoT) irrigation systems, including the alternate solutions previously introduced, have been discussed in detail. Then, the architecture for the proposed system is presented, which includes the areas of interest for the monitoring activities comprised of the canal and field areas. Moreover, the description and operation algorithms of the sensor nodes contemplated for each area is provided. The next chapter details the proposed heterogeneous communication protocol including the messages and alerts of the system. Additionally, a new tree topology for hybrid LoRa/WiFi multi-hop networks is presented. The specific additional functionalities intended for the proposed architecture are described in the following chapter. It includes data aggregation algorithms for the proposed topology, an overview on the security threats of PA systems, energy-saving and fault-tolerance algorithms, underground

communication for IoUT, and the use of drones for data acquisition. Then, the simulation results for the solutions previously proposed are presented. Finally, the tests performed in real environments for the presented heterogeneous protocol, the different deployment strategies for the utilized nodes, the energy consumption, and a functionality for fruit quantification are discussed. These tests demonstrate the validity of the proposed heterogeneous architecture and communication protocol.

Resumen

La introducción de soluciones tecnológicas en la agricultura permite reducir el uso de recursos y aumentar la producción de los cultivos. Además, la calidad del agua de regadío se puede monitorizar para asegurar la seguridad de los productos para el consumo humano. Sin embargo, la localización remota de la mayoría de los campos presenta un problema para proveer de cobertura inalámbrica a los nodos sensores y actuadores desplegados en los campos y los canales de agua para regadío. El trabajo presentado en esta tesis aborda el problema de habilitar la comunicación inalámbrica entre los dispositivos electrónicos desplegados para la monitorización de la calidad del agua y el campo a través de un protocolo de comunicación y arquitectura heterogéneos. La primera parte de esta tesis introduce los sistemas de agricultura de precisión (PA) y la importancia de la monitorización de la calidad del agua y el campo. Asimismo, las tecnologías que permiten la comunicación inalámbrica en sistemas PA y el uso de soluciones alternativas como el internet de las cosas bajo tierra (IoUT) y los vehículos aéreos no tripulados (UAV) se introducen también. Después, se realiza un análisis en profundidad del estado del arte respecto a los sensores para la monitorización del agua, el campo y las condiciones meteorológicas, así como sobre las tecnologías inalámbricas más empleadas en PA. Además, las tendencias actuales y los desafíos de los sistemas de internet de las cosas (IoT) para regadío, incluyendo las soluciones alternativas introducidas anteriormente, han sido abordados en detalle. A continuación, se presenta la arquitectura propuesta para el sistema, la cual incluye las áreas de interés para las actividades monitorización que incluye las áreas de los canales y el campo. A su vez, la descripción y los algoritmos de operación de los nodos sensores contemplados para cada área son proporcionados. El siguiente capítulo detalla el protocolo de comunicación heterogéneo propuesto, incluyendo los mensajes y alertas del sistema.

Adicionalmente, se presenta una nueva topología de árbol para redes híbridas LoRa/WiFi multisalto. Las funcionalidades específicas adicionales concebidas para la arquitectura propuesta están descritas en el siguiente capítulo. Éstas incluyen algoritmos de agregación de datos para la topología propuesta, un esquema de las amenazas de seguridad para los sistemas PA, algoritmos de ahorro de energía y tolerancia a fallos, comunicación bajo tierra para IoUT y el uso de drones para adquisición de datos. Después, los resultados de las simulaciones para las soluciones propuestas anteriormente son presentados. Finalmente, se tratan las pruebas realizadas en entornos reales para el protocolo heterogéneo presentado, las diferentes estrategias de despliegue de los nodos empleados, el consumo energético y la función de cuantificación de fruta. Estas pruebas demuestran la validez de la arquitectura y protocolo de comunicación heterogéneos que se han propuesto.

Resum

La introducció de solucions tecnològiques en l'agricultura permet reduir l'ús de recursos i augmentar la producció dels cultius. A més, la qualitat de l'aigua de regadiu es pot monitoritzar per assegurar la qualitat dels productes per al consum humà. No obstant això, la localització remota de la majoria dels camps presenta un problema per a proveir de cobertura sense fils als nodes sensors i actuadors desplegats als camps i els canals d'aigua per a regadiu. El treball presentat en aquesta tesi tracta el problema d'habilitar la comunicació sense fils entre els dispositius electrònics desplegats per a la monitorització de la qualitat de l'aigua i el camp a través d'un protocol de comunicació i arquitectura heterogenis. La primera part d'aquesta tesi introdueix els sistemes d'agricultura de precisió (PA) i la importància de la monitorització de la qualitat de l'aigua i el camp. Així mateix, també s'introdueixen les tecnologies que permeten la comunicació sense fils en sistemes PA i l'ús de solucions alternatives com l'Internet de les coses sota terra (IoUT) i els vehicles aeris no tripulats (UAV). Després, es realitza una anàlisi en profunditat de l'estat de l'art respecte als sensors per a la monitorització de l'aigua, el camp i les condicions meteorològiques, així com sobre les tecnologies sense fils més emprades en PA. S'aborden les tendències actuals i els reptes dels sistemes d'internet de les coses (IoT) per a regadiu, incloent les solucions alternatives introduïdes anteriorment. A continuació, es presenta l'arquitectura proposada per al sistema, on s'inclouen les àrees d'interès per a les activitats monitorització en els canals i el camp. Finalment, es proporciona la descripció i els algoritmes d'operació dels nodes sensors contemplats per a cada àrea. El següent capítol detalla el protocol de comunicació heterogeni proposat, així como el disseny del missatges i alertes que el sistema proposa. A més, es presenta una nova topologia d'arbre per a xarxes híbrides Lora/WiFi multi-salt. Les funcionalitats específiques addicionals concebudes per l'arquitectura proposada estan descrites en el següent capítol. Aquestes inclouen algoritmes d'agregació de dades

per a la topologia proposta, un esquema de les alertes de seguretat per als sistemes PA, algoritmes d'estalvi d'energia i tolerància a fallades, comunicació per a IoUT i l'ús de drons per a adquisició de dades. Després, es presenten els resultats de les simulacions per a les solucions proposades. Finalment, es duen a terme les proves en entorns reals per al protocol heterogeni dissenyat. A més s'expliquen les diferents estratègies de desplegament dels nodes empleats, el consum energètic, així com, la funció de quantificació de fruita. Els resultats d'aquetes proves demostren la validesa de l'arquitectura i protocol de comunicació heterogenis propost en aquesta tesi.

Résumé

L'introduction de solutions technologiques en agriculture permet de réduire l'utilisation des ressources et d'augmenter la production végétale. De plus, la qualité de l'eau d'irrigation peut être surveillée pour assurer la sécurité des produits destinés à la consommation humaine. Cependant, l'emplacement éloigné de la plupart des champs présente un problème pour fournir une couverture sans fil aux nœuds de capteurs et d'actionneurs déployés dans les champs et les canaux d'eau d'irrigation. Le travail présenté dans cette thèse aborde le problème de permettre la communication sans fil entre les dispositifs électroniques déployés pour la surveillance de la qualité de l'eau et le terrain à travers un protocole et une architecture de communication hétérogènes. La première partie de cette thèse présente les systèmes d'agriculture de précision (AP) et l'importance du suivi des champs et de la qualité de l'eau. De même, les technologies qui permettent la communication sans fil dans les systèmes de sonorisation et l'utilisation de solutions alternatives telles que l'Internet des objets souterrains (IoUT) et les véhicules aériens sans pilote (UAV) sont également introduites. Ensuite, une analyse approfondie de l'état de l'art est effectuée en ce qui concerne les capteurs pour la surveillance des conditions d'eau, de terrain et météorologiques, ainsi que les technologies sans fil les plus utilisées en AP. En outre, les tendances et les défis actuels des systèmes Internet des objets (IoT) pour l'irrigation, y compris les solutions alternatives introduites précédemment, ont été traités en détail. Ensuite, l'architecture proposée pour le système est présentée, qui comprend les zones d'intérêt pour les activités de surveillance, y compris le canal et les zones de terrain. A leur tour, la description et les algorithmes de fonctionnement des nœuds capteurs envisagés pour chaque zone sont fournis. Le chapitre suivant détaille le protocole de communication hétérogène proposé, y compris les messages système et les alertes. De plus, une nouvelle topologie arborescente pour les réseaux hybrides LoRa / WiFi multi-sauts est

présentée. Des fonctionnalités spécifiques supplémentaires conçues pour l'architecture proposée sont décrites dans le chapitre suivant. Ceux-ci incluent des algorithmes d'agrégation de données pour la topologie proposée, un aperçu des menaces de sécurité pour les systèmes de sonorisation, des algorithmes d'économie d'énergie et de tolérance aux pannes, une communication souterraine pour l'IoUT et l'utilisation de drones pour l'acquisition de données. Ensuite, les résultats des simulations pour les solutions proposées ci-dessus sont présentés. Enfin, les tests réalisés en environnement réel pour le protocole hétérogène présenté, les différentes stratégies de déploiement des nœuds utilisés, la consommation d'énergie et la fonction de quantification des fruits sont discutés. Ces tests démontrent la validité de l'architecture et du protocole de communication hétérogènes qui ont été proposés.

Acknowledgements

El proceso de realizar esta tesis ha comprendido estos últimos años, en los que he crecido tanto personal como profesionalmente. Primeramente, la realización de este trabajo habría sido imposible sin el apoyo de mi familia, quienes me han ayudado a avanzar en los momentos más difíciles. Todo lo que he conseguido ha sido gracias a ellos y a su certeza de que era capaz de lograr todos los retos que se me presentasen. También les quiero agradecer a mis amigos su compañía y apoyo a lo largo de este periodo. No puedo más que agradecer inconmensurablemente la ayuda de mi director de tesis PH. D. Jaime Lloret Mauri, quien me ha guiado en mi trayecto por el mundo académico y me ha aconsejado en los momentos más difíciles. A su vez, le doy todo mi agradecimiento a mi director de tesis Pascal Lorenz por todo su apoyo.

Asimismo, no puedo olvidarme de mis compañeros, con los cuales he compartido muchas horas de trabajo y muchas alegrías. Con los que he publicado artículos y he disfrutado de buenos momentos. Ellos han hecho que esta experiencia sea mucho más llevadera. Gracias a José Miguel Jiménez, Lorena Parra Boronat, Sandra Sendra Compte, Albert Rego Mañez y Miran Taha.

A su vez, me gustaría agradecer su ayuda al profesor Minho Jo, de Korea University, por su acogida durante mi estancia de investigación en su laboratorio.

Muchas gracias a todos.

Abbreviations

3G	Third Generation Mobile Networks
5G	Fifth Generation Mobile Networks
6LoWPAN	IPv6 over Low -Power Wireless Personal Area Networks
ACK	Acknowledgement
ADC	Analog-to-Digital Converter
AES	Advanced Encryption Standard
AFH	Adaptive Frequency Hopping
AI	Artificial Intelligence
ALOHA	Additive Links On-line Hawaii Area
AMQP	Advanced Message Queuing Protocol
ANFIS	Adaptive Neuro Fuzzy Interference System
AOP	Advanced Oxidation Processes
AP	Access Point
APP	Application
APTEEN	Periodic Threshold-sensitive Energy-Efficient sensor Network
ARE	Accumulate Relative Error
AWMA	Alternating Wireless Medium Access
BER	Bit Error Ratio
BLE	Bluetooth Low Energy
CAGR	Compound Annual Growth Rate
CAP	Common Agricultural Policy
CCTV	Closed-Circuit Television
CH	Cluster Head
CMAC	Cipher-based Message Authentication Code
CoAP	Constrained Application Protocol
CPP	Coverage Path Planning
CPS	Cyber-Physical Systems

CRBL	Cramer Rao Lower Bound
CRS	Cognitive Radio Systems
CSCC	Common Spectrum Coordination Channel
CSMA	Carrier Sense Multiple Access
CTR	Counter
D2D	Device-to-Device
D2M	Device-to-Machine
DAC	Digital-to-Analog Converter
DB	DataBase
DBPSK	Differential Binary Phase Shift Keying
DC	Direct Current
DDRMPC	Data-driven Robust Model Predictive Control
DD-WRT	DresDren-Wireless RouTer
DEBR	Distributed Energy Balanced Routing
DFCR	Distributed Fault-tolerant Clustering and Routing
DHCP	Dynamic Host Configuration Protocol
DMZ	Demilitarized Zone
DoS	Denial-of-Service
DPSK	Differential Phase-Shift Keying
DSC	Digital selective calling
DSL	Digital Subscriber Line
DPV	Disjoint Path Vector
DTIM	Delivery Traffic Indication Message
EESNR	Energy-Efficient Sensor Network Routing
EEZRP	Energy-Efficient Zone-based Routing Protocol
EU	European Union
EM	Electromagnetic
ET	Evapotranspiration
ETc	Evapotranspiration of the crop
ETo	Reference Evapotranspiration
FAO	Food and Agriculture Organization
FCAPS	Fault, Configuration, Accounting, Performance, Security
FN	Field Node
FTP	File Transfer Protocol
GPIO	General-Purpose Input/Output
GPRS	General Packet Radio Service
GPS	Global Positioning System
GSM	Global System for Mobile communications
HCP	Heterogeneous Communication Protocol
HMI	Human Machine Interface
HTML	Hypertext Markup Language
HTTP	HyperText Transfer Protocol
I2C	Inter-Integrated Circuit
I2S	Inter-Integrated Circuit Sound
ICSP	In-Circuit Serial Programming
ICT	Information and Communication Technology
IDE	Integrated Development Environment
IDFCA	Distributed Fault-Tolerant Clustering Algorithm
IETF	Internet Engineering Task Force
ILC	Iterative Learning Control

IoT	Internet of Things
IoUT	Internet of Underground Things
IR	InfraRed
ISM	Industrial, Scientific, and Medical
ISO	International Organization for Standardization
ISP	Internet Service Provider
ITU-R	International Telecommunication Union – Radiocommunication Section
KPBS	Konza Prairie Biological Station
LAA	Licensed-Assisted Access
LAN	Local Area Network
LBT	Listen-Before-Talk
LEACH	Low-Energy Adaptive Clustering Hierarchy
LED	Light Emitting Diodes
LLN	Low-Power and Lossy Networks
LDR	Light-Dependent Resistor
LoRa	Long Range
LoRaWAN	Long Range Wide Area Network
LPWAN	Low-Power Wide-Area Network
LQI	Link Quality Indicator
LRD	Lightning and Radio Emission Detector
LTE-U	Long-Term Evolution - Unlicensed
LTE-UL	Long-Term Evolution - UpLink
M2M	Machine to Machine
MA	Maximum Attenuation
MAC	Medium Access Control
MED	Modified Exponential Decay
MHRM	Minimum Hop Routing Model
MI	Magnetic Induction
MIC	Message Integrity Code
MITM	Man in the Middle
MODIS	Moderate Resolution Imaging Spectroradiometer
MQTT	Message Queuing Telemetry Transport
NDVI	Normalized Difference Vegetation Index
NZG	Nonzero Gradient
OLA	OverLap Avoidace
OLED	Organic Light-Emitting Diode
OTA	Over The Air
PA	Precision Agriculture
PA-RPL	Partition Aware- Routing Protocol for Low-Power and Lossy Networks
PCB	Printed Circuit Board
PIR	Passive Infrared Sensor
POP3	Post Office Protocol
PTA	Packet Traffic Arbitration
PSoC	Programmable System-on-Chip
PWM	Pulse-Width Modulation
RDI	Regulated Deficit Irrigation
RFC	Request for Comments
RFID	Radio Frequency Identification
RGB	Red Green Blue

ROS	Robot Operating System
RPA	Remotely Piloted Aircraft
RR	Radio Regulations
RSSI	Received Signal Strength Indicator
SD	Secure Digital
SFN	Sink Field Nodes
SMTP	Simple Mail Transfer Protocol
SNMP	Simple Network Management Protocol
SPI	Serial Peripheral Interface
TCP	Transmission Control Protocol
TDD	Time Division Duplexing
TDMA	Time Division Multiple Access
UART	Universal Asynchronous Receiver-Transmitter
UAV	Unmanned Aerial Vehicle
UDP	User Datagram Protocol
UNESCO	United Nations Educational, Scientific and Cultural Organization
USB	Universal Serial Bus
USD	Unated States Dolars
UWB	Ultra-WideBand
VLC	Visible Light Communication
VoIP	Voice over IP
VPN	Virtual Private Network
VRT	Variable rate technology
WAN	Wide Area Network
WDS	Wireless Distribution System
WLAN	Wireless Local Area Network
WMN	Wireless Mesh Network
WNA	Water Node After
WNB	Water Node Before
WPT	Wireless Power Transfer
WSN	Wireless Sensor Network
Wi-Fi	Wireless Fidelity
WHO	World Health Organization

Contents

List of Figures

List of Tables

Chapter 1

Introduction

1.1 Introduction

The predictions related to the world population, presented by different international organizations, suggest that there will be a large and constant increase in population in the coming years. Organizations such as the United Nations [1] predict that the world population will reach 8.5 billion people by 2030, and 9.7 billion by 2050. This increase in population brings with it the need for a very important increase in food production. In these forecasts, it is estimated that 70% more food than the food produced nowadays will have to be produced by 2050. Agriculture is the main way of obtaining food nowadays. More or less, 95% of the consumed food is produced directly or indirectly in the soil. In recent years, the growth rate of agriculture production and crop yield has declined. The decline in production can be explained by a lot of causes like intensive agriculture, which causes degradation in the soil, losing most of the nutrients in this process [2]. This has raised fears that the world will not be able to sufficiently increase the production of food and other products to ensure adequate food for the future population [3]. It is necessary to achieve greater efficiency, in order to be able to supply the entire population and optimize the consumption of resources such as irrigation water, fertilizers, or pesticides. But there are great difficulties to increase current production, among other reasons due to the important changes that are taking place over the last few years in meteorology, water resources are becoming increasingly scarce every day. To achieve such a significant percentage increase, it is necessary to apply the new agricultural techniques provided by Smart Agriculture. Farmers and agricultural

workers must implement measures to improve and control the state of crops and to optimize the utilized resources. In many countries, farmers are opting to implement solutions that apply technological means. For example, the European Union (EU) establishes in its 2020 strategy policies such as the Common Agricultural Policy (CAP) [4], which responds to the new economic, social, environmental, and technological challenges facing our society and, as a result, contributing to its development.

Due to the causes previously exposed, it is necessary that agriculture advances in the future and becomes intelligent agriculture. Smart agriculture is achieved by applying Information and Communication Technologies to traditional agriculture [5]. Thanks to their employment, farmers, and engineers can use smart tools [6], through which they can be more efficient and consume smaller amounts of natural resources. Countries with large tradition in agriculture are implementing smart agriculture systems. Implementing these types of solutions can optimize the moments to temporize vital actions in the harvests, like irrigation, sowing, or the moment to add fertilizers to the terrain. Precision Agriculture (PA) focuses on utilizing different sensors and actuators that are part of a system that monitors crops and takes decisions according to the readings. Fundamentally, it is about applying Information and Communication Technology (ICT) techniques to agriculture. It consists of observing, measuring, and acting on crops, regardless of the conditions of the site, and utilizing certain technologies [7, 8]. These decisions are reflected in the actions performed by the actuators.

PA systems aid in reducing water consumption and improving the quality and quantity of the produce. Most fields are located in rural areas with no access to internet connection resulting in difficulties in deploying PA solutions. Ad-hoc networks allow forwarding the information to a sink node by transmitting the data from node to node. However, deploying numerous sensing nodes is expensive and may not serve the needs of the farmer. The use of drones to gather the data from sensors deployed on the fields can be another solution for these remote fields [9]. However, this solution only allows to access the data at the time the drone flies over the field. Another option is to use robots that move through the fields to collect the data from the sensor nodes [10]. However, with the use of vehicles as gateways, the PA solutions cannot perform any actions in real-time or quasi-real-time. Therefore, there is the need to provide connection to remote areas in order to deploy PA systems with all their functionalities.

Automating the irrigation schedule is one of the main tasks of the PA systems. This is often performed with the use of agrometeorological data from meteorological stations that can be placed far from the fields. The introduction of soil monitoring nodes has led to the use of soil variables to make scheduling more precise. The water balance formula has been adjusted with data from soil moisture sensors to implement regulated deficit irrigation (RDI) strategies [11]. A homogenization of the production was achieved after applying the RDI strategies with the automatic irrigation system. The Van Genutchen model has also been utilized by some irrigation scheduling systems to determine moisture usage and obtain water savings between 56.4% and 90% [12]. Predictive irrigation scheduling systems have been developed as well utilizing AI and machine learning techniques. A data-driven robust model predictive control (DDRMPC) for irrigation needs prediction utilized learning-based techniques to create an uncertainty set

obtained from existing data logs [13]. The results of applying DDRMPC showed a reduction of 40% in water consumption. Machine learning has also been employed to calculate the reference Evapotranspiration (ETo) of the crop based on the data from soil moisture sensors, obtaining the best results with the randomizable filtered classifier technique followed by artificial neural networks [14]. Lastly, performing climate modeling [15] could also be utilized to predict the resource requirements of a crop.

1.1.1 Water quality and water treatment for irrigation

Water scarcity is a very important problem in the world. 4 billion people live under the condition of water scarcity at least one month per year [16]. Moreover, farming is the activity with the highest water consumption in the world with 70% of water usage [17, 18]. The lack of fresh water is a rising concern, particularly in the Mediterranean countries or southern Asian countries such as India. Among the countries in Europe, the Mediterranean countries are the most vulnerable to drought [19]. A connection has been established between climate policies and water management. Water management can be affected by different variables such as the water demand from the different sectors or the consequences of some degrees of warming on hydrological resources. Climate change and its effects are a recurrent topic in research papers regarding water resources and agriculture. The possible consequences of global warming have led to the consideration of creating water adaptation measures to ensure the availability of water for food production and people and to maintain ecosystems [20]. In the future, the increase of the population and global warming could be the cause of wars over water. To reduce the problems with water, there are three options I) decrease the use of water II) Increase the available water by reusing wastewater. III) Desalination of seawater. The high costs of water desalination make it impossible to use it for agriculture if it is not with public incentives. China has a long history of wastewater reuse [21]. In Spain and Greece, it is foreseeable that, in the future, the regeneration of water will become a routine practice [18]. However, as we have previously seen, the quality of these waters can cause problems. The irrigation with raw o diluted wastewater can cause problems in the environment and human health. Consequently, the governments have to take measures to manage the risks [22]. A study of reuse of wastewater concluded that with a good control of the pollutants and the use of this water for irrigating the appropriate species, the regenerated wastewater can be used without any problems [18]. Therefore, wastewater can be used for irrigation employing the correct methodologies.

Water quality is an aspect of great importance concerning crops. Generally, in Europe, the quality of the irrigation water is acceptable but in other regions, the quality of the water is not good for irrigation. The countries of North Africa and the Middle East are an example of this situation [23]. The safety of the water to be consumed by humans and to be returned to the environment must be ensured. Water quality may be affected by many aspects such as pollution from industries, agricultural fertilizers and pesticides, and waste produced by humans. United Nations Educational, Scientific and Cultural Organization (UNESCO) estimates the amount of contaminated water on the

planet as 12,000 km^3 [24]. Poorer regions of the planet are the most affected by contaminated water. Contaminated water is able to cause numerous health problems in the population. The World Health Organization (WHO) estimates the number of deaths caused by contaminated water consumption to be 842,000 [25]. Furthermore, it is estimated that there are 200,000 deaths per year due to pesticide consumption, with nearly 3 million people poisoned per year [26]. In India, 29% of the pesticide consumption is used on rice and 9% is used on vegetables. Thus, it is imperative to assure irrigation water is treated correctly so as to reduce water pollution as much as possible. The possible risks of climate change are an increase in water shortage, the reduction of water quality, the increase in water and soil salinity, the biodiversity loss, the increase in irrigation requirements, or the possible cost of emergency and remediation actions.

Considering the repercussions of water contamination on people, it is necessary to add a treatment process in irrigation systems. Even though irrigation water may have been treated prior to distribution, the characteristics of the distribution canals may not avoid the incursion of water pollutants during water transport. There is a variety of water treatment processes, including advanced oxidation processes (AOPs) [27], and adsorption, both organic and inorganic, among other water treatment processes [28]. Biosorption is a physicochemical process based on adsorption, surface complexation, adsorption, and precipitation, that employs biomass to adsorb chemicals, metals, and other pollutants [29]. This process may employ different types of biomass such as marine algae, bacteria, fungi, peat moss, bark, and yeast and each type may present better results with different types of pollutants [30]. This is highly important in biotreatment processes and can remove or recover organic and inorganic substances from a solution. The biological material can be living beings or parts of living beings that have suffered some treatment [31]. Bioabsorption is a very popular technique for eliminating the presence of heavy metals in the water. It is eco-friendly in nature and is considered a low-cost technique [32, 33]. The biosorption of cyanobacteria has been observed in Lake Dianchi (China) [34]. Other studies showed that the use of Acacia leucocephala (Lam) bark can be used for removing Cu(II), Cd(II), and Pb(II) ions of the water [35].

Agricultural waste materials are also being considered as an economic and ecologic biomass source. Agricultural waste biomass is abundant, reduces the waste generated from agriculture, and it has a low cost and high efficiency as an absorbent. Some of the already tested agricultural waste biomass absorbents are sawdust, coconut shells, rice bran, wheat bran, sugarcane bagasse, sugar beet pulp, maize corn cob, orange peels, waste tea leaves, and hazelnut shells, among other agricultural waste from different produce types [36]. The remnant of the wastewater biosorption process is treated with anaerobic digestion, dewatering, incineration, thermal drying, or pyrolysis [37].

1.1.2 Water quality and field monitoring

Monitoring the quality of the water that is going to be employed for irrigation has started to be considered for new smart agriculture proposals [28]. Treated wastewater is apt for crops irrigation and allows reducing water consumption [18]. However, in order to be able to use wastewater for irrigation, some water cleanliness requirements must be met. Therefore, monitoring water quality before performing irrigations tasks allows verifying the correct quality of the water.

In order to perform the aforementioned activities, different sensors must be utilized. These sensors are designed for the field or the water according to their purpose. For field monitoring, there are varied low-cost commercial sensors that allow monitoring soil moisture and humidity, as well as rain and other environmental conditions. A greater efficiency can be achieved by applying new technologies to crops. Using sensors, farmers obtain information on different parameters related to their crops and help them in making decisions [38]. The application of these new technologies in crops brings with it a significant reduction in production costs and an increase in the quality of the products. In addition, farmers may need to spend less time physically present in the crop fields, being able to obtain the crucial information that will allow them to perform data analysis in real-time. This will ultimately improve the quality of life of people and the productivity of their businesses. Initially, the tendency is that, due to the need for a return on investment, the products that reach a higher price in the market will be the ones that will be subject to greater investment in technology. In smart agriculture, it's vital to have information about multiple parameters that allow us to establish precision agriculture [39]. Among others, we can highlight as fundamental the obtention of information in real-time about temperature, humidity, precipitation or light as well as some aspects of the plants such as the amount of foliage, foliage color, plant height or stem width, the amount of available water and water flow through the pipes. According to the type of crop to be monitored, the design of the IoT system may differ. For citrus plots in the Mediterranean coast of Spain, nodes may need to monitor soil, the quality, and the amount of water in the irrigation canals and the environment [28]. Monitoring nodes may also be mounted on vehicles such as drones or robots [40]. This monitoring process can be performed not only on the field, but it may also follow the produce to monitor its manufacturing process [41].

Water quality monitoring can be performed with chemical or physical sensors. Physical sensors allow monitoring water quality in real-time and do not require continuous supervision and manipulation. Thus, physical water quality monitoring sensors are suitable for remote water quality monitoring in smart irrigation systems. Physical sensors use the electromagnetic field, optical properties, and resistance variations in order to assess changes in the characteristics of the monitored environment [42]. Therefore, optical sensors can be utilized to monitor turbidity or the presence of an oil layer. Coils can be employed to determine the conductivity of the water. Moreover, image processing performed on the images obtained from cameras can be utilized to detect the presence of objects or animals. However, the available commercial sensors for water quality monitoring present a very high cost which turns out in the resulting increase of the price of deploying a smart agriculture system. Nevertheless, recent research on water quality monitoring has provided inspiring results on low-cost sensors for turbidity [43] and conductivity [42] monitoring. The conductivity sensor proposed in

[42] can be used for determining the salinity of the water, which is a very important parameter for agriculture because irrigation with salt water can cause the loss of fertility of the soil. Another important parameter for detecting the quality of water is the presence of solids. This parameter is calculated indirectly with the turbidity of the water. However, not only is it important to know the value of solids but also their nature. In [43], a sensor with infrared and color Light Emitting Diodes (LEDs) to detect the value of the solids expressed in mg / l, differentiating between two species of algae and inorganic solids was proposed. Moisture sensors can prevent moisture stress conditions in the plants and reduce the excess of irrigation [44]. Furthermore, currently available low-cost sensors can be used to monitor water quality, with results comparable to those obtained from more expensive commercialized probes for water quality assessment. The use of low-cost sensors for smart and precision agriculture allows reducing the price of said systems and opens the door to the implementation of these systems in developing countries. Therefore, both the quantity of the production and the quality of the resulting produce would increase which, at the same time, could lead to better nutrition of the people of the area and a reduction in the prices of the produce.

Sensor node systems have the advantage of being able to capture information to observe a large number of environmental parameters 24 hours a day, 365 days a year, and their values can be monitored in real-time if necessary. The information can be stored and transmitted at any time, based on the developed system and the needs of crop control as long as there is an internet connection in the deployed area.

1.1.3 Wireless technologies in precision agriculture systems

The information from the sensors deployed on the field or in the water is gathered utilizing embedded boards such as those provided by Arduino. Due to the characteristics of agricultural environments, wired communication among the nodes is practically impossible. In addition, when using agricultural machinery, which is often heavy vehicles, it is very difficult not to deteriorate or break the copper or fiber-optic wires deployed in the fields. It is very easy for situations to appear where the tools attached to the vehicles can drag the cables, and animals and weather conditions would lead to the necessity of installing protections for all the wires of the system. For this reason, PA is one of the ideal areas where wireless technology should be used.

There are several low range and medium range wireless technologies such as WiFi, ZigBee, or Bluetooth Low Energy (BLE). WiFi is the most accessible technology due to the wide variety of devices and prices which makes it a good option for affordable solutions. Furthermore, its extensive documentation allows farmers and non-technicians to easily operate the devices. Wi-Fi has been thoroughly studied for agricultural applications considering different types of vegetation and different positions of emitter and receiver and, it is the most utilized wireless technology in PA IoT systems [45]. ZigBee would also be a good solution but its usage in PA is yet to grow. Long-rage technologies, such as LoRa, allows providing connectivity to remote areas. The Things Network was able to perform a Long Range Wide Area Network (LoRaWAN)

transmission that reached 766 km utilizing a transmission power of 25mW on two occasions [46]. Although the maximum theoretical distance would not exceed 6 km for the configurations required to achieve higher data rates in the 868 MHz frequency band [45]. Furthermore, the LoRaWAN protocol only considers a star topology, which presents a limit to the distance between node and gateway. Therefore, it may be necessary to add more hops to the LoRa network. In this regard, studies on multi-hop and mesh LoRa networks and protocols have been performed by some researchers [47]. The scenario of LoRa nodes for a water quality monitoring system intended for irrigation that presents an architecture with several hops has been studied in previous works [48]. Where clusters of nodes are deployed on the water canals to monitor the state of the water and avoid false positives and false negatives by comparing the data from all the nodes in the cluster. However, there can be a scalability problem due to possible collisions among the messages forwarded by each node in a shared coverage area. As it may be necessary to deploy several sensors on the fields, combining LoRa with a smaller range wireless technology may be a good solution.

Inexpensive nodes that include wireless technologies are available on the market. Among the most currently employed, we can find nodes that include IEEE 802.11n interfaces, BLE, and LoRaWAN. Furthermore, instead of just using one communication technology, two different wireless technologies may be used depending on the required communication distance, such as utilizing a gateway that receives the data from the sensors using WiFi and forwards it to the database using 3G. Nodes with both ZigBee and LoRa transceivers are currently being developed but they are not accessible [49]. On the other hand, nodes such as the Heltec LoRa WiFi v2 [50], allow the utilization of both wireless technologies at the same time at an affordable price. The use of nodes with transceivers of multiple technologies allows to provide more functionalities to the system and to address the peculiarities of each scenario.

Wireless networks for monitoring have specific characteristics and requirements. Therefore, specific protocols have been designed to assess these requirements. Constrained Application Protocol (CoAP) and Message Queuing Telemetry Transport (MQTT) are an example of recently developed protocols for IoT that are increasing in popularity. Both are application layer protocols but differ on the transport protocol they utilize. While MQTT utilizes Transmission Control Protocol (TCP), CoAP works on top of User Datagram Protocol (UDP). CoAP has been utilized in some implementations of smart environmental monitoring systems [51]. It is a simplified version of HyperText Transfer Protocol (HTTP) and thus it is possible to bridge both protocols. However, as it is intended for low-sized packets, the use of SigFox or LoRaWAN is more considered for CoAP. This fact has led to few implementation resources for CoAP with WiFi antennas. Furthermore, the observe option, which was further explained on a posterior Request for Comments (RFC) [52], is not fully implemented on the available libraries for CoAP over WiFi chips such as the ESP8266.

Aspects such as foliage density, which can change according to the seasons or depending on the growth state of the plant, should be considered as they can affect the wireless transmission. The coverage of the IoT devices deployed on the field may vary greatly based on the selected wireless technology, the height at where the devices are

located, and other factors regarding signal quality such as possible interferences, distance attenuation, absorptions, reflections, dispersion, or the multipath effect. Therefore, the effective range achieved by IoT devices deployed at crops can be considerably reduced. It is, therefore, necessary to know the limitations regarding the range of the devices when implementing a solution for agriculture so as to design the network according to the characteristics of the environment. The Received Signal Strength Indicator (RSSI) allows obtaining a measure of the quality of the wireless signal and can be utilized for the localization of the devices [53, 54]. Although there are varied metrics utilized for estimating link quality, RSSI is a good measure when the focus is on the coverage of a wireless connection and assessing the quality of the link that can be obtained establishing ranges that indicate if the connection is good or bad. For grass fields, the threshold that was established to indicate poor quality links was -90 dBm [55]. Authors in [55] also determined that no conclusion has been reached on whether RSSI or Link Quality Indicator (LQI) is better than the other as there are contradictory results and remarks in the literature. They state that each metric is able to provide information on some aspects regarding the quality of the link. However, there is no commonly used metric that is able to provide information on all available aspects regarding link quality unless it is a newly proposed metric that has, in turn, a big overhead. Therefore, RSSI can be considered a good enough metric for the purpose of performing coverage studies.

1.1.4 IoT in precision agriculture

The Internet of Things (IoT) technology represents a fundamental role. The main objective of the IoT is to establish the connection between devices to automate and control processes that are carried out on a daily basis. The scope of IoT has varied and, as the years go by, its applicability increases. Cisco [56], predicts that M2M (Machine to Machine) connections will grow 2.4-fold, from 6.1 billion in 2018 to 14.7 billion by 2023. There will be 1.8 M2M connections for each member of the global population by 2023. The increase, in their use, is due to the decrease in the costs of the devices and the means of transmission of the observed information. Its application in multiple areas makes it possible to adopt the most appropriate solutions to different problems. One of the areas in which this technology is increasingly implemented is in agriculture. For example, if environmental and crop health parameters are controlled, the use of both water resources and pesticides can be avoided, which will reduce the impact on the environment.

In the space of IoT applied to Agriculture, we can highlight for its novelty the studies presented on the Internet of Underground Things (IoUT). According to Vuran [57], IoUT consists of sensors and communication devices, partly or completely buried underground for real-time soil sensing and monitoring. Underground communications can be performed both by wired and wireless technologies. Wireless technologies are based on acoustic waves, electromagnetic waves (EM), magnetic induction (MI) and, visible light communication (VLC) while the wired technologies use coaxial cable and

optical fibers [58]. In its application to agriculture, underground sensors are used, which control different systems, both irrigation, and machinery, to help farmers and agronomists in making decisions. By using buried sensors, we can control crop parameters such as soil temperature and humidity, more efficiently than with the parameters that are only estimated on surface. Furthermore, due to the underground location of the nodes, there are major problems when working with machinery in their environment, because they can be unused or destroyed. When using IoUT, if EM is emitted, there are scenarios where the sensors are buried under a cultivated field, and the communication is performed between buried nodes, between some of the buried nodes and nodes or surface wireless devices that collect the signal emitted by the buried node, and the nodes or surface wireless device that send the signal via WiFi to other points. Therefore, the requirements of the soil medium and its characteristics should be considered for the design of an IoUT network. For that purpose, there are path loss prediction models specific to the underground channel [59].

Energy consumption is an important problem for IoT. Currently, when applied to agriculture, most of the time they are installed in areas where it is not possible to connect the device to the electricity grid. Energy is needed for the sensors and microcontrollers to work. For this reason, devices and technologies with minimal energy consumption are often used. To achieve this, in the field of communications it is ideal to use technologies such as Low-Power Wide-Area Network (LPWAN). In general, in order to power the IoT, there are two options: batteries or solar panels. Solar panels cannot always be used because, in some cases, light does not impact the panel directly. There is not an only way for saving energy in IoT. The strategies will depend on the needs that have to be monitored [60]. If the nodes remain active in real-time, to gather the values of the parameters that are needed, they will consume a large amount of energy. Assuming that the nodes are distributed in dispersed locations, where it is not possible to bring the energy at reasonable costs, the supply of electrical power can become a big problem. Depending on the needs of different crops, the observation time may vary. However, the amount of data may not be a problem.

The amount of information generated from these types of sensors and smart systems applied to precision agriculture can be significantly large. Thus, data processing algorithms are necessary to analyze the data and determine the actions that the actuators must perform. These algorithms may also consider reducing the amount of forwarded data in order to reduce energy consumption and the amount of generated traffic. On the other hand, the monitored parameters usually change at a slow pace. However, the consistent transmission of the data is necessary. Therefore, small-sized IoT devices with low energy consumption are usually employed for both data acquisition and actuator management. Moreover, low-power protocols can be utilized as well so as to reduce energy consumption as much as possible [61, 62]. Each communication protocol has its own transmission speed and range which implies greater or lesser energetic consumption. There are other energy-saving techniques such as radio optimization, data transmission reduction, sleep, and wake-up techniques, and energy conscious routing protocols [60, 63]. In this case, a communication protocol that does not consume a large amount of energy is needed in order to avoid replacing batteries. Fault tolerance is another aspect that is usually considered by the algorithms employed in wireless sensor

networks (WSNs) and IoT solutions. Moreover, some solutions consider soil moisture and other factors such as weather predictions to determine whether the irrigation system must start or stop [64].

In some situations, it is necessary to use a large number of sensor nodes. Obviously, the cost of the nodes, if they are used in large numbers, can be prohibitive. In addition, if mobile technologies are used to establish transmissions, such as 4G or any other, the cost of the node is significantly increased, and maintenance is also expensive. Furthermore, it would be necessary to hire the services of a mobile operator that has coverage in the space that will be monitored. Furthermore, the number of IoT devices deployed in the field must be minimized with the aim of reducing the cost while guarantying the performance of the system. One of the ways of minimizing the number of nodes is deploying the nodes at the maximum possible transmission distance for the selected wireless technology. Furthermore, the processing and storage capacities of IoT devices are generally very limited. When using Fog Computing a decentralized network structure is employed in which resources, including data and applications, will be found somewhere between the data source and the Cloud. By using Edge Computing, intelligence is brought into individual hardware systems such as sensors [65]. Using Edge Computing, the source devices are already in charge of filtering data. Redundant data and even false positives can be removed depending on the architecture. In the case of wanting to correct an error or wanting to optimize the performance of the observed elements or environments, after processing the data, the appropriate corrective measures are taken to optimize the observed functions. Lastly, the decision-making process that uses the monitored information to determine the actions that the actuators must execute has become easier. Artificial Intelligence (AI) is employed to process the data to provide recommendations and perform predictions [66]. For the case of intelligent irrigation systems for smart agriculture, data on temperature and humidity of the air and the soil can be analyzed to determine when to start and stop irrigation to optimize water usage.

1.1.5 The use of drones in precision agriculture

Gateways in PA systems can be deployed in different manners, i.e. on poles, on trees, on moving machinery such as tractors of pivot-center irrigation structures, and drones. For the cases where the gateway is located in a static position (poles and trees), the network would require a larger number of gateways to cover the expanse of the fields. Using moving manned vehicles and irrigation structures would be possible for crops that require those vehicles to go through the fields often enough or to be irrigated using pivot-center structures regularly. However, drones can be utilized in more comprehensive types of crops and are not restricted to specific moments of plant growth where the machinery is necessary. It also allows reducing the cost as only one gateway is required.

The use of drones, also known as Unmanned Aerial Vehicle (UAV) in the military field or Remotely Piloted Aircraft (RPA), has been increasing in recent years due to the

improvement in design and accessibility. Drones are primarily used to perform remote sensing and can capture photographs and videos to send them in real-time or to store it for its later analysis. These images can be utilized to perform mapping, navigation, and georeferencing [67] for applications such as agriculture, forestry, surveillance, location and rescue, environmental monitoring, photogrammetry, vegetation analysis, atmospheric monitoring, wildlife conservation, cultural heritage conservation, and urban environment monitoring [69]. In precision agriculture, remote sensing can be used to monitor growth vigor, drought stress, and nutrients, to detect weeds and pathogens, and to perform yield prediction using multispectral, hyperspectral, RGB (Red Green Blue), and thermal sensors [69]. Their use is being extended to the implementation of smart systems such as the system proposed in [70] where a drone took pictures of palm trees and communicated with smart insect traps to spray insecticide. They can also be used as tools for treatments with fertilizers or phytosanitary products or even to scare away birds. The agriculture drones market size is expected to grow from USD 1.2 billion by 2019 to USD 4.8 billion by 2024 at a CAGR (Compound Annual Growth Rate) of 31.4% [71].

Contemplating the increase in the use of drones for precision agriculture remote sensing activities, adding new functionalities to benefit from the itinerary of the drone is an aspect to consider. Precision agriculture includes the use of WSNs as well. The design of these WSNs can vary depending on the node density, the topology, or the communication technology. However, using the UAVs currently employed for image and video capture of the crops as a mobile gateway to gather the data from the sensor nodes deployed on the field is a solution to consider. These drones already have a flight plan designed to capture the required images to map the fields or detecting diseases, pests, or water stress on the plants. Furthermore, significant efforts have been made for implementing low-cost PA solutions in developing countries, in which the internet connection might not be as extended as in developed countries. In these cases, we can use the drone, which has an internet connection, to serve as a mobile gateway for the WSN deployed in the soil. Nevertheless, aspects such as the required flight height and speed to ensure good image captures, as well as local regulations, and the characteristics of the drone have to be considered. It is important to note that the flying parameters of the drone have been set to optimize the process of gathering pictures or video, and those parameters cannot be modified.

1.1.6 Security concerns for precision agriculture systems

Wastewater treatment systems for irrigation benefit from using different IoT technologies for monitoring and managing information of the irrigation process. A smart irrigation system relies on sensors and online services for improved efficiency. Users can control the system from a remote device and can configure it using a cloud service. However, there can be a variety of new security threats. Therefore, security solutions can be introduced to avoid the access of malicious third parties to the gathered data [72].

These systems face different types of attacks which can be physical attacks, network attacks, and system attacks. For physical attacks, the problem includes destroying or stealing the components of the IoT devices. For communication attacks, the lack of security and vulnerability of the channel for data communication allows the attacker to sniff information from the network. In the system, unsecured data storage allows the attacker to obtain information from the cloud environment. Therefore, unauthorized people may modify and steal information from the system.

Failures among the nodes affect the communication process and are another one of the problems that WSNs face. Sensor nodes can be broken or stolen, there can be communication link errors, malicious attacks or they may simply run out of power. In order to avoid fault problems, there are routing algorithms that act in case of failure (fault-tolerant algorithms). In a WSN, the fault-tolerance functionalities can be implemented in the software, hardware, network communication, and application layers [73]. According to the routing protocol, different techniques are used to reduce the consequences of the failures. In addition to the efficiency of the system, fault-tolerance solutions may have an impact on energy consumption. Therefore, a balance between energy consumption and efficiency must be sought after so as to implement fault tolerance functionalities.

1.2 Objectives and motivation

The aim of this work is to provide a new architecture and communication protocol to transmit data, actions, and alerts to the different elements that comprise a precision agriculture system with wastewater treatment functionalities. In order to achieve this goal, the following process was performed.

Firstly, the different elements of a PA system are identified so as to assess the devices that comprise the architecture of the system. The field area and the water canals where the water treatment process is performed are the differentiated zones of interest. The proposed sensor nodes are designed to be deployed in these areas. The operation algorithms applied to the sensor nodes allow reducing the amount of forwarded data while the necessary information is transmitted.

Furthermore, a heterogeneous communication protocol was designed to allow data, action, and alert transmissions among the different elements of the architecture. As the architecture is comprised of different areas with different requirements, WiFi and LoRa wireless technologies were utilized for zones with medium-range and zones with long-range requirements, respectively. A bridge node allows forwarding the messages of the protocol from the WiFi nodes to the LoRa nodes. Moreover, a multi-hop LoRa topology was created to allow the addition of edge-computing functionalities and to overcome the coverage limitations by adding more nodes to relay the messages of the protocol to the gateway deployed at the desired location. This solution has a great potential to provide connectivity to other systems in remote areas. It also expands on the use of LoRa

contemplating a tree topology instead of the point-to-point topology that is currently utilized.

The main objectives of this dissertation are:

- Identifying the key parameters for precision agriculture and water quality monitoring.
- Performing a study on the recent advances on smart irrigation and precision agriculture systems considering the utilized sensors, electronic devices, and communication technologies.
- Designing an architecture for the monitoring of water quality and the estate of the fields located in remote areas with limited access to the infrastructure of service providers.
- Design and development of a heterogeneous communication protocol for the designed architecture.
- Designing and developing algorithms for data aggregation and generation of alarms according to the monitored parameters.
- Evaluation of the performance of the proposal in simulated and real scenarios.

1.3 Precedents

WSN were the focus on past years and some works were performed regarding routing protocols for PA WSN. One of them is the PhD thesis presented by Yibo Chen in 2015 named "Routing algorithm dedicated to environmental data collection: precision agriculture". The author proposed an architecture for IPv6 low power and lossy networks for PA. Furthermore, a routing protocol was presented introducing energy-aware routing metrics. Experiments were performed through simulations and deployments in real environments to test the performance of the proposal.

More recent works propose IoT architectures for varied purposes. Diana Cecilia Yaccjirema Vargas presented in 2019 her PhD "Arquitectura de interoperabilidad de dispositivos físicos para el internet de las cosas (IoT)". She designed an interoperability architecture so as to communicate IoT devices. Furthermore, she developed a smart IoT gateway to perform data analysis and storage. On the other hand, David Fernando Sarabia Jácome defended in 2020 his PhD "Arquitectura de análisis de datos generados por el Internet de las cosas (IoT) en tiempo real". In his work, the author designed an architecture for Big Data management and has applied his solution to assisted living systems where artificial intelligence is applied to monitor sleep apnea.

Furthermore, other PhD thesis of the research group have been related to the introduction of technology in agriculture and the development of architectures and

communication protocols for varied purposes. Carlos Cambra Baseca presented in 2019 his PhD thesis “PLAtaforma Tecnológica Multimedia para la Agricultura de Precisión (PLATEM Precision Agricultre)”. The author developed a web platform for agriculture data integration that incorporates AI to process the data gathered from sensing nodes and drones. Furthermore, the data can be shared among farmers in order to expand the knowledge. José Miguel Jiménez Herranz defended in 2018 his PhD “Design of an architecture and communication protocol for video transmission and videoconference”. The architecture and protocol developed by the author are focused on Internet Protocol Television and use of HTML5 (Hypertext Markup Language). The Software Defined Network technology is utilized as well. Moreover, the proposal improves the Quality of Experience of the users. Juan Ramón Díaz Santos presented in 2016 his PhD “Design and Implementation of a Communication Protocol to Improve Multimedia QoS and QoE in Wireless Ad Hoc Networks”. In his dissertation, a protocol based on the organization of node clusters that maximize the utilization of the available resources for IP and multimedia traffic was implemented. Lastly, Miguel García Pineda presented in 2013 his PhD “A Group-Based Architecture and Protocol for Wireless Sensor Networks”. In his thesis, an architecture and protocol for collaborative group-based networks that avoid overheads and the transmission of unnecessary messages. The work presented in this dissertation is a continuation from the work performed by Miguel García Pineda.

Furthermore, the research group has been active in a project regarding the use of sensing nodes to monitor and transmit the data of a network for wastewater treatment of water intended for irrigation through the ERANETMED (Euromediterranean Cooperation through ERANET joint activities and beyond) project ERANETMED3-227 SMARTWATIR.

1.4 Thesis structure

After the introduction of the motivations and main objectives of this thesis, the rest of the dissertation is organized as follows:

In chapter 2, the state of the art on systems for water quality and precision agriculture monitoring is presented. Numerous works were analyzed to determine the most utilized sensors and electronic devices in precision agriculture systems. Moreover, varied architectures and protocols that consider the specific needs of providing connectivity to remote areas have been analyzed. Furthermore, the current trends and limitations of water quality monitoring for precision agriculture are discussed.

In chapter 3, the proposed architecture that contemplates the fields and the water channels that contain the water to irrigate the fields is presented. The topology for a heterogeneous network that includes a WiFi/LoRa bridge is provided as well. Furthermore, the electronic devices that monitor the varied elements of the system are described and the algorithms that determine their operation and data management are presented.

In chapter 4, the heterogeneous communication protocol is described. The protocol has a low overhead and allows the communication between WiFi and LoRa nodes. The design and the functionalities of the protocol are discussed and the message exchange for each phase is specified. Furthermore, the messages and the contemplated alarms are detailed.

In chapter 5, the study cases for special needs and functionalities are presented. Firstly, a multi-layer data aggregation fog computing framework to reduce the number of transmitted packages is presented. Then, the case of a network comprised of LoRa nodes is proposed. The security of different elements of the system is discussed as well. Furthermore, the case of heterogeneous networks that utilize WiFi, 3G, or CoAP are contemplated. Lastly, the case of the use of remote sensing drones as gateways is addressed.

In chapter 6, the simulation experiments are described and discussed. The effects of the proposal for data aggregation on the consumed bandwidth and the number of forwarded messages are presented. The results of the performance assessment of the protocol for a LoRa network for water quality monitoring are analyzed as well. The use of multiple WiFi nodes and their effects on consumed energy and bandwidth is also studied. Moreover, the collisions in WiFi WSN transmission for PA are evaluated as well. Lastly, the effects of different drone flight settings on the coverage of the drone as a gateway are discussed.

In chapter 7, the practical experiments are presented. The performance results that validate the proposed protocol are discussed. Coverage tests were performed as well with WiFi devices deployed on environments with different types of vegetation, different heights, and underground. Furthermore, LoRa coverage tests with low-cost devices and antennas were performed as well. Lastly, the results of a fruit quantification functionality are provided as well.

In chapter 8, the conclusions on the performed work are presented. Furthermore, the problems faced during the thesis, the personal contributions, and the future research lines are detailed. Lastly, the publications derived from this work are presented.

Chapter 2

State of the Art

2.1 Introduction

In this section, the state of the art is presented. In order to analyze the state of the art, the following research questions were considered: What are the current IoT solutions for smart irrigation for agriculture? What sensors, actuators, nodes, and wireless technologies are being utilized to develop IoT irrigation systems? Search engines and digital libraries were utilized by the authors to search manually for papers suitable for this survey. A total of 283 papers were obtained from Google Scholar [74], IEEE explore [75], Scopus [76], and the digital library of Sensors [77]. The keywords employed to obtain the total number of papers to be analyzed were IoT irrigation, IoT irrigation system, and smart irrigation. Furthermore, all papers were checked to ensure they included the keywords irrigation or water and IoT or smart in their content.

In order to discern which papers to use, only papers written in English were considered. Furthermore, to observe the recent evolution in this field, the selected papers were published from the years 2014 to 2019 (both years inclusive). Finally, a total of 178 papers were utilized to compile this review.

After the selection process, all papers were classified manually into IoT irrigation systems and architecture, protocol, and sensor proposals that were not used to create the figures in this paper but discussed relevant information. The papers from the first group (160) were then analyzed to determine the sensors and actuators that were employed to develop the IoT irrigation system, the parameters that were monitored, the type of

irrigation and agriculture, the type of node, the type of wireless technology and data visualization technique that was utilized to access the data and to manually choose the actions of the irrigation system. All the collected data has been then classified into different sections and converted into graphs and tables to provide a complete overview of the actual state of the art regarding IoT irrigation systems.

The distribution of the papers regarding the country of the first author is presented in Figure 2.1. As it can be seen, the countries that investigate IoT systems for irrigation are countries where agriculture is a major economic source. India is the country with the highest number of papers with a total of 92 papers, 57.5% of the total. China and Spain are tied with seven papers each. Costa Rica, Ecuador, Indonesia Thailand, and the USA have between three and six papers. The rest of the countries that have investigated IoT systems for irrigation have one or two papers.

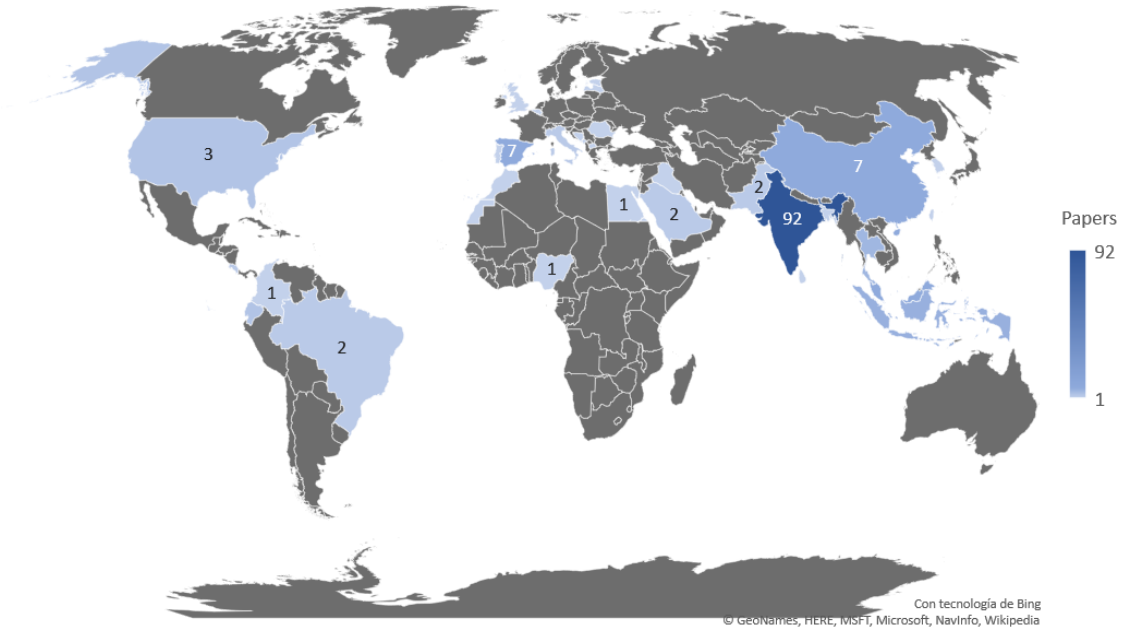

Figure 2.1. Number of published papers presenting IoT systems for irrigation per country.

It is remarkable that only one out of the five countries with the highest agricultural land area (China, USA, Australia, Brazil, and Kazakhstan) is included in the top five countries of our survey in terms of water management. India, which is the country with the highest production of papers that presents IoT systems for water management is the 7th country in terms of agricultural land area. With regard to the top six countries, in terms of published papers with irrigation systems, three of them (India, China, and Spain) have regions with high and moderate water scarcity problems. Again, there are some countries with regions affected by water scarcity that use irrigation systems in their agriculture and have published fewer papers on irrigation systems like the USA. Nonetheless, it does not mean that in these countries no efforts are done in order to reduce water use in agriculture. It is possible that in these countries the major efforts are

done by enterprises and their findings are directly patented and distributed in the market. Most of the papers are published by authors who come from developing countries.

As per the number of papers per year of publication, see Figure 2.2, the interest in this topic has been increasing over the years. The lower number of papers for 2019 is due to the year not being finished when the selection process of the papers was completed. Thus, not all the papers performed in 2019 had been published.

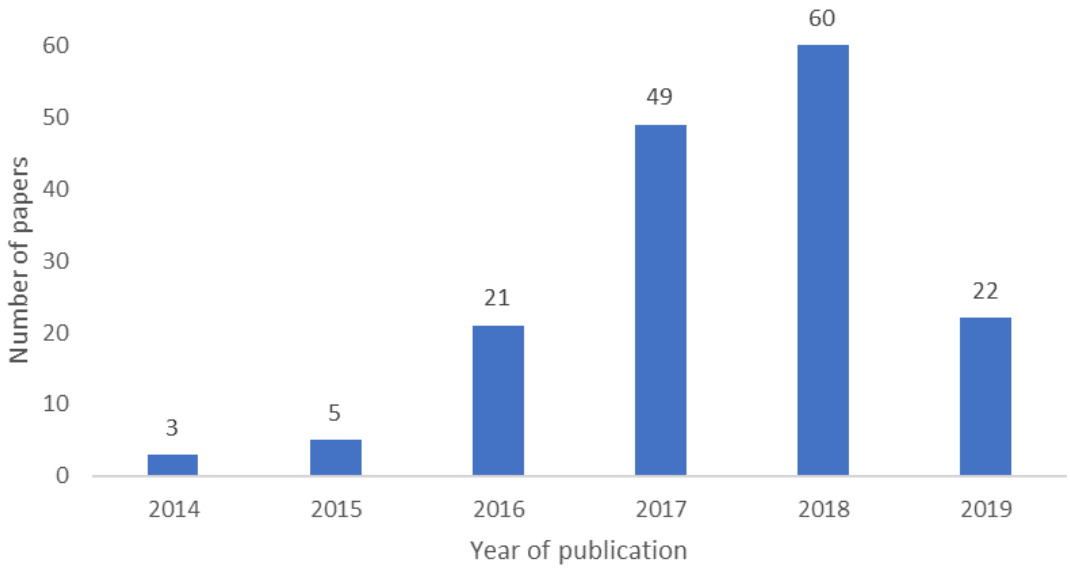

Figure 2.2. Number of published papers presenting IoT systems for irrigation per year.

After the review of the papers that met the aforementioned criteria, a discussion on the previous works regarding different topics concerning precision agriculture irrigation systems and wireless communication for these environments has been performed.

2.2 Water Management

In this section, we present the information and analysis of papers that present different techniques for water management in the irrigation process. For this analysis, we consider the papers that include any sort of water pumping actuator as an irrigation system. From a total of 178 evaluated papers, 107 of them present an actuator for irrigation. After analyzing the 107 papers we discard the ones that just offer partial information, a total of 89 papers are included in this section.

In the agriculture activities that use water inputs, also known as irrigated agriculture, there are different manners to distribute the water. The different options present different efficiency and, in some cases, a specific manner should be used for a specific crop. The specific manners to irrigate have a great variety but we can divide them into

the following categories: Attending to the way of water is distributed we can consider: (i) flood irrigation, (ii) spray irrigation, (iii) drip irrigation, and (iv) nebulizer irrigation. Regarding the existence of sensing systems, we can have (i) irrigation without any consideration, when the amount of water is not calculated or estimated, (ii) scheduled irrigation, when the water is supplied according to the estimated needs in a period of the year, (iii) Ad hoc irrigation, when the amount of water is calculated based on the sensors measurements. The vast majority of the papers included in this section propose to use pumps and valves to distribute the water in conjunction with sensors to measure environmental parameters in order to calculate the water needs. From the 89 evaluated papers in this section, 83 include clear information of the proposed irrigation system, the other six only mention that they include actuators for irrigation, see Figure 2.3. Those 83 include different levels of detail, there are 49 papers that only indicate that there are motor/pumps in their system (40 paper) or valves (nine papers) without more detail. From those papers which offer more details, 19 of them include sprinklers (the most used system) [5, 78–95], eight use drip irrigation [96–104], two propose the utilization of sprayers [96, 105], and the rest use very specific irrigation systems (robots [10], pivot [106], rain gun [107] or it can be applied to multiple systems [108]). In conjunction with the principal irrigation system, three papers propose the use of a fogging system [90, 92, 101] and two papers propose the use of fertigation in their systems [91, 102].

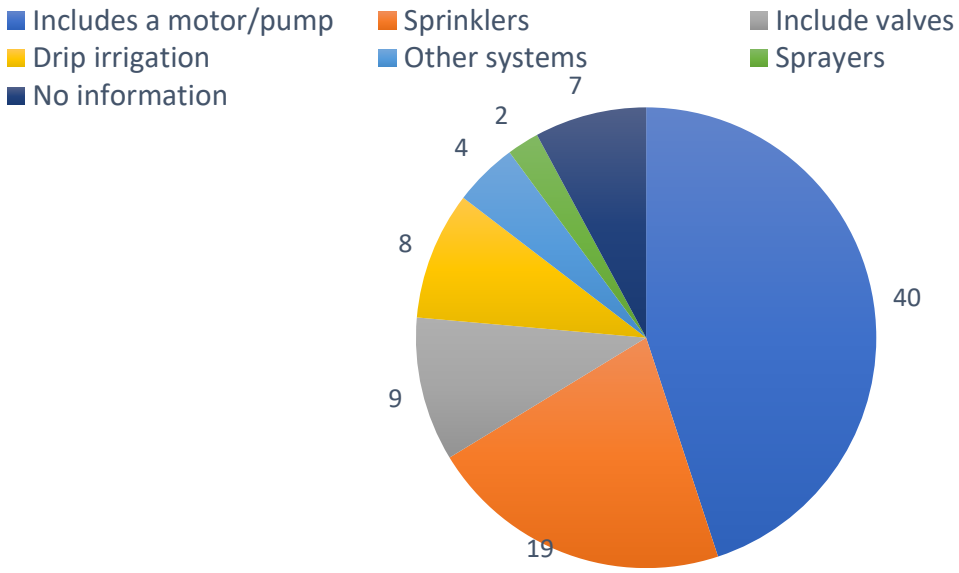

Figure 2.3. Number of papers that propose different irrigation systems.

In this paragraph, we describe the different agriculture systems that are included in the papers. Most of the included papers in this section do not describe the target agriculture system of their proposal. Nevertheless, there are 38 papers that include this information, see Figure 2.4. The most common use of irrigation systems is in outdoor agriculture, 50% of the proposed systems are for outdoor agriculture. Among this outdoor agriculture cases [5, 79, 81, 87, 89, 91, 95-98, 102, 106, 109-117], some papers

specify the agriculture products in more detail: general cereal [106], rice [98, 109], spinach, beans, carrots, walnuts, corn, barley and maize [97], and multi-height fields [110]. In addition, among the 14 papers about greenhouses [78, 82, 88, 90, 101, 118-125], five of them specify the type of crop. There are three cases of hydroponic crops [82, 118, 119], one case of mushroom cultivation [90], and one paper on flower farming [121]. Finally, there are five papers focused on gardening [85, 103, 105, 117, 126], one of them specifically about green walls [126].

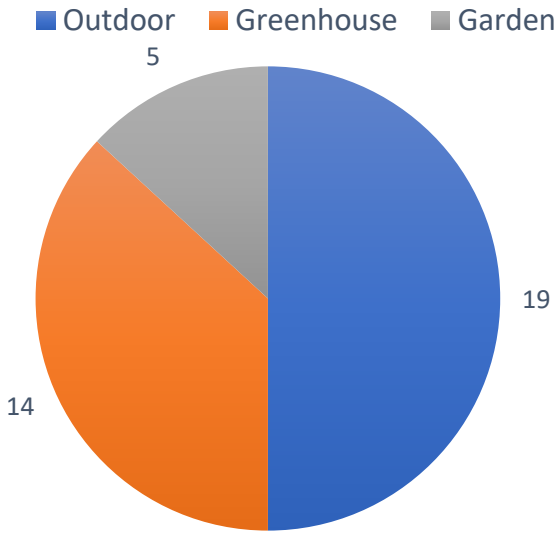

Figure 2.4. Number of papers that proposed irrigation systems for different sorts of agriculture.

Following, we describe the sensors used in the irrigation systems. From a total of 89 papers that include irrigation systems, there are six of them that do not describe or give information about the utilized sensors for their system. Those six papers are more focused on the node, telecommunication, or visualization aspects. As in this survey, we include several parameters, we will divide this information into two figures.

In the first graph, we are going to show what environments (air, water, soil, or plant) have been monitored in most papers. This information is presented in Figure 2.5. A paper that monitored the soil can measure one or more parameters, but this information is not included in Figure 2.5. The environment that has been monitored in more papers is the soil. It was measured in 76 papers, more than 85% of the cases. Weather is the second parameter in terms of the relevance of monitoring, it includes many parameters such as temperature, rain, and humidity among others. Weather is monitored in 60 papers, up to 68% of the proposals. Water is less measured in the proposals of irrigation systems. It is measured only in 26 papers, less than 30% of the included cases. Plant monitoring is the less measured factor. It is monitored only in four proposals. There are 15 papers that use the weather forecast to obtain data and include this data in their system.

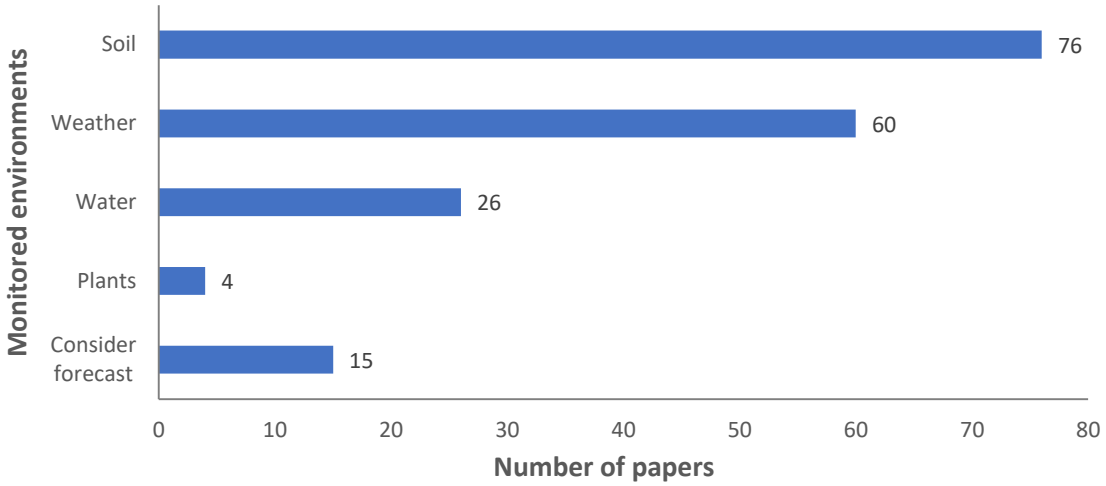

Figure 2.5. Monitored environments in papers that propose an irrigation system.

Following, the details about the number of monitored parameters are presented (see Figure 2.6). From the 89 included papers, more than half of the proposals measure between three and four parameters. Measuring fewer parameters (one or two) represents 31% of the cases (17% one parameter and 14% two parameters). There are some rare cases (10% of them) where more than four parameters are monitored. The papers where more parameters are measured are [114, 117], with six measured parameters, and [5, 94, 96, 111, 118, 125, 126] that measured five parameters. On the other hand, there are five papers (6% of cases) that do not measure any parameter [82, 90, 127–129].

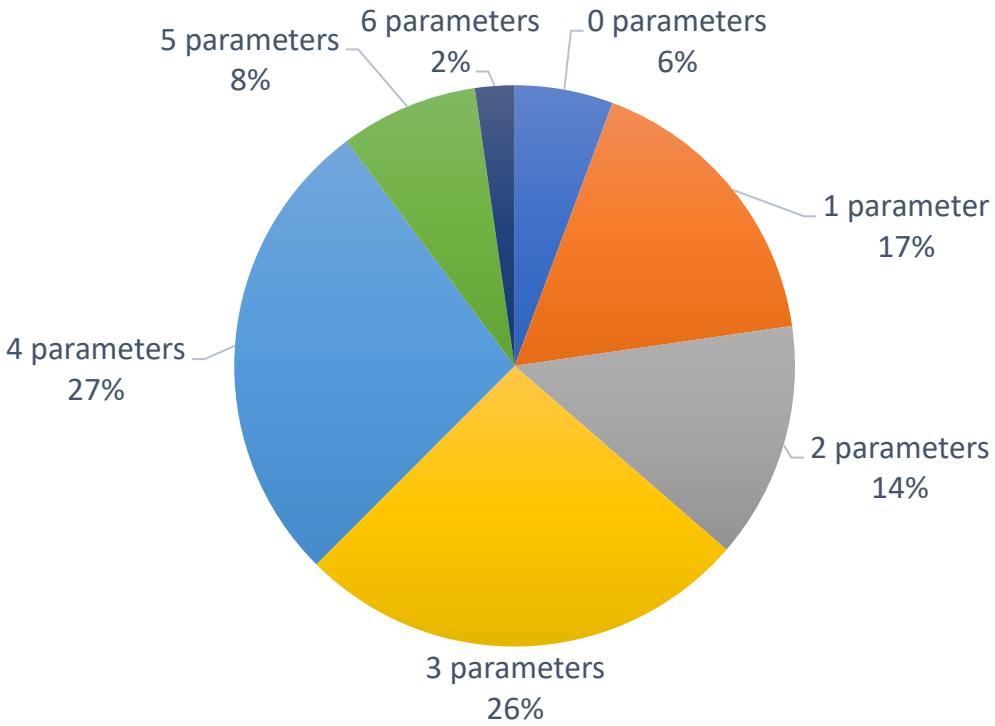

Figure 2.6. Number of monitored parameters in papers that propose an irrigation system.

Next, the details about the measured parameters are shown. Regarding the sensors of soil, plants, and water (see Figure 2.7), the most used sensor in the systems is the soil moisture sensor, which is used in 76 papers (more details in Section 4). First, we will analyze the data from soil and plant sensors. The soil temperature is much less considered in these systems, it is only measured in seven proposals. Attending to the soil characteristics, in one proposal the authors use a sensor that monitored the nutrients of the soil [130]. There are 14 proposals of IoT for irrigation management that include a pH sensor. However, not all of them specify if the pH sensors are for the soil or for the water [5, 91, 99, 104, 118, 120, 124, 125, 131, 132], only four of them indicate this (three for soil [116, 117, 122] and one for water [119]). Only four papers consider plant monitoring, in two papers the measured parameter is the plant height [114, 133], using an ultrasound sensor. In the other two cases, leaf wetness was considered in their system [95, 134, 135]. Different sensors are used, [134] used a sensor based on optical signals while [95] utilized a commercial FC-37 sensor.

Now, the data from the water sensor are presented. In this case, we will consider for the commentaries not only the data of the graphic (proposals with irrigation system) but also the information of the paper which measures the water quality, having or not the actuators for the irrigation system. The water level in the tanks is measured in 17 [81, 85, 101, 107, 108, 111, 112, 114, 119, 135–142] out of 88 papers that have a pumping system. There are different methods to monitor the water level in the tanks and the most used is the one based on ultrasound [81, 119, 139], the resistive methodology is used in one case [85], the rest of the cases do not offer information of how the data is measured. In the case of sensors based on ultrasound methods, the most utilized sensor is the HC-SR04 [119]. In addition, there are six papers that do not include an actuator for the irrigation system even when they have water level sensors [110, 143–147]. There are nine papers where sensors for monitoring water flow are utilized [5, 106, 91, 94, 100, 114, 125, 126, 132]. The sensors used are only described in two cases, the commercial Gems FT110 G3/8 sensor is used in [125] and the YF-S402 in the proposal presented in [126]. Both sensors are based on a Hall effect turbine. They have different prices and similar operational ranges. The Gems FT110 G3/8 [125] can measure flows between 0.5 to 5 L/min. The other sensor, the YF-S402 [126], is capable of measuring flows between 0.3 to 6 L/min. Moreover, water flow sensors are used in three other proposals that do not include actuators for irrigation systems [148-150]. Regarding water quality, the water conductivity is monitored in four proposals [101, 118, 119, 125]. Only in one case [125], the authors indicate the used sensor. They use commercial sensors for monitoring pH and conductivity from B&C Electronics [125].

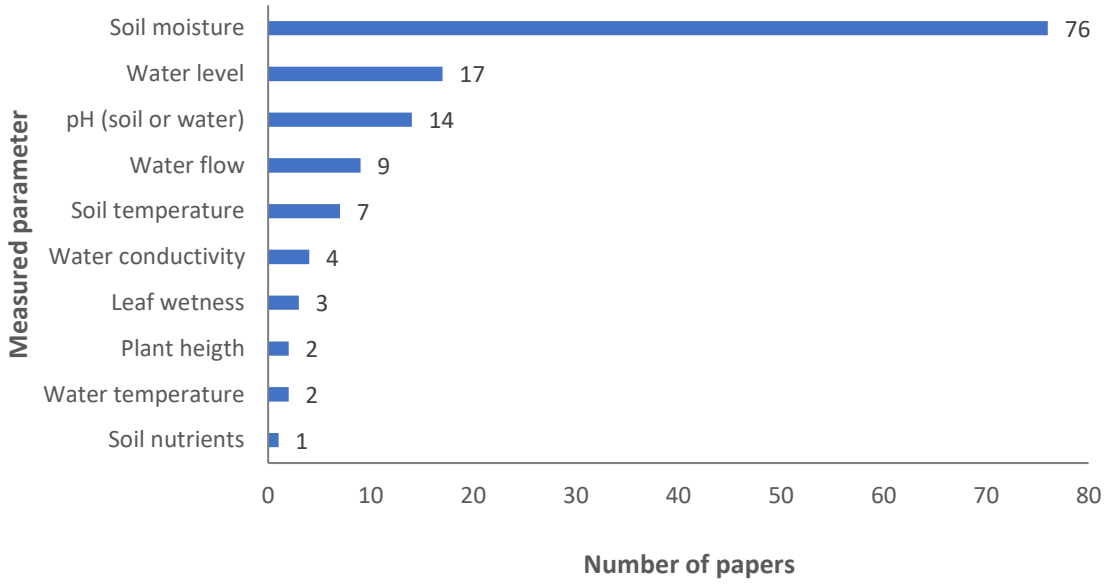

Figure 2.7. Monitored parameters from the soil, water, and plants in papers that propose an irrigation system.

Additionally, there are two papers without an actuator for irrigation systems that include in their proposals a sensor for conductivity [149, 151]. Nevertheless, no data regarding the equipment used are given. Regarding the pH of water, it is monitored in another three papers (apart from [119]) [150, 152, 153]. In one case, the authors specify the used sensor, the Lutron Pe-03 [150]. The temperature of the water is measured in two proposals [101, 119]. Only in one case did the authors specify that the used sensor is the DS18B20 [119]. No other proposals evaluated in this survey (having or not irrigation system) presented the use of temperature sensors for the water.

On the other hand, with regard to the proposals that monitored the atmospheric parameter, the data is presented in Figure 2.8. Next, we are presenting the importance of these sensors for irrigation systems. No details of which sensors are used in which papers are given in this section. This information will be further discussed in Section 2.4. The air temperature is the most measured parameter, it is monitored in 58 papers. A total of 51 proposals include a humidity sensor. Other parameters are less measured such as the rain, which is measured in eight out of 89 papers that proposed an irrigation system, or the wind, measured in only one paper. Meanwhile, there are 15 proposals that consider the weather forecast. From those 15 proposals, 10 of them use the data from the forecast in conjunction with the data gathered by sensors and five proposals use the weather forecast as the sole information for weather data/atmospheric parameters.

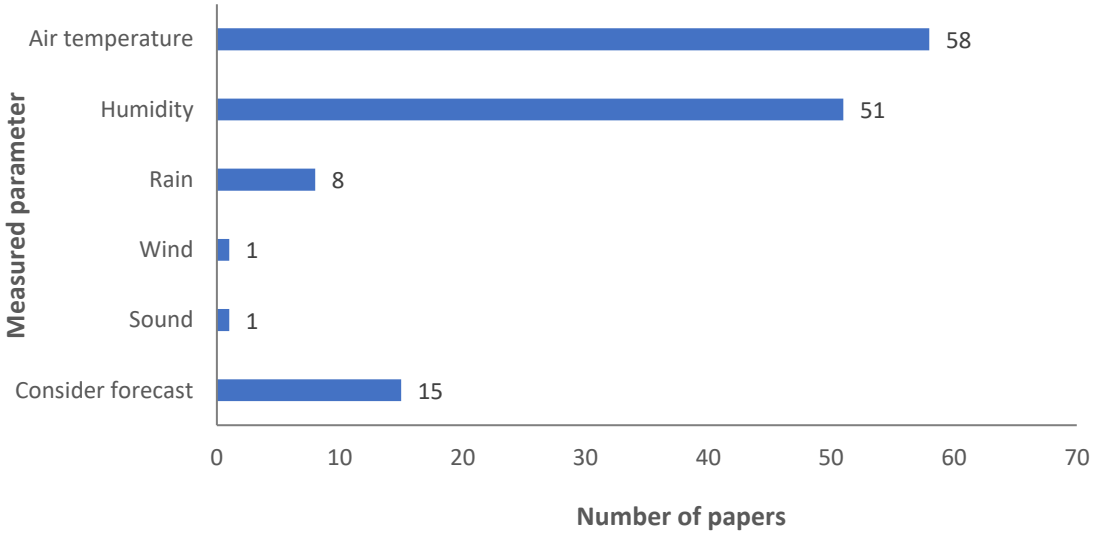

Figure 2.8. Monitored atmospheric parameters in papers that propose an irrigation system.

Next, the information related to the use of actuators in the papers that proposes an irrigation system included in this section is listed in this paragraph (see Figure 2.9).

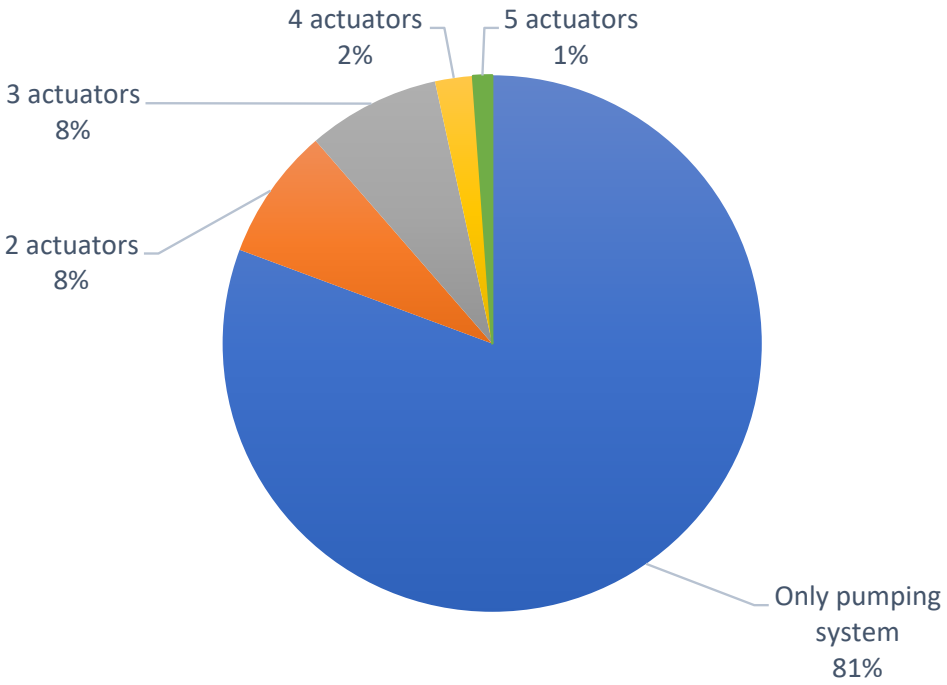

Figure 2.9. Number of included actuators in papers that propose an irrigation system.

The vast majority of the papers include only the actuator of the irrigation system (pump, valve, sprinklers, etc.). A total of 71 proposals (81% of cases) use only the irrigation system as an actuator. There are seven papers (8% of cases) that propose the use of two actuators (irrigation system plus another one). The use of three actuators is

presented in seven papers, the same percentage that the use of two actuators. Finally, there are some rare cases (3%) where authors have proposed the use of more than three actuators, in two papers they use four actuators [88, 122], and in one case the use of five actuators is presented [117].

Next, we present in Figure 2.10 the description of the selected actuators. Since we are considering only the papers that include an irrigation system, the most used actuator in the different irrigation systems. Therefore, we do not include the use of irrigation actuators in Figure 2.10. The most utilized actuator is the sound emitter, used in seven cases [81, 99, 108, 109, 111, 116, 154]. It is generally used as an alarm for the farmers or as a dissuasive measure to prevent the entry of animals into the farming lands. In the second position, we found the use of artificial light systems. They are used in six cases [85, 87, 100, 121, 122, 125]. The use of artificial light is mainly related to the generation of artificial photo- periods to increase productivity, but they can also be used for operational purposes. Fans are included in five proposals and their use is related to modifying the atmospheric conditions (temperature, humidity, or even the balance between CO_2/O_2). The proposals that include the use of fans are [88, 115, 118, 112, 125]. The use of ultrasonic sound emitter is found in four papers [32, 51, 64, 65]. The least utilized actuators in IoT irrigation systems are scarecrows [58, 115, 116], which are dummies or robots that are utilized or have the function of scaring birds and other types of animals to protect the crops, and heaters [78, 115], that modify the temperature to improve the performance or the health of the crops.

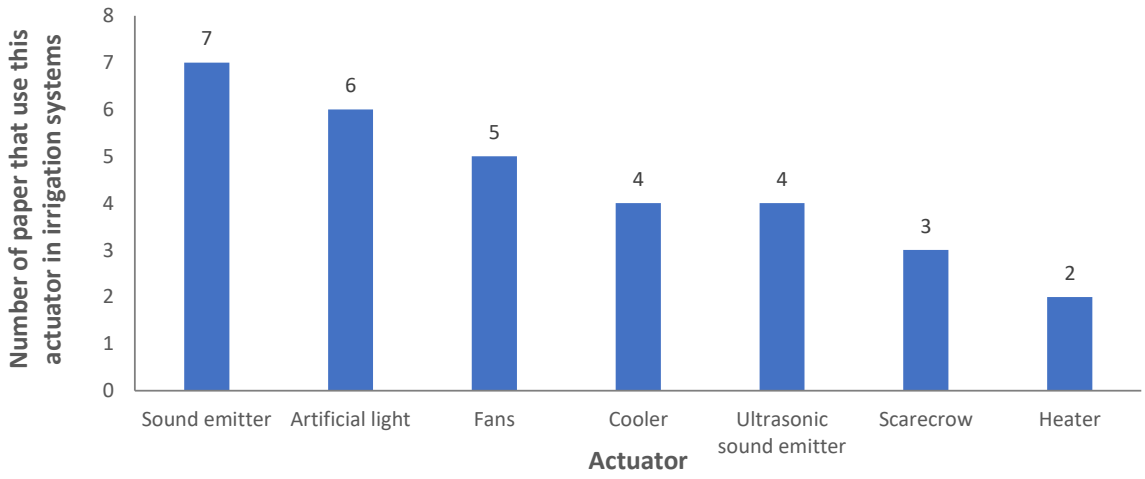

Figure 2.10. Used actuators in papers that propose an irrigation system.

In addition to the defined parameters, which are measured in different papers included in this survey, there is an important parameter that is crucial for irrigation scheduling. This parameter indicates the water loss due to the evaporation from the soil and transpiration through the stomata of plants; it is known as evapotranspiration (ET). Several authors measured both terms—evaporation and transpiration—separately, using different sensors to obtain the ET data [155]. It also can be estimated according to the vegetation and the climatic data by several mathematic models [156]. Some web-based

applications can estimate the potential ET given a location. For ET monitoring, remote sensing is the best option as many papers point out [157–159]. Among the possibilities for ET monitoring with sensors, the integration of soil moisture changes can offer evaporation data. Nonetheless, the measurement of transpiration is more complex; it can be estimated with the data of sensors that measure radiation, leaf area index, and vapor pressure deficit [160]. Due to the complexity of its measurement, it is not included as a monitored variable in most of the papers of precision agriculture. None of the papers considered by this survey includes all the necessary sensors for measuring the ET.

2.3 Soil Monitoring

An outline of the soil parameters considered for the IoT irrigation monitoring systems and the utilized sensors are detailed in this section. In this section, we include the data from those proposals that include at least one sensor for the soil, a total of 106 papers are included.

As indicated in the previous section, the most relevant parameter for the irrigation systems is soil moisture. The number of proposals that include different sensors is presented in Figure 2.11. The soil moisture is measured in all the 106 papers included in this section. The second parameter, in terms of relevance, is the soil temperature. The soil temperature is monitored in nine proposals. The pH is monitored in four papers [102, 116, 117, 161] and the nutrients of soil in only three cases [148, 130, 153].

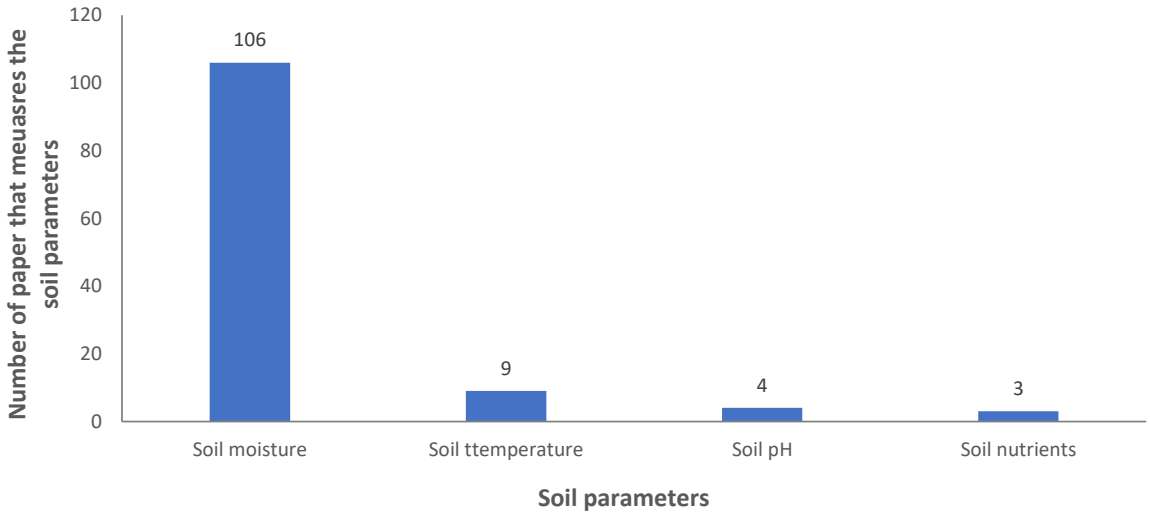

Figure 2.11. Monitored soil parameters in all the evaluated papers.

From the 106 proposals that include a soil moisture probe, 71 of them do not indicate the used equipment to measure the soil moisture, see Figure 2.12. In six cases [87, 152, 162–165], they only include a picture of the device, but they do not indicate the model and manufacturer. In all those cases, the sensors employed are based on the

measurement of the conductivity between two electrodes that are inserted in the soil. In one case [144], the authors proposed to use a 4-fork sensor, based on the same principle as the previous ones. Nonetheless, no extra information about the sensor used was included in the paper, such as the manufacturer or model. The proposal presented in [149] only indicates that the utilized sensor was manufactured by EB. In [114] the authors only mention that the sensor used was a hygrometer. A total of 24 proposals clearly indicate the used sensor for monitoring the soil moisture.

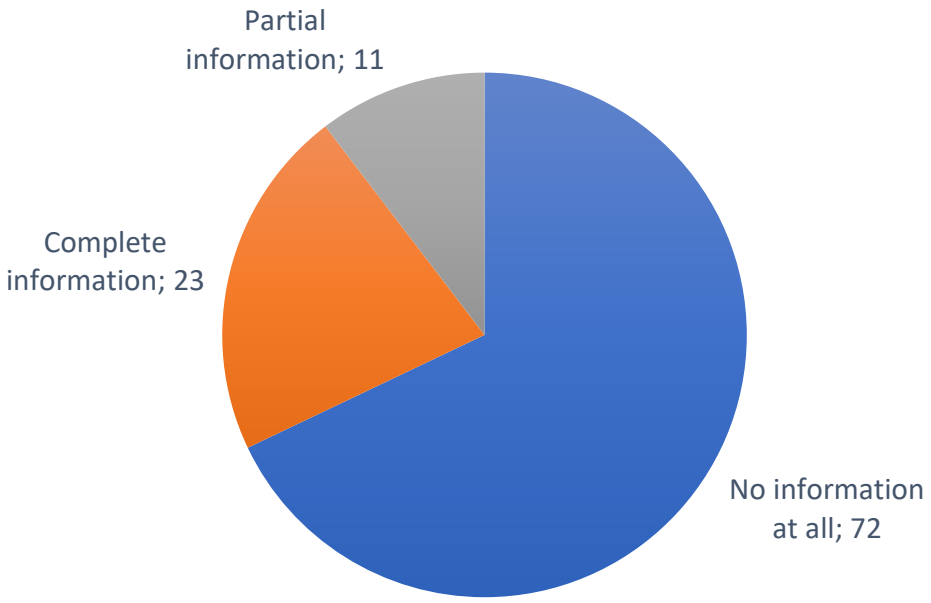

Figure 2.12. Information about the used moisture sensors in all the evaluated papers.

Most of those proposals use similar sensors based on the conductivity between two electrodes. Different models of the aforementioned sensor have been used in the proposals (see Figure 2.13). The most used sensor, based on conductivity, is the YL69. It has been used in nine proposals [10, 93, 121, 137, 145, 166–169]. This sensor is characterized by a low price, and it is created specifically to operate with Arduino (and similar nodes). The output voltage goes from 3.3 to 5 V and the output values are related to soil moisture (0 to 300 for dry soil, 300 to 700 humid soil). Nevertheless, it is not possible to have a measure that indicates exactly the value of moisture without performing new tests and calibration of the sensor. The same range of measure is found in the other used sensor based on the same principle, the FC-28 [83, 122, 126] and the SEN0114 [95]. The S-XNQ-04 [105] has a similar operation principle. However, it is composed of three electrodes. In this case, the sensor output voltage goes from 0 to 2 V and the sensor is capable of measuring the soil moisture giving as a response the relative saturation moisture content expressed in percentage (%). This sensor has an accuracy of 3% and it can measure from 0 to 100% of relative saturation. It can operate from −40 to 85 °C.

A device able to measure the temperature and the moisture at the same time, the VH400, is utilized in [86, 89, 139, 146, 170, 171]. These sensors can be used from 40 °C to 85 °C, but the accuracy and operational range of the sensor probe are not indicated in its datasheet. The operational principle of this sensor is based on the measurement of the dielectric constant of the soil using transmission line techniques to measure the moisture in any type of soil notwithstanding soil salinity. The output voltage of this sensor goes from 0 to 3 V. This output voltage is related to the volumetric water content in the soil. The sensor does not offer a linear relationship between the output voltage and the volumetric water content, but the sensor can measure from 0 to up to 60% of volumetric water content in the soil. This sensor has a relatively low price and can be implemented in Arduino systems (and similar).

A sensor with completely different operational principles, the 200SS, is used in two proposals [106, 172]. It is a solid-state electrical resistance sensing device that is used to measure soil water tension. The 200SS [106, 172] has a pair of highly corrosion-resistant electrodes, as a resistive device, the resistance of the sensor changes with the soil moisture. The electrodes are embedded within a granular matrix. The output values of the sensor go from 0 to 199 centibars. The higher the value of centibars the lower the water availability for the plants. The system presented in [104] uses an SM300 sensor. This device is able to measure two soil parameters (moisture and temperature). The SM300 [104] measures the soil moisture and temperature based on the generation and propagation of the electromagnetic field into the soil. The sensors measure the soil moisture as the volumetric water content, the operating range goes from 0 to 100% and the accuracy is ±2.5%. This sensor is manufactured by Delta-T Devices Ltd. This sensor is not specifically created to be integrated into an Arduino measuring system, even though it can be adapted since the output voltage goes from 0 to 1 V.

Finally, the system detailed in [173] used the HA2002 sensor, but no information is available on the internet about this sensor in terms of operational principle or range of measuring. The sole information that was found was that the sensor is an HA2001 [173] sensor manufactured by Handan Dingrui Electronics Co., Ltd.

Regarding the sensors used for monitoring the soil temperature, which are mentioned in [86, 89, 45, 94, 113, 117, 144, 173, 174], the different sensors are detailed in this paragraph. There are five papers that do not specify the sensors used [94, 113, 117, 144, 174]. The other four proposals indicate in the paper the sensors selected. Although in one paper no information could be found about the sensor utilized [173], the authors indicate that their system includes the HA2001 sensor.

In other cases, the information of the selected sensors is detailed. The proposal presented in [104] used an LM35 sensor. This device is able to measure temperature. The operating range is −40 to +125 °C and the accuracy is ±0.5 °C. The sensors offer an analogic signal and it is manufactured by Texas Instruments. The proposals presented in [86, 89] selected the THERM200 to measure the temperature. The operational range of these sensors goes from −40 °C to 85 °C and its accuracy is ±0.5 °C. The operation principle of this sensor is not specified in the datasheet.

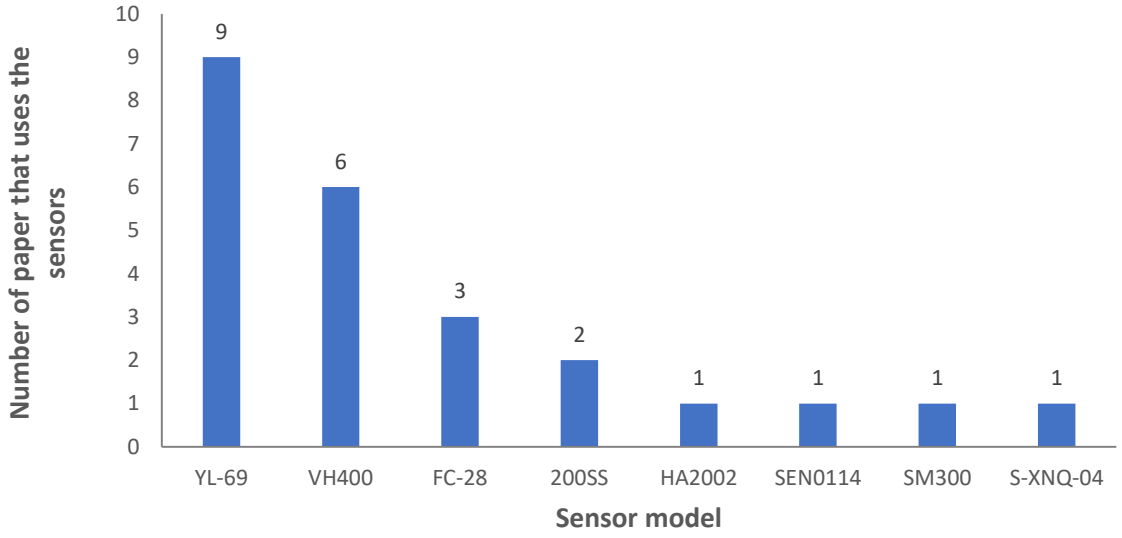

Figure 2.13. Number of papers that used different models of soil moisture sensors.

In terms of sensors for soil nutrients, three papers include in their proposals sensors for monitoring this variable [130, 148, 153]; nonetheless, not all of them indicate the used sensor. The only paper that clearly indicates the utilized sensor is the proposal presented in [130] includes an 1185 SunRom color sensor. This sensor is based on RGB color detection, in [130] authors relate the color of the soil with the nutrients. The pH of the soil is measured in four proposals [116, 117, 122, 161]. However, none of these proposals indicates the selected device or equipment in the paper.

2.4 Weather Monitoring

An overview of the weather parameters monitored in IoT irrigation monitoring systems and the most utilized sensors to monitor these parameters is provided in this section. The weather conditions are a key factor both in irrigation needs and in the performance of crops. Figure 2.14 shows the most monitored weather parameters in the currently available smart irrigation proposals. Temperature and humidity affect the evapotranspiration of the water in the soil. Air temperature is defined as the thermic level of the atmosphere and is usually measured in Celsius, Fahrenheit, or Kelvin degrees. It is the most monitored weather parameter with one hundred papers monitoring it. Humidity is the presence of water vapor in the air. The amount of water vapor in the air is expressed in percentage (%). It is the second most monitored weather parameter with 86 papers. Furthermore, luminosity is paired with temperature as direct radiation from the Sun raises the temperature and leads to more water loss in the soil. It is defined as the intensity or brightness of the light. It is measured in Lux. It is the third most monitored parameter with 28 papers. The amount of precipitation determines whether the irrigation is needed or not and the amount of water to be employed in the case of irrigation being necessary. It considers any form of hydrometeor that falls from

the atmosphere and reaches the earth's surface. Furthermore, it includes rain and snow. A total of 14 papers considered precipitation monitoring. Although temperature, relative humidity, luminosity, and precipitations are the most important factors regarding IoT irrigation systems for agriculture, many systems propose the monitoring of other environmental parameters. Table 2.1 details all the papers that utilized these parameters.

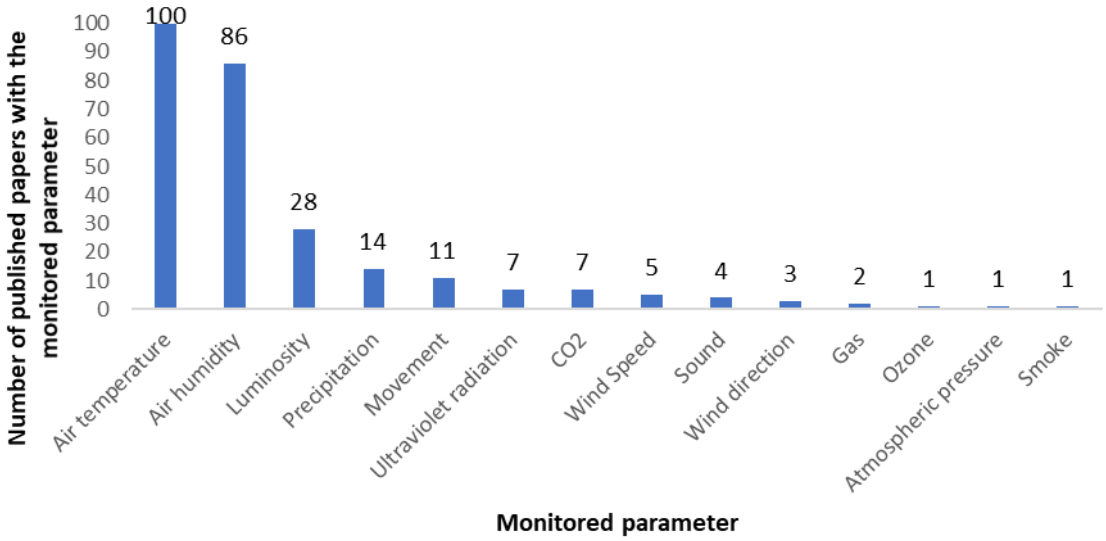

Figure 2.14. Most monitored weather parameters.

Table 2.1. Papers that measure the most monitored weather parameters.

Parameter	**References**
Air temperature	[10, 78, 81, 83, 84, 94–102, 107–109, 111–118, 121–126, 130–139, 141, 143, 144, 146–148, 149, 150, 153, 154, 162, 165, 166, 168–173, 175–213]
Relative humidity	[78, 83, 84, 91, 94–99, 101, 106–109, 111–118, 121–126, 131, 134–139, 141, 143–148, 149, 150, 153, 154, 162, 165, 166, 168–173, 176–178, 181, 182, 184, 186, 188–191, 193–197, 199, 201, 204–211, 213–216]
Precipitation	[80, 95, 98, 100, 111, 117, 126, 145, 165, 170, 188, 194, 208]
Luminosity	[78, 94, 98, 112, 113, 115–117, 121, 122, 126, 141, 149, 163, 169, 170, 176, 177, 180, 182, 187, 191, 195, 196, 205, 207, 208, 210]

As it can be seen, the four previously mentioned weather parameters are the most recurrent environmental factors in the literature. However, there are other weather factors concerning the air and climate that are monitored in some IoT smart irrigation systems. Ultraviolet radiation is electromagnetic radiation with wavelengths ranging from 10 nm to 400 nm and is monitored by seven papers [106, 116, 118, 125, 171, 189, 196]. Measuring wind speed [94, 95, 106, 117, 122], wind direction [94, 95, 117], and atmospheric pressure [209] is also considered by some papers. Air pollutants are

considered in some IoT irrigation systems as well. CO_2 [94, 113, 116, 117, 125, 189, 196], ozone [153], gas [145, 194] and smoke [175] are the types of air pollutant considered by the currently available smart irrigation systems. Lastly, other parameters that are monitored concerning the surrounding area are movement and sound. Movement [87, 91, 108, 111, 115, 178, 192, 194, 197, 199, 214] and sound [91, 189, 191, 214] are considered mostly for security purposes. Ultrasound sensors are deployed to detect intruders in the fields.

There are varied sensors that can be utilized to measure weather parameters. However, there are smart irrigation systems that opt for not including these sensors and choose to ask for the environmental information to web servers such as Yahoo [112, 178], which provide the weather and environmental data from meteorology agencies.

Temperature monitoring is one of the most common parameters regarding weather monitoring in IoT irrigation systems. As it can be seen in Figure 2.15, The DHT11, DHT22, and the LM35, are the most utilized temperature sensors with 27, 13, and 14 papers respectively. Al these sensors are low-cost sensors. On the one hand, the DHT11 and DHT22 provide both temperature and relative humidity readings. On the other hand, the LM35 and the TMP-36 [83, 203] have broader temperature ranges. The papers that utilized these sensors are detailed in Table 2.2. These sensors are low-cost which may be relevant to their extended use.

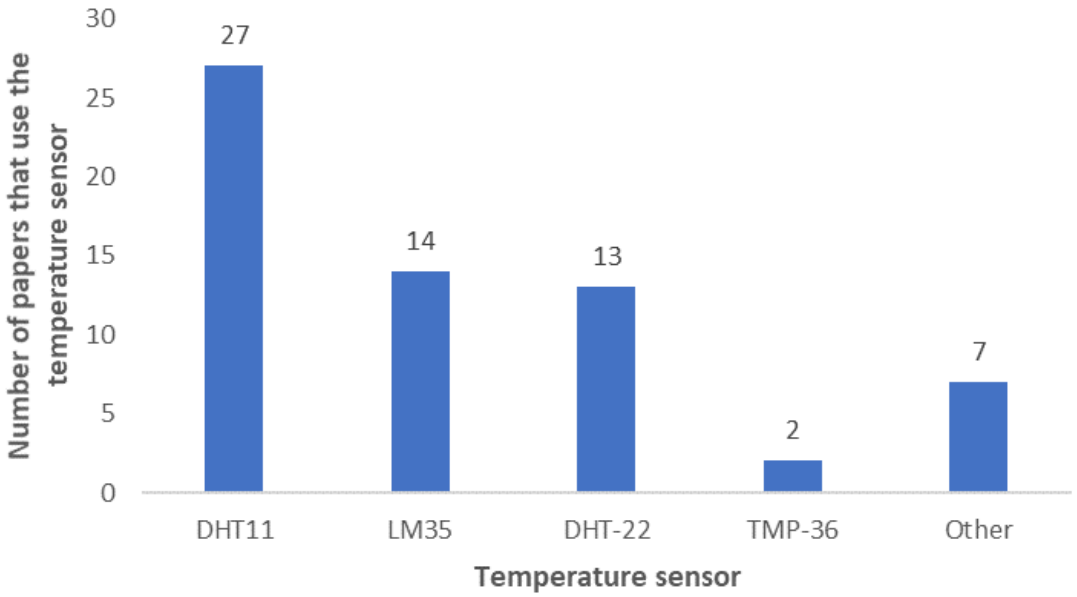

Figure 2.15. Most utilized temperature sensors.

Table 2.2. Temperature monitoring sensors.

Sensor	Temperature Range		Accuracy	Reference
	Min	**Max**		
DHT11	0 °C	50 °C	±2 °C	[78, 109, 111, 112, 114, 121, 137, 143, 144, 153, 154, 166, 168–170, 172, 181, 182, 186, 190, 194, 195, 199, 205, 210, 211, 213]
DHT22	−40 °C	125 °C	±0.5 °C	[126, 138, 145, 146, 165, 171, 177, 195, 197, 202, 206, 207, 209]
LM35	−55 °C	150 °C	-	[10, 98, 99, 103, 115, 130, 132, 134, 141, 149, 154, 180, 183, 216]

According to sensor type, thermistors such as the DHT11, the DHT22, and the AM2315 are the most utilized type of temperature sensors [106] (see Figure 2.16). The DHT11 and DHT22 are low-cost sensors. However, the AM2315 [106] has a higher price with the advantages of a higher range (−40 °C to 125 °C) has higher accuracy (±0.1 °C). Semiconductor-based integrated circuit temperature sensors like the LM35 and DS18B20 [100], and band-gap proportional to absolute temperature sensors, SH10 [84] and SH11 [95], are the next most utilized temperature sensors by type. The SH10 [84] and SH11 [95] sensors provide both temperature and relative humidity readings. Furthermore, compared to the DHT11, they present better temperature ranges and accuracy. They are however similar to the DHT22 in terms of temperature ranges, accuracy, and price. The TMP36 [83, 203] is a temperature sensor comprised of a diode and the EE160 [125] is a resistive temperature detector sensor. The FM-KWS [173] and the BME250 [208] are of an unknown type.

The most utilized relative humidity monitoring sensors are presented in Figure 2.17. As in temperature monitoring, the DHT11 and DHT22 sensors are the most utilized ones, with 29 and 13 papers that use them, respectively. As both sensors are able to monitor both temperature and humidity, most systems that utilize these sensors do not choose a separate sensor for each parameter. There are sensors with better accuracy. However, IoT irrigation systems generally do not need the highest accuracy levels available in the market. Table 2.3 presents the papers that utilize these sensors.

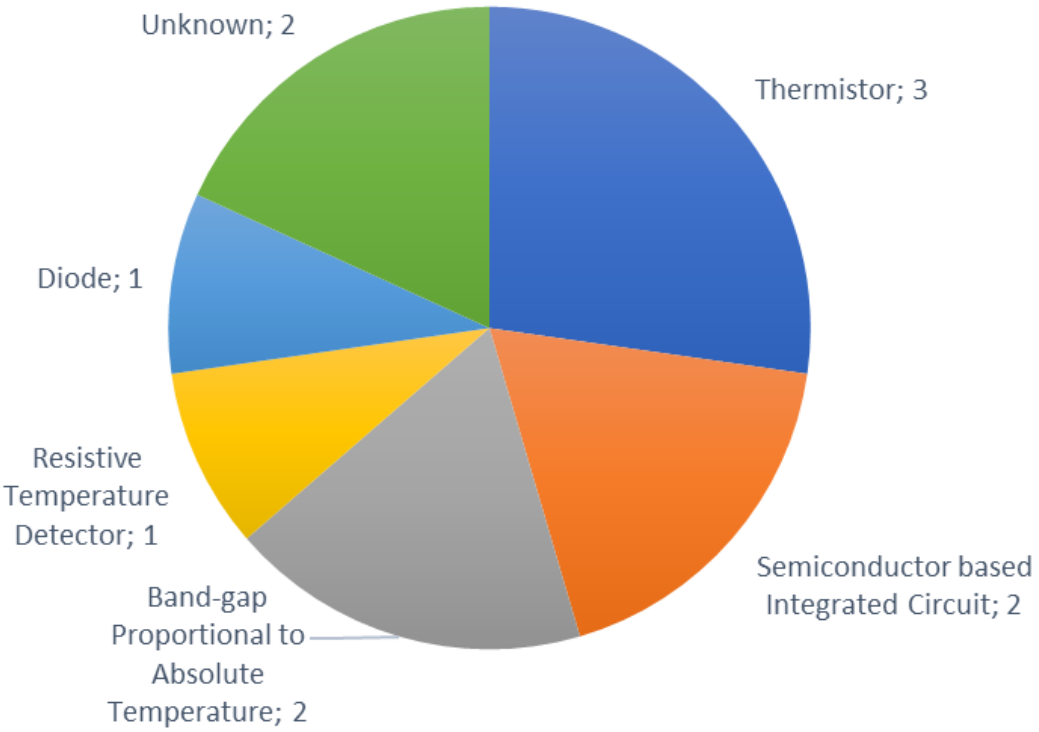

Figure 2.16. Most utilized temperature sensors by type.

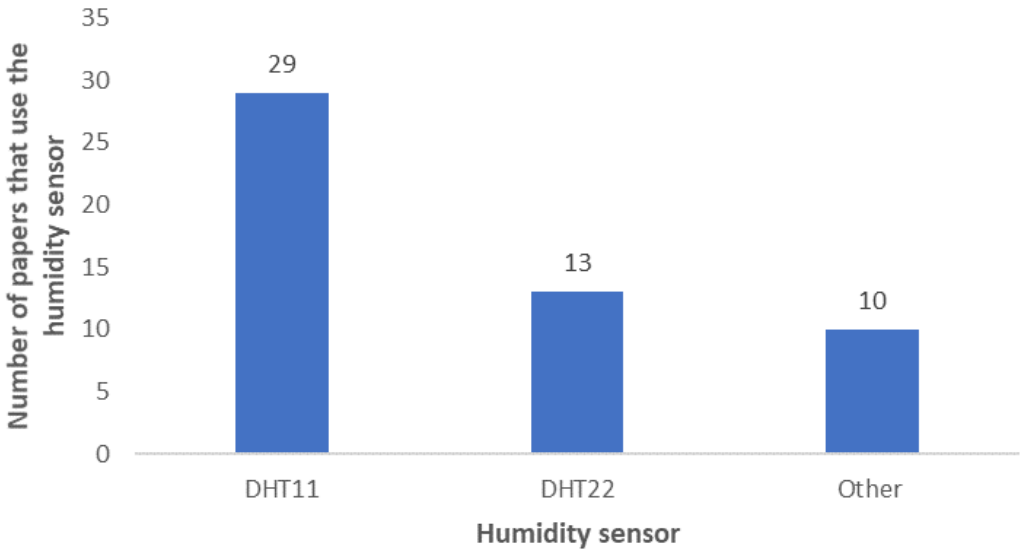

Figure 2.17. Most utilized humidity sensors.

Table 2. 3. Relative humidity monitoring sensors.

Sensor	Humidity Range		Accuracy	Reference
	Min	Max		
DHT11	20%	90%	±5%	[78, 109, 111, 112, 114, 121, 137, 143, 144, 152, 154, 166, 168–170, 172, 181, 182, 186, 190, 194, 196, 199, 205, 207, 210, 211]
DHT22	0%	100%	±5%	[126, 138, 145, 146, 165, 171, 177, 195, 197, 202, 206, 207, 209]

According to type (see Figure 2.18), the most utilized humidity sensors for IoT irrigation systems is the capacitive humidity sensor, which are the DHT11, the DHT22, the AM2315 [106], the SH10 [84], the HIH 4000 series [149] and the HH10D [217]. The DHT22, AM2315 [106], and SH10 [84] have the same range. However, the AM2315 has higher accuracy (±2%) than that of the DHT22 and the SH10 [84] (±5% and ±4.5% respectively). Resistive humidity sensors are another one of the types of available humidity sensors, such as the HR202 [98]. However, there are five humidity sensors employed for IoT irrigation systems that are of an unknown type. They are the FM-KWS [173], the BME280 [208], the EE160 [125], the HTU210 [95], and the SY-HS-220 [99].

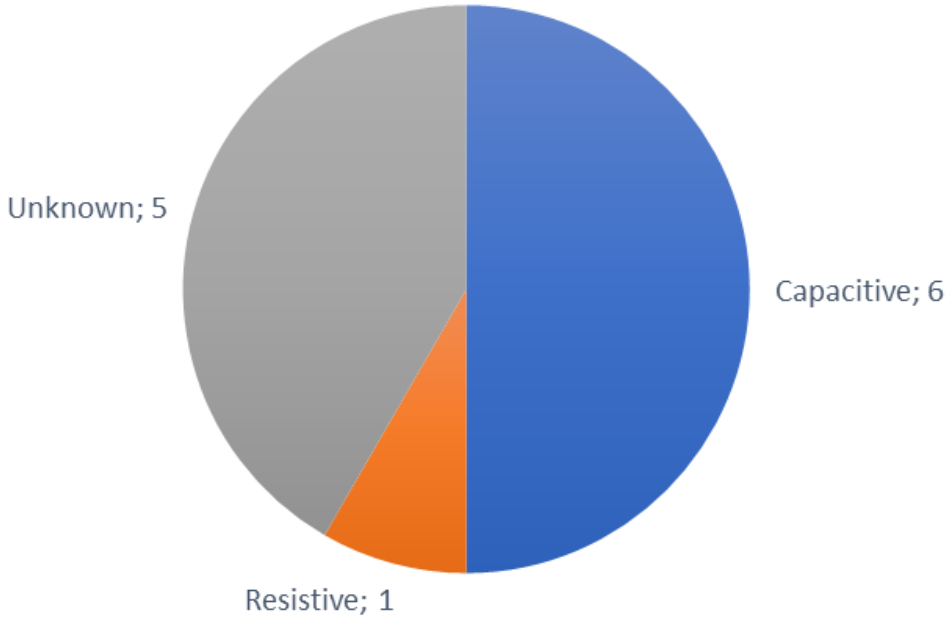

Figure 2.18. Most utilized humidity sensors by type.

Light intensity and UV radiation are another set of parameters that are frequently monitored in IoT irrigation systems. Figure 2.19 presents the most utilized sensors for light intensity monitoring. The light dependent resistor (LDR) is the most utilized sensor for light intensity monitoring [78, 98, 122, 126, 134, 170, 180, 182]. The second most used luminosity sensor is the BH1750 [112, 177, 197, 208] followed by the TSL2561 [196, 209] with one paper less. The LS-BTA Vernier was used as well in [149]. Among them, the BHT1750 [112] is the sensor with a broader range (1-65535 Lux). There is not a commonly utilized sensor for radiation, but the sensors currently utilized in IoT irrigation management systems are the SN-500 [106], the GUVA-S12SD [171], the 6450 TSR [196], and the SP110 [125].

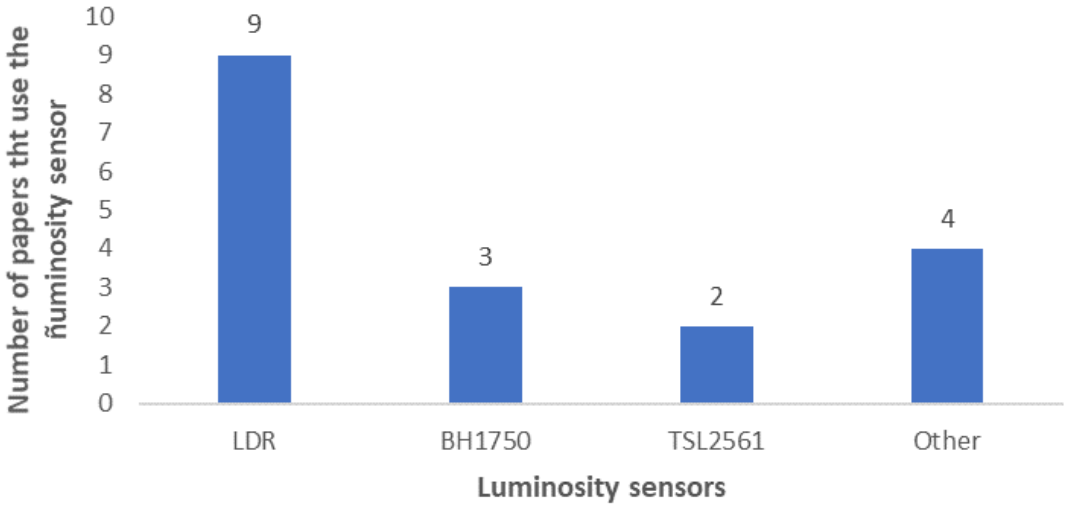

Figure 2.19. Most utilized luminosity sensors.

Regarding rain, one of the ways in which it is incorporated in the decision-making process of irrigation systems is to stop automatic irrigation if rain is detected to avoid overwatering [91]. The RSM3ALS sensor was utilized in [170]. It is an optical rain sensor comprised of an LED (Light Emitting Diodes), an LRD (Lightning and Radio Emission Detector), an electronic control unit, lenses, and an ambient light sensor. When the sensitive area is dry, a high intensity of light is received by the IR receiver. When the sensitive area is wet, the intensity of the received IR light decreases. It is manufactured by Bosch and it is commonly used in the automotive industry. The SEN-08942 [95] is a meteorology station manufactured by Sparkfun. It allows monitoring both wind speed and direction and it incorporates a pluviometer. The PRD180 [98] is comprised of a rain detecting board with two separate PCB (Printed Circuit Board) tracks and a control module that provides a digital and an analog output. The operating voltage is from 3.3 V to 5 V. It is manufactured by Elecmake. Like the PRD180 [98], the YL83 [126] is comprised of a series of conductive strands printed onto a Bakelite plaque. The water creates a short-circuit offering a low resistance between the lines connected to the ground and the lines connected to the positive polarity.

The type of agriculture most concerned with air and wind as a parameter concerning weather is greenhouse agriculture. For example, one of the aims of [118] is the sanitation of the air of the greenhouse from pathogens and chemical contaminants. This is then closely related to the activation of the actuators necessary to the regulation of the quality of the air. The contaminants that can affect the quality of the air are CO, CO_2, O_3, NO_x, $PM_{2.5}$, and PM_{10}, among others [114]. In the context of agriculture, air contaminants are monitored with the use of sensors that can be low-cost sensors such as the MQ135, MQ131, MQ2, or MQ9 sensors or commercial sensors that can be found in professional weather stations. The MQ135 [114, 194], used for benzene, alcohol, smoke, NH_3, NO_x, and CO_2 monitoring, and the MQ2 [114, 145], used for gas monitoring (propane, hydrogen, and LPG), are the most utilized low-cost sensors for air quality monitoring. The MQ131 [114] is utilized for ozone, Cl_2, NO_2 monitoring, and the MQ9 [114] is utilized for CO/combustible gas, methane, carbon monoxide, and LPG monitoring. Another sensor that can be used to monitor CO_2 is the CDM4161A [196].

Wind speed and direction may be of interest to IoT irrigation systems such as for the proposal in [95], that utilized the SEN-08942 sensor manufactured by Sparkfun. Barometric pressure can be of interest as well and can be measured by the BME280 sensor manufactured by Bosch [208].

Movement detection is often related to security measures or to the aim of scaring animals to avoid crop damage. The most utilized sensor for movement detection is a passive infrared (PIR) sensor [91, 145]. This sensor measures the infrared light that radiates around the objects placed at the front of the sensor. The change in infrared radiation is converted into changes in voltage that trigger the detection. It is often utilized for intrusion and pest detection. Ultrasonic sensors are often utilized to detect movement, such as the robot proposed in [115] that is able to perform some actions to scare the animals that may enter the fields. These sensors are comprised of a transmitter and a receiver that operate at the 40 kHz frequency. Its range is from 10 cm to 30 cm. Ultrasound at lower frequencies was utilized in [110] to repel the animals. Insects may cause great damage to the crops, for that reason some systems such as [94] include a pest warning functionality. The system in [184] is able to even detect the type of insect pests that are damaging the crops. These features are often accompanied by a buzzer to generate an alarm when intruders or animals are detected [111].

Depending on the type of agriculture, the values from the measures for each environmental parameter can be utilized to determine the actions of different types of actuators. It can be part of a model like the one proposed in [122] where the on-agriculture stage gathers the data on temperature, humidity, light, moisture, and wind speed in order to activate or deactivate fans, artificial light, a cooler, and water pumps. Many IoT irrigation systems have both a manual and an automatic mode to control irrigation. In [114], the amount of water released by the water pumps, or the duration of the irrigation can be selected in the manual mode. For the automatic mode, a preset value is utilized at the beginning. Then, the data is analyzed to determine the personalized settings. The most utilized actuators to modify the conditions of the climate that affects the crops or to protect the crops from animals and intruders are presented in Figure 2.20.

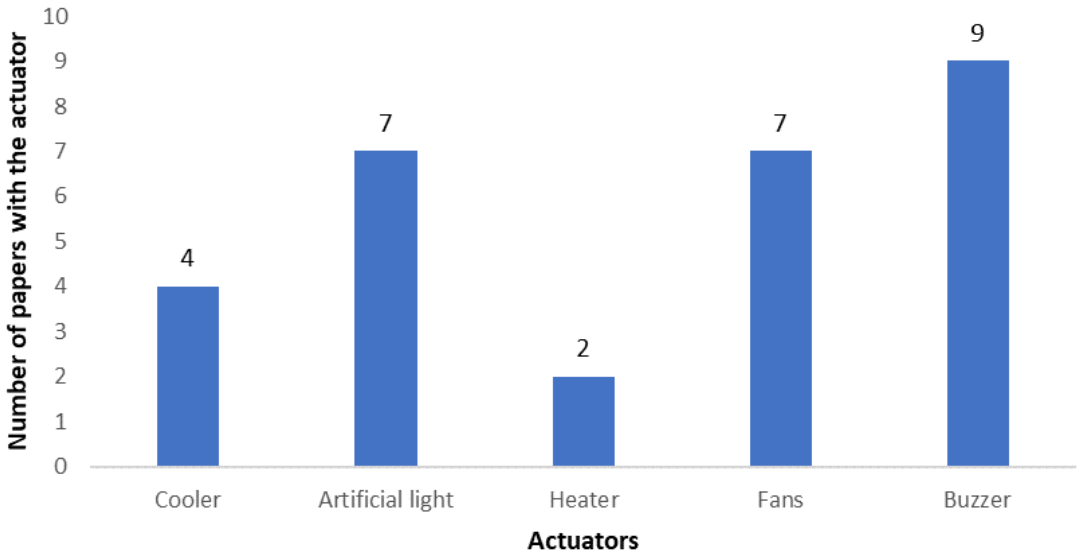

Figure 2.20. Most utilized actuators.

Buzzers are the most utilized actuators in IoT irrigation systems regarding external agents. These sound emitters are usually utilized to scare animals and to alert the user of anomalies in the system or the intrusion of animals or people [81, 99, 108, 109, 111, 116, 141, 145, 154]. Fans [88, 115, 118, 122, 125, 203, 217] and artificial lighting [88, 101, 121, 122, 125, 132, 205] are tied in first place with seven papers each. The fans can be utilized to cool the temperatures and to create a breeze or light wind to aid in the pollination process. Artificial light is utilized to aid plants in performing photosynthesis. Different colors may be good for different aspects of the plant growth such as blue for the leaves and a mix of red and blue for the flowers. Coolers are the third most employed actuator for weather conditions controlling, utilized for cooling the temperature and for aiding in the control of the relative humidity, with four papers [78, 88, 118, 122]. The least utilized actuators in IoT irrigation systems are heaters [78, 115], that modify the temperature to improve the performance or the health of the crops. Most of the actuators regarding weather conditions are usually placed inside greenhouses. Whereas buzzers and scarecrows can be placed in outdoor fields.

2.5 Sensor Networks for Irrigation Systems

In this section, an overview of the most utilized nodes for implementing sensor networks intended for irrigation systems is presented. Furthermore, the most employed wireless communication technologies are going to be presented as well. Lastly, the most frequent cloud systems for IoT in smart irrigation solutions and common architectures for these systems are going to be discussed as well.

2.5.1. IoT Nodes for Irrigation Systems

In this subsection, the most utilized IoT nodes for IoT irrigation systems are going to be presented. Figure 2.21 presents the most utilized nodes for the implementation of IoT irrigation systems. As it can be seen, Arduino boards are the most utilized nodes for the implementation of IoT irrigation systems. The Arduino UNO was utilized in 34 papers and the Arduino Mega was used in six papers. Furthermore, a total of 59 papers claimed to use an Arduino board. The references of the most utilized nodes are detailed in Table 2.4.

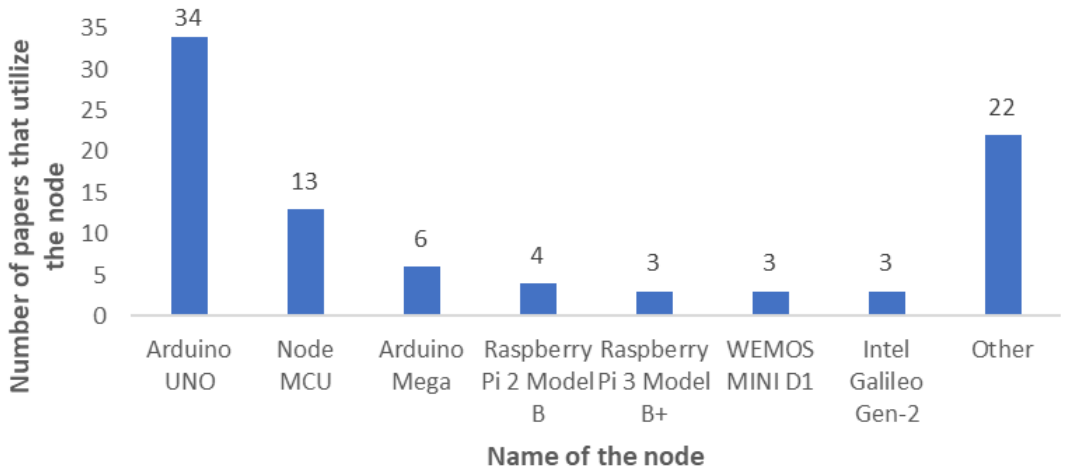

Figure 2.21. Most utilized nodes to implement IoT irrigation systems.

Table 2.4. Most popular nodes for IoT irrigation systems.

Node	Reference
WEMOS MINI D1	[121, 137, 139]
Node MCU	[90, 92, 136, 147, 164, 164, 178, 204, 206, 209, 218–220]
Arduino Mega	[102, 105, 106, 122, 221, 222]
Arduino UNO	[83, 85, 89, 93, 99, 104, 105, 111, 112, 114, 119, 126, 134, 141, 162, 163, 168, 170, 172, 178, 180, 190, 194, 195, 202, 204, 205, 207, 211, 217, 219, 223–225]
Raspberry Pi 2 Model B	[116, 119, 216, 226]
Raspberry Pi 3 Model B+	[108, 163, 227]
Intel Galileo Gen-2	[80, 101, 127]

Figure 2.22 shows the types of Arduino nodes utilized in IoT irrigation systems. In addition to the Arduino UNO and the Arduino Mega, the Arduino Yun [110], the Arduino Due [146], and the Arduino NANO [202] were utilized in other IoT irrigation proposals. However, 15 papers did not specify the model of the Arduino board utilized [79, 82, 101, 131, 132, 140, 148, 171, 175, 182, 189, 213, 215, 218, 228].

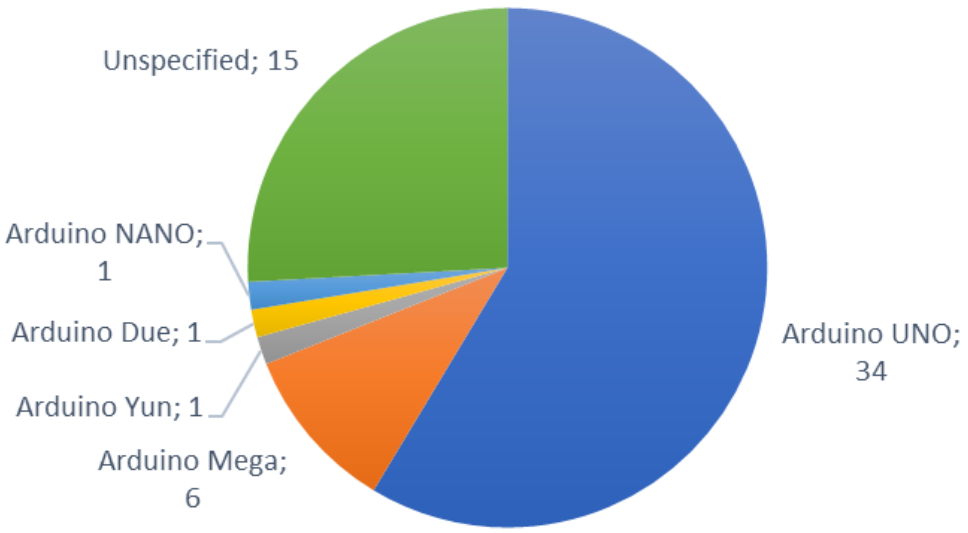

Figure 2.22. Arduino nodes utilized to implement IoT irrigation systems.

Some other popular boards are manufactured by other companies but can be programmed utilizing the Arduino IDE. One of these boards is the Node MCU, which was utilized in 13 papers. The other boards are the Wemos MINI D1 and the Galileo Gen-2 both utilized in three papers each.

The nodes from the Raspberry family were frequently utilized as well. The most utilized Raspberry node was the Raspberry Pi 2 Model B and the Raspberry Pi 3 Model B+, with four papers and three papers, respectively (see Figure 2.23). They are followed by the Raspberry Pi 3 Model B [183, 202], the Raspberry Pi 1 Model B [126, 168], and the Raspberry Zero [203]. There were however eight papers that utilized an unspecified Raspberry Pi 3 [78, 95, 105, 150, 161, 199, 210, 214] and 13 papers [88, 101, 109, 115, 146, 166, 171, 175, 185–187, 223, 229] that indicated that a Raspberry Pi node was utilized but the model of the node was not specified. The Raspberry Pi boards are more potent than the Arduino boards. Oftentimes, both Arduino and Raspberry Pi boards are utilized to implement an IoT irrigation system, using them according to the processing requirements of each task.

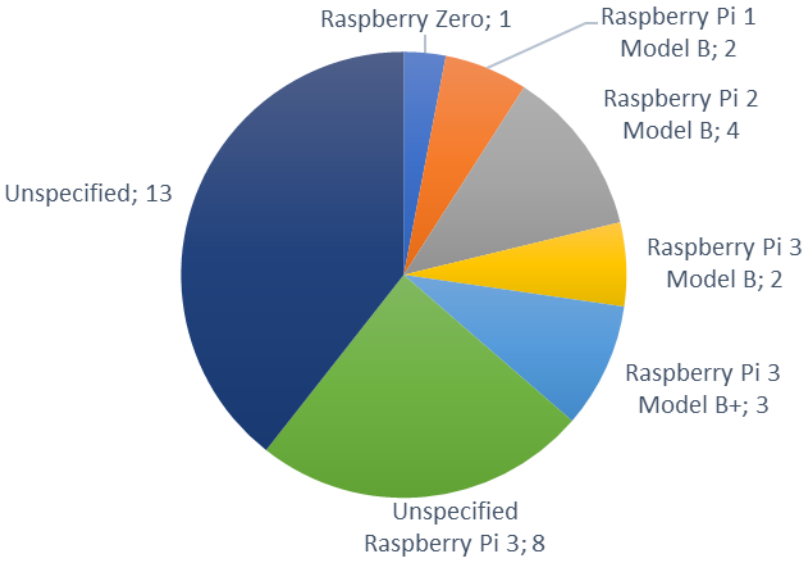

Figure 2.23. Raspberry Pi nodes utilized to implement IoT irrigation systems.

Furthermore, there are other less popular nodes utilized by other IoT irrigation proposals. These other nodes are the waspmote [208], the crowduino [87, 131], the LPC2387 [186], the IPex16 from OdinS [125], the Renesas [128], the Mica mote [86], the eZ430-RF2500 [64], the AESP ONE [144], the FORLINX OK6410 [173], the BeagleBone Black [145], the Edison [79], the CC3200 Simple Link [112, 230] and the CC1310 [198].

The selection of the best node for an IoT irrigation system will depend on the necessities and the characteristics the farmer wants for the system. Arduino nodes and similar nodes from other brands provide a low-cost solution that can be implemented in developing countries and smaller farms. On the other hand, Raspberries have powerful computing abilities that allow the implementation of more demanding software and algorithms.

Many works do not use a microcontroller board like the ones presented above and opt to implement their system with their circuit design. Figure 2.24 presents the most utilized processors for smart irrigation systems. The most utilized controllers are the ATmega328 [143, 154, 221, 231, 232] and the ATmega2560 [10, 122, 131] with five and three papers respectively. The Atmega1281 [184, 208] and the LPC2148 [98,174] are both utilized in two papers each. The other controllers comprise the LPC2138 [130], ATmega8 [152], the ATmega16/32 [115], the MSP430F5438A [117], the MSP430F5419A [64], the MSP430F2274 [64], the STM32L151CB [128], the STM32F205 [203] and the PIC16F877A [91]. The proposals that opt for developing their own designs for the nodes aim at addressing their own particular requirements. Therefore, the selection of the processor would depend on the characteristics of the IoT irrigation system considering the type of crop and its irrigation needs.

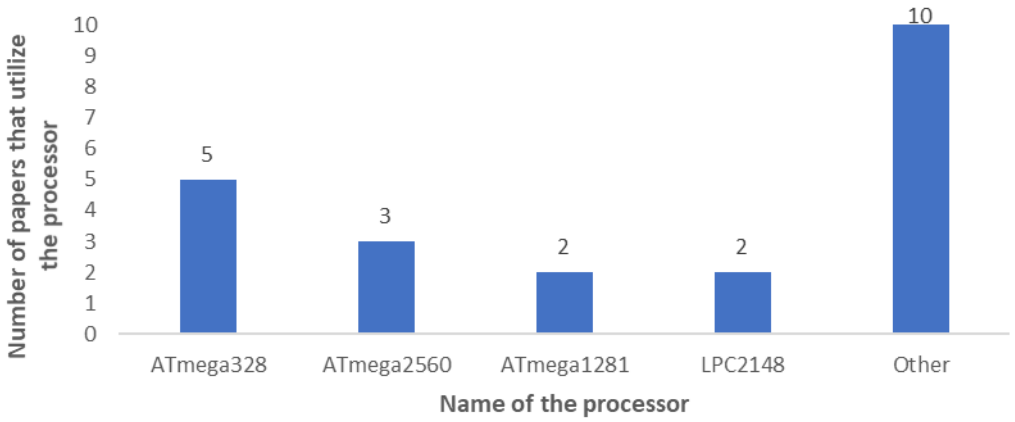

Figure 2.24. Most utilized processors to implement IoT nodes for irrigation systems.

2.5.2. Communication Technologies

In this subsection, an overview of the most employed wireless communication technologies is going to be presented as well.

According to the Machina research report, the number of connected agricultural devices is expected to grow from 13 million at the end of 2014 to 225 million by 2024 [233]. In addition, the report predicts that around half of those connections will use the newly emerging low power wide area network technologies which are particularly well suited to many of the applications in agriculture.

When IoT devices are implemented, the employed communication technologies are a key point to achieve successful operation. In a generic way, communication technologies can be classified according to the environment where they will be deployed, the utilized communication standard, or the utilized spectrum band.

If the scenario is considered, they can be classified into two types depending on the purpose of the IoT devices. On the one hand, we can distinguish the devices that function as nodes that transmit small amounts of data at short distances and have low energy consumption. On the other hand, there are devices that can transmit large amounts of data over long distances that have high energy consumption. Therefore, range, data rate, and energy consumption are some of the most important aspects to consider when deciding which technology to use.

If the utilized standard is considered, there are a large number of wireless standards that are used in the communications of IoT devices. A general classification can be established between devices that communicate at short or long distances. Short distance communication standards usually reach distances of up to 100 m. Long-distance communication standards reach distances of kilometers.

Also, another type of classification can be established based on the employed communication technology. In this way, three categories can be established. The first

category is formed by those that connect utilizing Ethernet or cable and WAN technology. The second category is comprised of those that connect via WiFi and WAN technology. Finally, the third category is formed by those that connect using both low power WiFi and WAN (Wide Area Network) technology. If the spectrum band used is considered, we can classify them into technologies that use the unlicensed spectrum or the licensed spectrum. Unlicensed spectrum bands are known as Industrial, Scientific, and Medical (ISM radio band bands, and are defined by article 1.15 of the International Telecommunication Union's (ITU) ITU Radio Regulations (RR) [234]. The ISM bands can vary according to the region and its permits. Its main advantage is its ease of installation and the main drawbacks are related to safety deficiencies and possible interferences. The licensed spectrum bands are assigned according to the different proprietary technologies. They offer greater security, greater coverage, and fewer interferences. However, the cost of using a licensed band is higher.

The most utilized communication technologies among the reviewed papers are presented in Table 2.5. In many of the proposals that we have studied, the authors combine several communication technologies instead of using one single protocol. As an example, it is very common for authors to start using either a wired or a wireless technology to connect the sensors with the nodes, and then, use a wireless technology to send data from nodes to remote or cloud storage centers.

According to the descriptions provided by the different authors of their own implementations, we have verified that the most used communication technology in the different proposals is WiFi, as it can be seen in Figure 2.25. The reason could be due to is accessibility. The currently available low-cost devices for IoT usually support WiFi and, although its range can be considered short for the average expanse of a farm, small farms could be able to provide enough wireless coverage with several low-cost devices. GSM (Global System for Mobile communications) and ZigBee are widely spread wireless technologies as well, with 25 and 23 papers that use them respectively. GSM provides long-range communication at the cost of a mobile plan of the service provider that operates in the area. ZigBee provides low energy consumption and allows implementing networks with up to 65000 nodes. However, it has lower data rates than other available technologies and its range would imply the deployment of many nodes. Lastly, there are two new technologies that have been getting popular recently. LoRa is able to provide very long ranges, which makes this technology a very good option for secluded areas with no service. Moreover, regarding specific protocols for IoT systems, it is a little bit surprising that even though MQTT is a widely spread protocol due to its low power consumption and low overhead, it is not a popular protocol for IoT irrigation systems at the moment. It is observed that a relatively high number of papers, exactly in 24 papers, did not describe the employed technology. In Figure 2.25 this group has been named as Undefined.

Table 2.5. Most utilized communication technologies in IoT crop irrigation systems.

Technology	References
Ethernet	[102, 112, 122, 150, 168, 182, 189, 190, 197, 203, 215]
GSM	[84, 85, 93, 98, 101, 107, 111, 114, 122, 123, 129, 135, 140–142, 154, 163, 180, 204, 208, 235–239]
Wi-Fi	[78, 83, 90, 92, 95, 97, 100–103, 106, 109, 110, 114–116, 119–121, 127, 132, 134, 138, 144, 145, 162, 163, 167, 168, 170, 171, 174, 176, 177, 178–180, 183, 185, 186, 190, 194, 202–205, 207–209, 211, 214, 216, 217, 219, 220, 224, 232, 237, 240–244]
ZigBee	[81, 88, 91, 113, 115–117, 143, 148, 170, 171–174, 189, 184, 188, 195, 202, 208, 226, 235, 241]
Bluetooth	[95, 103, 131, 169, 180, 183, 185, 207, 225, 231, 245, 246]
LoRa	[5, 106, 128, 145, 193, 195, 196, 200, 208, 246, 247]
GPRS	[64, 93, 94, 117, 123, 129, 149, 152, 173, 188, 208, 212, 222, 236, 240]
MQTT	[97, 125, 136, 164, 165, 211, 226, 227]
4G	[94, 106, 128, 189, 192, 196, 203]
6LoWPAN	[125, 198]
IEEE 802.15.4	[123, 153]

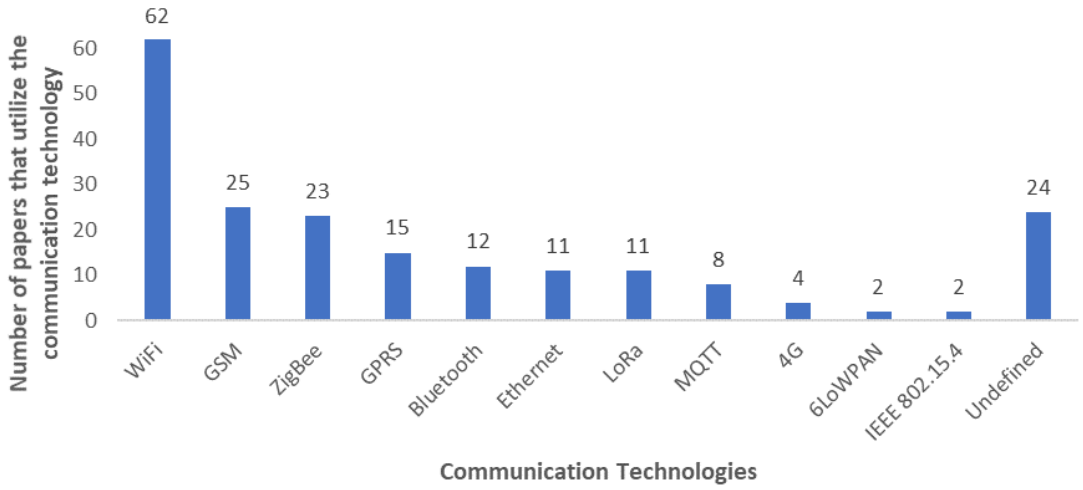

Figure 2.25. Communication technologies employed to implement IoT irrigation systems.

We also observe that, in a large number of works, the end-users access the data, obtained during the monitoring process or to carry out the control of the system, through APPs or WEBs. Most of these communications are done through mobile devices using wireless technologies.

Table 2.6 presents the communication modules that have been used in the reviewed articles. It is observed that most of the authors have not indicated the communication module employed. Furthermore, it can be observed that the most utilized module is the ES8266 WiFi module with 29 papers. It is followed by the SIM900 GSM module with nine papers and the NRF24L01 2.4 GHz module, the XBee S2 ZigBee module, and the SX1276 LoRa module with three papers each. Some other less utilized modules and chips for wireless communication include GSM modules such as the SIM800 [222, 237], the SIM300 [239], Ethernet modules such as the W5100 [132] or the Ethernet Shield utilized in [190], WiFi modules such as the ESP32 [170], the ESP1 [163], the ATWIN C1500 [241] and the Broadcom [203], LoRa modules such as the Feather 32u4 [241] and the LoRa ESP32 [246], 2.4 GHz RF modules such as the C2500 [64] and sub-1 GHz RF modules such as the CC1310 [198] and the CC1101 [201], Bluetooth modules such as the HC-05 [180,248] and near radio frequency nodules such as the NRF4L [231]. There are other modules that are compatible with several technologies such as the JN5139 that admits both WiFi and ZigBee [172] or the Dragino LoRa GPS (Global Positioning System) shield [195].

Table 2.6. Most utilized communication modules.

Technology	References
ESP82666	[10, 83, 92, 97, 114, 119, 121, 132, 134, 136, 137, 144, 147, 162, 164, 165, 167, 170, 174, 177, 178, 180, 209, 211, 217, 219, 220, 228, 232, 237, 243]
SIM900	[84, 85, 93, 111, 132, 173, 180, 230, 242]
NRF24L01	[175, 182, 224]
XBee S2	[170, 172, 195]
SX1276	[138, 145, 196]

2.5.3. Cloud Platforms

In this subsection, an overview of the most frequent cloud systems for IoT in smart irrigation solutions is going to be discussed. The two main storage systems used by the authors are traditional databases or cloud. In one article, the authors indicate that they store the data in a Raspberry Pi [175]. As it can be seen in Figure 2.26, a large percentage of the authors, more than 50%, have not defined the storage system they have used, there are 79 other papers where the storage system used is not specified.

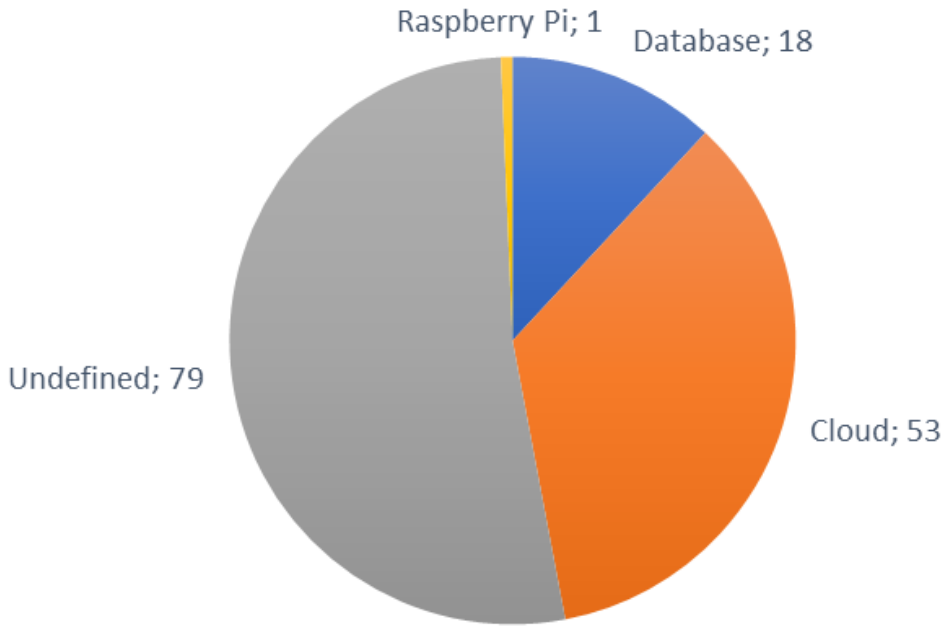

Figure 2.26. Number of papers per storage system.

To be able to provide the new services that are currently demanded in IoT, it is necessary to use middleware. Through middleware, it is possible to connect programs that initially had not been developed to be connected to each other. Bandyopadhyay et al. [249] presented a classification of the IoT-middleware, based on the various features and interface protocol support. One of the reasons why middleware is needed to connect IoT devices, which are initially autonomous, is to provide cloud services. We can take advantage of existing middleware using it on different cloud platforms.

When we talk about the cloud, we identify a place where data, which is collected through sensors and transmitted to remote locations, will be stored and processed. In most of the articles, it is indicated that the data is processed in the cloud itself, and the end-users view all the information by connecting to the cloud. Cloud storage has been done on different platforms as it can be seen in Figure 2.27. In 24 of the reviewed articles, the authors specified that they store the monitored data in the cloud, but do not identify the utilized cloud platform (see Table 2.7). Most of the works in which the authors define the employed cloud platform, the utilized platform is Thingspeak, with 14 papers. This platform is very intuitive and provides both free and paid options for storing, analyzing, and displaying the data on different devices. Algorithms can be developed using MATLAB to generate alerts. However, there are proposals that use other cloud platforms such as FIWARE [125, 200] and Dynamo DB [168, 210] with two papers each, and MongoDB [78], Ubidots [148], Amazon [141], M2X [250], NETPIE [92], SAP [251], InteGra [244], Firebase [205], InfluxDB [227]. These less-used platforms are either more expensive, provide fewer services or are less intuitive

than Thingspeak. Table 2.7 lists the cloud platforms that have been used in the reviewed articles.

Table 2.7. Cloud platforms.

Cloud	References
Unspecified Cloud	[82, 90, 100, 106, 114, 122, 127, 128, 138, 150, 161, 164, 165, 170, 172, 183, 193, 202–204, 207, 220, 226, 247]
Thingspeak	[93, 106, 149, 167, 169, 181, 194, 197, 209, 211, 217, 221, 224, 241]

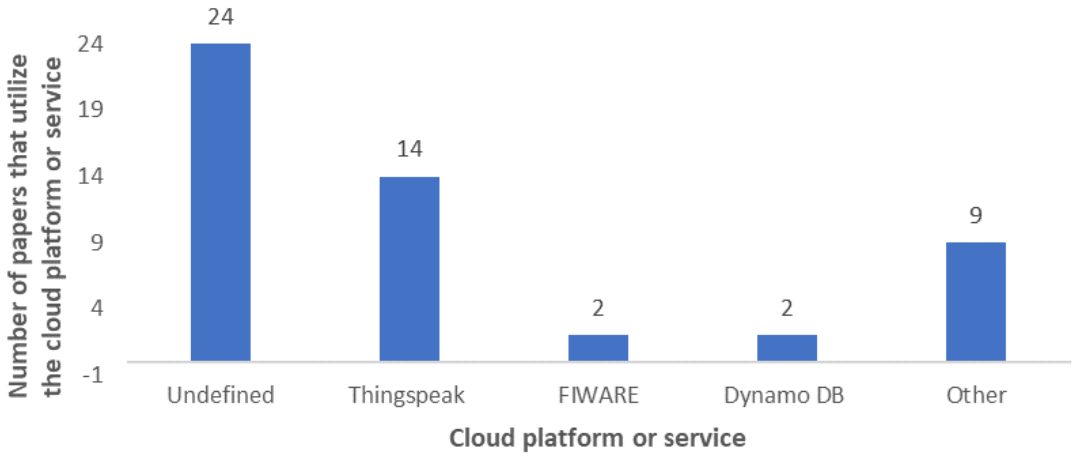

Figure 2.27. Number of papers that employ each clouds service or platform.

The rest of the articles where the authors identify the storage system utilize databases. As it can be seen in Figure 2.28, in 12 articles the information is stored in a database, but the name of the employed database is not specified. Other authors have identified the utilized databases. The most utilized one is MySQL [84, 95, 104, 108, 117, 126, 146, 161, 175, 177, 195, 209] 12 papers, followed by SQL [119, 170] with two papers. Other less utilized databases were SQLite [102] and a NoSQL database with JSON [235] with one paper each.

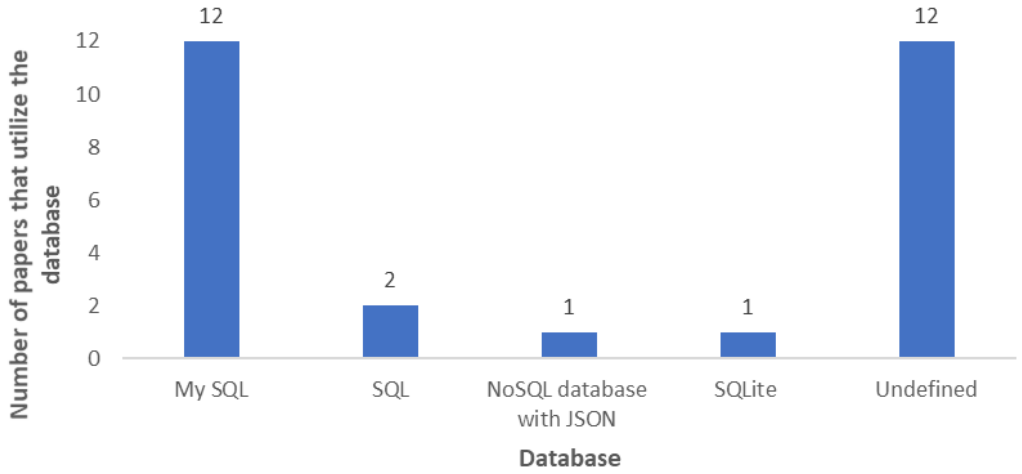

Figure 2. 28. Number of employed Databases to store data of IoT nodes for irrigation systems.

2.6. Discussion

In this section, current trends regarding IoT irrigation systems for agriculture are going to be presented.

2.6.1. Big Data Management and Analytics for Irrigation Optimization

IoT systems, in general, generate a great amount of data due to monitoring different parameters in real-time, and IoT irrigation systems generate big data as well. Therefore, it is necessary to provide mechanisms to manage and analyze big data. Ahad et al. [252] comment on the need for sustainable management of big data to avoid overusing natural resources. Using blockchain, powering IoT devices with solar energy, selecting useful data and discarding unnecessary and redundant data, employing clustering techniques to reduce the volume of the information, implementing time-efficient algorithms, and the utilization of sustainable resources as alternatives to the components that are employed nowadays are some of the suggestions they provide.

Although the data gathered from the sensors is already a big source of information, the analysis of this data is paramount to optimize the IoT irrigation system according to the crop and the weather conditions. For this purpose, Tseng et al. [253] presented a big data analysis algorithm to aid farmers in the crop selection process. Their proposal satisfied the five Vs (volume, velocity, variety, veracity, and value) of big data. They performed a 3D correlation analysis that evaluated the irrigation cycle to identify the irrigation practices performed by the farmer. Then, they calculated the soil moisture content to detect irrigation and to evaluate if the farmer applied pesticides or fertilizers. This information was coupled with data on the weather conditions and other aspects of the soil to provide the farmer with the cultivation risks of each type of crop.

Nonetheless, there are other technologies that are currently being utilized to analyze the big data produced by IoT irrigation systems for agriculture.

AI is currently the type of technology most companies are interested in for various purposes. In the case of irrigation, the use of AI is tied to the optimization of the available resources such as water, fertilizers or energy or to obtain information from the crops such as the presence of diseases or the correct growth of the plants, vegetables, and fruits. One of the techniques employed to analyze the data gathered from the sensors so as to perform decisions on the irrigation systems is fuzzy logic. Fuzzy logic has been employed to improve irrigation scheduling in greenhouses and control the drainage implementing it on the controller of the system [151]. The fuzzy rules were provided according to the water availability utilizing the QtFuzzyLite software (FuzzyLite Limited, Wellington, New Zealand). Another fuzzy logic controller is employed to determine the coverage error for the resources so as to determine if the effective watering of the plants can be guaranteed [146]. The system presented in [187] utilized fuzzy logic to determine the duration of the irrigation process once the soil moisture values go below the 20% threshold. Light and temperature lead to the least accuracy in irrigation (40%) whereas any combination with the soil moisture values reached an accuracy from 62 to 81%. The authors conclude that the subsoil moisture sensor is the most important sensor to determine irrigation. The irrigation time was predicted in [213] as well, using the adaptive neuro fuzzy interference system (ANFIS) to predict the irrigation time. This fuzzy logic technique was implemented employing the MATLAB software. However, outdoor temperature and light are important to avoid the evaporation of the water. Another irrigation system utilizes iterative learning control (ILC) arithmetic to make decisions regarding the opening of the water valves [117].

Machine learning is another technique that is utilized in irrigation systems to perform predictions. The prediction algorithm in [171] for soil moisture prediction obtained an accuracy of 96%. Prediction techniques can also be utilized to estimate the amount of available water for irrigation such as the case of [170], where the authors employ Fisher's LDA method for that purpose. Water usage is predicted as well in [100] employing regression algorithms. The regression algorithms consider the temperature of the environment and the water flow to produce a water consumption forecast that is then visualized by the user through a mobile app.

Feedforward neural networks and the structural similarity index were employed in [254] to develop an optimized smart irrigation system. The authors compared gradient descent and variable learning rate gradient descent optimization techniques to predict soil moisture and they determined that the latter was the best one. Furthermore, a study on machine learning applied to agriculture so as to perform predictions on irrigation was performed in [255]. Different machine learning techniques were applied to the data on the soil and the environment collected from jojoba plantations. The authors conclude that the boosted tree classifier was the best classification model was and the gradient boosted regression trees was the best regression model. They had 95% and 93% accuracy respectively. The authors suggest as well that different feature-sets would be better for different plots as some configurations achieved better results for different types of plots such as organic ones. Furthermore, the models considerably reduced their

accuracy when deliberated soil drying was performed. Moreover, the authors state that the data on the weather and the saturation could be not considered without it substantially affecting the accuracy of the models.

2.6.2. Low-Cost Autonomous Sensors

As we have seen in Section 2.1, the majority of the countries that dedicate more effort to researching IoT irrigation systems are countries where the farmers cannot afford commercial solutions. Therefore, most of the solutions for irrigation management are comprised of low-cost sensors and controllers so as to increase the scope of the benefits of utilizing smart irrigation systems. Apart from individual sensors, some shields integrate several sensors and connectors for irrigation and agriculture-specific IoT systems such as the OpenGarden shield [187]. It can be connected to an Arduino UNO and it is comprised of an LDR, a DHT22 connector, a soil moisture connector, a hydroponics connector, digital and analog pins, a DS18B20 [100] connector, and an antenna connector. This type of solution allows the easy implementation of low-cost smart irrigation systems.

2.6.3. Sustainable Irrigation Systems

Most irrigation systems do not have access to the power grid, therefore there is a need for alternative means of powering up the devices that conform the system. Even irrigation systems with access to the power grid may only receive power during a constrained time period. In India, for example, the system presented in [79] determines when access to electricity is available to turn on the irrigation motors. This system was designed to help farmers when access to electricity happens at irregular hours or even at night, when farmers may not be present in the field. To address the need for alternative ways of powering the irrigation systems in agricultural fields that are too far to access the power grid, many systems incorporate a solar energy functionality, making the system more sustainable [90]. Furthermore, the use of solar energy reduces the energetic costs which is an advantage for irrigation systems intended for developing areas. Considering those reasons, a total of 22 of the surveyed papers chose to utilize solar energy to power their proposed irrigation system [87, 90, 95, 96, 100, 106, 113, 116, 119, 138, 140–142, 146, 150, 152, 191, 196, 223, 229, 231].

Most of the energy consumption of the sensor nodes is produced by the data transmission. Thus, several studies focus on analyzing the energy consumption of wireless technologies. Ayele et al. [256] performed a simulated comparison of the energy consumption of BLE and LoRa in a Wildlife Monitoring System. The authors proposed a dual radio network model. The nodes were deployed on the collars of the animals. The communication between the nodes was performed over BLE until it reached a cluster head. Then, the cluster head communicated through LoRa to a Lora

gateway. The energy consumed by the LoRa star topology increased as the nodes increased, due to the overhead. However, the proposed solution eliminated the energy consumption caused by the overhead. The results showed a reduction of energy consumption of 97% compared to LoRaWAN. Bor et al. [257] presented an analysis of the parameters of LoRa transmissions. The authors focused on the effects of parameter selection on energy consumption and communication performance. The authors stated that a Spreading Factor (SF) of 8, a bandwidth of 500 MHz, 4/5 coding rate, and 8 dBm of transmission power (tx power) consumed 2.31 mJ and the optimal settings were an SF of 7, a bandwidth of 500 MHz, a coding rate of 4/5 and a tx power of 11 dBm which had an energy consumption of 1.60 mJ. Furthermore, the authors proposed an algorithm that was able to probe different settings and selected the best option in order to balance the energy consumption. Several experiments on the Carrier Sense Multiple Access (CSMA) channel access mechanisms of LoRa were performed by Phan [258]. The author presented an adaptation of the 802.11 CSMA protocol for LoRa and a new CSMA protocol. The energy consumption of the adaptation and the new proposal with different settings was compared as well. The results showed the new proposal had a lower energy consumption for all settings compared to the adaptation from 802.11. Moreover, Pötsch et al. [259] discussed the limitations of LoRa gateway deployment. The overhead caused by the LoRa gateways is analyzed as well. The energy consumption was compared for different spreading factors and bandwidths of 125MHz, 250 MHz, and 500 MHz. The results showed less energy consumption as the spreading factor decreased and the bandwidth increased. Furthermore, the energy consumption increased as the tx power increased, being 50 mA approximately for a tx power of 5 dBm and slightly above 120 dBm for a tx power of 19 dBm.

The energy consumption of WiFi nodes has been studied as well. Mesquita et al. [260] performed a study on the performance of ESP8266 WiFi modules which are branded as ultra-low power. The authors performed several experiments to measure the energy consumption with sleep modes and different transmission configurations. The authors stated that the usual configuration of a Delivery Traffic Indication Message (DTIM) period of 3 and a 100 ms beacon interval had the lowest average current consumption, namely 14.71 mA. They also stated that ESP8266 modules were able to operate for 2 to 4 days with a small battery of 1000mAh of capacity. Montori et al. [261] presented a performance study on WiFi for IoT systems. The authors utilized ESP-12 SoC modules to study their energy consumption under variations of the connectivity settings. Tests were performed with Lo-Po, alkaline, and NiMH batteries. The results showed similar performances for all batteries with the same configurations. Furthermore, the difference in energy consumption between awake and sleep mode was less than that stated on datasheets. Lastly, Putra et al. [262] performed an energy consumption comparison between BLE and WiFi with different settings for the beacons. Tests were performed for an iPhone device. The results showed BLE had 30% more energy efficiency than WiFi. Furthermore, the battery life of the smartphone was of 14 hours and 46 minutes for WiFi and 16 hours and 38 minutes for BLE.

Energy-efficient algorithms have been utilized as well to reduce the energy consumption of the nodes. Thar Baker et al. presented in [263] an energy-aware algorithm for IoT applications based on cloud called (E2C2). The algorithm allows

utilizing the least possible number of services needed to complete the requirement. The proposed algorithm was compared to four other existing proposals. Results showed a better performance of the proposed algorithm regarding energy efficiency and the least number of services used to complete a task in an optimal manner.

2.6.4. Frequency of the Data Acquisition

The frequency at which the parameters are monitored may be different for each proposal. Real-time monitoring [5, 121] has been surging as the cost of the devices, whether they are processors, devices for data storage, or sensors, has experienced a considerable reduction. Some proposals decide not to monitor the parameters in real-time so as to reduce energy consumption. Some authors have decided to take a measurement every 10 s [108].

2.6.5. New Forms of Data Acquisition

The advances in technology as lead to new ways of obtaining the data from the sensors deployed in the fields. One of the new ways of gathering data from the sensor nodes is by utilizing drones [5]. Drones also allow obtaining new data that could not be obtained in other ways such as aerial images of the fields.

Drones have been utilized for remote sensing activities for different purposes in vegetated areas. Andrew M. Cunlife et al. presented [264] a remote-sensing dryland vegetation quantification technique. The technique was able to employ structure-from-motion (SfM) photogrammetry of pictures taken from drones to obtain 3D models of the vegetation structure. The technique was able to identify grass tussocks with volumes of a few cm^3 employing canopy height models. Results showed the technique was able to predict biomass utilizing the detected canopy volume, obtaining coefficients of determination that ranged from 0.64 to 0.95. Moreover, Jian Zhuang et al. [265] proposed the use of lightweight drones for remote sensing of forests for ecological purposes. The system employed drone-derived canopy variables to detect patterns in the biodiversity of the forest. Results showed a correlation between canopy closure and stand basal area. Niche differentiation was performed utilizing edaphic and topographic variables. Lastly, the authors detected a correlation between canopy variables and light-demanding species. Urbahs et al. [266] described the structural characteristics and the parameters of a UAV developed for its use in environmental monitoring. Paulina Lyubenova Raeva et al. [267] presented a study in which a drone was utilized to obtain vegetation indexes and thermal maps, relating the temperature of the vegetation and the soil. In order to do so, they used multispectral and thermal sensors. Stehr et al. [268] assured that drones could monitor the fields more frequently than the satellites. They also stated that drones could take more detailed photographs, and clouds do not hinder their vision. They also predicted that at the time when the cost of drones decreases and

their technology improves, more drones would be used in the field of agriculture. Furthermore, Kurkute et al. [269] described the process of developing a mechanism for spraying from a drone.

Image processing techniques are implemented in farming to monitor the state of the crops. Parra et al. [270] showed the use of image processing techniques to detect the presence of undesired grass species. They utilize a drone with an Arduino module to take pictures. The obtained images are used to determine the best option to detect the presence of weeds. Their results pointed out that the combination of different layers of a single image can be used for detecting the presence of undesired plants. Ulzii-OrshikhDorj et al. [271] proved the utility of a computer vision algorithm to detect and count citrus on the tree using processing techniques. Their system was able to estimate the yield and compare the yield estimation results obtained through several methods. They collected 84 images from 21 trees. Mello [272] created a system, which includes an aerial platform including a spectral imaging device, a position sensor, an orientation sensor and includes a ground-based sensor platform including at least one soil sensor. Hutchinson et al. [273] presented a technique for monitoring vegetation changes and dynamics using satellite image time series analysis. The BFAST time series decomposition method was applied to a ten-year MODIS (Moderate Resolution Imaging Spectroradiometer) NDVI (Normalized Difference Vegetation Index) time series dataset for the Fort Riley military installation and Konza Prairie Biological Station (KPBS) in northeastern Kansas. Their results had shown that the generated indicators are useful for different uses in land management.

Other authors such as Puri et al. [274] made a study where they presented the best drones that can be used in monitoring and observation in agriculture so as to improve crops and prevent damage to the fields. Valente et al. [275] presented a collaborative system consisting of a WSN and an aerial robot that was used for real-time monitoring of frost in vineyards. Its solution was a mobile node that transported an aerial robot that ensured communication between the dispersed nodes and the base station of the robot. This method allowed them to overcome the limitations arising from the use of wireless networks.

There are authors, like the following, who present a classification of UAV applications in PA. Hunt et al. [276] present a classification of the applications of the unmanned aircraft systems (UAS) for precision agriculture. The authors define the following three niches or sectors in their classification: scouting for problems, monitoring to prevent yield loss, and planning crop management operations. Tsouros et al. [277] review recent applications of UAVs for Precision Agriculture. Rao Mogili et al. briefly review the implementation of UAVs for crop monitoring and pesticide spraying. Daponte et al. [278] propose a survey on techniques, applied to precision agriculture monitoring, through the use of drones equipped with multispectral, thermal, and visible cameras. For each application, the main limitations are highlighted, and the parameters to be considered before performing a flight are reported. Authors such as Boehm et al. [279] propose using an IEEE802.11n network to distribute the images captured from a UAV to their ground control station.

Furthermore, fields and remote areas can hinder the progress of other activities such as cultural heritage conservation, and drones have been considered as a solution to implement systems such as the remote-sensing system for an archaeological survey of remains in mountain areas presented by Tesse D. Stek [280]. The author concludes that the use of drones can substantially improve the surveying process of archaeological projects adding to the on-site activities. Furthermore, remote sensing provides advantages such as being non-destructive, reducing the time and cost of the surveyance process, and the ability to access areas located on agricultural fields with difficult access and fields where the farmer or the proprietor must grant the access.

The vegetation can also be in urban environments. For that reason, José Marín et al. presented in [272] a remote sensing system for urban lawn monitoring in smart cities. The system is comprised of an Arduino node with a camera mounted on a drone. Photographs are taken and classified into different grass qualities employing a rule-based algorithm that classify the grass into very low, low, and high coverage. The system was tested with a dataset of grass pictures resulting in success in the classification of 100%. Lastly, the authors concluded that their system reduced the execution time of the process of taking pictures of the garden, compared to the same classification system mounted on a vehicle, for areas larger than 1000 m2.

Another new form of data acquisition is the use of robots that can incorporate both sensors and actuators to perform activities such as soil moisture sensing, weeding, spraying water, or scaring the animals [115]. Robots can be utilized for the irrigation of precise areas due to their ability to travel to the desired location [87]. This robot is able to measure soil moisture and include proximity sensors to avoid collisions. The robot has a sprinkler system to irrigate the desired area. Furthermore, the wireless robot in [116] is comprised of both environmental and soil monitoring sensors and performs tasks such as water spraying, scaring animals and moving through the field. In order to improve the navigation of the robots for irrigation, the authors in [105] provided the robot with a coverage path planning (CPP) algorithm that has a map of the static elements and environmental data. The robot operating system (ROS) was utilized to develop the control system of the robot which is divided into three layers. The first layer reads the data from the sensors and controls the actuators, the second layer performs the communication among the elements of the system and the third layer performs the decision making and the path planning. This robot performs irrigation as a linear shower. Furthermore, these robots can be powered by solar panels [87, 116] to provide them with more autonomy.

2.6.6 Underground communications

IoUT is an IoT network comprised of at least one underground device with communication capabilities. In the case of the Over The Air (OTA) communication among the above-ground things, the communication can be affected by weather conditions, irrigation, and crop growth. Therefore, these aspects should be considered. On the other hand, underground communication has other requirements such as

adapting the transmission parameters to be able to transmit through the soil considering its changing conditions.

The architecture of IoUT applications may be comprised of static and moving elements such as machinery, drones, sensing nodes, radios, and cloud [57]. These elements should be integrated and can be utilized for both real-time sensing and automation.

The underground things are embedded systems with sensors for monitoring and a communication module. Underground things should be encapsulated in waterproof and weatherproof materials to avoid damages in the equipment from weather, animals, or machinery. They are powered by batteries, solar panels, or a combination of both and are expected to be low-cost. Underground things are deployed in large numbers to perform sensing in multiple places of the field. Base stations have a larger cost and are usually deployed at buildings or weather stations. They have access to more power as they have higher requirements.

The machinery and vehicles utilized on the field can carry mobile sinks to gather the information from underground things as they move through the field. UAVs and robots can be employed as well for this purpose. The data is usually forwarded to a cloud service for its storage and analysis.

Figure 2.29 shows a possible IoUT deployment for agriculture. Mehmet C. Vuran et al. in [281] determined the different components of an IoUT architecture as Underground Things for sensors and embedded systems deployed underground, mobile sinks that gather the data from underground things, base stations that act as a gateway, and cloud services that provide storage and data processing. However, there is no unified or standard IoUT architecture due to the different demands of the sectors that can employ this technology. One of the sectors that could benefit from IoUT is agriculture. In agriculture, IoUT is generally used for real-time sensing of soil moisture, ph, presence of organic matter, the composition of the soil, and nutrients [57]. It is also utilized for yield monitoring, precision planting, geolocation, map generation, soil sampling, drones, VRT (Variable rate technology), and auto steering. The usage of all these elements allows applications to divide the field into different areas according to the conditions of the field. Another sector is that regarding oil and natural gas extractions and transport. Oil and gas reservoirs can benefit from IoUT applications to perform temperature and pressure sensing and to detect pipe and gas leaks. However, localization is necessary to determine the position of the underground nodes. Nasir Saeed et al. resolved this problem using isometric scaling [282] and CRBL (Cramer Rao Lower Bound) in the closed-form to perform 3D localization as opposed to the existing two-dimensional solutions. Lastly, seismic exploration is another one of the uses of IoUT [58]. It differs from other uses such as agriculture in the required burial depth of the node.

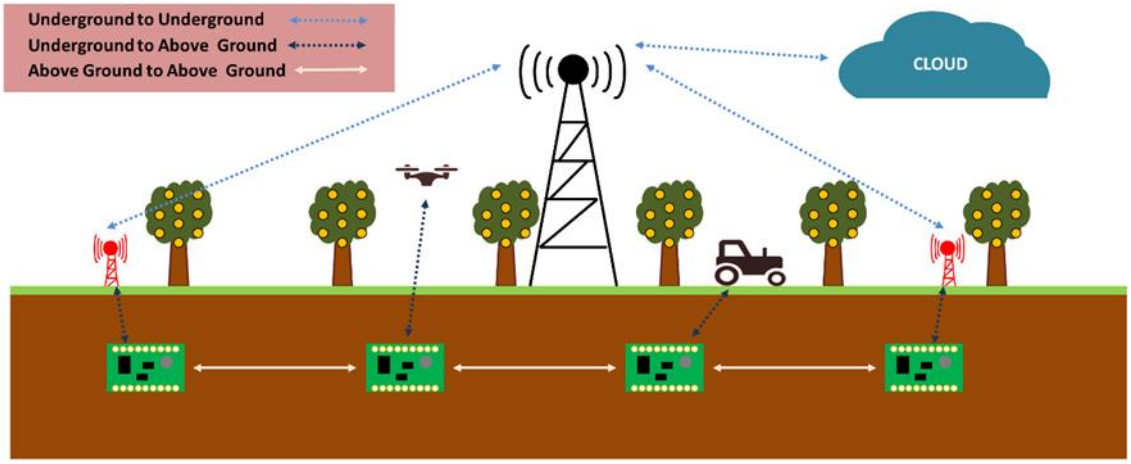

Figure 2.29. Example of IoUT using EM.

The wireless communication in IoUT systems can be performed among underground elements, among above-ground things, and between underground and above-ground elements. The latter one is not symmetric because of the soil-air interface. Vuran et al. determine the communication range for underground communication to be 12 meters [57].

The characteristics of the soil as the communication medium is the principal aspect to consider in IoUT. The parameters that characterize the underground channel are the propagation of electromagnetic waves, soil composition, water content, the multipath effect, and burial depth [283]. Furthermore, when the transmission is performed among underground things, the communication is performed through a direct wave, a reflected wave, and a lateral wave with a path that proceeds along the soil surface. The latter one is the wave with the highest contribution to the received signal power [284].

The behavior of the signal in the 0.3-0.9 GHz band was studied to perform underground channel propagation models [283]. The results show that the effects of the reflected wave decrease with increases in burial depths, being negligible at depths higher than 2 meters. Therefore, for burial depths up to 2 meters, a two-path model should be used and for depths from 2 meters on, a single-path model can be considered.

Regarding the distance between the nodes, the higher the distance, the higher the path loss. Furthermore, when the signal is reflected on the soil-air surface, its phase is changed and, when aggregated with the direct signal, ripples can happen. Another aspect to consider is the lack of uniformity of the soil. As the soil surface is not uniform and smooth both reflection and refraction occur. The multi-path effect can occur as well due to roots, stones, and air, resulting in random values of the phase and amplitude of the signal. Lastly, L. Li et al. conclude that the operating frequency and the soil composition are the key aspects for successful underground wireless communication and the existence of an optimal burial depth that minimizes the path loss for each operating frequency [283].

Several technologies have been studied to be utilized for wireless underground communications [58]. Electromagnetic signals have low ranges, are very susceptible to interferences and attenuations, and have lower data rates. Acoustic communications are less susceptible to interferences in comparison to EM waves. It has high coverage ranges and low data rates. Mud pulse has medium interferences and attenuation, a high coverage range, and low data rates. Magnetic induction has a medium coverage range, data ranges of kbps, and low interferences and attenuation. Lastly, VLC has low interferences but high attenuation. It has a medium coverage range and data rates of kbps.

N. Saeed et al. utilized magnetic induction to establish wireless communication between underground things for oil and gas reservoirs [282] to perform 3D localization based on the CRLB that considers channel parameters. The considered depth is 1.8 Km. The results show that the channel and parameters such as transmission power, error variance, coil size, and the number of underground things affect the localization accuracy. The performance is improved by increasing the number of turns in the coils, the transmission power, and the number of anchors. When the ranging error variance stays between 10 and 30%, the proposed solution is robust, but higher values are not accurate. In summary, the proposed solution is able to improve the localization accuracy by 30%. However, M. C. Vuran et al. determine that magnetic induction is not an option for IoUT systems [57].

A. Salam et al. studied the effects of soil type and moisture on the quality of wireless communication among the Underground Things [284]. From experiments performed both indoors and outdoors, results showed that lower soil moisture led to an increase of the channel capacity by 180%. Adapting the sub-carrier bandwidth to the soil conditions led to increases in capacity ranging from 56% to 136%. From experiments performed with sandy soil, silt loam soil, and silty clay soil with a system bandwidth of 20 MHz for all soils, the achieved capacity was 233 Mbps for sandy soil, 195 Mbps for silt loam soil, and 178 Mbps for silty clay soil. Furthermore, when studying the changes in capacity when increasing the distance from 50 cm to 100 cm, a decrease of 22 % was detected in sandy soil, a decrease of 29% in silt loam soil, and a decrease of 27% in silty clay loam soil. The water holding capacity of the soil is the principal soil parameter in the attenuation of electromagnetic waves. The higher the clay content of the soil, the higher the EM attenuation due to the small pore size. Moreover, the signal travels through both soil and air, with their respective conductivity and permittivity values, and through multiple paths. This results in an increase in the delay spread as the distance increases, obtaining less coherence bandwidth. Lastly, distance is another parameter that determines the channel capacity. Experiments were performed with antennas buried at 20 cm of depth in silty clay loam soil using an empirical antenna bandwidth of 20 MHz. Results showed a decrease from 678 kHz to 411 kHz in the coherence bandwidth when the distance was increased from 50 cm to 12 m, and an increase in the number of subcarriers from 30 to 49. Moreover, a real-time permittivity and soil moisture monitoring for wireless underground communication called Di-Sense was presented in [285]. In order to do so, the propagation path loss and the velocity of wave propagation were utilized. Experiments were performed in a greenhouse with burial depths of 10, 20, 30, and 40 cm, a frequency ranges between 100 and 500 MHz, and slit loam, silty clay

loam, and sandy soils. Results showed high accuracy for depths up to 40 cm and distances ranging from 1 to 15 meters. Lastly, a study on the performance of varied modulation schemes in underground communications was performed in [286]. Multiple antennas were utilized to exploit the direct, lateral, and reflected components of the wireless underground channel. Results showed bit errors rates of 10-3 for delay spreads below 0.05. Results showed that equalization impacts the performance of the IoUT communication with the 8-Tap Decision-Feedback Equalizer as the best one. Furthermore, DBPSK (Differential Binary Phase Shift Keying) and DPSK (Differential Phase-Shift Keying) presented a better performance for channels without adaptive equalizations. Lastly, the authors presented two new receiver designs for IoUT communications named Lateral-Direct-Reflected and 3W-Rake. The three antenna LDR design achieved a BER of 10-5.

Regarding the future challenges of IoUT, N. Saeed et al. commented on the difficulty in deploying IoUT nodes and accessing them for activities such as battery replacement [58]. Therefore, batteries should have a high enough capacity to reduce as much as possible the need for accessing the nodes and, the utilized protocols should implement energy-efficient functionalities. Furthermore, the nodes can get damaged if digging activities are performed. Another aspect is the transmission range that can be obtained in wireless underground communications, which is reduced due to the attenuation caused by the characteristics of the soil. Security in IoUT is not a topic that has been thoroughly studied yet. The physical security of the nodes is one of the security aspects that have to be considered as the nodes must be protected from corrosion, machinery, and digging activities. Furthermore, regarding cyberattacks, the interest in blockchain has been increasing. There are also problems regarding scalability and robustness. N. Saeed et al. also comment on the use of Software Defined Networks and cloud and fog computing to optimize data traffic, analysis, and data storage. Moreover, Rita de C. D. Leles et al. presented in [287] a summary of the challenges of IoUT for railways networks. The authors performed a coverage test in a tunnel where signal intensities of -55 dB were reached for 100 m of distance. The considered challenges are the environmental requirements such as power supply, electromagnetic compatibility, and the mechanical and thermal requirements, the mobility, the use of an independent frequency network that should provide enough bandwidth for the transmitted data, the QoS, the safety of the network and the energy efficiency.

2.6.7. Security in IoT Systems for Irrigation

Depending on the characteristics of the environment where the implementation of the IoT system is carried out, securing the system may become a challenging task as different types of threats must be considered. On the one hand, all the security issues of any IoT system can be applied to an IoT irrigation system for agriculture. Therefore, current works with their focus on securing IoT describes the security challenges that IoT irrigation systems may face. For example, organizations such as the Internet Engineering Task Force (IETF) study the different problems that affect this.

Furthermore, authors such as Garcia-Morchon et al. [288] present in their work the following list of security threats and managing risks: vulnerable software/code, privacy threats, cloning of things, malicious substitution of things, eavesdropping attacks, man-in-the-middle attack, firmware attacks, extraction of private information, routing attack, elevation of privilege, denial-of-service (DoS) attacks. Regarding DoS attacks, Kamienski et al. [100] highly stressed the importance of protecting the irrigation system from DoS attacks or avoiding attackers from accessing the collected data or the system with the intention of damaging the crops.

In order to face the above threats, it is necessary to apply the appropriate security measures, but as new threats and attacks appear daily, [288] propose using methodologies such as analyzing the business impact of the attack, assessing the threats considering their impact and probability, its impact on the privacy of the collected information and the process of reporting and mitigating incidents.

However, on the other hand, when considering just the currently available studies on securing IoT irrigation systems specifically, it is possible to discern which aspects of IoT security are prioritized for this type of system.

Jimenez et al. [289] identified the security threats specific to an intelligent wastewater purification system for irrigation. Apart from the previously mentioned security threats [288], the authors of [289] contemplate physical attacks that the IoT deployment may face. The IoT devices must be protected from the weather and possible animals that access the fields. However, strong weather conditions such as floods or animals such as wilds boars may result in the IoT device being damaged or lost. Furthermore, the IoT devices may also be damaged by the operators when they are performing their activities or be the aim of a person with malicious intentions. Another threat to the devices deployed on the field is the possibility of them being replaced with malicious nodes, providing the attacker with access to the network [79]. The deployed devices may also be susceptible to malicious code and false data injection, leading to wrong results and the malfunction of the system. Sleep deprivation attacks are aimed at depleting the battery of the devices. The deployed nodes are susceptible to booting attacks as well. Furthermore, attackers may also perform eavesdropping and interfere with the deployed devices. The concern of securing the physical devices deployed on the fields has led to many systems incorporating PIR sensors, scarecrows, and buzzers to detect intruders, either humans or animals, and to alert of their presence [109, 290].

Privacy is another aspect to consider. The data managed by IoT irrigation systems may not need as much privacy as the data managed by other IoT applications such as those for health. In fact, Jimenez et al. [289] remark that it may not be necessary for the gathered data of some irrigation IoT systems to remain private, but the correct performance of the system must be ensured, which is avoiding DoS attacks. However, the owners of the fields may be implementing new techniques they would prefer to remain private, or the water quality management system could be regarded as a critical infrastructure as the produce that results from the fields irrigated with that water would be consumed by people. Therefore, considering this aspect, Ahad et al. [252] and Barreto et al. [291] remark the need for user privacy, as the obtention of this information may lead to attacks to the owner or the personnel of the farm. Ahad et al.

[252] consider data and device privacy as well, because of the need for guaranteeing the ownership of the data to avoid repudiation and ensuring data availability. Barreto et al. [291] remark on the burden that could be originated from the exposure of the GPS locational data captured by IoT devices as attackers may gain information on the location of the farm to perform physical attacks. Lastly, Ahad et al. [252] also comment on the need for a secure storage system for the information, with particular emphasis on distributed data storage systems. Attacks such as SQL injections can lead to the obtention of private information from storage systems [292].

As cloud computing often goes hand in hand with IoT systems, threats to cloud services may compromise the IoT irrigation system as well. Flooding attacks and cloud malware injection are some of the attacks that can be intentionally executed to compromise the data and the performance of the cloud [292].

Ransomware is another security threat that could affect irrigation systems for agriculture [291]. All the data regarding pesticides and the fertigation system could be encrypted until a ransom is paid. For this reason, having a backup in a remote location is greatly advised.

Barreto et al. [291] also remark some security threats that are not usually commented on when discussing the security of IoT systems for agriculture. One of these threats is the damage that can be caused by social engineering as the users of the IoT irrigation system could provide login information to people posing as technicians or click on malicious links on their e-mails. The other threats are agroterrorism, cyber-espionage, mostly related to accessing intellectual property or confidential information regarding aspects such as genetically modified crops. Other security requirements specific to IoT systems include network security, identity management, privacy, trust, and resilience [293]. They presented mechanisms that ensure data confidentiality, integrity, origin authentication, and freshness for each IoT technology. A large selection of IoT technologies was analyzed, from single-layer protocols to full protocol stacks.

In WSN, failures that prevent the correct operation of the network may occur in the sensor nodes. Hereafter, some algorithms that reduce these problems are analyzed. Bagci et al. [294] developed a new distributed fault-tolerant topology control algorithm called Disjoint Path Vector (DPV) that is used for heterogeneous WSNs. These have two layers. The first one is a layer of nodes with low-cost ordinary sensors, limited power, and short transmission range. The other layer is comprised of supernodes with more energy reserves and better processing, data capacity, and actuators. These collect the information of the nodes. In the topology, each sensor is connected with at least one supernode by k-vertex disjoint paths (Paths with common endpoint but that have no other vertices in common). The typology is tolerant to a failure of k-1 in the worst case. The simulation showed that the algorithm is more efficient than other algorithms. DPV has a 4-fold saving in total transmission power of distributed anycast topology control under the assumption of no packet losses and a 2.5-fold saving with a packet loss rate of 0.1. Azharuddin et al. [295] showed an algorithm called Distributed Fault-tolerant Clustering and Routing (DFCR). This algorithm is proposed for WSNs. The sensor nodes are grouped in clusters and a sensor node of the cluster is selected as cluster head (CH). The CH changes in each round of information forwarding. This is selected based

on the residual energy of the CH, the distance between the sensor node and the CH and the distance from the CH to the base station. In case of failure, the sensor nodes send a help message to other clusters and, if they receive replies, they join this new cluster. They compared their algorithm with Minimum Hop Routing Model (MHRM) and Distributed Energy Balanced Routing (DEBR) with simulations. The results of the simulation showed that DFCR is better with regard to the number of live sensor nodes, energy consumption, etc. Authors in [296] proposed a lightweight algorithm, which is based on a set of rules to detect the characteristics of the packets in the network. The proposed approach can detect the malicious packets that are sent to the network. Furthermore, authors of [297] reviewed the architecture and features of fog computing, including real-time services and fog-assisted IoT applications based on the different roles of fog nodes. They presented security and privacy threats towards IoT applications. Kaur and Garg [298] developed an improvement of the DFCA, the Improved Distributed Fault-Tolerant Clustering Algorithm (IDFCA). In DFCA, when the CH fails, the operation is moved to the neighboring CH, causing a greater workload in it. In this study, when a CH fault happens, the sensor node selects the CH that was going to be chosen in the next round. Furthermore, the security level of LoRaWAN is studied in [299]. It is focused on the security of LoRaWAN. The LoRaWAN protocol is a MAC (Medium Access Control) layer protocol for LoRa, which provides the communication infrastructure and interfaces for gateway-sensor topologies, node coordination, and medium access. They proposed several countermeasures and changes to the LoRaWan protocol, which rendered all these attack vectors harmless. Many of these countermeasures can be implemented with minimal changes to the LoRa ecosystem.

Blockchain is a new technique that is being applied to secure IoT systems [292], which allows secure data storage and communication. In agriculture, it is mostly utilized to secure the supply chain [300], although there are other proposals that use it to secure a greenhouse [301] or to secure the overall smart agriculture framework [302]. Regarding IoT irrigation systems for agriculture, blockchain has been applied in [303] to track and trace the information exchange of their proposed smart watering system.

2.6.8 Common Architecture Designs for IoT Irrigation Systems for Agriculture

In this subsection, an overview of the most frequent architectures for these systems is going to be discussed.

Multi-agent architectures are popular in IoT solutions for irrigation management [226,230]. These types of architectures make a distinction among the different elements they are comprised of. Typically, the distinction is made according to the layer of the architecture the elements are encompassed in. For example, nodes positioned higher in the hierarchy may act as a broker for those lower in the hierarchy [226].

Most architectures are divided into layers or functional blocks that represent the main actions to be carried out [304]. These blocks or layers can be considered as generic and are utilized in most of the available architecture designs for IoT systems intended for

irrigation management. The main elements of these architectures are devices, communications, services, management, applications, and security.

IoT systems are comprised of devices located in a certain environment to perform multiple activities such as detection, monitoring, control, and action. The devices must have interfaces that allow their connection with other devices to transmit the necessary information. The data obtained through different sensors will generally be treated and their results will be applied to different actuators. Then, it is necessary to transmit the monitored data and response actions between the devices. Communication protocols are used for this task. In most cases, different communication protocols are used working together on the same IoT system. In order to perform activities such as device discovery, device control, or the analysis of the collected data, the use of services may be necessary as well. The applications allow the interaction of the user with the system. From the applications, the user will be able to visualize the information, both obtained by monitoring and that extracted from the data once they have been processed. On many occasions, the user can execute the actions that he considers appropriate to the situation presented by the data, the actions can also be carried out automatically. Lastly, providing security to the system may also be considered.

Traditionally, the IoT architecture has been considered to be divided into three layers, which are the perception, network, and application layer. Later on, an intermediate layer placed between the network and application layers has been introduced in multiple studies. This layer, called service layer, is employed to store and process data using cloud and fog computing. For the last few years, authors such as Ferrández-Pastor [305] presented a new architecture proposal, based on four layers: things, edge, communication, and cloud. In these latest architectural proposals, the authors use the edge layer to locate critical applications and perform basic control processes. Also, as indicated by [305], cloud (internet/intranet) can provide Web services, data storage, HMI (Human Machine Interface) interfaces, or analytic applications. Figure 2.30 shows an image where the architecture models are shown.

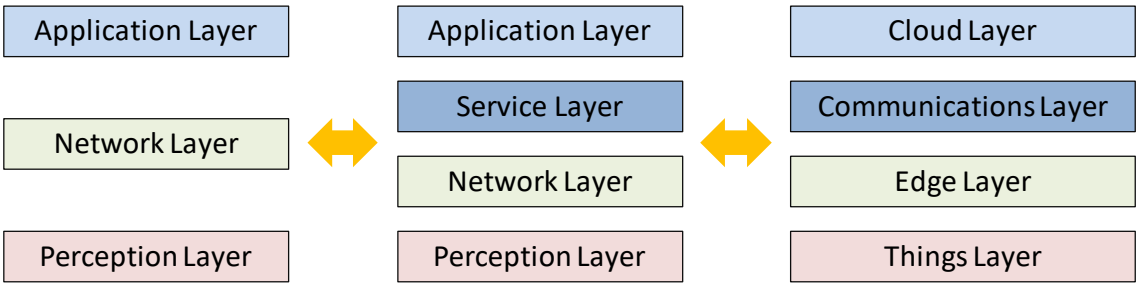

Figure 2.30. Evolution of the layered model in IoT architecture.

In the case of the reviewed IoT systems for irrigation, both 3-layered [95, 133, 169, 306, 307] and 5-layered architectures [230] are available. Commonly, the lower layer is comprised of the sensor nodes and the actuators. The middle layer is comprised of a gateway and contemplates data transmission. Lastly, the third layer is usually tasked

with performing data storage and analysis. Typical third layers are conformed of cloud services, databases, or applications.

A novel take on IoT deployments for precision agriculture is being considered on the Internet of Underground Things [281]. The authors define the functionalities as in-situ sensing, wireless communication in underground environments, and the connection between the elements of the architecture such as sensors, machinery, or the cloud. In the case of IoUT, the sensors are deployed underground. The authors performed a study on wireless communication among above ground and underground devices. The path loss link between above ground and underground devices reached -80 dBm for 50 m. The distance between underground devices reached approximately 10 m for -80 dBm. The authors also comment on the effects of soil moisture on path loss.

2.6.8.1 Field monitoring WSN

Sensor nodes are a widely spread technology utilized in many agricultural monitoring systems to implement their solutions. Some authors have presented a review of the state of the art of the use of WSN in agriculture [308-312]. Tamoghna Ojha et al. [308] studied applications of WSN and its problems and challenges for the improvement of agriculture. Antonis Tzounis et al. [309] presented a survey on the latest IoT technologies and their implementation in the agricultural sector, as well as the challenges that arise in their implementation. Aqeel-ur-Rehman et al. [310] studied the need of using sensors in agriculture and the utilization of WSN in that field. Luis Ruiz-Garcia et al. [311] reviewed wireless sensor technologies and standards for their communications in the agri-food sector, focusing on WSN and Radio Frequency Identification (RFID). Barcelo-Ordinas et al. [312] also presented the state of the art of WSN technology applied to precision agriculture, reporting hardware, and software solutions from the technological point of view.

Other authors presented designs for new WSN architectures for agriculture [313-315]. Authors such as Srbinovska et al. [313] proposed a WSN architecture for a greenhouse of vegetables, achieving the monitoring of environmental parameters in crops and a reduction in costs. Xiaoqing Yu et al. [314] presented a hybrid WSN architecture applied to agriculture. A hybrid network of wireless sensors consists of wireless sensors that communicate through the ground in addition to wireless terrestrial sensors. Chaudhary et al. [315] have proposed and analyzed a programmable System-on-chip (PSoC) microcontroller that they integrate into a WSN network and use to monitor and control parameters in greenhouses. J. A. López-Riquelme et al. presented in [316] a FIWARE cloud-based software architecture for precision agriculture. Authors discussed the advantages of FIWARE and its open-source modules and enablers for agriculture. The hardware architecture was performed utilizing the MEWiN Mainboard with a SIM900 Module. Experiments were performed both in the laboratory and on real crops. The average power consumption of the node was 4.29 mA. Another architecture for precision monitoring intended for potato crops and based on Cyber-Physical Systems

(CPS) is presented by Ciprian-Radu RAD et al. in [317]. Their proposed architecture was divided into four layers being application, analyzing, networking, and sensing. The data obtained from the system has then to be processed so as to perform the decision making and control the system in real-time. The aims of the proposed architecture were the optimization of water and chemical usage, the increase in production and sustainability, and the reduction of costs. H. Navarro-Hellín et al. presented in [318] an architecture for WSN intended for water management. The system utilized ES-2 sensors for water temperature and conductivity, GS3 and HP II sensors for moisture, temperature, and conductivity, 10HS sensors for soil moisture, LMK sensors for pressure, and MPS-2 sensors for temperature and soil matric potential. The communication was performed over GSM/GPRS (General Packet Radio Service) and the data was stored both in a database and in SD (Secure Digital) cards. A web application allowed monitoring the data remotely.

Furthermore, there are authors [38, 319-323] that present monitoring systems in agriculture based on WSN. Escolar Díaz et al. [319] proposed a methodology to implement WSN in agriculture and define the phases that cover the life cycle of WSN applications. Yingli Zhu et al. [320] presented the design of a real-time agricultural monitoring system based on WSN. They also provided the hardware design of the sensors and the software flow diagram. Manijeh Keshtgari and Amene Deljoo [321] also developed a WSN system for agriculture, through which they detected environmental data and made control decisions in real-time. Hwang et al. [322] proposed a monitoring system for agriculture that used a WSN, which collected soil and environmental information through sensors, image information using CCTV (Closed-Circuit Television), and finally GPS location information. Garcia-Sanchez et al. [323] proposed a new platform called Integrated WSN Solution for PA, in which a WSN is deployed with IEEE 802.15.4 technology. It allowed the monitoring of the crop and its video surveillance. Garcia et al. [38] presented the design of a wireless network that was responsible for monitoring the crops and their irrigation system; the network consisted of a WSN and a wireless mesh network (WMN). Marco Mancuso et al. presented in [324] a WSN for environmental monitoring in a tomato greenhouse. Sensicast devices were utilized as the nodes. Their proposed system considered air and soil temperature and humidity. For data transmission, the proprietary SensiNetTM protocol was utilized over ZigBee. Results showed a relation between temperature and humidity and determined that both of them are non-linear. Another WSN for smart agriculture that utilizes ZigBee is proposed in [325]. The authors addressed the necessity of precision agriculture systems so as to reduce water consumption. The monitored variables were soil temperature and moisture. Several modules with ZigBee radios such as TelosB, ATmega256RFR2, and OpenMote-CC2538 were considered. The data was stored every 15 minutes on an SD card for further analysis. Due to some data loss, the resulting efficiency of the system was 94.79%. Abd El-Kader, and Mohammad [326] studied the use of WSN in the potato crop in Egypt. They demonstrated that the cost of the WSN is compensated by the increase in profits and the reduction of costs. The sensor nodes contain sensors for temperature, humidity, light intensity, soil pH, and soil moisture. The sensor nodes are placed in the tubs of potato crops with a distance of 6 meters between them. The different sensor nodes communicate through radio frequency. The

Periodic Threshold-sensitive Energy-Efficient sensor Network (APTEEN) is used for routing strategy. In this protocol, node sensors are regrouped in a cluster and a sensor node has the responsibility of receiving, aggregating, and transmitting the data of cluster members to the gateway. They used APTEEN because it is the most suitable routing idea for their needs. In [327], Achouak et al. showed the use of a wireless network composed of sensors and actuators for controlling the requirements of crops in a greenhouse.

The use of WSN to monitor the irrigation needs of crop fields is very common as well. Dursun and Ozden, [44] developed a low-cost WSN (US$ 96) to control the irrigation in dwarf cherry trees. The system has been based on 3 units i.e., a sensor unit, a base station unit and, a valve unit. The sensor unit has a moisture sensor and sends the data to the base station. The base station analyzes the data and decides the parts that need irrigation and opens or closes the valve units. This system allows to eliminate the moisture stress and reduce excessive irrigation. Yao et. al. [328] proposed a WSN for monitoring irrigation in agriculture and saving water. The sensor nodes are composed of soil moisture, air temperature, pressure, and light intensity sensors. The sensor node transmits the data to the gateway node and the latter, forwards it to a LAN or WAN. For decision making, they used a fuzzy neural network. The self-learning ability of the neural network and the employed fuzzy logic techniques are good for irrigation monitoring. Simulation results confirm that the system can be used for irrigation monitoring. Finally, Rocher et al.in [329] presented a sensor for monitoring the fertigation in smart irrigation systems for fruit-bearing trees which can be used jointly with our system.

WiFi is a widely spread wireless communication technology. Many agricultural monitoring systems use WiFi for their communication between the different agents of their architectures such as the one proposed in [330] by Gerard Rudolph Mendez et al. They presented a WiFI Wireless Sensor Network for agriculture monitoring where temperature, humidity light, soil moisture, and water level data collected by the nodes. Furthermore, the data was forwarded to a server so it could be accessed later. Therefore, studying the coverage of WiFi in different agricultural environments is of great interest.

2.6.8.2 Water monitoring WSN

WSNs can also be used for monitoring water quality. He and Zhan [294] designed a water quality monitoring system for an environmental protection department. They used a CC2430 microprocessor and many different sensors, like water temperature, pH, turbidity sensors, etc. The employed wireless network transmission protocol is Zigbee. The sensor sends the data to the internet. Fustine et. al. [331] explained the need to monitor the Lake Victoria Basin which has increased due to anthropomorphic pressures. Thus, the authors presented a WSN for monitoring the Lake Victoria Basin. An Arduino microcontroller, water quality sensors (water temperature, dissolved oxygen, pH, and conductivity), and a wireless network connection compose the system. They used open

source hardware, a web portal, and a mobile phone platform to display the value of the sensors. The experiments showed that their proposal can be used for monitoring in real environments.

Regarding sensor networks for water quality monitoring and wastewater treatment, the contamination of the wastewater may not only affect the quality of the water but also the treatment plants or the sewer systems. Therefore, it is important to deploy a monitoring network to detect contamination and contain the affected areas. In their study, Mariacrocetta Sambito et al. [332] compared different sensor positioning techniques intended for nonconservative immanent pollutants. The results showed that the optimal solution could be reached with less computational effort by implementing pre-screening and gray information techniques. Stefania Piazza et al. utilized an optimization approach by using the NSGA-II algorithm to compare the positioning of the sensor probes to the results obtained from experimental tests [333]. The results showed that the sensors positioned at the center of the network minimize the redundancy and maximize the detection likelihood.

2.6.8.3 Meteorology monitoring WSN

Due to the importance of meteorology monitoring, researchers have developed several meteorology monitoring systems. F. J. Mesas Carrascosa et al presented in [334] an environmental monitoring system for precision agriculture. The system is comprised of the Arduino ATMega2560 microcontroller, analog, and digital temperature and humidity sensors, a light sensor that detects the presence and absence of light, a clock, a Bluetooth module, an SD card module, and a photovoltaic panel. The system was able to forward the data to a database for further processing. Real measurements were performed on a farm located in the Spanish city of Cordoba. The price of their proposal is below 100 € and the results were similar to those of a real meteorological station Furthermore, a wireless weather station that included a web interface for users was developed by Hardeep Saini et al in [335]. The system was able to monitor temperature, humidity, pressure, wind direction, and wind speed. Zigbee was employed for data transmission and alerts were generated according to the measured parameters. Results showed the accuracy of the proposed system.

2.6.9 Effects of vegetation on coverage and signal quality

The effects of vegetation on radio signals have been discussed by and analyzed by many authors. Jose Antonio Gay-Fernández et al. performed in [336] wireless propagation and path loss modeling for environments with vegetation for the 2.4, 3.5, and 5.5 GHz frequencies in a peer-to-peer configuration. Tests were performed in different environments, where the results showed better propagation models for

grasslands followed by forests and scrublands. However, the authors remarked the importance of vegetation density. The attenuation caused by the foliage of tropical vegetation for frequencies 2 to 18 GHz and 26.5 to 40 GHz was assessed by Hairani Maisarah Rahim et al. in [337]. The results showed that the obtained attenuation depended on the frequency with results varying from 10.99 dB at 15 GHz to 24.23 dB at 9 GHz. J. Acuña et al. presented in [338] a study on the interferences caused by vegetation barriers to wire-less networks with the aim to reduce the signal strength at the areas where coverage is not wanted. Several species of shrubs with different dimensions were studied. Results showed attenuations reaching 10 dB for 2.4 GHz and 21 dB for 5.8 GHz. Leire Azpilicueta et al. performed in [339] a studio on the propagation of radio waves at the 2.4 GHz band through inhomogeneous vegetation environments. Measures were simulated in a park environment with grass, trees, and concrete as the elements that introduce attenuation using ZigBee and Bluetooth wireless technologies. The experimental measures were performed with Zigbee mote was placed at the trunk of a tree. The results verified that their proposed 3D ray launching algorithm was good enough for radioplanning in such environments. A model for radiowave propagation through the foliage of different tree species and locations for frequencies of 1 to 60 GHz was presented by Jürgen Richter et al. [340]. Results showed that the estimated RMS error was 8.38 dB compared to the 11.51 dB of the ITU-R (International Telecommunication Union – Radiocommunication Section) 833-3 model. A study of wideband signal propagation from 1 to 60 GHz through different types of trees was performed by D. L. Ndzi et al. in [341]. The signal power is obtained with an omnidirectional antenna. Results showed that the signal path depends on the width and height of the vegetation. A simulation of the effects of vegetation on radiowave propagation for WSN was performed by Naseer Sabri et al. in [342]. The authors utilized the Free Space Path Loss Model and added foliage models to simulate the attenuation. The simulations were performed for frequencies from 1 to 3 GHz, distances up to 20 meters, and heights between 0.5 and 2 meters for the receiver and 3.5 meters for the transmitter.

The factors that create signal attenuation in wireless transmissions through vegetation at 1.3, 2 and 11.6 GHz were discussed by Nick Savage et al. [343]. The maximum attenuation (MA), the nonzero gradient (NZG), and modified exponential decay (MED) were utilized to model the attenuation caused by vegetation. A wideband channel sounder was utilized to perform the measures at heights varying from 2.5 to 7.5 meters. Results showed that vegetation density, the measurement geometry, and the state of the leaf are the factors that most contribute to the attenuation. The 11.6 GHz frequency was the one that presented a greater attenuation due to the leaves. A study on the radio wave propagation of 433 MHz signals at potato fields utilizing RSSI measures was performed by John Thelen et al. [344]. Results showed a communication range of 78 meters and advise to place nodes between a 23 m range when the crop is on its return and a 10 m range when the crop is flowering. Furthermore, a characterization of vegetation movements on radiowave propagation was performed by M. H. Hashim et al. in [345]. The measures were taken in an anechoic chamber at 0.9, 2, 12, and 17 GHz with two types of trees and four different settings for wind. The results showed that the behavior of the signal propagation varied with calm and windy conditions, but it didn’t

vary much among different windy conditions. The comparison of the different studies on the effects of vegetation on the wireless signal is presented in Table 2.8.

Table 2.8. Comparative of testbeds of studies on the effects of vegetation on the wireless signal.

Ref	Environments	Heights	Frequency	Transmitter	Receiver
Jose Antonio Gay-Fernández et al. [336]	Forests, scrublands, and grasslands	0.9, 1.2, and 1.6 m	2.4, 3.5, and 5.5 GHz	Rhode-Schwarz SMR-40 signal generator and an Electronics EM 6865 wideband antenna	Robde-Schwarz FSH-6 spectrum analyzer
Muhammad A. et al. [346]	Urban areas, rural areas, forests, and plantations	-	2.4 GHz	-	-
Hairani Maisarah Rahim et al. [337]	Tropical vegetation foliage	2m	2-18 GHz and 26.5-40 GHz	Anritsu MG3694C Signal Generator	Spectrum Master MS2730T
J. Acuña et al. [338]	Shrubs	1.25 m	2.4 GHz and 5.8 GHz	Rohde&Schwarz radio signal generator SMR-40	Rhode&Schwarz FSP-40 spectrum analyzer
Leire Azpilicueta et al. [339]	Park	1 m	2.4 GHz	Zigbee mote	Agilent N9912 Field Fox portable spectrum analyzer
Jürgen Richter et al. [340]	Trees	5-17 m	1-60 GHz	-	-
Nick Savage et al. [343]	Trees	2.5-7.5 m	1.3, 2, and 11.6 GHz	Channel sounder	Channel sounder
John Thelen et al. [344]	Potato crop	0 m	433 MHz	Mica2Dot	Mica2 with MIB510 programming board and an antenna with an 11.7 dB gain
B. Dhanavantha n et al. [347]	Cornfields and coconut gardens.	2 cm, 15 cm, and 1 m	2.4 GHz	Agilent N5182A Vector Signal Generator	Agilent N9010A Vector Signal Analyzer
Andrew	Sports facility	0 - 130.8	2.45 GHz	National	National

Szajna et al. [348]	and a forested area covered by snow.	cm		Instruments PXI-5670	Instruments PXI-5690 low noise preamplifier paired with National Instruments PXI-5660 RF vector signal analyzer.
Daihua Wang et al. [349]	A plaza, a sidewalk, and a grassland.	3 cm, 1 m	2.4 GHz	RF transceiver working at 2.4GHz	Agilent N9912A spectrum analyzer
Weisheng Tang et al. [350]	Concrete road, flat grass, and undulating grass.	5 cm, 50 cm, and 1 m	470 MHz	Silicon Labs Si4432 radio frequency chip	MSP430F5438 as the Microprogramed Control Unit (MCU) chip
Seun Sangodoyin et al. [351]	Rural flat and hilly terrains.	10 cm, 20 cm, 50 cm, and 2 m	3–10 GHz	Tektronix AWG 7122c waveform generator	Agilent DSA91304A Digital Sampling Oscilloscope
Amir Torabi et al. [352]	Ground plain, yard, and grass park.	13 cm	315 MHz, 915 MHz, 2.4 GHz	-	-
Daniel P. Luciani et al. [353]	Concrete, grass field and hallway.	15 cm, 30 cm, and 1 m	2.48 GHz	STMicroelectronics STM32W-RFCKIT	Laptop
Hicham Klaina et al. [354]	Soil, short and tall grass fields	20 cm and 40 cm	868 MHz, 2.4 GHz and 5.8 GHz	ZigBee nodes	ZigBee nodes
Peio Lopez-Iturri et al. [355]	Oak and pine tree fields.	1 m, 2 m, and 3 m	2.4 GHz	-	-
D. L. Ndzi et al. [356]	Mango and palm plantations.	1.3 m, 1.7 m, 2.2 m and 2.6 m	0.4-7.2 GHz	Agilent E8267D signal generator	Agilent E4405B spectrum analyzer
Jaime Lloret et al. [357]	Rural and forest areas.	3 m	2.412-2.472 GHz	wireless multisensors and wireless IP cameras	802.11g access points
Our testbed [358]	Orange field, scrubland, and grassland	0, 0.5, 1 m	2.4 GHz	ESP 32 Doit devkit v1	ESP 32 Doit devkit v1

2.6.10 Communication protocols intended for irrigation and agriculture monitoring systems

WSNs have specific requirements and several protocols were developed specifically for these types of networks. Many systems for agricultural monitoring employ these protocols to forward the data obtained from the sensors. U. B. Nagesh et al. presented in [359] the usage of a MQTT protocol applied to precision farming and weather monitoring. The proposed system monitored humidity, temperature, and power and utilized a Raspberry Pi as the controller. The Eclipse Paho MQTT client was utilized to implement the subscriber and an open-source MQTT broker was utilized to access the data. A system for controlling and monitoring a smart greenhouse employing IoT and the MQTT protocol was presented by Dipen J. Vyas et al. in [360]. The system comprised an ESP8266 Wi-Fi module and an Atmega328 board with temperature, humidity, and soil moisture sensors. For the MQTT broker, the authors utilized Mosquitto. Ravi Kisore Kodali et al. introduced in [165] a low-cost smart irrigation system that employed MQTT as the communication protocol. The system comprised the ESP8266 NodeMCU-12E, a soil moisture sensor, a temperature and humidity sensor, and a relay. Junsung Park et al. presented in [361] a greenhouse monitoring and control system. Communication among the nodes was performed over ZigBee employing the UDP-based CoAP communication protocol. Nodes sent the gathered information from the sensors to the gateway which converted the CoAP message into an HTTP one so as to forward the data to the server. Finally, A. Paventhan et al. performed in [362] a comparison of two different protocols for WSNs in agricultural environments. The authors compared the simple network management protocol (SNMP) and CoAP in its message format, security and resource management, and the user interface. They concluded that the CoAP presented better integration with the web and was expected to grow in usage for WSN applications.

Other protocols were created so as to address specific requirements of precision agriculture. Awais Ahmed et al. presented in [363] a routing protocol for WSNs to improve energy efficiency in environmental monitoring deployments. The energy-efficient sensor network routing (EESNR) protocol reduced the overhead of control messages. All the nodes were able to become the cluster head as long as the constraint on energy life and the established criteria was met. The authors performed simulations in NS3, comparing the proposed protocol to other existing protocols for WSNs like LEACH (Low-Energy Adaptive Clustering Hierarchy) and its variations. The results showed an improvement of 27.8% of the lifespan of the sensors compared to the other protocols. A routing protocol for sensor networks intended for agriculture monitoring based on the efficient zone was developed by Lutful Karim et al. in [364]. An energy-efficient zone-based routing protocol (EEZRP) assigned different zones to the nodes depending on their distance to the base station and considering that nodes closest to the base station consume more energy. The proposed protocol considered the sensing range. The number of active nodes was fewer than in other protocols, but it might perform more processing and control operations. Simulations were performed to compare the energy consumption of the nodes to other protocols intended for WSNs like LEACH and DSC

(Digital selective calling). The results showed a significant reduction of the consumed energy compared to other protocols. S. Bhagyashree et al. proposed, in [365], Apteen, a protocol intended for expanding the lifetime of the nodes in WSNs for precision agriculture. It is a cluster-based hierarchical routing protocol that groups the nodes into clusters comprising a cluster head and member nodes. The sensed parameters, thresholds, time division multiple access (TDMA) schedules, and the count time were broadcast from the cluster head. The messages were for-warded utilizing ZigBee in order to send the data to a database. Karim Fathallah et al. presented, in [366], partition aware RPL (PA-RPL), a routing protocol for IoT in precision agriculture. It was a version of the routing protocol for Low-Power and Lossy Networks (LLN) (RPL) protocol that considered the partitions in farmlands to perform the routing topology. The protocol only considered one sink node. Simulations were performed employing the Cooja simulator. The results showed that the protocol was able to construct the network covering all the parcels. Lastly, a MAC protocol for precision agriculture based on storage and delivery intended for airground collaborative wireless networks (SD-MAC) was introduced by Song-Yue Liew et al. in [367]. In their proposal, a UAV flew over the sensors in order to collect the gathered data. This way, a re-duction in the duplication of data was obtained and the cost was reduced as a single UAV was able to gather the data from a large area. The proposed protocol forwarded the packets only when the UAV was within the range of the sensor. Sensors were deployed outside of the range of other sensors so as to avoid interferences. When the UAV was not close to the sensor, the sensor stored the information until the UAV was within range. Simulations were performed, comparing the proposed protocol to ALOHA (Additive Links On-line Hawaii Area). The results showed that the proposed protocol outperformed ALOHA.

Furthermore, implementations of monitoring systems employing IoT protocols such as CoAP are starting to be performed. Adarsh B. U. et al. performed in [368] an implementation of a water quality monitoring system utilizing CoAP over 6LoWPAN (IPv6 over Low-Power Wireless Personal Area Networks). The Contiki OS cooja simulation environment was utilized to design the system. The monitored parameters were conductivity, pH, temperature, and ORP (Oxidation Reduction Potential). A TelosB mote was utilized so as to gather the data from the sensors and transmit it to the database. Actuators were utilized so as to add acid or basic solutions to the water according to the sensed data. The data could be accessed through a web interface. An environmental monitoring system that utilized CoAP as the communication protocol was developed by Tomislav Dimčić et al. in [369]. The authors utilized a Telit GSM-GPRS modem with a Python engine and implemented CoAP on the application layer of the M2M system. Comparisons were performed with CoAP and HTTP where CoAP obtained a considerably lower transmission time. Lastly, a comparison of application protocols for IoT systems was performed by Nitin Naik in [370]. CoAP, MQTT, HTTP, and AMQP (Advanced Message Queuing Protocol) were compared according to message size and overhead, power consumption and resource requirements, bandwidth and latency, contrasting reliability vs. interoperability, security vs. provisioning, and IoT usage vs. standardization. CoAP presented the lowest size, power consumption, and bandwidth usage followed by MQTT, AMQP, and HTTP. However, MQTT was the most reliable, and HTTP and CoAP were the ones that presented more interoperability.

MQTT was the most secure protocol followed by CoAP and the most utilized for IoT systems. However, it is also the least standardized protocol, being HTTP and CoAP the most standardized ones.

2.6.11 Unlicensed bands occupation and coexistence

Some of the most employed wireless technologies operate on unlicensed bands. The most common is the 2,4 GHz ISM band but the 5GHz band is started to be more employed, as it can be seen in Figure 2.31. Some of the problems that arise from channel occupancy are addressed in [371]. They determine that the main problems of a crowded spectrum are achieving high performance, supporting overlapping WSN, and managing interferences. Authors propose establishing more unlicensed frequency bands or using spread spectrum techniques. The presence of IEEE 802.11 technologies can increase IEEE 802.15.4 packet loss however, failures are negligible employing -10 dBm transmit power [372]. Higher power transmissions could be a solution, but they could not be indicated for some applications like BANs due to electromagnetic energy absorption by the human body. It also would increase interference with other users of the 2,4 GHz ISM band and be susceptible to attacks like eavesdropping. Some suggestions presented in [373] include keeping low the power levels in order to allow coexistence and frequency reuse and employing Cognitive Radio Systems (CRS) to utilize the gaps with low spectrum occupancy. Employing this technique is advised for short range communications for it not to interfere with other users of the spectrum.

Bluetooth, ZigBee, and WiFi share the 2.4 GHz band. Bluetooth and UWB (Ultra-WideBand) employ adaptive frequency hopping to avoid interferences (channel collision) and ZigBee and WiFi use dynamic frequency selection and transmission power control. There are three types of solutions to avoid interference between Bluetooth and WLAN (Wireless Local Area Network) [374]. The first one is collaborative solutions where Bluetooth and WLAN have to exchange messages. They are called Packet Traffic Arbitration (PTA), where time slots are assigned to avoid collisions and Alternating Wireless Medium Access (AWMA) where TDMA is employed. The non-collaborative solutions do not perform a message exchange between Bluetooth and WLAN. Adaptive Frequency Hopping (AFH) changes the hopping sequence to avoid channels with high interference. Listen-Before-Talk (LBT) employs CSMA/CA so the channel is checked before transmitting. However, the radiation power of Bluetooth is lower than the access point (AP), so the WLAN may not detect the Bluetooth device and begin the transmission, resulting in collision. The OverLap Avoidace (OLA) Mechanism considers the Bluetooth device and the AP separately. The slot size of the Data-link is adjusted in order to avoid collision. Several experiments have been performed in order to determine the effects of interferences between Bluetooth and Wi-Fi. In [375], data traffic, a Bluetooth voice application, and the performance of the WLAN are considered. They conclude that packet loss is higher when the Access Point and the Bluetooth device are closer. They also study interference mitigation techniques such as the backoff strategy (BIAS) and adapting the frequency

hopping pattern for Bluetooth devices. Their results show that there is not any technique that can improve the performance for all applications and suggest employing a combination of both. In [376], an analysis of the packet error rate under interferences from WLAN and Bluetooth is performed. They state that when the distance between the source and destination of a WLAN transmission is less than 3 m, there is no interference from a ZigBee network. The higher the number of WLAN APs, the higher the packet error rate of ZigBee. Their studies show that the major interference for ZigBee comes from WLAN. Bluetooth interferences decrease abruptly when the distance between devices increases.

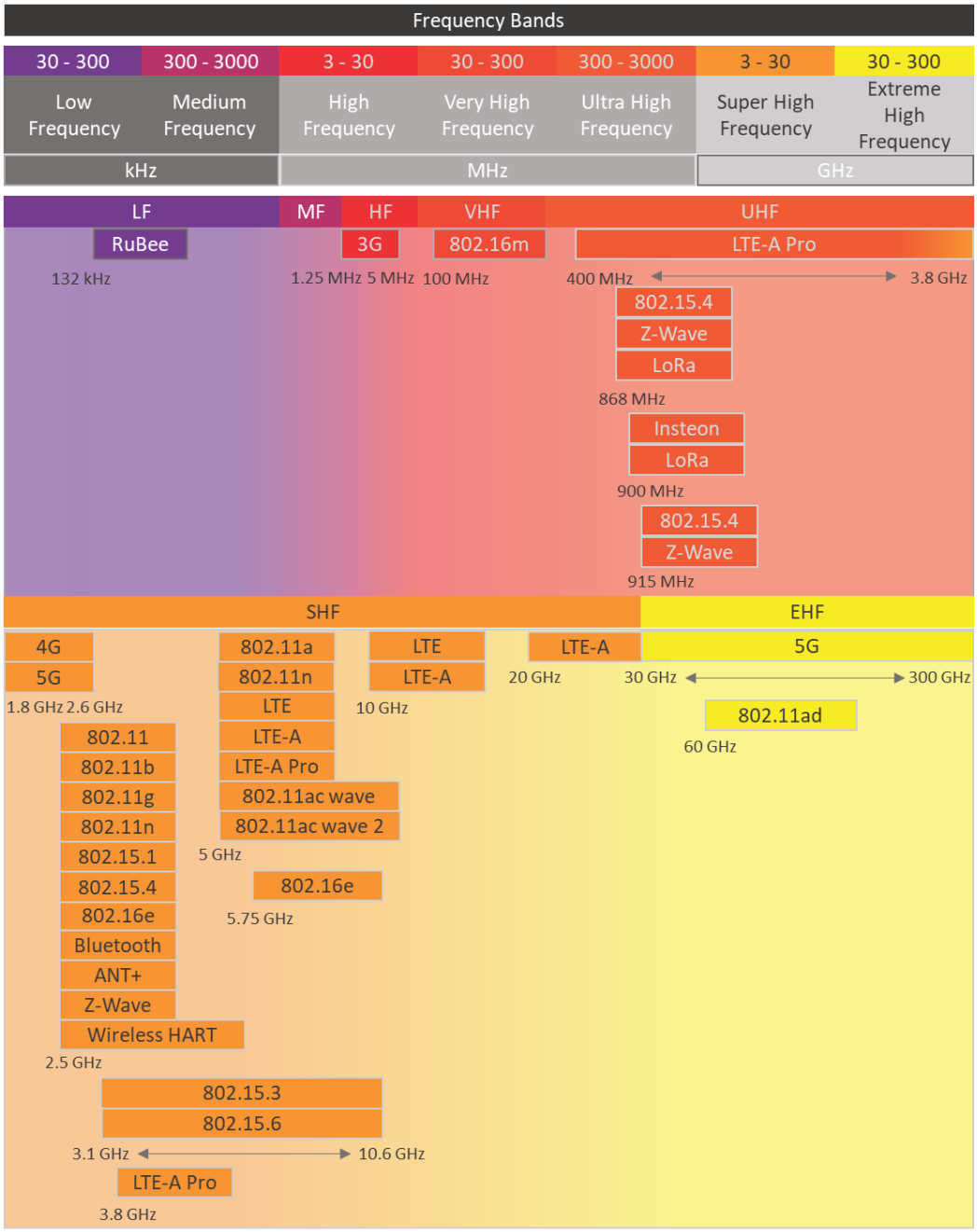

Figure 2.31. Wireless technologies in the frequency spectrum.

The coexistence between IEEE 802.15.4, IEEE 802.11, and BLE considering the distance, packet interval, and channel separation is analyzed in [377]. The comparison of the distance of short and medium ranged technologies is shown in Figure 2.32 and the one for long-ranged technologies is available in Figure 2.33. BLE is more affected by IEEE 802.15.4 interferences for distances around 7 m. IEEE 802.15.4 is more affected by IEEE 802.11 with distances up to 12 m. When the packet interval is varied, BLE networks are more affected by IEEE 802.15.4, being around 5 times less affected by IEEE 802.11. When considering interferer channel separation BLE is again more affected by IEEE 802.15.4 than by IEEE 802.11. An experiment is performed in [378] to determine the effects of interferences between IEEE 802.11 and IEEE 802.15.4. Results show that WLAN technologies can interfere greatly with ZigBee and interferences created by ZigBee devices are barely noticeable to WLAN technologies. They suggest a 7 MHz offset between operational frequencies in order to avoid interferences. Authors in [379] propose an adaptive radio channel allocation scheme that improves the coexistence between IEEE 802.11 and IEEE 802.15.4. Reaching between 97% and 86% of success rate. Employing multiple channels is considered in [380] in order to overcome interference and obtain a higher performance.

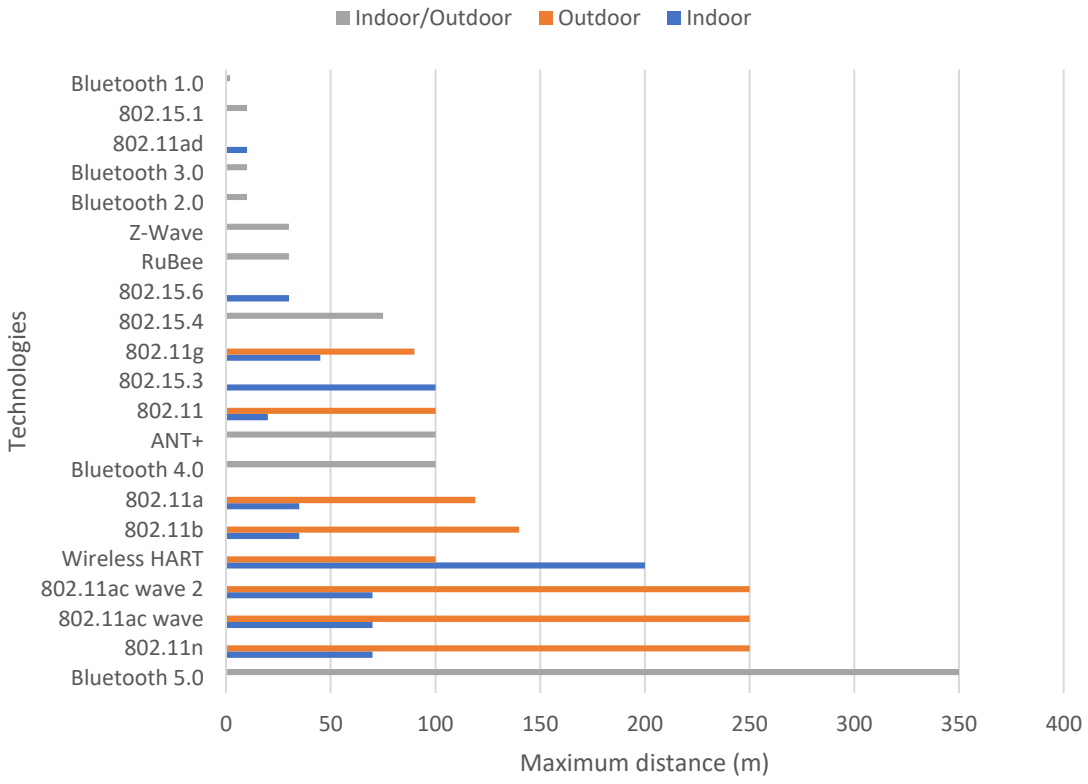

Figure 2.32. Maximum distance for short and medium ranged technologies.

Figure 2.33. Maximum distance for long-ranged technologies.

A study of the co-existence between IEEE 802.11 and IEEE 802.16 was performed in [381]. Results show only in the scenario with 0 dB energy threshold and high connectivity, IEEE 802.16 technologies are unaffected. Otherwise, IEEE 802.11 and IEEE 802.16 coexistence suffers when utilizing the same channel. The interferences between IEEE 802.11 and IEEE 802.16 result in just a 40% of available capacity in the simulations performed in [382]. They also propose a coexistence algorithm that increases channel utilization up to 20% providing fairness among both technologies. Another solution is presented in [383] where authors employ the Common Spectrum Coordination Channel (CSCC) etiquette protocol to reduce interference between IEEE 802.11 and IEEE 802.16 technologies sharing the 2,4 GHz ISM band. Results also show that CSCC can solve the hidden-receiver problem and improve system throughput.

As data traffic increases cellular networks are considering employing unlicensed bands to provide multimedia services, specifically the 5 GHz frequency band. However, although this band is not as highly used as the 2,4 GHz ISM band, LTE-U (Long-Term Evolution – Unlicensed) technologies employing the 5GHz band may be faced by interferences caused by WiFi. The results provided by [384] show that LTE-U can obtain high throughput for small cell users while allowing WiFi networks to perform well. The coexistence between WiFi and LTE is also studied by [385]. They perform several simulations considering WiFi, Licensed-Assisted Access (LAA), Time Division Duplexing (TDD), and LTE Uplink (LTE-UL). When operating in the same frequency band, results show WiFi has higher performance than LAA. They also conclude that some configurations of LTE TDD and LTE UL can improve WiFi performance at the cost of slightly reducing LAA performance.

2.6.12. Future Challenges of IoT Irrigation Systems

The IoUT is a new view of the IoT [57]. It consists of deploying both underground and above ground IoT devices that communicate among themselves with underground-underground, underground-above ground, and above ground-above ground communication. It is especially useful and applicable to irrigation and precision agriculture IoT systems as the devices would not be impeding the work of machines and farmers and it would reduce the amount of physical damage the nodes deployed on the fields may receive. Although WiFi surprisingly allows underground-above ground communication in short distances and depths above 30 cm [386], it would be necessary to study the performance of other existing protocols or even the creation of a new protocol that employs lower frequency bands to transmit the information through the soil medium.

The use of LoRa is increasing for irrigation and precision agriculture applications due to its long-range, which allows wireless communication to remote fields. However, the advances in 5G may lead to a decrease in the interest in LoRa technology. On the one hand, if the designed irrigation system produces lower amounts of data, as these types of systems present low variability in the data, LoRa presents itself as a very good solution. However, on the other hand, for IoT systems that require the transmission of large amounts of data, 5G would solve the problem of the limited amount of data that LoRa can transmit. Considering these aspects, a possible future is the use of LoRa and 5G hybrid wireless networks to attempt in satisfying those needs [387].

There are diverse opinions on the existence and effects of climate change on earth. However, there is no doubt that many governments, companies, and the citizens themselves are increasing their awareness regarding sustainable consumption. This not only affects their view on the energy consumption of IoT systems for irrigation but also, the origin of the components of the devices and the impact of IoT devices on the environment and the fauna of the area where they are deployed. Therefore, the reduction in energy consumption and the use of alternative powering methods will continue to be a research trend. Furthermore, it may be a challenge to find new materials that are weather-resistant and do not increase severely the cost of the devices, but the use of recyclable materials in some of the elements of the IoT devices is to be expected [253].

As it has further been commented in Subsection 2.6.1, blockchain and AI will be incorporated into most IoT services [292], including those aimed at irrigation and precision agriculture. These technologies provide not only increased security but also optimization to the management of the IoT systems. This will lead to an increased understanding of the crops and a faster way to characterize genetically modified crops and the effects of new fertilizers and pesticides. Furthermore, it will aid in optimizing and reducing water consumption and improving the new mechanisms that are being proposed to determine if treated wastewater can be used for irrigation and which crops can be irrigated with wastewater depending on its composition.

Lastly, farmers usually have a very small profit and thus, these IoT systems may not be affordable to them. Therefore, the cost of IoT devices and the overall system

implementation should have a decreasing tendency for these types of systems to have a commercial future.

2.7 Conclusion

In this chapter, the state of the art on IoT irrigation systems for precision agriculture. The most monitored parameters to characterize water quality for irrigation, soil, and weather conditions have been identified. The utilized sensors, actuators, wireless technologies for communication, protocols, and the challenges of deploying WSNs on these environments have been presented. Moreover, the current trends and challenges on the implementation of IoT systems for irrigation and crop management have been examined as well.

After the in-depth analysis of the existing works, the proposed solution of this thesis will be presented in the following chapters.

Chapter 3

Design of an Architecture for Irrigation

3.1 Introduction

In this chapter, the proposal of an architecture for water quality monitoring and field monitoring intended for irrigation is presented. The architecture contemplates a Canal area with groups of water monitoring nodes, a Field area with groups of field monitoring nodes and a meteorology monitoring node, and an Urban area where the gateway is located. Moreover, the topology considers WiFi clusters that obtain the data from the fields and the water channels and transmits it over a multi-hop LoRa wireless network to the gateway by utilizing a WiFi-LoRa bridge. The node sensors for each area are described as well. Then, the operation algorithms of the system are presented. Lastly, the irrigation algorithm that determines the irrigation requirements of the crop is presented.

3.2 Architecture description

The architecture for a wastewater treatment and field monitoring system intended for irrigation is presented in this subsection.

3.2.1 Areas and elements of the architecture

The disposition of the area and the distribution of each of the zones we have identified are presented in Figure 3.1. As shown in Figure 3.1, we identify several urban areas, a canal area, and the fields. These areas communicate using wireless technologies. The wastewater disposed of by the population inhabiting the urban areas is transported to a purification station before being released to the irrigation canals. However, the quality of the resulting water may not be optimal and non-treated waters and different contaminants may worsen the quality of the water before reaching its destined field. Thus, an in-situ water purification system is needed to ensure the quality and the healthiness of the produce.

In Urban Area 0, the gateway will establish a wired connection to transmit the data to the data center for storage and data analysis. We have chosen cabled communication because the performance of the data transmission is better, and the urbanized area allows easy access to the infrastructure of the service provider. The data that is received with information from the different nodes will be treated and analyzed to respond with appropriate measures in our system. Lastly, the adopted measures will be forwarded to the actuator nodes to let the contaminated water go through the biosorption process. The Canal area designates the zones where the irrigation canals are located. Auxiliary canals connecting to the principal one have been designed in a comb-shaped structure to perform the biosorption process. Then, the decontaminated water would be released again to the main canal ready for its use in irrigation. Lastly, at the Field area, soil and meteorological parameters are monitored to determine the necessary amount of irrigation.

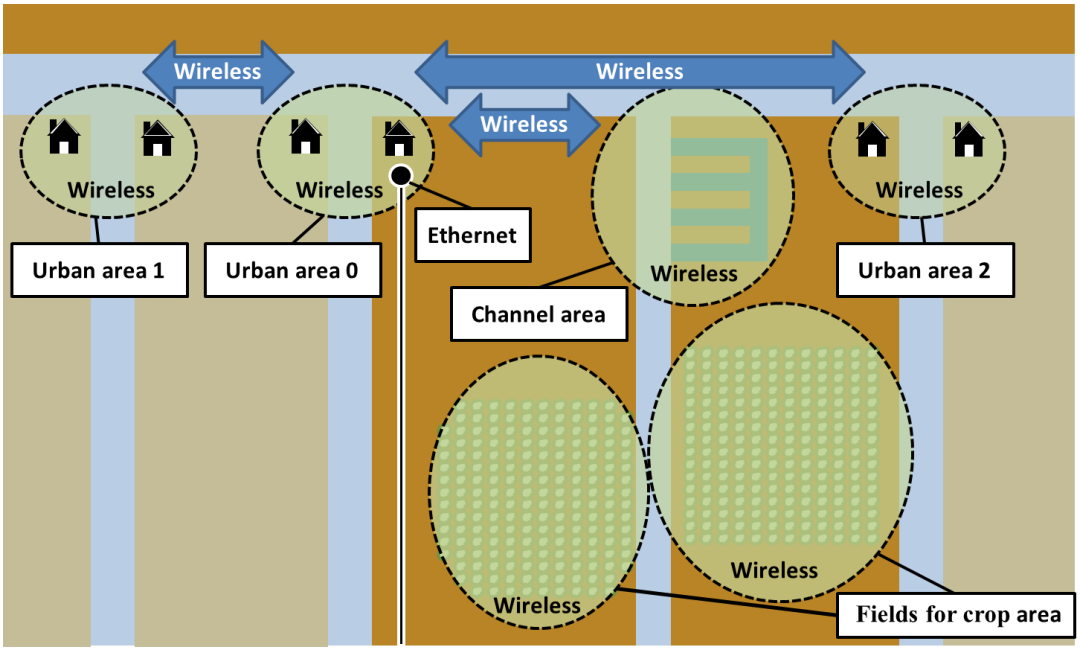

Figure 3.1. Deployment of node areas.

The detailed view of the Canal area is provided in Figure 3.2. This is the area where the different types of nodes will be deployed. Three models of sensor nodes can be identified. The Sensor nodes are comprised of a microcontroller and the different sensors that allow quantifying the contamination in the water. The actuator nodes are comprised of a microcontroller and the necessary actuators to open and close the gates to return the water to the main canal. The Cluster head is the node that receives the information from the rest of the nodes and forwards it to the gateway situated in Urban area 0.

The auxiliary canals that contain the biosorption materials are deployed in a comb-shape. As it can be seen in Figure 3.2, all the auxiliary canals have the same structure and are connected to each other for the water to go through the biosorption process several times if necessary. In order to determine if the water from the canal needs to be processed in the biosorption canals, the sensor nodes check for water pollution at the entrance of the canal. When contaminants are detected, the gates are opened to let the water flow into the biosorption canals. Once inside the biosorption canals, the water is treated to remove the contaminants. At the end of the auxiliary canal, another set of sensor nodes monitor the water to decide if the water can be returned to the main canal or if it needs to go through the biosorption process again. The actuator nodes are connected to the lock-gates that allow regulating the passage of the water flow.

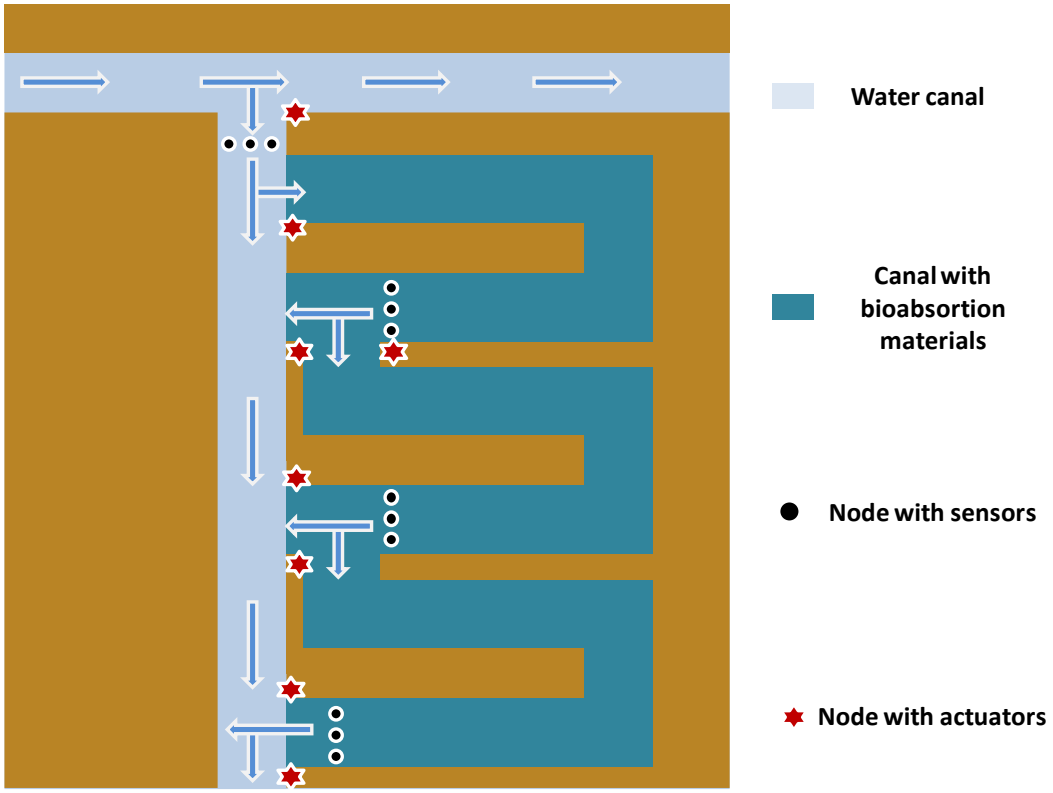

Figure 3.2. Example of canal zone in detail.

The Field area is depicted in Figure 3.3. The fields are divided into sectors and each sector has a deployment of a soil sensing cluster comprised of two Soil Sensing Nodes and a soil Sensing Cluster Head that aggregates the data from the soul sensing nodes and transmits it to the Aggregator node. The moisture sensors of the Soil Sensing Nodes and the Soil Sensing Cluster Head are deployed at different depths to determine if the water has reached the needed depth or if there is water stress. The Soil Sensing Cluster Head is placed at the same spot as the dripper with its sensors located on the vertical of the dripper [316]. The Soil Sensing Nodes are located at the mid-point between to drippers, which is at a distance of 45 cm from the dripper. All the Soil Sensing Nodes forward the data to the Aggregator node. This node aggregates the data from all the sectors to forward it to the gateway in the Urban Area. Lastly, the actuator node controls the opening of the gates and the water flow.

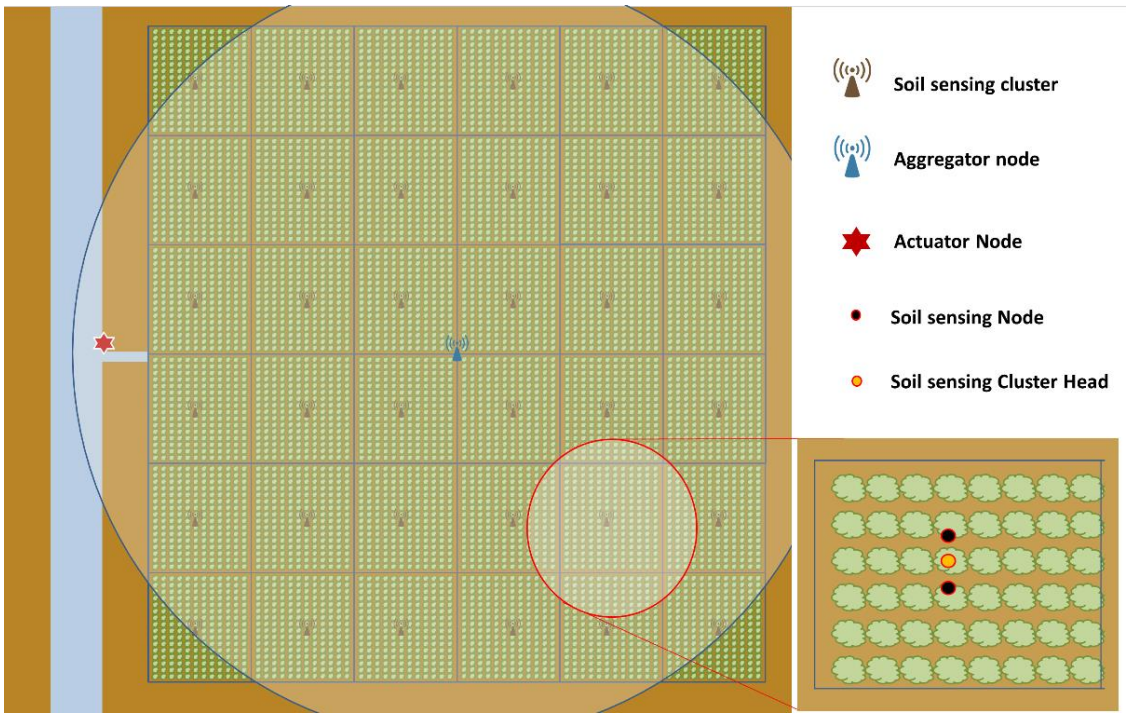

Figure 3.3. Example of Field zone in detail.

In this proposal, there are different types of nodes that can be grouped into sensor nodes and actuator nodes. In the sensor nodes, different physical sensors will be connected so as to allow, in some cases, to study the need for irrigation in fields so that the crop develops properly and does not get lost and, in other cases, to detect the quality of the water transported in irrigation water canals and be able to study and control its debugging. The sensor nodes will be distributed forming groups of three nodes. Three nodes are utilized for reliability reasons. If any of the measures estimated in a group is not validated by at least two of the group's nodes, it is not considered valid. The actuator nodes will be connected to the gates to open or close the water passage in a canal. The

nodes are strategically placed, to maximize the impact of the measures taken in the studied area. At the same time, they must be located so that they can be connected correctly through a wireless transmission.

The proposed architecture, formed by three layers, being Nodes Sensors & Actuators, Storage & Activation, and Artificial Intelligence, is shown in Figure 3.4. In the Nodes, Sensors & Actuators layer, all the nodes of the network are located. The different sensors that take measures of the water quality are connected to the nodes. Then, the data are periodically forwarded to the data center situated in the upper layer, where the data are stored. Furthermore, the actuators are connected to the nodes that are located at the gates of the canals so that the appropriate actions that have been decided in the higher layers are performed. On the other hand, the Storage & Activation layer hosts the devices where the information received from all the sensors is stored. Furthermore, this layer also hosts the system that allows for sending orders to the actuators so as to carry out the actions established by the decision-making process that is performed in the upper layer. Lastly, the systems that allow for processing the data that were stored in the lower layer are located in the Artificial Intelligence layer. This layer oversees the decision-making process whose result will be sent to the action functionality in the lower layer.

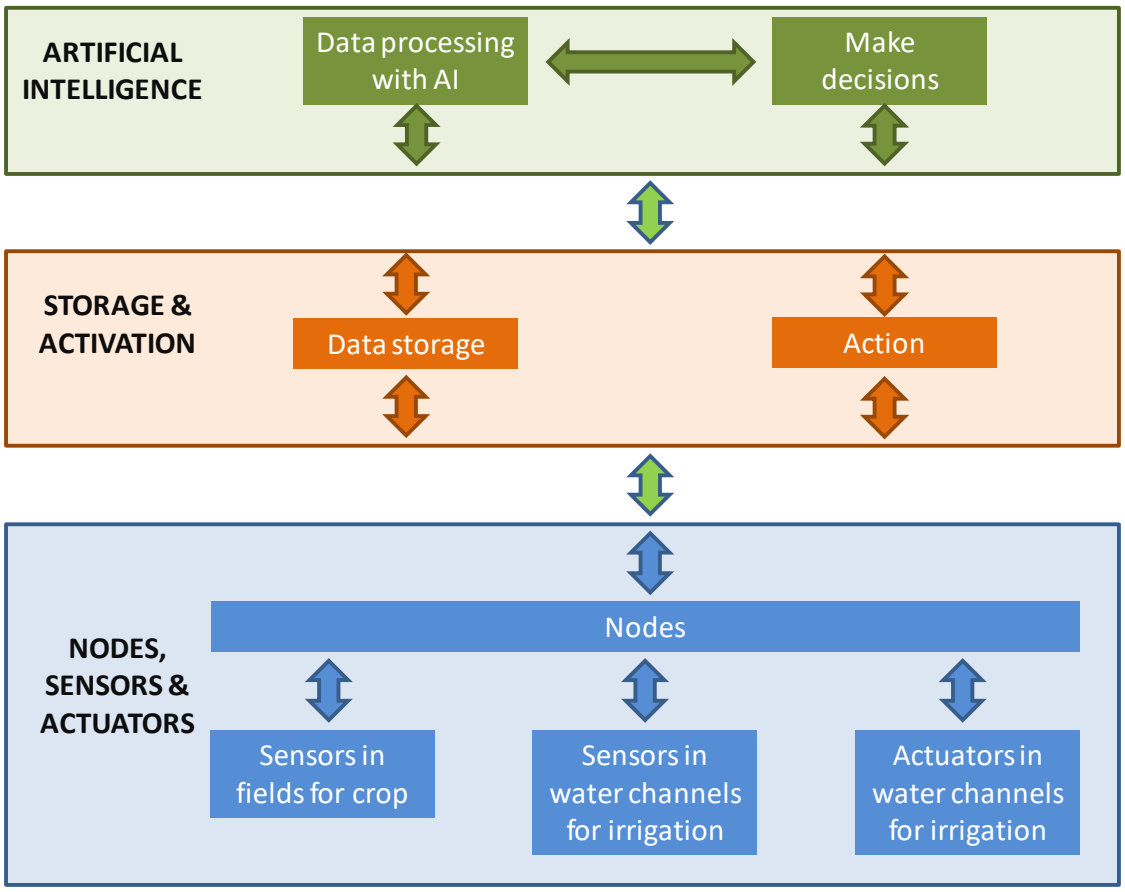

Figure 3.4. Proposed architecture.

3.2.2 Topology

In this subsection, we will detail the proposed topology for our wastewater purification system for irrigation purposes. The topology of the system is presented in Figure 3.5. The near-range communication is performed using WiFi and the long-range communication is performed utilizing LoRa. Due to the low amount of data that needs to be transmitted, to obtain the highest possible WiFi coverage and to increase the robustness, the nodes can adjust the WiFi connection to 2 Mbps. On the other hand, the AP can be set to 54 Mbps as it needs to manage the messages from several nodes. In the case the WiFi nodes do not need high distances, other WiFi settings can be utilized. The communication between the data center and the gateway is performed using a wired connection. As it can be seen, the system presents a star topology. This is due to the need of implementing a low-cost system where the number of nodes that can be employed is limited. In a star-topology of LoRa Nodes, there can be collisions and thus, losses due to all the nodes emitting in the same channel. As the system does not require performing in real-time, a delay can be introduced to avoid collisions. Furthermore, as a LoRa node can send the data to the data center through multiple gateways, more gateways would be installed if necessary.

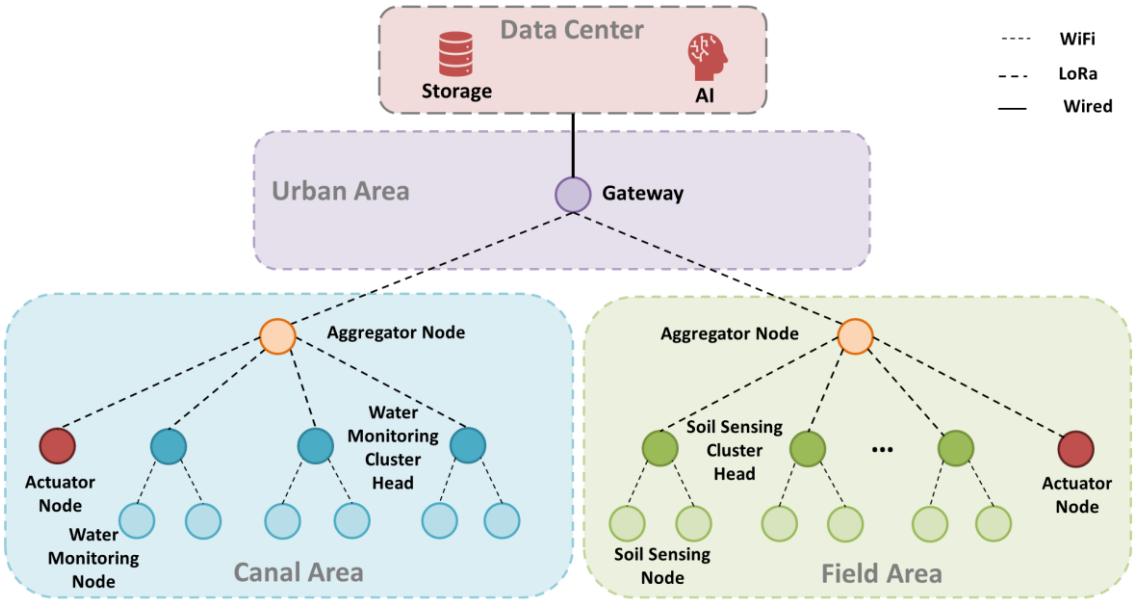

Figure 3.5. Topology of the system.

The system is comprised of the following elements:

- *Water Monitoring Node:* This node is comprised of an embedded board, an SD card module with an SD card for data storage, a turbidity sensor, a

salinity sensor, an oil sensor, a battery, and a solar panel for energy harvesting. This node communicates with the Water Monitoring CH using WiFi.

- *Water Monitoring CH:* This node has the same elements as the Water Monitoring Node. However, this node has more capacity for data storage and processing as it receives the data from the Water Monitoring Node and a LoRa transceiver. It communicates with both the Water Monitoring Node and the Aggregator Node of the Canal Area.

- *Soil Sensing Node:* This node is comprised of an embedded board, a soil humidity sensor, a soil temperature sensor, an SD module, an SD card, and a solar panel. This node monitoring the state of the soil and forwards the data to calculate the water requirements of the trees.

- *Soil Sensing CH:* This node has the same elements as the Soil Sensing Node with more storage and processing capacity as it processes the data from the Soil Sensing Nodes and a LoRa transceiver. It communicates with the Soil Sensing Nodes through WiFi and the Meteorology Monitoring Aggregator Node through LoRa.

- *Aggregator Node:* The Aggregator Node is a LoRa node with high processing capabilities and data storage resources to manage and aggregate the data received from all the sensors. It also has an energy-harvesting module to ensure it has enough energy to operate. Using a LoRa node to relay data in a LoRa network has been studied in works such as [317-319]. Adapting the LoRa SF and BW settings according to the data that needs to be transmitted can be done.

- *Meteorology Monitoring Aggregator Node:* This node adds functionalities to the Aggregator Node described before. It has an air temperature and humidity sensor, a light sensor, a rain sensor, and a wind sensor to provide the Data Center with the necessary data to calculate the water requirements of the fields. It communicates with the CH Nodes, the Actuator Nodes, and the Gateway using LoRa.

- *Gateway:* It is a commercial LoRa gateway connected to the internet through an Ethernet connection.

- *Data Center:* The Data Center can be either a cloud service of a service provider or a private server that performs storage and data analysis to determine the water requirements of the fields. The results of the data analysis are then forwarded to the deployed nodes and the users.

- *Farmer User:* This user is the owner or the manager of the fields. Thus, the Farmer User needs to know the problems of the nodes on the field area to replace them when necessary. Furthermore, the Farmer User needs to know the water requirements of the fields as well.

- *Hydrographic Confederation User:* This user is the owner or the manager of the canals. They are responsible for replacing the broken nodes in the canal area and they can only access the information of the quality of the water and the state of the actuators of the canal area.

The protocol Stack of the system is presented in Figure 3.6. The Cluster Head is the node that acts as a bridge between the elements of the network that utilize WiFi and the elements that use LoRa. Regarding the LoRa network, LoRa™ defines the Physical Layer. Our proposed Heterogeneous Communication Protocol (HCP) is part of the Application Layer. Regarding the WiFi network, HCP is encapsulated in UDP.

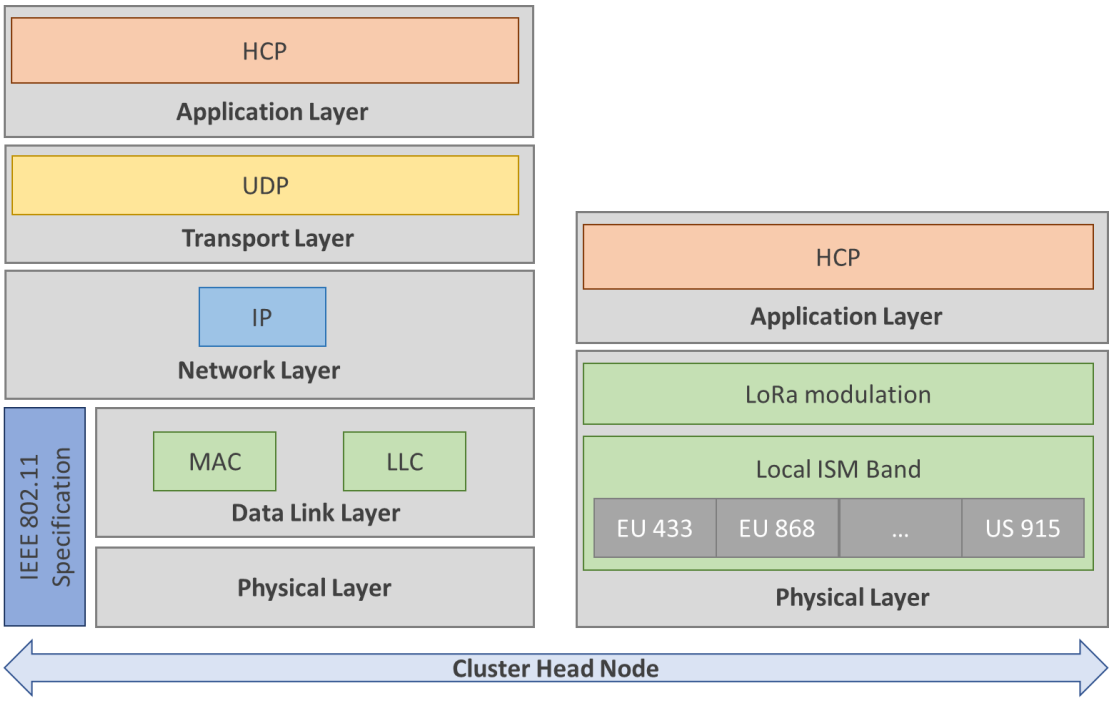

Figure 3.6. Protocol Stack.

3.2.3 Alternative architectures for specific needs

Due to specific needs of the farmers, alternative architectures may be necessary to address the functionalities that are required. In this subsection, the architecture designs to provide other functionalities are described.

3.2.3.1 WSN for monitoring numerous trees

When the deployment of numerous sensor nodes is necessary, utilizing wireless technologies such as LoRa may present a problem as there can be collisions among the packets transmitted by all the nodes within the coverage area. Therefore, mesh networks of nodes utilizing medium-range technologies such as WiFi would be a possible solution to the requirement of monitoring a great number of fruit trees.

The proposed system uses the information collected by the sensors of a WSN. The data from the sensor network will be sent through a WMN formed by APs located in environments where irrigation canals exist in urban and rural areas. In addition, in a centralized location, the network devices that allow the WAN connection to send the collected dataset to an external location will be installed, where it will be stored and processed. Also, in that location, equipment will be deployed to automatically respond to alarms that have been previously detected and where the action that must be carried out in response is known. The utilized communication technology is that of device-to-device (D2D) and device-to-machine (D2M). The included features are:

- Independent of communication technology.
- Supports different manufacturers.
- Adaptable to different physical environments.
- Low power consumption. We avoid the need of the nodes of an external power supply.
- Low bandwidth consumption.
- Scalable, supporting the aggregation of new nodes.

In the proposed architecture (See Figure 3.7), each sensor node gathers measurements from each one of the sensors that it has connected. All these data will be used later in the decision algorithms. The sensor nodes are installed in two areas, mainly in the water canals for irrigation and in the crop fields. The deployment of the sensor nodes in the water canals is that detailed in the previous section. Whereas the nodes in the field area are placed in a manner of one node per tree that is monitored. When a sensor node generates an alert, due to the exceeding of a threshold value of one or more of the parameters, the measurements of all the parameters of that node are sent at that moment. The information will be sent from a single device to another device. The algorithms of the nodes allow reducing the number of forwarded messages to a minimum to obtain high energy savings.

The WSN nodes collect information from the sensors connected to each one of them. The collected data will be stored in an SD card that will be included in the node hardware. In addition, the data will be sent periodically, through a WAN connection, to the place where they will be stored and processed, using AI. The AI uses the processed information to know what is happening and to use it in the decision algorithms. The actions that must be taken, as a result of the application of AI, are sent back to the WSN so that they receive nodes with actuators and carry out the appropriate actions. Previously, different parameters and thresholds that allow an optimal functioning of the

system were defined. Depending on the type of crop and the types of area, different corpus are created for different crops. For example, a corpus is defined for growing citrus, another for rice, or another for vegetables. Once the nodes have been identified and the different sensors and actuators labeled, information will begin to be collected. After a training phase, a casuistic series is obtained. Using a decision algorithm and rules that include all the possible cases, we determine the actions that the actuators must carry out. The system will be able to predict actions before receiving specific alarms from the nodes indicating an anomalous situation.

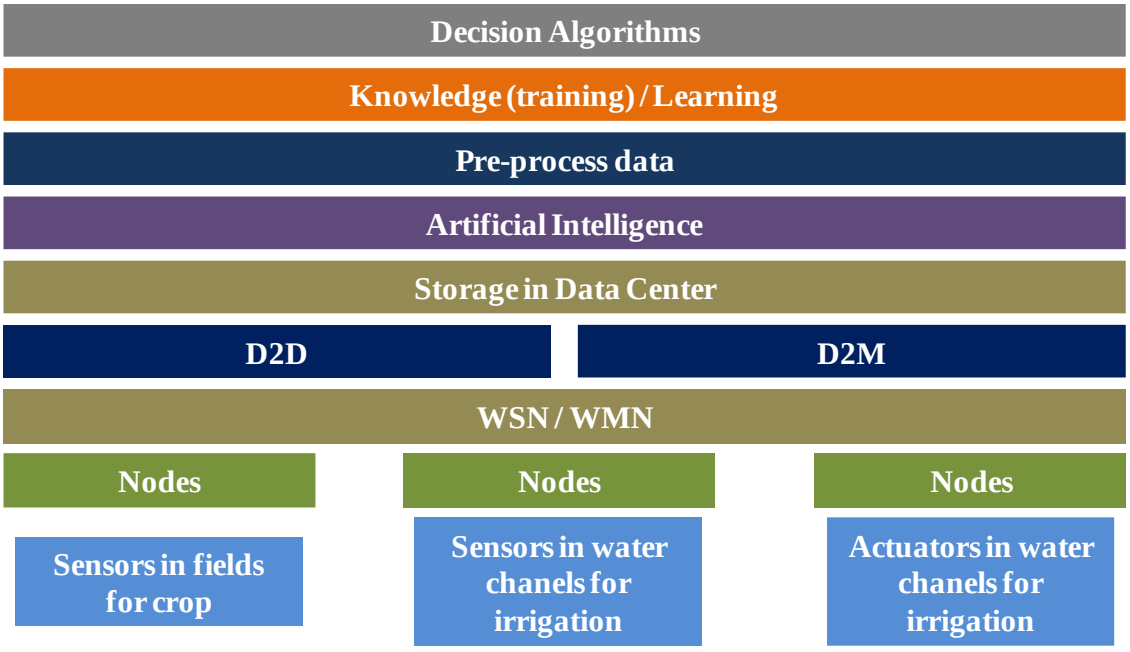

Figure 3.7. Proposed Architecture.

Figure 3.8 shows the 4 principal phases of the PA system, which include sensor nodes, data storing, AI, and actuator nodes. Firstly, the data acquisition from all the distributed sensor nodes is performed. Periodically, the data acquired in the previous phase is stored on the remote storing servers. Then, the different characteristics of the data such as location, date, time, humidity, temperature, and turbidity are extracted so as to be processed by applying the decision rules designed by experts. The processed information will be utilized to obtain models and predictions and its results will be stored increasing our database. Lastly, the corresponding actions are performed on the actuator nodes according to the obtained predictions.

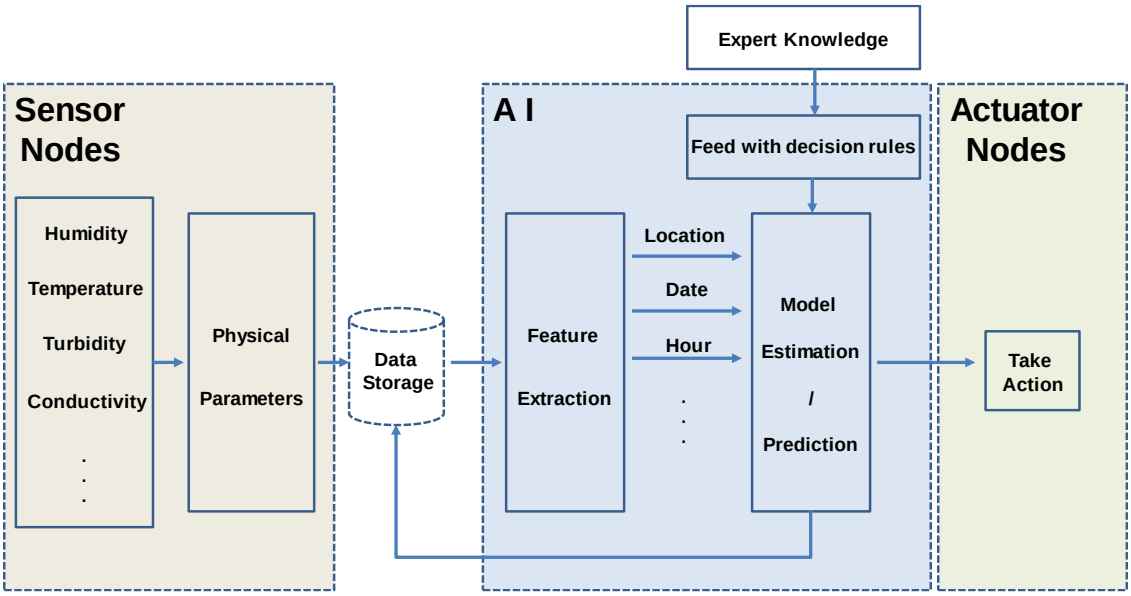

Figure 3.8. Phases of our system.

Figure 3.9 shows the flow of the data. Initially, the data is collected by the physical sensors. The algorithms will process the data and make the appropriate decisions based on the previously created rules. Finally, the action to be carried out will be decided. It will be sent to the actuators so that it is carried out properly.

IEEE 802.11 technology is utilized. Due to the power consumption of IEEE 802.11 technology, the published recommendations for WLAN in [320] are considered. To communicate the groups of nodes, use APs are used, which will allow us to extend the distance to which the nodes can be connected and, to extend the size of the network as well since there will be deployed as many APs as necessary for the transmissions to be carried out correctly. Therefore, a WMN is established.

In case of being in a land with hills or mountains, the AP will be deployed in the highest areas so that the coverage will be maximum while using the least number of devices. Although, tentatively, most of the areas where they are going to be deployed are flat. An example of the location of an AP is shown in Figure 3.10, it can be seen that the AP is placed in a centralized position from which it makes a circular coverage of 100 meters. As in a plantation of orange trees, the distance between the trees is 4x6 meters, in an area of 200x200 meters that is the one represented in the figure, there are 1600 planted trees. To cover all the trees, the use of more APs is needed, but in this way, 1250 nodes can be theoretically connected.

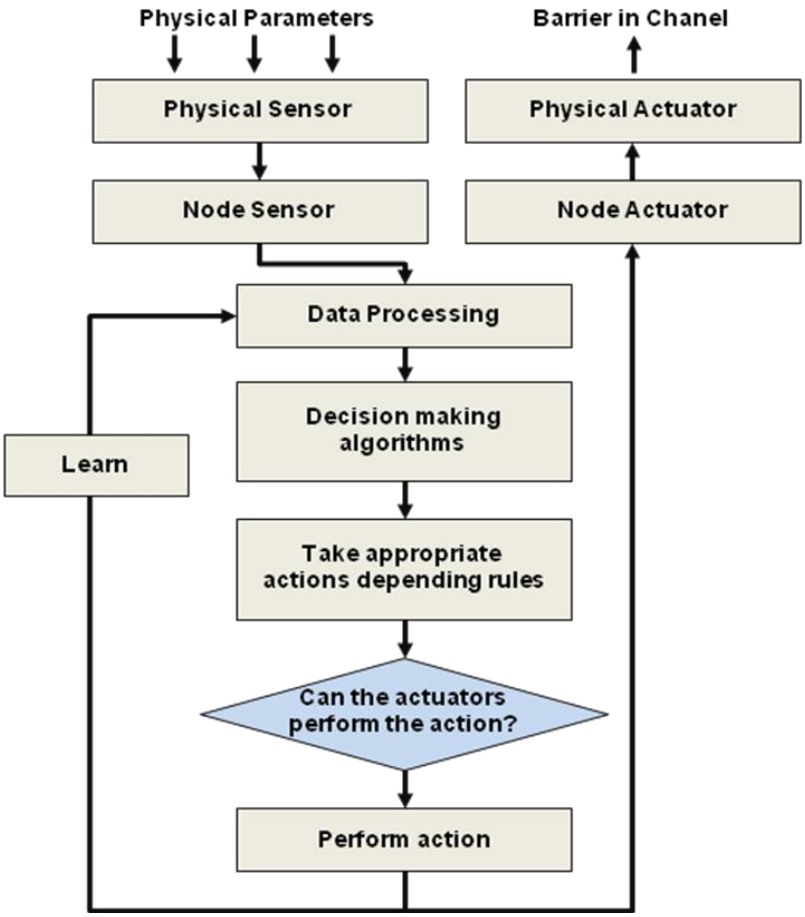

Figure 3.9. Data Flow.

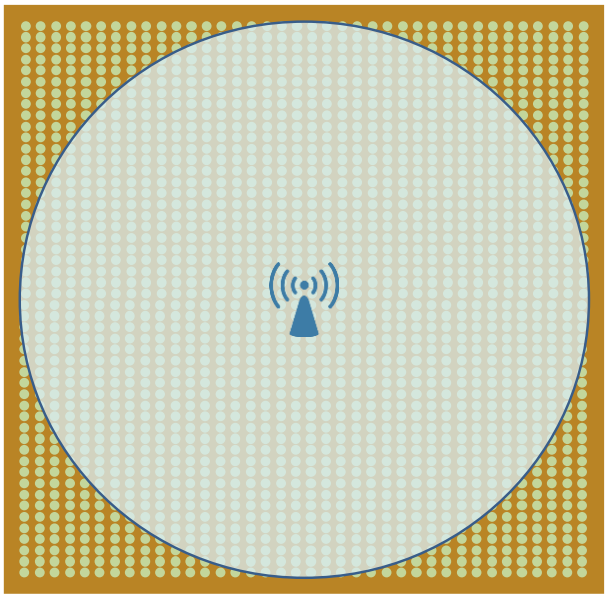

Figure 3.10. AP coverage in field of oranges of 200 x 200 meters.

All groups of sensor nodes will connect wirelessly with a group of sensors located in an urban area, which we will call the "Urban area 0" group. To achieve this purpose, APs with DD-WRT (DresDren-Wireless RouTer) [321] firmware will be implemented. It is an open source firmware based on Linux that can be used with embedded systems and routers that provides multiple functionalities for security, QoS, bridging, and the use of SD-cards. Thanks to the firmware, a Wireless Distribution System (WDS) is activated. The WDS, working in repeater mode, will allow the APs to communicate with other APs (forming the WMN) and with nodes simultaneously.

The group "Urban area 0", has as a distinguishing feature from the rest of the nodes that, being in an urban area, it can receive a power supply and establish a permanent wired or wireless WAN connection. The rest of the groups of nodes will send the measures to this special group so that they are forwarded to a remote location where our data storage systems and the equipment necessary to perform their treatment through AI will be located.

Once the AI system makes a decision regarding the action that must be carried out, it will store the adopted measure and send it at the same time to the "Urban area 0" group using the WAN connection. Together with this group of nodes and the network devices that allow us to connect to the WAN network, a team will be implemented that will allow us to store all the actions that the AI has already dealt with, with the appropriate response. So, when an alarm is generated in any group of sensors, when exceeding the thresholds allowed in any of the parameters studied, if the same event was previously produced, the associated action will be carried out immediately employing fog computing so as to avoid unnecessary latencies. Lastly, from the central node of the "Urban area 0" group, the order of the action will be sent to the affected node or actuating nodes, so that they carry out the recommended action.

3.2.3.2 Architecture for remote fields with cellular connection

The use of cellular technologies can be considered as well for field monitoring in PA systems. Figure 3.11 shows the four layers that form the proposed architecture where the ESP32 nodes are located. The ESP32 nodes are located in the lower layer, which have the necessary sensors connected to them to obtain the information from the environment. The characteristics of the utilized nodes and their antenna are depicted in the specifications of the nodes in [322, 323]. These nodes perform the transmission using the IEEE 802.11 standard, with a maximum data rate of 150 Mbps in the 2.4 GHz band. Their low cost makes their use in agricultural systems affordable to farmers. Furthermore, power consumption can be optimized by programming the nodes to go to sleep mode when measures are not being taken. Moreover, these applications do not usually record video or transmit data in real-time as variations in the state of the crops are slow, resulting in a reduced amount of data for transmission [28]. In the immediate upper layer, a network of wireless APs is available through which the data is sent to an AP that acts as a gateway to the Internet. That gateway receives the data from the node

and uses 3G to forward the data to the database. The Internet is in the next layer. Finally, the upper layer is where the data is stored, and its consultation and treatment of the obtained data is performed. The farmers can access the data through a web or a mobile interface.

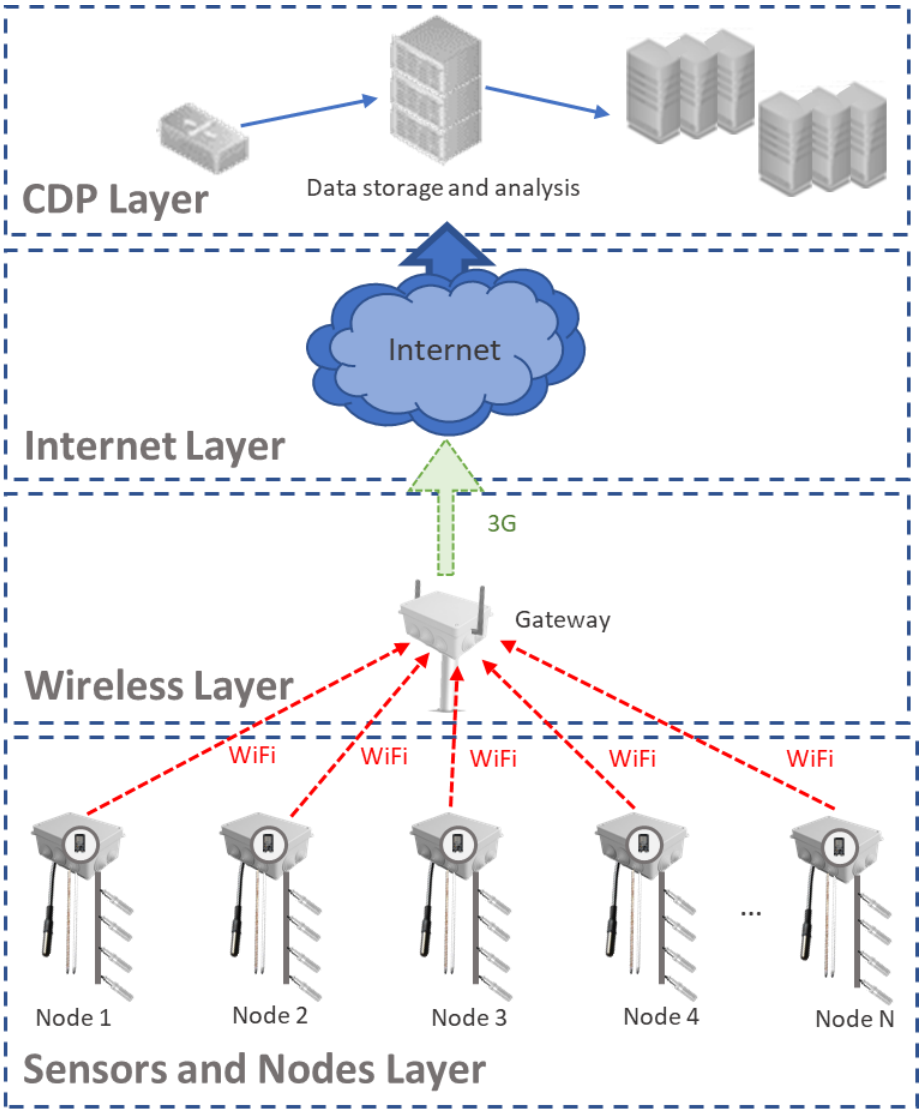

Figure 3.11. Architecture.

3.2.3.3 Architecture for IoUT functionalities

In this section, the proposed architecture for an IoUT solution for agriculture is presented. Figure 3.12 shows the different levels of the proposed architecture. It is formed by four levels: Nodes and Sensors, Wireless Network, Internet, Data Center, and Artificial Intelligence.

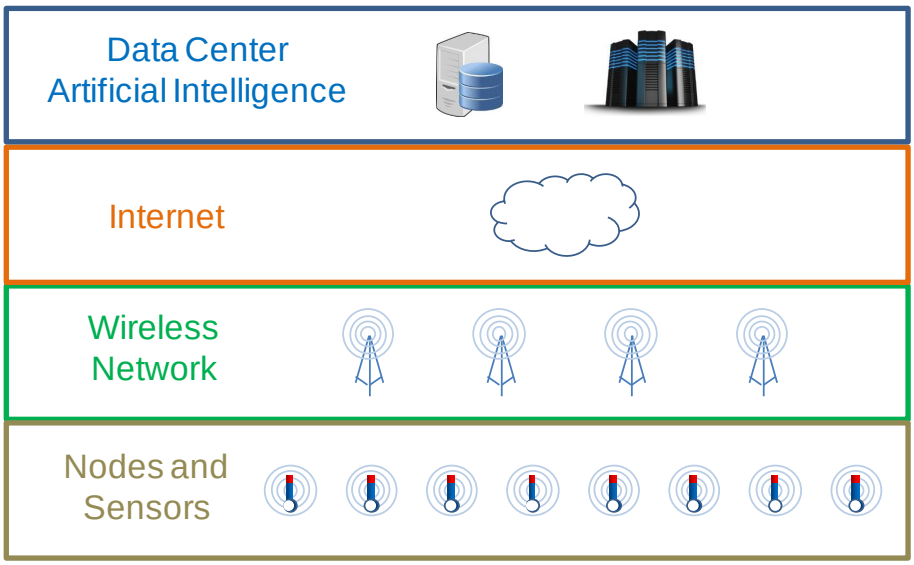

Figure 3.12. Architecture for IoUT.

The nodes are located in the lower level with the sensors connected to them. These sensors will obtain all the necessary information of the crops for a later decision-making process, in which Artificial Intelligence is used in order to perform smart agriculture. The level above the first one is the level of the wireless network. At this level, the transmission of data, obtained in the fields of agriculture through the sensors by using a wireless network, is performed. At this level, the APs are located, which collect the signals sent by the nodes and transmit them until they reach a gateway device. The gateway allows the connection through the Internet to a remote location. The next level is the Internet, where the obtained data is transmitted using an Internet Provider connection to the location where they are stored. This connection can be achieved using different technologies, such as DSL (Digital Subscriber Line), wireless technology, and 3G / 4G mobile data. We select the one that fits our requirements with the lowest costs depending on the location of the crops. Finally, in the upper layer, we locate our Data Processing Center that employs Artificial Intelligence. At this level, the information storage and treatment systems are located. In this location, the data will be stored so that it can be retrieved at any time and then be processed. With this data, the farmers and engineers can obtain relevant information for decision making.

3.2.3.4 Architecture for the use of drones for data acquisition

The architecture of the precision agriculture scenario is divided into four layers, which are: the Sensor Node Layer, the Drone Layer, the Internet Layer, and the Data Center Layer. Figure 3.13 shows the different layers.

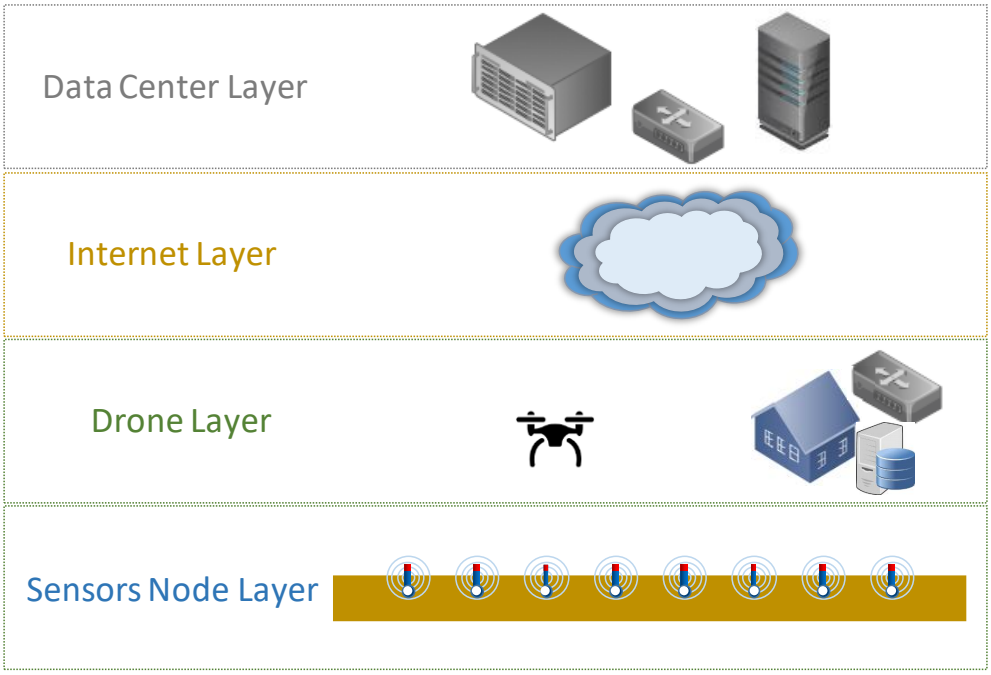

Figure 3.13. Architecture layers.

The Sensors Node Layer is the bottom layer. All the sensor nodes deployed in the crops are located in this layer. The layer immediately above is the Drone Layer. It is comprised of the remote sensing drone that is responsible for obtaining images of the crops and collect the information stored by the nodes through its wireless interface, the location where the drone has its base station, the IT equipment where the information that the drone has collected during its flight is stored, and the network devices that allow us to connect to the Internet. The connection to the Internet is performed by employing a Service Provider. Depending on the location of the crop fields, the technology used to connect to the Internet may vary, choosing among cable or wireless technologies to establish the connections. The following layer is the Internet. The Internet is accessed through the Operator to send all the acquired data to a remote location, where the information will be processed. The connection to the remote location is made by establishing a Virtual Private Network (VPN). This way, the data will be protected when crossing the Internet. Finally, the Data Center Layer, where we store the obtained information is located at the remote location. This information can be processed using AI to ensure that decision making is optimal.

3.2.3.5 Architecture for IoT irrigation system with security and management functionalities

In this subsection, an architecture proposal for an IoT irrigation system for irrigation with security and management functionalities is presented. In order to ensure the correct performance of the IoT irrigation system for precision agriculture, the architecture should provide interoperability, scalability, security, availability, and resiliency.

After having carried out an exhaustive study of works presented by other researchers, our architecture proposal is divided into four layers that we define as devices, communication, services, and application, as shown in Figure 3.14. Furthermore, the aspects related to management and security should be treated jointly between the communication and services layers.

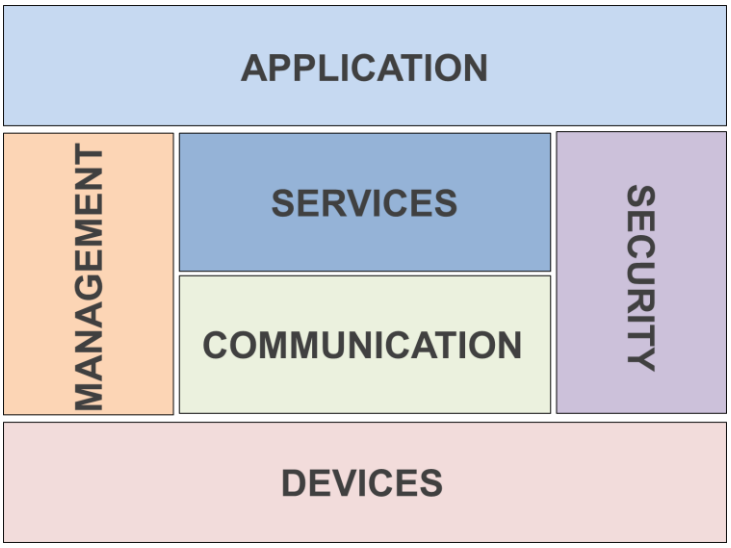

Figure 3.14. Architecture proposal for an IoT irrigation system for agriculture.

The first layer is the Device layer, where all the devices that will perform the functions of detection, monitoring, control, and action are located. We would have four types of nodes. The water monitoring node would monitor water quality to determine if the water is apt for the irrigation of the crops. The soil monitoring node would monitor soil moisture, soil temperature, and other parameters that aid in the irrigation schedule decision process. The weather monitoring node would measure air temperature and humidity, precipitation, luminosity, radiation, and wind parameters so as to aid in the decision-making process. Lastly, the actuator nodes would perform the actions resulting from the decision-making process.

The second layer is the communication layer, comprised of three blocks. The Hop-to-Hop communication block allows defining data link layer technologies and to transmit the frames that contain the data of the device layer. From this block the frames will be sent to the network communication block, to reach the remote locations. The routing function can be assumed in this block in mesh networks, such as 802.15.4 networks. The end-to-end communication block is responsible for delivering the capabilities of the transport and application layers of the TCP/IP model when communication crosses different network environments. Finally, the network communication block is responsible for the communication (routing) between the networks, of the hop-to-hop at end-to-end blocks, using the address, for example, IPv4 and IPv6, and the ID resolution. In addition, it will be responsible for managing the QoS.

The next layer is the services layer, which is comprised of three blocks. The services block includes the IoT services and operability for their discovery and search. The organization block performs the assignment of the services according to the needs of the users or the available resources. At last, in business environments that relate to IoT, the modeling and execution of service block will be invoked from the execution of the applications.

There are two blocks, management, and security, that act on both the previously described communication and services layers. The management block is based on the fault, configuration, accounting, performance, security (FCAPS) model, and framework. This is a model of the ISO (International Organization for Standardization) Telecommunications Management Network [324].

The security block guarantees both the security and privacy of the systems and is comprised of four blocks. The authentication block is responsible for the authentication of users and services. The authorization block manages access control policies. Furthermore, access control decisions will be made based on access control policies. The key exchange & management block is used to achieve secure communications between peers. Finally, the trust & reputation block is responsible for scoring the user and calculating the level of trust of the service.

The last layer is the application layer. It allows users to interact with the IoT system. From this layer, users can receive alarms, visualize the gathered data in real-time, or activate the actuators or actions that have not been programmed automatically.

3.3 Sensor nodes

In this section, the different nodes, sensors, and actuators proposed to collect data from the field and carry out the corresponding actions that allow treating the water are described.

3.3.1 Soil monitoring node

The state of the soil is critical in agriculture. Monitoring known parameters that characterize the soil is key for precision agriculture systems as they are needed to determine the amount of water for the irrigation of the crops and to optimize the production. The available sensors to monitor the characteristics of the soil can perform their measurements through the physical characteristics of the soil or its chemical characteristics. However, chemical sensors are not adequate for these systems as they would require the assistance of a person to clean, calibrate, and perform the measurement. Therefore, a precision agriculture system will usually be comprised of sensors that need low maintenance.

Soil quality depends on several aspects and its degradation is mostly caused by soil compaction, acidification, and salinization. The salinity, acidity, and water holding capacity of the soil are some of the most considered aspects when monitoring the state of the soil but other factors such as nutrient availability, labile and organic carbon, rooting depth, soil structure and texture affect the quality of the soil as well [325].

Most precision agriculture systems focus then on three factors to characterize the soil. The PH of the soil is measured to determine its acidity or alkalinity. Very acid soils can lead to deficiencies in nutrient availability despite the addition of fertilizer. Low PH levels can result in aluminum toxicity leading to poor growth, smaller quantity, and produce size. Moreover, the persistence of herbicides can be affected by the PH levels as well. Lastly, microbial activity can be affected as well leading to unhealthy plant conditions.

Soil humidity is measured to determine if the crops are suffering from water stress due to a lack of water in the soil. High humidity results in root diseases and the waste of irrigation water. On the other hand, low humidity can cause yield loss and even the death of the plant. Furthermore, the movement of the water in the soil determines how the nutrients will reach the plants whether they are added to the irrigation water or through other means. The content of clay, sand, and silt of the soil determines its water holding capacity.

Soil temperature experiments change within the day and throughout the year. Solar radiation and air temperature are determinant factors on the temperature of the soil. Soil temperature can affect the chemical and physical properties of the soil. The PH increases with soil temperatures between 25ºC and 39ºC [326]. The moisture content, salinity, and the structure and aeration of the soil are affected as well. The organisms and the organic matter in the soil are influenced by soil temperature resulting in more soil respiration between temperatures of 10ºC and 28ºC, an increase in the activity of micro-organisms and macro-organisms between temperatures from 10ºC to 24 ºC and the decomposition of the organic matter with temperatures between 2ºC and 38ªC. Furthermore, the water uptake of the plants gets reduced with high soil temperatures and the nutrient uptake decreases with low soil temperatures. Lastly, high soil temperatures lead to an improvement in root growth whereas low soil temperatures result in a decrease in root growth.

The proposed soil monitoring system is presented in Figure 3.15. The data acquisition and transmission are performed with the ESP 32 Devkit v1 node. Although this node is not an industrial node, the low-cost nodes can also be utilized in realistic agricultural environments considering real-time data transmission is not necessary for the proposed system. Furthermore, the node is placed inside a protective box to avoid damage from the weather, animals, or machinery. Utilizing low-cost nodes and sensors in precision agriculture solutions also allow farmers to improve the performance of their crops and optimize resources without investing large amounts of money, which makes the proposed solution more accessible. Temperature is measured with a soil temperature monitoring sensor probe such as the THERM200 [327]. The soil humidity multi-sensor array is comprised of low-cost soil humidity sensors such as the FS200-SHT10 sensor [328] at depths of 20 cm, 30 cm, 40 cm, and 50 cm in a manner similar to that presented

in [329] for the scenario of a sensor buoy. Lastly, a low-cost soil PH sensor is connected to the node to monitor the PH of the soil as the MS02 [330]. The probes are inserted into the soil to gather the measurement. These probes act as a fixing structure to ensure that the box does not move due to meteorological conditions, mainly wind and rain, or due to the pass of fauna. Moreover, due to the general characteristics of citrus orchards, we do not expect high soils erosion, which might alter the location of the sensor or the generation of disturbances in our measures.

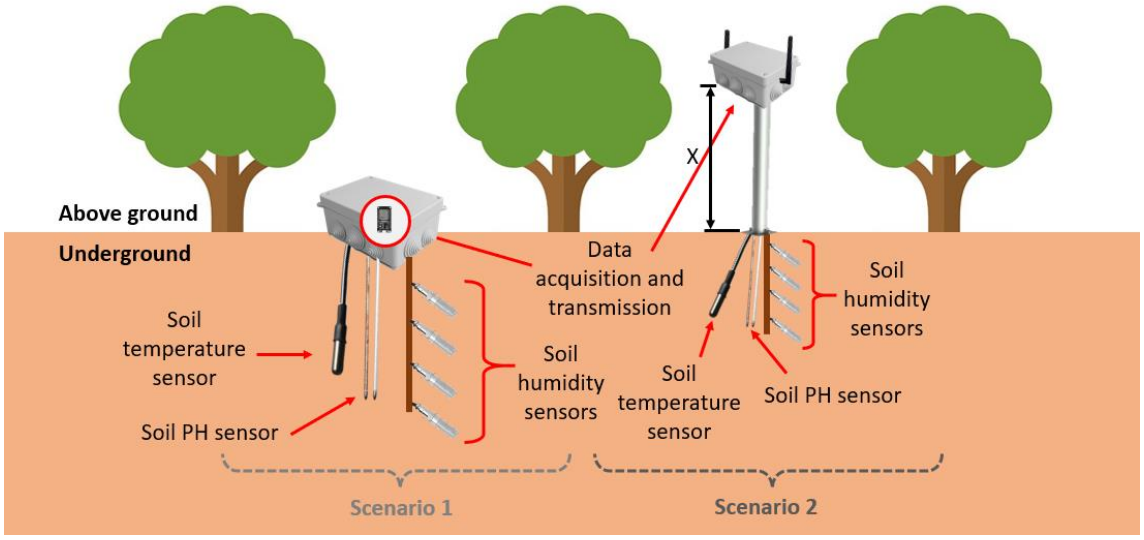

Figure 3.15. Proposed soil monitoring node for scenarios 1 and 2.

Two scenarios are contemplated, one with the node placed in an on-ground position and the other with the node located above-ground at different heights. The tests have been performed considering a deployment strategy that is focused on the field area, where the nodes are located among the crops both on the surface of the soil and above the ground contemplating that the sensors must be buried into the ground. There are other areas in PA systems such as the canals where the irrigation water is transported that can be monitored with sensors such as the conductivity sensor presented in [331]. However, they are not the focus of this paper.

3.3.2 Water monitoring node

In this subsection, the sensors used for monitoring water quality and irrigation needs in the farmland are described.

The sensor used to monitor water quality will be used to monitor turbidity and conductivity. For the detection of turbidity, optical sensors are used, while for conductivity monitoring, inductive sensors are used. For the detection of turbidity, optical sensors are used, while for conductivity monitoring, inductive sensors are used. The turbidity sensor is based on that presented in [43]. It is made with two LEDs that emit at different wavelengths and two light detectors. One of the LEDs has a maximum wavelength of 612–625 nm and the other of 850 nm. The light detectors are a light-dependent resistor (LDR) that responds to the visible light of the first LED and a photodiode that responds to the infrared (IR) light of the second LED. The turbidity sensor is placed before and after the application of the filters to treat the water. The LEDs are powered at 3.3 V using the 3.3 V output voltage.

The conductivity sensor is based on the prototype described in [42]. It is composed of two copper coils. The first coil is powered with a sine wave and the second coil is induced. The induced voltage depends on the conductivity of the water. The powered coil is powered with the Arduino using an analog output (PWM) pin. The generated voltage in the induced coil is measured. Both the turbidity sensor and the conductivity sensor are connected to the same node. They are placed before and after the filters and will monitor the correct operation of the wastewater treatment filters by registering the changes in water quality. Additionally, we use a sensor to detect the presence of hydrocarbon in the water. The sensor is based on the photoluminescence effect linked to the hydrocarbons. In the design of the sensor, different light colors are used to excite the molecules of a hydrocarbon. The light source is an LED and a photodetector is used as a receptor of the emitted light.

In the proposed system, the nodes are deployed throughout the expanse of the canals, both for urban areas and farming areas. The quantity of nodes depends on the number of canals and their specific needs. The Arduino Mega 2560 is one of the options of embedded systems that execute the algorithm that indicates how to gather, manage, and forward the data (See Figure 3.16) [332]. The node has 16 analog input pins and 54 digital input/output pins, allowing for connecting many sensors to one single node. Moreover, it provides a universal serial bus (USB) connection, 4 universal asynchronous receiver-transmitter (UART) serial ports, a power jack, a 16 MHz crystal oscillator, an in-circuit serial programming (ICSP) header, and a reset button. However, as the node does not provide an integrated wireless interface, it is necessary to incorporate wireless modules. The nodes can be provided with WiFi connectivity through a ESP8266 module [333] or with LoRaWAN connectivity by employing the module F8L10D-N [334] which transmits in the 868 Mhz band.

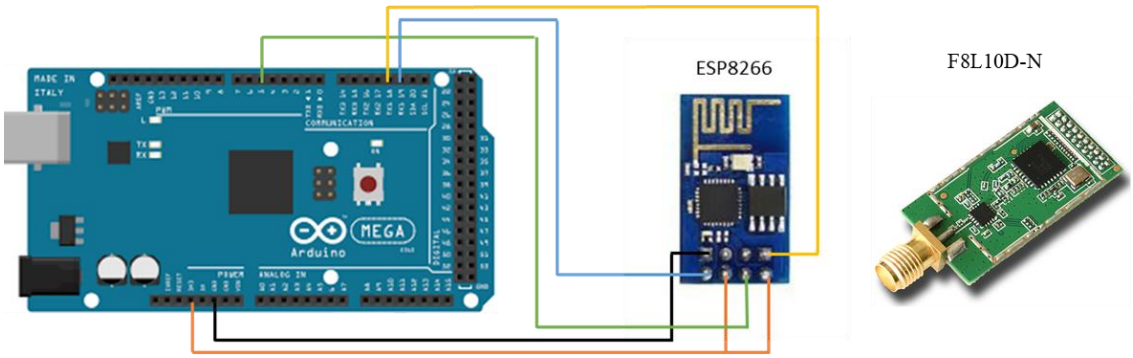

Figure 3.16. Example of the Arduino Mega 2560 and the ESP8266 and F8L10D-N modules.

3.3.4 Meteorology monitoring node

In this subsection, the description of the meteorology monitoring node for agriculture is going to be presented.

There are several environmental parameters whose knowledge is important to farmers and the development of a comprehensive system for precision agriculture. Temperature is one of the most important factors that affect plants. The correct growth of plants, blooming, photosynthesis, or water and nutrient absorption are some of the aspects that depend on the temperature of the environment. To measure temperature, on this prototype the DHT11 sensor has been utilized. This sensor has been utilized to measure humidity as well. Humidity affects plant transpiration, its photosynthesis, and its growth. Low levels of humidity are related to withered plants, small sized leaves, or burnt or dried leaf tips. High humidity levels are related to higher root and leave diseases, nutrient deficiencies, or weak growth. The rain determines whether the irrigation should be activated or not. Furthermore, high amounts of rain should be accompanied of the implementation of proper drainage so as to avoid excess of humidity in the soil. A rain sensor was utilized so as to determine the presence or absence of rain. Lastly, the amount of light is related to the photosynthesis process of the plants and may affect the constitution of the fruit.

Apart from the sensors described previously, the system is comprised of an ESP32 Devkit V1 microcontroller [335]. Furthermore, an SD card is incorporated to the prototype so as to store the information in case of the malfunction of the wireless connection or the server and the power is provided through a 12V solar panel and a set of batteries. The connection of all the sensors and modules is presented in Figure 3.17 and the node prototype is shown in Figure 3.18. The DHT11 sensor is located inside a protective plastic with open spaces to let the air flow. The open spaces are protected with a net to avoid the incursion of insects. The other sensors are located on the bigger encapsulation. The solar panel is supported by an aluminum structure and the rest of the circuit, and the microcontroller is located inside the encapsulation.

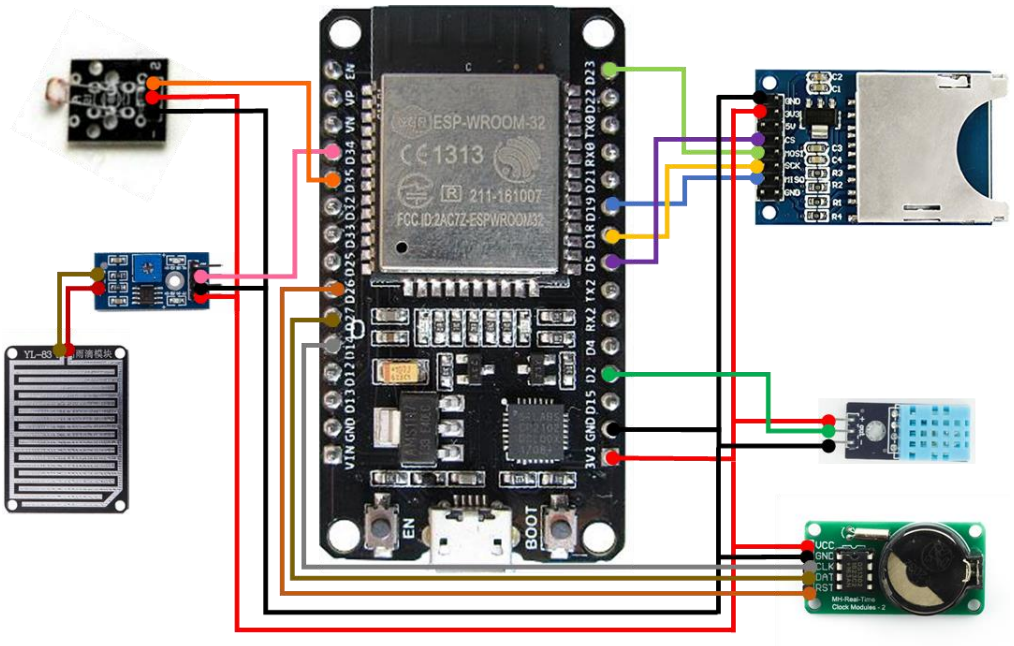

Figure 3.17. Connection of the elements of the system.

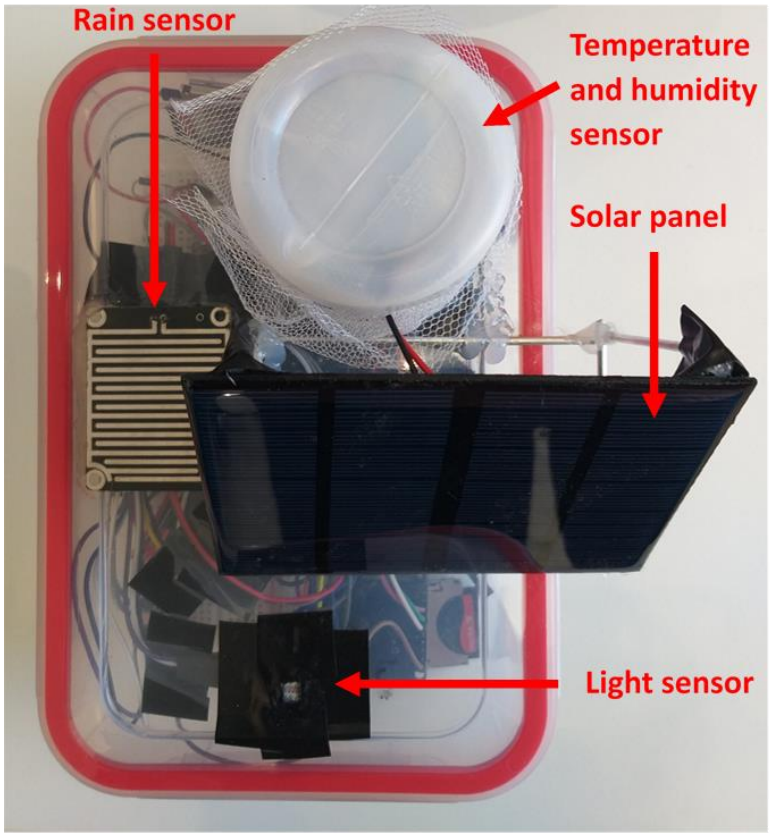

Figure 3.18. Prototype of the meteorology monitoring node.

The algorithm of the system is presented in Figure 3.19. This algorithm determines when the data is forwarded according to the variations in the monitored values. Therefore, the number of forwarded messages is reduced. Firstly, the thresholds of the parameters are set. These thresholds indicate the limits in the variations so as to assess if a message with the value of the parameter is forwarded. Then the initial values are measured and used as reference values. The counter and variables of the different metrics are initialized afterward. The system starts taking measures and calculates the averages of temperature and humidity, and the maximum value for luminosity. As each parameter has different variations throughout the day, the decision for the data transmission is different for humidity and temperature, luminosity, and rain. For humidity and temperature, the average value in the determined period is calculated. When the counter reaches the specified time, the variations in the gathered data are evaluated. If the variation does not surpass the threshold, the data is not forwarded, and the previous values are maintained. If enough variation has been detected, the standard deviation is calculated, and the data is forwarded. For the luminosity, increases in luminosity are determined to obtain the maximum luminosity value. When the counter reached the determined time, the variations are evaluated, and the data is forwarded if the threshold is surpassed. Lastly, for the rain, when the counter reaches the set time, the data is forwarded if there are changes. If there have not been any changes, the previous values are maintained.

3.3.4.1 Determination of data acquisition frequency

To determine the best *dt* for each parameter, the followed approach has been to evaluate the accumulate relative error (ARE) of the data in the database (DB) for 15 hours. The data is real environmental data gathered by our environmental monitoring system presented in the previous section. The algorithm has been applied to the gathered data to determine the best *dt*. The 15-hour period includes two time lapses with big changes at the beginning and at the end of the experiment (sunset and sunrise), and a long time lapse with minor changes (the night). We consider that the best *dt* is the highest one that allows to have an ARE lower than 5%. Therefore, we minimize the number of packets and keep a good data accuracy in the DB.

First, the data about temperature when different *dt* are utilized in the algorithm is presented. The values of temperature in de DB with different dt are presented in Figure 3.20. We can see that, at the beginning, of the data set the data values of temperature are decreasing slowly due to the sunset. During the night, the temperature still decreases more leisurely. At the end of the experiment, after sunrise, the temperature starts to increase. When different dt are used, the values of temperature in the DB change, and some fluctuations are lost. For example, for the *dt* of 50, 55, and 60 min, the minimum temperature (7ºC) is not recorded in the DB, and the increment of temperature during the sunrise is not correctly gathered with *dt* higher than 25min.

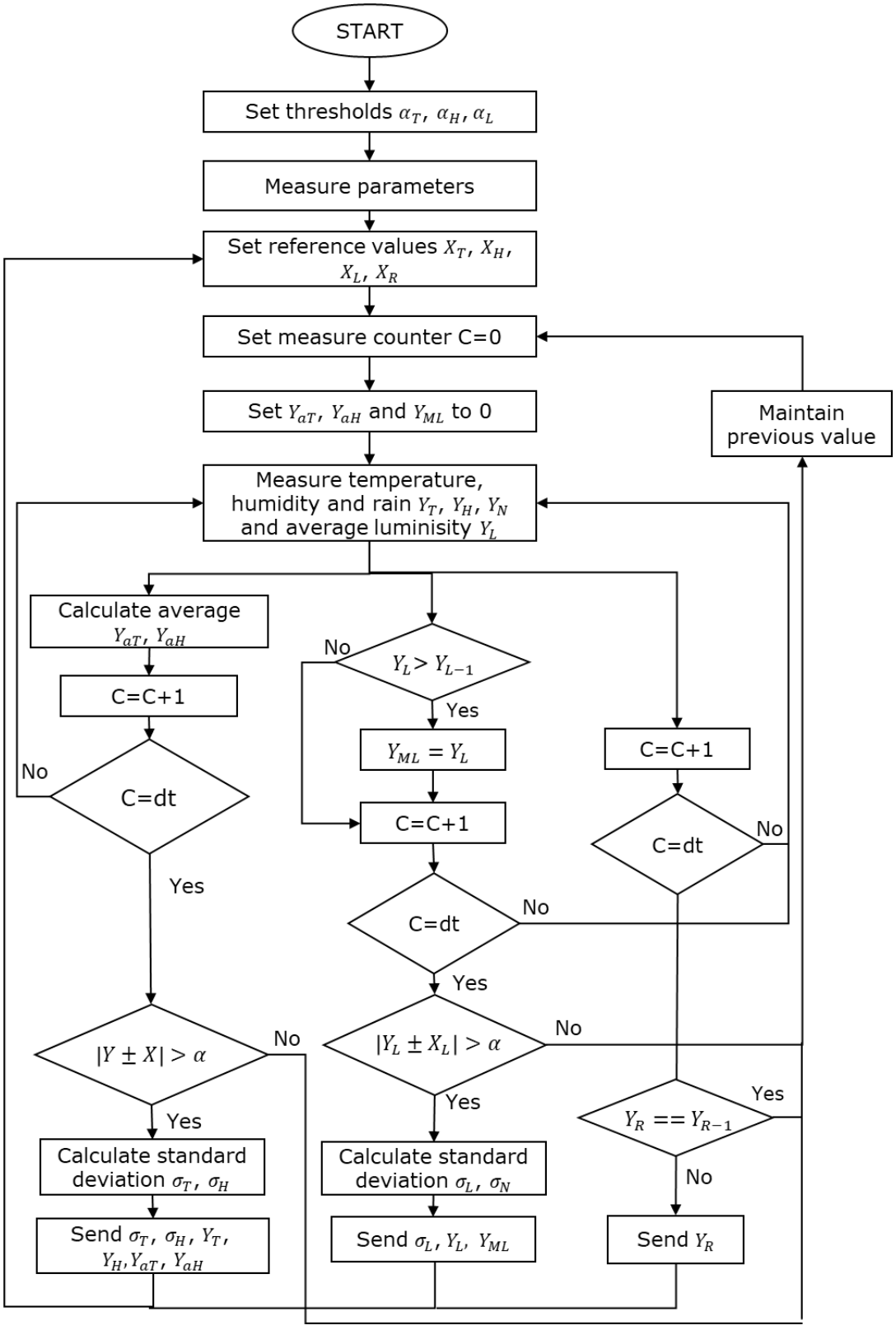

Figure 3.19. Algorithm of the system.

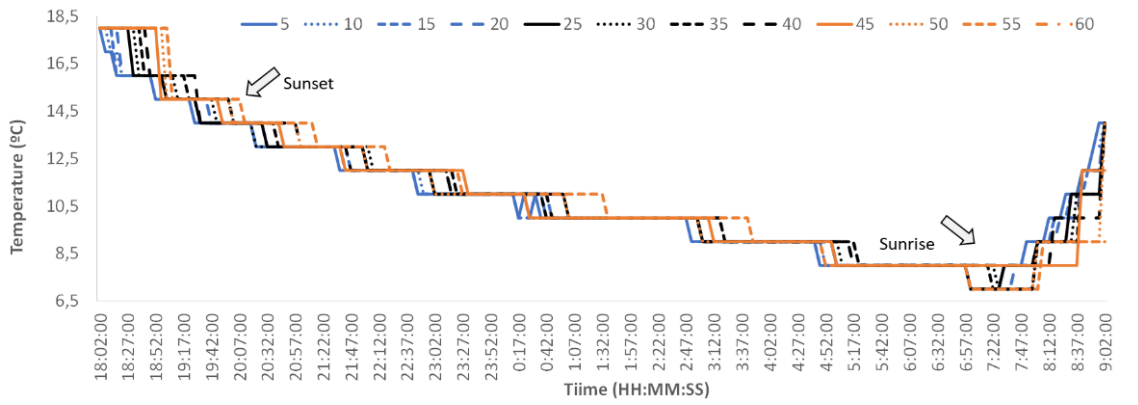

Figure 3.20. Value of Temperature in the DB with different *dt* in the algorithm.

Regarding the ARE in temperature values of the DB, see Figure 3.21, we can affirm that, ARE increases dramatically when the *dt* is higher than 25 min. ARE for *dt* between 30 and 55 min are almost the same and increases again with *dt* of 60 min. Therefore, considering the ARE during this experiment and the aforementioned information in Figure 3.21, the best *dt* for temperature sensing, according to our data, is 25 min.

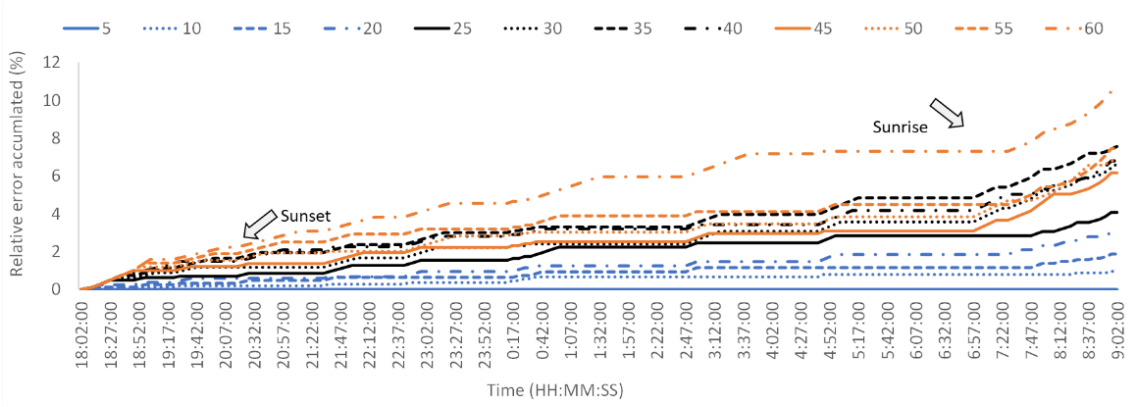

Figure 3.21. ARE of Temperature in the DB with different *dt* in the algorithm.

Following, the data stored in the DB that is gathered by the Humidity sensor is shown, see Figure 3.22. During the sunset and the first hours of the night, the humidity increases. Then, after the sunrise, the humidity decreases due to the increase of temperature. As the changes in humidity are slower than in the case of temperature, no big differences can be seen in the values of the DB with the different *dt* beyond a delay on the notification of the changes. The maximum and minimum values are gathered with all the *dt* and a good representation of data variability is archived in all the cases.

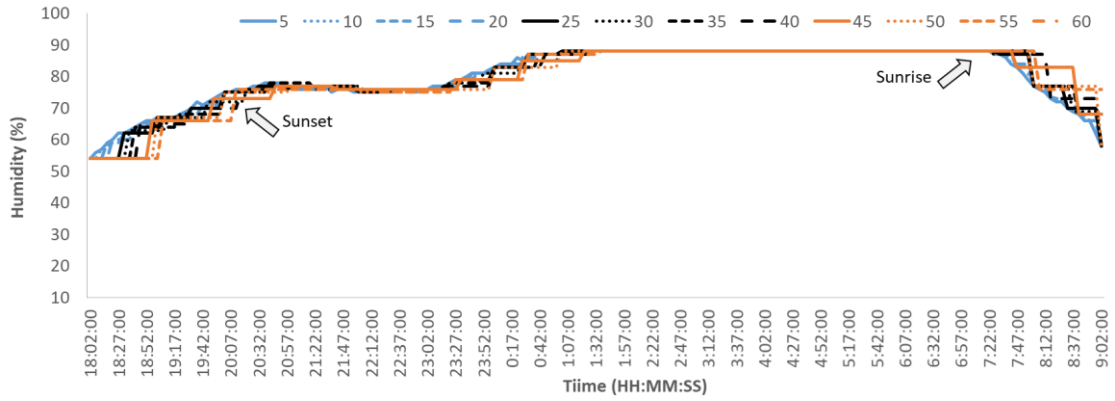

Figure 3.22. Value of Humidity in the DB with different *dt* in the algorithm.

In terms of ARE of humidity data, see Figure 3.23, it increases almost constantly as the *dt* upsurges. The only *dt* that overtakes the limit of 5% is the *dt* = 60 min. Nonetheless, the *dt* of 50 and 55 min are close to reaching 5%. Therefore, we can say that to ensure that ARE do not exceeds the 5%, it is better to use a *dt* of 45 min for the data of humidity.

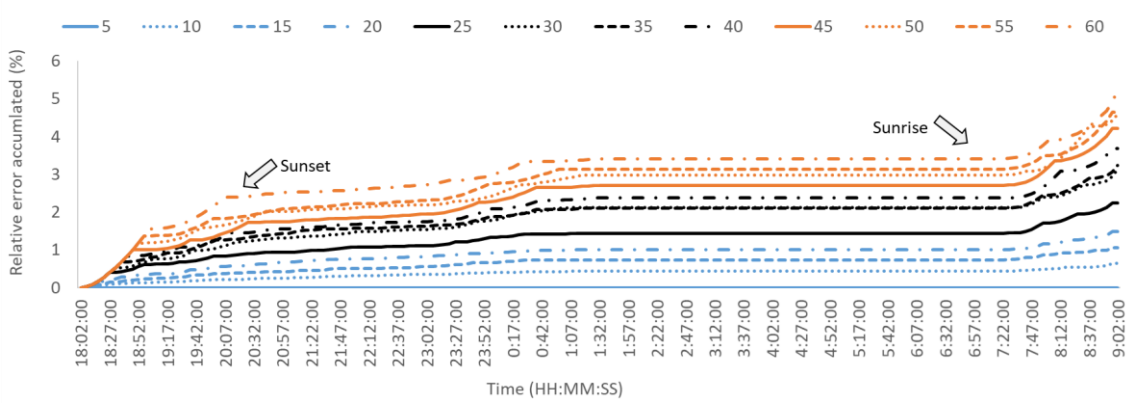

Figure 3.23. ARE of Humidity in the DB with different *dt* in the algorithm.

Finally, we focus on the data of illumination, see Figure 3.24. This data presents the highest changing rate in sunrise and sunset. Consequently, we expect to have high mismatches in the data when high *dt* are used. In this case, the dt higher than 5 (the original data) are not able to record the maximum light value. Moreover, the dt higher than 15 min cannot gather properly the abrupt changes in the sunrise and the sunset. Thus, according to the capability to record the maximum, minimum values, and the variations in the data, the maximum acceptable *dt* is 15 min, as seen in Figure 3.25.

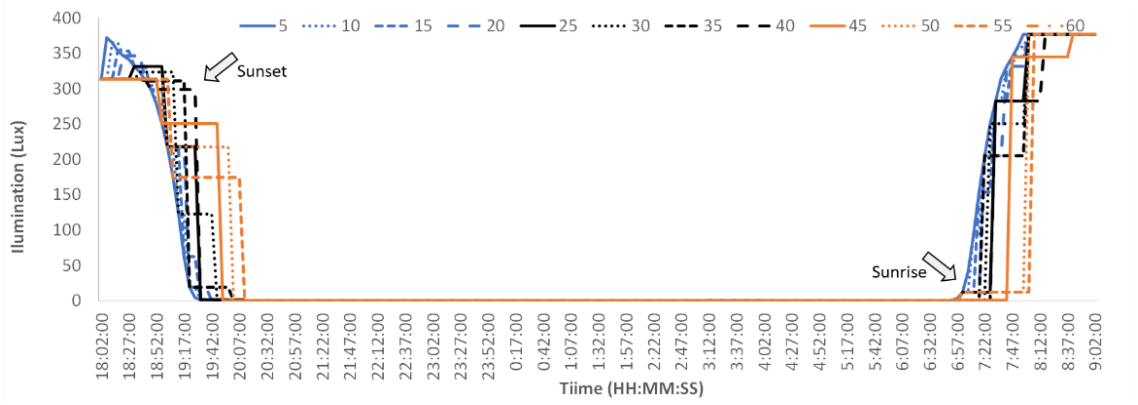

Figure 3.24. Value of Illumination in the DB with different *dt* in the algorithm.

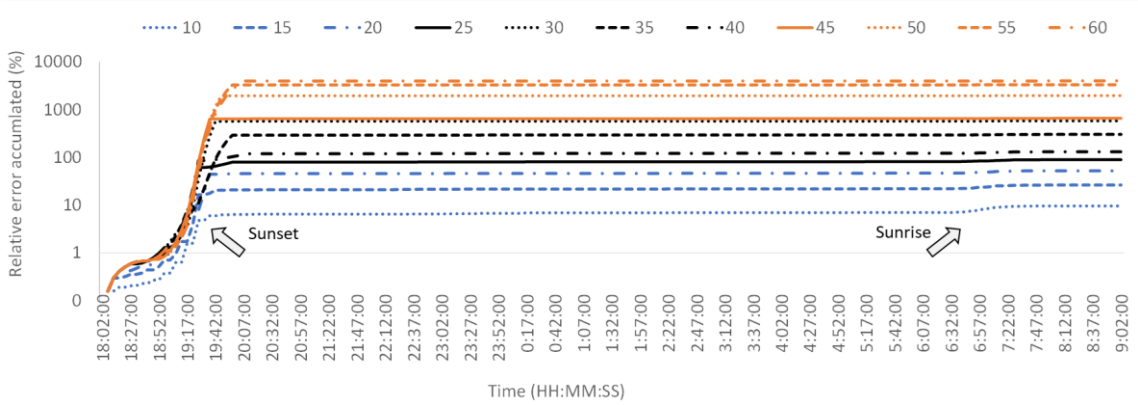

Figure 3.25. ARE of Illumination in the DB with different *dt* in the algorithm.

As it can be seen, the obtained results vary from 45 minutes to 5 minutes depending on the parameter. Other environmental monitoring systems such as [336], perform a measure each hour. The selected time period must serve the required purpose. Our results indicate the best time period for each parameter in the Spanish Mediterranean weather in order to preserve the information of the changes in the weather. However, other climates may require different settings and other applications may not need much accuracy.

3.3.5 Actuator node

To carry out the design of the actuator nodes, several factors must be considered. The actuator node must have a linear actuator. The linear actuator is a device that converts the rotational motion of a low-voltage direct current (DC) motor into linear motion. This allows us to operate a hydraulic or pneumatic actuator that will move the gates to open or close the canals. Furthermore, an SD card will be needed as well. The hardware

necessary to receive and transmit the actions must be arranged. Furthermore, for its operation, it must have a self-powered system for power generation. The energy system consists of rechargeable batteries and small solar panels which are responsible for recharging the batteries. In this way, we ensure a long service life of the devices in operation. It will also have a USB port so that administrators can connect directly to the node.

3.4 System operation algorithms

In this subsection, the performance algorithm of the elements of the proposed system is presented. The proposed algorithm has been divided into two parts. The first part shows the algorithm used by the sensor nodes to obtain the data and transmit them to a central node. This node is called Central Node and it is located in Urban Area 0, from which the data and alarms are sent to the AI and storage systems. The second part presents the manner in which the data are stored in the Storage Server and treated in the AI computers so as to later send the response action to the actuator nodes.

The algorithm presented in Figure 3.26 shows the operation process of a group of nodes. As can be seen in Figure 3.2, a sensor node is not deployed on its own but in a group of three nodes that measure at the same point. This group is formed by one sensor node named Central Node, and two more sensor nodes. All sensor nodes are capable of detecting different parameters related to water pollution. All the sensors connected to the nodes take measurements every minute. If there are variations with respect to the reference values, the data are sent to the Central Node of the group, and at the same time, the data are stored in the SD card. In addition to performing the usual functions of any other sensor node, distributed Central Nodes are responsible for sending data and alarms with information from any node in their group. These alarms and information are forwarded to the Central Node located in Urban Area 0, via wireless communication. This grouping of nodes allows for guaranteeing fault tolerance. If only one node detects pollution, the node sends an update to the Central Node of their group, and this Central Node checks if itself or the other sensor of the group has also detected pollution. If pollution is not detected by more than one node, it is considered a false positive.

All the groups of nodes located in the different areas, urban or canal, can send updates to their Central Nodes via wireless communication. The Central Nodes send the information, via wireless communication as well, to the Central Node of Urban Area 0. The Central Node of Urban Area 0 is responsible for sending all information and alarms collected in all areas to the data center through a wired/wireless transmission medium. The data center is primarily responsible for storing the data, which can be consulted at any time, and generating analytical and machine learning models. In addition, it is also responsible for generating the actions that the actuator nodes must take.

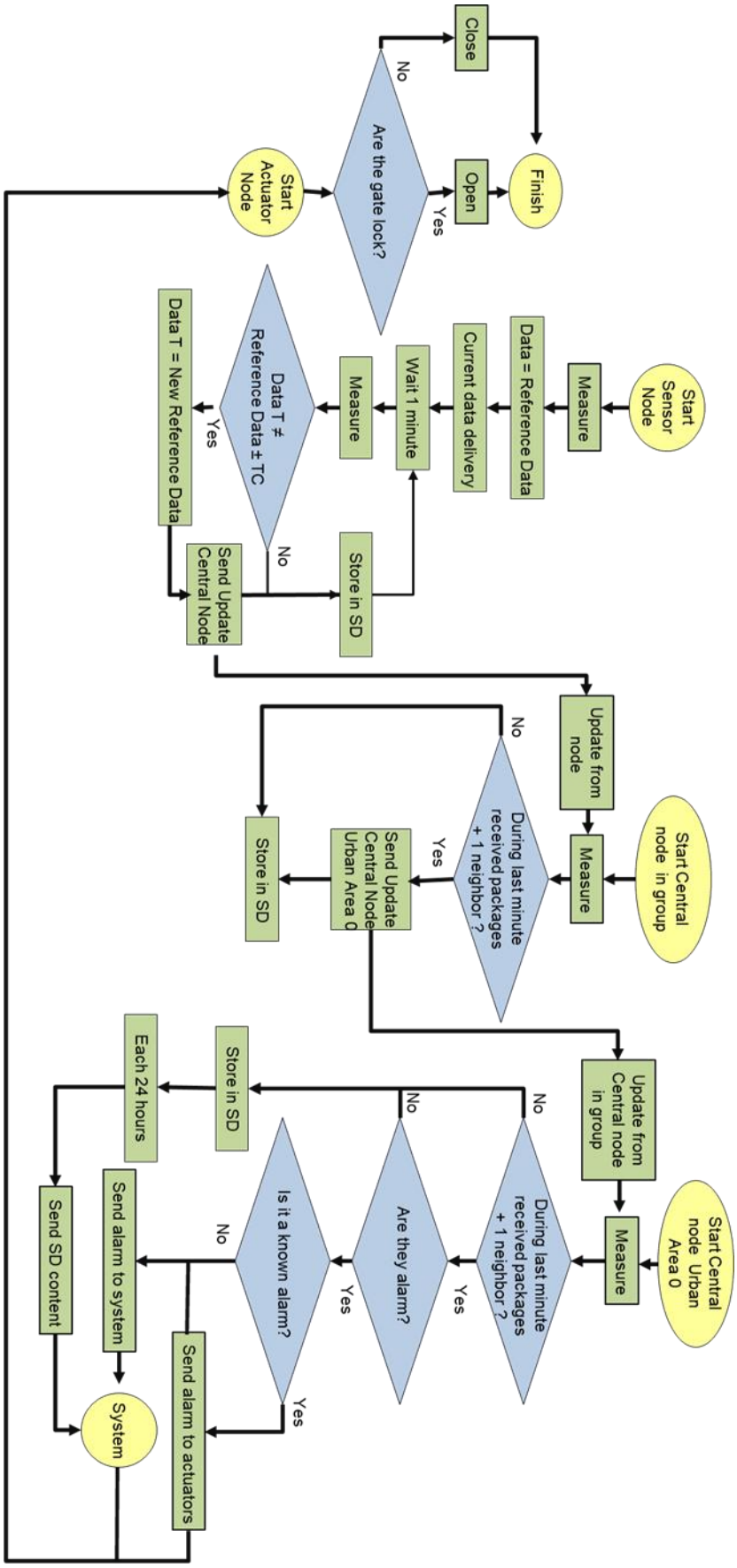

Figure 3.26. Algorithm for node groups.

Generally, the action resulting from the detection of an alarm is associated with the start-up of one actuator node at least in one area. When the Central Node of Urban Area 0 receives an alarm, if it is known and has been previously treated, this node decides an action and makes an order to the actuator nodes so that the corresponding action is carried out. Moreover, the Central Node of Urban Area 0 sends the alarm to the storage and AI data analysis system.

The second algorithm that we propose so as to store the data and alarms that are generated in the sensor nodes is provided in Figure 3.27. Once saved, they are processed by AI, and then the decisions that are made are forwarded to the actuator nodes.

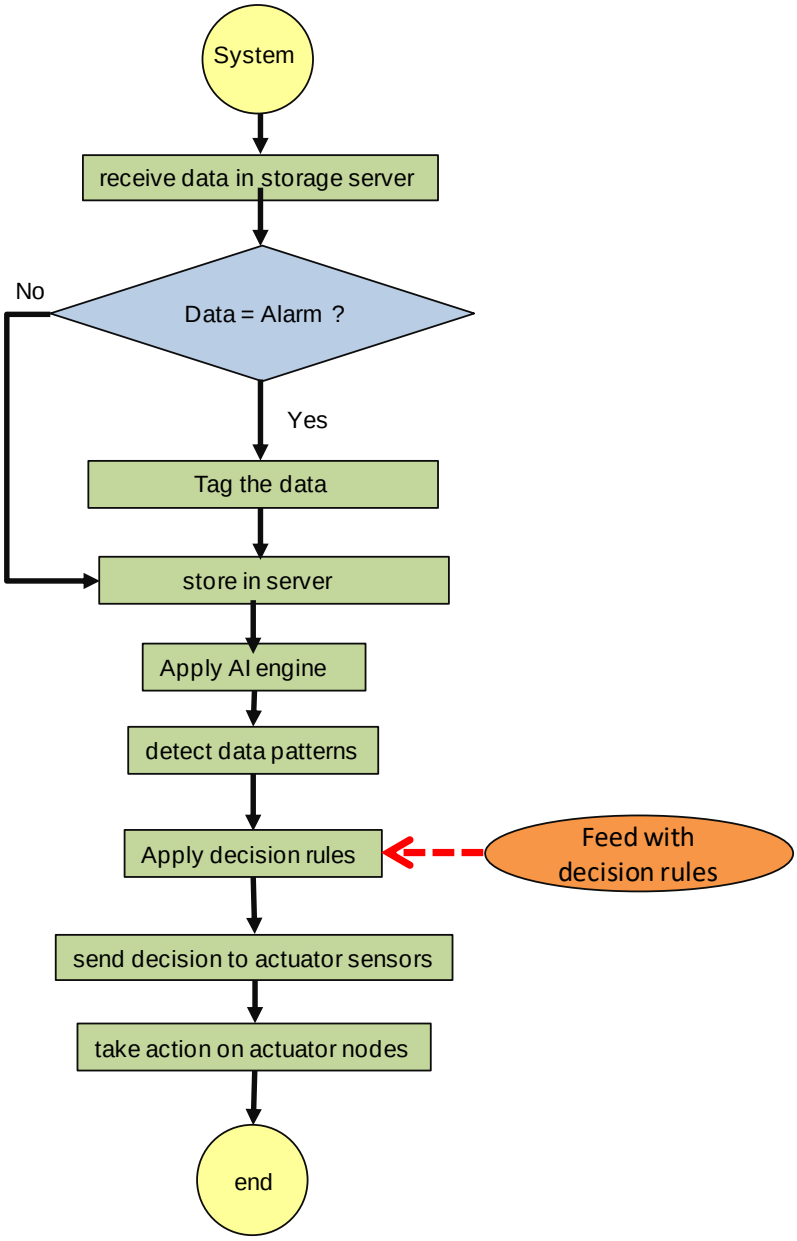

Figure 3.27. Algorithm for storage data, obtain patrons' big data and take decision to actuator nodes.

Initially, when the data are received in the Storage Server, the system must differentiate if it is an alarm or if it is the data that have been obtained during an observation period. In case of an alarm, the received data will be tagged before being stored. If it is not an alarm, the data are stored directly. Then, they go to the computer where they are treated by AI. In this way, patterns of behavior can be detected. Depending on the problems that can be detected and the place where actions should be applied, several decision rules have been created. Those rules are applied based on the detected patterns. Finally, the decisions that have been made based on the rules are sent to the actuator nodes so that they are put into action in an appropriate manner.

3.5 Proposed algorithm for irrigation

In this subsection, the performance algorithm of the irrigation system is depicted.

The presented system determines the irrigation requirements of the fields according to the weather and the state of the soil. For the field area, an irrigation software was created to analyze de data from the fields at the Data Center so as to determine the amount of water required by the fields. The flow chart of the performance of the Data Center is presented in Figure 3.28. After the network establishment, all the variables, fixed and obtained from both the user and the sensors, are initialized. All the required variables are listed in Table 3.1. Then, the Data Center receives all the data from the sensors and stores it for later analysis. The system generates an alert if some variables such as the salinity of the soil or the water surpass a threshold. Therefore, if the data center receives any Alert Notification, the notification is processed and then, an Action is decided and forwarded to the relevant actuator. If there is no alert notification, the system checks if the calculation timer is reached. The calculations for the irrigation requirements need to be performed once a day as the irrigation is done each morning. Therefore, when that time is reached, all the data is processed to create reports for the user. Then, the intermediate variables are calculated. Lastly, the calculated irrigation requirements are forwarded to the Field Actuator for it to irrigate the fields the following morning. The PA system may include irrigation water monitoring and an agrometeorological monitoring node to obtain more precise irrigation schedules for the intended fields. However, this paper is focused on the field area.

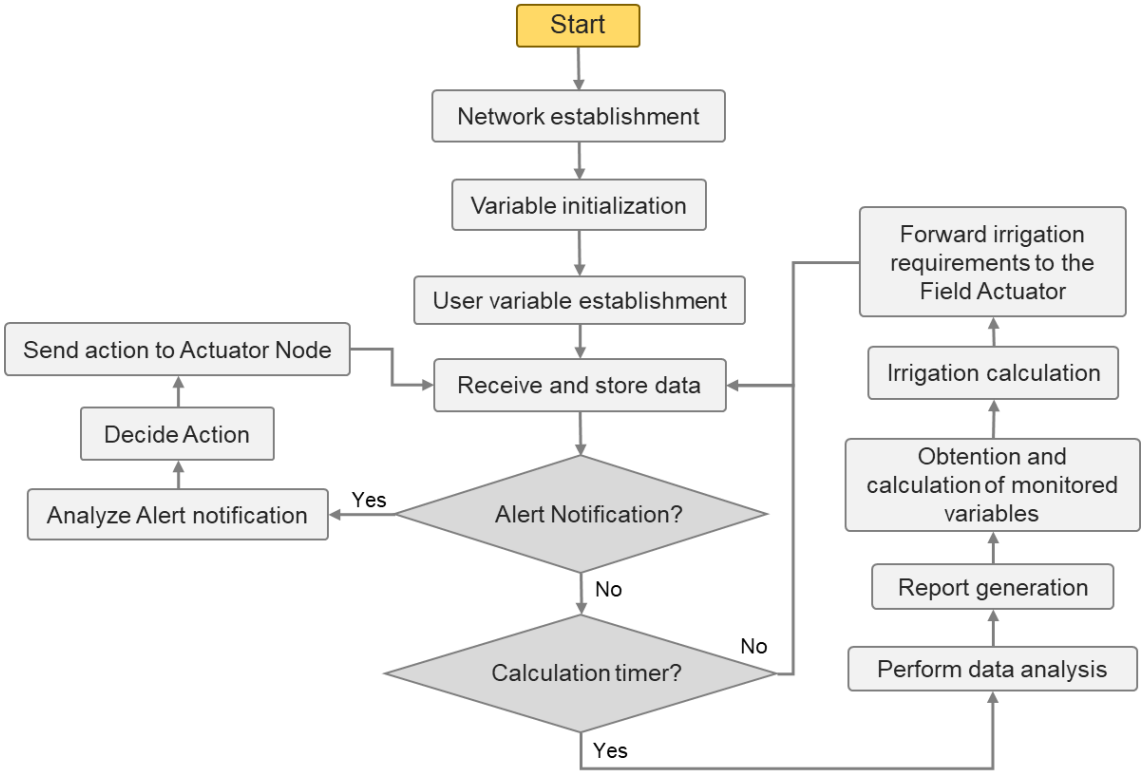

Figure 3.28. Flow chart of the Data Center.

Table 3.1. Variables required by the system.

Fixed Variables	Variables set by the User
Elevation above sea level	Height of the tree
Date	Selection of soil type
Latitude	Time period for irrigation calculation
Height of wind speed measurement	Selection of Single Coefficient Approach or Dual Coefficient Approach for ETc calculation
Variables obtained from the monitored data	
Maximum air temperature of the day	Water salinity
Minimum air temperature of the day	Soil conductivity
Maximum relative humidity of the day	Soil humidity
Minimum relative humidity of the day	Soil temperature
Hours of sunlight of the day	Mean temperature of the actual month
Wind speed	Mean temperature of the previous month
Precipitation amount	Estimated mean temperature of the following month
Hour of the precipitation	

Algorithm 3.1 presents the algorithm that determines the irrigation needs of the crops. The basis of the calculations of the irrigation requirement of a crop is presented on the FAO (Food and Agriculture Organization) Irrigation and Drainage Paper No. 56 on Crop Evapotranspiration [337]. For our system, we introduced the monitored parameters as variables of the equations for irrigation calculation presented by the FAO. Although the FAO does not contemplate the use of sensors deployed on the field to acquire the necessary data for the calculations of the evapotranspiration of the crop (ETc), many papers have implemented varied forms of ETo (reference evapotranspiration) and ETc calculations using the data from sensors deployed on the fields [12, 13, 316].

Algorithm 3.1. Irrigation algorithm

```
1)  Variable initialization
2)  User parameter initialization
3)  ETo calculation
4)  Determination of the Crop Stage
5)  If Water stress then
6)    Calculate irrigation adjustment due to water stress
7)  end if
8)  If High salinity levels then
9)     Calculate irrigation adjustment due to salinity
10) end if
11) If Precipitation then
12)   Determine the precipitation amount
13)   Determine the hour of the precipitation
14)   Calculate irrigation adjustment due to precipitation
15) end if
16) Calculate ETc
17) Calculate Irrigation requirements of the crop
18) End.
```

Algorithm 3.1 is executed once a day after the data center receives the data gathered throughout the day. This is done because some variables require the minimum and maximum value of a day to perform the calculations, such as temperature and relative humidity, and other variables require a total of the day, such as sunlight hours and precipitation amount. Therefore, the monitoring process and the reception of the data at the specified intervals is contemplated in the flow chart in Figure 3.27. Whereas Algorithm 3.1 receives the processed data of the day with the variable initialization process, as well as the fixed variables. Then, the variables set by the user are initialized. Using all the gathered data, the ETo is calculated. Then, the crop stage is determined. The crop stage differs among crop types and the time of the year. Then, the presence of water stress and salinity stress is determined according to the readings from the soil sensors so as to adjust the irrigation requirements as stated in the recommendations of

the FAO. Water stress and salinity stress can result in higher water requirements in an effort to counteract the caused damage. Furthermore, if precipitation is detected, the amount of irrigation water may be reduced, or the irrigation day may be postponed according to the amount of precipitation. This is calculated utilizing the irrigation adjustment due to precipitation as recommended by the FAO. Lastly, the ETc is calculated, and the irrigation requirements are determined.

Figure 3.29 presents the case of an irrigation schedule for an orange orchard in a Mediterranean climate for one month. The climate data were obtained from the agrometeorological station MO12 in Región de Murcia, Spain [338] for the month of October 2020. During the period of one month, there were four precipitation events and one water stress event. As it can be seen, the irrigation scheduling begins with one initial irrigation event. Then, the Root zone depletion is calculated to determine the irrigation needs of the orange trees. Water stress is detected on day 15 and another irrigation event is scheduled for day 16. It is noticed that the Root Zone Depletion is reduced by both irrigation and precipitation events.

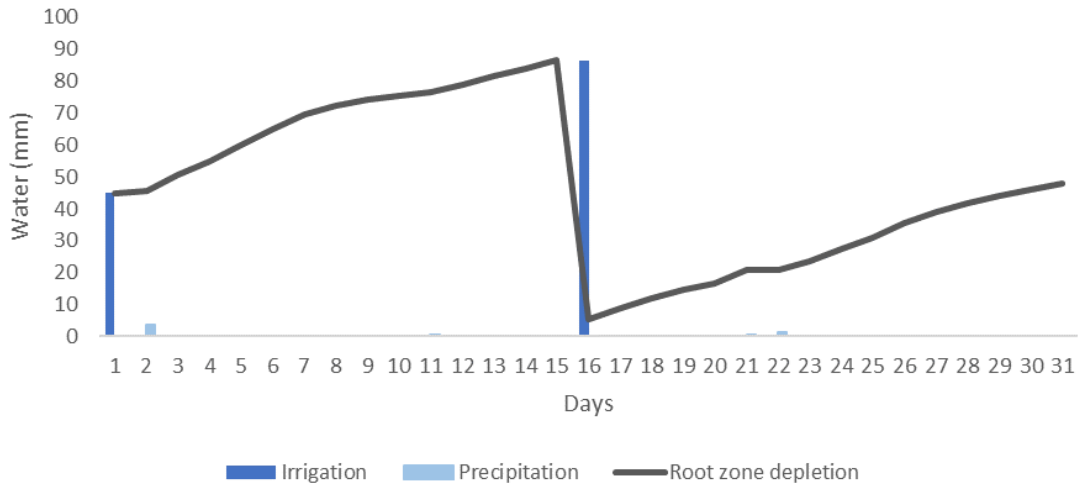

Figure 3.29. Simulation of an irrigation schedule for an orange field in Murcia.

The case of the irrigation of an orange field in the area of the station of Gandía Marxuquera, Comunidad Valenciana, Spain [339] for the month of October 2020 is presented on Figure 3.30 as well. In this case, in the area of Gandía, situated in a norther region, there were seven precipitation events. However, four of them were 0.1 mm and thus, are not visible on the graph. Considering a first irrigation of 45 mm as in Figure 3.28, as it can be seen, the next irrigation event is scheduled for day 19 instead, three days after the irrigation event of the MO12 station. In that manner, the algorithm takes into consideration the different weather conditions of each area to provide the necessary amount of irrigation water for each field.

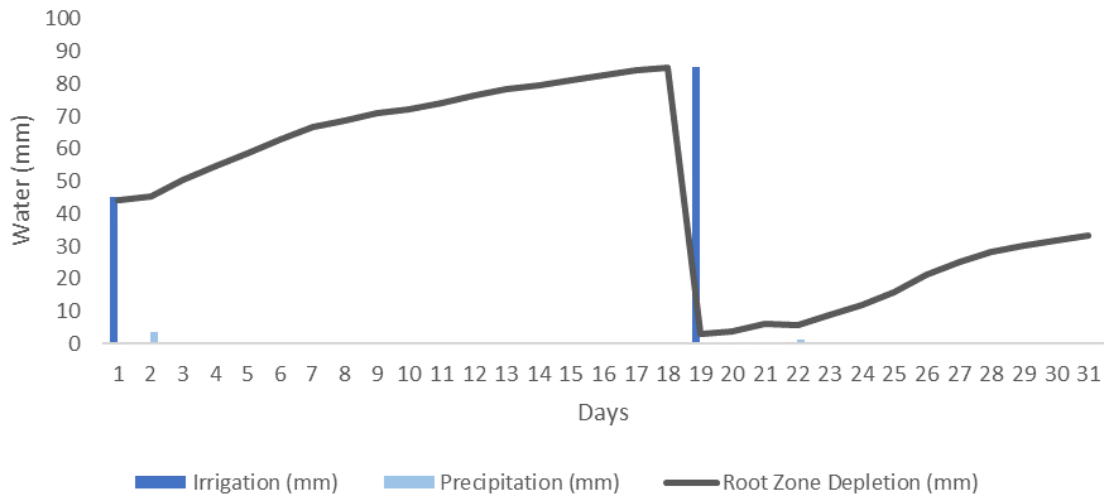

Figure 3.30. Simulation of an irrigation schedule for an orange field in Gandía.

3.6 Conclusion

In this chapter, the architecture for water quality monitoring for an irrigation PA system and has been presented. Three areas have been considered being the Canal area where the water quality is monitored, the field area where the state of the crops is monitored, and the Urban area where the gateway is located. The data is forwarded utilizing both WiFi and LoRa wireless technologies, where the CH node is the WiFi/LoRa bridge that allows the connection between the WiFi and the LoRa nodes. Furthermore, a tree topology for LoRa has been introduced. This allows reaching further distances and reducing the amount of data and the number of messages forwarded from one node to the following node. Furthermore, specific scenarios have been contemplated as well. Then, the sensor nodes for monitoring water quality, soil conditions, and meteorology conditions have been described. Lastly, the operation algorithm for the system and the algorithm that calculates the irrigation requirements have been presented as well. The aforementioned work has been published in several papers authored in several publications: [28, 38, 45, 48, 340, 341]. Moreover, the communication protocol for the presented architecture will be described in the following chapter.

Chapter 4

Protocol Design

4.1 Introduction

In this chapter, a new communication protocol for the architecture presented in Chapter 3 intended for PA systems located in remote areas is presented. It is intended for heterogeneous networks comprised of both WiFi and LoRa devices, including a WiFi/LoRa bridge to perform the conversion between each wireless technology. Thus, the proposed protocol is encapsulated over UDP and LoRa. Furthermore, this protocol has a low overhead, which is beneficial for the LoRa transmissions. The structure of the header and the messages is detailed. Furthermore, the alerts caused by water salinity, water pollution, malfunctioning elements of the nodes, low battery, or down nodes are contemplated.

4.2. Protocol description

In this section, the proposed protocol for a precision agriculture system is presented.

The message format is described in Figure 4.1. The first field of the Header is the NODE_ID field. It is one byte long and has the specific ID of each node. This field is set to 0 when the node has not yet been registered or when the sender is the Data Center. It is followed by the NODE_TYPE field which is 4 bits long. Table 4.1 depicts the

different node types and the value at the NODE_TYPE field. The MESSAGE_TYPE field is 3 bit long and determines the type of message the nodes or the Data Center is sending (See Table 4.2). The next field is the Priority Field. The messages with priority have this flag as 1. All messages have the priority flag activated except the DATA message. The DATA message does not have priority unless access to the data has been requested by the user. The next field is the Payload which has the information that is forwarded in the message. Not all messages have a payload.

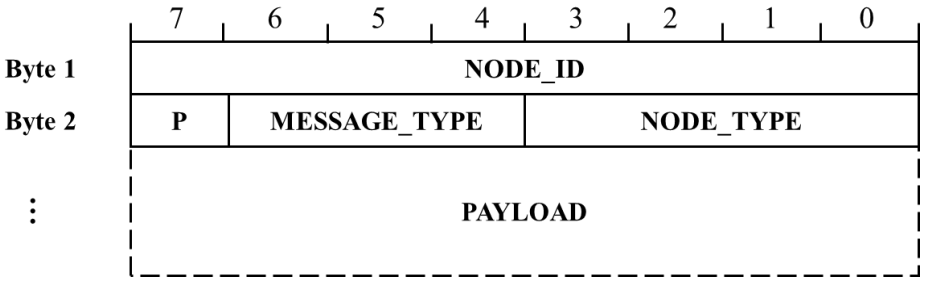

Figure 4.1. Message format of the protocol.

Table 4.1. Values of the NODE_TYPE field.

Value	**Node Type**	**Bit**			
		3	**2**	**1**	**0**
0	Data center	0	0	0	0
1	Gateway	0	0	0	1
2	Aggregator Node of Canal Area	0	0	1	0
3	Aggregator Node of Field Area	0	0	1	1
4	Actuator Node of Canal Area	0	1	0	0
5	Actuator Node of Field Area	0	1	0	1
6	Water Monitoring CH	0	1	1	0
7	Water Monitoring Node	0	1	1	1
8	Meteorology Monitoring Aggregator Node	1	0	0	0
9	Soil Sensing CH	1	0	0	1
10	Soil Sensing Node	1	0	1	0
11	Farmer User	1	0	1	1
12	Hydrographic Confederation User	1	1	0	0

Table 4.2. Values of the MESSAGE_TYPE field.

Value	Message Type	Bit			Description	Priority
		6	**5**	**4**		
0	REGISTER	0	0	0	This message is sent when creating the topology for the node to be assigned an ID.	Yes
1	DATA	0	0	1	This is the message format to forward data.	Both options
2	ACTION	0	1	0	This is the message that is sent to the actuators with the actions they have to perform.	Yes
3	MALFUNCTION	0	1	1	This is an Alert message that is forwarded to the Data Center when a malfunction in one of the elements of a node is detected but the node is able to perform other activities.	Yes
4	IS_DOWN	1	0	0	This is an Alert message that is forwarded to the Data Center to notify that a node is not functioning.	Yes
5	LOW_BATTERY	1	0	1	This is an Alert message that is forwarded to the Data Center to notify that a node has a low battery and thus, there is a problem with the energy-harvesting functionality.	Yes
6	POLLUTION	1	1	0	This is an Alert message forwarded to the Data Center by the nodes in the Canal Area to notify that pollution has been detected.	Yes
7	SALINITY	1	1	1	This is an Alert message forwarded to the Data Center by the nodes in the Canal Area to notify that high levels of salinity have been detected in the water.	Yes

A scheme of the phases of the protocol is presented in Figure 4.2. When the system is deployed, the first process performed by the protocol is the Activation Phase to connect all the devices. Then, the Verification Phase is performed to ensure all devices work properly. Then, the User Registration Phase is performed to add all the Users to the system. The Data Acquisition Phase, the Data Transmission Phase, the Action Phase, and the Alert Phase can happen at the same time between the different elements of the architecture. Lastly, the Verification Phase is performed periodically to assess the state of the devices. Hereunder, an in-depth description of each of the phases is provided:

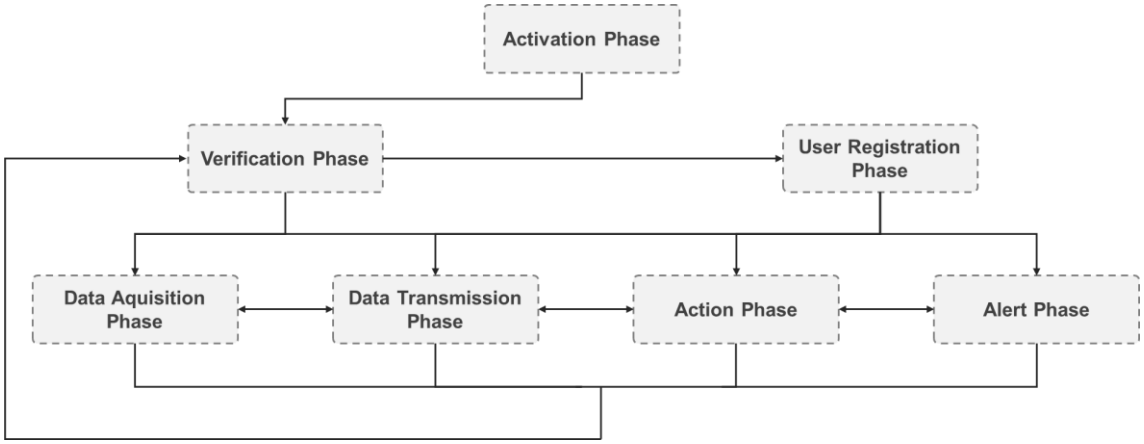

Figure 4.2. System diagram flow chart.

1. **Activation phase:** In this phase, the topology presented in Figure 3.5 is established. The nodes detect their neighbors and establish a connection with the other nodes. The initial set-up of all the variables necessary for the correct functioning of the system is established as well.

All the nodes have a static address assigned by the network designer. The nodes establish the connection with one another according to the specifications of the WiFi/LoRa technology. Once the topology has been established, the nodes send a REGISTER message to obtain the Node ID from the Data Center (See Figure 4.3). The Register process begins with the Gateway, followed by the Aggregator Node, then the CH, and, lastly, the Sensing Nodes. As it can be seen in Figure 4.3, the NODE_ID is set to 0. The NODE_TYPE is part of the initial configuration of the node. Therefore, depending on the type of the node, the NODE_TYPE field in the REGISTER message will have a different value. The MESSAGE_TYPE is the REGISTER message, and the P flag is set to 1. Lastly, in order to know which of the nodes has forwarded the message, the payload of the REGISTER message will be a Byte with a random number. The answer from the Data Center will substitute the random Byte with the Node ID assigned to the node. An example of the REGISTER message for a Water Monitoring Node is provided in Figure 4.4.

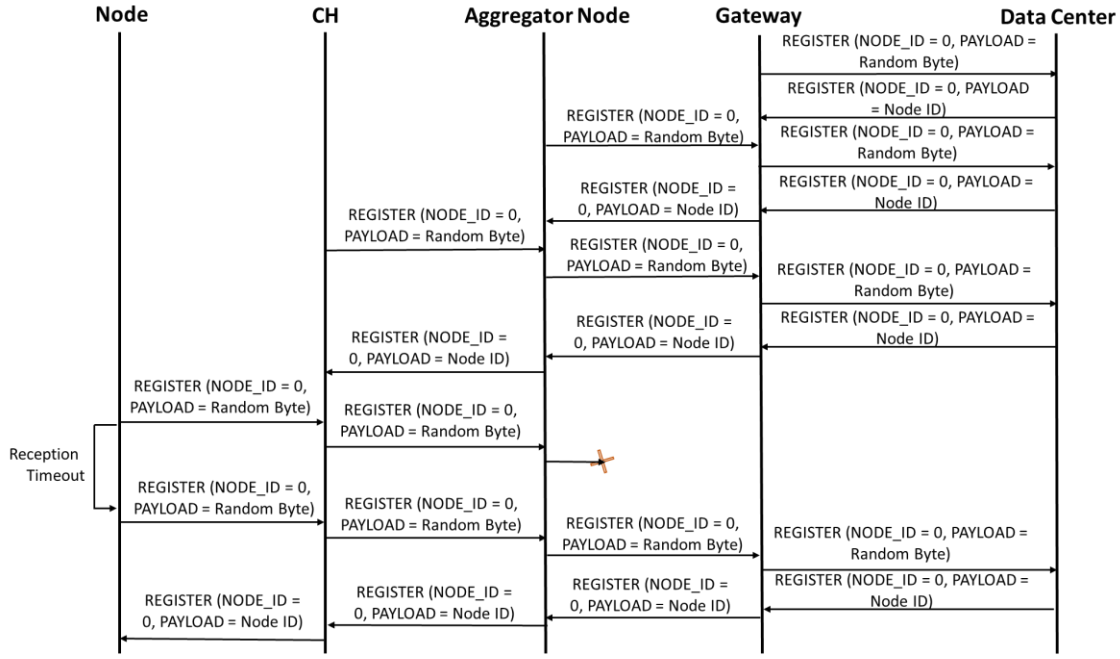

Figure 4.3. Message exchange in the Activation phase.

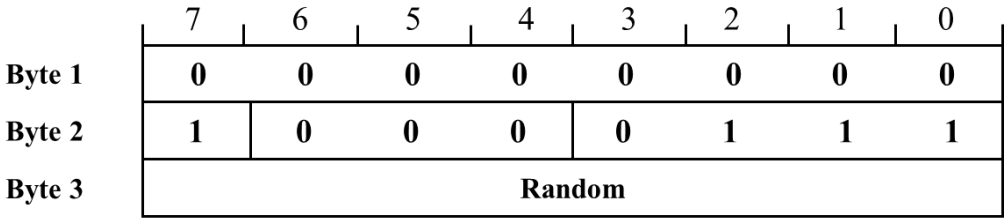

Figure 4.4. Example REGISTER message for a Water Monitoring Node.

2. **Verification phase:** The nodes verify that all the sensors, the solar panel, the radio, and the communication are functioning correctly. If any of the elements of the system has a problem, a notification is generated.

Once the nodes receive the NODE_ID, they begin the verification process to check if all the sensors and elements that comprise the node are working properly. If there is not any problem, no messages are sent. However, if there is a problem with any of the elements of the node, a MALFUNCTION notification will be sent to the Data Center (See Figure 4.5). The Verification phase is performed periodically to assess the performance of the system as it is exposed to the elements, animals, and machinery of the workers of the farm.

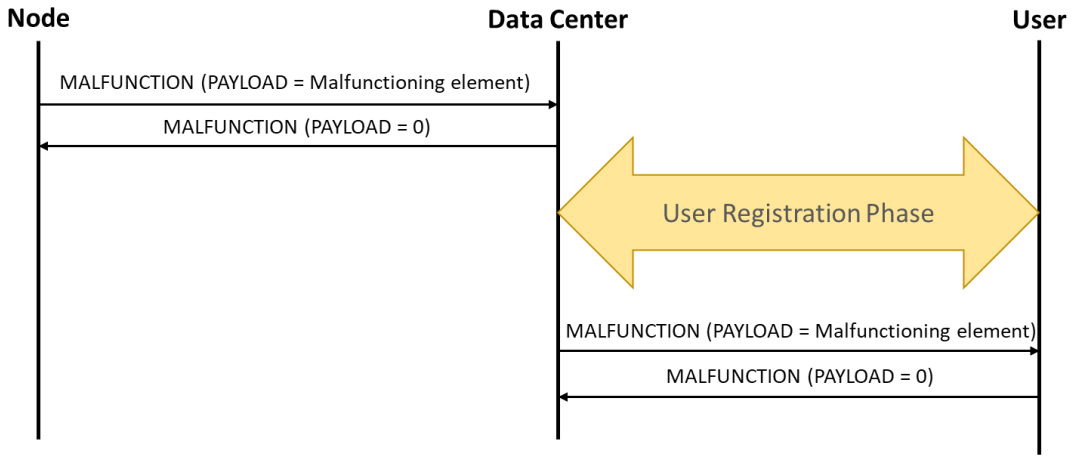

Figure 4.5. Message exchange in the Verification phase.

The payload of the MALFUNCTION message is different according to the Node Type. It consists of a set of flags that indicate which sensor is malfunctioning (See Table 4.3). The Actuator Nodes only have two flags while the Soil Sensing Node and CH, and the Meteorology Monitoring Aggregator Node have 5 flags. When one of the sensors is not working correctly, the MALFUNCTION message is forwarded with the flag of the broken sensor set to 1. The sensors that are working properly have their flags set to 0.

Table 4.3. Payload of the MALFUNCTION message according to Node Type.

Node Type	**Bit**				
	4	**3**	**2**	**1**	**0**
Actuator Node of Canal Area	-	-	-	Gate 2	Gate 1
Actuator Node of Field Area	-	-	-	Flux sensor	Gate
Water Monitoring CH/Node	-	-	Oil sensor	Turbidity sensor	Salinity sensor
Meteorology Monitoring Aggregator Node	Wind sensor	Luminosity sensor	Rain sensor	Humidity sensor	Temperature sensor
Soil Sensing CH/Node	pH sensor	Temperature sensor	Humidity sensor 3	Humidity sensor 2	Humidity sensor 1

3. **User registration phase:** The user is registered at the Cloud platform to access the data from the sensors and to indicate any changes in the initial variables. If any new information is provided by the user, the data is forwarded to the nodes that need that information.

In this phase, the user is registered to the system. There are different types of users with different privileges. Table 4.4 presents the types of users and the nodes they have access to. As it can be seen, the Farmer user has access to the nodes deployed on their farm whereas the Hydrographic Confederation User has access to the nodes deployed on the water canals.

Table 4.4. Nodes that can be accessed by each User Type.

User Type	**Node Type**
Farmer User	Meteorology Monitoring Aggregator Node, Aggregator Node of Field Area, Actuator Node of Field Area, Soil Sensing CH, and Soil Sensing Node
Hydrographic Confederation User	Aggregator Node of Canal Area, Actuator Node of Canal Area, Water Monitoring CH, and Water Monitoring Node.

The message exchange between the User and the Data Center is presented in Figure 4.6. As it can be seen, the employed message is the REGISTER message. In the case of the user, The NODE_TYPE field has the values of the User Type. The NODE_ID and Payload fields are used in the same way as the nodes on the Activation phase.

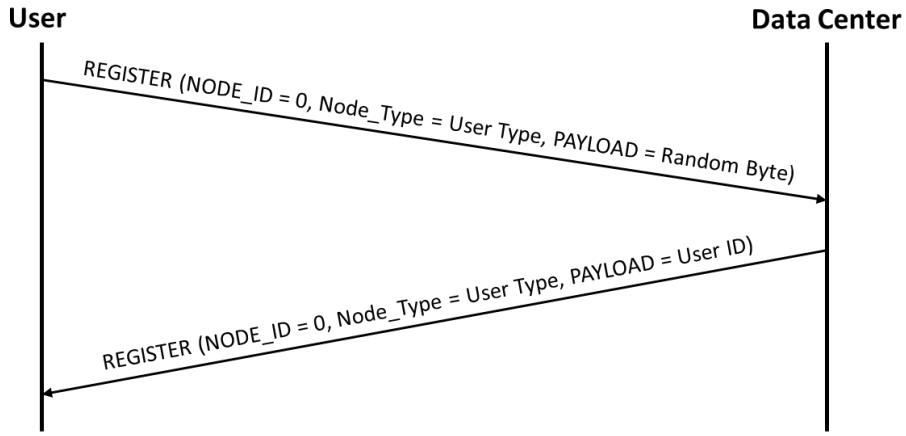

Figure 4.6. Message exchange in the User registration phase.

4. **Data acquisition phase:** The nodes of the cluster gather the data from the sensors. The sensing nodes send the data to the Cluster Head for its latter transmission to the data center. The system enters this phase more regularly than the Data transmission phase. Depending on the activities performed by the node, it can vary from minutes to hours.

According to the NODE_TYPE, the payload of the DATA message is different. The bits required for each of the parameters are the minimum size necessary according to the resolution required for the calculations. This way, the size of the message is reduced as much as possible while ensuring the desired functioning of the system. The P flag of this DATA message is set to 0. The message exchange for this phase is presented in Figure 4.7. No Acknowledgement (ACK) are forwarded to reduce energy consumption. Instead, The CH has a Reception Timeout to assess if the messages from the Monitoring Nodes have been received within the expected time. This is a parameter that is configured at the establishment of the network. When the Reception Timeout is reached, a DATA message is forwarded to the Monitoring Node with a Payload of 1 bit set to 1 (See Figure 4.8).

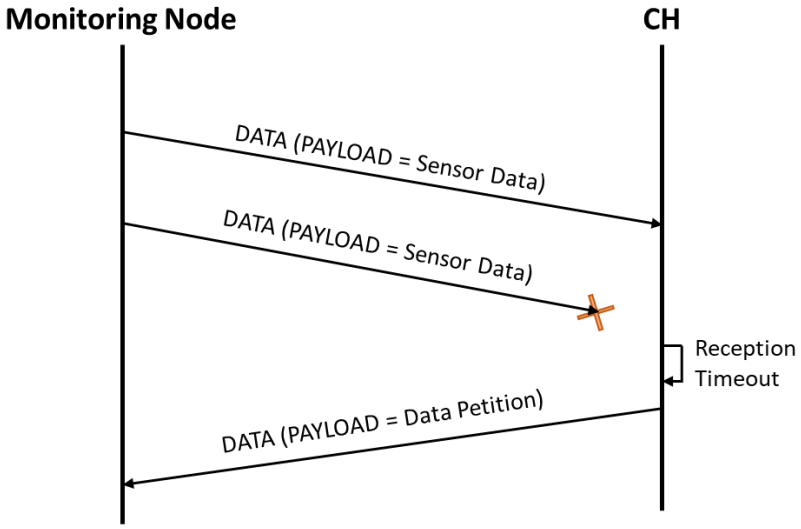

Figure 4.7. Message exchange for the Data Acquisition phase.

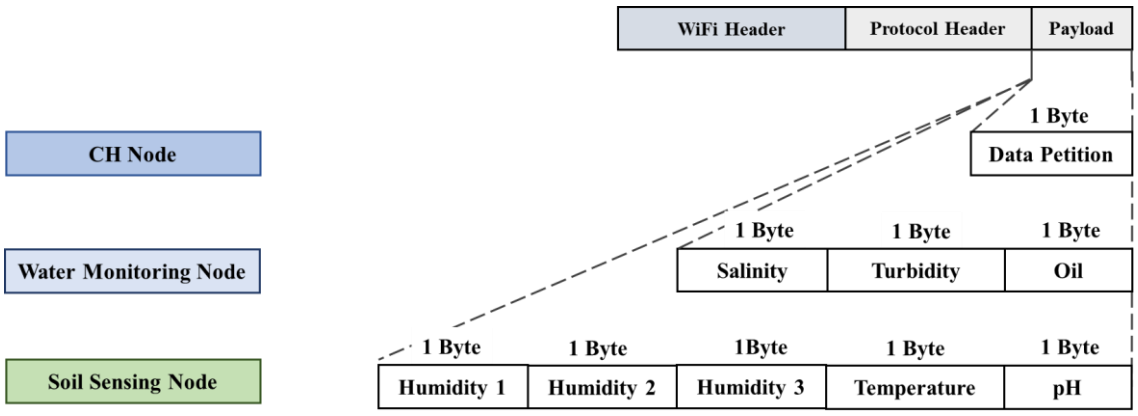

Figure 4.8. Payload format of the Data messages at the Data transmission phase.

5. **Data transmission phase:** The nodes start gathering the data from the sensors. This data is stored on an SD card. Then, all the local analysis is performed, and the data is transmitted to the specified node. For the Cluster Heads, the data from the sensor nodes is aggregated and forwarded to the gateway. If any alerts arise during this phase, then an alert notification is forwarded. There are different types of alerts. This phase is entered when a notification occurs and once a day to forward the data stored in the SD card. Unless it is a message with priority, the information is forwarded to the Data Center once a day. The message exchange for the Data Transmission phase is shown in Figure 4.9.

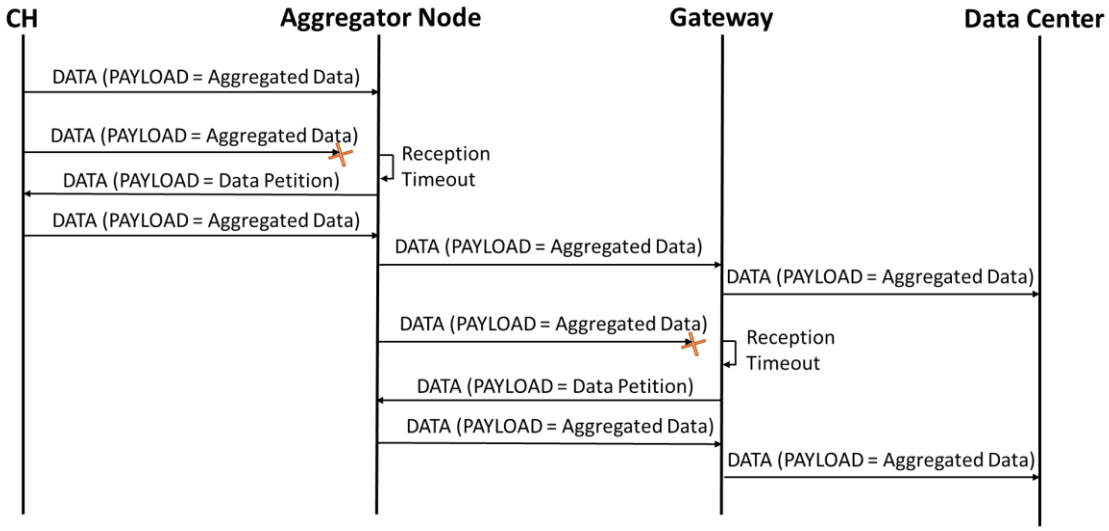

Figure 4.9. Message exchange for the Data Transmission phase.

6. **Action phase:** Once the data reaches the data center, it is stored and processed using AI based on a dataset of preestablished values of the correct performance. With the correct performance in mind, decisions are taken throughout the performance time. When actions are required, the specific action is forwarded to the actuator nodes.

The message ACTION is forwarded from the Data Center to the Actuator Node (See Figure 4.10). The payload of the ACTION message is the new values of the Actuator Node, such as an open or closed gate. The Actuator Nodes of the Canal Area are LoRa Class B nodes so they can receive an ACTION message when necessary, with a latency below 30 seconds, which is an acceptable latency for our system. The Actuator Nodes of the Field area are LoRa Class A nodes. As the calculations for the amount of water needed for irrigation are performed for the next day, the Actuator Node will forward an empty DATA message so it can receive any queued ACTION messages from the Data Center. The Aggregator Node will discard the empty DATA message and forward the ACTION message.

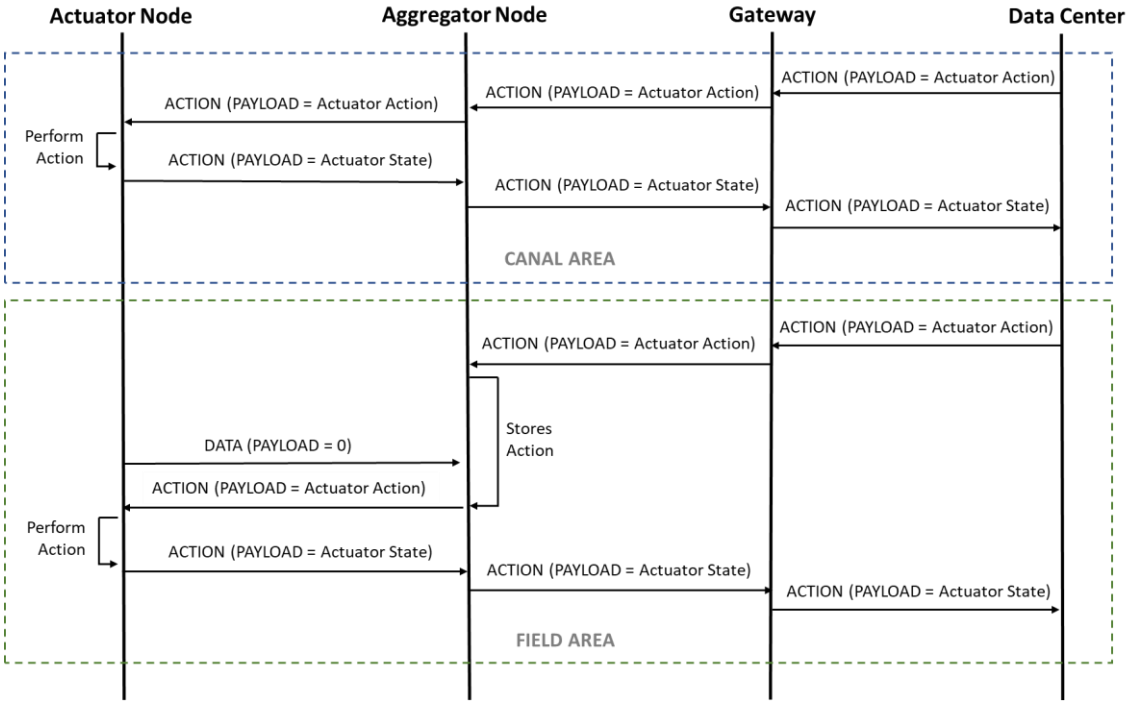

Figure 4.10. Message exchange for the Action phase.

7. **Alert phase:** When the system receives an alert notification, the system processes the notification and determines the action that has to be taken to solve the problem. Depending on the type of alert, the action that has to be taken by the element of the network that has reported the alert will be forwarded. The alert messages have priority over the rest of the messages. Therefore, if an alert is received, the node will send the alert before continuing with sending other information. There are different types of alert messages according to the detected problem.

a. **Pollution detected:** When the water is contaminated, an alert message is forwarded to the data center and the user that has access to the information of the nodes in the canal area. The data center will decide the necessary action and forward it to the actuators that need or take the action. This alert generates a response from the Data Center as described in the Action phase.

When pollution is detected in the water, a POLLUTION message is forwarded to the Data Center (See Figure 4.11). The payload of this message is the measured pollution levels. The Data Center uses this information to determine the required action. Furthermore, the priority messages need to be acknowledged to ensure the message has been received. The acknowledgment is done by forwarding a message with the same header as the POLLUTION message and the payload set to 0.

b. **High salinity levels detected:** When high salinity is detected, a SALINITY message is sent to the Data Center (See Figure 4.11). The payload of this message is the salinity levels detected by the node that sends the alert. The message is acknowledged by a message with the same header and the payload set to 0. Then, a decision is taken to modify the amount of irrigation water so the salinity levels of the soil, resulting from the irrigation, are reduced in comparison

to those that would result from taking no action. This alert generates a response from the Data Center as described in the Action phase.

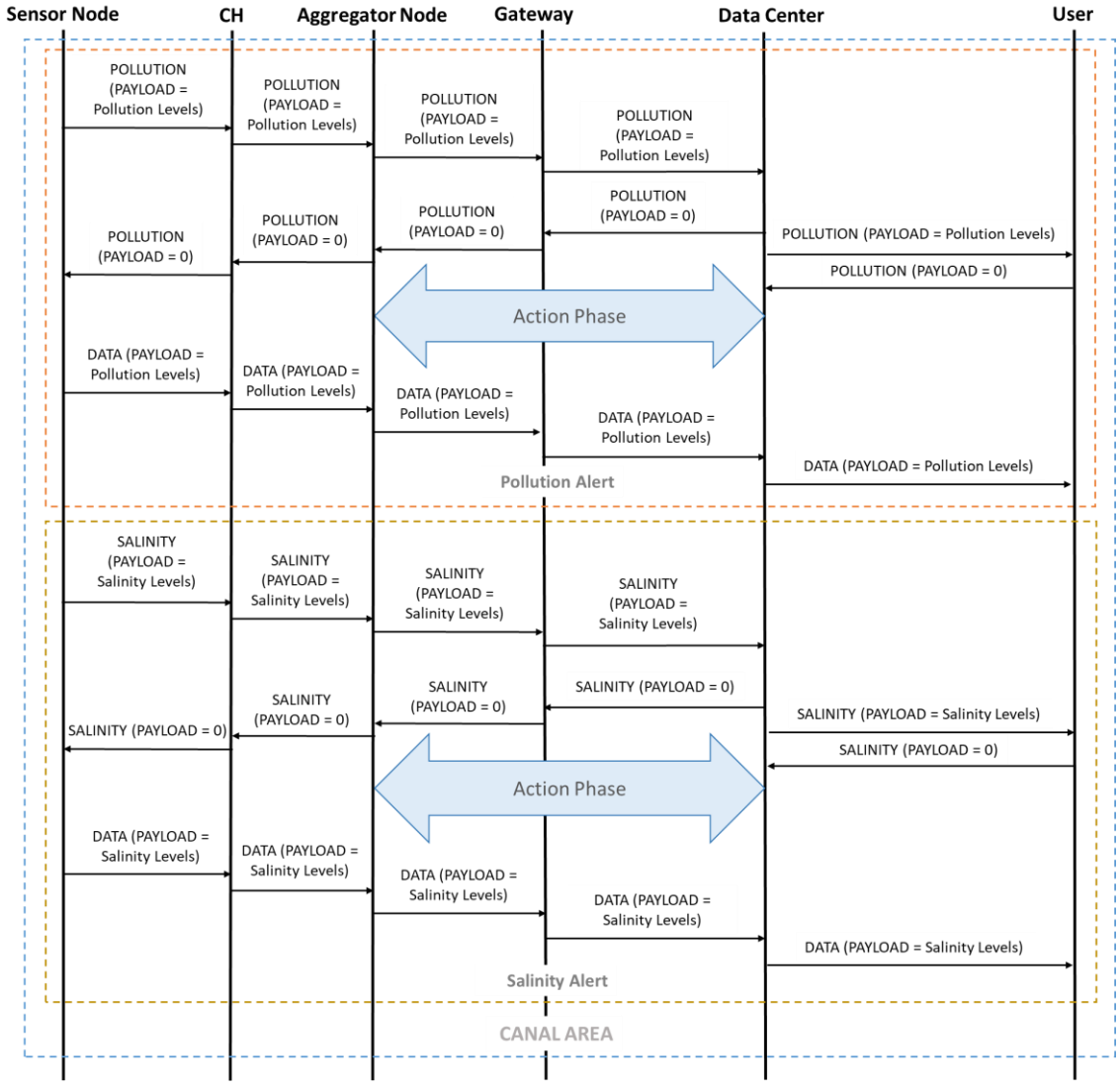

Figure 4.11. Message exchange for the Pollution and the Salinity alerts.

c. **Cluster Head node is not operative:** When the Cluster Head Node is detected to be down, the system generates an IS_DOWN message to notify the user (See Figure 4.12). The message is acknowledged with an IS_DOWN message with the payload set to 0. The sensing nodes that send their data to the Cluster Head will store the information on their SD card until the CH node is replaced.

This message is forwarded from the Aggregator Node to the Data Center when the Aggregator Node detects that no messages are received from the CH Node. Therefore, the NODE_ID of the message is the ID of the Aggregator Node and the payload of the message is the NODE_ID of the CH Node.

d. **Sensing node is not operative:** The CH node sends an IS_DOWN message to notify the user and continues with its operation (See Figure 4.12). The payload of the IS_DOWN message is the NODE_ID of the Sensing Node. For the acknowledgment of the message, the payload of the message is 0. If decisions need to be taken, the CH will only consider the operative nodes.

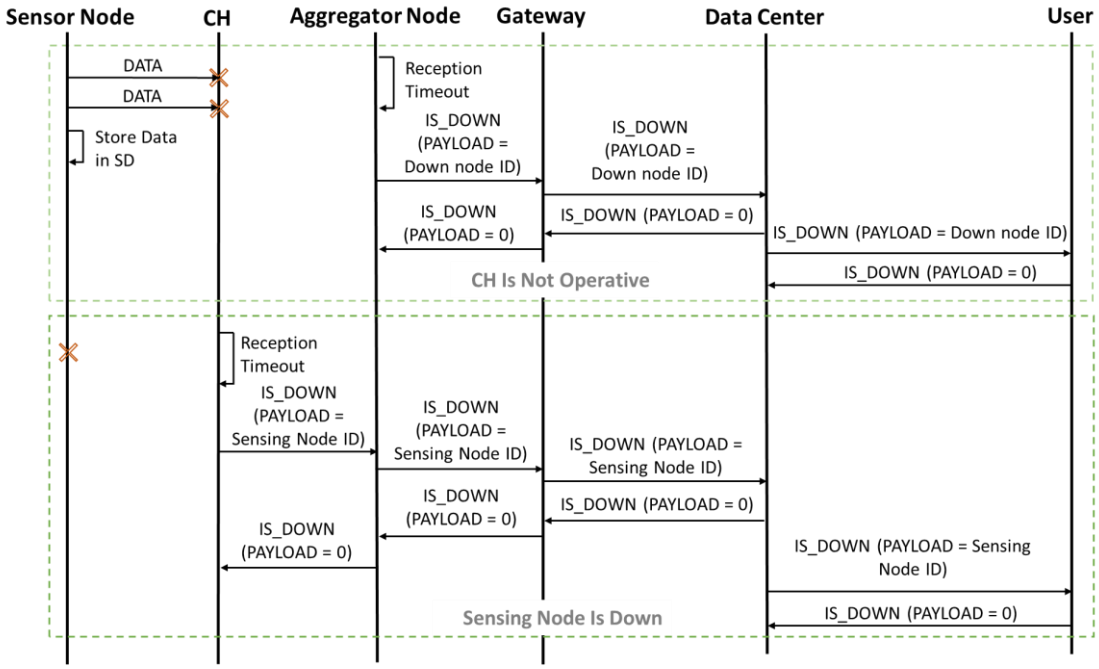

Figure 4.12. Message exchange for the CH is not operative and the Sensing node is down alerts.

e. **Actuator node is down:** The gateway sends an IS_DOWN message to the Data Center and to the Actuator Node of the next canal to operate as indicated by the sensing nodes of the previous canal (See Figure 4.13). The payload of the IS_DOWN message is the NODE_ID of the broken Actuator Node. For the IS_DOWN acknowledgment, the payload of the message is 0. In case of malfunctioning, the water will always go through the biosorption process to ensure water quality.

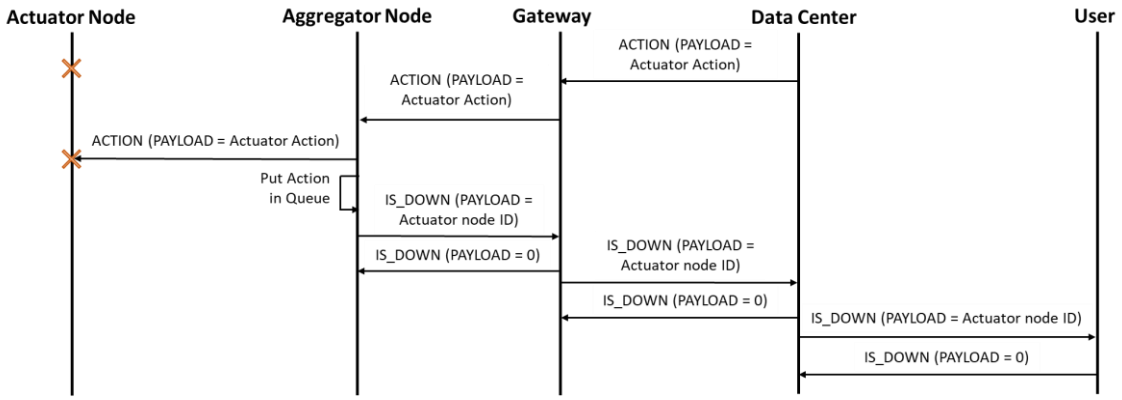

Figure 4.13. Message exchange for the Actuator node is down alert.

f. **Aggregator node is down:** If the Aggregator Node is down, the Gateway will generate an IS_DOWN message and send it to the Data Center, which will send the IS_DOWN message to the user for the node to be repaired (See Figure 4.14). The message is acknowledged by an IS_DOWN message with a payload of 0. Then, The Cluster Head nodes will store the data until the Aggregator node is active again. As the CH nodes cannot receive any decision from the data center, the nodes will decide if the water needs to go through the biosorption process locally. On the field area, the last irrigation schedule provided by the data center is maintained.

g. **The gateway node is down:** If the Gateway Node is down, the clusters and the Aggregator Node will perform fog computing and make independent decisions based on the information gathered up to the gateway being down (See Figure 4.14). When the Gateway is operative, the stored data is forwarded, and the decision process is again performed by the data center. If there is more than one gateway, the Aggregator Nodes and the Actuator Nodes will forward the data to the available Gateway. When the Data Center detects that the Gateway Node is down and sends an IS_DOWN notification to the User with the ID of the Gateway for the User to replace it.

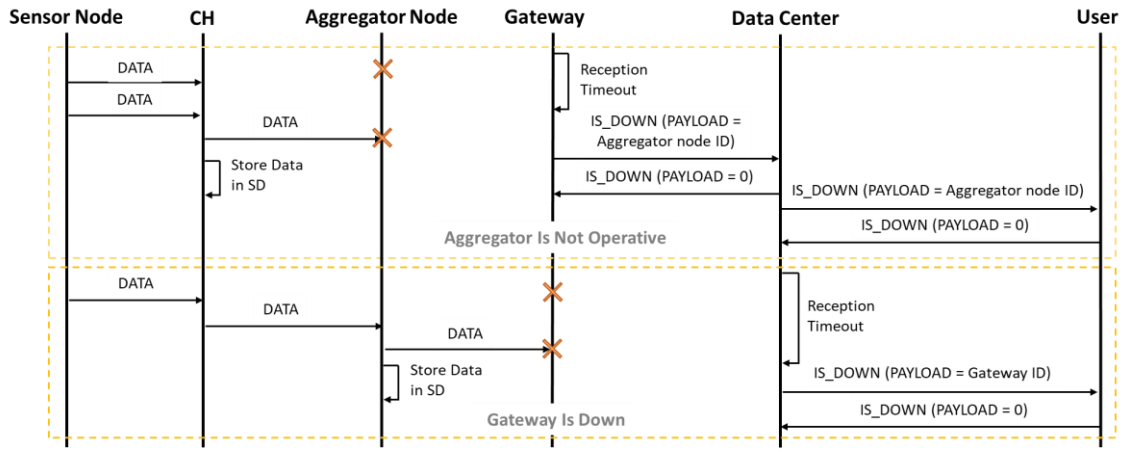

Figure 4.14. Message exchange for the Aggregator node is down and the Gateway is down alerts.

h. **Node with low battery:** If the energy harvesting system of the node is malfunctioning and the node detects a low battery or the battery is malfunctioning and it is not charging, a LOW_BATTERY notification is forwarded to the Data Center, which conveys the notification to the user (see Figure 4.15). If there is enough energy available, the node will forward all the stored data. The node will continue functioning until the battery expires. The node of the layer above will store the data of the node with a low battery until it is down. This problem may be caused by weather conditions damaging the node, or elements blocking the solar panel, such as soil or leaves.

Unlike the IS_DOWN message, the LOW_BATTERY message is forwarded by the node with the problem and thus, the payload of this message is 1 as the NODE_ID in this message is that of the node with a low battery. Furthermore, the message is acknowledged with a message with the same message and the payload set to 0. However, if bad weather conditions were detected by the Meteorology Node and the LOW_BATTERY message is received, the message forwarded to the User by the Data Center will indicate this aspect in its payload.

i. **Malfunction detected:** If the node detects a malfunction in one of its elements, a MALFUNCTION message is forwarded to the Data Center as specified in the Verification phase (See Figure 4.15). A message with the same header and the payload set to 0 is forwarded as an acknowledgment.

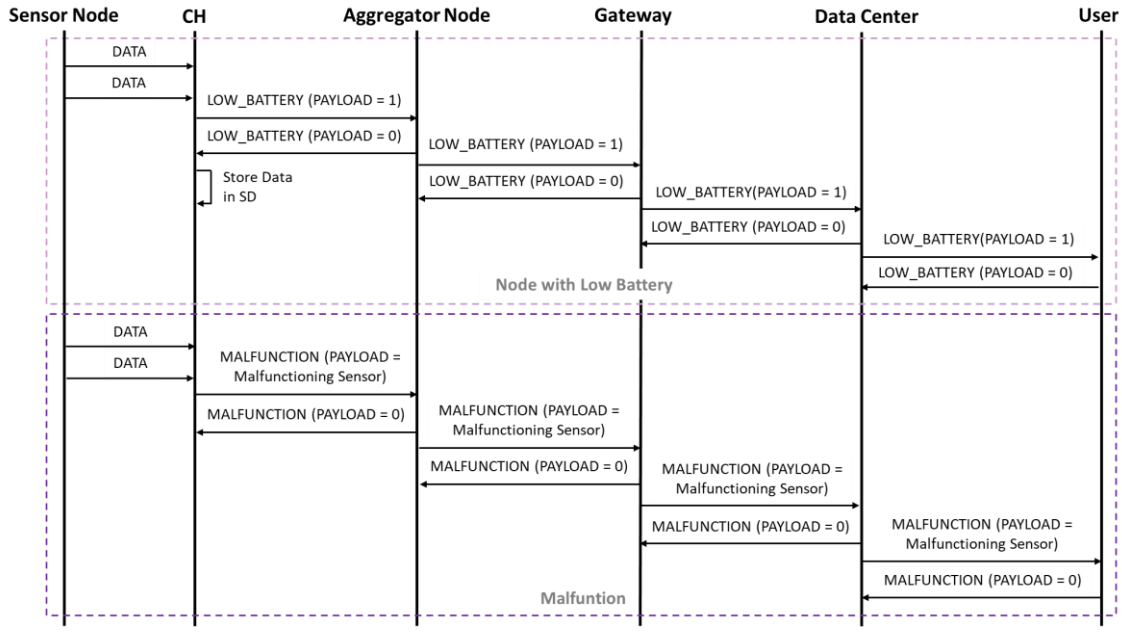

Figure 4.15. Message exchange for the Node with Low Battery and the Malfunction alerts.

j. **Data center down:** This is not a habitual problem as data centers have backup systems. However, if the data center is not a hired service from a service provider and it is a server created by the user, it is possible for it not to have a backup and the data center could be susceptible to blackouts, failures of the equipment, and accidents such as fires. In case this problem arises, the User application will notify the User that the Data Center cannot be accessed. Furthermore, The Aggregator Node will perform fog computing and make independent decisions based on the information gathered up to the Data Center being down. This way, the system can operate independently until the Data Center is running again.

k. **User not available:** If the user is not available, the system will function in an autonomous manner. The notifications intended for the User will be queued at the Data Center until the User is active again.

4.3 States of the nodes

According to the varied nodes and the functionalities they have, the states of the nodes are different.

The Gateway and the Aggregator node can have four states (See Figure 4.16):

- Activation state: This is the first state. The nodes send the REGISTER message to the data center and receive their Node ID.
- Verification state: This state is reached for the first time after the activation state. The node verifies the correct functioning of its elements and the correct communication with its neighbors. If any malfunctions are detected, a report is forwarded to the data center. If all the elements of the node work properly, no message is forwarded. This state can be accessed again by request of the data center or the user.
- Data transmission state: The nodes send DATA messages to the Data Center with the information received from the Sensing and CH nodes.
- Alert state: This state is reached when the node detects a malfunction either on its elements or when communicating with other nodes. The forwarded messages are detailed in the Alert phase in the previous section.

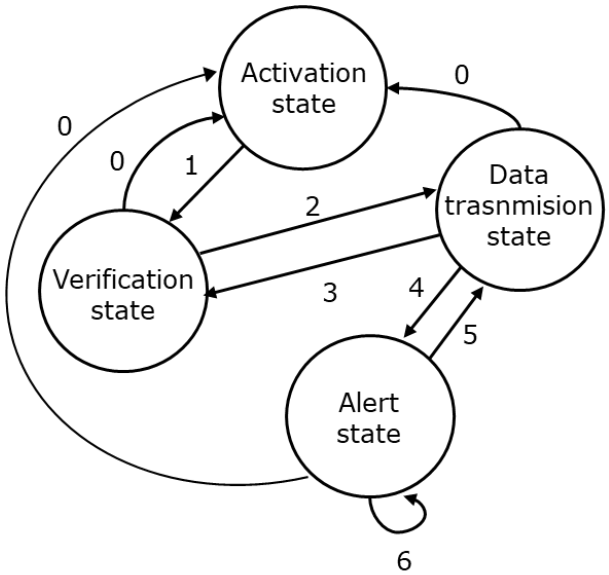

Figure 4.16. States of the Gateway and Aggregator nodes.

Events are detailed as follows:

- **Event 0:** This event occurs when the node has a failure or when it reboots.
- **Event 1:** This event happens when the Activation process where the connection is established has been completed.

- **Event 2:** This event happens when the node verifies its correct functioning.
- **Event 3:** This event occurs when verification of correct functioning is requested from the Data Center or the User.
- **Event 4:** This event happens when an alert is detected.
- **Event 5:** This event occurs when the node finishes communicating the alert.
- **Event 6:** This event happens when the alert is not solved, and the alert is related to a failure that inhibits communication with other nodes.

The Actuator has three states (See Figure 4.17):

- Activation state: This is the first state. The Actuator sends the REGISTER message to the data center and receives their Node ID.
- Verification state: This state is reached for the first time after the activation state. The node verifies the correct functioning of its elements. If any malfunctions are detected, a report is forwarded to the data center. If all the elements of the node work properly, no message is forwarded. This state can be accessed again by request of the data center or the user.
- Action state: This state is reached when the Actuator receives an action. Then, the Actuator performs the action and forwards a message with the current state of the Actuator.

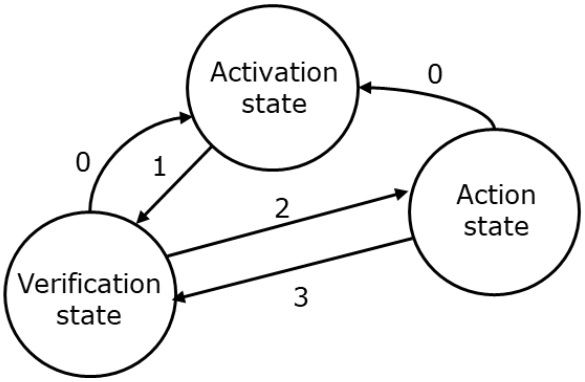

Figure 4.17. States of the Actuator nodes.

Events are detailed as follows:

- **Event 0:** This event occurs when the node has a failure or when it reboots.
- **Event 1:** This event happens when the Activation process where the connection is established has been completed.
- **Event 2:** This event happens when the node verifies its correct functioning.
- **Event 3:** This event occurs when verification of correct functioning is requested from the Data Center or the User.

The Sensing nodes have four states (See Figure 4.18):

- Activation state: This is the first state. The nodes send the REGISTER message to the data center and receive their Node ID.
- Verification state: This state is reached for the first time after the activation state. The nodes verify the correct functioning of their elements. If any malfunctions are detected, a report is forwarded to the data center. If all the elements of the node work properly, no message is forwarded. This state can be accessed again by request of the data center or the user.
- Data acquisition state: The nodes send DATA messages to the CH node with the information obtained from the sensors.
- Alert state: This state is reached when the node detects a malfunction on its elements. The forwarded messages are detailed in the Alert phase in the previous section.

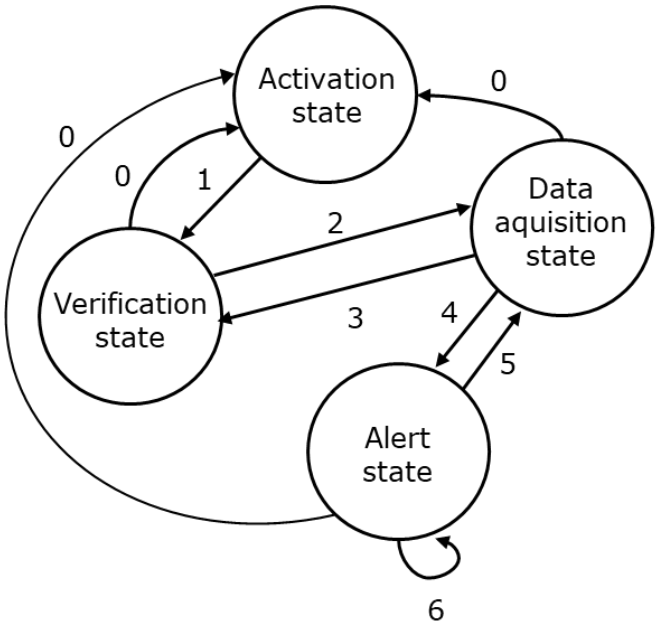

Figure 4.18. States of the Sensor nodes.

Events are detailed as follows:

- **Event 0:** This event occurs when the node has a failure or when it reboots.
- **Event 1:** This event happens when the Activation process where the connection is established has been completed.
- **Event 2:** This event happens when the node verifies its correct functioning.
- **Event 3:** This event occurs when verification of correct functioning is requested from the Data Center or the User.
- **Event 4:** This event happens when an alert is detected.

- **Event 5:** This event occurs when the node finishes communicating the alert.
- **Event 6:** This event happens when the alert is not solved, and the alert is related to a failure that inhibits communication with other nodes.

The CH nodes and the Meteorology Monitoring Aggregator node have five states (See Figure 4.19):

- Activation state: This is the first state. The nodes send the REGISTER message to the data center and receive their Node ID.
- Verification state: This state is reached for the first time after the activation state. The node verifies the correct functioning of its elements and the correct communication with its neighbors. If any malfunctions are detected, a report is forwarded to the data center. If all the elements of the node work properly, no message is forwarded. This state can be accessed again by request of the data center or the user.
- Data acquisition state: The nodes obtain the data from the sensors.
- Data transmission state: The nodes send DATA messages headed to the Data Center with the information received from the Sensing nodes and the information gathered from its sensors.
- Alert state: This state is reached when the node detects a malfunction either on its elements or when communicating with other nodes. The forwarded messages are detailed in the Alert phase at the previous section.

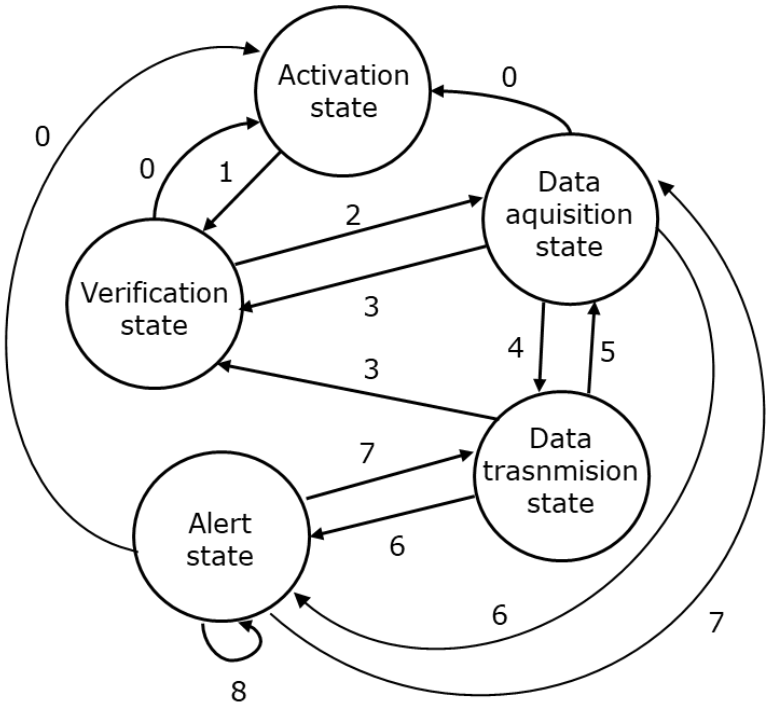

Figure 4.19. States of the CH nodes and the Meteorology Monitoring Aggregator node.

Events are detailed as follows:

- **Event 0:** This event occurs when the node has a failure or when it reboots.
- **Event 1:** This event happens when the Activation process where the connection is established has been completed.
- **Event 2:** This event happens when the node verifies its correct functioning.
- **Event 3:** This event occurs when verification of correct functioning is requested from the Data Center or the User.
- **Event 4:** This event happens when the node needs to transmit data.
- **Event 5:** This event occurs when the node finishes forwarding the queued information.
- **Event 6:** This event happens when an alert is detected.
- **Event 7:** This event occurs when the node finishes communicating the alert.
- **Event 8:** This event happens when the alert is not solved, and the alert is related to a failure that inhibits communication with other nodes.

4.4 Conclusions

In this chapter, a heterogeneous communication protocol for a precision agriculture system was presented. The protocol designed to communicate devices that employ WiFi and LoRa communication technologies has low overhead with a header of only 2 Bytes. The format of the header and the messages has been specified. Furthermore, the different messages and the message exchange between the varied elements of the architecture have been specified. Lastly, the states of the nodes have been detailed. The performance of the protocol will be further explained in Chapter 7 section 7.2.

Chapter 5

Study Cases

5.1 Introduction

There are specific needs of PA systems that require specific designs to address those needs. In this chapter, different functionalities for the main architecture and for the specific architectures presented in Chapter 3. Firstly, a multi-layer fog computing framework for architecture presented in subsection 3.2.1, and the topology presented in subsection 3.2.2 is described. Then, a protocol for a PA system with a wireless network comprised entirely of LoRa nodes is designed. After that, the security aspects of LoRa networks are analyzed and the security actions to be taken are proposed. The case of heterogeneous WiFi/3G networks and how to provide fault-tolerance and energy-saving functionalities is proposed as well. Furthermore, the use of CoAP for IEEE 802.11 networks for PA is discussed. Lastly, the use of drones for the data acquisition of WiFi nodes deployed on the fields is addressed.

5.2 Multi-layer fog computing framework for constrained LoRa networks

In this section, our multi-layered fog computing proposal for the precision agriculture and irrigation water quality monitoring system described in Chapters 3 and 4 is presented.

The deployment of the water quality monitoring system for irrigation purposes and the precision agriculture system is presented in Figure 5.1. The Canal Area is comprised of a series of subcanals in a comb shape where the biosorption process for water purification is performed. The Field Area is where the fields are situated. These fields can be further divided into different zones to apply different processing to each of the areas and have a more detailed overview of the state of the plants. The Urban Area is the zone where the Gateway is located and connected to the Data Center. There are clusters of sensing nodes at each subcanal and deployed on each zone of the fields, with a cluster head for each cluster. Actuator nodes are deployed as well at each subcanal to manage the gates to the biosorption process and to control the amount of water for the irrigation of the fields. Furthermore, the cluster head forwards the data to the aggregator of their Area. Then, the aggregator forwards the data to the Gateway destined to the Data Center. The CH nodes and Actuators at each Zone are detailed in Table 5.1. The system is scalable, and more zones can be added when necessary. If monitoring more fields is necessary, more gateways could be added so that the data transmission is divided into the deployed gateways and a bottleneck scenario is avoided.

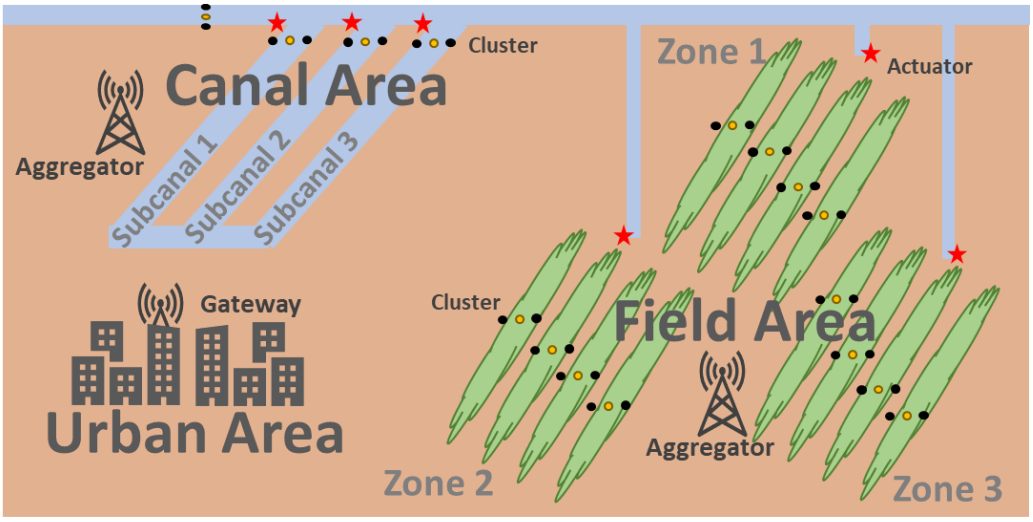

Figure 5.1. Water quality monitoring and precision agriculture system.

The topology of the system is presented in Figure 5.2. It is comprised of the following layers:

- Layer 1: The first layer is the layer comprised of the sensor and actuator nodes. These devices forward all data to the next layer and do not perform any computations. The data acquisition is performed at different frequencies depending on the selected settings. These settings are the Research Mode, the Advanced Farmer Mode, and the Regular Farmer Mode. Table 5.2 presents the characteristics of each mode. For the case of the actuators, the actions are performed when the message with the new action is received. Then, a message with the new state of the actuator is forwarded to the data center.

Table 5.1. CH nodes and Actuator nodes at each Zone.

Zone	**CH**	**Actuator**
Main canal	CH 1 Canal Area	Actuator Node 1 &2
Secondary Canal 1	CH 2 Canal Area	Actuator Node 3 &4
Secondary Canal 2	CH 3 Canal Area	Actuator Node 5 & 6
Secondary Canal *n*	CH *n*+1 Canal Area	Actuator Node 2*n*+1
Biosorption Output	CH *n*+2 Canal Area	Actuator Node 2*n*+2
Field Area Zone 1	CH 1 Field Area	Actuator Node Field Area 1
Field Area Zone 2	CH 2 Field Area	Actuator Node Field Area 2
Field Area Zone *m*	CH *m* Field Area	Actuator Node Field Area *m*

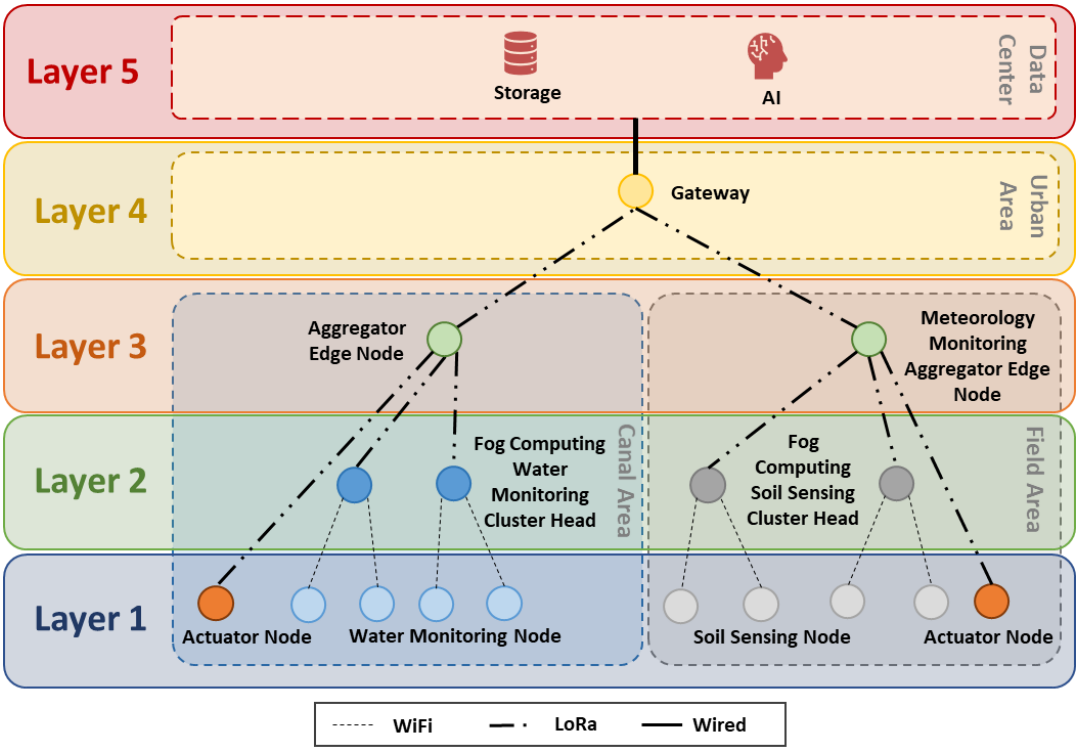

Figure 5.2. Multi-layered fog topology of the precision agriculture and irrigation quality monitoring system.

Table 5.2. Data forwarding and aggregation settings.

Settings	**Data Acquisition Frequency**	**Data Aggregation**	**Data Forwarding Frequency**
Research Mode	10 minutes	Data driven aggregation at layer 2	4 times a day + Alerts
Advanced Farmer Mode	30 minutes	Data driven aggregation at layer 2 and layer 3	2 times a day + Alerts
Regular Farmer Mode	1 hour	Data driven aggregation at layer 2 and layer 3	Once a day + Alerts

- Layer 2: This layer is comprised of the Cluster Head nodes. These nodes receive the data from the sensing nodes and perform the first data aggregation process detailed by the Algorithm 5.1. For the Canal Area, these nodes evaluate the quality of the water by considering the values obtained by all the nodes at the cluster. The CH node receives the turbidity or salinity levels from the sensor nodes of the cluster. The outlier values are discarded. This is performed by calculating the variance σ_i^2 and determining if it surpasses the Th_{sigma2} threshold. Then, the CH compares all the received values using the $C_{Positive-var}$ variable to obtain a final result of the salinity or turbidity levels of the water. If the turbidity or salinity surpasses the $Th_{variable}$ threshold, an alarm is forwarded to the next layer. For the case of the CH nodes of the field area, the same process is performed with soil moisture and soil salinity. That way, the Aggregator nodes at layer 3 and the Data center are able to determine if the variations in the calculations due to water stress or salinity should be applied when determining the necessary amount of water for irrigation.
- Layer 3: This layer is comprised of the Aggregator nodes. These nodes receive the data from each of their areas, being the canal area or the field area. This node performs the decision-making process that determines the actions of the actuator of their areas. In the case of the canal area, the Aggregator node sends a message to the actuator node of the specific canal to open or close the gates. At the field Area, The Aggregator node calculates the water requirements for a time frame of one month and forwards the actions to the Actuator when irrigation is required. The data exceeding the time frame of one month is deleted from the storage system of the Aggregator node. The data is aggregated as detailed in Algorithm 5.2 and forwarded to the data center when the data forwarding timer is reached so the user can access the history of all the variables. According to the state of the actuators in the Canal Area and the selected settings, the amount of data forwarded to the data center varies.

Algorithm 5.1. Data Aggregation at layer 2

1) Gather data from the sensors of the CH node
2) Receive the data from the *n* sensors of the cluster
3) **for** each variable *var* **do**
4) **for** each node *i* in the cluster **do**
5) $\sigma_i^2 = \frac{\sum_1^j (s_j - s_i)^2}{n}$
6) **if** $\sigma_i^2 > Th_{sigma2}$ **then**
7) Discard data from sensor *i*
8) **end if**
9) **If** $V_i > Th_{variable}$ **then**
10) $C_{Positive-var} = C_{Positive-var} + 1$
11) **end if**
12) **end for**
13) **if** $C_{Positive-var} \geq {}^{3n}/_{2}$ **then**
14) Add the average of the value for the variable V_{Avg} to *Alert-Payload* string
15) **else if** $V_{Avg} > Th_{variable}$ **then**
16) Add the average of the value for the variable V_{Avg} to the *Alert-Payload* string
17) **else**
18) Store aggregated data V_{Avg}
19) **end if**
20) **end for**
21) **if** there is data on the *Alert-Payload* string **then**
22) Send Alert message with the content of *Alert-Payload*
23) **end if**
24) **if** timer for data forwarding has been reached **then**
25) Forward stored aggregated data
26) **end if**
27) **End**

- Layer 4: This layer is comprised of the gateway. This node will store all the data in the rare case the Data Center or the connection to the data center is down. This layer does not perform data aggregation nor performs computing as all the necessary data aggregation and computation have been performed on the lower layers.
- Layer 5: This layer is comprised of the Data Center. The data center stores all the data and processes the information to perform analysis and predictions on water quality, water requirement, and quality of the soil, among others.

By providing a multi-layered fog computing functionality to the topology of the water quality monitoring and precision agriculture system, the obtained benefits are twofold. On the one hand, it provides the system with fault-tolerance capabilities by providing autonomy to each of the layers of the topology in case any of the elements of the network gets damaged or stops functioning and the decision made at the Data Center cannot be forwarded. This is a key aspect considering the tree topology of the system.

Algorithm 5.2. Data Aggregation and decision-making at layer 3

```
1)  Update Actuator decision making rules from the Data Center
2)  Receive data from the devices in layer 2.
3)  Receive Actuator State
4)  if Canal Area Alert received then
5)      Forward Action message to the required actuator so as to open the gates of the
    biosorption canal closest to the CH node that activated the alarm
6)      Forward Alert message destined to the Data Center
7)  end if
8)  if Field Area Alert received then
9)      Store Alert for further processing
10)     Forward Alert Message destined to the Data Center
11) end if
12) if data_forwarding_timer is reached then
13)     if Research Mode then
14)         if all gates are closed then
15)             Add the data from the Main Canal to the Payload string
16)         else
17)             Add data from all CH nodes at canal area to the Payload string
18)         end if
19)         Add data of the CH nodes at the field area to the Payload string
20)     else if Farmer Mode then
21)         Add data of the Main Canal and the Biosorption Output to the Payload
22)        for each field area do
23)          for each Zone at Field area do
24)            Calculate average of the variables measured by all CH nodes at the same zone
25)          end for
26)         end for
27)         Add average data of the field zones to the Payload
28)     end if
29)     Forward message with the data stored at the Payload string
30) end if
31) If water_requirement_calculation_timer is reached then
32)     For each zone in field area do
33)         if water_stress alert && Salinity alert received then
34)             Calculate water requirements with water-stress and salinity modifications
35)         else if water_stress alert received then
36)             Calculate water requirements with water-stress modifications
37)         else if Salinity alert received then
38)             Calculate water requirements with salinity modifications
39)         else
40)             Calculate water requirements
41)         end if
42)         if irrigation_day is true then
43)             Forward Action message to the actuator nodes of each area with the amount of
    water needed for the next irrigation
44)         end if
45)     end for
46) end if
47) End
```

On the other hand, it reduces the energy consumption by filtering the data and limiting the number of messages that are forwarded to the data center. This reduction in data and messages also helps to reduce the collisions that may be caused when different LoRa nodes transmit at the same time. It also allows the system to meet the duty cycle requirements of LoRa.

5.3 Protocol design for LoRa nodes

In this subsection, a protocol for a water quality monitoring system comprised by nodes that communicate through LoRa is presented.

The proposed protocol, as can be seen in Figure 5.3, is divided into four fundamental phases, which are: Discovering Neighbors, Send Data, Storage and Data Processing, and Action. As its name suggests, in the Discovering Neighbors phase, the different sensor nodes send wireless signals to discover the nodes that are part of the group. Then, the sensor nodes determine the Central Node, and the Central Node identifies the gateway which is the Central Node in Urban Area 0. Therefore, a LoRa multi-hop network is established as in [318, 342].

Once the nodes are activated and their connection is established, they go into the Send Data phase. The different sensors that are connected to each node begin to measure their respective parameters. The data collection period has been set to take place every minute. If the observed data differ by an amount greater than a previously established threshold, the measurement is sent to the Central Sensor Node of the group, and this node will store the data and compare them to check if they exceed the alarm threshold. It also checks if the alarm has been detected by more than one of the sensors of the group in order to provide fault tolerance capabilities. In case of exceeding the alarm threshold, the data are forwarded to the Central Sensor Node of Urban Area 0. Then, it is forwarded to the central storage system in the data center. In case of not exceeding the alarm threshold, the data are stored in the Central Sensor Node of the group until all the data are sent every 24 h period. Every day, the Central Sensor Node of Urban Area 0 will send all data to the Storage Server through the wired network.

The next phase is responsible for making the decisions to correct anomalies. It is the Data Processing phase. In this phase, the data are sent from the Storage Server to the AI system. This system will be responsible for making the pertinent decisions that will be sent to the actuators.

Finally, during the Action phase, the operation that the AI system considers adequate to solve the problem detected by the sensors will be sent to the Actuator Nodes.

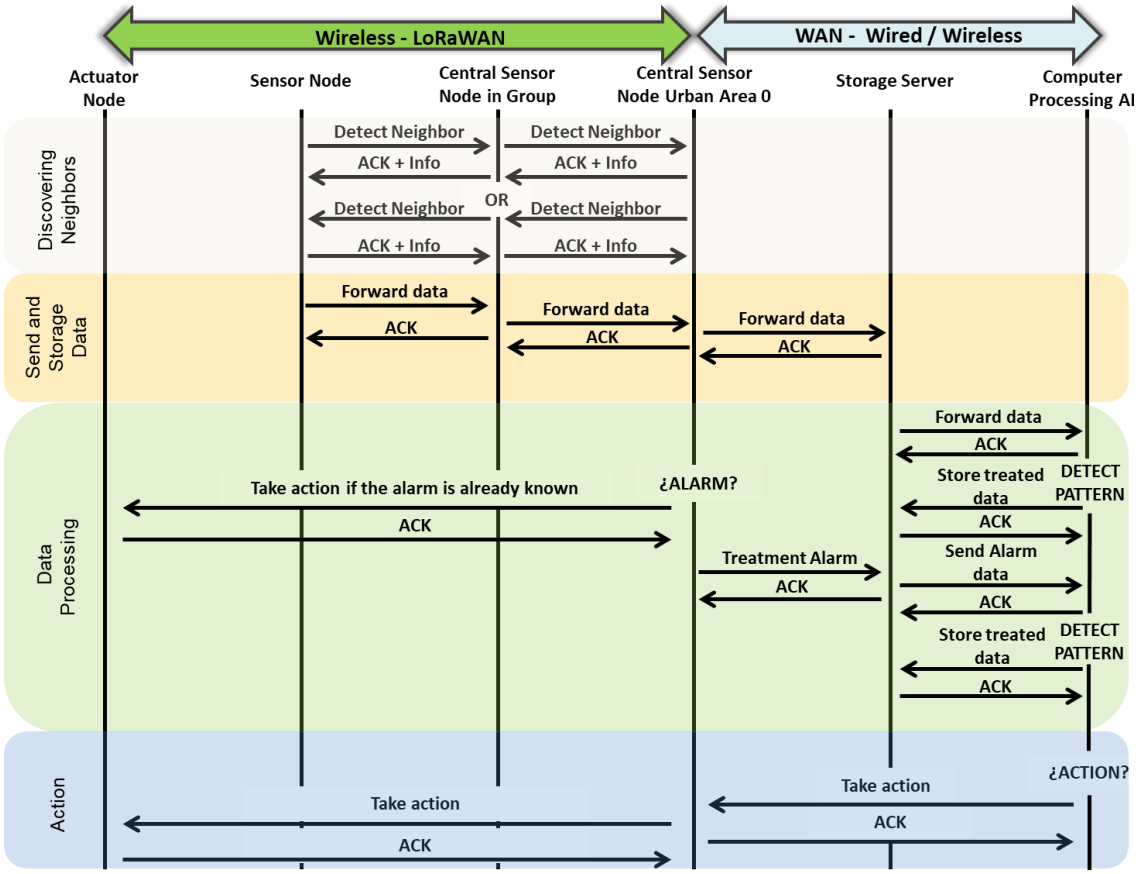

Figure 5.3. Proposed protocol.

The protocol stack is presented in Figure 5.4. As it can be seen, the Network Interface layer uses an ethernet protocol in the wired network, and a LoRaWAN protocol to perform wireless transmissions. The wired network is based on the stack defined by the TCP/IP reference model. IPv4 and IPv6 protocols are used in the Network layer. The protocols TCP and UDP are used in the Transport layer. Finally, the Application layer can use any protocol of this layer to implement the proposed system. On the other hand, for the wireless network, the physical layer utilizes the LoRa modulation. Then, the Medium Access Control layer utilizes LoRaWAN. Lastly, the Application layer employs the proposed protocol.

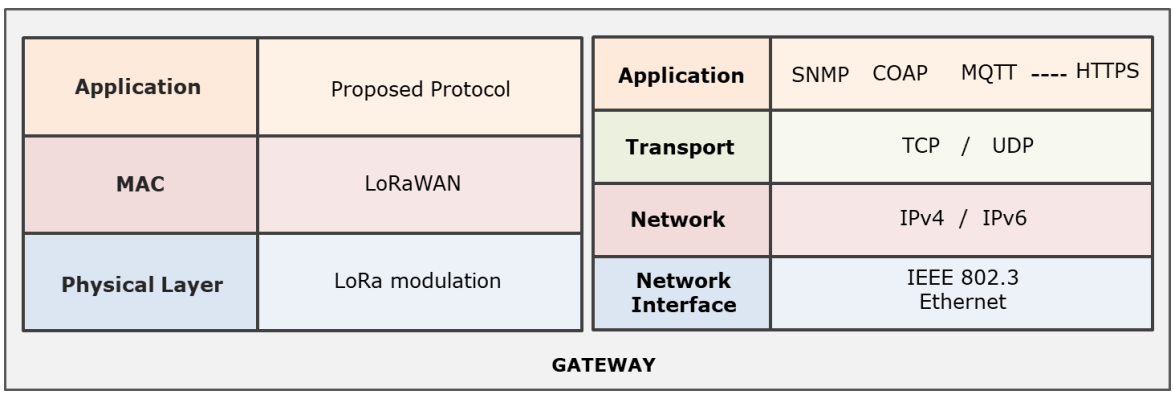

Figure 5.4. Protocol stack.

5.4 Comprehensive security framework for a LoRa network for wastewater treatment

In this subsection, a security framework for a LoRa network intended for a wastewater treatment system for irrigation is presented.

5.4.1 Overview of the system

As it can be seen in Figure 5.5, our system is distributed in different locations. In some of them, we have implemented groups formed by nodes that can contain sensors or actuators. Red circles with black dots inside identify groups of sensor nodes. The black dots of each circle represent a sensor node. Stars identify actuators nodes. The data is transmitted wirelessly using LoRaWan between all the nodes and among the node groups. Besides, there is a remote location, which will be reached through wired technology, where our data storage center and the equipment to carry out the work with AI are located.

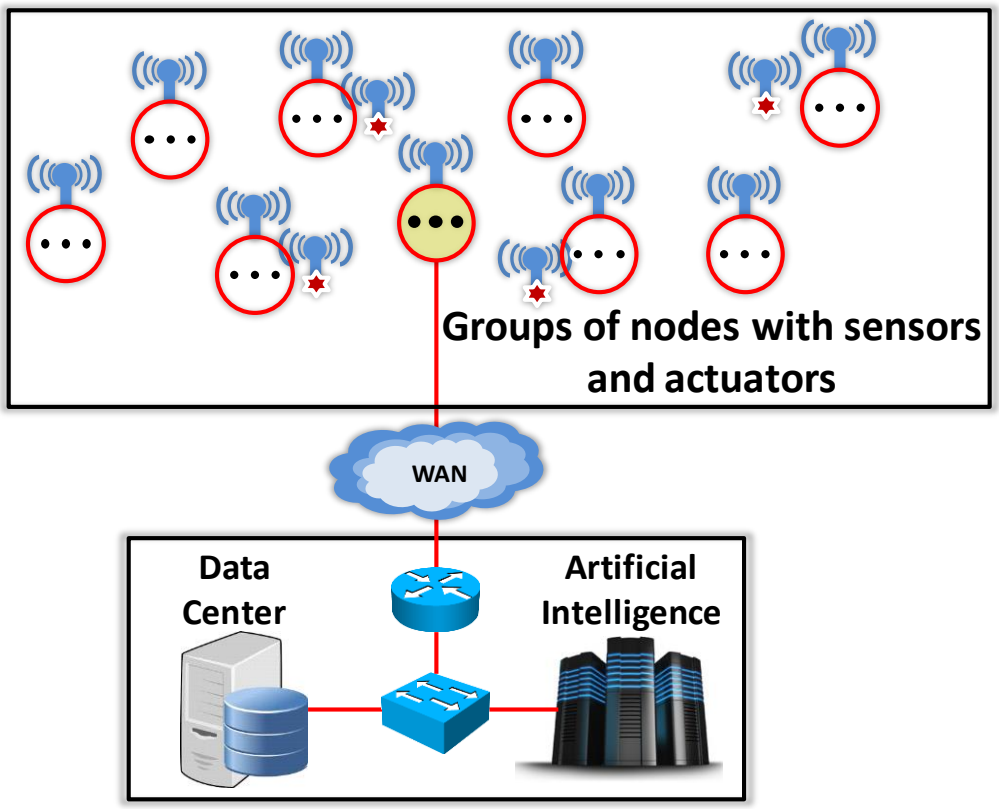

Figure 5.5. Location of devices and equipment.

Both the sensor nodes and the actuator nodes are distributed in external locations. For this reason, they will be protected by integrating them in watertight boxes to withstand water, weather variations, and possible animal attacks.

From one of the groups of nodes, that is located in an urban area, a WAN connection is established with the remote location through an Internet Service Provider (ISP). In the remote location, the network devices that are connected to the ISP and to the different available equipment are deployed. The Data Center and the equipment that utilizes AI to process the information collected by the sensors is deployed at the remote location as well. Behavior patterns will be detected through AI and decision rules will be applied in the actuator nodes according to the detected patterns.

The vulnerabilities of the systems to control water, which is performed through actuator nodes in our water management proposal, may compromise the objective of our system. Severe problems of both irrigation saturation and shortage as well as an unwanted lack of control of the water purification system may be generated. Furthermore, attackers may obtain the control of the nodes so as to perform massive attacks, which may affect the Internet.

5.4.2 Securing the system

For the system, it is paramount to guarantee the availability and accessibility to all the devices at any time.

In the report in [343], an attack on a water and wastewater treatment plant managed by an international company, the attackers compromised the internal network by launching an attack from a server located on the demilitarized zone (DMZ). It was discovered that the attackers performed the following steps:

- The DMZ server had been violated due to a bad policy that allowed establishing RDP connections.
- The server was violated and controlled through different IPs (Internet Protocol) by different attackers that were enemies to the company.

Those attackers performed more attacks on other plants of the same company.

All systems that manage information or provide a service are susceptible of being attacked. Irrigation and water management systems may not manage information that must remain private but ensuring the correct performance of the system is crucial. Furthermore, these systems are not only susceptible of attacks from people with malicious intentions but also may be affected by animals, weather conditions and people that accidentally compromise the system. The scenario where people is interested in controlling the waterflows of the canals according to their own interests is also possible.

The main problem with IoT devices is that they are not designed considering that their security is paramount in certain fields. Once the network security is established, it is important to perform a penetration test on the different components that comprise the system so as to verify the effectiveness of the solution.

In the next sections, we describe and propose the solutions for our system. Figure 5.6 shows the basic security scheme that we will implement on our system. The three network areas that we are going to utilize can be observed. They are the IoT network area, the ISP network area, and the network area of the data center and the AI equipment.

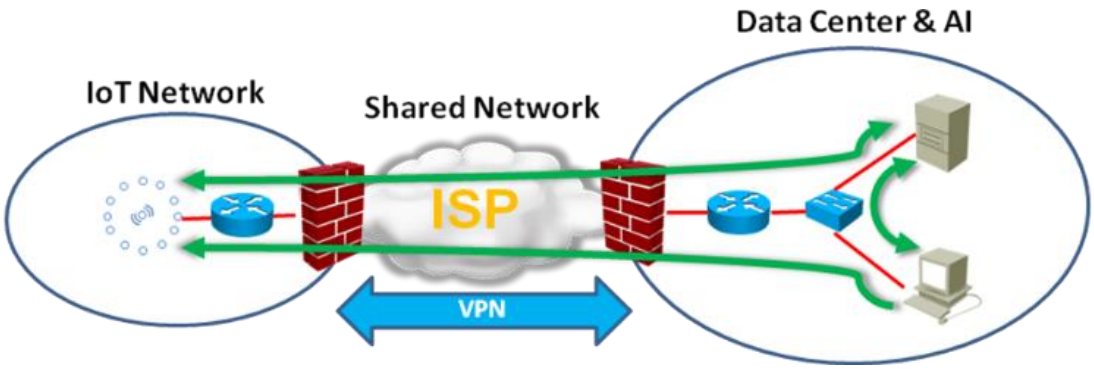

Figure 5.6. Basic scheme of security and data flow.

As it can be seen, two firewalls will protect the areas of the network that belong to us from the shared network. The green arrows represent the data flows that will be established between the IoT network, the data center, and the AI. Considering the way the system performs its functions and its vulnerabilities, attacks can be classified into four categories: physical attacks, attacks on the data in transit, attacks on the management system, and attacks on the data.

5.4.2.1 Physical attacks

Physical attacks comprise those attacks that require physical access to the device. In the case of our proposed system, removing the sensors, accessing the nodes through the serial port, or removing the batteries are some of the physical attacks that can be performed.

Another important thing to consider in our system is the possible presence of animals that could bite the wires or take the devices. Thus, nodes should be enclosed on a protective box so as to protect the device from possible attackers and the elements. The box should include a combination lock and the password to the lock should only be known by the administrator of the system. Moreover, considering that the nodes are deployed over several irrigation canals, there is a possibility of losing the devices in case of flooding or extreme rain. This security issue cannot be avoided, but the system includes the mechanisms so as to alert of malfunctioning or lost nodes. Therefore, the administrator would know to replace the damaged devices in case of these types of events.

It is also important to consider that most of the nodes, as well as network devices and the computers employed on our system, are provided with different access ports. For all the equipment, we will only utilize the ports necessary to transmit the information or to access the administration of the different devices and equipment. We will disable the rest of the ports so as to avoid the unauthorized access from attackers external to the project.

Another important remark is reducing the usage of USB memory drives or other external memory devices. These elements are connected to the computing resources and may be infected with malware. By utilizing just the necessary ports and previously analyzing them, it is possible to avoid subsequent attacks. Furthermore, physical security is also very important at the transmission network and at the different storage and computation devices.

5.4.2.2 Attacks on the data in transit

These attacks would aim at making the system unable to communicate or intercepting the transmitted data so as to gain knowledge on the information gathered by the system.

It is necessary for our system to be protected against eavesdropping and tampering. In order to achieve it, the combination of forwarded data encryption and the protection of the networks where the transmission is performed should be performed. Attackers may try accessing through the physical network infrastructure or through the software components provided by the services of the network itself. The impact of an attack performed utilizing software components would probably be greater [344].

Our proposed system utilizes both wired and wireless communication, and both types of communication should be secured. The most effective way of establishing greater security over the wired network is having a proprietary telecommunications service comprised of an optic fiber network. However, this proposal is not viable. For this reason, for the wired communication, a VPN will be established so as to avoid eavesdropping and access to the network.

As for LoRaWan, replay attacks, jamming techniques, and wormhole attacks could compromise the communications [299]. Replay attacks consist of fooling the device by utilizing old information that has been retransmitted. However, the attacker should know the channels and the employed frequencies so as to sniff the transmission. This attack is addressed by keeping track of frame counters as seen in Figure 5.7. Jamming consists of disrupting radio transmissions by transmitting high power radio signals in the vicinities of the nodes. The spreading factor and transmissions on the same frequency may cause interferences among the devices. Although this attack is difficult to avoid, it is easier to detect, and proper actions can be taken so as to re-establish communication. If the nodes of the network begin to lose the connection, the communication frequency should be changed. Lastly, wormhole attacks consist of capturing packets and replaying to the source so as to avoid them reaching the gateway.

Regretfully, this type of attacks is hard to detect but utilizing previous analyzed data, abnormal behaviors could be detected.

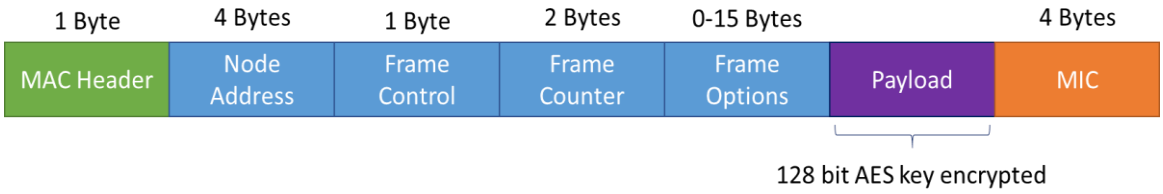

Figure 5.7. Frame counters.

Authentication between the end-device and the network is one of the implemented security measures. Moreover, LoRaWAN also incorporates end-to-end encryption [345]. It utilizes AES (Advanced Encryption Standard) with CMAC (Cipher-based Message Authentication Code) and CTR (Counter) to provide integrity and encryption, respectively. The authentication is performed with a unique identifier and 128-bit AES key. AES-CMAC is utilized to compute the Message Integrity Code (MIC). Furthermore, LoRaWan already addresses some security issues by implementing several security measures.

5.4.2.3 Attacks on the management system

Our proposed system utilizes Fog computing so as to manage alerts and control the nodes from the edge. However, an attack on the Fog server could compromise the correct functioning of the system. Fog servers are susceptible to attacks of DoS, Man in the Middle (MITM), or placing a rogue gateway [346].

The structure of Fog computing implies that DoS attacks would affect the closest networks but not the whole system if several Fog servers are utilized. Furthermore, the utilized protocols and their security mechanisms have to be considered and will become determinant in the success or failure of the attack. Man in the middle attacks could intercept data such as the alerts of the system, resulting in the system not taking the corresponding actions to resolve the problem if these messages are not forwarded. Tracking the messages and detecting abnormal behavior could help in detecting these types of attacks.

If this attack is utilized for eavesdropping, proper encryption techniques should be utilized. Furthermore, the system should be designed so as to avoid the introduction of rogue gateways that could disrupt the correct functioning of the system.

Moreover, all devices must be configured with passwords and access codes that will only be known by the authorized management personal. As usual, the personnel entrusted with the management and administration of the system will employ different

passwords to access the devices and their personal accounts. Furthermore, different access levels to management privileges will be established according to the activities related to each job position.

If our devices are not provided with a strong authentication system, some of the previously addressed problems may arise. These attacks may be denegation of service, modification and/or data thief, brute force attacks, etc. Device monitoring, freezing accounts, and throttling are some of the common measures that we will employ so as to avoid fraudulent access to the devices. Actualizing firmware and the operating systems of all the utilized devices is critical. All devices and equipment must update throughout their lifespan. Furthermore, the amount of equipment with external access to the Internet browser must be reduced.

5.4.2.4 Attacks on the data

The data gathered from the system could be compromised by a third party. Unauthorized people could acquire the data or modify it so as to disrupt the correct performance of the system. The aspects that concern data security are integrity, confidentiality, and availability [347].

In the case of our proposed system, the integrity and availability of the data is preferred to its confidentiality. However, enough encryption techniques should be utilized so as to provide the system with enough confidentiality. Furthermore, the information stored on Fog servers and the cloud should be properly protected. Secure passwords to access the data, authentication, encrypted data forwarding, and guaranteeing that user accounts cannot be duplicated are some of the measures to be considered.

At the data center, our data is previously protected by a firewall that prevents the connection of unauthorized users from the shared network (ISP). Moreover, the access permissions and updates of operating systems and firewall software of the different equipment must be adequate. These tasks must be performed on all implemented proprietary network resources as well.

The data of our system must be isolated from the data from any other network at all times. This way, a direct transfer can be avoided. Table 5.3 summarizes the proposals to reject the attacks. Furthermore, Figure 5.8 shows the summary of the phases of our security system. At the start, the proposals defined in Table 5.3 should be applied to the different equipment and devices.

Table 5.3. Proposals to Rejects Attacks.

Attacks	**How our proposal refuses the attack**
Access to physical device.	Hardening devices and facilities. Access control in the facilities. Alarms. Periodic inspections of the sensor nodes.

Compromised physical Device.	User/password access. Visual identity verification (authentication phase).
Compromised node.	Use of algorithms to detect compromised nodes. Change of trust level. trust elimination.
Malfunctioning or lost the nodes or equipment.	Replacement of the damaged devices.
Power failure.	Equipment protection against failure to supply power. Persistent storage.
Lost data because of failures or battery discharge.	Persistent storage. Authentication.
Access to user date in physical device.	User/password access. Privileges management.
Infestation with Malware.	Reducing the usage of USB memory drives or other external memory devices Control ports.
Loose of connectivity.	Persistent data storage. Authentication.
Identity impersonation.	Visual identity verification (authentication phase). Control ports. Use of short-range technologies. Firewall. Trust policies.
Phishing, active spoofing, compromised data	Hashing and authentication. Use of a trusted chain. VPN IPSec. Firewall.
Network data access using passive spoofing.	Control ports. Ciphered using session key. Key management. Firewall.
Access to network key using passive spoofing. (man-in-the-middle)	Asymmetric encryption. Key-regeneration using trusted chains. Firewall.
Access to private user delivered data using passive spoofing	Asymmetric or symmetric encryption guaranteeing confidentiality. VPN IPSec.
Data modification. Compromised data	Hash function to guarantee data integrity. VPN IPSec.
Overload and/or loose of resources.	Capacity plan and forecast. Control the number of asymmetric operations. Firewall. Persistent data storage.
Erroneous packets delivery	Control sent and received packets. Packet retransmission.
Data storage overload	Distributed data management and storage.
Denial-of-Service / Data availability	Distributed data management and storage. Distributed access to data services. Distributed security processes. Firewall.
Access to not reliable data. Data disclosure.	Data access only through trusted nodes. Session key regeneration.

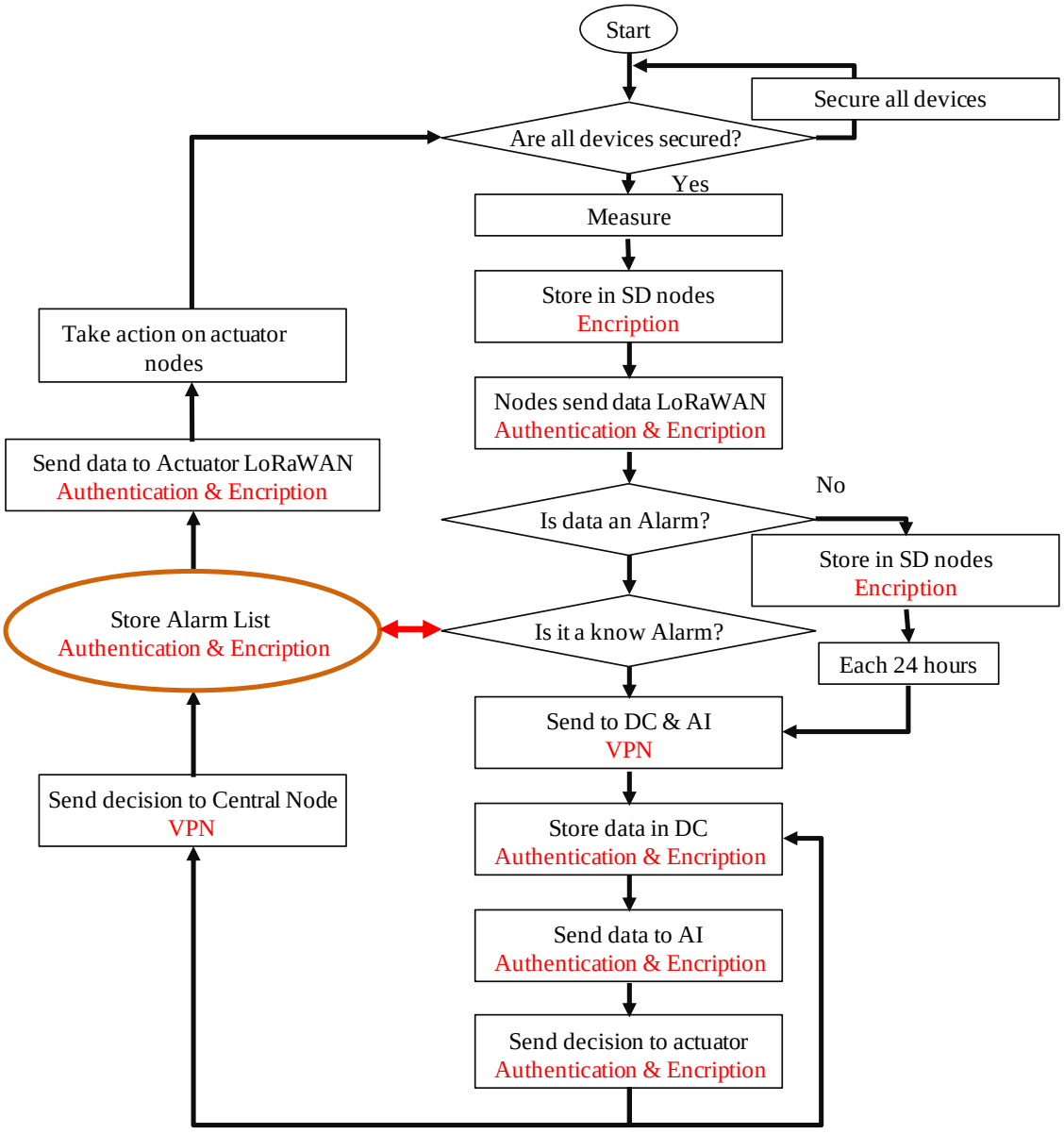

Figure 5.8. Phases of the security system.

5.5 WSN for smart irrigation in citrus plots with fault-tolerance and energy-saving algorithms

In this section, the case of a heterogeneous network with IEEE 802.11 and 3G that contemplates the deployment of numerous nodes on the fields is presented. Furthermore, fault tolerance and energy saving algorithms will be presented.

In Figure 5.9, an example of deployment of the different nodes in an orchards area is shown. The black dots represent the nodes with the field sensors, the Field Node (FN). They are measuring soil moisture at different depths along with the temperature sensor.

One node with a moisture and temperature sensor is placed at the base of each orange tree. In each plot, one or more nodes will be used as Sink Field Nodes (SFN). The sink node is in charge of collecting the data from each node via Wi-Fi and forwarding the data to the DB using 3G technology. Moreover, the sink node has also a rain sensor. Along the river, different channels are used to get the water to the different plots. At the beginning of each channel, the filters for water purifying are placed. Two nodes are placed to measure water quality. One before the filter named as Water Node Before (WNB) and one after the filter, named as Water Node After (WNA). The nodes that measure water quality have a Wi-Fi antenna and they send the data to the closest FN, which will transmit this information until it gets to the SFN.

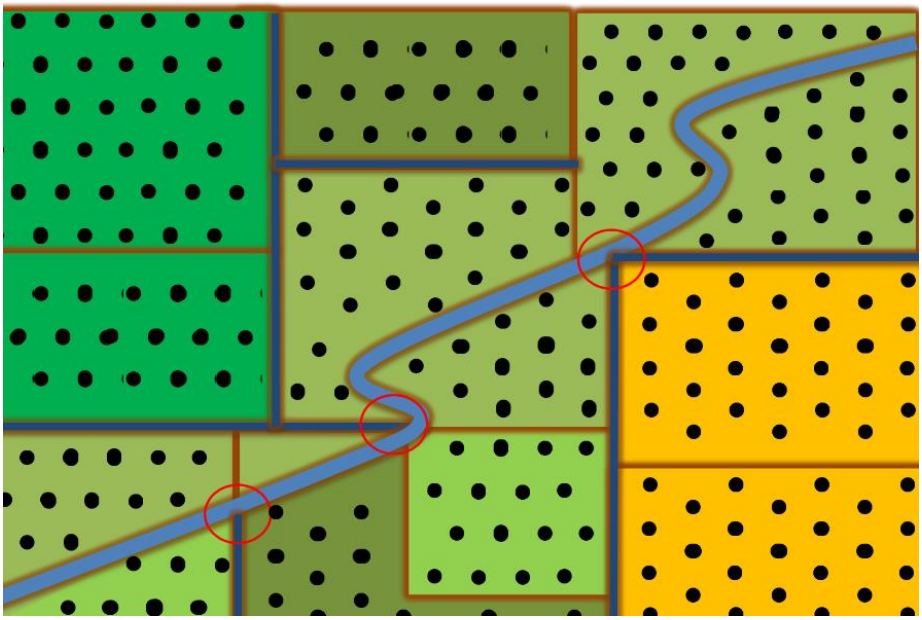

Figure 5.9. Example of location of nodes in the field.

The path that follows the data from a WNB to the DB can be seen in Figure 5.10. In blue, we can see the nodes that measure water quality. In light orange, the sensors that measure the data from soil status can be seen. Finally, the sensor that measures the data from soil and rain are colored in dark orange and the database is colored in grey.

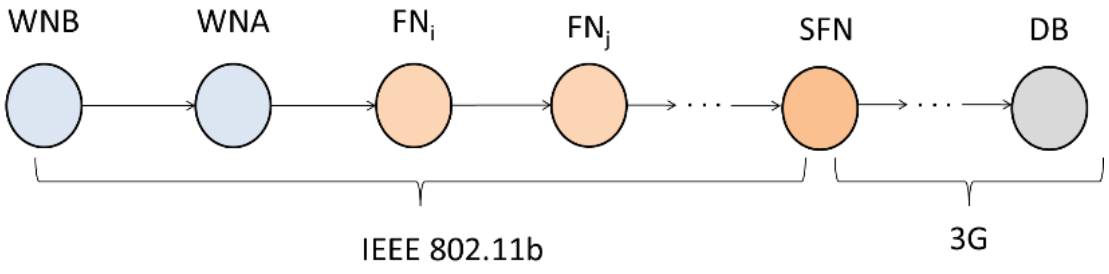

Figure 5.10. Data forwarding from the WNB to the DB.

Next, the operation algorithm applied in the nodes that monitor water quality, the WNB and WNA, and activate the filters when needed are described. The algorithm presented in Figure 5.11, shows the operation process of the nodes. Firstly, the WNB gathers data from salinity and turbidity. Then, the node evaluates if it is necessary to send the data or not. This will be performed applying the algorithm described in the following subsection. If the data changes from the previous sent value, the WNB must send the new gathered data to the WNA. Thus, the WNA will evaluate the needed action. The actions are meant to activate the filters to purify the water, if pollution is detected, or irrigate with river water if the water is clean. To determine the pollution of the water, the data from the WNB is compared with established thresholds. However, if it is not necessary to send the data from the WNB to the WNA, the data is not sent, and no actions are taken on the filters. If no data is received, the WNA gathers new data as usual. If data from WNA is higher than a threshold, it indicates that the filters are not operating properly, then an alarm is sent. The last step is to evaluate if it is necessary to send the data gathered by the WNA. Then, according to the need of sending the data of WNA and WNB, the WNA will forward the data that requires to be sent.

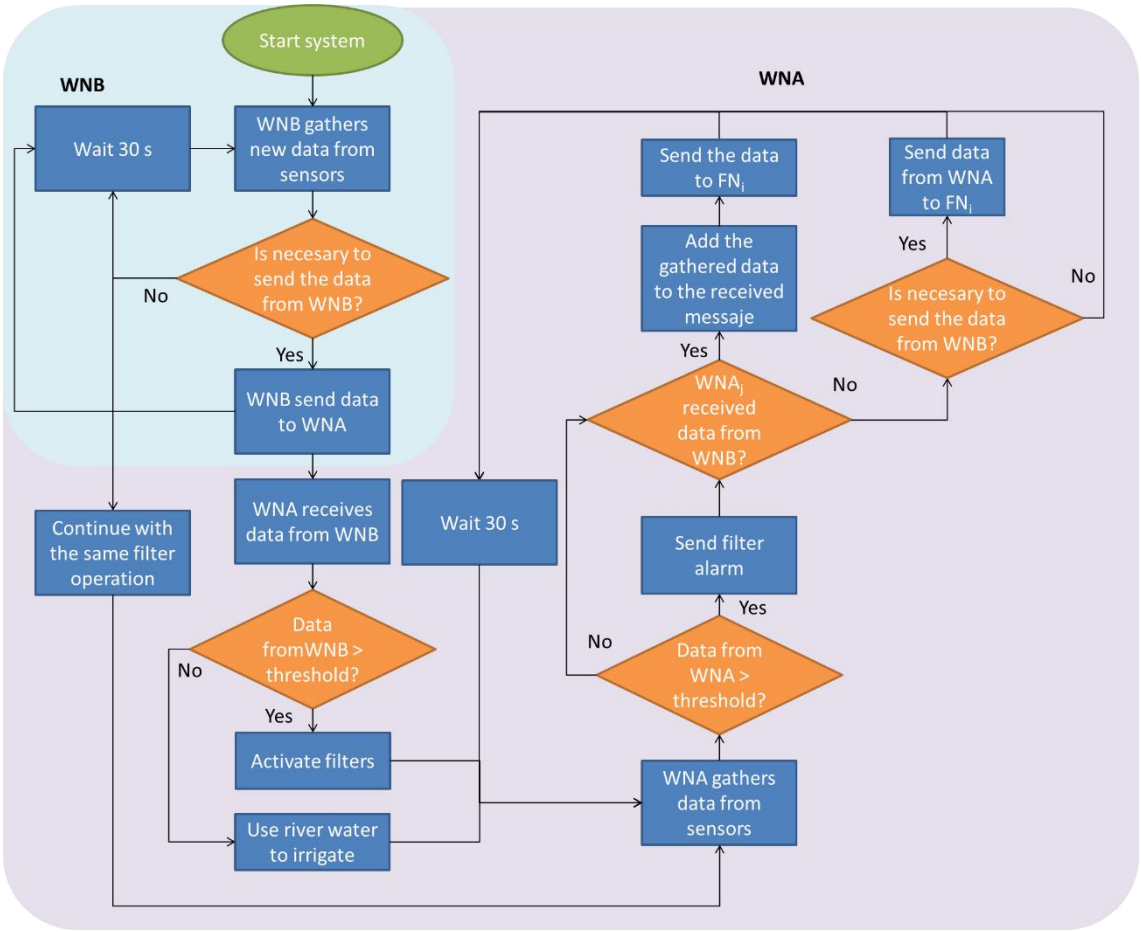

Figure 5.11. Operation algorithm of WNA and WNB.

In the FN, the operation algorithm includes the gathering of new data, the activation of the local irrigation, and the need of sending data. The algorithm can be seen in Figure

5.12. First, the node gathers new data. If the humidity level is lower than the established threshold, the node activates the local irrigation. If the soil moisture is higher than the threshold level, no action is taken on the irrigation system. Then, the node checks if, in the last 5 minutes, any message with data from another node was received. If data were received, the node adds the gathered data to the received message and forwards it. If no data were received, the node evaluates if the gathered data must be forwarded or not. If the data must be forwarded, the node sends it to the next node. Then, the node waits 5 minutes to gather new data.

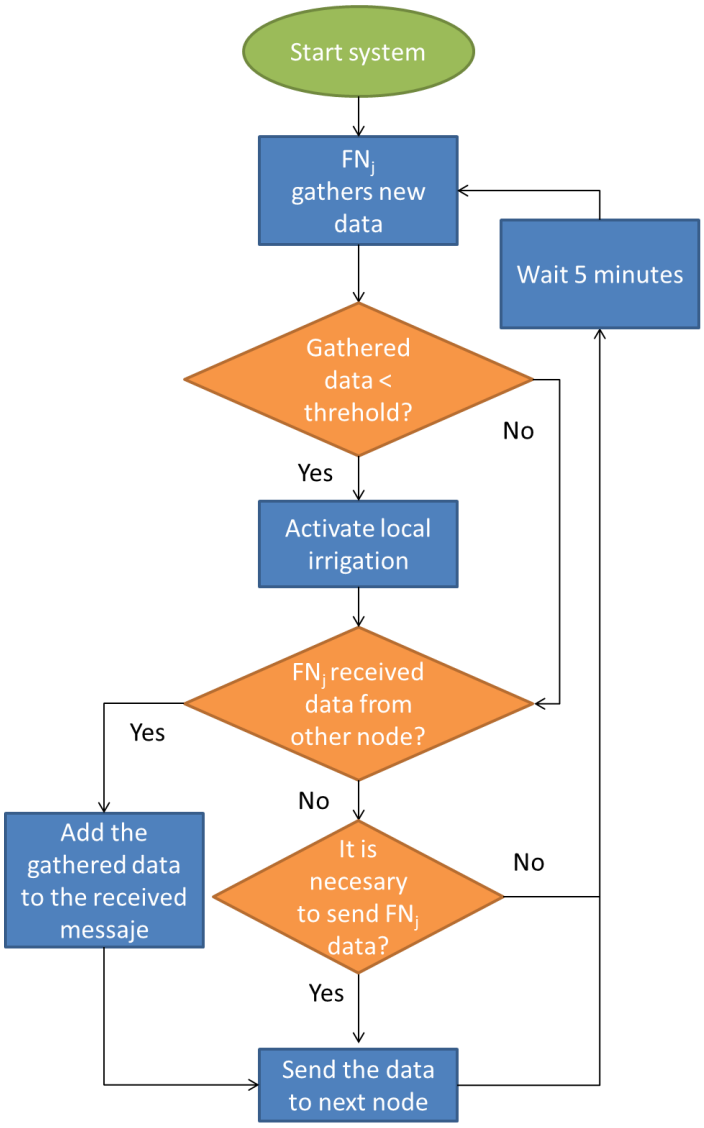

Figure 5.12. Operation algorithm of FNs.

5.5.1 Fault tolerance algorithm

Figure 5.13 presents the fault tolerance algorithm for the nodes deployed throughout the crops. The nodes employed are Arduino Mega provided with WiFi connection employing the ESP8266 module. Firstly, the connection is established between the

nodes. Nodes detect their neighbors and ask for the metrics to determine the shortest path to the base station. When the node determines the next hop, it starts performing its sensing activities. Then, the forwarding decision algorithm presented in the next section of this paper is applied. When necessary, data is forwarded to the next hop. If the ACK is received, the node continues with its normal functioning. If an ACK is not received, the data is forwarded again. If after three tries an ACK is not forwarded, the process of detecting the neighbors and selecting the one closest to the base station is performed again. Then, the data and a warning are forwarded so as to inform that there is a broken node.

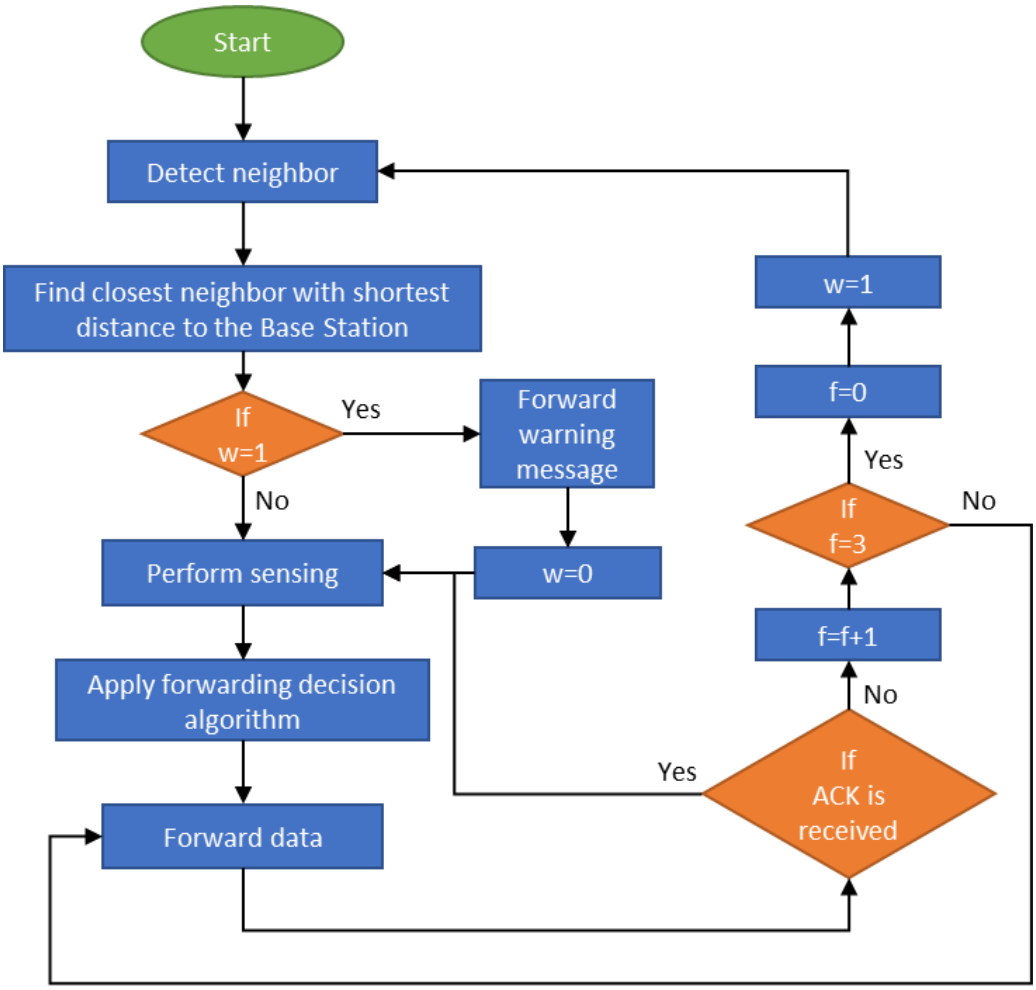

Figure 5.13. Fault tolerance algorithm.

Figure 5.14 presents the message exchange between the components of the architecture of our proposed system. Firstly, the connection establishment process is performed where nodes send a broadcast message to reach the other nodes. Then, the nodes send the metrics indicating the distance to the base station. When the nodes perform correctly, the data is forwarded to the next hop and an ACK is received. Then, the information is forwarded from node to node to the router in the base station, where the information from the nodes is received employing Wi-Fi. 3G is employed to

forward the information to the database. When there is a failure in a node, the data is forwarded three times in order to ensure the error was not caused by interferences. The neighbor discovery process is performed again and when the next hop is selected, the data is forwarded as usual including a warning to alert of the broken node.

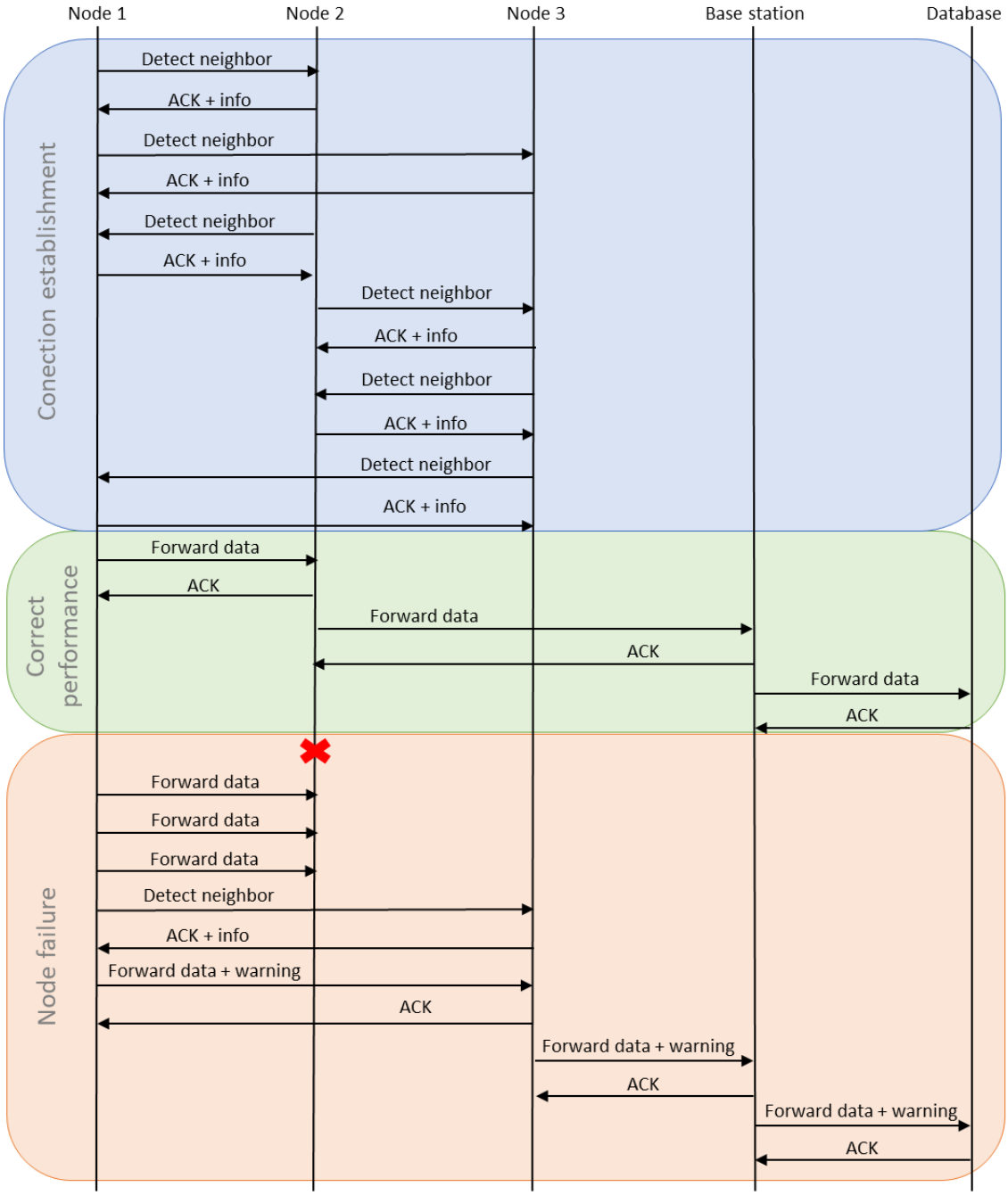

Figure 5.14. Message exchange among the elements of the system.

5.5.2 Energy saving algorithm

In this section, the energy saving algorithm is described. Many algorithms have appeared in the last years for WSNs to diminish the energy usage. The majority of those algorithms are based on the selection of different transmission settings, using different routing protocols, or using specific protocols with fewer communication requirements or less packet size. However, the best way to save energy is to avoid unnecessary packet exchanges. In WSNs, when the sensors are measuring a parameter, the node usually sends the gathered data without considering the relevance of this data.

It is extremely important to consider the relevance of the gathered data in order to know if it is important to forward it. The reason is that if the node sends this data a high energy consumption in this and other nodes will be generated. The data transmission is considered as the procedure that requires more energy. Thus, the rest of the processes as processing, coding, and decoding the data can be despised. In another paper, [348], the authors have proposed a smart algorithm that decides if the gathered data must be transmitted or not. Based on their algorithm we propose a simplified version adapted to our proposal.

The adapted algorithm is shown in Figure 5.15. In our case, the decision algorithm is applied to all the nodes during its operation algorithm (Figures 5.11 and 5.12). These algorithms start with the new gathered data and must decide to send it or not. The gathered data corresponds to two variables, *m* and *n*. The new gathered data is set as *Xm* and *Xn*. Those variables are, in the case of WNB and WNA, the conductivity and the turbidity and, in the case of FN, soil moisture and temperature. Then, the algorithm searches in the node memory for the established thresholds for each variable (*Δm* and *Δn*). These thresholds represent the minimum variation in the parameter that must be overcome to consider the new information as relevant. Next, the algorithm searches in the node for the previous transmitted values. If there were no previous transmitted values, the new values are set as the last transmitted values (*Ym* and *Yn*), and the values are transmitted. If there were *Ym* and *Yn* in the node memory, the algorithm compares the *Xm* and *Xn* with the *Ym* and *Yn*. If the difference exceeds *Δm* or *Δn,* the gathered data is transmitted. Otherwise, the data is not transmitted because it is considered that the gathered data does not contain relevant information.

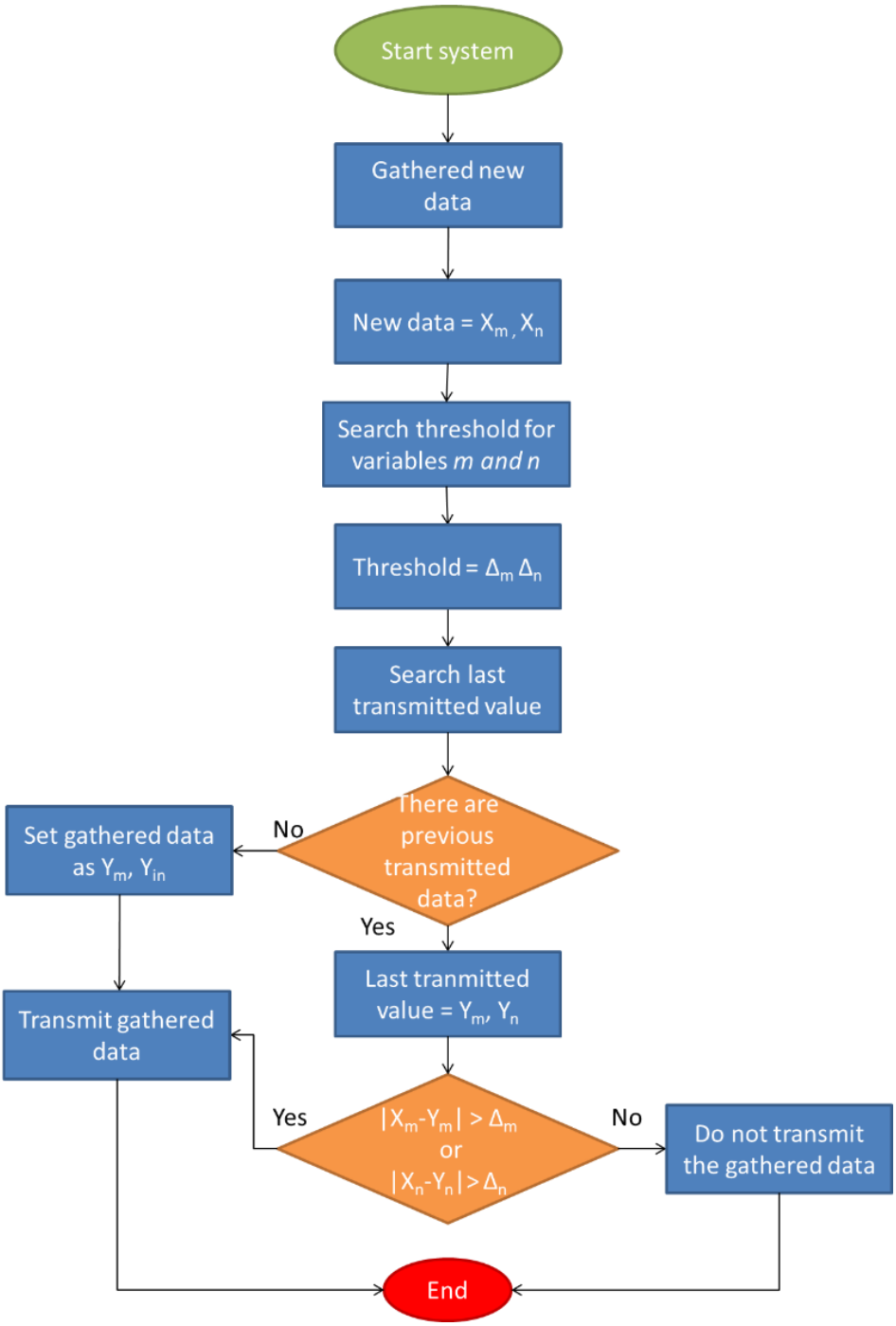

Figure 5.15. Energy saving algorithm.

5.5.3 Protocol description

Nodes communicate employing IPv4. For this proposal, a modification of the TCP protocol is presented. It incorporates on the TCP datagram the fields presented in Figure 5.16. In the data forwarding message, the TCP header is followed by the W Node ID field. This field is employed if there is a warning. The W Node ID indicates the ID of the node that is malfunctioning. Node 1 ID indicates the ID of the first node that wants

to forward information, which has a size of 1 Byte. The next field is sensor ID and has a size of 1 bit. The Sensor data field is where the data gathered from the sensor is positioned on the datagram. There are two types of sensors. For WNA/WNB sensors, the size of the data field is 6 bits whereas, for FN sensors, it is 8 bits. Sensor 2 ID has a 1-bit size and indicates the ID of the second sensor. Lastly, Sensor 2 Data is employed to transmit the information gathered from the second sensor. Its size is 4 bits for both types of sensors.

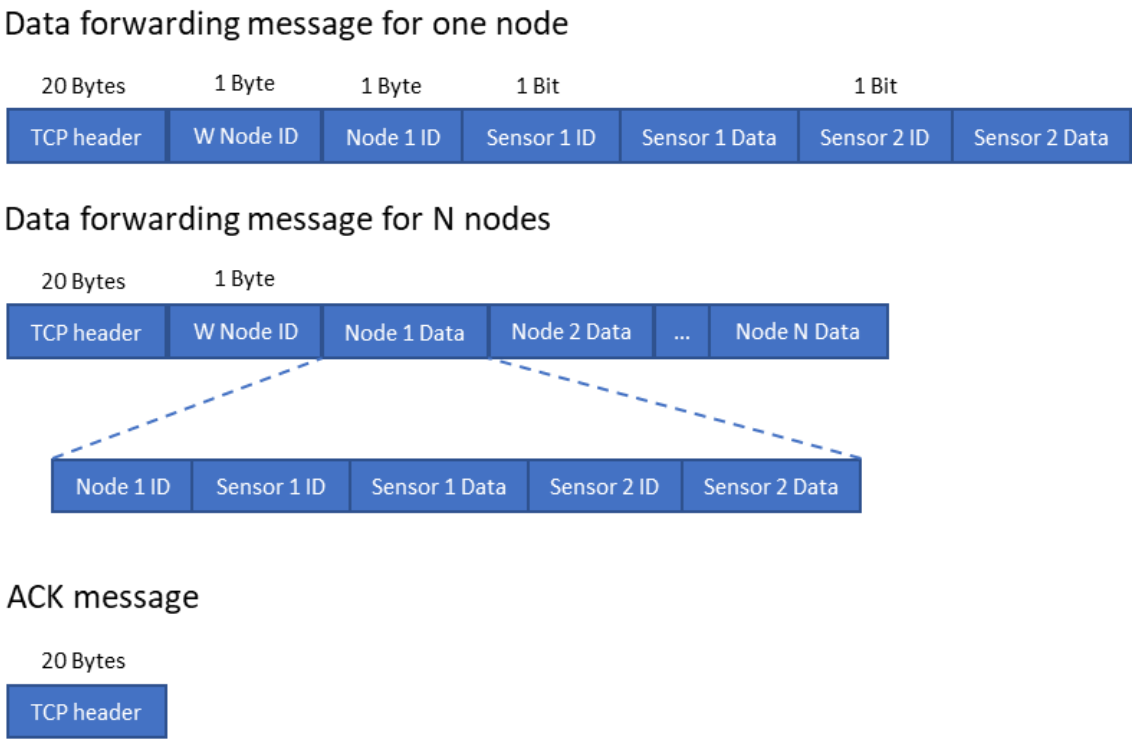

Figure 5.16. Message structure.

When a node receives information from other nodes in order for it to be forwarded, the information is placed on the datagram following the data from the other nodes. As it can be seen in Figure 5.16, where Node 1 Data is followed by Node 2 Data and so on depending on the number of nodes that are forwarding data at the moment. The W Node ID field is only employed when there is a warning. Finally, the ACK message is composed of only the TCP header, without adding any more data.

5.6 Utilizing CoAP in IEEE 802.11 networks for PA

In this subsection, the association problem of the nodes to de AP of the architecture presented in Chapter 3 subsection 3.2.2.1 is presented.

The problem that arises when trying to connect a large number of nodes to the "Urban area 0" is the distance at which it can be found. To solve this, a WMN is utilized as shown in Figure 5.17. Here, we can see the nodes that will connect as clients to the APs. The whole set of APs will form the WMN that in the "Urban area 0" will be connected with cable to a switch that will allow reaching a server. The server is responsible for managing the number of users that are associated with each AP. When the nodes associated with an AP reach a threshold, the server ensures that the nodes that exceed this threshold are associated with another AP.

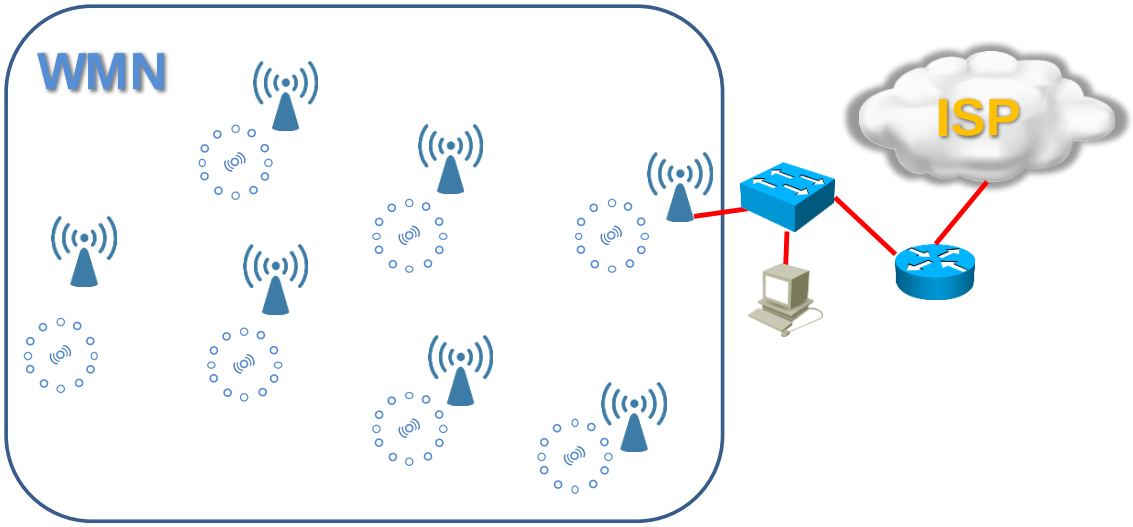

Figure 5.17. Network architecture of our nodes-balanced system.

One of the main obstacles, historically speaking, at the time of using wireless technology if we compared it with the wired, was the shortage of bandwidth. Since the appearance of this technology, the transmission speed has increased remarkably. The initial 1Mbps of the IEEE 802.11 standard has developed into the theoretical 7 Gbps that can reach the IEEE 802.11ac standard, including the future standard IEEE 802.11ax that will provide speeds of up to 11 Gbps.

With these transmission speeds, the problem of bandwidth is beginning to disappear in certain environments. For example, in practice, if we use the IEEE 802.11ac standard, we can transfer 900 Megabytes per second. It is achieved by using eight 256 QAM channels of 160 MHz each. These channels can transfer a maximum of 870 Mbps, although it is usual to use no more than 2 or 3 of the eight channels.

This network is not a usual network in which very varied types of traffic and with different requirements, such as HTTP, multimedia streaming, SMTP (Simple Mail Transfer Protocol), POP3 (Post Office Protocol), FTP (File Transfer Protocol) or VoIP (Voice over IP), which may require large bandwidths are found. Although the bandwidth of an AP is shared for the transmission of different groups of nodes, because the bandwidth required by CoAP for the transmission of the information of the IoT devices is very low, we will not find limitations from the point of view of bandwidth. Actually, the frames will have a maximum size of 1077 bytes, which is lower than the

maximum size of a CoAP packet (1125 Bytes). Figure 5.18 shows an IPv4 CoAP frame, with the different fields that form it and the size of each of them. In this case, the token has a length of 1 Byte and the Observe option is utilized.

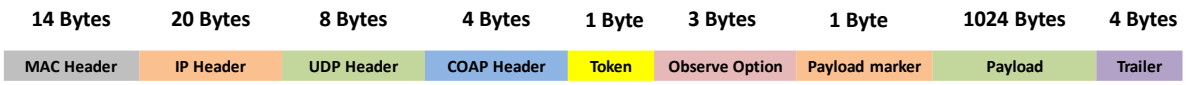

Figure 5.18. CoAP frame.

If the APs that meet the IEEE 802.11n standard are utilized, using the 20 MHz channel, a transmission of 72.2 Mbps can be achieved theoretically. However, the real transmission rate is approximately 50 Mbps. Since the maximum size of a COAP datagram is 8616 bits, at a speed of 50 Mbps the transmission is performed in 0.000172 seconds. Theoretically, there can be transmitted approximately 5800 datagrams in a second.

The main challenge of our proposal, when associating groups of nodes with APs, is to know the maximum number of simultaneous connections that APs can establish, together with a design that covers all the observed space with the minimum amount of AP needed. Generally, the limitation is given by the manufacturer. For example, if the Linksys WRT600N v1.1 [349] APs which work in the 2.4 and 5 GHz bands with the a / b / g / n standards are used, a theoretical maximum of 253 users that are assigned by DHCP (Dynamic Host Configuration Protocol) are supported, although by default only 50 are allowed.

In response to the initial proposal, for example, when the number of nodes associated with an AP exceeds 50, from the server located in "Urban area 0" through the WMN, it will be indicated to the surplus nodes that they must be associated with another AP.

5.6.1 COAP

CoAP is an application protocol for IoT systems that works over UDP. It is a simplified version of HTTP so it provides interoperability with it. However, CoAP has not been widely implemented utilizing WiFi. In fact, the available libraries for WiFi chips are scarce. Particularly, for the ESP8266 chip, there is the ESP-CoAP library [350] that allows implementing CoAP and provides the biggest number of functionalities compared to other available libraries. However, one of the things to consider with CoAP is that the client has to make a request to obtain the data. Therefore, clients could be requesting data when it would not be necessary, making the system forward more messages than necessary and increasing the energy consumption. For that reason, CoAP provides an “observer” option that would allow the system to forward the information regularly to the client once the client subscribes to a resource.

Although the ESP-CoAP library allowed observing one resource, the ability to observe more than one resource was found necessary. Therefore, the library for the server was modified so as to allow observing several resources as well as allowing several observers to one resource and canceling the observe if wanted.

The notification class was modified so as to allow observing several resources as shown in Figure 5.19.

```
void coapServer::notification(String url, char *payload)
{

    response->version=request->version;
    response->type=COAP_ACK;

    response->messageid=messid++;

    response->code = COAP_CONTENT;
    response->payload = (uint8_t *)payload;
    response->payloadlen = strlen(payload);
    response->optionnum = 0;

    obsstate=obsstate+1;

    response->options[response->optionnum].buffer =&obsstate;
    response->options[response->optionnum].length = 1;
    response->options[response->optionnum].number = COAP_OBSERVE;
    response->optionnum++;


    char optionBuffer2[2];
    optionBuffer2[0] = ((uint16_t)COAP_TEXT_PLAIN & 0xFF00) >> 8;
    optionBuffer2[1] = ((uint16_t)COAP_TEXT_PLAIN & 0x00FF) ;
    response->options[response->optionnum].buffer = (uint8_t *)optionBuffer2;
    response->options[response->optionnum].length = 2;
    response->options[response->optionnum].number = COAP_CONTENT_FORMAT;
    response->optionnum++;

    for(uint8_t i=0;i<obscount;i++){
            for (int j = 0; j < rcount; j++){
//send notification
            if(observer[i].observer_url==resource[j].rt && url==resource[j].rt){
                response->token=observer[i].observer_token;
                response->tokenlen=observer[i].observer_tokenlen;
                sendPacket(response, observer[i].observer_clientip, observer[i].observer_clientport);
            }
        }

    }
    if(messid==5000)
        messid=0;
```

Figure 5.19. Code for observing several resources.

ParseOption was modified as well so as to enable the possibility of canceling observing a resource (see Figure 5.20).

```
if(request->options[num].number==COAP_OBSERVE){


    if(*(request->options[num].buffer)==1){

        for(uint8_t i=0;i<obscount;i++){
            if(observer[i].observer_clientip==Udp.remoteIP()  && observer[i].observer_url==url){
                    if(obscount==1){
                        observer[i]={0};
                        obscount=0;
                    }else{

                        observer[i]=observer[i+1];
                        observer[i+1]={0};
                        obscount=obscount-1;
                    }
                }
            }
```

Figure 5.20. Code for canceling the observation with a GET message.

5.7 Decision-making algorithm for underground communication

In this section, a data transmission decision technique is going to be presented according to the characteristics of the underground transmission.

One of the key functionalities of precision agriculture systems is soil monitoring. Soil monitoring nodes are the elements more susceptible of being deployed underground in an IoUT system. These nodes incorporate sensors to monitor soil humidity, temperature, ph, and nutrients. Particularly for irrigation systems, nodes such as the Arduino UNO or the Node MCU are the most utilized in scientific papers. Considering the extended use of low-cost nodes for IoT precision agriculture systems, as high soil moisture values lead to high signal attenuation in underground communications, the decision-making process regarding the transmission of the data gathered by soil monitoring IoUT nodes can be improved making use of the soil moisture values provided by the sensors.

The decision-making algorithm is presented in Figure 5.21. After obtaining the information from the sensors, the humidity threshold (Hth) is evaluated. According to the selection of the settings performed by the user, humidity values are divided into three different ranges as it is exemplified in Figure 5.22. If the value of Hth is 3, then the humidity of the soil is high, and the data is stored. Then, if the value stored at the variable that indicates the time of the last transmission (TLT) surpasses the maximum time the node can stay without forwarding any data (Max Time), the urgent transmission (UT) flag is activated. If the maximum time has not been surpassed, the node goes into sleep mode. If the value of the humidity threshold is 2, the settings of the transmission mode (TM) are checked. A value of 1 indicates the default mode and the value 0 indicates the energy-saving mode. When the normal mode is activated and the value of the humidity threshold is 2, the transmission power (TP) of the antenna is set to high (value 1). The high setting depends on the characteristics of the utilized antenna and should be specified at the preliminary setup. This is done to increase the quality of

the signal that reaches the receiver when there are medium levels of soil moisture. Then, the urgent transmission flag and the counter of the last transmission time are set to 0 and the node goes to sleep. Lastly, if the humidity threshold is set to 1, the transmission power of the antenna is set to default, and the data is forwarded. In this manner, the soil monitoring node is able to decide when and how to transmit the gathered data according to the moisture levels of the soil.

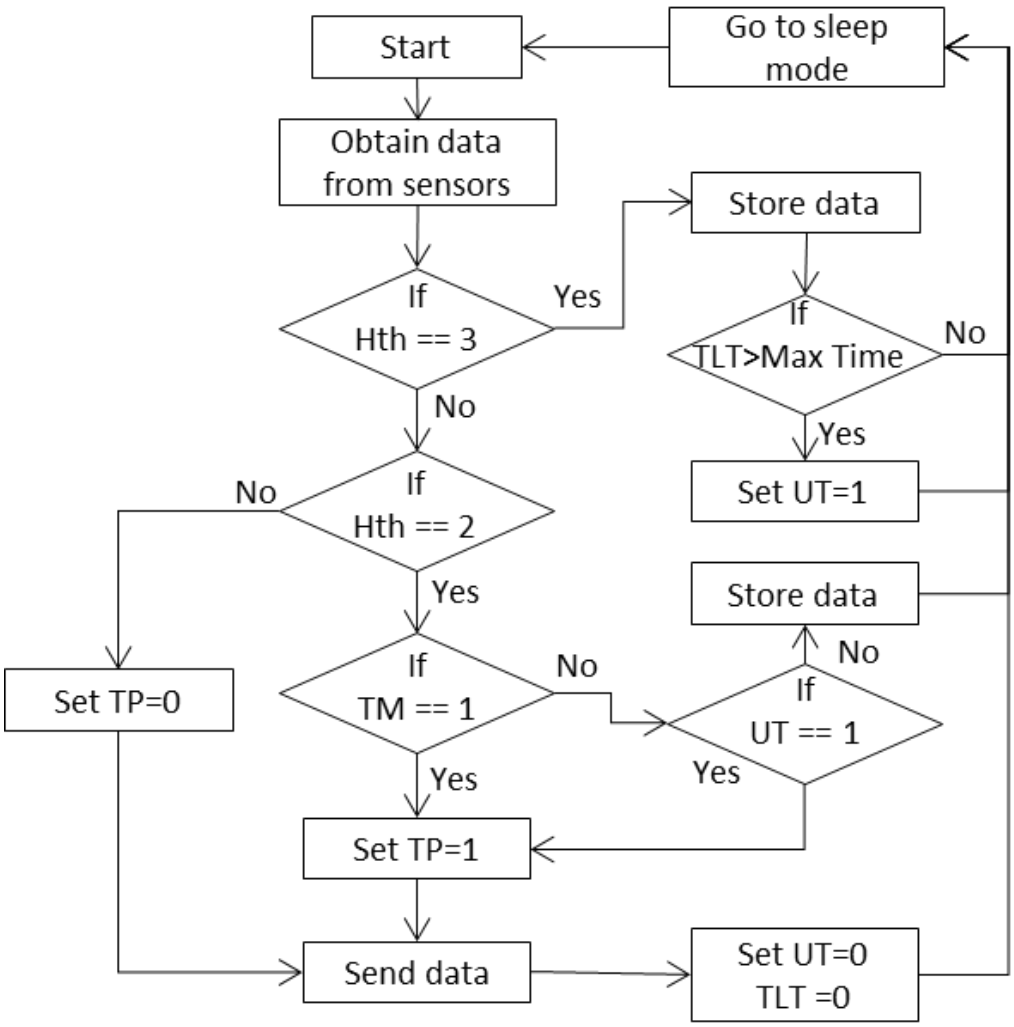

Figure 5.21. Underground transmission decision-making algorithm.

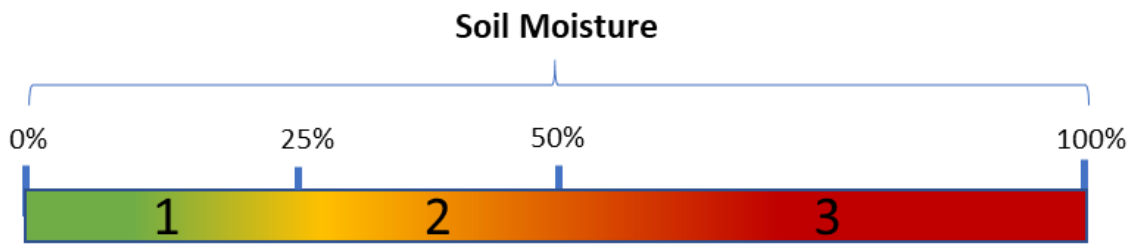

Figure 5.22. Humidity threshold example from soil moisture values.

5.8 The use of remote sensing drones as mobile gateway for WSN in precision agriculture

In this section, the parameters and elements considered when employing drones for data acquisition are presented. In the first subsection, an overview of the available types of drones that can be utilized in PA and the description of the flight plan of the considered scenario is provided. In the second subsection, the characteristics of commercial nodes that can be utilized for our proposed scenario are detailed. In the third subsection, the background on the antenna radiation model and the best antenna types for the scenario are presented. Furthermore, the theoretical framework used to perform the calculations is described.

5.8.1. Drone parameters

Drones in PA have been mainly used for remote sensing by image gathering. However, drones can be utilized as well for data gathering of nodes deployed on the field. These drones can have fixed or rotary wings, which determines how they fly as well as other parameters such as the ones detailed in Table 5.4.

Table 5.4. Characteristics of commercial drones for PA systems.

Drone	Nominal endurance	Cruise speed	Typical climbing speed	Max wind speed	Typical range altitude	Wing type
Swinglet [351]	30 min	10 m/s	3 m/s	7 m/s	20-500 m	Fixed
Phantom 3 advanced [70]	23 min	16 m/s	5 m/s	-	120 m	Rotatory
SenseFly eBee [352]	45 min	15.84 m/s	-	-	-	Fixed

Fixed-wing drones can fly for hours and long distances on a limited amount of energy [353], which makes them popular for precision agriculture purposes, including taking pictures of the fields, as it provides good autonomy. However, stationary flights are not possible with fixed winged drones. Furthermore, this type of drone requires a drone catapult to launch it if a person cannot do it, and a big enough surface for landing.

On the other hand, rotatory winged drones are the most common. They can stay in one place to perform inspection activities. This type of drone is available with 3 to 8 motors. They can take off and land vertically. However, these drones have less

autonomy with endurances below 1 hour. Other solutions opt for using their developed drone [354]. This allows detailed customization of the UAV for the required PA solution.

The intended purpose of the drone will determine its flight plan. For the drone to carry a node that acts as a gateway, the drone must be in the area of coverage of the node long enough for all the data to be transmitted. For small amounts of data, a straight flight plan where the nodes are flown over can work. However, for significant amounts of data, flight plans where the drone circles the node until all the data is transmitted may be necessary [355]. In Figure 5.23, these two types of flight plans are shown. In the scenario considered in this paper, the flight plan follows straight lines that fly over the nodes deployed on the field. The flight plan that circles the node for a fixed-wing drone or hovering over the nodes for a quadcopter would solve the problem of having enough connection time to perform the connection and transmit all the data before the node is out of the coverage area of the drone. However, as previously stated, in this paper we consider the challenge presented by the scenario where an imaging drone that has a previously defined flight plan that covers the field following straight lines while carrying the gateway node.

Figure 5.23. (**a**) Flight plan with straight lines, (**b**) Flight plan circling the nodes.

Furthermore, each country has its regulations for drones. Some countries require the obtention of a license that may distinguish between recreational and professional use. The height, areas allowed for flights, and weight of the drone may also be restricted depending on the type of license.

5.8.2 Low-cost nodes for precision agriculture deployments

Nowadays, there is a wide variety of low-cost nodes that can be employed for PA purposes using WiFi communication. Some of the most utilized ones are presented in Table 5.5. In the scenario contemplated in this paper, low-cost nodes are utilized both for the field monitoring and for the gateway mounted on the drone. As can be seen, the

characteristics of the nodes can vary greatly. The weight and size of the nodes should be considered to determine if the chosen drone would be affected by it or if it is able to carry the node without interfering with its flight. If no sensors are connected to the node carried by the drone and a big processing capacity is not necessary, nodes such as the WEMOS MINI D1 would be best to reduce the energy consumption due to its low weight and size.

Table 5.5. Characteristics of popular nodes for PA systems.

Controller	FLASH	RAM	EEPROM	Weight	Size	Operating Voltage	Reference
WEMOS MINI D1	4MB	-	-	3 g	34.2 x 25.6 mm	3.3V	[356]
Node MCU	4MB	520kB	-	10 g	48 x 26 x 11.5 mm	3.3V	[357]
Arduino Mega	256 kB	8 kB	4 kB	37 g	101.52 x 53.3 mm	5 V	[358]
Arduino UNO	32 kB	2 kB	1kB	25 g	68.6 x 53.4 mm	7 V-12 V	[359]
Raspberry Pi 3 Model B+	-	1GB	-	50 g	85x 56 x 17 mm	5V	[360]

Other wireless technologies such as LoRa and 5G would reduce the need for using drones for data collection or completely eliminate it in small fields due to their wider range. However, these technologies are more costly and, therefore, less accessible for farmers with lower budgets.

Furthermore, multiple parameters can affect the communication system, such as the transmitted power, the protocol, or the link budget. Regarding the transmitted power parameter, it would fundamentally affect the drone coverage, as it would consume a greater amount of energy, and its flight capacity would be reduced. Using different protocols would affect the total connection time since, depending on the transitions between different states, which are associated with the actions implemented by the nodes, the connection time necessary between the nodes and the drone can be altered. On the other hand, the link budget would be defined as an addition of transmitted power and gains minus the losses. The received power is based on the losses, which occur when the signal is transmitted through the medium and can be affected by aspects such as the weather or the objects that interrupt the line of sight between the emitter and the receiver. However, in the studied scenario, there are no objects between the emitter and the receiver, and the drone would not fly with adverse weather conditions. Therefore, in this scenario, the losses would be constant. Lastly, the transmitted power and the gains

will be based on the antennas and their configuration and, therefore, they would not vary unless that different types of antennas or nodes with their configuration were used in order to increase the transmitted signal.

5.8.3 Antenna radiation model

There are many types of antennas available to transmit at the 2.4 GHz band. However, not all of them are advised for the scenario of a gateway carried on a drone. In Figure 5.24, the Theoretical WiFi Coverage Area (TWCA) and the Assumed WiFi Coverage Area (AWCA) for both an omnidirectional and a directional antenna are displayed. Common radiation patterns for both antennas are displayed as well. For the scenario, the gateway node is considered to be carried by the drone, placed in a manner so that the antenna emits its energy in a downward direction, towards the earth. For the case of the directional antenna, the radiated energy is focused on a specific direction. Whenever the gain of a directional antenna increases, the coverage distance increases, but the effective angle of coverage decreases [361]. On the other hand, omnidirectional antennas have a radiation pattern that is given based on the directive gain. This type of antenna provides uniform radiation in one of the reference planes. Therefore, regarding directivity, omnidirectional antennas are better suited for the scenario as it allows the node to be in the coverage area of the gateway for a longer time than that of directional antennas. For other scenarios such as that of a flight plan that circled the nodes on the ground, directional antennas would be a better fit as the drone could remain in a zone where the node is inside the coverage area, and the radiated energy would remain on the intended spot.

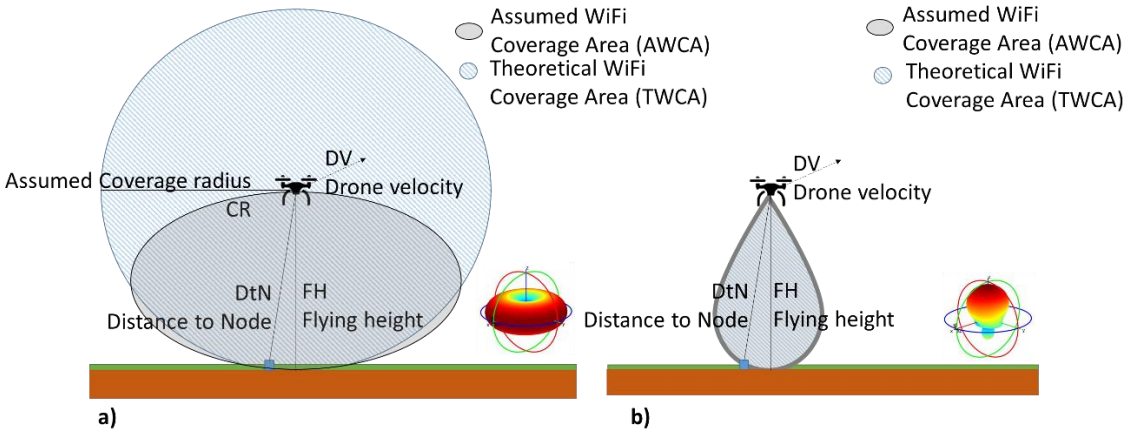

Figure 5.24. Area covered by the sensor antenna located on the drone (**a**) Omnidirectional Antenna case, (**b**) Directional Antenna case.

Furthermore, the antennas can have linear or circular polarization. Depending on the type of polarization, their coverage area will vary. The polarization of the antennas from both the emitter and receiver should match to avoid loses. In our scenario, the antennas

are placed at the same position in a horizontal manner with the same polarization for the antennas of the gateway node on the drone and the nodes on the field.

Some low-cost nodes incorporate built-in WiFi antennas such as the PCB antenna while others need a communication module or an external antenna, such as a whip antenna, to provide better performance. The antenna gain and the selected transmission power determine the Coverage Radius (CR). Therefore, it is essential to determine the distance that must be covered to select the antenna. For lower flying heights, the required coverage radius is lower, and the built-in PCB antenna has been utilized in IoT applications for distances up to 30 meters in most low-cost modules for RSSI values below -80 dB and, up to 120 m for the best performing module [362]. For higher flying heights, the area to be covered is wider, and whip antennas would provide better performance but, its size is bigger and should be placed in a manner not to interfere with the flight of the drone.

From the point of view of the node in the soil, the radiation pattern of the gateway in the drone can be compared with a sphere. Based on this assumption, we can use a trigonometrical problem to calculate the time that a single node has a wireless connection to the mobile gateway, in different scenarios (different drone flying heights, flying velocities, etc.).

The concept of sagitta (s) of a circular arc is widely used in architecture and optics. The sagitta of a circular arc is the distance from the center of the arc to the center of its base, see Figure 5.25.

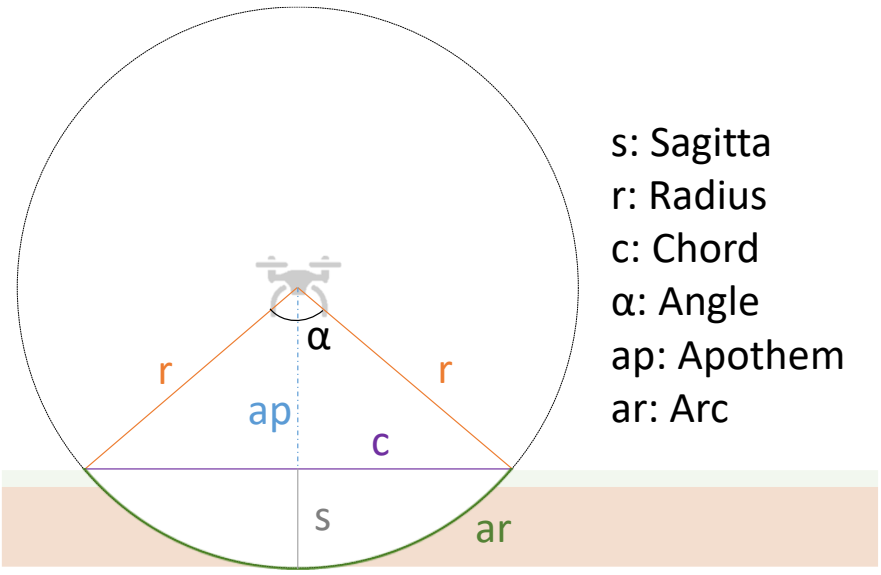

Figure 5.25. Sagitta of the circular arch described by the coverage of the drone.

The mathematical equations of this problem are equations 1 to 7. The *s* can be calculated as the difference between the radius (*r*) and the apothem (*ap*), see equation (5.1). According to the Pythagorean Theorem, s can also be calculated as a function of r and chord (*c*), see equation (5.2). Moreover, it is possible to apply the versine function

to obtain the value of s according to equation (5.3) where α is the angle formed by the two r which forms the triangle with the *c*. alternatively, there is one last method to calculate the *s*, see equation (5.4).

$$s = r - ap \tag{5.1}$$

$$s = r - \sqrt{r^2 - \left(\frac{c}{2}\right)^2} \tag{5.2}$$

$$s = r \times versin\frac{\alpha}{2} = r \times \left(1 - \cos\left(\frac{\alpha}{2}\right)\right) \tag{5.3}$$

$$s = \frac{c}{2} \times \tan\frac{\alpha}{2} \tag{5.4}$$

In our problem, the *ap* represents the flying height (*fh*), the *r* is the radius of the drone coverage (*dc*), and the chord represents the coverage in the soil. The known variables are the *fh* and *dc*, and our objective is to calculate the value of c. Therefore, the employed equations in our calculations will be equation (5.1) and equation (5.2). Combining them, we can obtain equation (5.5), which can be expressed as equation (5.6) to obtain the value of *c*. Finally, considering the flying velocity (*fv*), we can calculate the time (*t*) during which a single node has coverage from the gateway mounted on the drone (equation (5.7)).

$$dc - fh = dc - \sqrt{dc^2 - \left(\frac{c}{2}\right)^2} \tag{5.5}$$

$$c = 2\sqrt{dc^2 - (-fh)^2} \tag{5.6}$$

$$t = {2\sqrt{dc^2 - (-fh)^2}}\Big/{dv} \tag{5.7}$$

Now we can use equation (5.7) to calculate the time during which a node has coverage for different scenarios. In our calculations, we include values of *dc*, *fh*, and *fv*, which can be found in real applications. The selected values are dc from 200 to 25 m; *fh* from 5 to 100 m and *fv* from 5 to 20 m/s.

5.8.4 System description

One of the main problems in the considered scenario is that the drones may face collisions between the sensor nodes located within the coverage range of the drone. To solve this problem, in this section, we propose a data acquisition system for precision agriculture deployments where the sensor nodes forward the data to one sole mobile gateway mounted on a remote sensing drone. Furthermore, the message exchange between the elements of the architecture introduced in Chapter 3 subsection 3.2.2.4 is presented.

The PA scenario is comprised of multiple sensor nodes deployed in several agricultural fields. No networking structure is established among the nodes. Thus, the nodes do not communicate in any way among themselves. A sensor network where the nodes deployed on the field forward the data through relay nodes located in between the soil monitoring nodes would address the problem of sending the information to the base station, but it would significantly elevate the cost of the deployment. More so for node densities where large distances separate the nodes. The nodes incorporate various soil monitoring sensors that are able to obtain data on the physical parameters necessary to manage and monitor the crops. Depending on the node model, like the ones previously presented in Table 5.5, the node may use an embedded antenna to communicate, or it may need a separate communication module from the ones available at the market. The data is stored in the SD cards connected to each one of the nodes until the remote sensing drone retrieves the information. Figure 5.26 presents an example of a soil monitoring drone with a temperature and a humidity sensor.

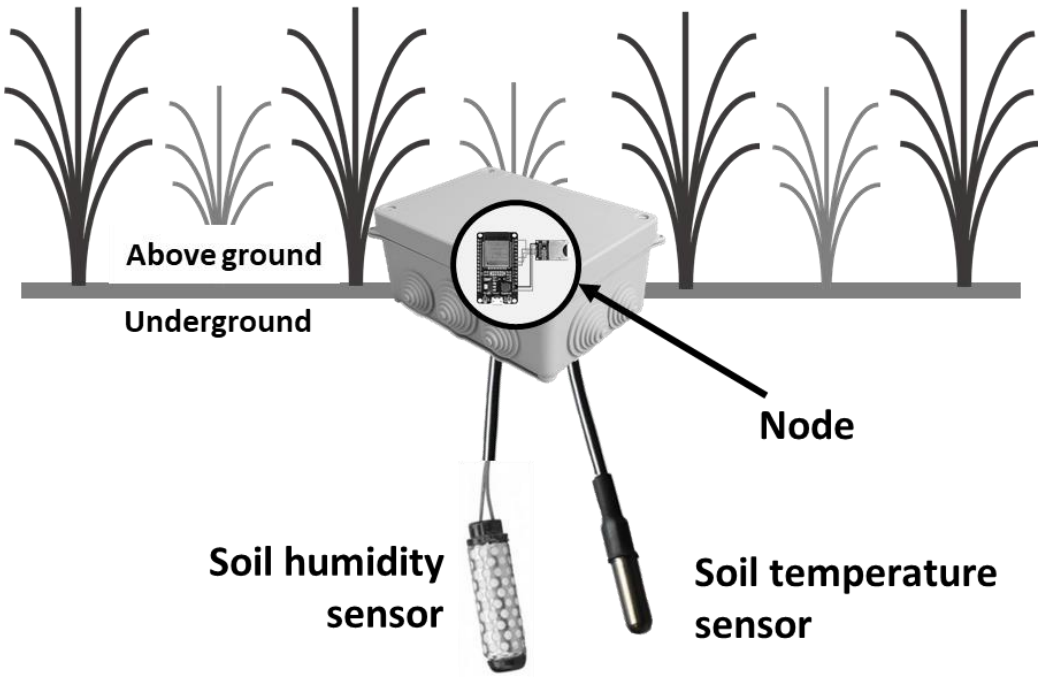

Figure 5.26. Design example of the soil monitoring node.

The drone is located on a base station, where the route begins and ends. The drone takes photographs of the fields and the terrain during its flight. When the drone reaches the base station, all the retrieved information is forwarded to the data center where the information is stored on a database for further analysis.

A connection between the sensor node and the drone, with a good enough quality to ensure the data is transmitted successfully, is one of the requirements of a PA system that employs a drone to gather data from sensor nodes deployed on the field. Other requirements include low energy consumption for the drone to complete its route, the availability of the operating frequency band, and good weather conditions to avoid signal attenuation and damages to the drone and sensor nodes.

Regarding the data rate, it is crucial to consider that the parameters measured in PA systems vary at a slow pace. Therefore, continuous monitoring is not necessary, and the data can be captured each minute or at larger time intervals such as 5, 10, or 30-minute intervals. Therefore, the information stored in the SD card is not a large amount, and the necessary data rate would hardly surpass 1 Mbps. Furthermore, works such as [363] show real data rates obtained at different flying heights and distances that surpassed 1 Mbps for heights of 20 m and distances of 45 m, with the drone acting as an intermediary node and therefore, with more chances of experiencing interference and signal attenuation. A fixed-winged drone is utilized in [352] to capture images from the fields and forward them using WiFi, where a UDP throughput up to 176 Mbps was obtained from real experiments. Therefore, although parameters such as flying height and speed are undoubtedly determinant in the success of the data transmission, once the connection between the sensor node and the drone is established, the necessary data rate is not high.

Low energy consumption should be sought on both the drone and the sensor nodes. The sensor nodes can go to sleep mode during idle time to reduce energy consumption. Furthermore, if the settings of the drone indicate a fixed time for the drone to gather the data from the sensor nodes, the nodes can activate at that time to avoid being in sleep mode when the drone flies over them. Lastly, the lifetime of sensing nodes can surpass a year if the energy consumption is optimized, and the battery is chosen to ensure it. Using solar panels to power the sensor nodes would even nearly cease the problem of battery-less sensor nodes. Choosing between using batteries or solar power would be determined by the type of crop or the desired size for the sensor node. Trees remain productive each year without needing to plant new ones, but other crops are not used after the harvest, where the field is left to rest until the planting season. Therefore, the nodes could be fixed or be removed and deployed again according to the type of crop and its characteristics.

Most fields are far from populated areas, and interferences from other networks are lower than industrial or urban environments. However, testing the area for other networks is a good practice to choose the best settings and communication technology for the PA system.

Lastly, extreme weather conditions are unavoidable, but some measures can be taken to reduce the damage that can be caused by the elements of the PA system. For example, if a weather station is incorporated into the PA system, the drone could decide whether

it is safe or not to fly. The sensor nodes should have a protective encapsulation and be able to store the data of several days to ensure no data is lost. Furthermore, if the drone were to be lost due to extreme wind or rain, the SD cards in the sensor nodes would ensure the data can be accessed manually.

The information monitored in each one of the sensors is unique and, as we have previously commented, it must be forwarded to a remote location where the data center is deployed. Due to the limitations intrinsic to the deployed network which has a limited processing and storage capacity, limited power availability, and a short time interval for the communication between the node and the drone, we consider a system comprised of soil monitoring nodes. These remote sensing drones obtain video and photographs of the fields and gather the data from the nodes, the base station of the node that includes a gateway to send the data to the remote location, and the data center situated in a remote location where the data is stored and analyzed.

The functioning algorithm of the drone is presented in Figure 5.27. Firstly, the drone loads the flight plan, which can be designed using the existing software for flight plan designs and considering crop requirements. After the setup, the drone asks for the weather information gathered by the weather station. If the wind speed is greater than the threshold value (*wth*), the flight is canceled, and the drone waits until the next scheduled flight. If the wind speed is correct, the rain amount is then checked. If the threshold value (*rth*) is surpassed, the flight is canceled as well. If everything is correct, the drone checks the available energy. If there is enough energy, the drone begins the route through the fields. If there is not enough energy, the drone cancels the flight. The drone then checks if a node is asking for a connection. If there is no node to connect with, a photo of the field is taken, and the available energy is re-evaluated. When a node is detected, a connection is established, and the drone receives the data. When all the data has been received, the drone sends a disconnect message to the node to indicate that the connection is terminated and that the node should go to sleep mode and should not try to connect to the drone for the time determined in the settings. By doing this, the possible interferences caused by other nodes deployed in the fields in the coverage range of the drone are avoided. Although interferences among the nodes for the configurations of node coverages for orchards of fruit-bearing trees, as contemplated in this scenario, would only be possible with the case of 1 node per 60 m^2 of node density. The detailed explanation of the different node densities considered for different types of crops is presented in section 6.6.1. After that, an oblique photo of the field is retaken, and the drone looks for another node. When the route was finalized, the drone goes to the base station and forwards the data to the database at the remote location for further analysis. Then the drone waits at the station until the scheduled time for the next flight is reached.

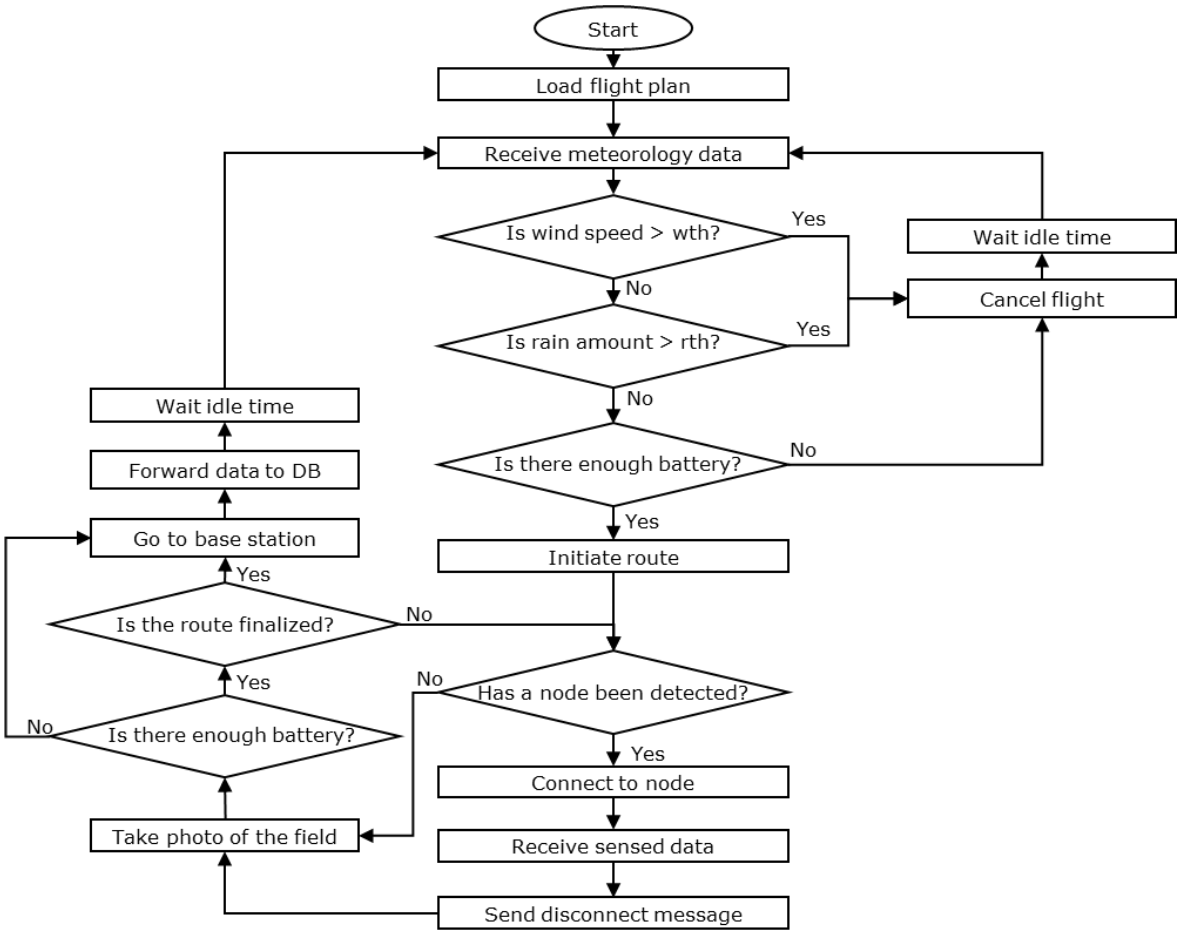

Figure 5.27. Algorithm of the drone.

The functioning algorithm of the node is presented in Figure 5.28. After the setup has been completed, the node starts gathering the data from the nodes and storing it on an SD card. If it is the scheduled time for the drone flight, the node gets activated to wait for the drone. If it is not the scheduled time, the node goes into sleep mode for the time specified in the setup parameters. If a drone is detected, all the data stored on the SD card is forwarded to the drone. When the node receives a disconnect message, the node disconnects from the drone and deletes all the data stored in the SD card. Then, the node goes into sleep mode for the time stipulated on the settings so as to save energy and to avoid the drone having interferences with other nodes. While the node does not detect the drone, it checks if the maximum time activated time is reached to determine if it needs to go to sleep mode. This way, the node is not constantly activated if the drone decides to cancel the flight due to weather conditions. Then, it keeps gathering the data from the sensors each time the time interval between measures loaded from the setup has been reached.

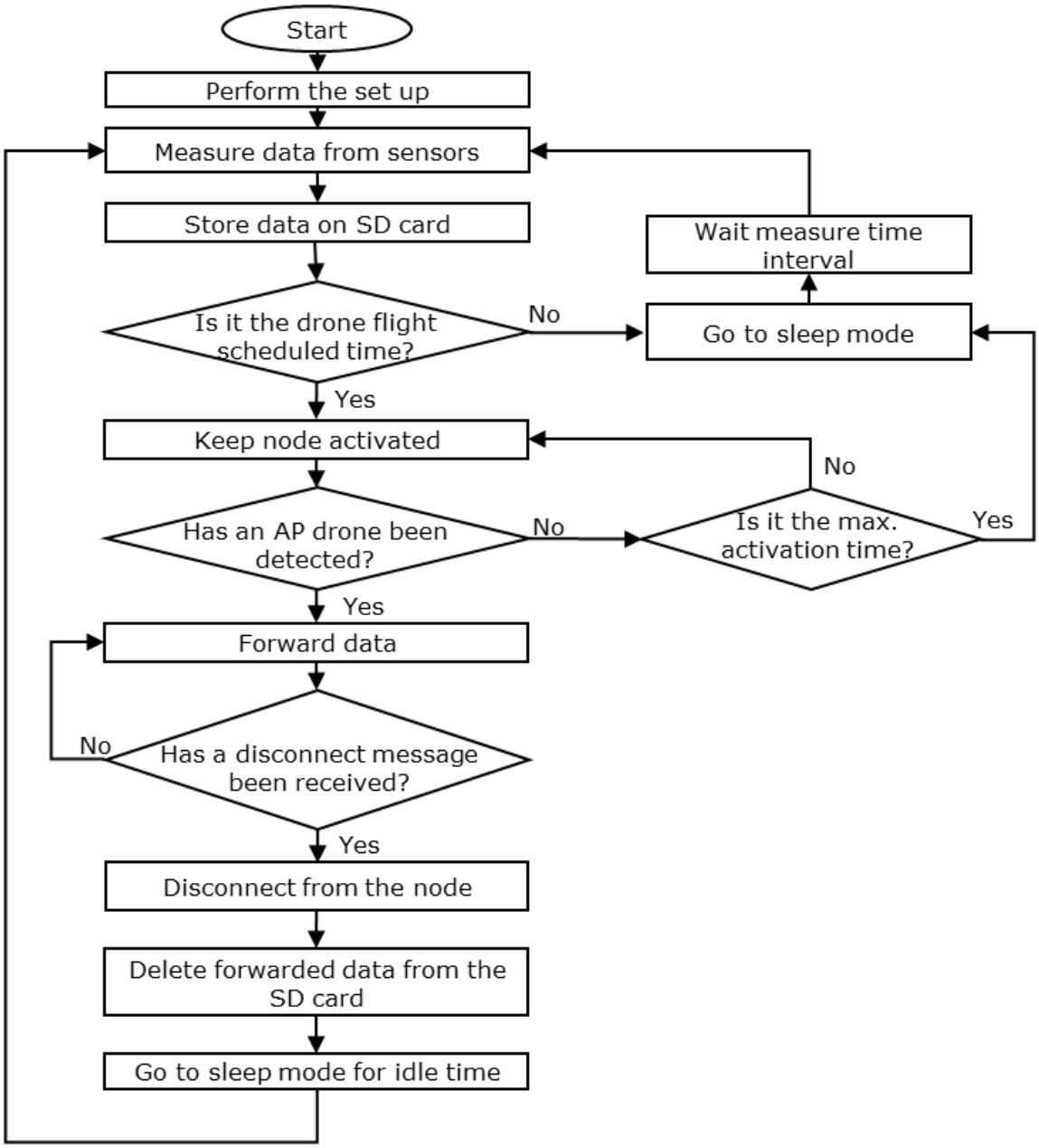

Figure 5.28. Algorithm of the node.

The message exchange between the elements of the architecture is presented in Figure 5.29. The drone sends beacons so the nodes can detect it and ask for a connection. When the connection establishment is performed, the node sends the data to the drone. The drone then sends an ACK and a Disconnect message to indicate that the node should go into sleep mode for the stipulated time. After that, the node sends an ACK to the drone to indicate that the Disconnect message has been received correctly. The process is repeated with all the nodes deployed on the field within the coverage area of the drone as it follows its route. When the node reaches the base station, the data is forwarded to the database, and the database confirms the reception of the data with an ACK.

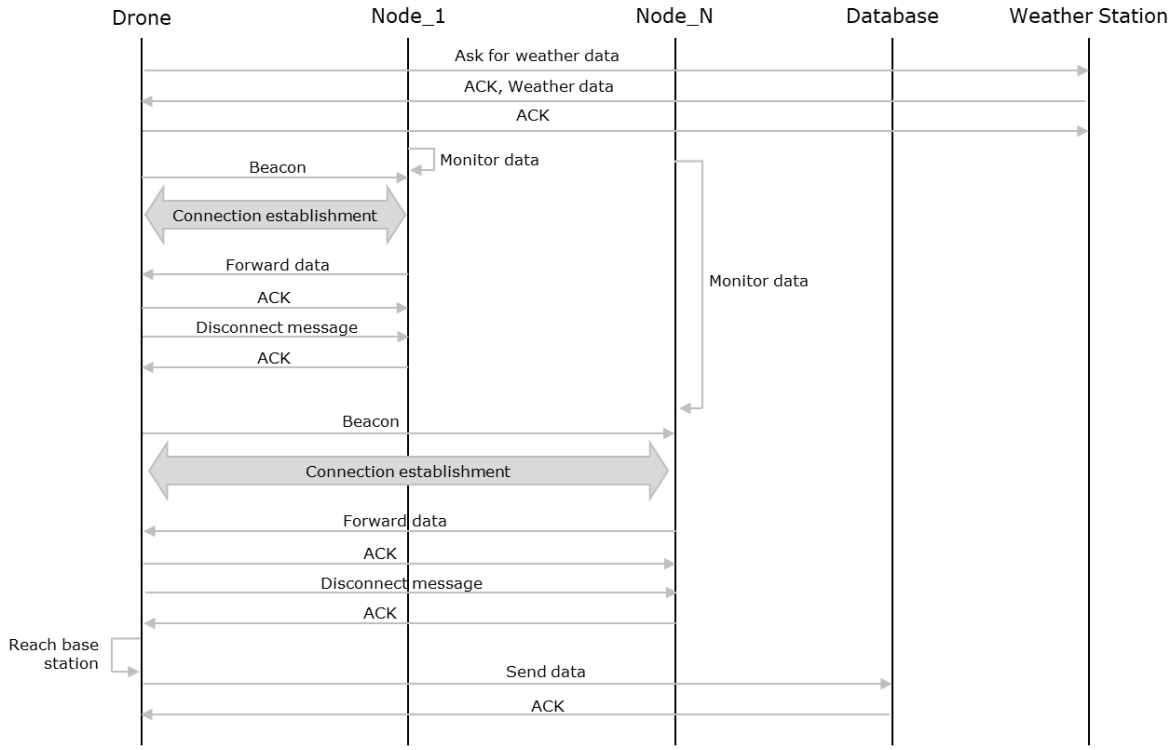

Figure 5.29. Message exchange between the elements of the architecture.

5.9 Conclusion

In this chapter, the proposed solutions for different specific cases have been provided. The cases that have been addressed are the following:

- A multi-layer fog computing framework has been proposed [364]. It provides fog functionalities to the nodes deployed on the canal and field areas in order to reduce the amount of data and messages that are forwarded in the network. The simulation results will be detailed in Chapter 6 section 6.2.
- A protocol for a network entirely comprised of LoRa nodes has been proposed as well. This work has been published in [48]. Moreover, the simulation testbed and the obtained results will be detailed in Chapter 6 section 6.3.
- The security threats that LoRa networks for PA systems may face have been discussed. Physical attacks, attacks on the data in transit, attacks on the management system, and attacks on the data have been considered. Furthermore, the actions that can be taken to address these security issues have been presented. This work was published in [289].
- A WSN for the case of WiFi/3G heterogeneous networks for the monitoring of citrus plots has been presented as well. Furthermore, fault-tolerance and energy-saving algorithms have been provided as well. This work was published in [28] and the simulation results on bandwidth consumption and consumed energy will be commented in Chapter 6 section 6.4.

- A discussion on the use of CoAP for PA systems comprised of IEEE 802.11 nodes, previously published in [38], has been performed. The simulation results will be depicted in Chapter 6 section 6.5.
- An algorithm for underground communication for IoUT networks has been presented [365].
- The use of remote sensing drones to gather de data from WiFi nodes deployed on the field while maintaining the designed flight plan for the remote sensing activities has been presented as well [9]. The simulation results on the best parameters to achieve a successful data transmission will be analyzed in Chapter 6 section 6.6.

Chapter 6

Simulation Results

6.1 Introduction

In this chapter, the simulation experiments of the proposals described in the previous chapters are presented. Firstly, simulations of consumed bandwidth and the number of forwarded messages are performed to assess the effectiveness of the proposal for data aggregation. Then, the case of a protocol for a network where all the nodes transmit the data utilizing LoRa is contemplated. Simulations are performed to assess the amount of data that is stored on the SD cards of the nodes, the energy consumption, and the consumed bandwidth. Then, the consumed bandwidth and energy consumption for deployments of multiple WiFi nodes are presented. After that, the collisions that may happen in WiFi WSN for PA are evaluated. Lastly, different configurations of flight settings for remote sensing drones have been considered to determine the adequacy of the remote sensing node as a gateway.

6.2 Results for a multi-layer fog computing framework

In this section, the simulation results from the study case presented in Chapter 5 subsection 5.2 are presented.

The Canal area is comprised of four clusters that forward the data to one aggregator node. There are eight actuator nodes in this area. For the Field area, three zones were considered with three clusters per zone, one aggregator node which is an agrometeorological station as well, and three actuator nodes. The sensing nodes and the CH nodes communicate through WiFi. The CH nodes and the Aggregator nodes communicate through LoRa at the EU 863-870 frequency band, with a bandwidth of 125 kHz and a spreading factor of SF8. These LoRa settings allow a maximum payload of 222 Bytes including the LoRa header. Furthermore, as collision management is not part of the scope of this paper, it is assumed that there are no collisions.

The Researcher mode performs the data acquisition process every 10 minutes and thus, the high amount of forwarded data (See Figure 6.1). As it can be seen, the nodes in Layer 1 forward all the data to the CH nodes in Layer 2. The state of the Actuator nodes is forwarded each hour. The Researcher Mode obtains a reduction of 35% at the forwarding times compared to not performing any data acquisition (See Figure 6.2). In this case, no data aggregation was performed at Layer 3. Furthermore, there is a water salinity alarm on the first day. At the times the data forwarding timer is reached, the data forwarded nearly reaches 20000 Bytes for an hour.

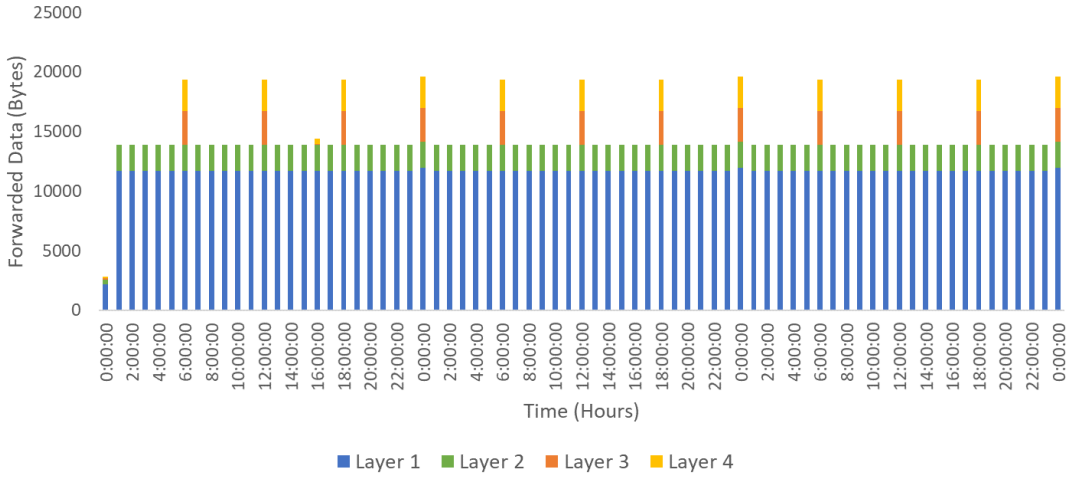

Figure 6.1. Data forwarded by each layer at the Researcher Mode.

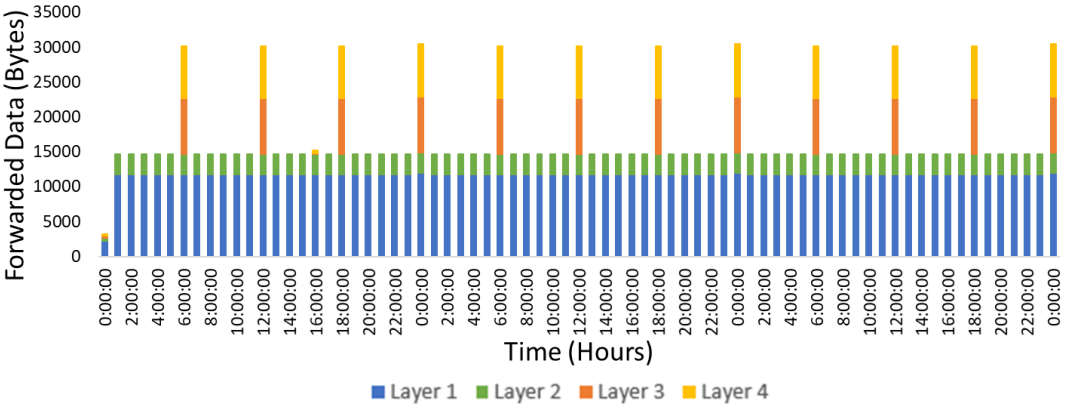

Figure 6.2. Data forwarded by each layer at the Researcher Mode without data aggregation.

At the Advanced Farmer Mode, as it can be seen in Figure 6.3, the amount of forwarded data is decreased due to the data acquisition frequency of 30 minutes. The state of the Actuator nodes keeps being forwarded each hour. Thus, there is a fluctuation in the amount of data forwarded each time the timer is reached. Furthermore, the data is aggregated at Layer 3 as well and the data is forwarded to the data center twice a day. With this mode, compared to not performing data aggregation, a reduction of 60% was achieved when the forwarding time is achieved (See Figure 6.4). With data aggregation, a reduction of 66% of the forwarded data was obtained compared to the Research mode. The reduction reached a 76% at the times where the de states of the actuator are forwarded.

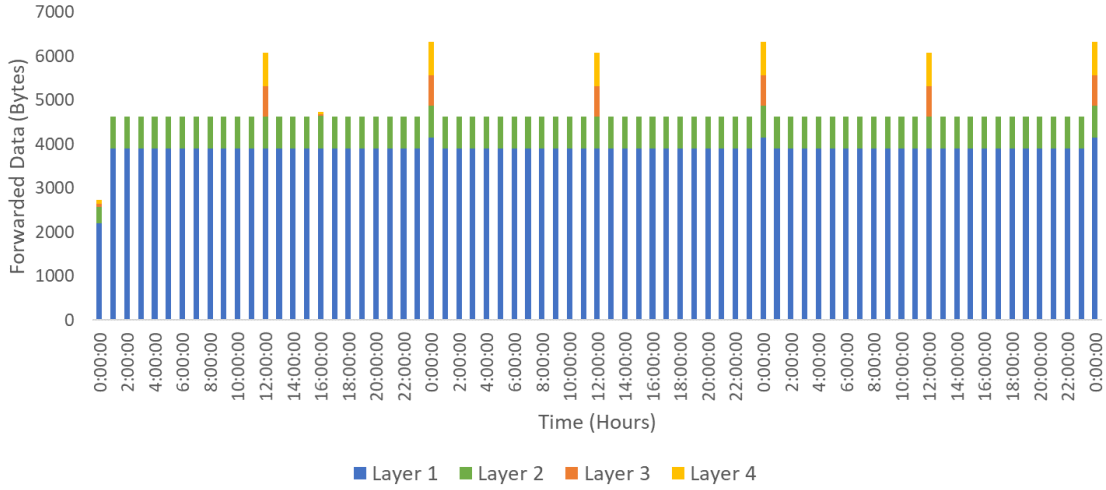

Figure 6.3. Data forwarded by each layer at the Advanced Farmer Mode.

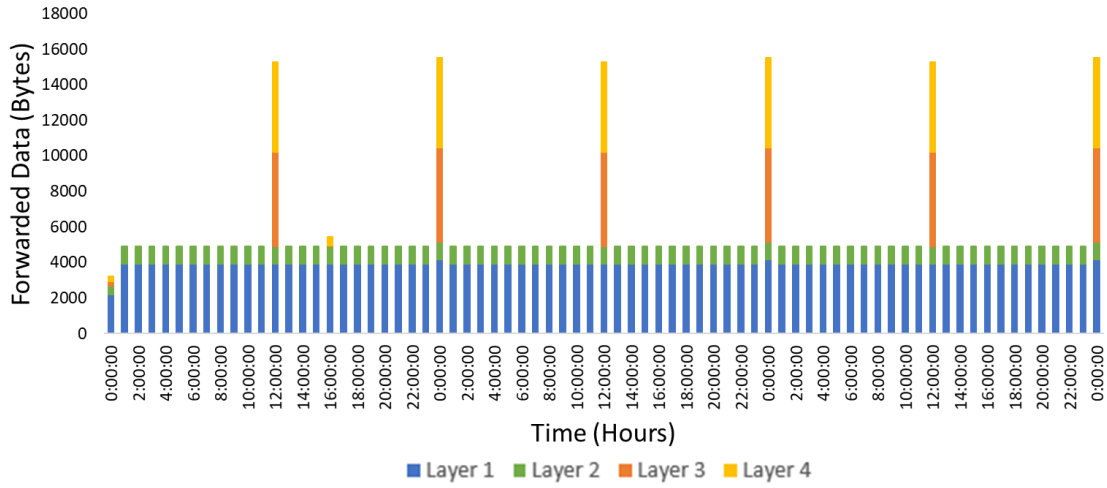

Figure 6.4. Data forwarded by each layer at the Advanced Farmer Mode without data aggregation.

Lastly, the data forwarded by each layer to the next layer of the hierarchy on the Regular Farmer Mode is presented in Figure 6.5. The algorithms allow reducing substantially the amount of data forwarded by the higher Layers to the Data Center with an 83% for layers 1 and 2 and an 80% when the data forwarding timer is reached. Furthermore, a reduction of 69% in the transmitted data at the forwarding time is obtained compared to not performing data aggregation (See Figure 6.6). This reduction in the forwarded data leads to a reduction in the energy consumption of the devices as the higher energy consumption is produced when data is transmitted.

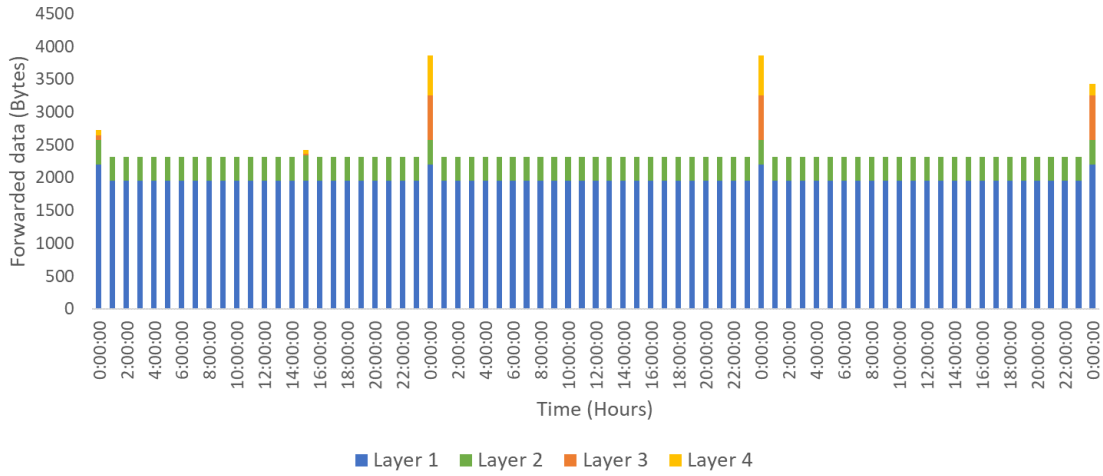

Figure 6.5. Data forwarded by each layer at the Regular Farmer Mode.

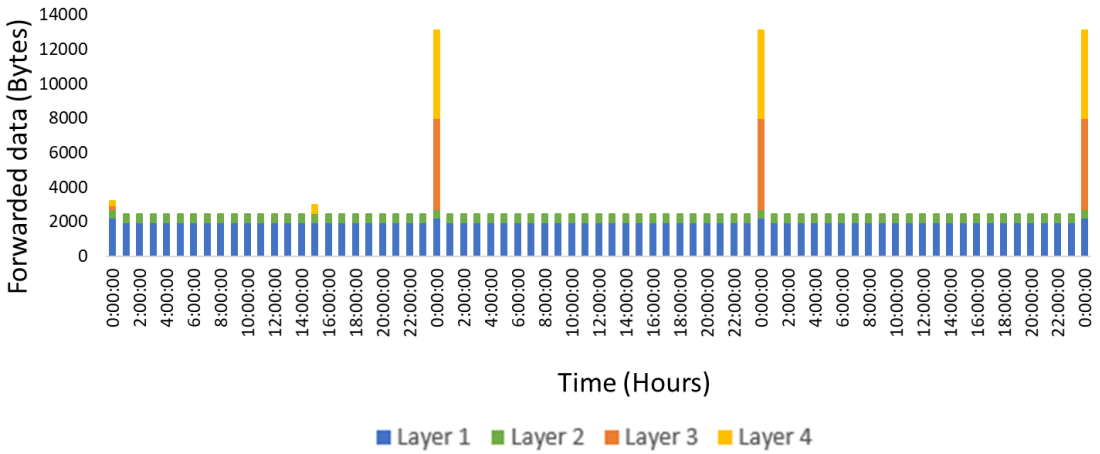

Figure 6.6. Data forwarded by each layer at the Regular Farmer Mode without data aggregation.

Regarding the number of forwarded messages, the results of the Researcher Mode are presented in Figure 6.7. Between 234 and 249 messages are forwarded per hour except when the system is firstly activated where 53 messages are generated. As it can be seen, the hierarchical structure of the framework allows reducing the number of forwarded messages at each layer. Furthermore, a reduction of 9% of the messages at

the peaks compared to not performing data aggregation was achieved (See Figure 6.8). This is important regarding LoRa as there is a limitation in the number of messages that can be forwarded due to the duty cycle. Other LoRa settings would not support the Researched Mode. This is a key aspect if longer distances need to be reached as higher spreading factor values would be necessary and thus, the number of messages that could be forwarded would decrease.

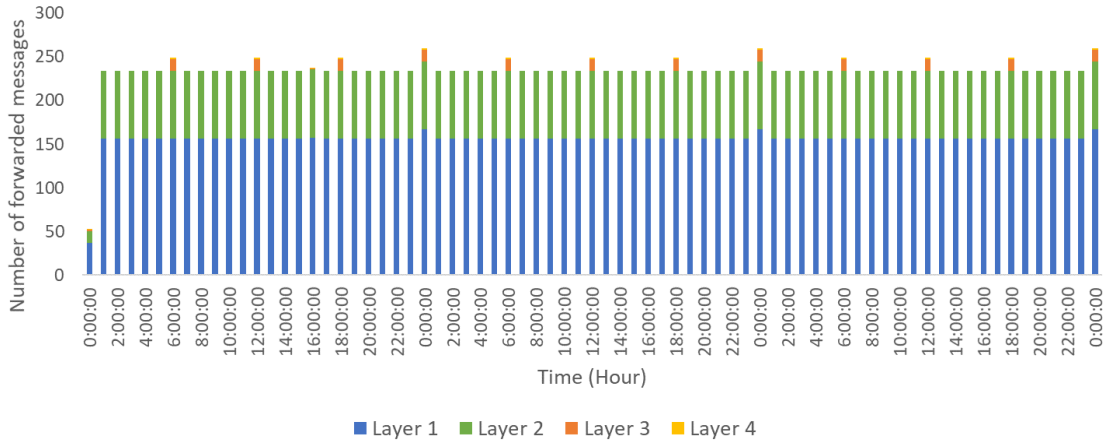

Figure 6.7. Number of messages forwarded by each layer at the Researcher Mode.

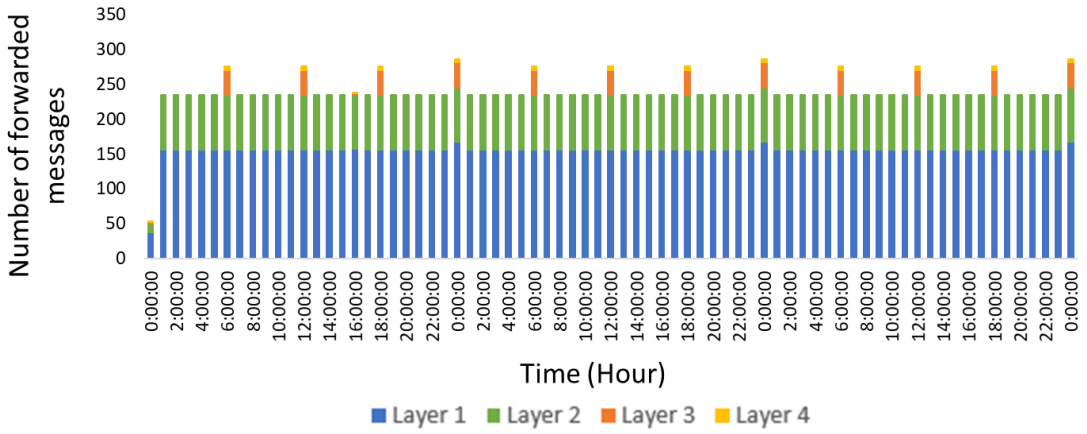

Figure 6.8. Number of messages forwarded by each layer at the Researcher Mode without data aggregation.

At the Advanced Farmer Mode, the number of messages oscillates between 78 and 83 messages per hour except for the first hour with 53 messages (See Figure 6.9). The reduction of messages at the peaks is 68,67% compared to the Researcher Mode and 21% compared to not performing any data aggregation (See Figure 6.10).

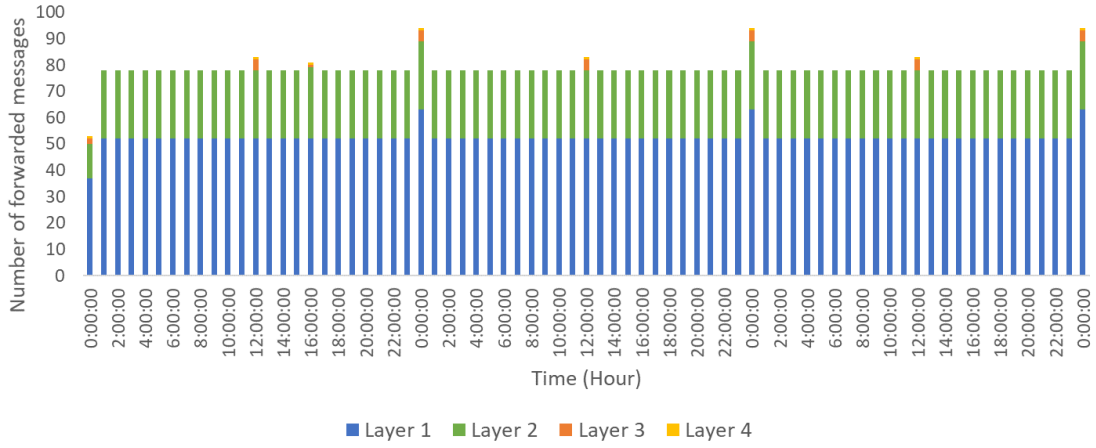

Figure 6.9. Number of messages forwarded by each layer at the Advanced Farmer Mode.

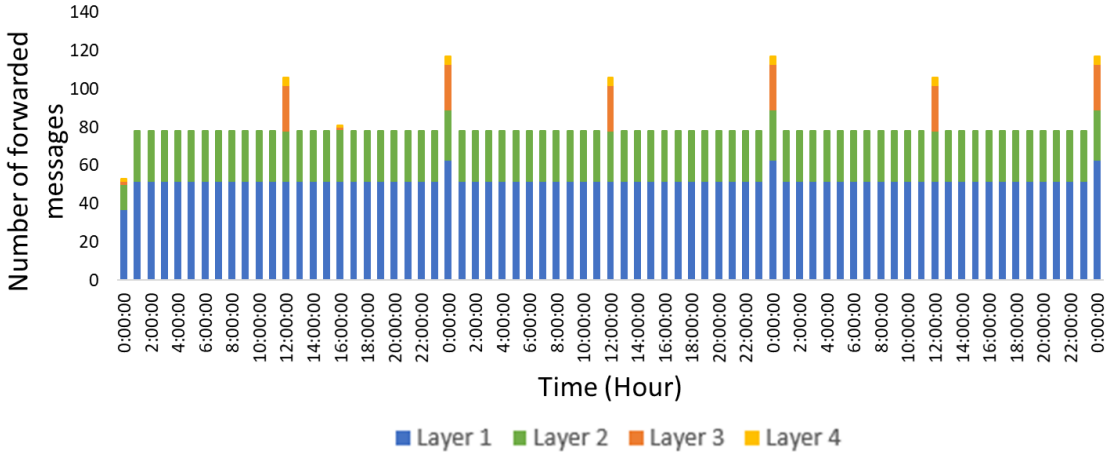

Figure 6.10. Number of messages forwarded by each layer at the Advanced Farmer Mode without data aggregation.

Lastly, at the Regular Farmer mode, the number of forwarded messages remains between 39 and 55 messages per hour (See Figure 6.11). With an 85.33% of reduction at peaks compared to the Researcher Mode and 29% compared to not performing data aggregation (See Figure 6.12). This mode is optimal for remote areas as it would allow other LoRa settings with more restrictions regarding the number of messages that can be forwarded by each device. Furthermore, it would not be detrimental to the farmer as the calculations of the irrigation requirements only need one measure of each variable per day except for the meteorology data where the maximum and minimum values of temperature and relative humidity are necessary.

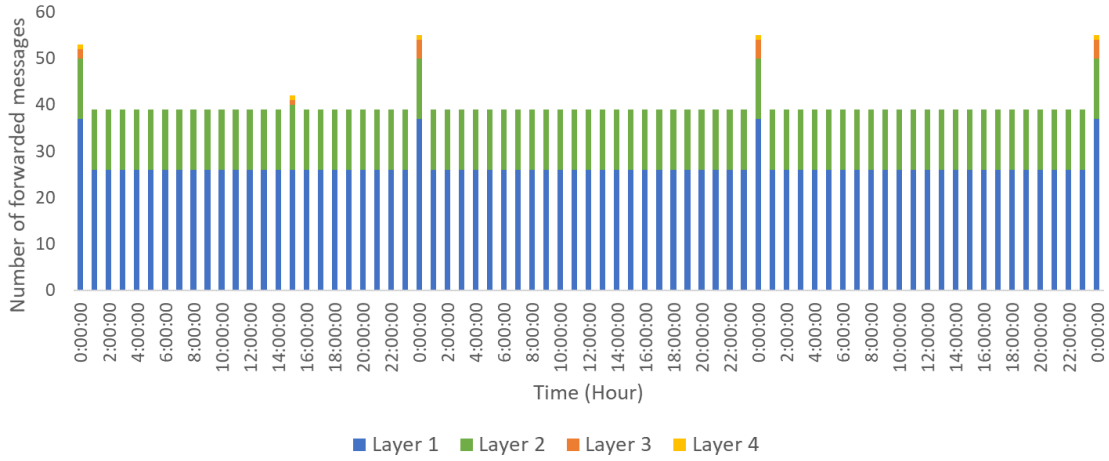

Figure 6.11. Number of messages forwarded by each layer at the Regular Farmer Mode.

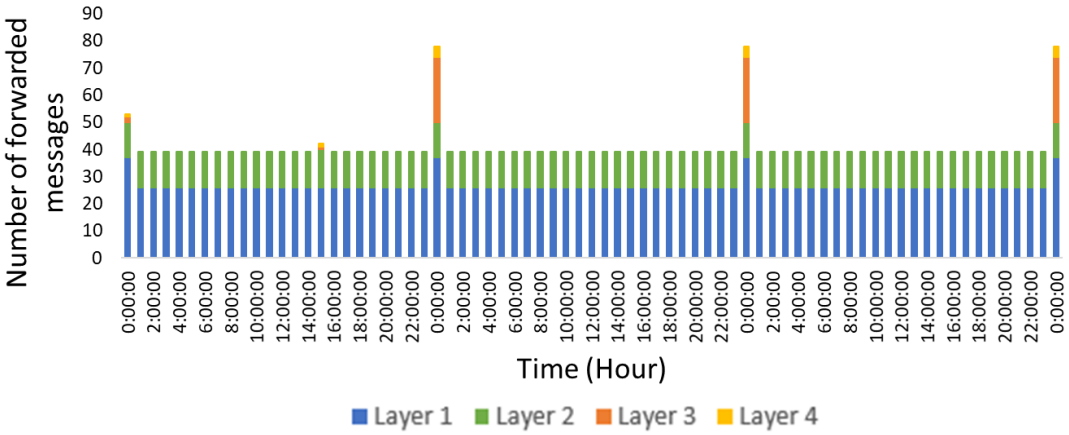

Figure 6.12. Number of messages forwarded by each layer at the Regular Farmer Mode without data aggregation.

6.3 Simulations of a LoRa protocol for wastewater treatment

In this section, the simulation results for the protocol presented in Chapter 5 subsection 5.3.

6.3.1 Simulation Description

The considerations under which the simulation was conducted are detailed in this subsection.

6.3.1.1 Water Details

For the simulation, we have considered a region that entails two urban areas (UAs) with their channel to collect the water, the main channel, and one irrigation channel (IC) with the small pools (POs) in which water is treated. A total of 6 locations are considered in this simulation: 2 urban areas (UA1 and UA 2), the irrigation channel (IC 1), and the 3 pools (PO 1, PO 2, and PO 3.). In each one of these areas, a total of three nodes (a cluster) is located. The cluster comprises three nodes with LoRa interfaces. The six locations are close enough to ensure good coverage with a single LoRa gateway.

Since we are going to simulate our results using the algorithms described above, we need to generate different values of pollution in the monitored areas. To generate these values, we have included in our simulations the movement of water from point to point and some pollution inputs generated by random numbers at different intervals. The generated pollution coming from UAs and the pollution from the IC is diluted into the channel and flows to the next station. The pollution levels are maintained along with the IC. They only decrease in the pools where biosorption material is cleaning the water. Each pool has the capacity to reduce 50% of the pollution present in the water.

The following consideration is the probability of a false positive or a false negative due to an abnormal monitored value of one of the sensors. We have defined the chance of giving a false positive as 5% and 1% for a false negative.

The simulation has a duration of one week in which each sensor measures the water quality once per minute. This timing is required since the arrival of pollution to the fields can transfer the problem of pollution from the water to the soil, and in this medium, the recovery is more complex. The simulation is carried out in two different periods of the year, in summer and in winter. This will affect only the energetic-related parameters.

6.3.1.2 Network Details

Regarding the packets sent through the network, we consider that the sensed data have a length of 37 bits for each measurement. The headers of the packets sent through LoRa comprise a preamble of 8 bytes and a header of 13 bytes. The data packets that are forwarded over LoRa will have a minimum size of 141 bits, which corresponds to a message with one measurement. Furthermore, the maximum packet size is 4176 bits, which is the maximum size allowed by LoRa. Lastly, the LoRa ACKs have a size of 21 bytes which corresponds to the preamble and the header.

The simulation for the energy consumption of the LoRaWAN nodes is performed according to the energy consumption model presented in [366]. The total energy consumption of the node is presented in Equation (6.1).

$$E_{Total} = E_{Microcontroller} + E_{Sensors} + E_{tx} + E_{rx} \quad (6.1)$$

where $E_{Microcontroller}$ is the energy consumed by the microcontroller, $E_{Sensors}$ is the energy consumed to activate the sensors and gather the data, E_{tx} is the energy consumed to transmit the data, and E_{rx} is the energy consumed to receive the ACK from the gateway, which according to [366] is 0.27 mJ.

Equation (6.2) is utilized to determine the energy consumption per bit at the transmission.

$$E_{bit} = (\text{Power Consumption x ToA})/(8 \text{ x } (\text{Preamble + Header + Payload})) \quad (6.2)$$

As for the LoRaWAN parameters, considering that our system requires a minimum range of 2 km, all possible settings would meet the requirement in the scenario of free space for a frequency of 868 MHz (See Figure 6.13). However, as there are vegetation and trees in the area, we consider a scenario with few obstacles, as presented in Figure 6.14. Therefore, for a transmission power of 7 dBm, the settings of BW250-SF7 and BW500-SF7 would not meet the requirement. For the case of 433 MHz, the required maximum theoretical distance is reached with all settings.

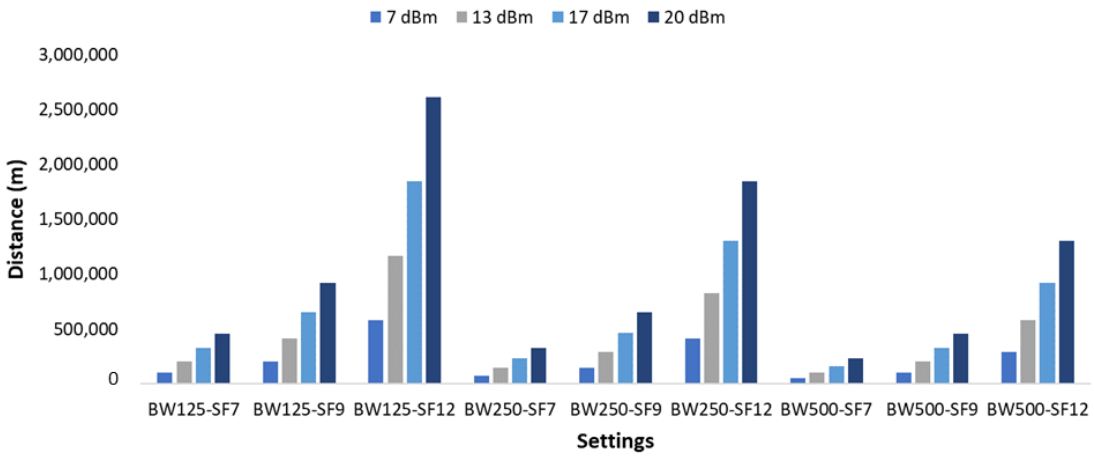

Figure 6.13. Maximum theoretical distance at 868 MHz for free space.

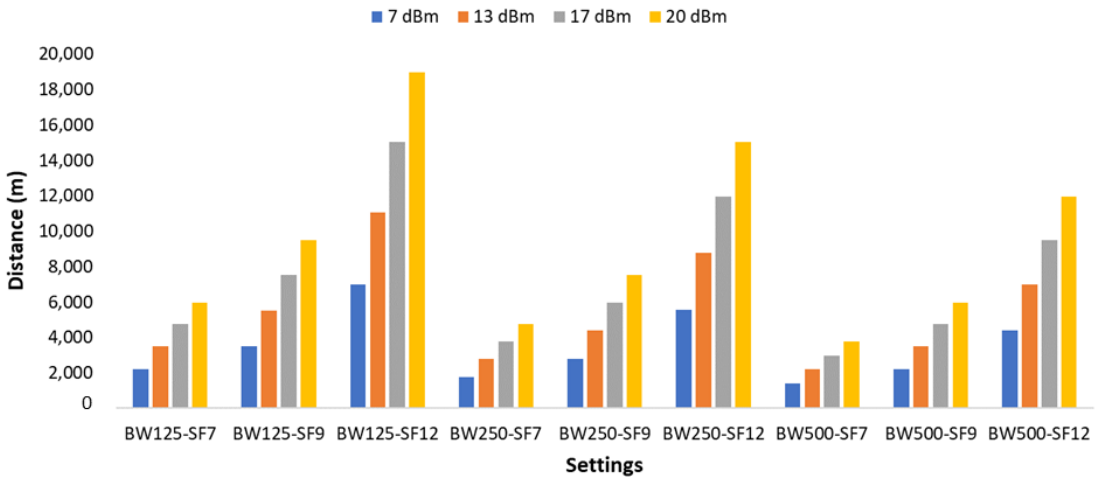

Figure 6.14. Maximum theoretical distance at 868 MHz for few obstacles.

Considering the results of the theoretical distances for each LoRa setting, the settings selected for our system are the EU 863–870 frequency band, BW 125 kHz, and SF 8. Therefore, for the selected settings and a selected transmission power of 13 dBm with its power consumption of 92.4 mW/h, the energy consumed per bit for each sensor is 45.55 μJ.

6.3.2 Results

In this subsection, the results of the simulation are presented. First of all, the storing and sending procedure of each node is represented as the SD status. Then, the bandwidth of the full network is depicted. Finally, the issues related to the remaining energy in the node are evaluated.

6.3.2.1 Status of the SDs

Considering the protocol described in Chapter 5 subsection 5.3, one of the main aspects of this protocol is storing data, instead of sending it, waiting until the moment in which the water quality changes to send all stored data. We have to consider that the nodes which are not a CH store the data before sending them to the CH once the node detects a change. This procedure implies that the CH node stores large amounts of data just before sending them. Figures 6.15 and 6.16 show the stored information in the SD of each one of the included nodes in our topology. While Figure 6.15 focuses on the first 60 min of the simulation, allowing for seeing some of the processes in detail, Figure 6.16 summarizes the whole simulated period.

In Figure 6.15, we can identify the stored information in the SDs of the clusters of six included locations: (a) UA1, (b) UA2, (c) IC1, (d) PO1, (**e**) PO2, and (**f**) PO 3. Focusing on Figure 6.15 a), we can identify that the three nodes store information until minute 35. In minute 35, Node 3 and Node 2 detect a change in water quality. Node 1 has a false negative. Node 3 sends data to Node 2 and erases the data. Then, Node 2 checks that both nodes registered a change and sends all the data stored in the SD to the gateway. We can identify that Node 3 continues storing information during the rest of the period. In UA2, in Figure 6.15 b), we can see the same case in minute 5, in this case, Node 3. Then, we identify a case in which the three sensors detect a water pollution change, see minute 52. In that case, the two nodes (Node 1 and Node 3) send the CH node data. Thus, the stored information is incremented three times. At that moment, the SD of the CH node stored 5550 bits of information. Similar cases can be seen in Figure 6.15 c) in minutes 41, 47, 51, and 59, and in Figure 6.15 d) in minutes 51 and 57. This delay of 10 min between IC1 and PO1 is the simulated time that the water remains in each pool. Finally, Figure 6.15 e), f) show the normal data storage process in the SDs. Since water is treated twice and three times, there are fewer water quality changes.

On the other hand, Figure 6.16 shows the SD usage for each node along the simulated period of one week. We can identify that locations UA1, UA2, and IC1 have a similar trend. All these areas, in Figure 6.16 a)–c), have low volumes of data stored in the SDs due to the constant exchange of information with the gateway caused by changes in water quality. Meanwhile, PO1, PO2, and PO3 are clusters characterized by larger amounts of data stored in the SDs, particularly during the second day of our simulation. In general terms, we can see that areas characterized by a lot of change follow the patterns seen in Figure 6.15. We can have false positives, false negatives, or true positives related to the water quality, which induce the sending event of stored data. In addition, we can see a secondary pattern here, mainly in the areas characterized by a lower degree of change. In these cases, when no changes are detected, Node 1 and Node 3 send all the information to the CH at midday to free their SDs, and as a method of control, as explained in Chapter 3 Figure 3.26. This behavior can be particularly identified in the node of PO3, in which the unique movements of data in the SDs are related to the process. Thus, we identify a pattern of storing information until midday when all the data are sent to Node 2, and then Node 2 sends data to the gateway to free its SD. The maximum amount of stored information is 106,486 bits (13.3 Kbytes).

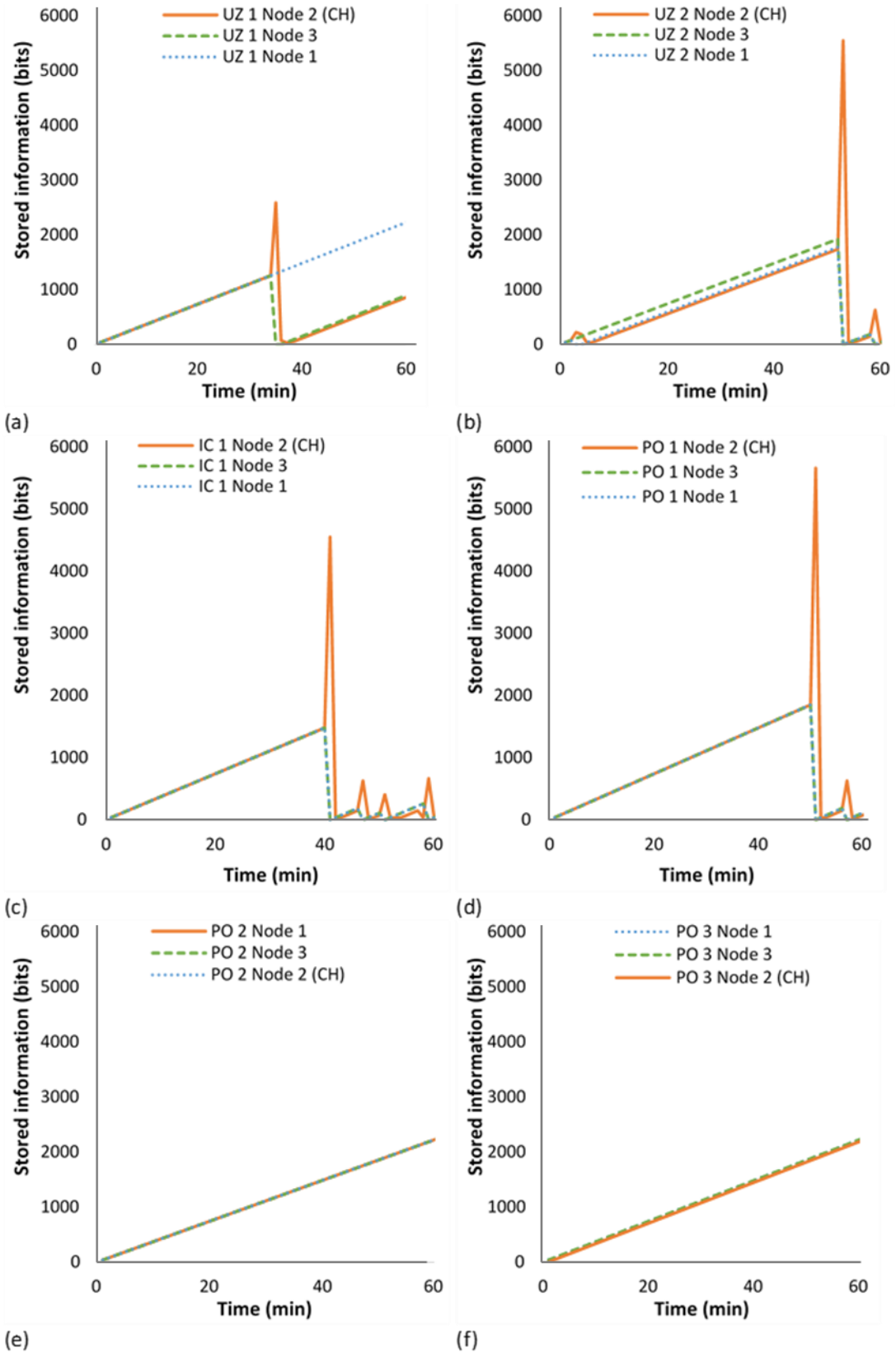

Figure 6.15. Stored information in the SDs cards of nodes. Details of the first 60 min of operation. Different letters (**a**) to (**f**) denote the different locations of the cluster: (**a**) UA1, (**b**) UA2, (**c**) IC1, (**d**) PO1, (**e**) PO2, and (**f**) PO 3.

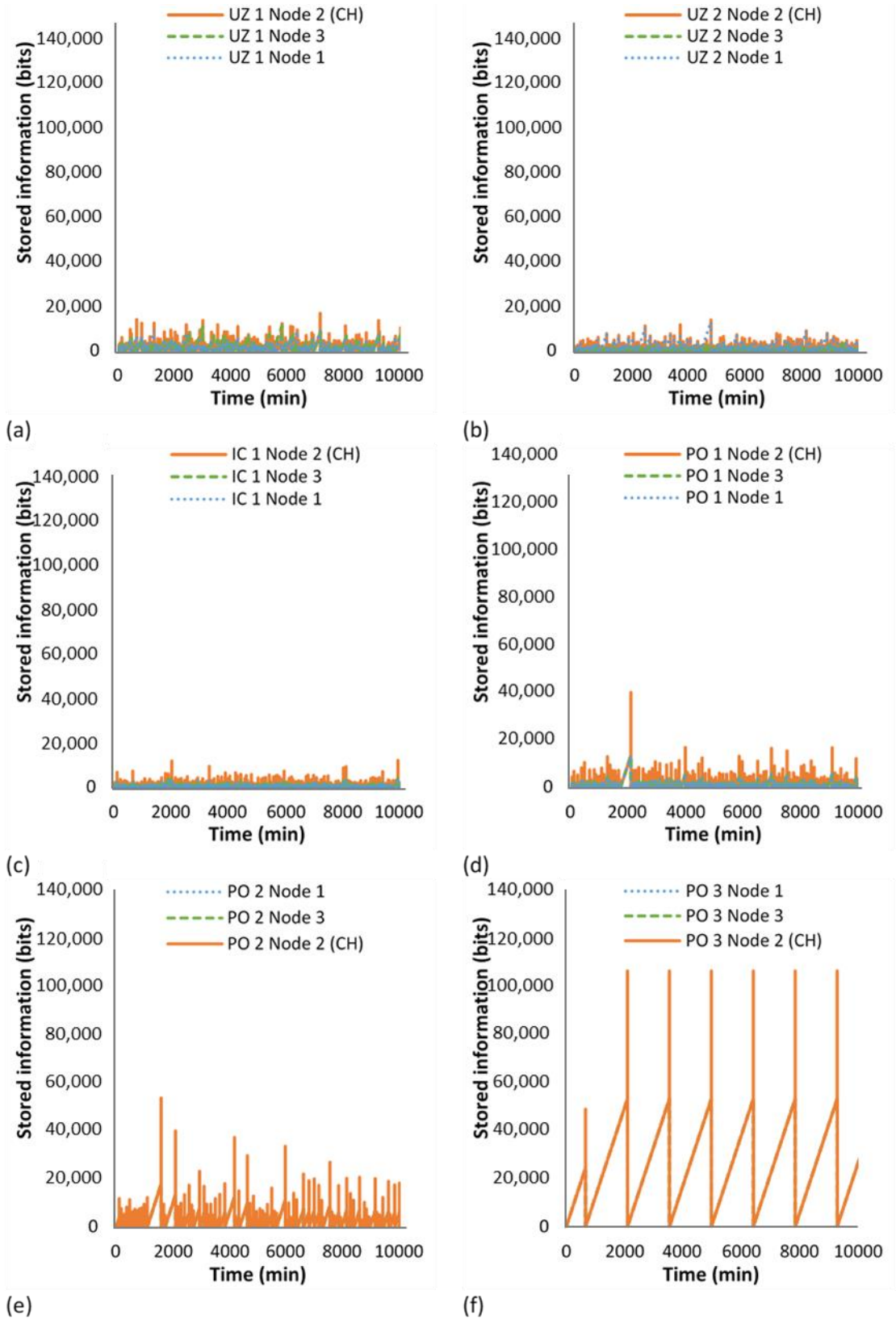

Figure 6.16. Stored information in the SDs cards of nodes. Summary of the whole simulated period. Different letters (**a**) to (**f**) denote different locations of the cluster: (**a**) UA1, (**b**) UA2, (**c**) IC1, (**d**) PO1, (**e**) PO2, and (**f**) PO 3.

6.3.2.2 Consumed Energy

Figures 6.17 and 6.18 show the node energy. The nodes have an energy harvesting system that has been dimensioned to ensure that it can cover the node's energy requirements. In comparison, Figure 6.17 shows the remaining energy along with the simulation in each location in the worst scenario (winter with three consecutive days with a reduced energy harvesting). We can see the different locations in Figure 6.17 a)–f). In all four locations, we identify a similar trend. Node 2 is the node that consumes more energy since it receives the information of Nodes 1 and 3 and sends all the information to the gateway. Nodes 1 and 3 of each location have the same tendency in their energy levels in general terms. No significant differences can be seen among the energy levels of Nodes 1 and 3, along with the locations. Nonetheless, the energy of CHs differs from one location to another.

The CHs of locations with greater changes in water quality (Figure 6.17 a–c) send more packets which are translated into more energy consumption. The CH with higher energy consumption is the CH of UA2 (Figure 6.17 b). This node reaches a minimum energy of 12,320 mW/h just before the sunrise of the fifth day. The rest of the CHs, located in areas with fewer or no changes in water quality (Figure 6.17 d–f) have higher energy levels. Another interesting trend can be identified in PO3 (Figure 6.17 f). We can see a sharp decrease in energy levels at midday due to the large amounts of data sent at that moment. The absence of water quality conditions causes this during the rest of the day. Since the other CHs send data when the nodes detect a change, this decrement of energy level is distributed throughout the day.

Finally, Figure 6.18 shows the energy level of CHs in three different simulations for which we have modified the energy harvesting conditions. Figure 6.18 a) represents the worst conditions, the winter period with just 9 h of energy harvesting and three consecutive days with a reduction of 50% in the energy harvesting. These results summarize the data shown in Figure 6.17. Figure 6.18 b) shows a period of winter but without attenuated energy harvesting. We can identify that the CH of UA2 still has lower levels of energy than the others. Nevertheless, the difference is lower than in the previous scenario. On the other hand, Figure 6.18 c) shows a period of summer without attenuated energy harvesting. In this case, we have 14 h of energy production. We can see that the energy levels of CHs are similar to those in previous cases. During summer, nodes have their batteries full for most of the day.

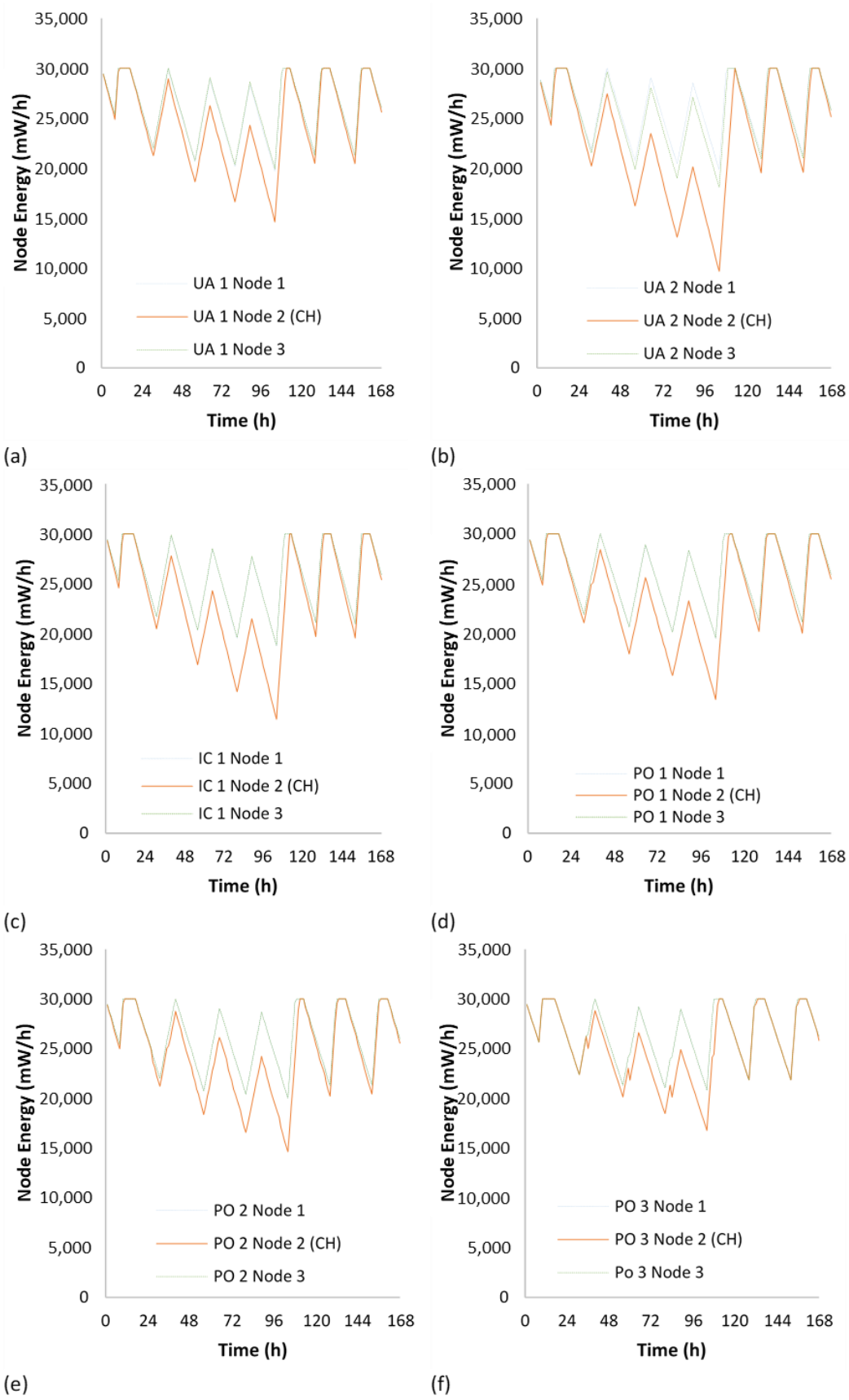

Figure 6.17. Energy consumed by the nodes. Summary of the whole simulated period. Different letters (**a**) to (**f**) denote different locations of the cluster: (**a**) UA1, (**b**) UA2, (**c**) IC1, (**d**) PO1, (**e**) PO2, and (**f**) PO 3.

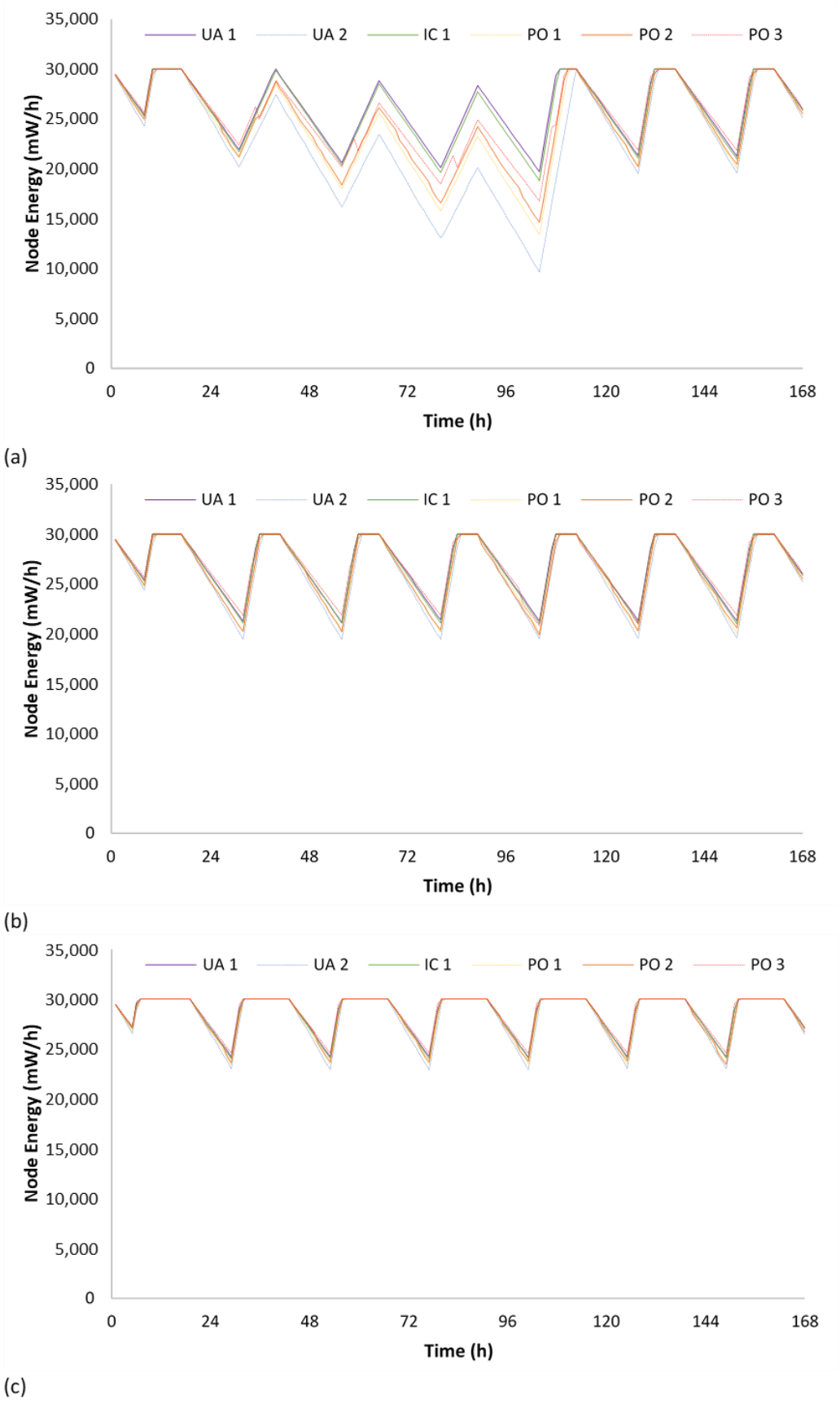

Figure 6.18. Energy consumed by the nodes. Summary of the whole simulated period. Different letters (a–c) denote different ambient conditions: (**a**) winter period with reduced energy harvesting for three days, (**b**) winter period with full energy harvesting, (**c**) summer period.

6.3.2.3 Consumed Bandwidth

Figure 6.19 portrays the entire network's consumed bandwidth, including the communication inside each cluster and the communication between the CHs and the gateway. A detail of the consumed bandwidth of a short period can be seen in Figure 6.19 a). It represents the first 720 min of the simulated network, the first half of the day. We can see that in a considerable amount of time, the network does not generate any packet exchange due to the application of the algorithm. In this simulation, during the first 720 min, we can identify that in 612 min, there is no exchange of information in our network. Minute 661 is the moment when all the information is sent to the gateway. At this moment, we reach the maximum bandwidth usage, 177,187 bits/min (2.95 kbps).

Considering Figure 6.19 b), we can identify the consumed bandwidth during the whole simulated period. We can find seven peaks in the consumed bandwidth, which correspond to the seven middays. The maximum peak in this period is found on the second day. At that moment, a consumed bandwidth of 381,357 bits/min (6.35 kbps) can be identified. It is important to note that among the 40 performed simulations, we have represented the one with the highest maximum bandwidth. Figure 6.19 c) shows the box and whiskers diagram of the maximum bandwidth of all the 40 simulations. The average maximum bandwidth is 306,411 bits/min (5.1 kbps). With the selected LoRa settings, the maximum data rate is 3125 bps [367]. Therefore, we conclude that the data of the third cluster should be forwarded in two periods to avoid peaks of bandwidth consumption above 3125 bps.

A second simulation was performed to verify that changing the data forwarding settings of cluster three to two data forwarding times, being 9 h and 21 h, allows the bandwidth to remain below the maximum 3125 bps. The consumed bandwidth in the second simulation is presented in Figure 6.20. Figure 6.20 a) shows the results for a short period of time. In this case, the first 1400 min are shown as the system spends more than 1100 min with low bandwidth consumption. Then, there is a peak of 155,011 bits/min (2.58 kbps). The results for the complete simulated period are shown in Figure 6.20 b). The peak with the highest bandwidth consumption is the same as the one displayed in Figure 6.20 a). The second highest bandwidth consumption peak reached 142,764 bits/min (2.37 kbps).

Another 40 simulations were performed to obtain the box and whiskers diagram of the maximum bandwidth for this simulation scenario (See Figure 6.20 c). The average maximum bandwidth was 128,204 bits/min (2.13 kbps). Furthermore, the change produced in the simulation does not have relevant repercussions on the global energy consumption of the proposed system.

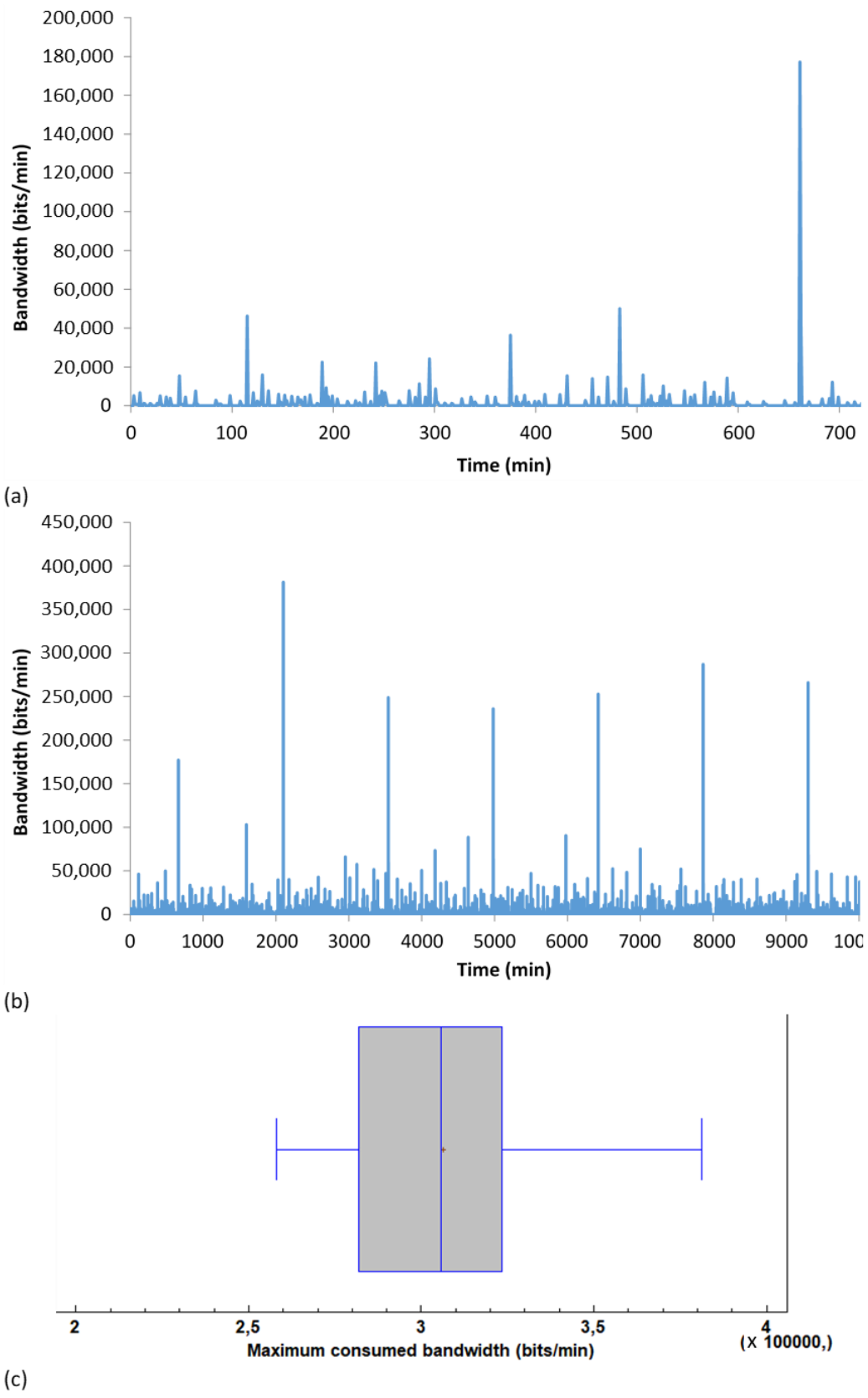

Figure 6.19. Details of consumed bandwidth in our simulation. Different letters denote different details: (**a**) initial period, (**b**) whole period, (**c**) summary of the maximum bandwidth of 40 simulations.

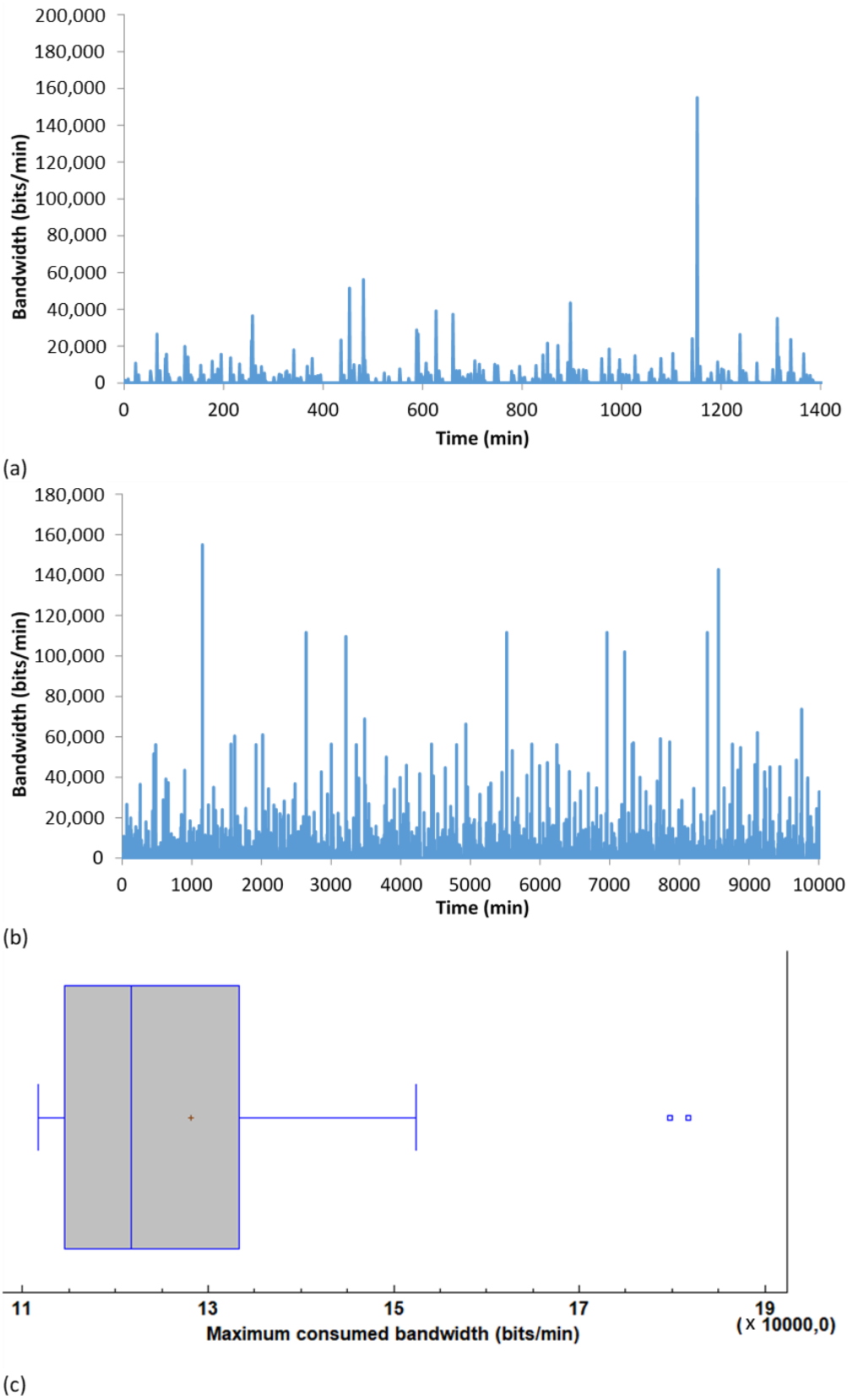

Figure 6.20. Details of consumed bandwidth in second simulation. Different letters denote different details: (**a**) initial period, (**b**) whole period, (**c**) summary of the maximum bandwidth of 40 simulations.

6.4 Simulations of WSN with fault-tolerance and energy-saving functionalities

In this section, the simulation performed with the protocol and algorithms proposed in Chapter 5 section 5.5 is going to be described.

6.4.1 Simulation description

First, the number of employed nodes and the topology are described. In our simulation, we include a total of 23 nodes. From those 23 nodes, there are different types of nodes such as WNA (1 node), WNB (1 node), FN (20 nodes) and FNS (1 node). In Figure 6.21, we show the location and type of the nodes. In blue, we can see the WNA and WNB placed in the Jucar River and in the channel used to transport the water to the orchards. The FN are represented in red dots and are numbered in letters, from "*a*" to "*u*". The node "*k*" is the FNS, which will collect the data from the rest of the nodes.

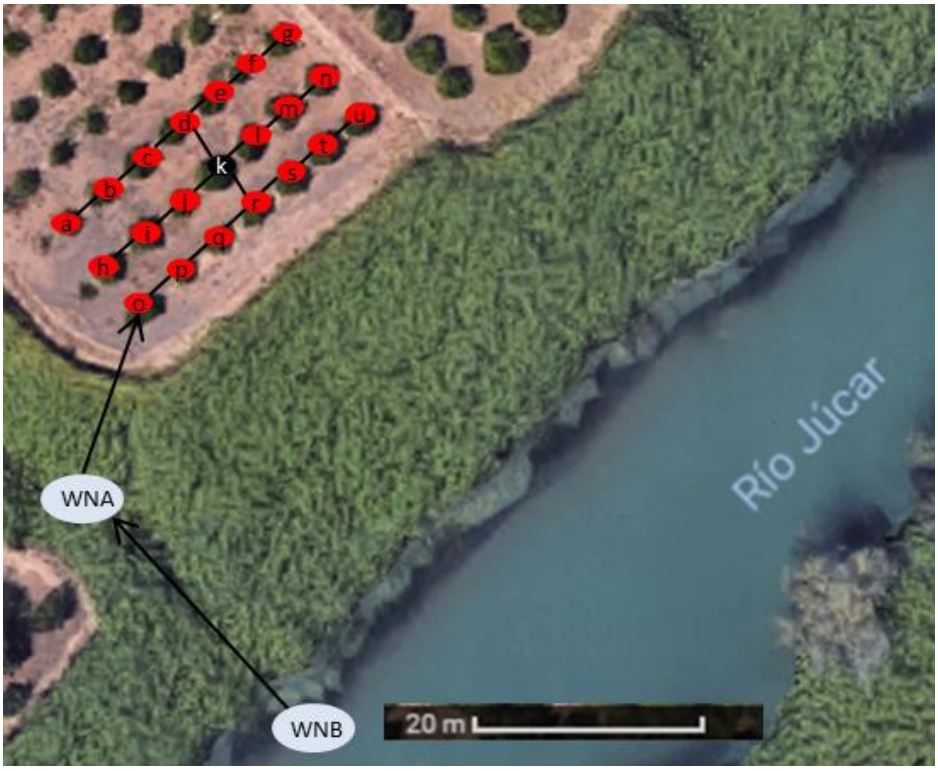

Figure 6.21. Topology for the simulation.

According to [348] we assume that the energy used for transmission and reception is 50nJ/bit, and 100pJ/bit/m2 considering a distance of 3m between FNs. In our simulations, we are not going to use any type of encryption to avoid energy use. The

initial battery of the FNs is 0.1J and the FNS has a different battery with 0.5J. We consider that the nodes gather data each 5 min. The data is sent only if the gathered data is relevant, see Chapter 5 Figure 5.11. For the simulation, we consider a 10% chance that the gathered data is relevant and must be sent.

When one node sends information, according to Chapter 5 Figure 5.11 and 5.12, the following nodes in the topology have to add their gathered data to the received information and send it. The length of the TCP header is 160 bits. The length of the data gathered by WNA or WNB is 20 bits. The length of the data gathered by FNs is 22 bits. The ACK packet length is 160 bits.

The same scenario will be tested with different energy configurations. The first configuration is the previous one, with 0.1J in all the FN nodes and 0.5J in the FNS. The second configuration gives 0.5J to FNS and 0.25J to nodes *d* and *r*. In the last configuration, nodes d and r have 0.425J, the nodes *c, e, j, l, o, p, q,* and *s* have 0.15J, the FNS 0.5J, and the rest of the nodes 0.05J. The number of iterations will be 20000. A total of 9 simulations will be performed for each configuration.

6.4.2 Results

In this section, we present the data obtained from the aforementioned simulation, including the total bandwidth consumed from the FNs and the remaining energy after 10000 iterations.

Firstly, we are going to present the results from the bandwidth consumed by the network. Figure 6.22 presents the consumed bandwidth during 5000 iterations. The mean consumed bandwidth is 1938 bits. The maximum consumed bandwidth is 7252 bits at iteration 4165. The minimum consumed bandwidth is 0 bits, this occurs many times in the 5000 iterations.

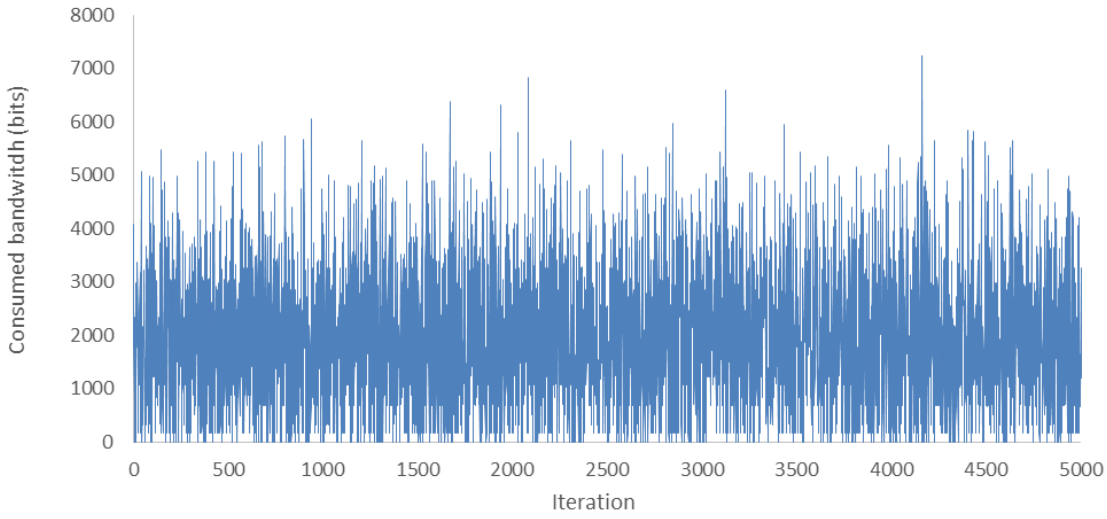

Figure 6.22. Consumed bandwidth.

Next, the remaining energy in the nodes is shown (see Figure 6.23). The node represented by a k in Figure 6.23 is the FNS and has 5 times more energy than the rest of the nodes. In Figure 6.23, we are representing the energy use related to the data transmission and reception. The nodes j and f consume the energy much faster than the other normal FNs. The node with less remaining energy is the r node, with 0.028J. The average remaining energy in the FN is 0.081J. The FN with higher remaining energy is the h node with 0.95J. The FNS has a remaining energy of 0.36J.

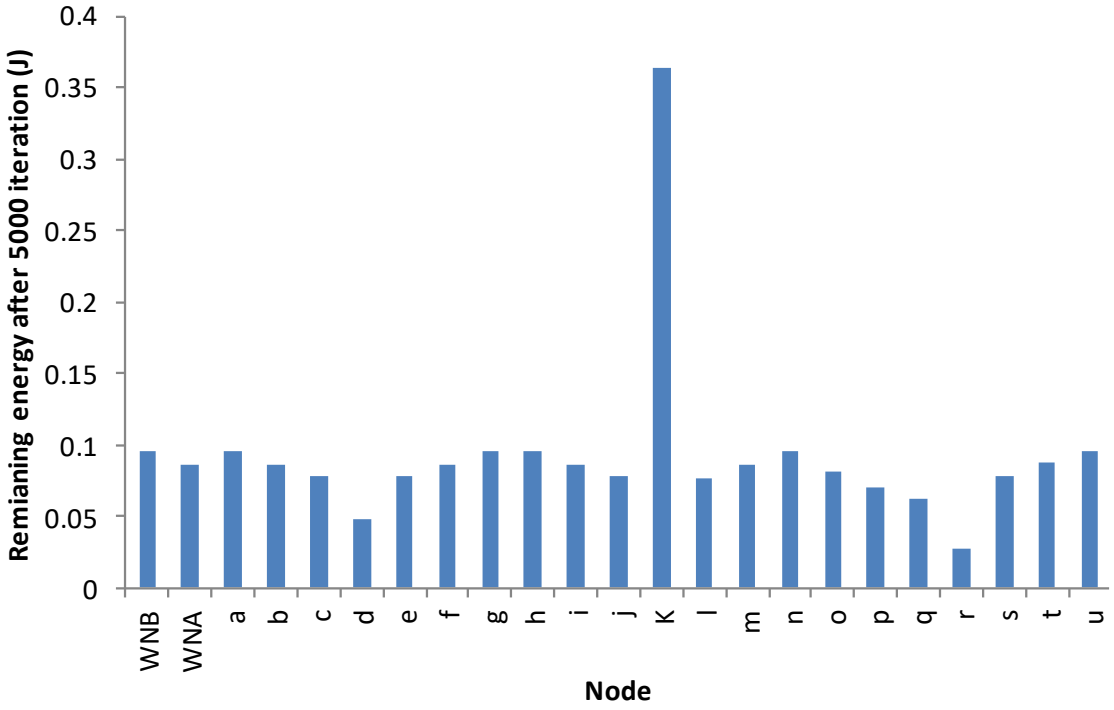

Figure 6.23. Remaining energy in nodes after 5000 iterations.

Now, we are going to evaluate the different energetic configurations. Table 6.1 shows the iterations before the first node dies. In the first configuration, the first node that dies is node r. The first node dies between iterations 6762 and 6919. The mean lifetime of the network is 6841 iterations. For the second configuration, the first node that dies is node q. This happens between iteration 1306 and 13609. The mean lifetime of the network is 13300 iterations. For the last configuration, the first node that dies is k node. The mean lifetime of the network is 18126 iterations, the minimum and maximum are 18079 and 18189. In Figure 6.24, we can see the maximum remaining energy in one node and the mean remaining energy in all the nodes for the different configurations. The configuration that uses the energy less efficiently is configuration 1, where there is one node with up to 3J when the first node dies. The second and third configurations have almost the same maximum remaining energy in one node. However, configuration 2 has a higher mean remaining energy in the nodes, 0.06J, while configuration 3 only has 0.04J. In addition, configuration 3 is the one that presents the longer lifetime.

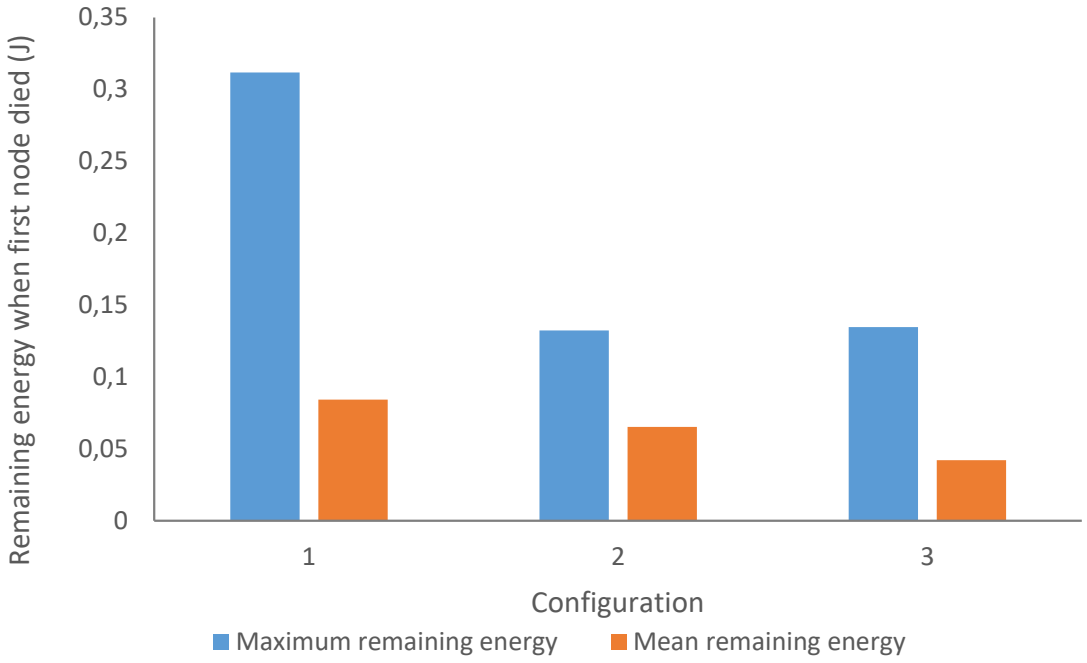

Figure 6.24. Remaining energy in nodes after 5000 iterations.

Table 6.1. Number of iterations before first node dies with different energetic configurations.

	Iteration first node died		
Simulation	***Conf 1***	***Conf 2***	***Conf 3***
1	6919	13236	18094
2	6862	13153	18189
3	6844	13326	18158
4	6765	13409	18129
5	6875	13343	18098
6	6762	13414	18114
7	6833	13609	18079
8	6850	13144	18146
9	6861	13065	18124
Mean	6841	13300	18126

6.5 Simulations of collisions in IEEE 802.11 WSN for PA

In this section, the obtained results after simulating the scenario described in Chapter 5 section 5.6 are presented. For our simulation, we consider a different number of nodes that send data to a single AP. Firstly, the number of nodes that are unable to send their data because another node is sending data is calculated. Then, we calculate the number of nodes that, after applying the CSMA/CA, are still unable to communicate their data to the AP. Finally, we show the number of attempts of sending data that failed during 1 second in the network.

The number of nodes that are unable to send the data when it is expected is shown in Figure 6.25. We consider that each node has a different clock time, and they have to send the data every second, as long as we are considering the worst case when the orange trees are being irrigated. Due to the different clock times, each sensor sends the data at a different moment. Our purpose with this graphic is to evaluate the effect of increasing the number of nodes in the number of nodes that are unable to send the data.

First of all, the number of nodes that are unable to send their data when it is expected because the network is currently being used by another node is evaluated. As it is expected, the higher the number of nodes, the higher the nodes unable to send the data. This is because as more nodes are in the network for more time the channel is used. In blue bars, the mean value after 30 different simulations (with different clock times) is represented and the line represents the minimum and maximum simulation results. The number of nodes unable to send the data increases following a second order polynomial relation. If we consider the percentage of nodes unable to send the data, the relation is still positive and increases following a linear relation. In the first case, with only 25 nodes, our simulation indicates that 4% of the nodes are unable to send the data when it is expected. In the most extreme case, with 250 nodes, 32% of the nodes detect a message when they try to send their data.

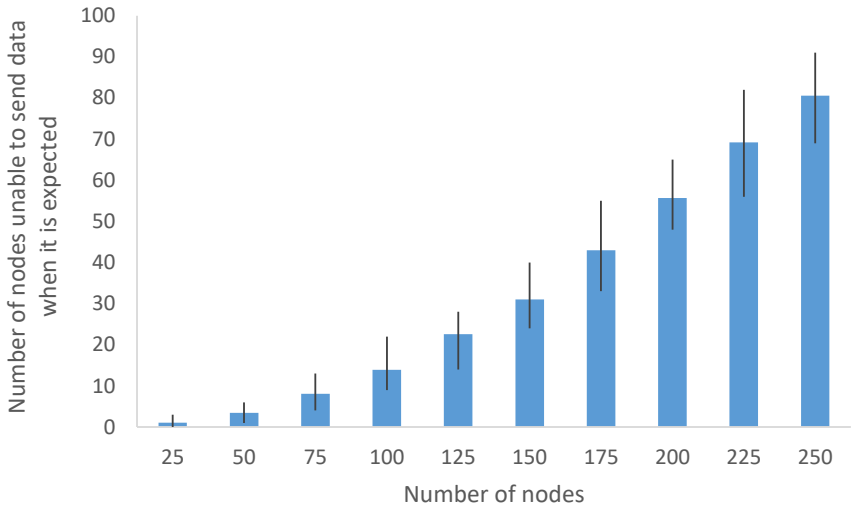

Figure 6.25. Number of nodes unable to send data when it is expected.

Next, we present the number of nodes that are unable to send the data after the application of the CSMA/CA algorithm using an exponential Backoff algorithm to calculate the waiting time, see Figure 6.26. The used Backoff algorithm gives 5 attempts before considering that the connection is unreliable. Again, we present in the graphic the mean, the minimum, and the maximum of 30 simulations. The results show that when there are less than 75 nodes (25 or 50) no node was unable to connect to the AP and send the data. However, when we connected up to 75 nodes to a single AP with the network parameters set in the previous section, some nodes were unable to connect and forward their data. As it is expected, the higher the number of nodes connected to the same AP, the higher the number of nodes unable to connect after applying the CSMA/CA. The relation between the number of nodes and the number of nodes unable to connect follows a potential relation. The number of nodes unable to send the data is up to 23 for a network with 250 nodes. If we consider the percentage of nodes instead of the number of nodes, the values are 0%, 0.04%, 0.33%, 1.07%, 1.60%, 3.03%, 4.95%, 7.60% and ,52%.

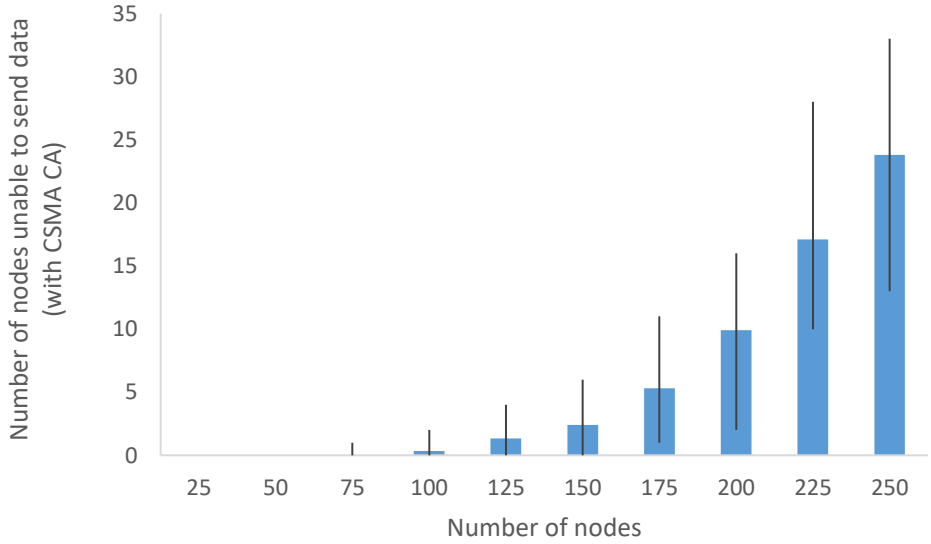

Figure 6.26. Number of nodes unable to send data after the CSMA/CA.

Finally, we present the data of the number of failed attempts in all the network during 1 second. This value is important because it represents the number of times that a node must apply CSMA/CA and the Backoff algorithm. This process not only consumes time but also consumes energy. Even it is performed in the microprocessor, and they are energy efficient, some energy is consumed and if this process should be repeated many times in one second (a maximum of 5 times) it will have an effect on the battery lifetime. Moreover, the time that the microprocessor remains to apply the algorithm is time that cannot be utilized to perform other actions. Therefore, it is important to consider the number of failed attempts to send the data in the network, see Figure 6.27. The number of attempts that fail, increases with the number of nodes in the network. With 250 nodes a total of 267 attempts failed during 1 second (mean value). It means that to send 250

packets with data 267 attempts failed and 226 attempts succeeded (250 less the number of nodes unable to send the data, see Figure 6.26). For the best case, with the lowest number of nodes, the mean number of failed attempts is almost 2, the maximum and minimum are 6 and 0.

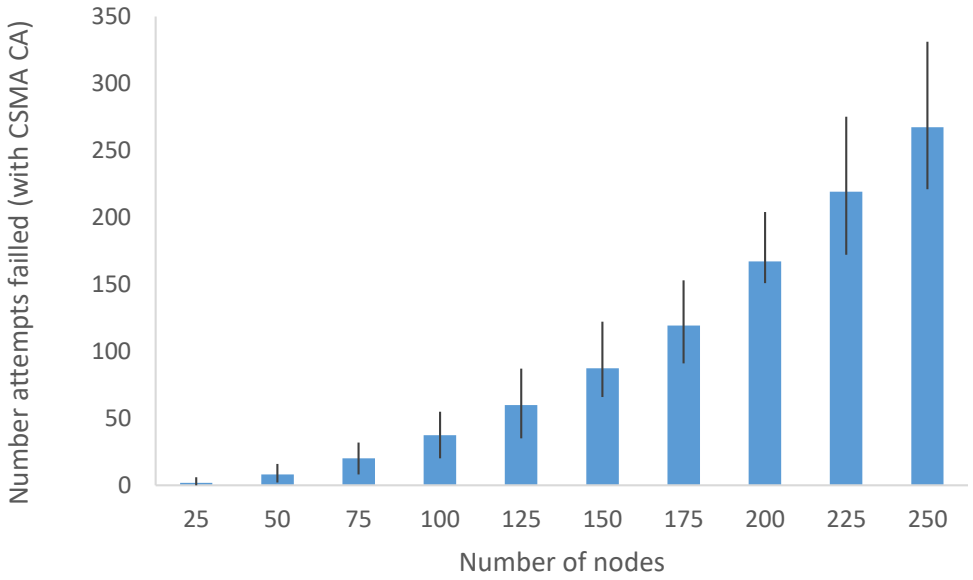

Figure 6.27. Number of failed attempts of sending data to avoid collisions.

Observing the obtained results, we propose the connection of a maximum of 50 nodes to each one of the AP, so that no collisions appear, and the operation of the network is optimal.

6.6 Drone coverage analysis

In this section, the theoretical values obtained after applying the equations described in Chapter 5 subsection 5.8.3 are analyzed. Furthermore, the energy consumption of the drone is analyzed, as well.

6.6.1. Coverage analysis

In this subsection, we first calculate the time during which a node has coverage from the gateway. Then, we calculate from those cases and with different bandwidths the amount of exchanged information between the node and the gateway and evaluate if this is enough to send the data stored in the node during the day.

Before starting to analyze the theoretical results, some assumptions must be made related to the connection and the density of nodes on the soil.

- First, we must consider the time required to establish the connection. We performed tests in real environments to determine the time required by Arduino nodes to establish the connection between each other. The results showed connection establishment times, ranging between 2 and 4 seconds. To ensure the connection of the nodes, we will consider the worst-case scenario of connection time of 4 seconds. Since the data is forwarded after the connection establishment, we will consider 5 seconds of total required time for connection establishment and data transmission. Therefore, all the combinations of dc and *fh*, which gives, as a result, a time in coverage equal to or less than 5 s are considered as unfeasible scenarios for connection. Since the current velocities in WiFi have increased in the last years and the gathered data by the sensors are small, we can consider that all the information can be sent in this period of 5s.
- Moreover, all the coverage areas do not have the same properties in terms of signal strength. The further points have lower Received Signal Strength Indicator (RSSI) values, and the connection will be difficult in those situations. Nonetheless, the estimation of the effects of RSSI on the establishment of the connection is not the purpose of this paper.
- Finally, regarding the density of nodes, we must consider the number of nodes that will be able to connect to the drone at the same moment and which have to share their time in coverage. There is a different type of scenarios regarding node density in precision agriculture. The densest cases are related to the intensive agriculture of fruit-bearing trees as orchards. The farmers use to grow their trees in a density of one tree each 16 to 20 m^2. In the case that we have one node per tree, the node density will be one node each 16 to 20 m^2. Nonetheless, this is not usual, since the conditions of the soil and irrigation techniques are relatively homogeneous. Therefore, we can expect that in the densest networks, we have one node every 3 or 4 trees, having a density of 1 node each 60 m^2. Other scenarios can include cereal or energetic crops. In these cases, the crops create a uniform soil coverage, and it is not possible to differentiate the individual plants. Moreover, as the outcomes of these crops are much lower than in the case of fruit-bearing trees, the investment in precision agriculture is lower. In addition, if we consider that most of the cereals and energetic crops do not need irrigation, the node density can be further lower. It is no exaggeration to say that in these cases, we can have only one node in each field having node densities of one done each 5000 m^2 or even more. In between both cases, we can find another example of fruit-bearing trees as olive trees. The density of trees in the field is lower than in the case of orchards. Moreover, since no irrigation systems are used in the culture of olive trees, the monitoring requirements are lower. Thus, we can expect densities of one done each 750 m^2 in the cropping of this type of crop. Nevertheless, the final density will be a factor that the farmer will define. To select the density of the nodes, the farmer will consider the environmental parameters (soil proprieties, homogeneity of the terrain, and past climate events), culture parameters (crop resilience, irrigation requirements, and susceptibility to specific diseases or pests among others), and economic constraints (benefits of the crops and the required investment).

Therefore, and to facilitate the comprehension of the results section, we detail the included parameters and their range in our model in Table 6.2. In Table 6.2 we describe if the parameter is considered as fixed-parameter or no, which means if this parameter is previously defined by the scenario or not. The defined parameters are the node density, the flying parameters (velocity and height), and the required time for communication. Furthermore, we have detailed the calculated parameters in our model based on the abovementioned variables.

Table 6.2. Parameters included in our model.

Parameter	Fixed parameter	Acronym	Units	Range
Flying height	Yes	fh	(m)	4 to 104
Flying velocity	Yes	fv	(m/s)	1 to 20
Drone coverage	No	dc	(m)	25 to 200
Node density	Yes	nd	(nodes/m^2)	60 to 5000
Time in coverage	No	-	(s)	Calculated
Required time for communication	Yes	-	(s)	5
Nodes in coverage	No	-	(nodes)	Calculated
Connection feasibility	No	-	No Units	Calculated

Now, we are going to analyze the results of applying the equations to calculate the time in coverage for different scenarios. The time in coverage of a node placed on the soil when the drone is moving at 20 m/s can be seen in Figure 6.28. The higher the dc, the higher the time in coverage. The maximum time in coverage is 20 s in the case of dc=200m. The *fh* has a relatively low impact in the time in coverage for gateways with dc of 150 to 200 m. The increase of *fh* from 0 m to 100 m reduces the time in coverage by less than 25%. For the drone with dc of 25 m, even with the lower *fh*, the time in coverage is only 4 s which handicaps the correct establishment of the communication and the data sending. Thus, assuming this minimum time for establishing the connection, at *fv* of 20 m/s, the gateways with dc of 25m cannot be used no matter their *fh*. When the used gateway has a dc of 50 m, the maximum possible *fh* is 39 m. For dc of 75m and 100 m, they can be used with *fh* from 4 to 64 m and 4 to 89 m respectively.

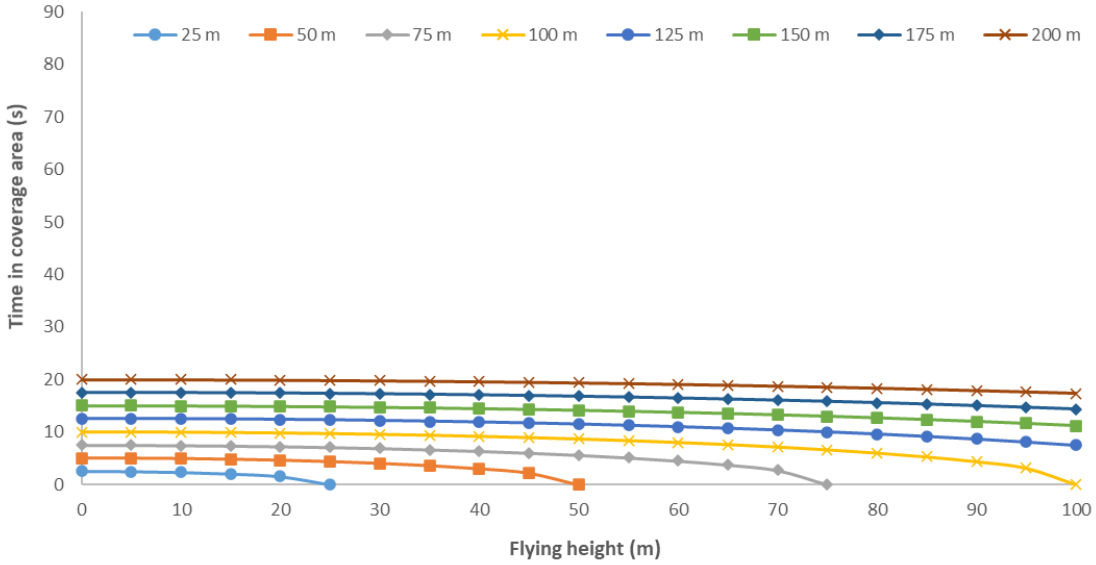

Figure 6.28. Time in coverage when a drone flies at 20 m/s and different *dc*.

Following, the time in coverage for *fv*=15 m/s is presented in Figure 6.29. Compared with Figure 6.28, as the drone is moving slowly, the time in coverage increases. The highest time in coverage for this scenario is 27 s, 7 s more than in the previous case. For the minimum dc, the time in coverage when the *fh* is the lesser is the same as in the previous case, 4 s. For this combination of dc and *fh*, the decrease of *fv* does not produce a relevant change in the time in coverage. Thus, with dc of 25m, the communication with this velocity is not possible, no matter the *fh*. For the other dc (50 to 100m), the maximum *fh* that offers enough time in coverage to ensure the communication increases from 34 to 39m (*dc* = 50 m), from 64 to 69 m (*dc* = 75 m), and from 89 to 94 m (*dc* = 100 m).

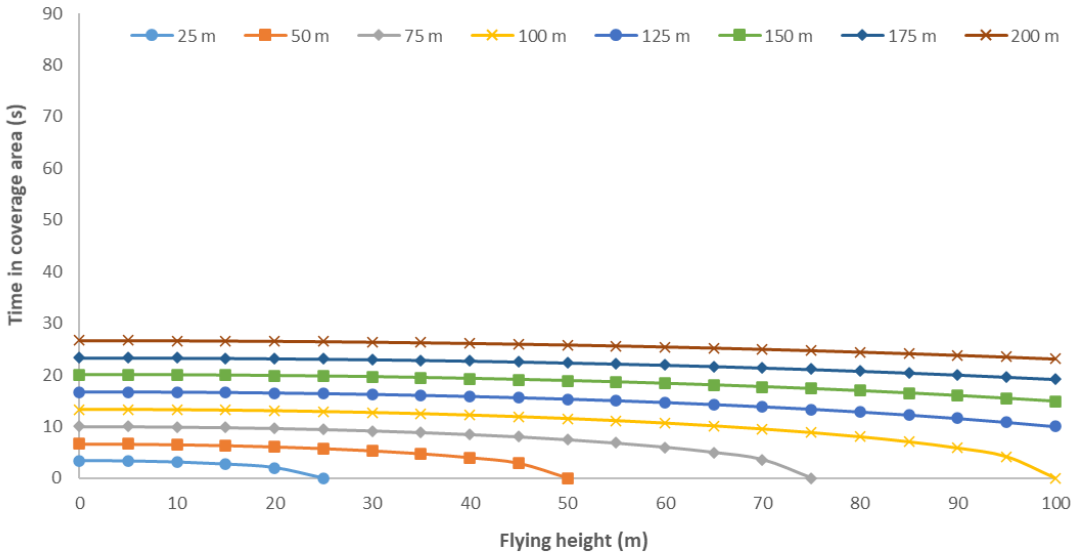

Figure 6.29. Time in coverage when a drone flies at 15 m/s and different *dc*.

The results of time in coverage when the drone flies at 10 m/s can be seen in Figure 6.30. In this case, the maximum time in coverage is 40 s. On the other hand, from the minimum dc and *fh*, the time in coverage is 5 s and can be used for receiving data from one node. With this *fv*, the maximum *fh* for different dc increases significantly compared with previous velocities for dc = 25, 5 m the maximum *fh* are 14, 44 m. Nonetheless, for *dc* of 75 and 100 m, the maximum *fh* is the same as in the previous velocities, and for dc higher than 100 m the communication is feasible at all the *fh*.

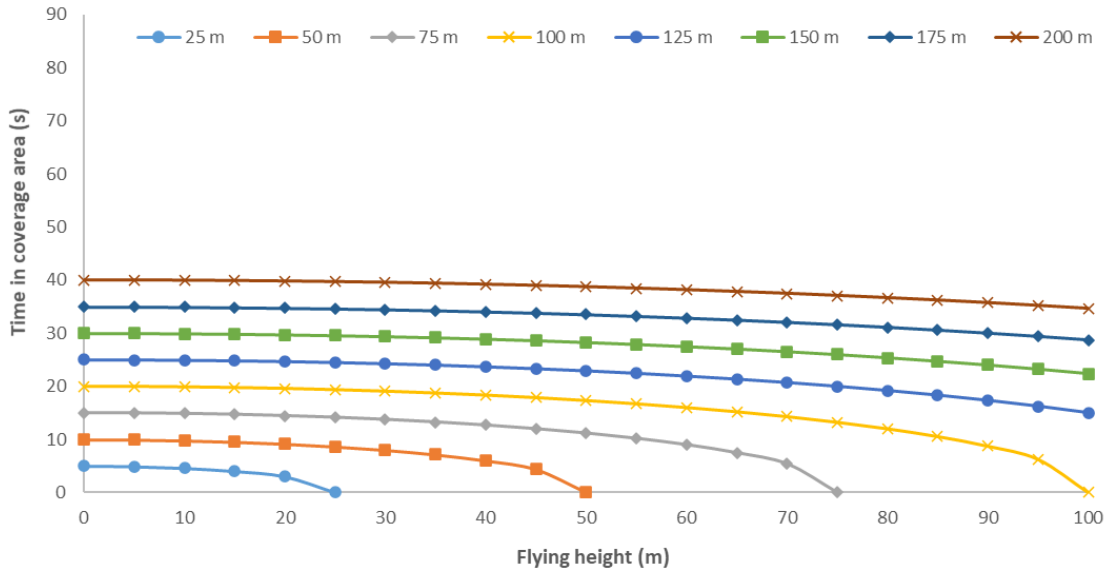

Figure 6.30. Time in coverage when a drone flies at 10 m/s and different *dc*.

Following, in Figure 6.31, we can see the theoretical values of time in coverage for *fv* = 5 m/s. The maximum time in coverage increases to 80 s with dc of 200 m and *fh* of 4 m. For the dc of 25 m, the maximum *fv* where it is possible to establish a communication with a single node is 19 m. For other dc in all the cases where there is coverage for the sensor, the time in coverage is high enough to establish the connection and communicate the data.

In Figures 6.28 to 6.31, we presented the time in coverage of a single node and evaluated if this node will be able to transmit the information or not according to the required time to establish the connection and send data, which has been set in 5 s. Next, we are going to analyze for each combination of dc and *fh*, the area in the soil which has coverage. Then, according to the aforementioned node densities in Table 6.2, we calculate the number of nodes that will have coverage in a certain period and need to send their data to the gateway. According to the time in coverage, the minimum required time to establish a connection, send the data and close the connection, and the number of nodes, we estimate if the drone can be used to receive all the data of the WSN or not. The summary of different considered scenarios and the results in terms of the success or not of the connection is presented in Figure 6.32. In Figure 6.32, we can identify in different rectangles the different scenarios, which combine different node

densities and *fv*. In each scenario, we can consider the combination of *dc* and *fh* in the x and y-axis. Thus, we cover all the parameters that affect the success or not of the gathering of all data stored in the nodes placed in the soil. The success of the connection is indicated in colors; the area colored in grey indicates that there is no coverage (NC) for this combination of *fh* and *dc*. This is found when the *fh* is higher than the *dc*. The areas in red represent combinations of *dc* and *fh* when even that we have coverage, the time in coverage is too short of ensuring the transmission of data from all the nodes. It means that the time in coverage of the nodes contained in the area in coverage is lower than 5s for each one and the gathering of data contained in the nodes cannot be attained. Combinations colored in yellow represent the combination of *dc* and *fh* that can be used to receive the data but with very adjusted time. Therefore, if an unexpected problem as a punctual loss of connection appears during the communications can endanger the collection of the data of certain nodes. In green, we present the optimal combination of *dc* and *fh* that ensure the data gathering.

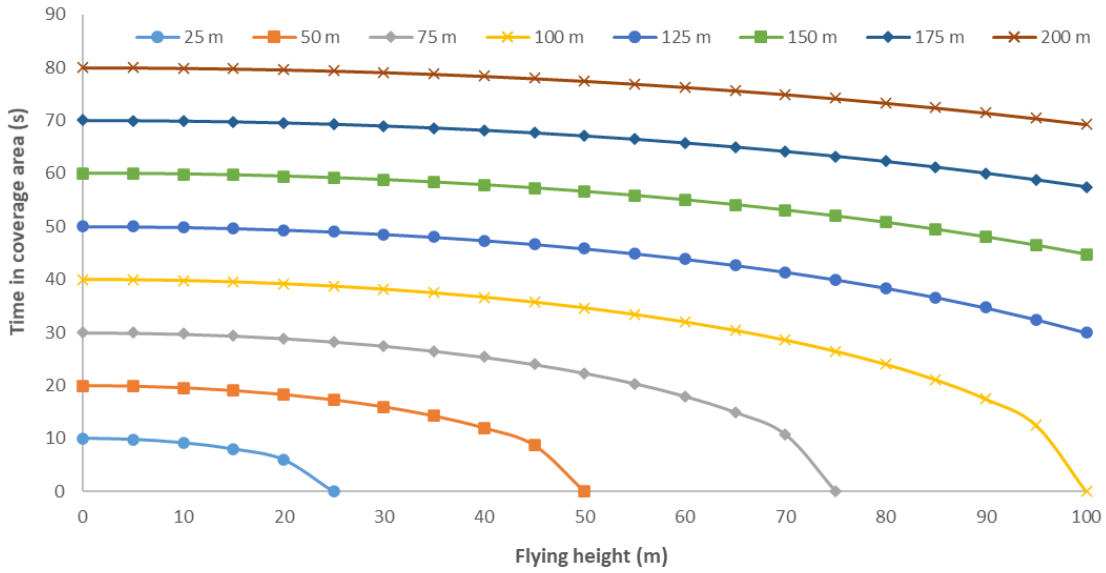

Figure 6.31. Time in coverage when a drone flies at 5 m/s and different *dc*.

According to Figure 6.32, we can determine for a given *fv*, *fh*, and node density if we will be able to communicate and receive the data from all of our nodes or not with different types of *dc*. Now, we are going to analyze the different scenarios, for the scenario with the maximum node density (1 node each 60 m2) there is only one combination that allows the communication. This combination is found for the lowest *fv* (1m/s) at *fh* = 24m and *dc* = 25m. The result of this combination of parameters is good coverage (yellow). For the other node densities, we can find more combinations. For node densities of 1 node every 750 m2 and the maximum *fv* no combination allows the communication. For other *fh* of 15 and 10 m/s few combinations allow a good connection. Meanwhile, when the *fv* decrease to 5m/s we can identify some combinations of *fh* and dc that result in an optimal connection (*fh* = 24 m and *dc* = 25 m). For the lowest *fv* several combinations allow good and optimal connectivity. Finally,

for the scenario with the lowest density of nodes (1 node every 5000 m2) we can identify some combinations that allow optimal connection even with the highest *fv* with *fh* equal or smaller than 100 m. For the other *fv* (15 to 1 m/s) several combinations of *fh* and dc ensure that the drone can act as a mobile gateway and gather the data of nodes placed in the soil.

In case that none of the combinations of the given parameters (*fh*, *fv*, and node density) with different dc values offers us a good (yellow) or optimal (green) solution, it will be necessary to evaluate if the possibility to modify the given parameters (fixed parameters) exists. For example, decreasing the *fv* or increasing the *fh* can be useful to ensure communication; meanwhile, we maintain the original purpose of the drone. These adjustments must be carefully considered to guarantee that the original purpose of the drone surveillance of the crop is possible. To do so, there will be necessary to evaluate the loss of image resolution due to the increment inf the *fh* and the reduction of overlapping between obtained images due to *fh*.

Otherwise, in case there is no possibility to change the given parameters, it will be necessary to use some other communication process in the nodes placed on the soil. For example, it will be possible to use a clustering algorithm to communicate all the gathered data from the cluster to the cluster head and this cluster head sends the data to the node. This will minimize the time consumed to send the data as fewer processes of communication establishment must be done. Nonetheless, this solution is limited to the coverage of WiFi antennas of nodes placed in the soil, and it can only be applied in cases with high node densities.

6.6.2 Energy consumption

In this subsection, the energy consumption of the drone is presented.

The energy consumption of a quadcopter drone is presented in equation (6.3), where the minimum flight power for hovering at the lowest height (β) is 30, the multiplier for the velocity of the motor (α) is 10.5, and the maximum power that the motor can achieve (P_{max}) is 85, according to [368]. The flying time (t) will be set to 20 minutes as it is the typical nominal endurance for quadcopter drones.

$$Energy = (\beta + \alpha * fh)t + P_{max}(fh/fv) \tag{6.3}$$

For quadcopter drones, the energy consumption of the drone is highly dependent on the flying height. To increase the coverage time, some authors have presented proposals for flights plans where the drone circles the node on the ground until all the data is transmitted. In our case, we consider the transmission of small amounts of data gathered from soil monitoring sensors. Therefore, that type of flight plan is not necessary for our scenario.

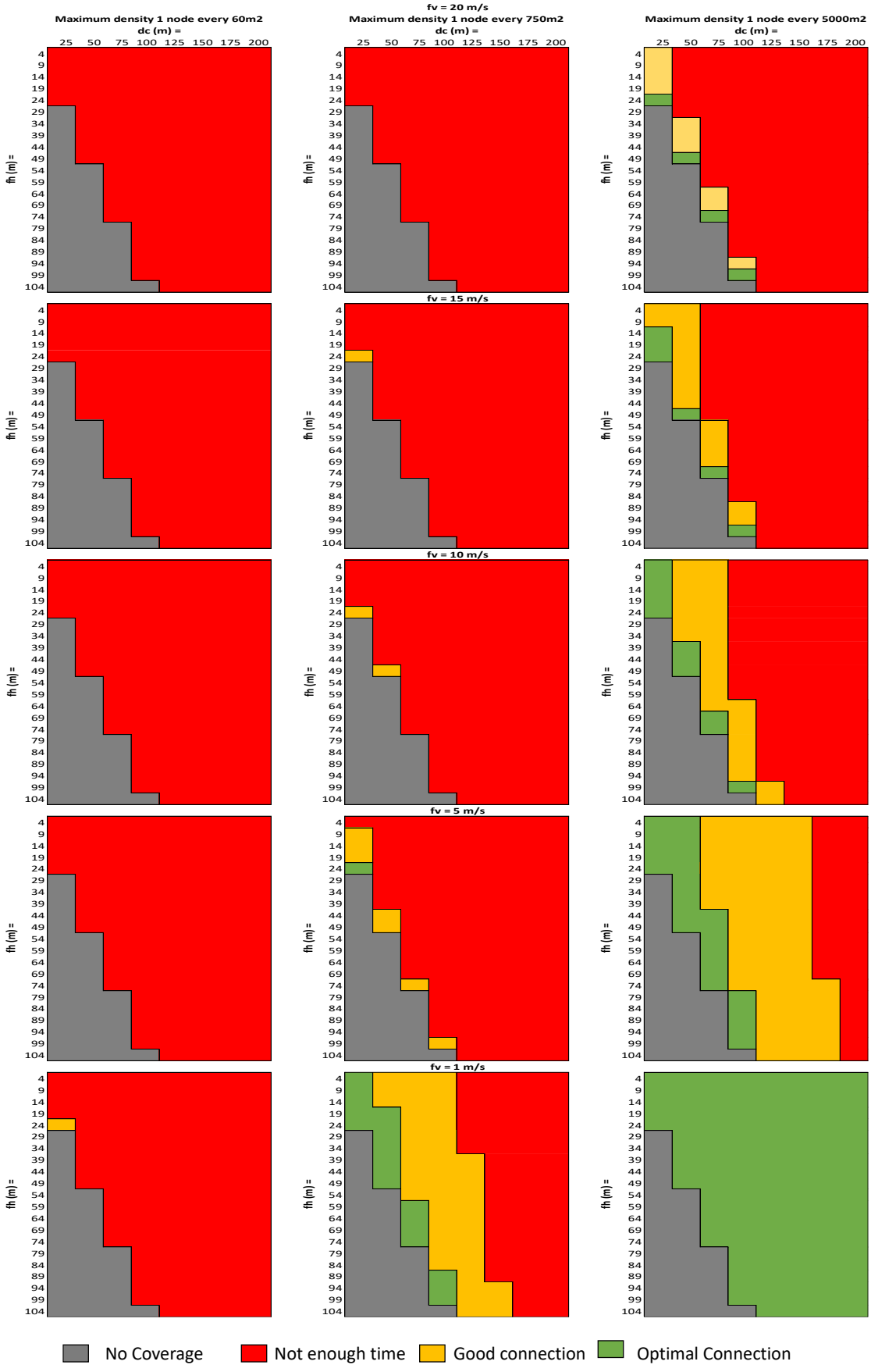

Figure 6.32. Summary of communication in different scenarios, grey is N.C., red is not enough time in coverage.

The energy consumption of the quadcopter drone for a flying time of 20 minutes is presented in Figure 6.33. The energy consumption is height dependent, and the speed of the drone barely creates a difference in energy consumption. Considering that flying heights between 15 m ad 25 m provide better coverage, the selection of a flying height within that range would minimize the energy consumption while maximizing the coverage of the node placed at the drone.

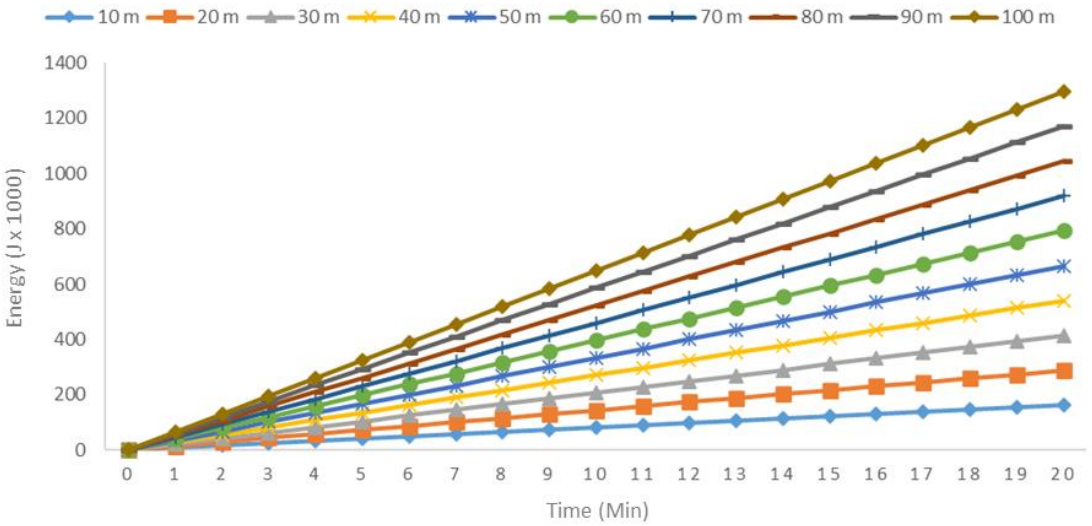

Figure 6.33. Energy consumption of a quadcopter drone at 10 m/s for different fh.

Considering the different node densities studied in this paper, the approximated number of nodes that the drone can cover in a flight of 20 minutes at different *fv* is presented in Table 6.3. This calculation was performed determining the space covered by the drone at each *fv* taking into account that the nodes are placed at the center of a square sector of 60 m^2, 750 m^2 or 5000 m^2, according to the node density, and the drone flies over them in a straight line to gather the information. Therefore, for a node density of 1 node per 60 m^2 the number of nodes that can be covered is considerably greater than that of the other two configurations.

Table 6.3. Nodes covered in a 20-minute flight for different fv and node densities.

Velocity	**1 m/s**	**5 m/s**	**10 m/s**	**15 m/s**	**20 m/s**
1 node per 60 m^2	19	99	199	299	399
1 node per 750 m^2	-	7	15	23	31
1 node per 5000 m^2	-	-	1	2	3

6.7 Conclusion

Firstly, the results of the simulations of the algorithms for a multi-layer fog computing framework for water quality monitoring and precision agriculture have been presented [364]. The results show a significant reduction for each of the modes compared to not using the data aggregation algorithms. Furthermore, the effects of utilizing different modes for data acquisition have been presented as well.

Regarding the use of a LoRa network with multiple nodes in a tree topology, the results show that the proposed system is able to transmit the necessary information and alerts with a low bandwidth generation [48]. However, the scheduled data forwarding of the central node of the last auxiliary canal had to be modified to two transmissions instead of one to ensure the fair access policy of LoRa. Lastly, the system is able to sustain energy consumption even on winter days with fewer hours of light and adverse weather conditions.

For the case of deployment with multiple WiFi nodes [28, 38], the results show that the energy consumption was able to be maintained with the established battery. However, different energy configurations show different network lifetime and different remaining energy in the rest of the nodes. Furthermore, regarding the collisions that may happen among IEEE 802.11 nodes, an association of a maximum of 50 nodes to each AP is proposed for optimal performance.

Lastly, different scenarios were simulated to determine the optimal drone parameters for the drone to be able to gather the data from the sensor nodes [9]. The results indicate that for the highest node density there is only one case in which the drone can be used when the drone has a flying height of 24m or lower and velocities equal or lower to 1m/s and we include an antenna with coverage of 25m. For the rest of the node densities, we can find several combinations that ensure that the drone can be efficiently used as a mobile gateway. Nonetheless, in maximum flying velocity, no connectivity is achieved for the medium node density.

Chapter 7

Practical Experiments

7.1 Introduction

In Chapter 4 the proposed protocol was presented. In this chapter, the results that validate the performance of the protocol are detailed. Furthermore, different coverage tests were performed to determine the best locations for the nodes deployed on the fields. These tests consider different vegetation types, different vegetation densities, and underground, on-ground, near-ground and aboveground locations for the nodes. In addition, the energy consumption for WiFi and LoRa transmissions utilizing low-cost nodes is tested as well. Lastly, as an added functionality, a proposal for fruit quantification is provided, where images of fruit trees are analyzed utilizing the histogram.

7.2 Results from tests on real devices of the proposed protocol

This section presents the performance results of the protocol presented in Chapter 4.

7.2.1 Testbed description

The tests have been performed in a real environment. Two types of nodes were utilized. The Wemos Mini D1 [356] and the Heltec LoRa WiFi 32 v2 [50] (See Figure 7.1). The Wemos Mini D1 is an embedded system with 1 analog input, 11 digital input/output pins, and 4MB of flash memory. This node includes the ESP 8266 chip and has Wi-Fi connectivity. The Heltec nodes have both LoRa and Wi-Fi connectivity through the ESP32 microprocessor and a SX1276/SX1278 LoRa chip. Furthermore, it is comprised of an OLED (Organic Light-Emitting Diode) display, 18 ADC (Analog-to-Digital Converter) input ports, and 2 DAC (Digital-to-Analog Converter) output ports, with 3 UART, 22 GPIO (General-Purpose Input/Output), 6 GPI, 2 I2C (Inter-Integrated Circuit), 2 SPI (Serial Peripheral Interface), and 2 I2S (Inter-Integrated Circuit Sound). The Heltec devices are available for both the 433 MHz and the 868 MHz bands. Therefore, the tests were performed for both 433 MHz and 868 MHz for the LoRa nodes of the network with the antenna shown in Figure 7.1. Furthermore, a preliminary test was performed to test the coverage of the utilized LoRa nodes with the antennas provided by the vendor.

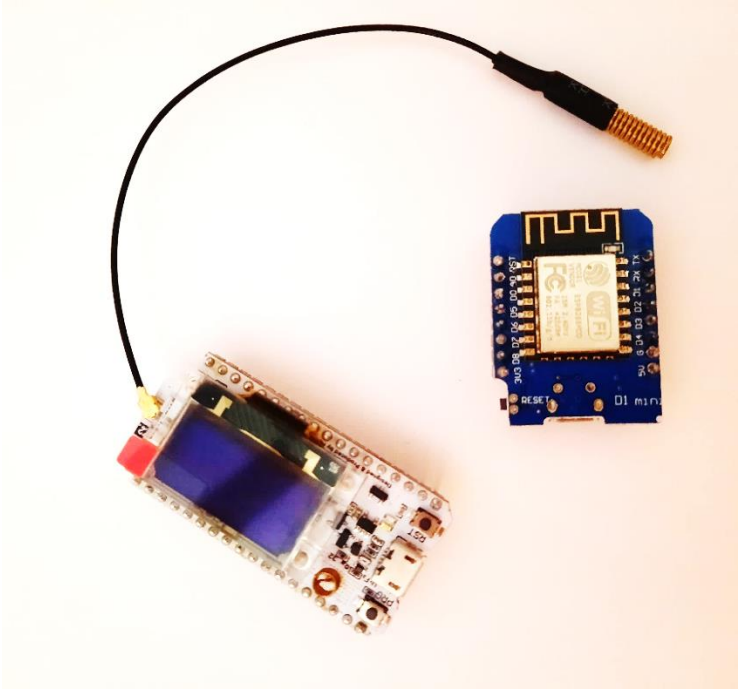

Figure 7.1. Nodes utilized to implement the protocol.

The topology utilized for the tests (See Figure 7.2) corresponds to one of the branches of the topology proposed in Chapter 4 subsection 4.2.1. Several libraries were created using the C++ programming language in order to implement the protocol on the aforementioned nodes. Each node type has its own library that specifies implements the state of the nodes introduced in Chapter 4 subsection 4.2.3. The environment where the tests were performed is shown in Figure 7.3. For the normal performance of the system,

the time between messages would be high, however, in order to test the performance in a worst-case scenario, the number of forwarded messages was incremented. Both WiFi sensing nodes forward the data message each minute. Then the WiFi 1 node sends the LOW_BATTERY message at minute 7 and the IS_DOWN message at minute 9, and the WiFi 2 node sends the LOW_BATTERY message at minute 6 and the IS_DOWN message at minute 8. The total time for each test was 10 minutes. The REGISTER messages are forwarded at the beginning when the nodes are connected. Lastly, the alarms are generated according to the data. The payload of the data messages was generated in a random manner within the range of each parameter with the addition of a range extension of values that would not be possible for the parameter in order to trigger an alert. Therefore, the forwarded alerts are more numerous than those of normal performances. For the case of LoRaWAN, there is a 1% policy to avoid collisions. With the proposed protocol, this policy is not considered.

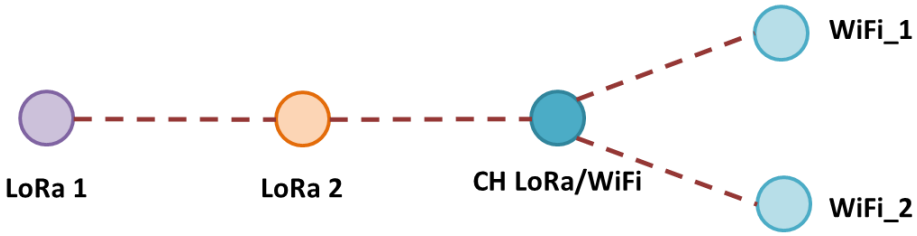

Figure 7.2. Topology of the testbed.

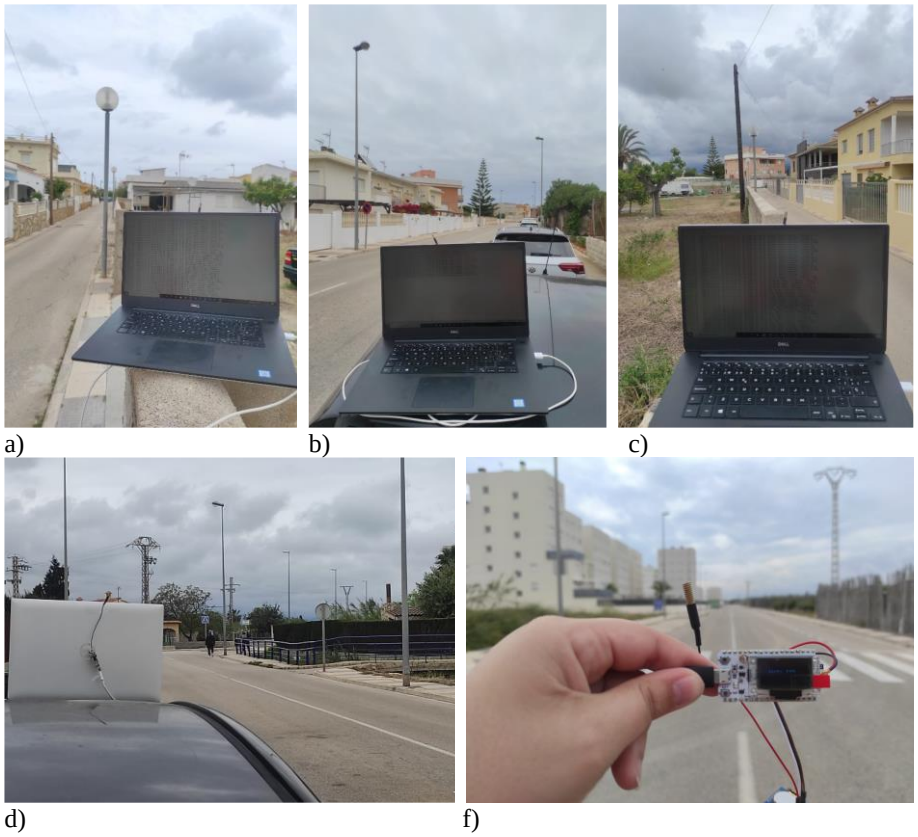

Figure 7.3. Nodes utilized to implement the protocol.

7.2.2 Test results

In this subsection, the test results of the proposed protocol are presented.

7.2.2.1 Consumed bandwidth

For LoRa networks, the consumed bandwidth is an important metric as the maximum data rate can be very limited depending on the LoRa settings. The data rate for the most restrictive settings for the EU 433 and the EU 868 frequency bands is 250 bps [369]. Therefore, maintaining lower data rates facilitates the selection of a great variety of configurations. The tests for both frequency bands were performed with variations in the packet forwarding delay of the CH node so as to reduce de number of lost packets due to collisions.

The results for the tests performed for the 433 MHz frequency with a packet delay of 0ms at the CH node are presented in Figure 7.4. As it can be seen, for the two nodes that only transmit in LoRa (see Figure 7.4 a and b), the maximum data rate remains below 250 bps considering that the tested scenario has more packet transmissions than that of the normal performance of the system. For the LoRa 1 node, the maximum data rate was 112 bps and the average data rate for the duration of the test was 1.68 bps. For the LoRa 2 node, the maximum data rate was 160 bps and the average data rate in the 10 minutes of the test was 2.63 bps. The rest of the nodes transmit using WiFi and LoRa for the CH node and only WiFi for the monitoring nodes. Therefore, the overhead of utilizing WiFi and UDP leads to an increased data rate compared to that of the LoRa nodes. The CH node reaches a peak of 760 bps when both WiFi and LoRa packets are received within the same second (See Figure 7.4 c) and an average of 13.69 bps for the duration of the test. Lastly, for the WiFi nodes, both of them reached a maximum data rate of 256 bps (See Figure 7.4 d and e) with an average of 2.49 bps and 1.25 bps respectively for the tested time. The total consumed bandwidth is presented in Figure 7.4 f). The peak in bandwidth consumption reaches 760 bps corresponding to the CH node and the average data rate for the duration of the test was 21.64 bps.

Figure 7.5 shows the results for the tests performed with the 433 MHz frequency band and a packet forwarding delay of 250 ms for the CH node. For the LoRa 1 node, as it can be seen in Figure 7.5 a), the maximum data rate is 112 bps, and the average value for the duration of the test is 2.21 bps. For the LoRa 2 nodes, the maximum data rate reaches 216 bps and the average reaches 3.61 bps (See Figure 7.5 b). The maximum data rate for the CH node is 808 bps and the average value is 15.47 bps (See Figure 7.5 c). For both of the WiFi nodes, the maximum data rate was 256 bps with an average of 2.08 bps in both cases (See Figure 7.5 d and e). For the total consumed bandwidth in the network (See Figure 7.5 f), the maximum data rate was 1056 bps, and the average value was 25.89 bps.

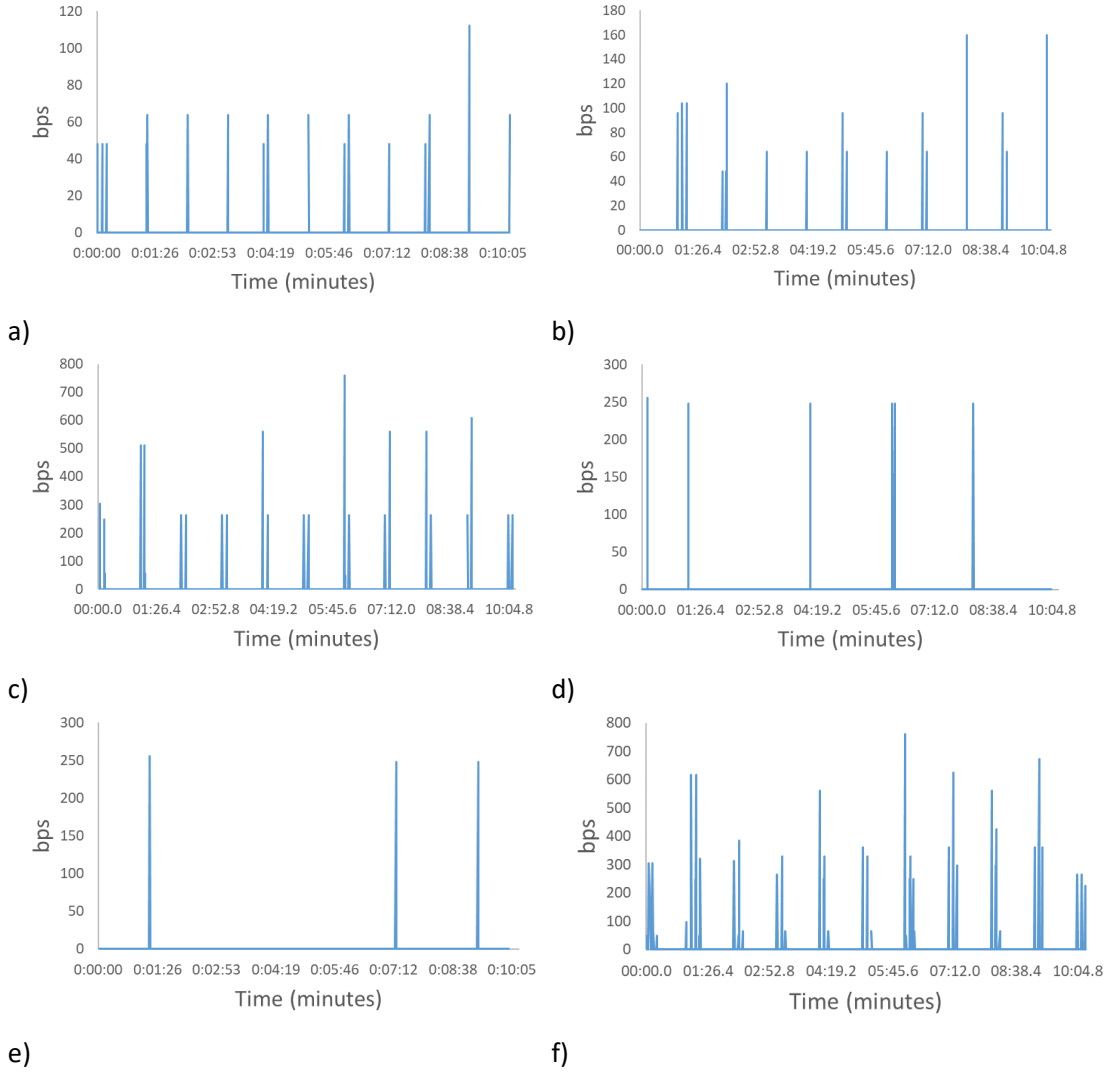

Figure 7.4. Consumed bandwidth of input packets for the 433 MHz LoRa notes and transmission delay at the bridge of 0 ms for a) LoRa 1 node, b) LoRa 2 node, c) CH LoRa/WiFi node, d) WiFi 1 node, e) WiFi 2 node, and f) for the complete network.

The consumed bandwidth from the tests performed in the 433 MHz frequency band and a packet delay of 500 ms at the CH node is presented in Figure 7.6. As seen in Figure 7.6 a), the maximum data rate for the LoRa 1 node is 160 bps. The resulting average data rate is 2.24 bps. In Figure 7.6 b) it can be seen that the maximum data rate for the LoRa 2 node is 304 bps. It is higher than the value of 250 bps for the most restrictive LoRa settings regarding the data rate. However, the data rate obtained at the test does not surpass the data rate for the second most restrictive LoRa settings. The maximum data rate for the CH node is 824 bps with an average of 15.17 bps (See Figure 7.6 c). In Figure 7.6 d) and e) it can be seen that the maximum data rate is 256 bps with an average for the duration of the test of 3.32 bps and 1.25 bps respectively. Regarding the total consumed bandwidth in the network, the peak data rate was 984 bps with an average of 25.62 bps (See Figure 7.6 f).

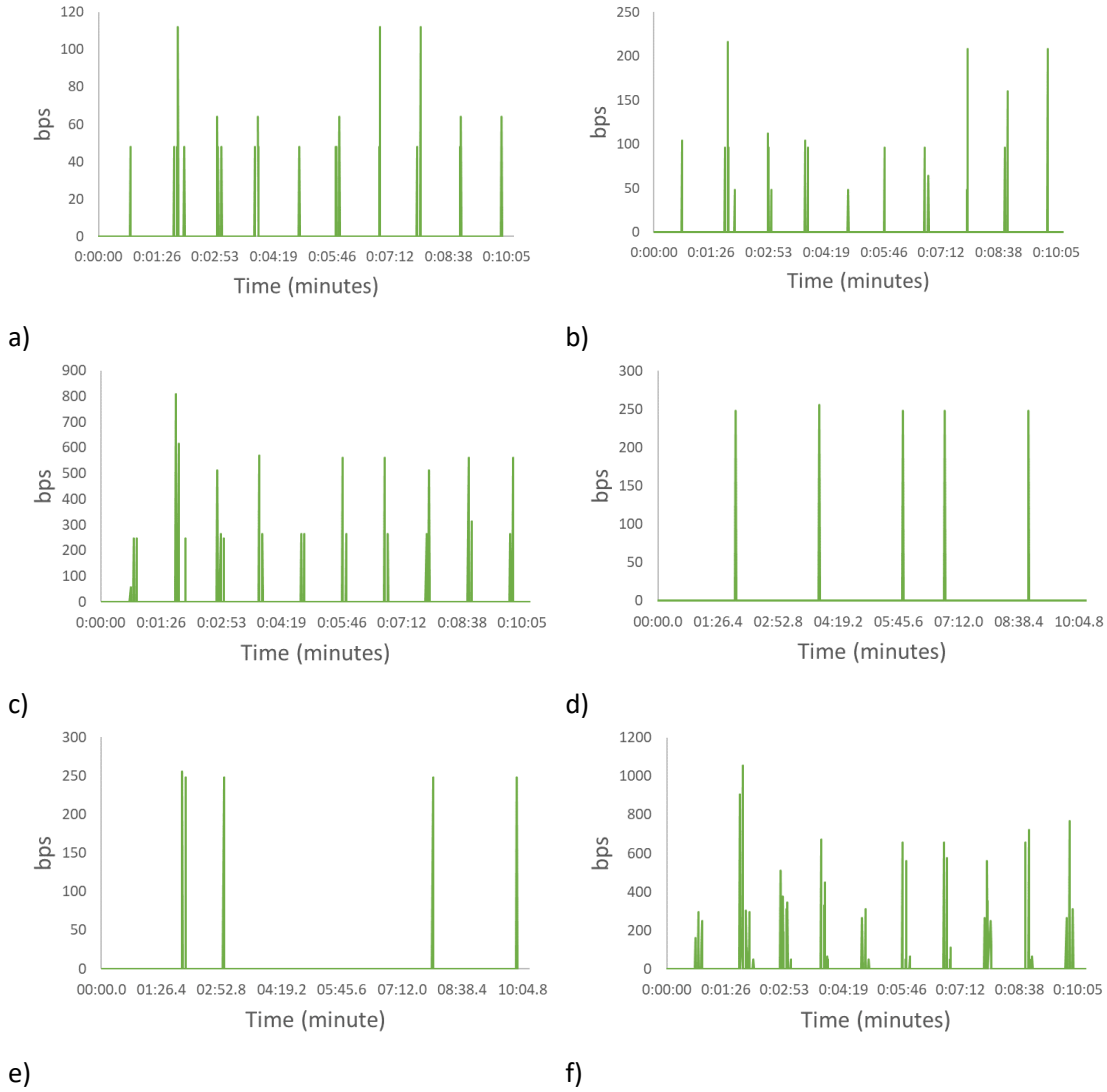

Figure 7.5. Consumed bandwidth of input packets for the 433 MHz LoRa notes and transmission delay at the bridge of 250 ms for a) LoRa 1 node, b) LoRa 2 node, c) CH LoRa/WiFi node, d) WiFi 1 node, e) WiFi 2 node, and f) for the complete network.

Figure 7.7 presents the results for the test performed with the 868 MHz LoRa nodes and a packet delay of 0 ms for the CH node. Figure 7.7 a) shows the results for the LoRa 1 node where the peak data rate is 112 bps and the average data rate for the duration of the test is 2.1 bps. The results for the LoRa 2 node as shown in Figure 7.7 b) indicate that the maximum data rate is 208 bps and an average data rate of 3.21 bps. For the CH node, the maximum data rate is 608 bps and the average for the 10 minutes of the test is 14.68 bps (See Figure 7.7 c). For the WiFi nodes, the maximum data rate is 256 bps, and the average data rate is 3.32 bps and 1.25 bps respectively (See Figure 7.7 d and e). Lastly, Figure 7.7 f) presented the results of the total network where the peak data rate is 872 bps with an average of 23.63 bps.

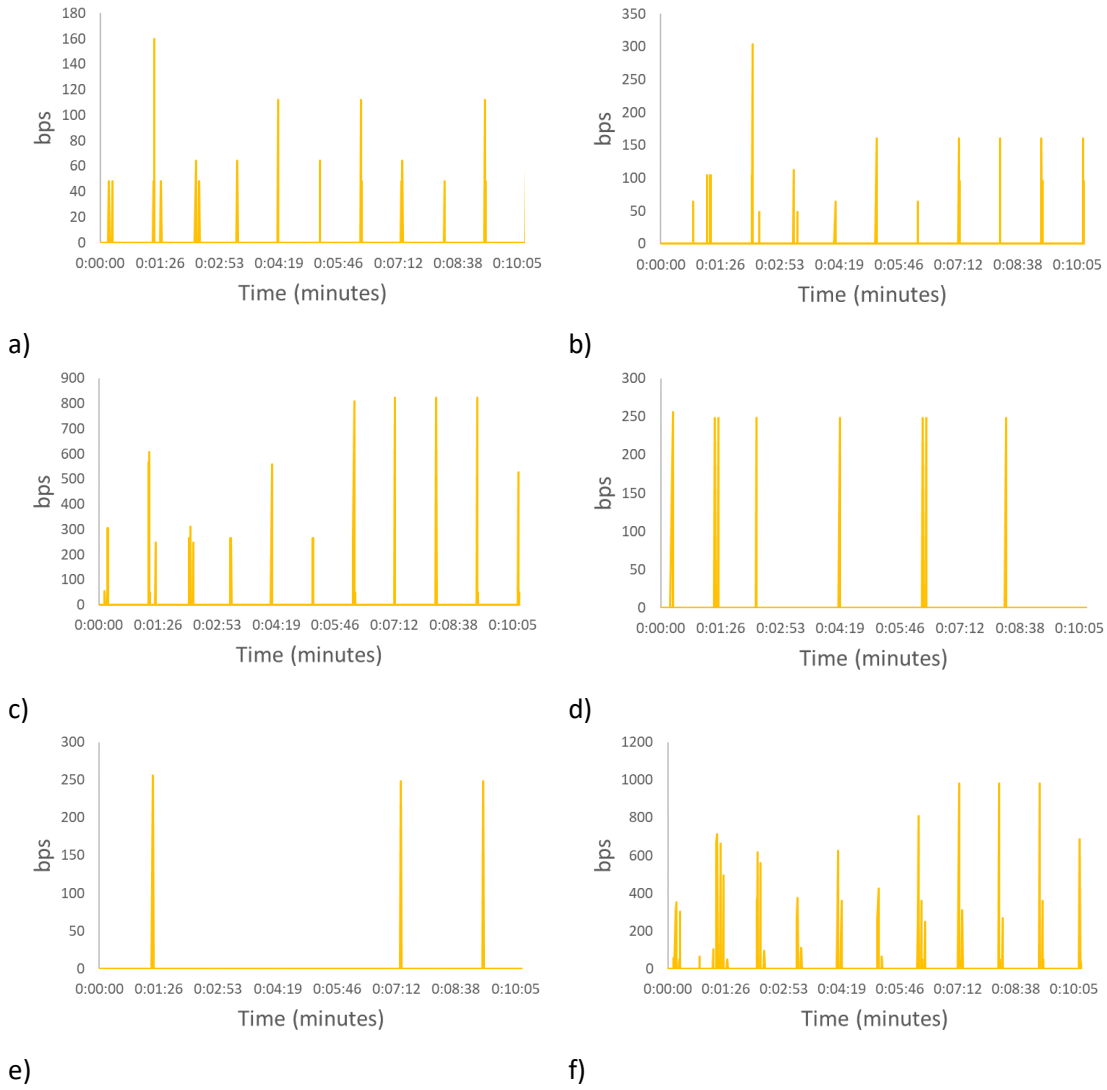

Figure 7.6. Consumed bandwidth of input packets for the 433 MHz LoRa notes and transmission delay at the bridge of 500 ms for a) LoRa 1 node, b) LoRa 2 node, c) CH LoRa/WiFi node, d) WiFi 1 node, e) WiFi 2 node, and f) for the complete network.

The results of the test performed utilizing the 868 MHz frequency band and with 250 ms of packet delay at the CH node are presented in Figure 7.8. As it can be seen in Figure 7.8 a) for the LoRa 1 node, the maximum data rate is 160 bps and the average data rate for the duration of the test is 2.05 bps. The maximum data rate for the LoRa 2 node is 256 bps and the average data rate is 3.56 bps (See Figure 7.8 b). For the CH node, as seen in Figure 7.8 c), the maximum data rate is 808 bps and the average data rate for the duration of the test is 15.05 bps. For the WiFi nodes, the maximum data rate is 256 bps, and the average data rate is 3.73 bps and 1.25 bps corresponding to the WiFi 1 and the WiFi 2 nodes (See Figure 7.8 d and e). For the complete network, the peak data rate value was 872 bps with an average data rate of 25.57 bps (See Figure 7.8 f).

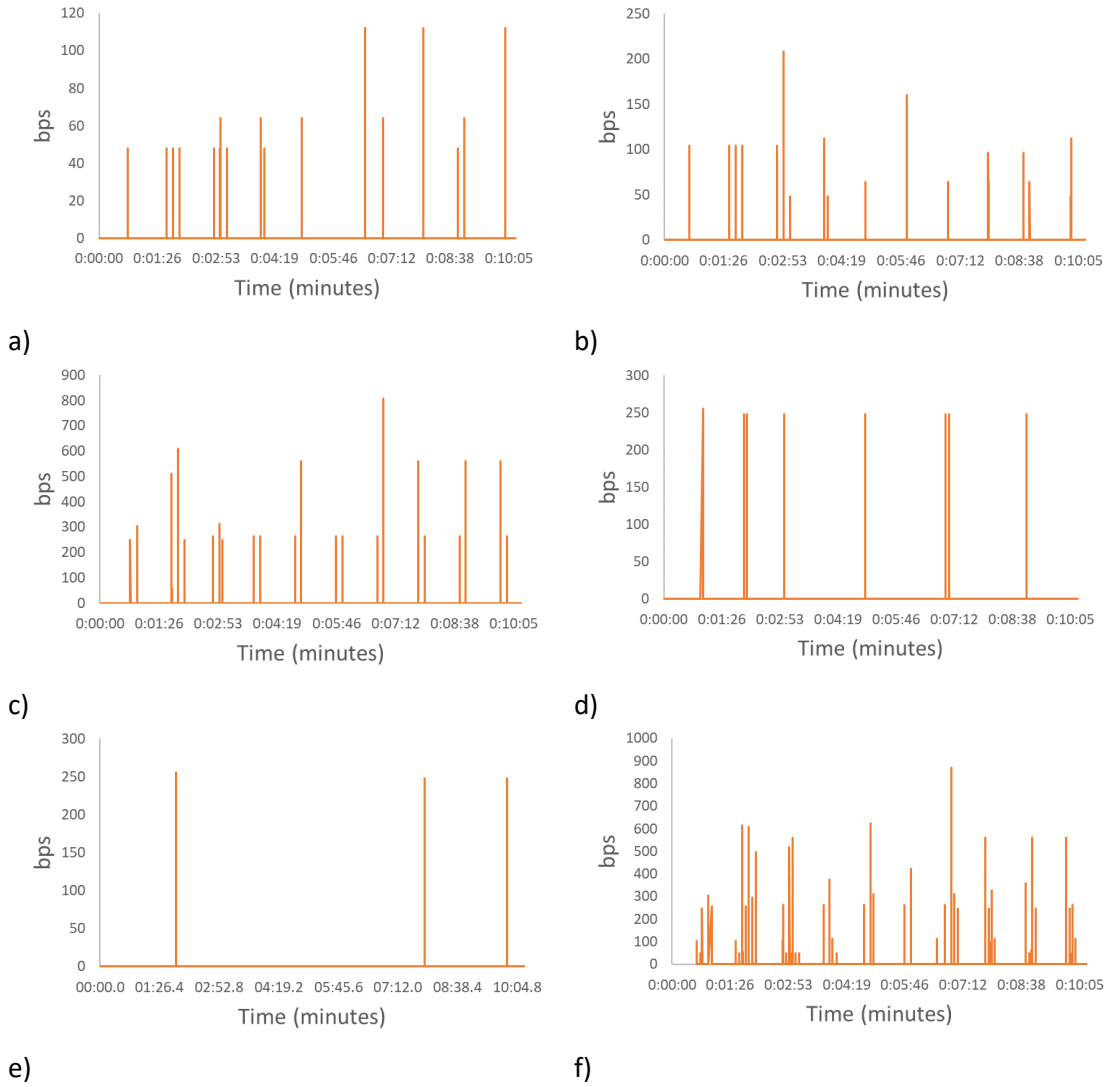

Figure 7.7. Consumed bandwidth of input packets for the 868 MHz LoRa notes and transmission delay at the bridge of 0 ms for a) LoRa 1 node, b) LoRa 2 node, c) CH LoRa/WiFi node, d) WiFi 1 node, e) WiFi 2 node, and f) for the complete network.

The results for the tests performed with the 868 LoRa nodes and a 500 ms packet delay at the CH node are presented in Figure 7.9. As it can be seen in Figure 7.9 a), for the LoRa 1 node, the maximum data rate is 160 bps and the average data rate for the duration of the test is 2.24 bps. For the LoRa 2 node, as seen in Figure 7.9 b), the maximum data rate is 256 bps, and the average data rate is 3.57 bps. For the CH node, as shown in Figure 7.9 c), the maximum data rate is 760 bps, and the average data rate is 13.77 bps. For the WiFi nodes, the maximum data rate is 256 bps, and the average data rate is 3.32 bps for the WiFi 1 node and 1.25 bps for the WiFi 2 nodes (See Figure 7.9 d and e). Lastly, for the complete network, the peak data rate is 968 bps, and the average data rate is 24.16 bps (See Figure 7.9 f).

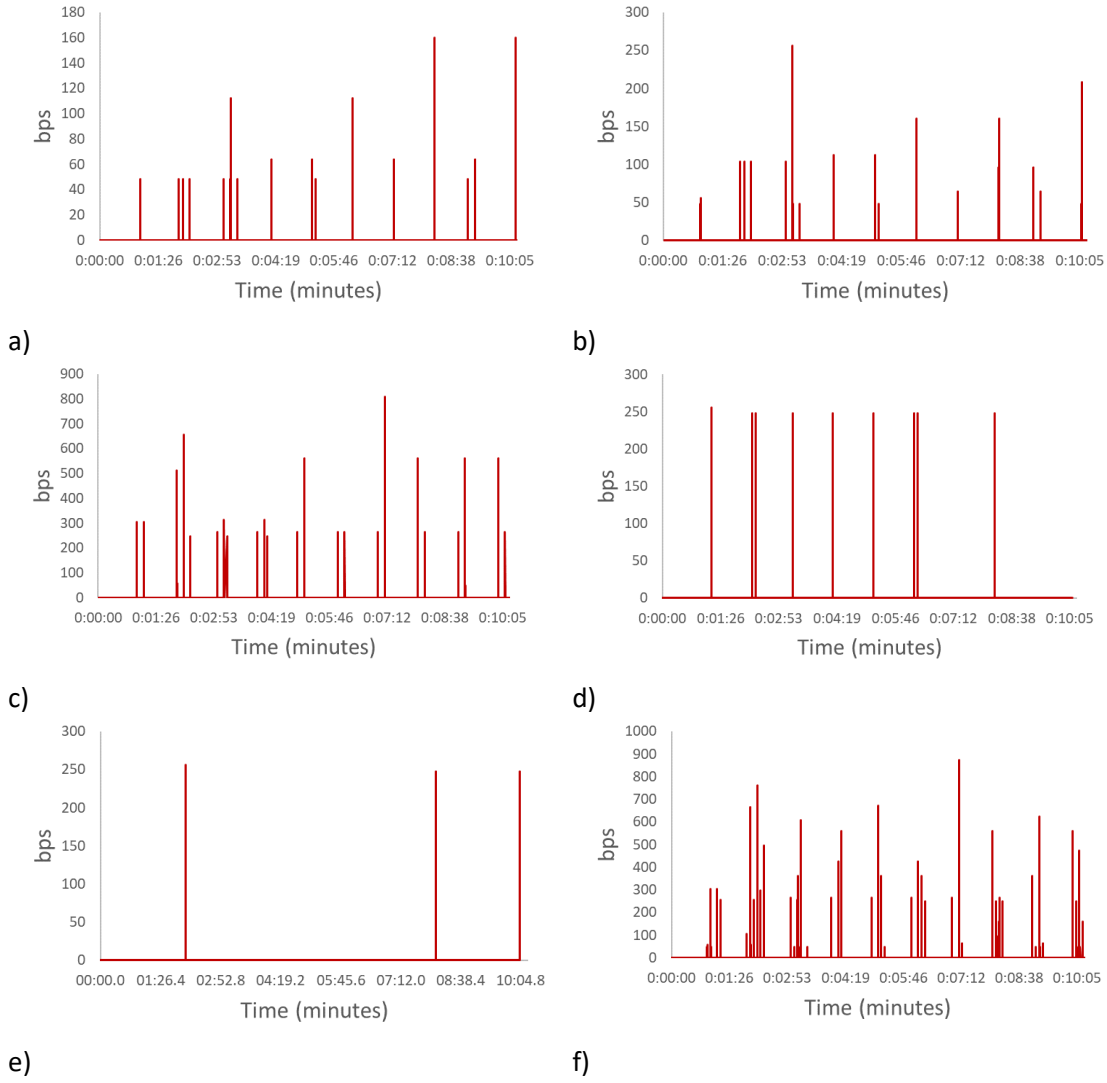

Figure 7.8. Consumed bandwidth of input packets for the 868 MHz LoRa notes and transmission delay at the bridge of 250 ms for a) LoRa 1 node, b) LoRa 2 node, c) CH LoRa/WiFi node, d) WiFi 1 node, e) WiFi 2 node, and f) for the complete network.

The data rate values for all the tests remain very similar. Thus, it can be concluded that the proposed system is viable and adequate for heterogeneous networks intended for water quality and field monitoring in order to automate and improve irrigation. However, it is necessary to determine the packet loss that can occur due to the characteristics of LoRa.

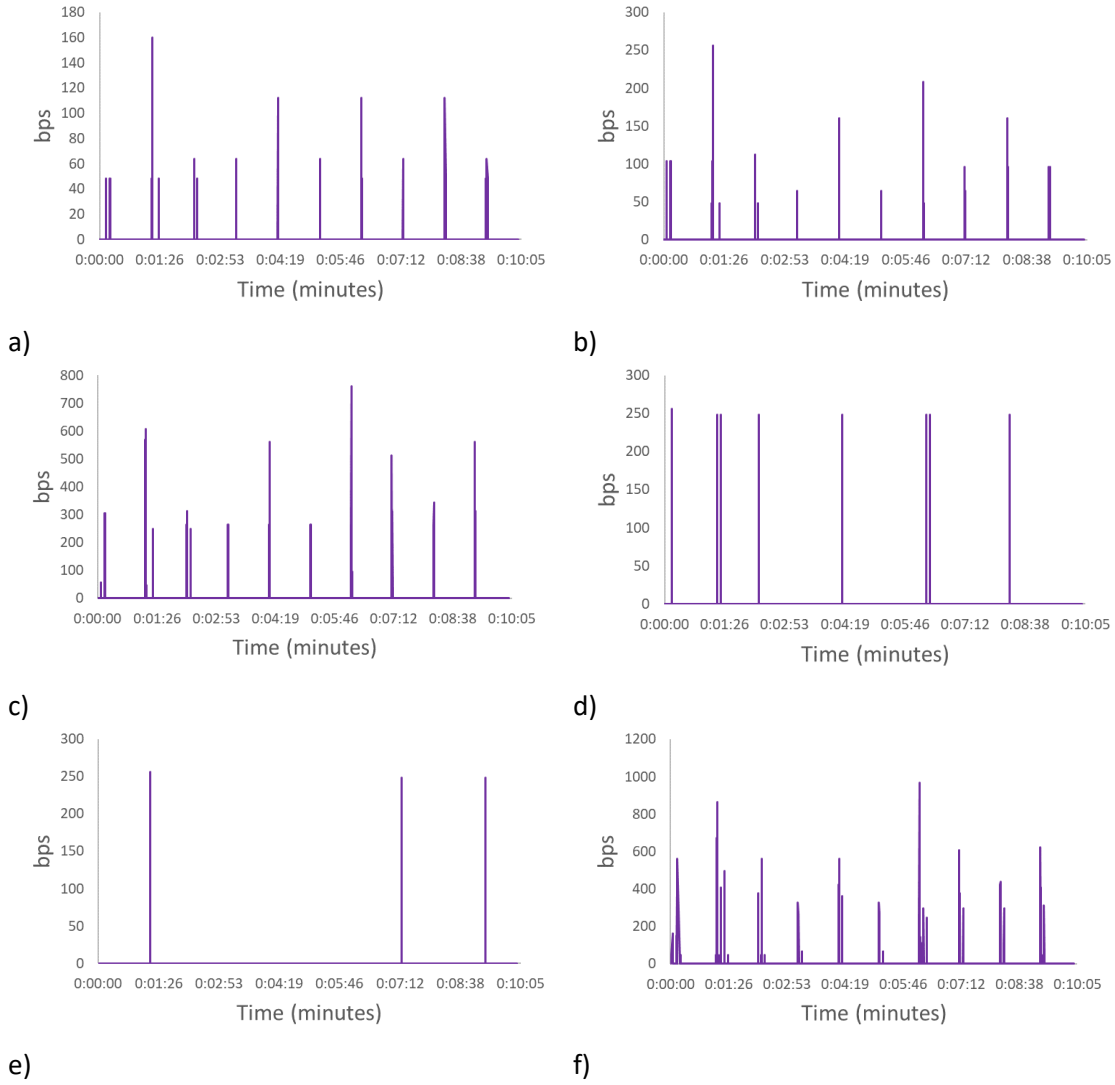

Figure 7.9. Consumed bandwidth of input packets for the 868 MHz LoRa notes and transmission delay at the bridge of 500 ms for a) LoRa 1 node, b) LoRa 2 node, c) CH LoRa/WiFi node, d) WiFi 1 node, e) WiFi 2 node, and f) for the complete network.

7.2.2.2 Packet loss

The utilization of LoRa can lead to packet loss due to the collisions that occur when two or more packets are forwarded at the same time. The successful packet delivery rate of each test has been determined. The results are shown in Figure 7.10. As it can be seen, the high delivery rates were obtained for all tests, but the additions of delays help in improving the number of successful packet deliveries. For a delay of 0 ms, 91.26% of the packets were successful for the 433 MHz frequency band and a 94.02% successful packet delivery rate was obtained for the 868 MHz frequency band. For a packet delay at the CH node of 250 ms, the successful delivery rate was 93.33% and 98.43% for the 433 MHz and 868 MHz respectively. Lastly, for a delay of 500 ms, the successful

packet delivery rate for the 433 MHz was 98.46% and for the 868 MHz frequency band the obtained result was 98.37%. As it can be seen, for the 868 MHz frequency band the delay of 250 ms allowed reaching a high delivery rate but for the 433 MHz frequency band a delay of 500 ms was necessary.

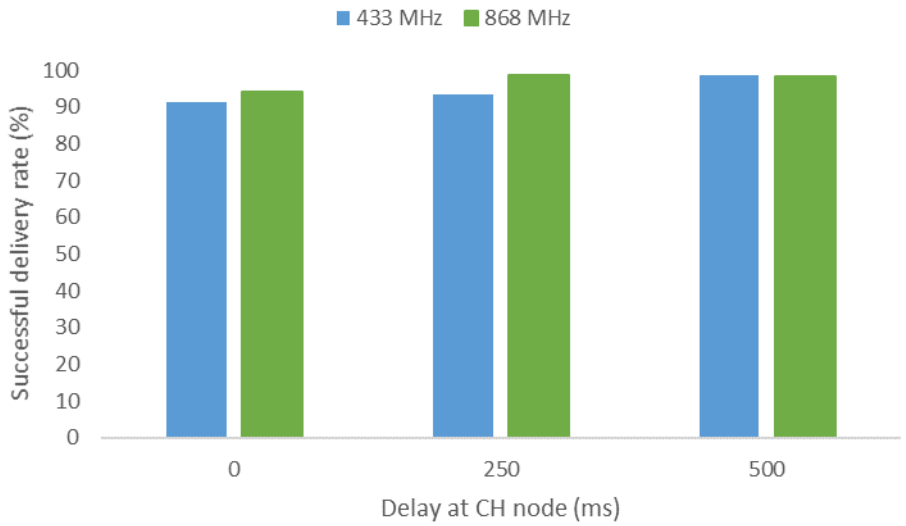

Figure 7.10. Successful delivery rate of the performed tests.

The addition of transmission delays helps in avoiding the collisions of the LoRa packets. As the performed tests contemplate a worst-case scenario, better successful delivery rates are expected with the normal performance as fewer packets would be forwarded, making it more difficult for two packets to collide. Furthermore, as our system includes mechanisms to ensure all data is delivered, the lost packets can be recovered.

7.3 Coverage studies for different deployment strategies in varied environments

When deploying devices for PA systems, the foliage of the plants may reduce the obtained coverage. Furthermore, other node placements such as underground nodes may be contemplated. In this section, a coverage study of low-cost WiFi nodes with different types of vegetation and different deployment configurations is presented. Furthermore, the coverage of low-cost LoRa nodes with different low-cost antennas is presented as well.

7.3.1 Coverage results for deployments with vegetation obstructions

The tests were performed at three different types of environments as seen in Figure 7.11 The first one is a grass field with low vegetation and a regular terrain. The second one is the field with thicket. The terrain of this field presents irregularities in height and a big amount of thicket that obstructs the direct vision between the transmitter and the

receiver. The third field is a citrus plot. Orange trees are organized in rows that cover the expanse of the area in an ordered manner. Depending on the position of the emitter and the receiver, trees may or may not obstruct the direct vision between them.

The signal strength was measured utilizing the ESP 32 Devkit v1 programmed utilizing the RSSI () function of the Arduino WiFi library and transmitting using the in-built antenna with a time span of 5 seconds between each transmission. The placement of the nodes inside the protective box can be seen in Figure 7.12. Five radio transmissions were performed per measurement and spot and results were averaged to avoid instability in the results as in reference [370].

Figure 7.11. a) Grass field. b) Thicker field. c) Orange field.

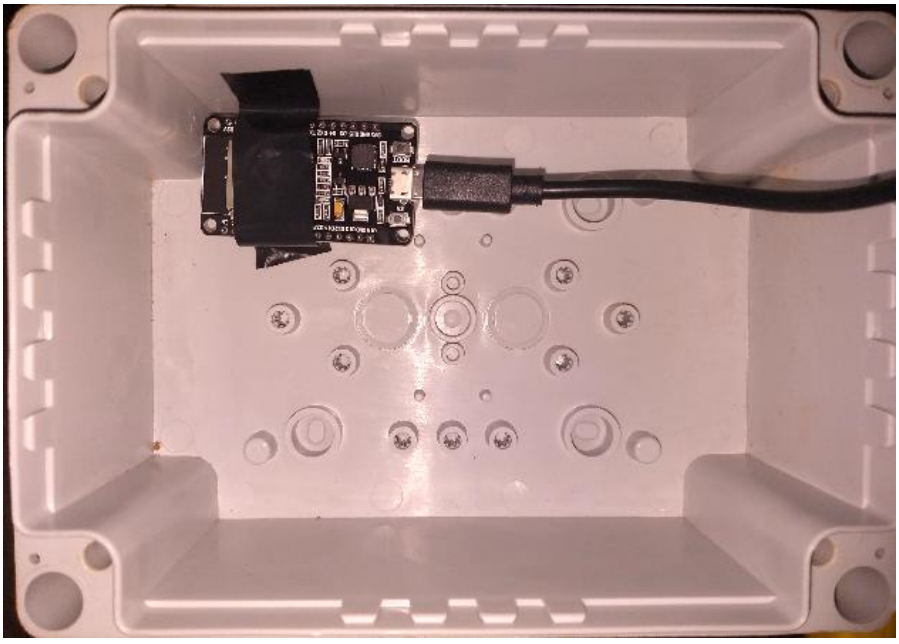

Figure 7.12. Placement of the node inside the box.

Two different scenarios were considered as previously shown in Chapter 3 subsection 3.3.1. In the first scenario, both transmitter and receiver were placed on the ground to consider the possible disturbance that the nodes may cause if they are positioned at higher heights with some agricultural applications, the machinery, and the

usual activities that can be performed by farmers. Furthermore, it is a deployment position that has been considered in soil monitoring scenarios such as [371] that employ drones to collect the data from the on-ground nodes. The aim of testing on-ground deployment strategies with different vegetation types is to determine the feasibility of the communication with nodes placed using this configuration. The measures performed on this scenario were taken with an angle of 0 and 15 degrees to obtain data on how results may change with varied degrees and a variation in vegetation density. Due to the arrangement of the trees in the orange field, it was not possible to make 360-degree measurements, so it was decided to replicate the measurements at 0 and 15 degrees for all vegetated environments in scenario 1. Furthermore, the measures were taken separating the emitter from the receiver, creating more distance between them with each measurement.

In scenario 2, on-ground, near-ground, and above-ground placements of the receiver with varied emitter heights were tested on the citrus plot. The aim of the second scenario is to assess different deployment strategies for crops comprised of trees as opposed to vegetation that present the bulk of its foliage closer to the ground such as wheat fields [372]. The layout of how the measures were taken is presented in Figure 7.13 a). Due to the differences in the amount of foliage and the structure and layout of the vegetation, the signal strength for each type of vegetation will differ. The satellite image of the fields with vegetation is presented in Figure 7.13 b). It is a Mediterranean area with great extensions of citrus plots and surrounded by mountains. This climate has warm to hot temperatures in summer and cool to warm temperatures in winter, where no below-freezing temperatures are normally reached. Furthermore, the precipitation is low and irregularly distributed. All the measures of each scenario were done on the same day, the temperature remained almost constant at 20 degrees Celsius as the data was gathered during the central hours of the day. Moreover, there was no presence of precipitations.

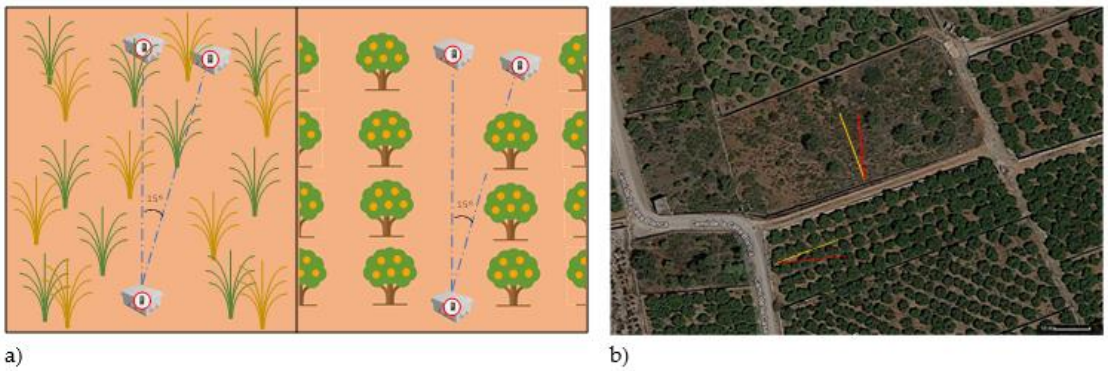

Figure 7.13. a) Layout of the measures. b) Satellite image of the fields.

7.3.1.1 Results

In this subsection, we show the results of analyzing the received signal strength with different deployment strategies positioning the nodes at several distances in different

environments. First, the data gathered in each of the environments (grassland, scrub, and orange field) at two different orientations are evaluated. This way, we study the signal attenuation in the aforementioned environments to show the possible positive and negative effects of having different types of vegetation. Second, we evaluate the signal at different heights of the emitter and receiver at the orange orchard.

7.3.1.1.1 Scenario 1: On-ground deployment with different types of vegetation.

Firstly, the results from the on-ground nodes deployed on grasslands are presented. The RSSI of the measures performed at 0º and 15º are shown in Figure 7.14. As the height of the grass is mostly uniform, the results at both degrees are quite similar. The differences are mainly explained by the irregularities of the terrain and the different irradiation pattern of the antenna. Initially, no objects in the studied area can cause any rebound or reflection of the emitted signal. Thus, we can consider this signal attenuation as the attenuation when both nodes are placed on the soil with no interferences. When the signal is transmitted over grasslands with very low grass, less than 1.5 cm, the RSSI at the maximum measured distance, 20 m, is -81 and -82 dBm at 0º and 15º respectively. The attenuation is higher in the first 6 to 7 meters decreasing 30 dBm approximately. Then, the attenuation occurs at a slower pace and the RSSI values are similar, -80 dBm, until 13 m. The last measured points present lower RSSI, less than -80 dBm.

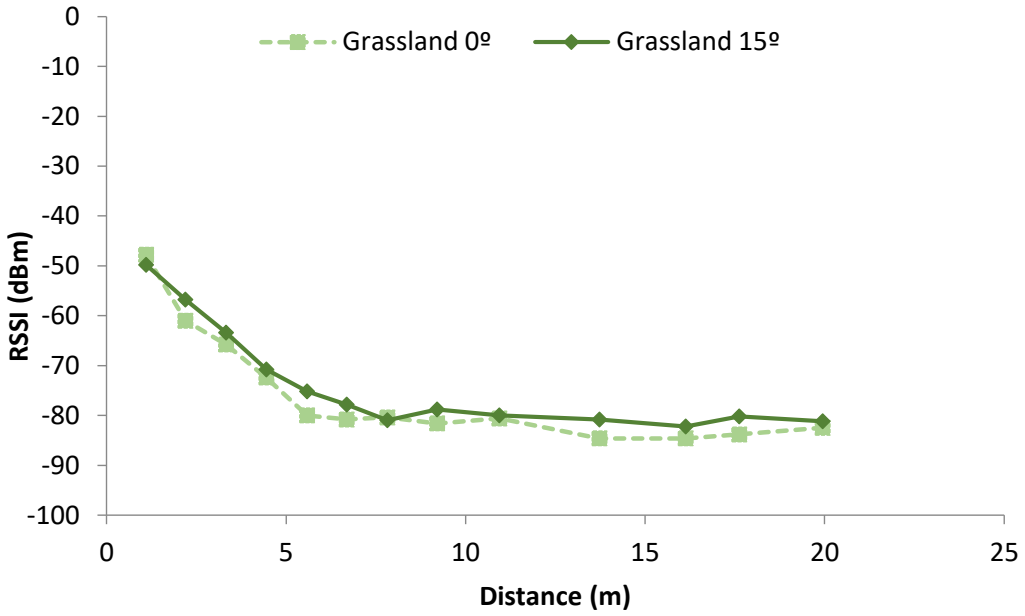

Figure 7.14. RSSI in grasslands.

The results of the RSSI measures performed in the scrub environment are shown in Figure 7.15. Initially, as it can be seen, the results from the different orientations show different RSSI values due to the different foliage patterns. As the scrub is not distributed

uniformly along the terrain, the RSSI in both orientations is not the same. Furthermore, the data does not present a regular attenuation as in the grassland case. At some points, farther distances present higher RSSI values than those obtained at measurement points situated closer to the emitter. Both observations are mainly explained by the effects of scattering and absorption of this vegetation, which causes shadow areas, and the reflection and refraction might lead to the multipath effect. A clear shadow area can be seen between 4 m and 6 m in the case of scrub 15º, where suddenly two points have lower values (-73 dBm and -72.5 dBm). At the maximum distance, the observed RSSI are -83 dBm and -85 dBm. They are quite lower than in the case of grasslands.

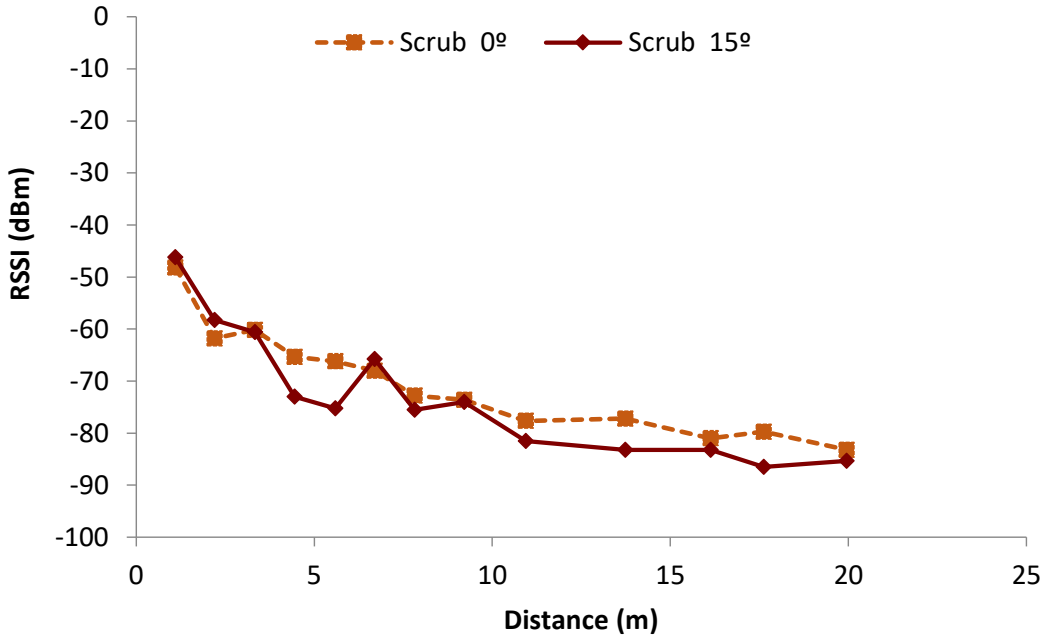

Figure 7.15. RSSI in scrubs.

Therefore, it is possible to conclude that the shrubs present in the scrub field cause alterations in the attenuation. Furthermore, the multipath effect can be affecting the RSSI received in each measurement greatly, causing the fluctuations in RSSI values. In some cases, for the same measurement point, a variation of more than 10 dBm was found between the maximum and minimum gathered values. Thus, with the data obtained in this study, changes in the vegetation or even some events as blooming, shedding, and growing, or just the wind moving the shrubs might be affecting the RSSI. Consequently, when the WSN is installed in scrub areas, it is important to note that the RSSI mean values might not be a good indicator and the minimum values should be considered when making the network planning. Further studies will focus on this aspect.

The attenuation of the WiFi signal in the orange fields is now analyzed. As it is explained in the previous section, the data gathered at 0º was taken having direct vision between the node configured as AP and the node configured as the receiver. On the other hand, the data gathered at 15º was taken without having a direct vision in all the cases as the trunks of the orange trees obstruct the path between the emitter and the

receiver. Figure 7.16 presents the mean of the RSSI data gathered both at 0º and 15º. We can note that in the first meters, the RSSI is higher in the data gathered at 15º than at 0º. Nonetheless, from 7 m, the RSSI is higher at 0º than at 15º. It is important to note that at 0º, from 16 m, the RSSI starts to decrease very abruptly losing the connection between 17 m and 20 m. In the case of data gathered at 15º, in the last 2 measured points, there was no connection. In order to represent the data in the graphics, the points where the connection was lost are represented as -100 dBm.

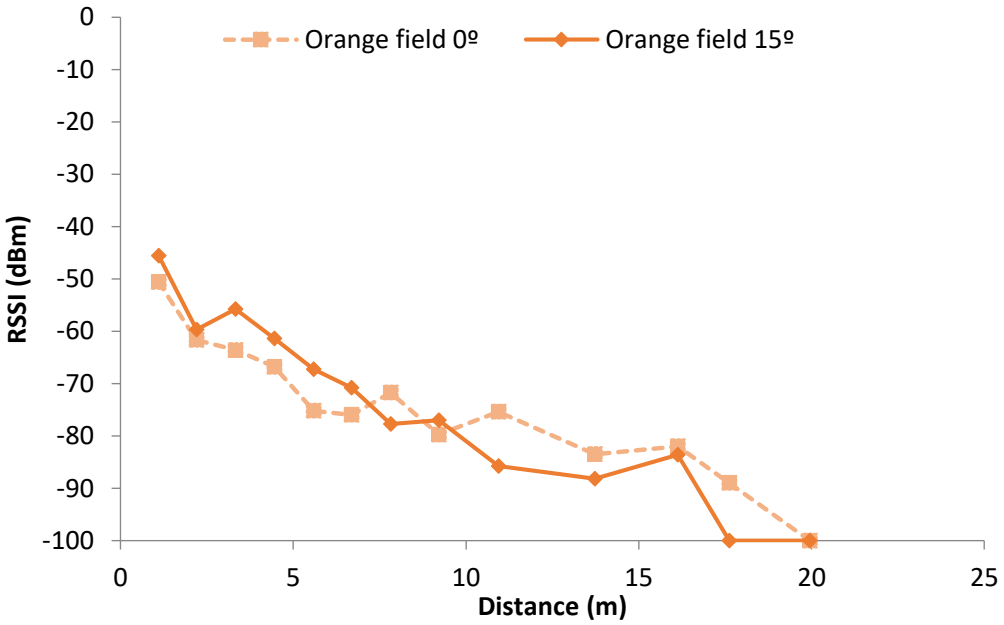

Figure 7.16. RSSI in Orange fields.

Thus, in the orange fields, we can conclude that the RSSI of on-ground deployments decreases faster than in grasslands or scrubs. Furthermore, from the obtained data it is appreciable that, in the first meters, the orange trees may cause constructive interferences at 15º. Nevertheless, at higher distances, the interferences cause negative effects, and the connection is lost earlier than in other environments and it is lost earlier when there is not direct vision between both devices. This effect will be the object of study for our future works as this type of crop are abundant in the Mediterranean area and agriculture systems will be deployed in similar fields.

Finally, a comparison of the data from the grassland, scrub, and orange fields in the same graphics is shown in Figure 7.17 to determine the differences in the signal attenuation for each type of vegetation. The multipath effect can cause constructive and destructive interferences. As it has been commented on the previous figures, the multipath effect can be considered as the cause of the fluctuations in the measured RSSI values as there is not only attenuation but also signal recoveries after obstacles and dense vegetation. From the obtained results it can be seen that, in the first meters, there is a positive effect on RSSI, with possible constructive interferences that would increment the RSSI. However, after 10 m, there are interferences that cause negative effects. As a result, the RSSI is lower than in environments without vegetation. This can

be due to the characteristics of the vegetation. As it can be seen in Figure 7.11, although the scrubs on the field do present thicker vegetation, there are areas where it is sparser. This type of scrubs and their layout is typical of Mediterranean areas. Therefore, there may be areas where the vegetation is not as thick and present less attenuation. Furthermore, both 0º and 15º measures were similar at many points so, at the position of the sender and receiver, the signal at the scrub field may present elements that introduce less attenuation than that of the grass field. Considering the position of the emitter and receiver at the grass field, the structure of the grass creates a rough surface where the signal is less likely to be reflected, similar to the walls of a small anechoic chamber, whereas the areas with dirt on the scrub field present less vegetation and as the dirt is compacted, the signal may be reflected. Other studies that perform measures at grasslands and scrublands such as [373] perform their measures in fields with other characteristics. In their case, the scrubland is an area with thick tropical vegetation and the grass field do not present common grass like that of parks and golf fields. Therefore, as stated before, the characteristics of the vegetation, a thicker, uneven surface in the case of grass and a sparser heterogeneous amount of vegetation in the case of the scrubs, may lead to the obtained results.

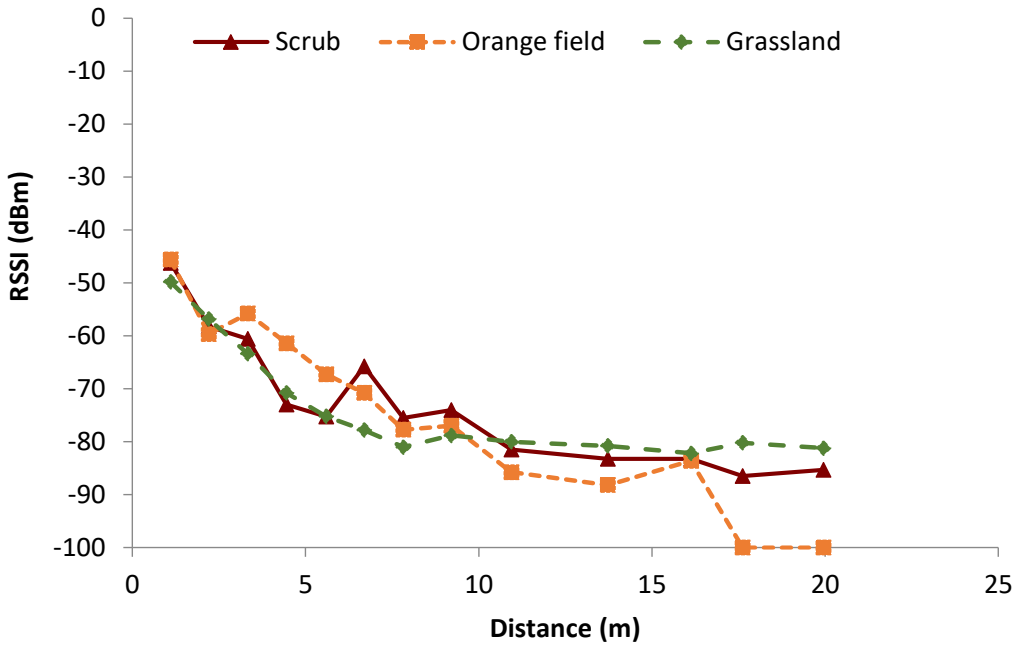

Figure 7.17. RSSI in all fields.

After discussing the results obtained from the RSSI measures of the on-ground deployment strategy in different vegetation environments, a model of the signal quality for each vegetation will be obtained to determine the theoretical maximum coverage for the on-ground deployment.

Equation (7.1) describes the power balance formula that determines the received signal power (Prx) according to the transmitted power, the gain of both the transmitter and receiver antennas, and the losses from air transmission, humidity, and vegetation as

in [374]. However, unlike in [374], the signal loss produced by the vegetation, in this case, is not that of [375] but will be obtained from the real measures performed in different environments.

$$P_{rx}(dB) = P_{tx\text{-}1m}(dB) - 10n \log d\,(m) - L_{humidity}(dB) - L_{vegetation}(dB) \quad (7.1)$$

Most of the values are known such as the transmitted power (Ptx-1m) that for the ESP32 it is -45.75 dBm, which can be theoretically calculated through equation (7.2). Where the frequency is expressed in Hz and c is 3*108 m/s. The characteristics of the ESP32 chip are depicted in [322]. When the medium is air, the value n equals 2. The distance between transmitter and receiver is d. Lastly, $L_{humidity}$ is 0.026 dB for the hydrometric H and K areas of Spain [376].

$$P_{tx\text{-}1m} = 20 \log_{10} d + 20 \log_{10}(f) + 20 \log_{10}(4\pi/c) \quad (7.2)$$

In order to determine the signal loss caused by each type of vegetation, the mathematical model for the Prx for each type of vegetation needs to be obtained.

The data from Figure 7.14 can be adjusted to a mathematical model, which will be our signal attenuation model with no interferences. As the observed differences at the same distance but with different orientations are minimum, we are going to consider that the RSSI does not change with the orientation of the antenna. We have observed that this happens with low vegetation environments in contrast to high vegetation environments where the results may vary with different angles. Thus, for the case of the grasslands, both sets of data are to be used for the mathematical model, see Figure 7.18 a). The mathematical model is a logarithmic model, and its expression can be seen in equation (7.3). In Figure 7.18, the gathered data is represented in squares and the lines represent the model, its confidence intervals, and its prediction intervals. The correlation coefficient of this model is 0.98, the R2 is 96.68%, and the mean absolute error is 1.44.

$$P_{rx\text{-}grass}\,(dBm) = -52.25 - 12.24 \ln d(m) \quad (7.3)$$

As in the grassland, we can obtain a mathematical equation that models the gathered data. As in the previous case, the mean of both sets of data is used. The obtained model follows the same pattern as the previous one and is shown in equation (7.4). The mathematical model, with the intervals of confidence and prediction, can be seen in Figure 7.18 b). The correlation coefficient of this model is 0.93, the R2 is 87.86%, and the mean absolute error is 3.40.

$$P_{rx\text{-}scrub}\,(dBm) = -47.95 - 12.25 \ln d(m) \quad (7.4)$$

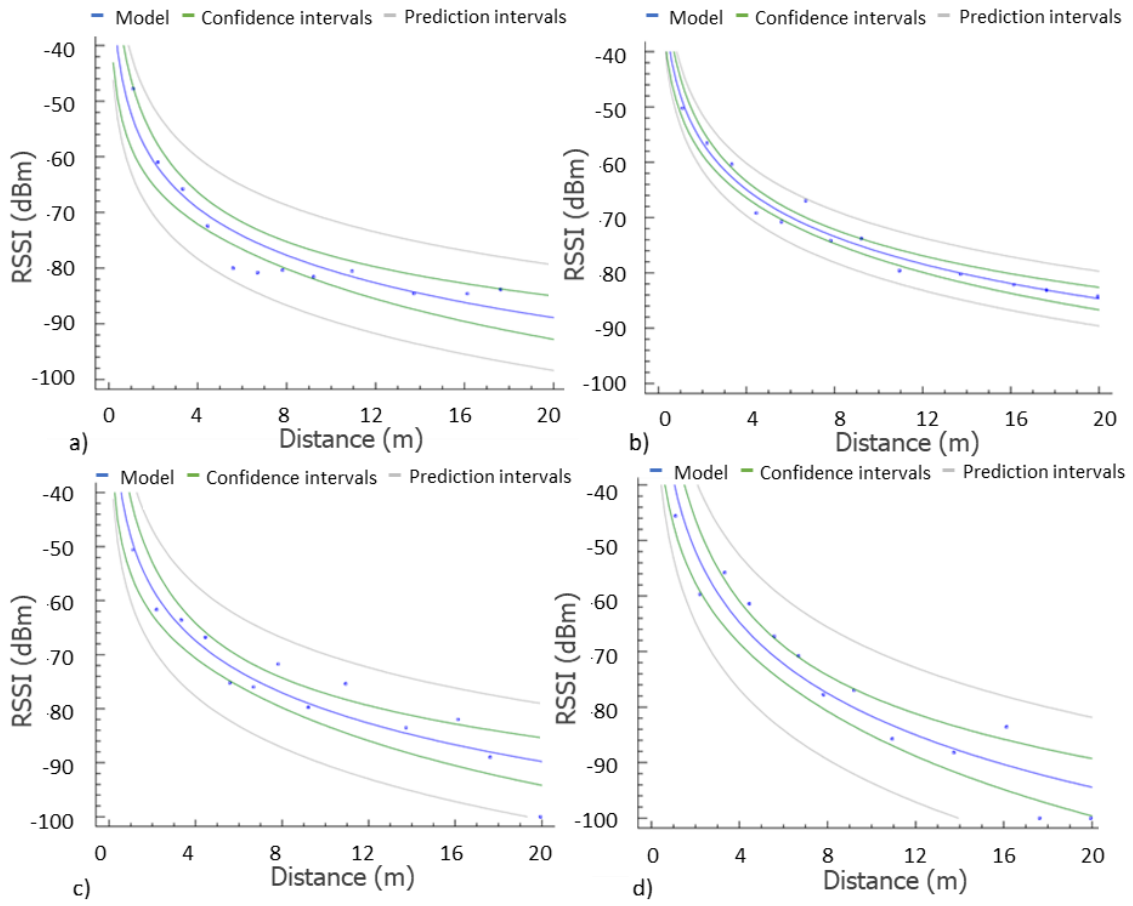

Figure 7.18. Model of RSSI in a) grasslands b) scrubs c) orange fields at 0º d) orange fields at 15º.

Regarding the orange fields, as we consider that the interferences are different at 0º and 15º, the gathered data is going to be utilized separately to build two mathematical models. The first one would be for a deployment strategy where the nodes are located at the line of sight, placed on the streets between the rows of trees. The mean of the data gathered at 0º is utilized to create a model, see Equation (7.5) and Figure 7.18 c). The correlation coefficient of this model is 0.94, the R2 is 88.84%, and the mean absolute error is 3.10.

$$P_{rx\text{-}orange\ 0^o}\ (dBm) = -48.15 - 13.89 \ln d(m) \quad (7.5)$$

Secondly, the model for the deployment where the trajectory between the emitter and receiver is obstructed by the tree trunks is obtained. The model from the data gathered at 15º is presented in equation (7.6) and Figure 7.18 d). The correlation coefficient of this model is 0.95, the R2 is 91.08%, and the mean absolute error is 4.29. We can compare both models and see that they are similar, but the slope is more pronounced in the second case.

$$P_{rx\text{-}orange\ 15^o}\ (dBm) = -39.12 - 18.74 \ln d(m) \quad (7.6)$$

From the obtained models, the signal loss caused by each type of vegetation can be obtained. Therefore, the theoretical equation and the model are equivalent as shown in equation (7.7), which is obtained for the grass mathematical model.

$$P_{tx} - 10n \log d - L_{rain} - L_{grass} = -52.25 - 12.24 \ln d \quad (7.7)$$

Therefore, the signal loss caused by grass can be expressed as Equation (7.8).

$$L_{grass} = P_{tx} - 10n \log d - L_{rain} + 52.25 + 12.24 \ln d \quad (7.8)$$

When the known values are replaced in equation (7.8) the resulting equation for the signal loss caused by grass is equation (7.9).

$$L_{grass} = 6.474 - 20 \log d + 12.21 \ln d \quad (7.9)$$

Equation (7.9) can be then simplified to equation (7.10).

$$L_{grass} = 3.554 \ln d + 6.474 \quad (7.10)$$

Following the same process, the resulting equations for the rest of the vegetation types are equation (7.11) for scrub, equation (7.12) for the orange trees at 0 degrees, and equation (7.13) for the orange trees at 15 degrees.

$$L_{scrub} = 3.5641 \ln d + 2.174 \quad (7.11)$$

$$L_{orange\_tree\_0} = 5.2041 \ln d + 2.374 \quad (7.12)$$

$$L_{orange\_tree\_15} = 10.0541 \ln d - 6.656 \quad (7.13)$$

In other to determine the maximum distance between nodes for each type of vegetation, the aforementioned expressions for signal loss for each type of vegetation should be applied to equation (7.14).

$$D = 10^{(Ptx - Lrain - Lvegetation - Prx)/\ 20} \quad (7.14)$$

Where $L_{vegetation}$ is replaced by L_{grass}, L_{scrub}, $L_{orange0,}$ and $L_{orange15}$ accordingly. The results for the maximum distance for each type of vegetation can be seen in Figure 7.19. Although results show distances greater than those of the empirical data, the real data for RSSI values between -90 and -100 is harder to obtain due to the nodes not connecting to each other. However, the model does not regard that. But, as it can be seen, for the orange field, values above -90 stay within the 20 m limit. Considering a signal strength between -90 and -100 is of bad quality and would not be considered when designing the network, values are reflecting the empirical case.

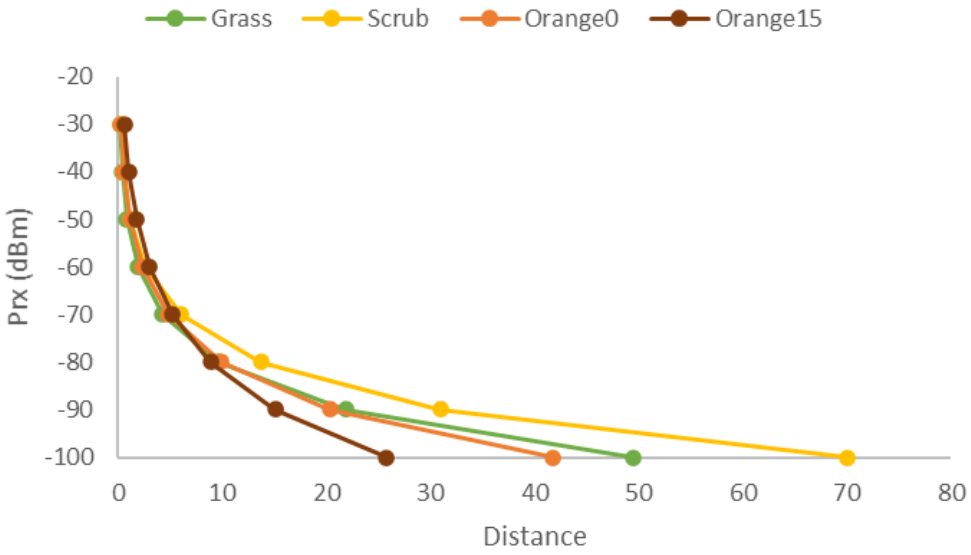

Figure 7.19. Maximum distance for desired Prx.

7.3.1.1.2 Scenario 2: On-ground, near-ground, and above-ground deployments for orange tree monitoring.

In this subsection, the results for the scenario with on-ground, near-ground, and above-ground deployment strategies with different emitter heights at an orange orchard are presented.

In this scenario, the results have been classified according to the height of the receiver as there was more variability with changes in the height of the receiver than with changes in the height of the emitter. The different receiver heights that were measured were on-ground (0 meters), near-ground (0.5 meters), and above-ground (1 meter). While the different heights of the emitter were 0.5 m, 1 m, 1.5 m, and 2 m.

The results for the receiver on the on-ground position and different positions of the emitter are presented in Figure 7.20. As it can be seen, the higher signal qualities were obtained for the emitter height of 50 cm for most distances. Good results were obtained as well for the height of 1 m. The lower RSSI values obtained at a height of 1.5 m and 2 m are due to a high density of the foliage of the trees. The average height of the orange trees was 2.5 meters. Therefore, the bulk of the foliage was between 1 and 2.5 meters. That led to great interferences for those heights when a tree was reached. It can be seen as well how the RSSI fluctuates at different distances alternating between lower and higher RSSI values. This effect can be due to the multipath effect as a result of the reflection on leaves and fruits as well as the attenuation caused by the foliage. One of these fluctuations is the peak reached at the 0.5-meter height for a distance of 9 meters at an area with abundant foliage. For the 0.5-meter case, the signal is boosted, however, for the rest of the emitter heights, the quality of the signal was reduced as the emitter was placed among the foliage. It is noticeable as well how the quality of the signal is recovered after an area with abundant foliage.

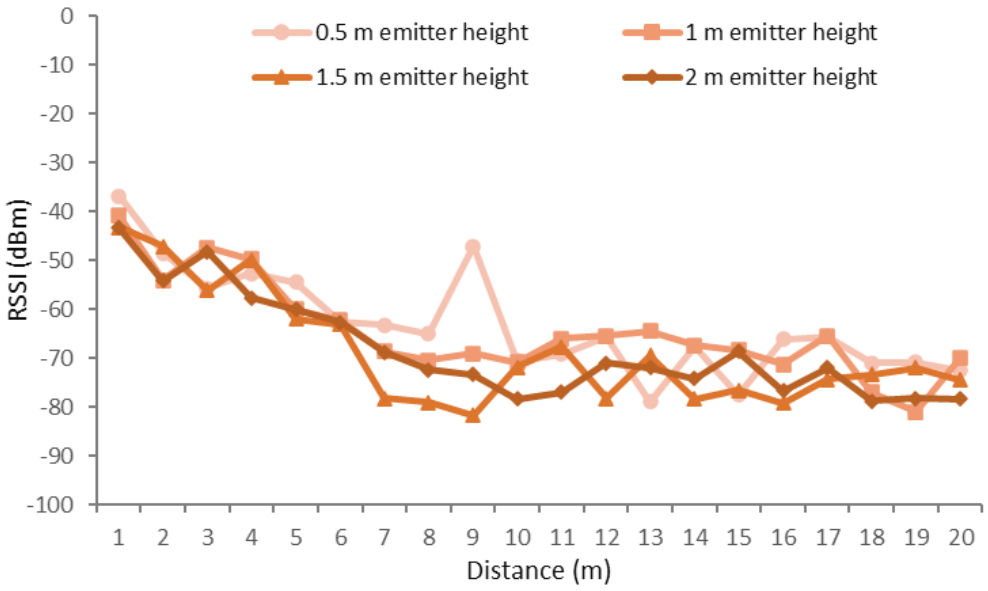

Figure 7.20. RSSI for on-ground receiver and different configurations for the emitter.

For the near-ground configuration of the height of the receiver (0.5 m), the results showed in Figure 7.21 were obtained. In this case, the best RSSI values were obtained for the emitter at a height of 1 m. The overall signal quality is better than that of the on-ground position of the receiver. However, the signal quality is less stable, resulting in high fluctuations along the different measurement spots as the distance between emitter and receiver increases. Particularly, the fluctuations of the RSSI at different heights, compared to those of the on-ground receiver position shown in Figure 7.21, are more evident with acute fluctuations of 27.4 dBm at the 1.5 m emitter height and 23.24 dBm at the 1 m emitter height. The lowest RSSI values were on the range between -80 and -70 dBm for the 1.5 m height. These values were due to a highly dense mass of foliage from the top of the orange trees. However, when the highly dense foliage is surpassed,

the signal is recovered. Particularly, after the low values reached at meter 17 for the emitter height of 2 m, the signal was recovered in 11.5 dBm.

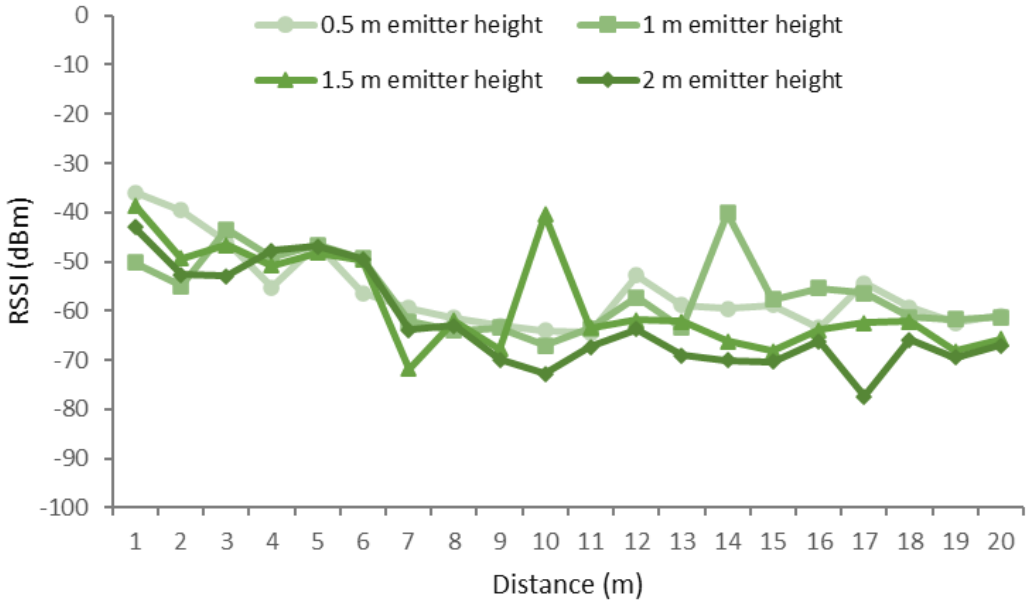

Figure 7.21. RSSI 1for near-ground receiver and different configurations for the emitter.

Lastly, Figure 7.22 presents the RSSI values for the receiver at the above-ground position (1 m) and the emitter at different heights and distances. This configuration presents worse signal quality than those of Figures 7.20 and 7.21 as the line of sight between the emitter and receiver nodes is at the same height as the bulk of the foliage. In the case of the above-ground position of the receiver, the emitter heights of 1 and 0.5 m are the best options as the RSSI values indicate better signal quality than those of the emitter heights of 1.5 and 2 m. This is due to the attenuation caused by the highly dense foliage of the treetops that obstructed the line of sight between emitter and receiver. As the signal was attenuated by a more constant density of foliage, the fluctuations in signal quality are in most cases less prominent than those of the on-ground and near-ground deployments. However, for the emitter height of 0.5 m, as it was not obstructed with dense foliage, there are great variations with several peaks. The first peak presents a degradation of the signal, which reaches a low value of -71 dBm at a distance of 4 m to the receiver. Then, the signal recovers and reaches a peak with a high value of -55.16 dBm at a distance of 8 m from the receiver. Then, another high peak is reached with a value of -41.66 dBm at a distance of 12 m from the receiver, which is a fluctuation of 20.34 dBm. Lastly, another low peak happens at a distance of 16 m from the receiver with a value of -73.16 dBm.

Considering all the receiver deployment strategies, it can be seen that for emitter heights of 0.5 m and 1 m, with no obstruction of the line of sight between emitter and receiver, the signal presents high fluctuations that may be caused by the multipath effect. For the case of the 1 m emitter heights, the fluctuations are less prominent than for the

case of 0.5 m with similar RSSI values at the points with no peaks. Therefore, due to the stability of the signal and the good RSSI values, the emitter height of 1 m is the best option for all on-ground, near-ground and above-ground receiver positions. While emitter heights of 1.5 m and 2 m are more stable, they are also more affected by the attenuation of the highly dense foliage as it is to be expected. Thus, the obtained RSSI values are generally lower than those of the 0.5 m and 1 m emitter heights.

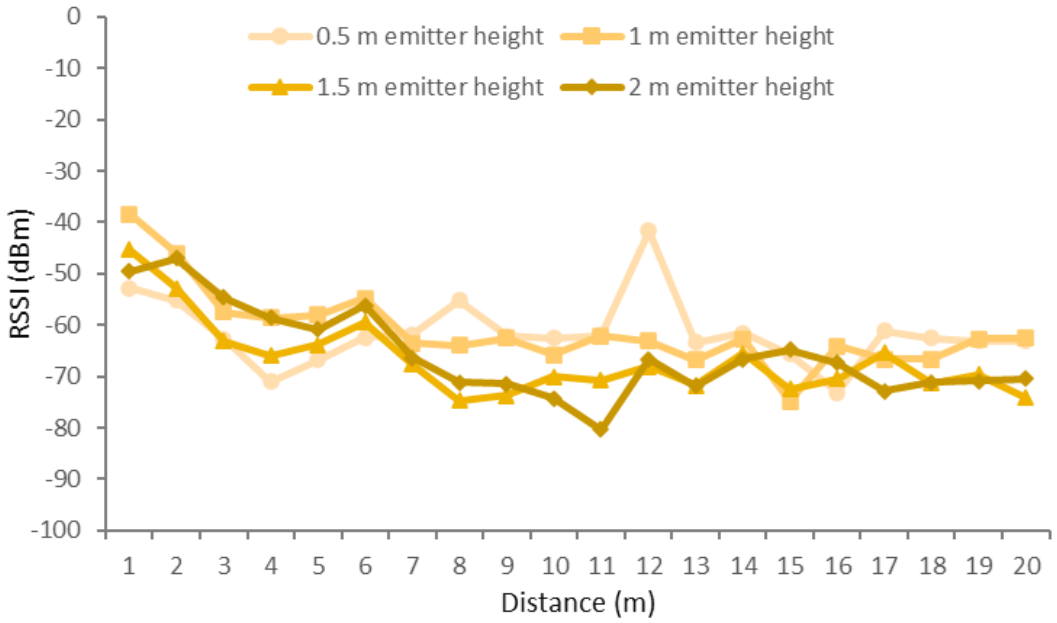

Figure 7.22. RSSI for above-ground receiver and different configurations for the emitter.

From the obtained signal quality results, a heuristic signal attenuation model was obtained for the on-ground, near-ground, and above-ground deployments after discarding the outlier values. As in the first scenario, the aim to obtain a theoretical maximum coverage to aid in the design of a soil sensing network deployment. The model presented in equation (7.15) was obtained for the on-ground deployment. In Figure 7.23 a), the data gathered from the tests performed in real environments is presented as dots. The model, confidence intervals, and prediction intervals are provided as well. For the near-ground deployment, the model presented in Figure 7.23 b) is expressed as equation (7.16). As it can be seen, this is the configuration with better signal quality. Lastly, the model for the above-ground deployment is presented in equation (7.17). The graphic representation of the model, the confidence and prediction intervals are shown in Figure 7.23 c).

$$P_{rx\text{-}on\text{-}ground}\,(dBm) = -42.05 - 11.53 \ln d(m) \quad (7.15)$$

$$P_{rx\text{-}near\text{-}ground}\,(dBm) = -41.55 - 8.10 \ln d(m) \quad (7.16)$$

$$P_{rx\text{-}above\text{-}ground}\,(dBm) = -49.80 - 6.68 \ln d(m) \quad (7.17)$$

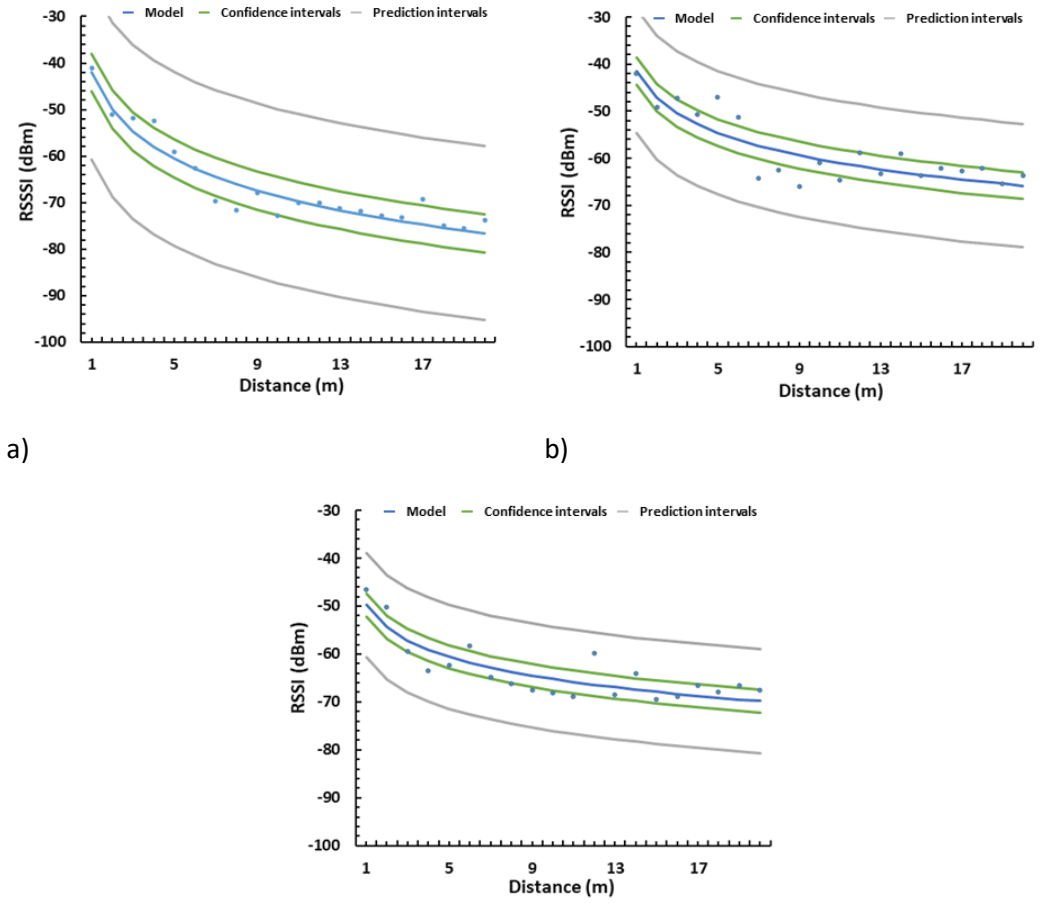

Figure 7.23. Model of RSSI in the orange field with emitter a) on the ground b) at 50 cm of height c) at 1 m of height.

Utilizing equation (7.1) and the models presented in equations (7.15), (7.16), and (7.17), the vegetation losses caused by the foliage of the trees at the on-ground, near-ground, and above-ground deployments are presented in equations (7.18), (7.19) and (7.20) respectively.

$$L_{veg\_on\_gorund} = 20.22 \ln d + 12.03 \quad (7.18)$$

$$L_{veg\_near\_ground} = 16.79 \ln d - 2.68 \quad (7.19)$$

$$L_{veg\_above\_ground} = 15.37 \ln d + 17.18 \quad (7.20)$$

Lastly, applying equation (7.14), the maximum theoretical distance for a determined Prx is obtained (See Figure 7.24). Where $L_{vegetation}$ is replaced by $L_{veg\_on\_gorund}$, $L_{veg\_near\_ground}$, and $L_{veg\_above\_ground}$. Acceptable signal quality would be obtained up to 26 meters for the on-ground deployments, 115 meters for the near-ground deployments, and 91 meters for the above-ground deployments. Considering these results, it can be

concluded that near-ground deployment strategies are the best option for soil monitoring network deployments in crops comprised of trees, such as orange orchards. The 0.5 m and 1 m height were found to be the better option for emitter positioning which could be expected as it is a height with a low presence of foliage. However, even with no or few obstructions of the line of sight between emitter and receiver, the signal quality presented high fluctuations, which were less acute for the case of the emitter placed at a height of 1 m.

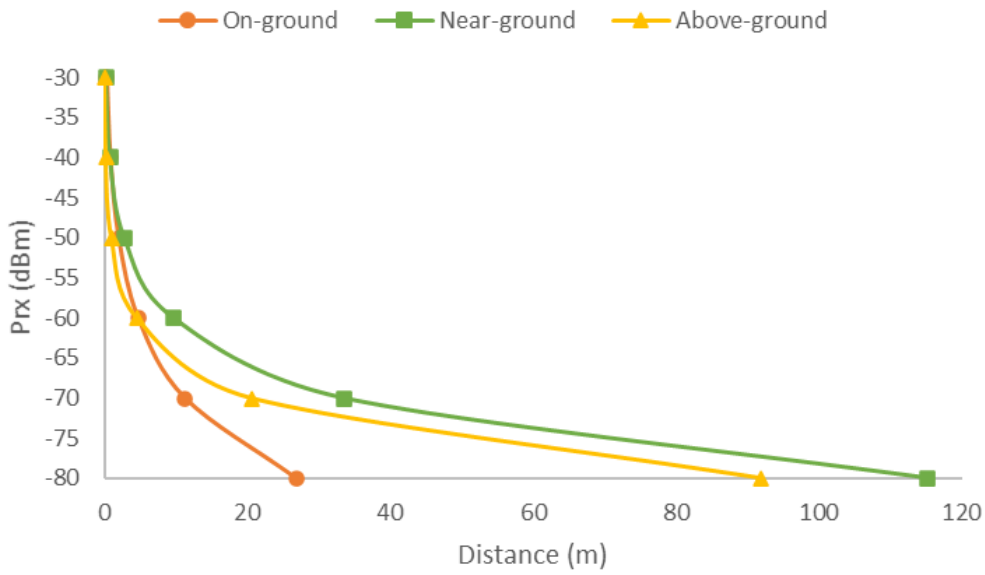

Figure 7.24. Maximum distance for desired Prx at on-ground, near-ground and above-ground deployments.

7.3.1.2 Discussion and challenges

In this subsection, a discussion on transmitting at different heights in environments with vegetations is provided. Furthermore, the challenges of deploying wireless sensor networks for precision agriculture are presented.

Node height is one of the key factors of sensor network deployments in rural and vegetated areas due to multiple reasons. Coverage and signal quality are one of these reasons as the main objective of the sensor network deployment is to gather and forward the data so it can be accessed by the user. However, other aspects such as the amount of foliage [377, 378, 379], the plant height [378], the machinery utilized at the fields, the presence of animals, or the irrigation system may present some challenges. Thus, the aim when designing the sensor network deployment for a determined rural environment is to consider the specific challenges and needs of the area while opting for the best signal quality and coverage configuration. The need of performing preliminary tests to determine the real performance of the nodes in contrast to the advertised by the manufacturer was also stressed in other studies [372], with an emphasis on low-cost nodes such as the ones utilized in our testbed. As there are many variables to consider,

other testbeds have focused on specific environments, node height, and frequencies to study how the signal is affected (see Chapter 2 subsection 2.5.9).

The crop type is always described on the testbeds presented in Chapter 2 subsection 2.5.9 as it is an indicator of the plant height and possible foliage density. Particularly, the effects of the attenuation caused by high foliage density were remarked in [380]. Though many studies have been performed regarding the effects of vegetation on signal quality, each study provides new insights on a specific type of crop, wireless technology, the response of a specific node, or the performance of the deployment strategy among other variables. Furthermore, a useful and interesting use of monitoring signal quality in vegetated environments is to use RSSI to identify vegetation growth [372]. Nonetheless, the deployment strategy is to be considered as the height of the node that is measuring the signal quality should be known to establish the reference height value of the crop. Crops such as lettuce or potatoes [381] have a low height, present a uniform foliage density for the height of the plant, and are planted with a small distance between plants. Thus, on-ground deployments would not be suitable for the characteristics of this type of crop. Asparagus, like some types of shrubs [382], present a medium height, the foliage density is uniform as well, and the separation between plants can be greater between rows. In this case, on-ground deployments would be possible if the nodes are deployed between rows. However, as the distance between rows is small, it could be an inconvenience for the farmers to access the plants. Therefore, above-ground deployments with posts placed on the plant row would be the best solution. Lastly, plants with high heights such as orange trees are planted with a separation between 3 and 5 meters and can reach heights above 7 meters. The bulk of the foliage is at the treetop, with space without foliage at the tree trunk level. Therefore, above-ground deployments would be susceptible to more signal interferences and would interfere with farming activities such as pruning. Furthermore, considering the results of the presented testbed, a near-ground deployment strategy would be the best option. However, the results show a high fluctuation of the signal quality at emitter heights of 0.5 m and 1 m with no obstructions in the line of sight between emitter and receiver that can be caused by the multipath effect.

The node density is another aspect to consider. Deploying one node per plant is neither necessary nor affordable. The data that is necessary to calculate irrigation needs or other aspects such as fertilizer needs does not vary significantly from plant to plant. Therefore, the field can be divided into different zones with a node or a cluster of nodes per zone. Moreover, the cost of deploying nodes all over the field can be too elevated for most of the farmers. As such, the nodes can be deployed as clusters that monitor one area and communicate with an AP or gateway that forwards the data to the user or the data center. Furthermore, if the nodes in the cluster are utilized to detect false positives and false negatives or to evaluate the area reached by the water in the case of drip irrigation, the distance between the nodes will not be very high as well. Lastly, as meteorology data is also necessary for the calculation of the irrigation needs and the data cannot be measured near the ground, if a node for meteorology monitoring is utilized, the node should be deployed above-ground and in an exposed area as it is recommended by the FAO [337].

The type of irrigation may also influence the decision-making process when designing a WSN deployment for a field. Flood irrigation would make on-ground deployments impossible as the nodes could get damaged or could move even when placed in protective boxes. For pivot irrigation, the node cannot be placed at a height higher than the shortest point of the structure of the irrigation system. Furthermore, for drip irrigation, wet areas can be avoided which facilitates the deployment of the nodes.

Energy consumption is a recurrent topic regarding WSN. Although the amount of daily data necessary for irrigation calculations can be as few as one value for each variable, most systems will gather data in real-time or at frequencies of 10 minutes, 30 minutes, or 1 hour. Therefore, energy harvesting solutions such as the use of solar panels have been widely implemented [383]. Furthermore, the performance of the energy harvesting solutions can be monitored by the nodes to ensure there is enough energy [384]. However, the foliage of the plants could create a shade on the panel resulting in a reduction or the absence of harvested energy. Therefore, this aspect should also be considered when selecting the height of the node. There are however new solutions that allow charging the batteries of the nodes in a fast manner without the need of connecting the nodes to any device or removing the insulation, such as utilizing Wireless Power Transfer (WPT) [385].

Finally, the selection of the wireless technology to be used on the precision monitoring system is also to be considered. Aspects such as coverage distance, data rate, energy consumption, equipment cost, and the simplicity of implementation are often evaluated when taking this decision. Regarding coverage, there are low range technologies such as Bluetooth, mid-range technologies such as Zigbee or Wi-Fi, and long-range technologies such as LoRa. High data rates are not often necessary for PA monitoring systems; therefore most technologies could be utilized. Regarding the cost of the devices, WiFi has been the technology with the most options regarding price ranges. However, ZigBee and LoRa devices have had a cost reduction in recent years, making them more affordable. Lastly, Wi-Fi is the easiest technology to use regarding implementation simplicity due to both the available options in the market and the extensive documentation, removing in many cases the need for an expert to deploy the network. This accessibility results in this technology being significantly the most utilized in IoT systems for PA [383], followed by GSM and ZigBee. In terms of energy consumption, Bluetooth Low Energy (BLE), ZigBee, or LoRa are presented as low-power technologies. Among these technologies, ZigBee is the most used low-power technology in agriculture networks [383] and its performance in vegetated environments has been studied in detail [372]. WiFi presents higher energy consumption. However, for Ad Hoc networks WiFi was found to have more energy efficiency than LoRa in shorter distances [386]. Being LoRa more efficient for distances greater than 300 m. Furthermore, as it was commented previously, energy harvesting solutions help in alleviating the higher energy consumption of non-low-power technologies. It could be argued that ZigBee would be the best technology for PA systems, and it is the best option regarding energy consumption, but the convenience of Wi-Fi often wins in deciding the wireless technology if the requirements for coverage and energy consumption are met, which it does for many architectures and the few data that needs to be forwarded. Furthermore, Wi-Fi is convenient for the user as well if there is a need to connect directly with a device utilizing a smartphone, tablet, or laptop. Which is the

case for remote areas, and countries without a well-developed communication infrastructure.

7.3.1.3 Limitations of this study

Precision agriculture systems have specific needs that require the consideration of specific aspects of the agricultural environment to be monitored. This paper provides a first approach to identify the aspects that affect the deployment of wireless networks for precision agriculture systems. It is thus limited to the specific types of vegetation that were considered in the testbed and to a specific low-cost ESP32 WiFi node. Furthermore, this study is limited to sunny weather conditions with medium temperatures which is the predominant weather in the Mediterranean coast of Spain. Although similar results are to be expected with a replication of this testbed utilizing low-cost WiFi nodes, more tests and replications are needed to determine the exact influence of certain aspects such as weather conditions, different stages of the crops where there is presence of flowers and fruits, and the use other types of low-cost nodes to determine if there are significant differences among them. However, although this study provides a first approach to perform soil monitoring wireless node deployments, we consider that our study provides some insights to wireless sensor deployments in orange fields that could be of interest to those interested in deploying a precision agriculture system to monitor citrus crops or other types of tree crops.

7.3.2 Coverage results for underground deployments

As Vuran described in [282], IoUT may be comprised of underground and aboveground elements. In this study, we test the signal strength between an underground and an aboveground node so as to determine the possible use of low-cost Wi-Fi nodes for IoUT purposes. As it can be seen in Figure 7.25, four RSSI-meter nodes were buried underground at distances 10 cm, 20 cm, 30 cm, and 40 cm deep into the ground. They were placed in the same hole one on top of the other and adding the necessary soil between each protective box so as to reach the required depth. Then, the AP was placed at heights of 50, 100, 150, and 200 cm for each of the measures. One meter was added to the separation of the AP and the initial point for each measure. The orientation of the antennas and the position of the nodes was always the same for all the measures. The images of how the nodes were placed on the field are presented in Figure 7.26. When the RSSI-meter nodes were buried, the soil was slightly compacted, and the soil of the surrounding areas was not disrupted.

To perform this test, four nodes were programmed to measure the RSSI and one node was programmed as an AP. The utilized node was the Mini D1 ESP 8266 node for both the AP and the RSSI-meter. The Mini D1 presents 11 digital input/output pins and has an operating voltage of 3.3 V. The specifications of the ESP8266 chip and the antenna can be found in [387].

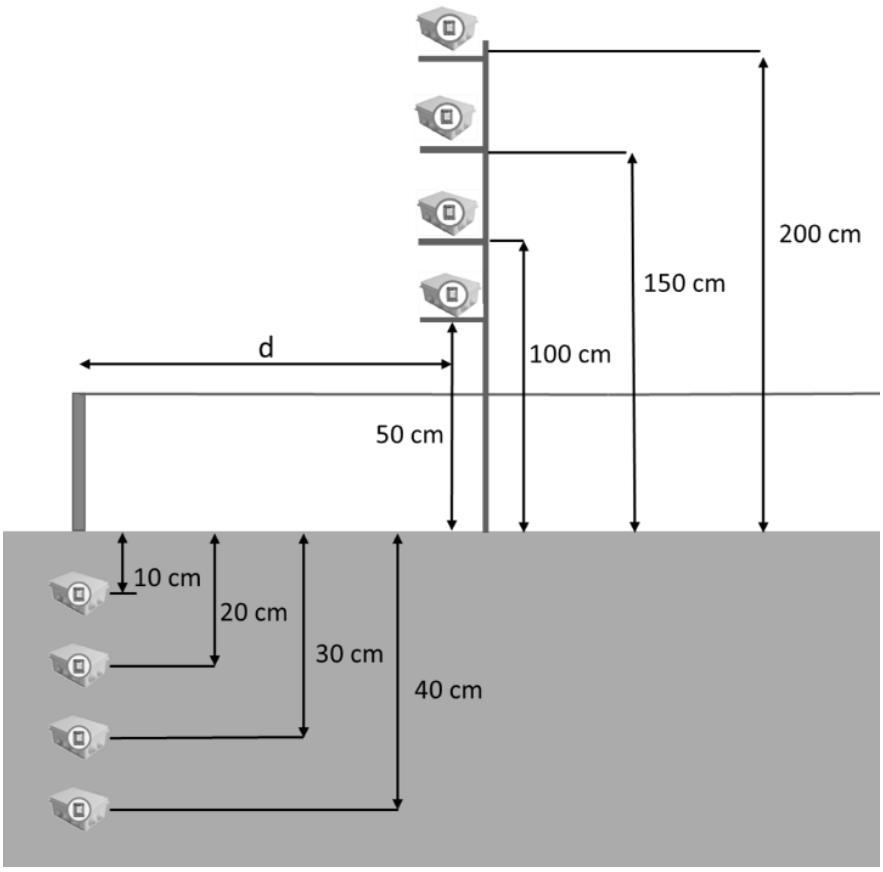

Figure 7.25. Diagram of the testbed.

Figure 7.26. Deployment of the nodes.

The nodes that measured the RSSI were placed on 80x80x36 mm sized protective boxes and the AP node was placed inside a 155X105X62 mm protective box that included the power supply. The power supply was a DC 5V-1000mA power bank with a capacity of 2000mAh. The ESP8266 nodes were placed inside the box with the antenna placed upwards. The nodes were taped in order to avoid any movement of the node inside the box at the time they were buried. A cable that connected the node to a laptop went through a hole of the box that was sealed afterwards so as to avoid the soil getting to the node. The data on the RSSI was gathered through the serial port of the node using the Arduino IDE.

The test was performed in a Mediterranean area in a field where a citrus plot used to be. The satellite image of the field can be seen in Figure 7.27. As it can be seen, the area is used for agriculture and several citrus fields surround the field where the tests were performed. That area of the field was selected due to the lack of thicker and other types of vegetation. The soil was a predominantly sandy soil and has the appropriate qualities for citrus plantations. There is no presence of housing in the area and the use of IoT systems for agriculture was unknown. Therefore, a preliminary test was performed to confirm the absence of any other signal from other networks in the area.

Figure 7.27. Field where the experiments were performed.

7.3.2.1 Mathematical model for deployments with a height of 50 cm

This subsection presents the results of the experiment. We show the gathered RSSI at different distances. Then, the attenuation effect of the soil is described.

First, the values of RSSI are presented for each set of data (10, 20, 30, and 40 cm of buried depth). The mean, maximum, and minimum of the RSSI gathered at different

distances are shown. This step is necessary in order to evaluate the variance of the data. Figure 7.28 presents the data of the RSSI gathered by the node buried at 10 cm. Even though we can expect to have a uniform decrease in the signal as no vegetation or building are in the studied area, the soil itself can cause multipath effect. The soil is not uniform, and it can have different densities at different points which can cause those constructive and destructive interferences. In the first measured point, at 1m of the node in horizontal distance, the mean RSSI was -66 dBm. The RSSI decreased quickly and uniformly to -84 when the node was placed at 3 m from the AP. This signal is considered as a poor or unstable signal, and the communication between both devices might have further problems. From this point, 3m, the signal is affected by the multipath effect and the attenuation is not uniform. In some points, 4, 6, and 9 m the RSSI increases. It is important to note that some points as 1 or 4m have a big difference between the maximum and the minimum RSSI values, with a standard deviation higher than 4 in both cases. The mean standard deviation of this set of data is 3.21. At distances 10 and 11 m, the connection between the node and the AP was lost.

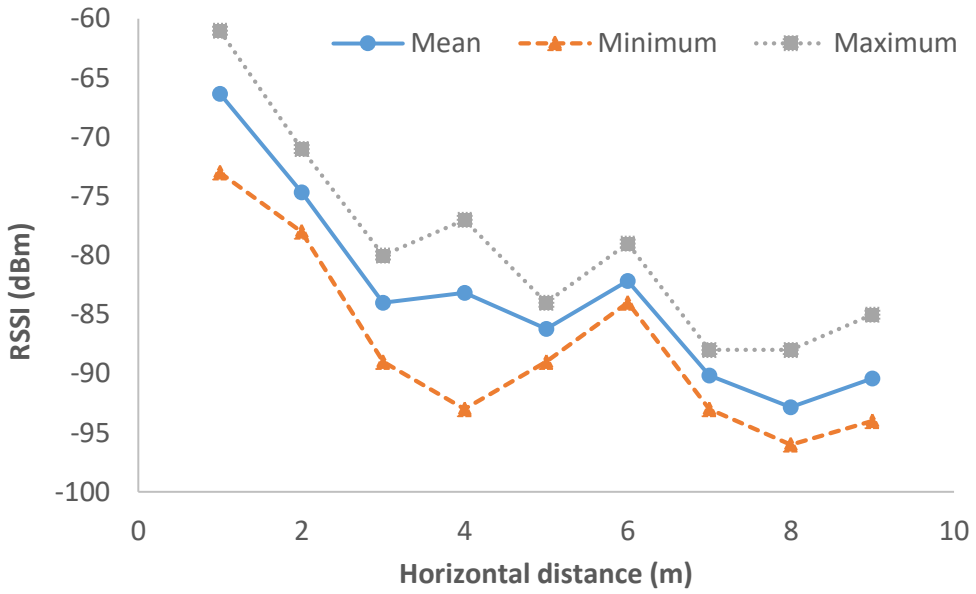

Figure 7.28. RSSI with node buried at a depth of 10 cm.

Figure 7.29 details the data gathered with the node buried at a depth of 20 cm. In this case, the signal attenuation is more uniform than in the previous case. The RSSI in the first measured point is -61 dBm (with a minimum of -62 dBm and a maximum of -60 dBm). The last measured point where the node is connected to the AP is 8m with a RSSI of -90 dBm. In this case, no clear evidence of multipath effect is found. We suspect that, as in the previous case, there were different densities in the soil which might cause it. Nonetheless, the data (mean, maximum, and minimum) follows a uniform attenuation. The standard deviation of this data is 1.67. Apparently, in this case, the standard deviation increases with the distance.

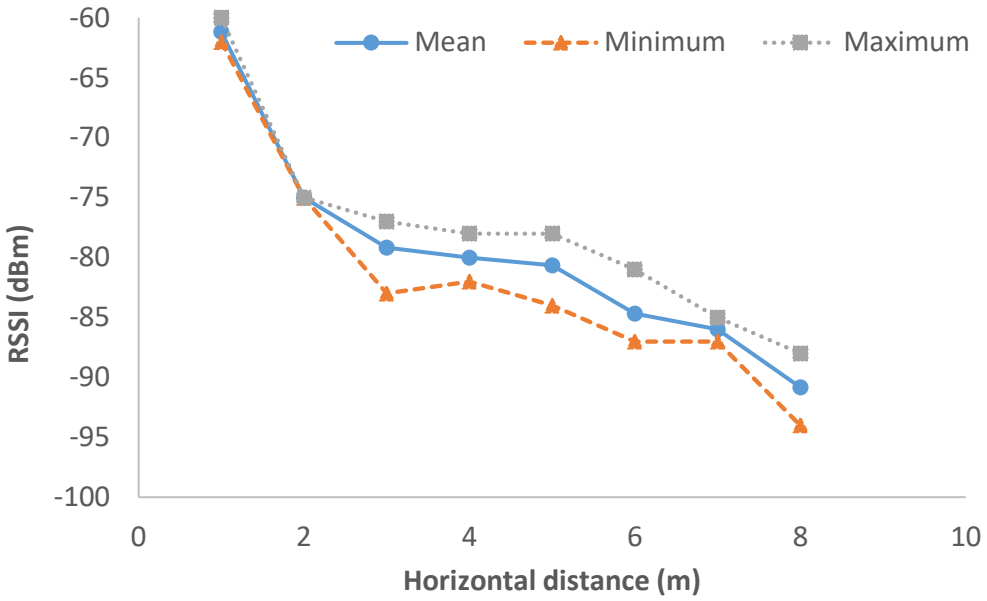

Figure 7.29. RSSI with node buried at a depth of 20 cm.

The data of RSSI from the node buried at 30 cm can be seen in Figure 7.30. In this case, the attenuation follows almost a linear relationship. There is one measured distance, 5m, where the RSSI increases, but in the rest of the cases it decreases with the distance. The mean RSSI at 1 m is 71 dBm (minimum and maximum are -68 dBm and -74 dBm). The last measured point where the node was connected to the AP was at 7 m, with a mean RSSI of -95 dBm. The mean standard deviation of this data is 1.75, which is similar to the standard deviation with the node buried at depth of 20 cm.

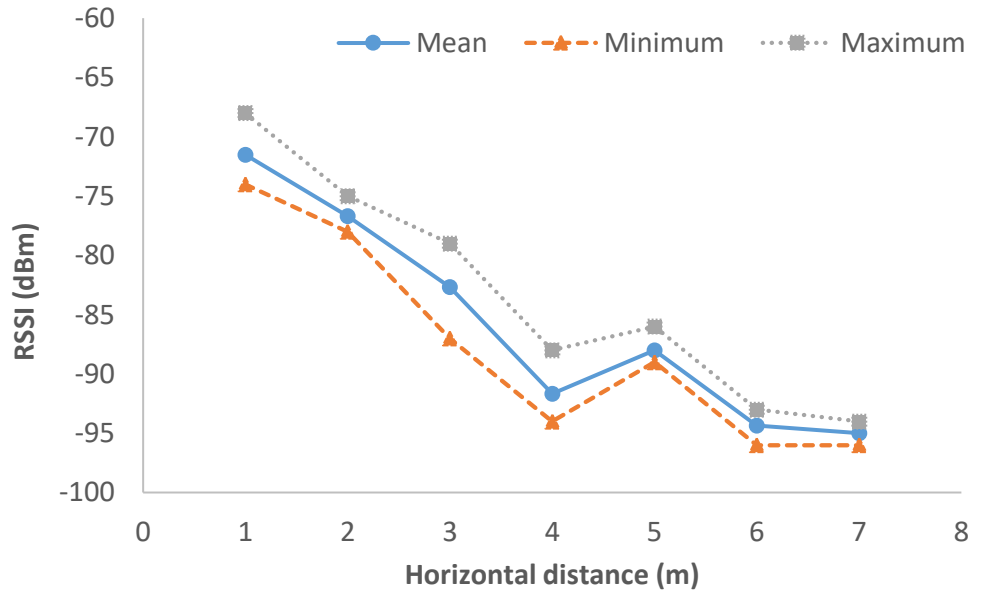

Figure 7.30. RSSI with node buried at a depth of 30 cm.

Figure 7.31 presents the data gathered with the node buried at a depth of 40 cm. The mean RSSI at 1m was -72 dBm, the minimum was -73 dBm, and the maximum -71 dBm. The RSSI indicates a signal attenuation with the distance following a uniform behavior. Besides, at 4 m, the RSSI increases because a possible multipath effect could be causing a constructive interference. The signal of the AP was lost after 6 m. The last measured RSSI was -92 dBm. The standard deviation of the data gathered at a depth of 40 cm was 1.57. This data has almost the same standard deviation as the data from the nodes buried at a depth of 20 cm and 30 cm.

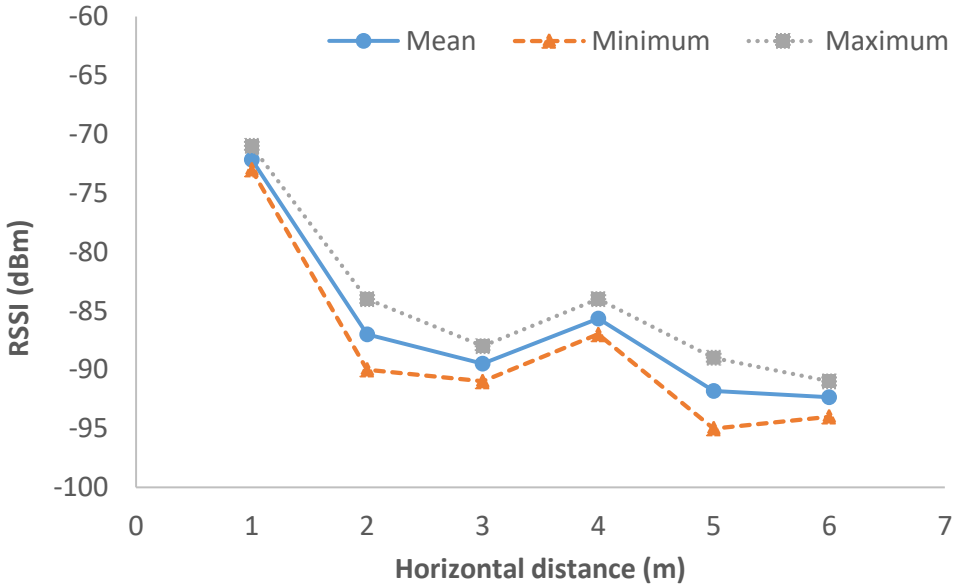

Figure 7.31. RSSI with node buried at a depth of 40 cm.

Finally, we can use the data shown in Figures 7.28 to 7.31 to create a visual model by interpolating this data. The model can be seen in Figure 7.32. The points where the signal was lost are entered as -110 dB to generate this model. Even though we can expect the best results with the shallowest node, the node buried at 20 cm seems to have better signal in the first 8m. Although the node which has coverage at further distances is the node buried at 10cm, we must consider not only the link existence but also the coverage in terms of RSSI. The values of RSSI lower than -70 dBm are considered as fair, lower than -80 dBm are considered as unstable signal, and lower than 90 are considered as a very unstable connection. Thus, although the node buried at 10cm has coverage until 9 m, we should only consider the values higher than 90 dBm. Therefore, the node which has higher coverage is the node buried at 20 cm. The explanation is that probably the signal of the node buried at 10 cm is highly affected by the air-soil interface.

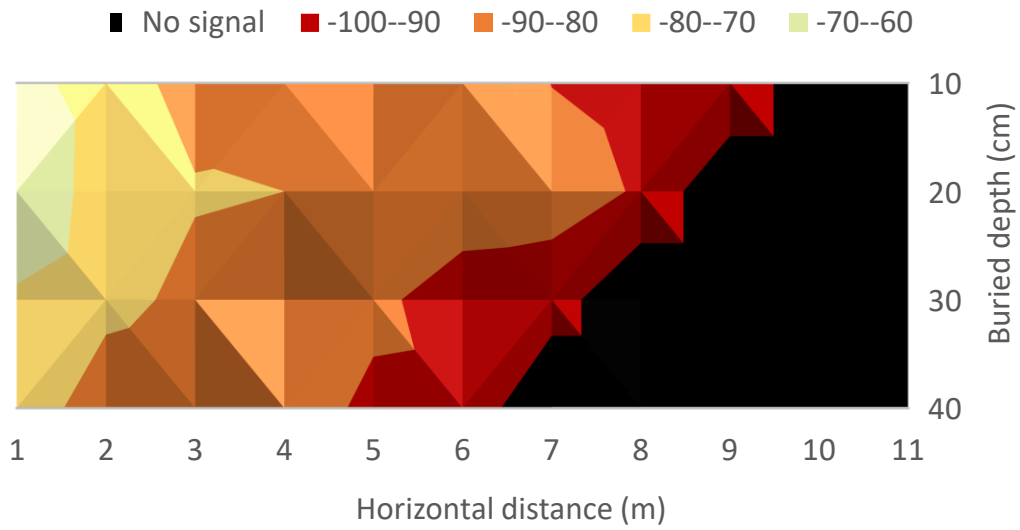

Figure 7.32. Visual model of the RSSI at different depths.

7.3.2.2 Mathematical model for deployments at a height of 50 cm

In this section, the mathematical model of the received power is presented. The received power is obtained utilizing the power balance formula [388, 389] provided in equation 7.21.

$$P_{rx} = P_{tx-1m} - n * 10 * \log d - L_{humidity} - L_{soil} \quad (7.21)$$

Where P_{rx} is de received power expressed in dBm, $P_{tx\text{-}1m}$ is the transmitted power at 1 meter in dBm which is -59,857 dBm for the ESP8266 nodes, n is the attenuation variation index which is 2 for air, d is the distance between transmitter and receiver expressed in meters, $L_{humidity}$ is the losses due to humidity for the two main hydrometric areas of Spain, areas H and K, which is 0.0026 dB [376] and L_{soil} are the losses due to the underground propagation of the signal. The theoretical received power at 1 meter is obtained with equation 7.22.

$$P_{tx-1m} = 20\ \log_{10} d + 20 \log_{10}(f) + 20 \log_{10}\left(\frac{4\pi}{c_0}\right) \quad (7.22)$$

Where c_0 is $3*10^8$ m/s and f is the operational frequency in Hz. Furthermore, the 100 mW power commonly used for WiFi transmissions should be considered. The losses due to soil, L_{soil}, are presented in Equation 7.23 [284].

$$L_{soil} = L_m + L_\alpha \tag{7.23}$$

Where L_m is the attenuation caused by the variation in wavelengths and L_α corresponds to the losses due to the attenuation constant. Each of them is presented in equations 7.24 and 7.25 respectively.

$$L_m = 20\log\left(\frac{\lambda_0}{\lambda}\right) = 20\log\left(\frac{\frac{c_0}{f}}{\frac{c}{f}}\right) = 20\log(\sqrt{\mu_r \varepsilon_r}) \tag{7.24}$$

$$L_\alpha = 8.69\alpha d_{soil} \tag{7.25}$$

The attenuation constant is given by equation 7.26.

$$\alpha = \frac{1}{5.31*10^{-3}*\frac{\sqrt{\varepsilon'}}{\sigma}} \tag{7.26}$$

Obtained from the expressions of penetration depth d=1/α and the expression simplified expression for mediums where μ=1 as soil [390], expressed as $d = 5.31 * 10 - 3(\sqrt{\varepsilon'}/\sigma)$. The real part of the permittivity for a sandy soil ε' is 6.53 (TDR), the imaginary part of the permittivity ε'' is 1.88 (TDR) and the conductivity σ is 2.32 (mS/m).

The results of the model for a depth of 10 cm are presented in Figure 7.33. As it can be seen, the results are very similar to the real measures obtaining a determination coefficient r^2 of 0.8256. The results of the model for a depth of 20 cm are presented in Figure 7.34. The r^2 for this depth is 0.8259. Figure 7.35 presents the results of the model for the depth of 30 cm. The obtained determination coefficient r^2 for this depth is 0.6084. Lastly, the results of the model for the depth of 40 cm are presented in Figure 7.36. The r^2 of this depth is 0.0158. This is the depth where the model is the least approximated, however, it is still useful for an estimation. The heterogeneity of the soil and possible stones or other materials that change the dielectric characteristics of the soil may introduce further losses that do not affect the other depths.

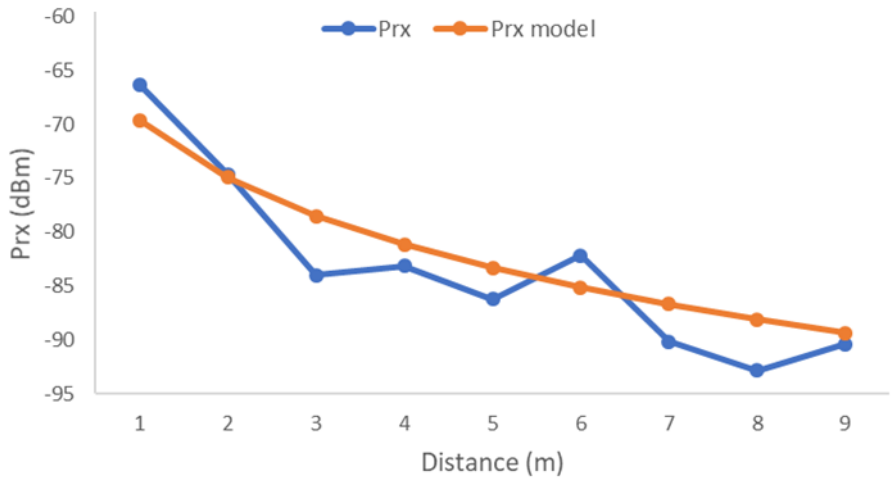

Figure 7.33. Results for the model at a depth of 10 cm.

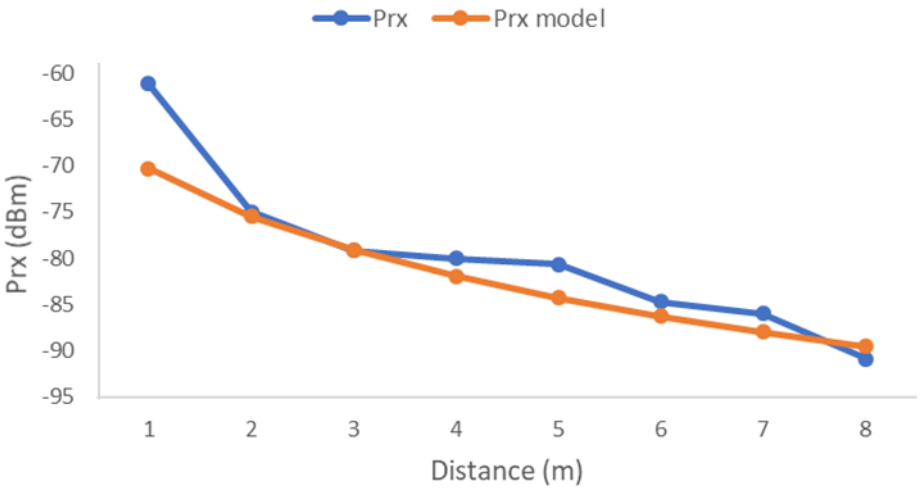

Figure 7.34. Results for the model at a depth of 20 cm.

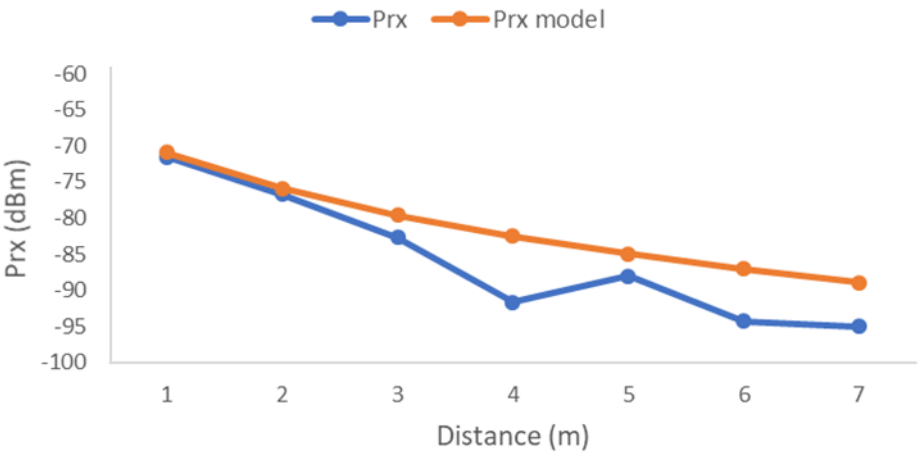

Figure 7.35. Results for the model at a depth of 30 cm.

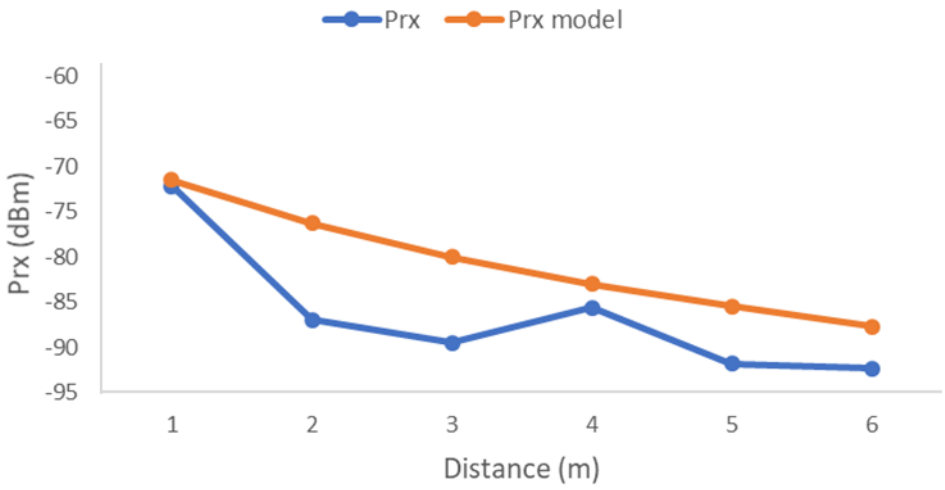

Figure 7.36. Results for the model at a depth of 40 cm.

7.3.2.3 Coverage results for all heights

In this section, the results from the coverage experiments performed between an underground node and an above-ground AP at different depths and heights are presented.

The RSSI values for each depth and each AP height are presented in the following figures. The measures at each height and length were taken five times and the average was calculated for each case.

Figure 7.37 presents the RSSI obtained from the node buried at 10 cm of depth. As it can be seen, the signal was able to reach 10 meters of length the node getting disconnected from the AP. The good quality RSSI signal values reach a length of 2 meters for a height of 1.5 meters. This height is also the best for the range between -70 and -80 dBm. Furthermore, there is a noticeable difference between the quality of the signal below and above the height of 1 meter. For the heights below 1 m, acceptable signal quality only reaches the 2-meter mark. However, for heights above 1 meter, it reaches up to 7 meters of length. For the RSSI values between -80 and -90, the maximum distance is up to 7 meters for heights below 1 meter and up to 9 meters for height above 1 meter.

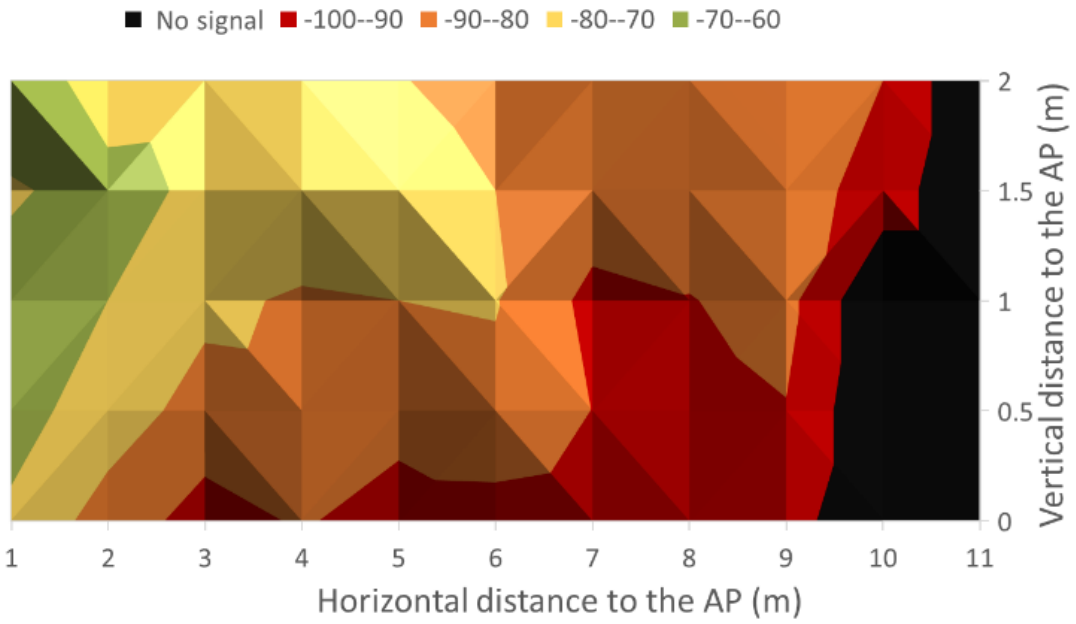

Figure 7.37. RSSI at 10 cm of depth.

The RSSI obtained from the node buried at 20 cm of depth is presented in Figure 7.38. In this case, there is a similar pattern to that of the node buried at a depth of 10 cm. However, the signal reaches 9 meters of length before getting disconnected. 1 meter less than in the case of the node buried at 10 cm of depth. However, it is important to remark that acceptable RSSI values reached up to 8 meters, 2 meters more than the node situated above. Good signal quality values reached a similar distance. Lastly, the signal reached RSSI values between -80 and -90 dBm further than in the previous case for the AP located at heights below 1 meter.

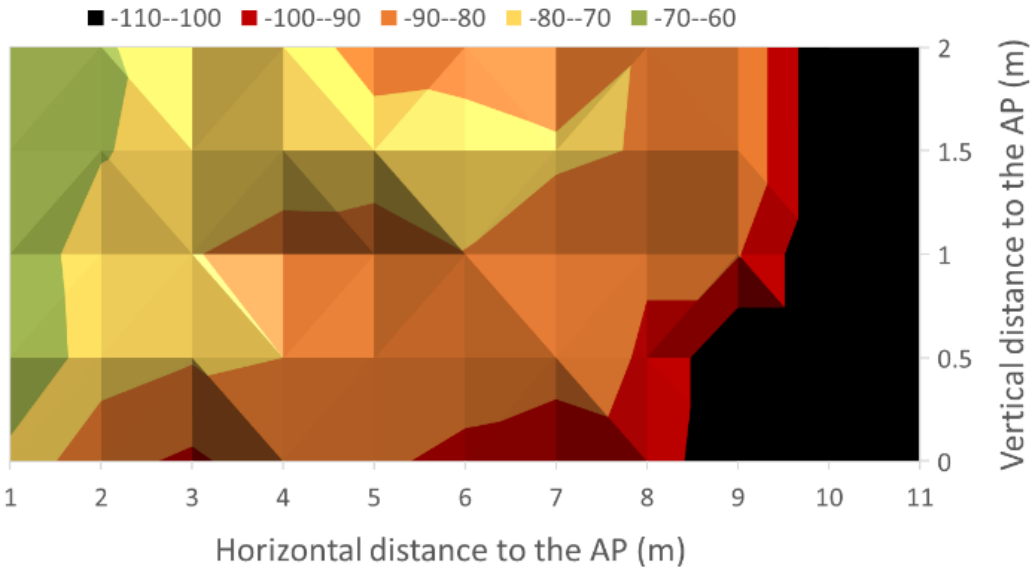

Figure 7.38. RSSI at 20 cm of depth.

Figure 7.39 presents the RSSI obtained from the node buried at 30 cm of depth. The reduction of the quality of the signal is evident with the node buried at this depth. No good-quality signal values were obtained. The signal was able to reach up to 7 meters of length before disconnecting. Furthermore, the signal was considerably better for heights above 1 meter, with acceptable RSSI values up to 6 meters of length.

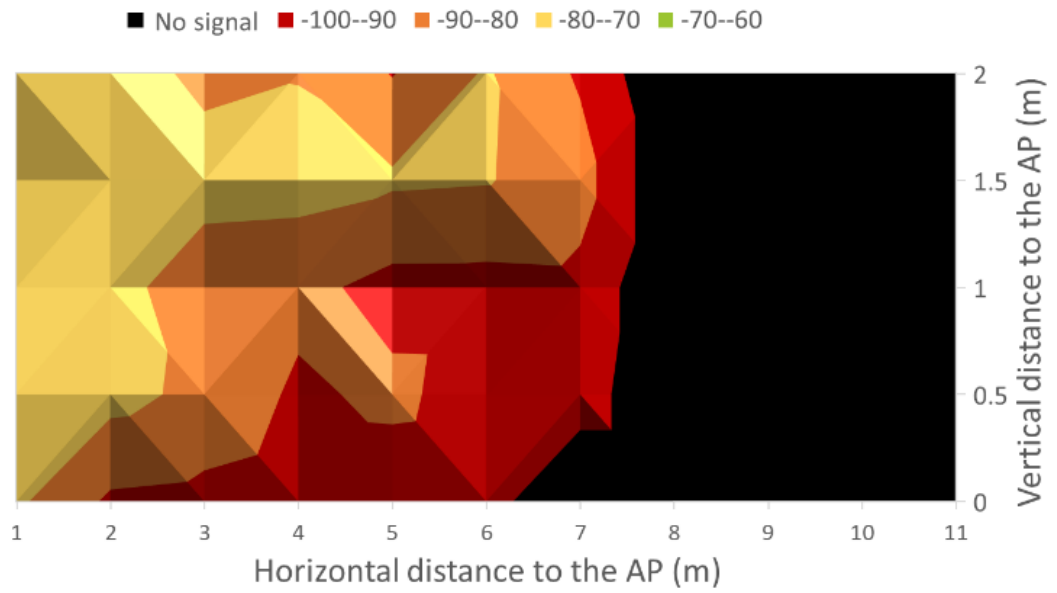

Figure 7.39. RSSI at 30 cm of depth.

Lastly, Figure 7.40 presents the RSSI obtained from the node buried at 40 cm of depth. Similar to the node located at 30 cm of depth, the signal was able to reach 7 meters before getting disconnected. However, acceptable RSSI values only reached the 3-meter mark.

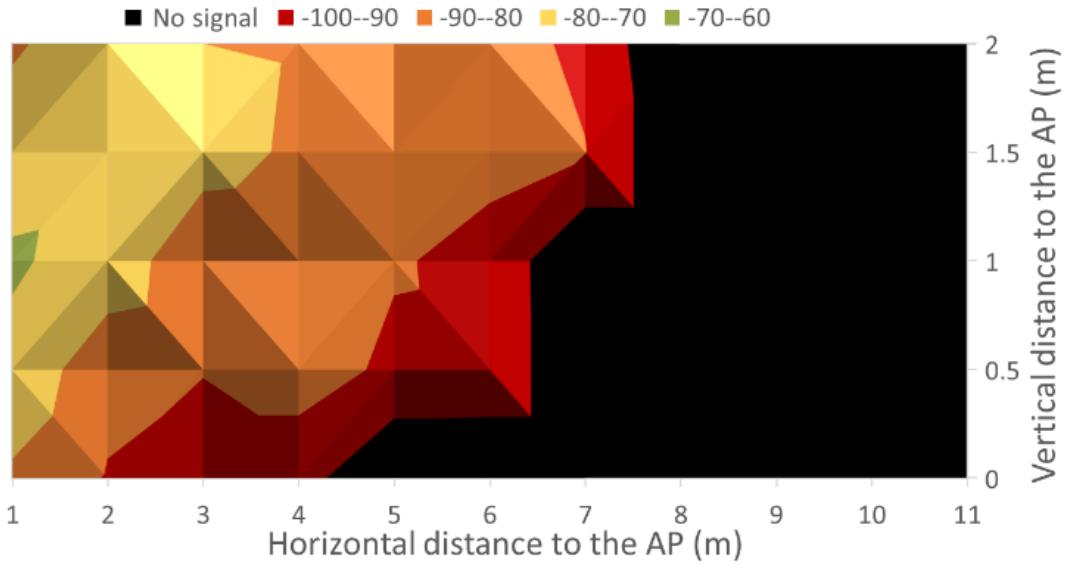

Figure 7.40. RSSI at 40 cm of depth.

7.3.3 Coverage results for LoRa low-cost nodes

In this subsection, the coverage results for the tests performed with low-cost LoRa nodes and antennas are presented.

The coverage tests performed with LoRa nodes were done using the Heltec LoRa WiFi 32 [50] nodes. For the antennas, different low-cost antennas for the 433 MHz and 868 MHz frequency bands were utilized (See Figure 7.41). The characteristics of the antennas are presented in Table 7.1. The tests were performed in the location shown in Figure 7.42, which is a wide and long street with fields at one side and buildings on the other side. The nodes were placed in a line-of-sight manner where the emitter remained static, and the receiver moved to the different measuring points. The RSSI was measured at each measuring point.

Figure 7.41. Utilized antennas for a) 433 MHz and 3 dBi gain, b) 433 MHz with 5 dBi gain and c) 868 MHz with 3 dBi gain.

Table 7.1. Characteristics of the antennas.

	Antenna 1	**Antenna 2**	**Antenna 3**
Frequency band	433 MHz	433 MHz	868 MHz
Gain	3 dBi	5 dBi	3 dBi
Voltage Standing Wave Ratio	≤ 1.5	≤ 1.5	≤ 1.5
Input impedance	50 Ω	50 Ω	50 Ω
Maximum input power	10 W	50 W	10 W

The results for the 433 MHz frequency band are presented in Figures 7.43 and 7.44. For the antenna with a 3 dBi gain, the best signal quality is obtained with the Spreading Factor of 7 (See Figure 7.43 a). The next SF configuration with the best signal quality is SF 10 (See Figure 7.43 d). The worst case is that of SF 11 (See Figure 7.43 e). In this case, as there is a great difference between the quality of the signal obtained with SF 7 and the rest of the SF configurations, the selection of the best SF for a transmission with these low-cost devices should be considered.

Figure 7.42. Location of the tests.

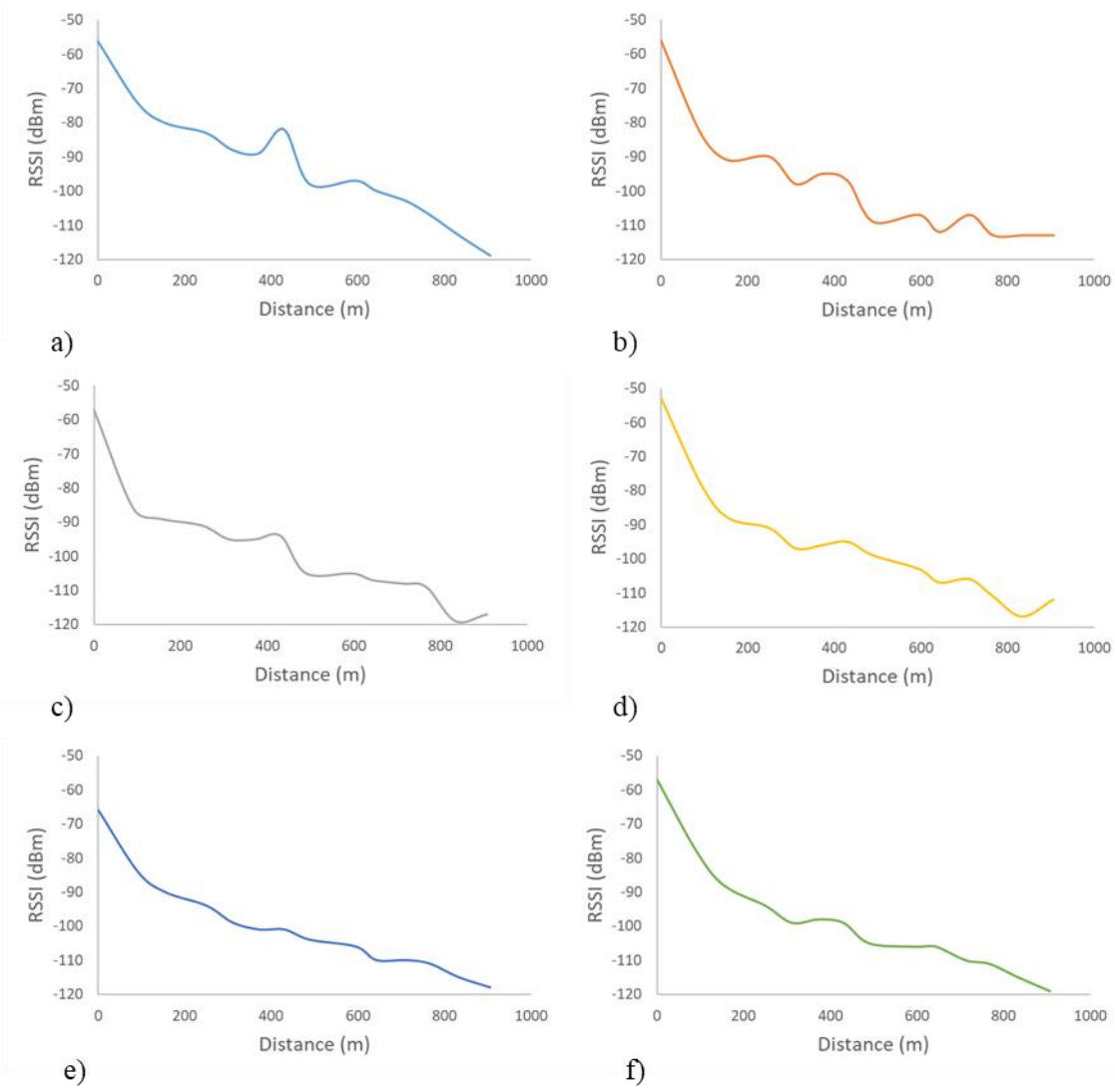

Figure 7.43. RSSI values for 433 MHz nodes with antenna of 3 dBi for a) SF 7, b) SF 8, c) SF 9, d) SF 10, e) SF 11 and f) SF 12.

Figure 7.44 shows the results for the antenna with a gain of 5 dBi. In this case, the SF 7 and SF 10 configurations have the best signal quality as well (See Figure 7.44 a and d). However, the RSSI values obtained with this antenna are not as differentiated as in the previous case. Therefore, with the use of this combination of node and antenna, other aspects should be considered to select the best LoRa parameters. The SF configurations with the lowest RSSI values are the SF 11 and SF 12 (See Figure 7.44 e and f).

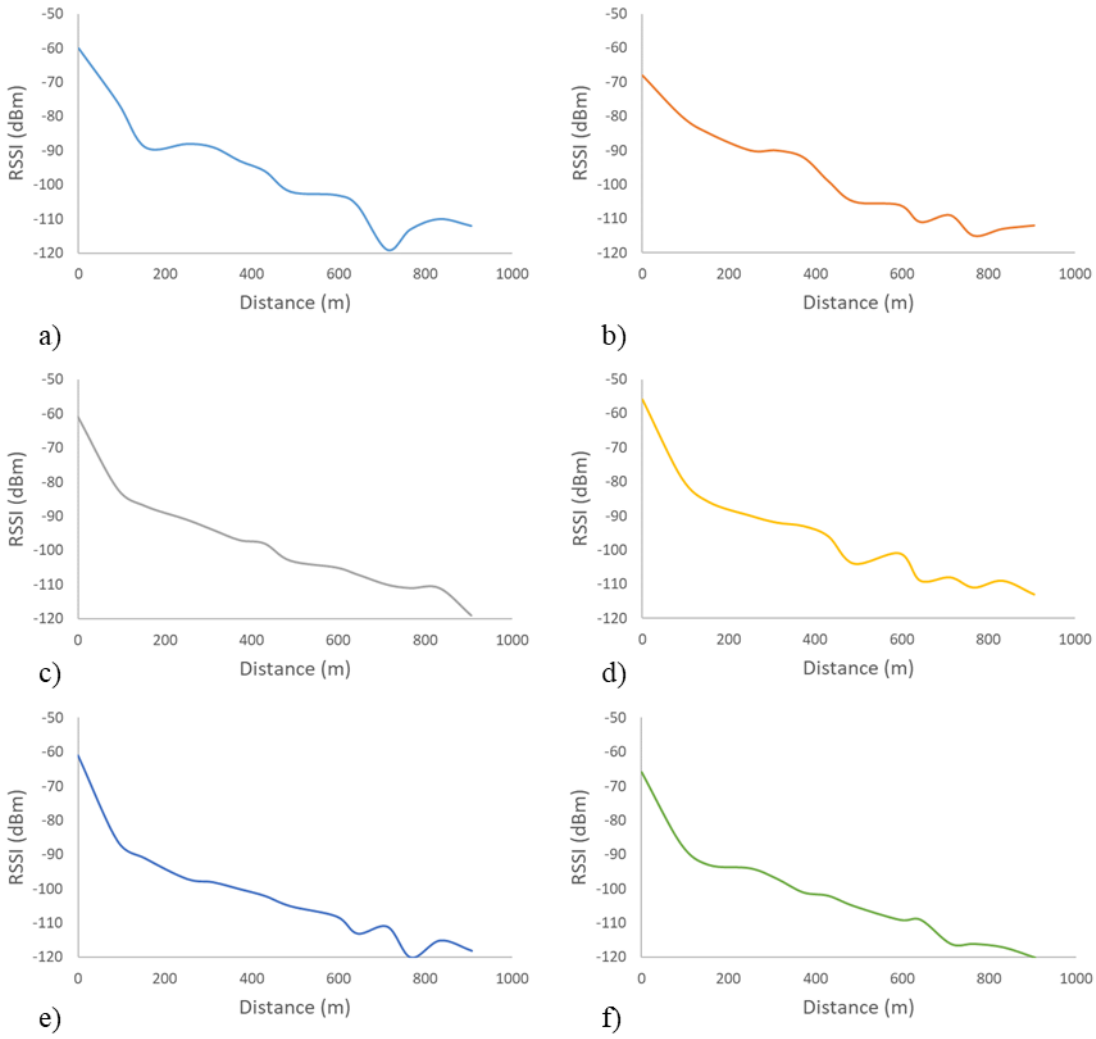

Figure 7.44. RSSI values for 433 MHz nodes with antenna of 5 dBi for a) SF 7, b) SF 8, c) SF 9, d) SF 10, e) SF 11 and f) SF 12.

Finally, the results for the 868 MHz frequency band are presented in Figure 7.45. These tests were performed with an antenna that had a gain of 3 dBi. In this case, Sf 7 had the best signal quality as well (See Figure 7.45 a). The configuration with the worst signal quality was SF 11 (See Figure 7.45 e). As in the previous case, other aspects should be considered when selecting the best parameters for LoRa transmissions as the RSSI values for all the SF configurations are similar.

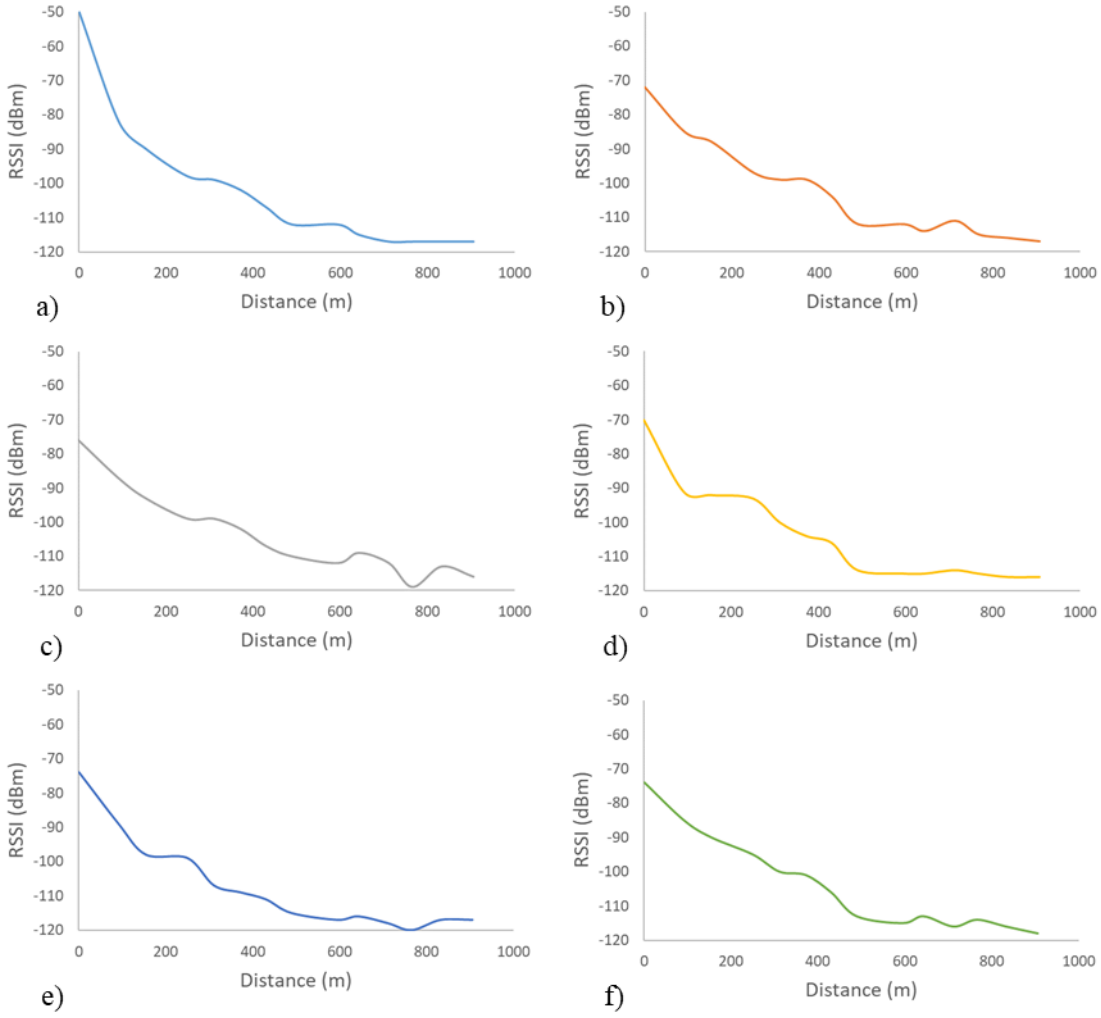

Figure 7.45. RSSI values for 868 MHz nodes with antenna of 3 dBi for a) SF 7, b) SF 8, c) SF 9, d) SF 10, e) SF 11 and f) SF 12.

Among the three studied cases, the node transmitting at 433 MHz and the antenna of 3 dBi had the best performance on average. The worst performance was that of the 868 MHz frequency band. Furthermore, all nodes reached the lowest RSSI values possible before the 1 km mark. Therefore, nodes with better quality or topologies such as multi-hop LoRa networks should be utilized to reach greater distances.

7.4 Energy consumption comparison between WiFi and LoRa

In this section, the energy consumption of transmitting with WiFi and LoRa utilizing affordable nodes is going to be presented.

In order to perform the tests on energy consumption, we utilized the Heltec WiFi LoRa 32 node which is presented in Figure 7.46. It is able to transmit with both WiFi and LoRa. This node has an ESP32 microprocessor and a LoRa SX1278 node chip. It

has an SH1.25-2 battery interface onboard as well and an integrated management system for lithium batteries so as to manage charge and discharge, switch automatically between USB and battery power, protect against overcharge and detect battery power. It also has an integrated OLED display, a CP2102 USB to serial port chip, and supports the Arduino IDE (Integrated Development Environment). It is comprised of 29 general GPIO ports. It has 3 UART (Universal Asynchronous Receiver-Transmitter) ports, 2, SPI ports, 2 I2C (Inter-Integrated Circuit) ports, and one I2S port. It also has a 4 MB flash memory. Table 7.2 shows the energy consumption provided by the manufacturer [50].

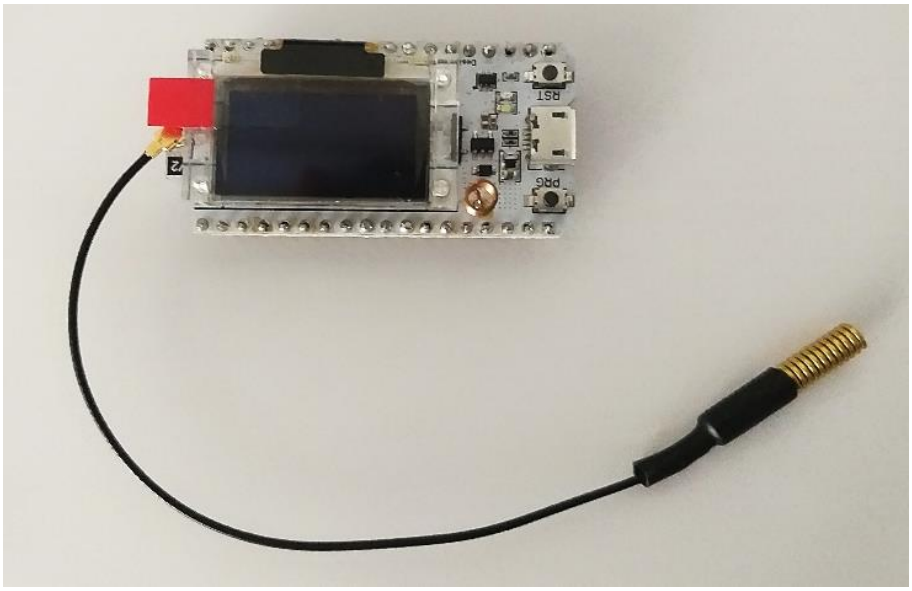

Figure 7.46. Utilized Heltec WiFi LoRa 32 node.

Table 7.2. Energy consumption of the node.

Mode	**Energy consumption**
LoRa 10 dB tx power	50 mA
LoRa 12 dB tx power	60 mA
LoRa 15 dB tx power	110 mA
LoRa 20 dB tx power	130 mA
WiFi AP mode	135 mA
WiFi scan mode	115 mA

In order to perform the tests, the Heltec WiFi LoRa 32 v2 was programmed using the Arduino IDE. The WiFi.h and LoRa.h libraries were utilized to establish the connection between the two Heltec WiFi LoRa 32 v2 nodes. The default settings were utilized for

both WiFi and LoRa. Table 7.3 shows the default settings for LoRa. The forwarded data was the same for both WiFi and LoRa transmissions and it had a length of 80 bytes.

Table 7.3. Default settings of LoRa.

Tx Power	17 dB
Frequency	433 MHz
SF	7
Signal Bandwidth	125 KHz
Coding rate	4/5
Preamble length	8 Symbols

Tests were performed forwarding a packet with a 5-second interval and a 30-second interval. The utilized battery was a 4955 power bank with a capacity of 2000 mAh and an output of 5V DC and 1000 mAh.

The tests on the energy consumption of WiFi were performed for the two selected transmission time intervals. Figure 7.47 shows the average battery life for each transmission interval. As it can be seen, a difference of 1 hour was obtained between transmitting with each time interval. For the time interval of 5 seconds, the obtained battery life was 10 hours and 10 minutes whereas 11 hours and 14 minutes of battery life was obtained for the 30 seconds time interval. Therefore, the transmission interval can severely affect the energy consumption of the devices that utilize WiFi for their communication.

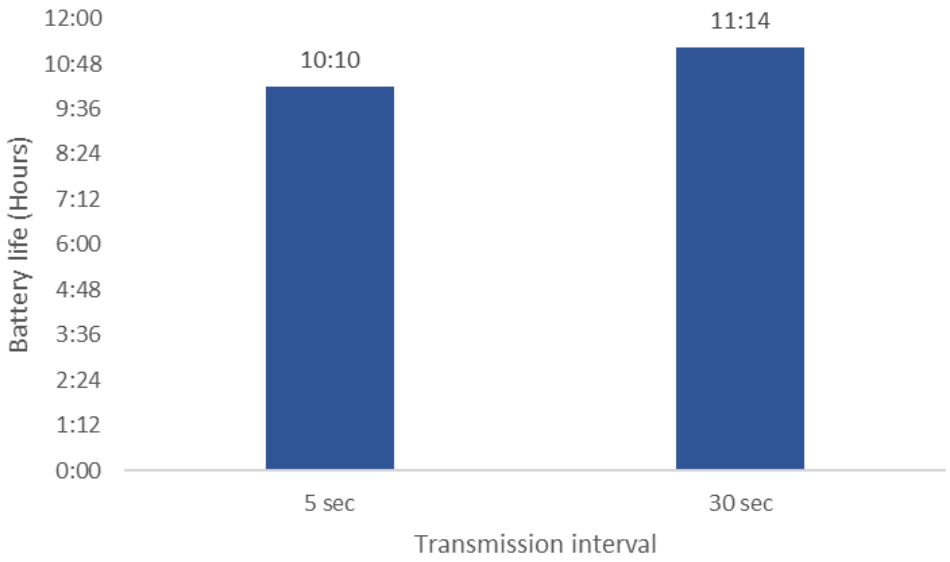

Figure 7.47. Battery life with WiFi communication.

The tests performed with LoRa considered 5 seconds and 30 seconds time intervals as well. However, no significant differences were obtained between both transmission intervals. In fact, the average battery life for the 30 seconds transmission interval was 26 minutes less than that of the 5 seconds transmission interval. As it can be seen in Figure 7.48, the lifetime of the battery was approximately 10 hours.

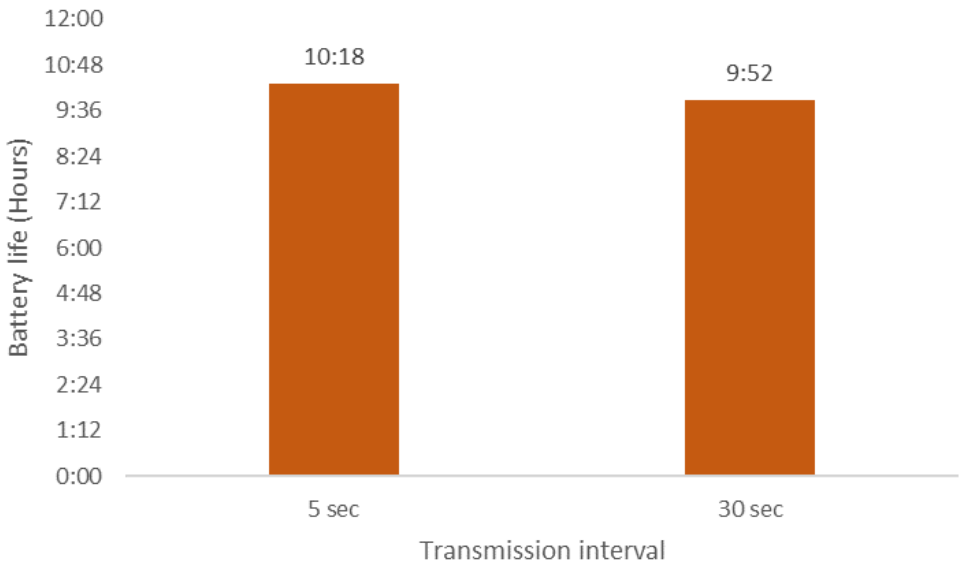

Figure 7.48. Battery life with LoRa communication.

As the manufacturer stated, the power consumption for both WiFi and LoRa transmissions is practically the same with transmission powers of 17 dBm or 18 dBm. It is surprising as LoRa is branded as a low-power consumption communication protocol. Therefore, the transmission power of LoRa has to be decreased so as to improve its battery consumption, which leads to less coverage.

To assess if the battery life was increased when transmitting with less transmission power, another test was performed changing the tx power of the LoRa transmissions to 10 dBm. The time interval for this test was 30 seconds. The average battery life for this case is presented in Figure 7.49. As it can be seen, the battery life improved compared to that with a transmission power of 17 dB, obtaining more than one hour more of battery life. Furthermore, the battery life surpassed that of WiFi with a transmission interval of 30 seconds in 20 minutes. The difference would be then more noticeable when utilizing batteries with more capacity. However, the overall difference between the power consumed by both technologies is not that great. Therefore, other factors, such as the range that can be reached with each technology or the data rate may be the factors to be considered when selecting the wireless technology to be utilized in an IoT system.

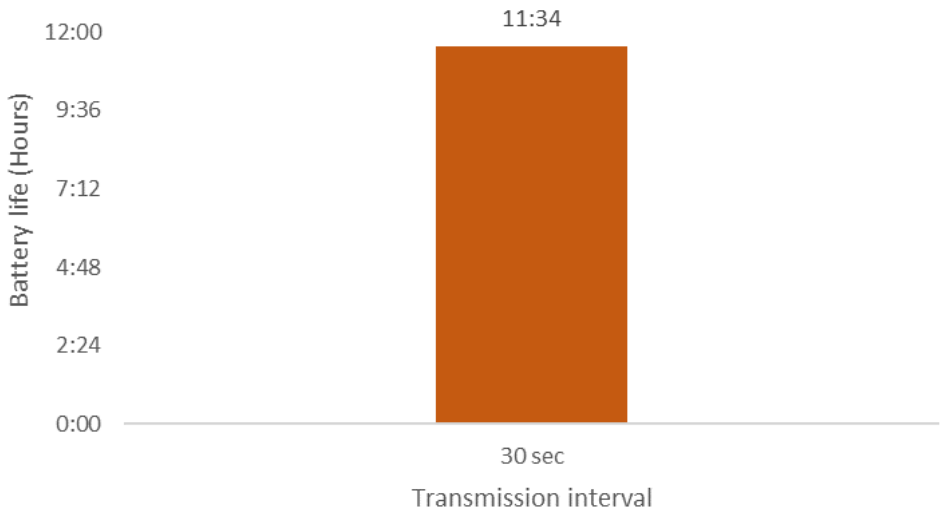

Figure 7.49. Battery life with LoRa communication and 10 dBm of tx power.

7.5 Quantification of fruit production through image processing

In this section, the description of a system for fruit production quantification is presented. Furthermore, we show the obtained pictures and the processing techniques used to quantify the fruit production. First, the combination of bands to find the best composition for fruit detection is presented. Following the correction of the effect of distance is described. Finally, we show the correlation between the number of pixels and production.

As this is a preliminary test, to minimize the use of resources, the pictures will be taken in the horizontal plane using a camera. In the future, the pictures will be taken in the vertical plane with a drone. To carry out our proposal it has been necessary to use a "curtain" of an opaque material. It allows us to hide the trees behind the tree to be studied. Furthermore, a mobile device has been used from which the images are obtained, which will then be treated.

As we take pictures in different fields and the distances between trees might are not always the same, the distance between the camera and the trees is not constant in all the cases. To solve this problem, we propose to use a reference object. Using this reference object, we will be able to correct the distance effect, which may appear when acquiring the images. Figure 7.50 shows how a tree image is captured.

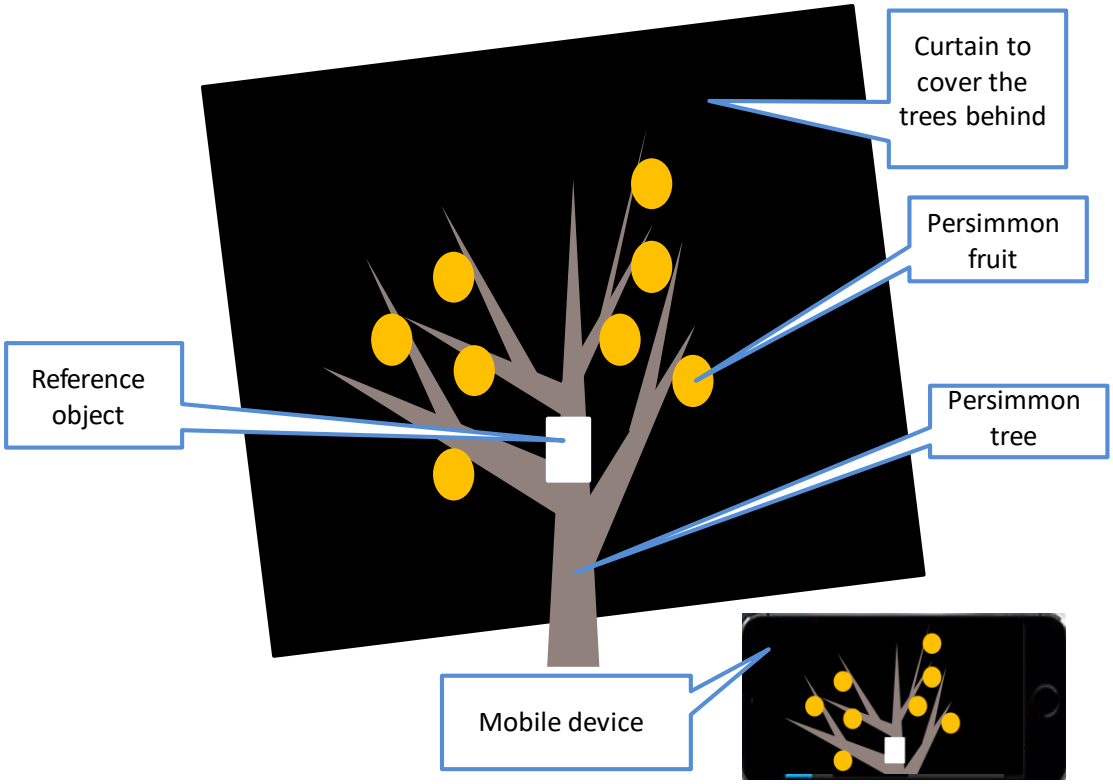

Figure 7.50. Scenario description.

Our experiment is based on the fact that these fruit trees, when the fruit is collected, have lost their leaves. Due to this phenomenon, it is possible to recognize and differentiate the fruits from the rest of the objects that may appear in the images. Therefore, the possible effects of overlapping structures are minimized. The branches are the sole overlapping structure and, since they are thinner than the fruits, their possible influence in the prediction model can be despised. Moreover, as the trees are similar in shape and height, the possible underestimation is a constant value. Therefore, it will not affect our prediction model.

Once the images were obtained, they have been processed. Decomposing them in the basic colors R, G, and B layers (or rasters). The RGB images are to be combined using mathematical operations to obtain new rasters. Then, the histograms of these new rasters are obtained. In this way, it will be possible to detect the region of the histogram that represents the fruit and does not represent the soil.

Subsequently, the histogram is normalized by the surface of the reference object. Finally, the histograms of the difference images are compared with the real kilograms of fruit that were harvested from the tree. A regression model is used to relate the histogram and fruit production.

The data obtained can be used by the farmer as a tool, because he can estimate the harvest he is going to obtain. In addition, this system allows the irrigation to be adjusted according to the observations made.

7.5.1 Evaluation of best band combination

The first step is to evaluate which band or bands of the image can be used for fruit detection. The coloration of Persimmon in the moment of yield is between orange and red, therefore we expect to find high pixel-values in the band of red, intermediate values in the green band, and low values in the blue band. In Figure 7.51, the RGB composition and the representation of single bands are presented. The representation of a single band is shown as a color ramp from black (when the pixel value is low) to white (when the pixel value is high). As expected, the fruits have been clearly identified in the red band. Nonetheless, the color of clouds and soil is similar to the color of fruits. The spectral signature is a well-known term, used in remote sensing, which is used to identify different surfaces by comparing the data of two or more bands. It has been used to identify fruits [391].

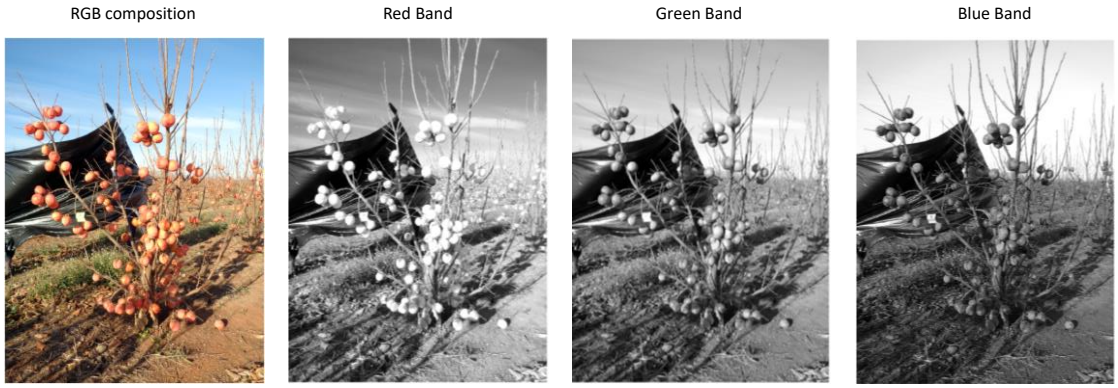

Figure 7.51. System description.

Therefore, it is necessary to combine the red band with a second band (green or blue). In order to evaluate which is the best band composition, it is necessary to represent and compare the different options. In this paper, and with the purpose of maintaining the system operation as simple as possible, we are going to evaluate the combination of only two bands and using the mathematical operators of addition, subtraction, multiplication, and division.

Figure 7.52 summarizes the different combinations of R and G or B bands in greyscale. The fruits can be distinguished in five out of ten combinations. From those combinations where fruits can be distinguished, in two of them the differences between fruits and soil are higher (R - B and R - G). The highest difference between the value of fruit pixels and soil pixels is observed in the R - G combination. Moreover, in Figure 7.52, we can observe the effect of the curtain, and how the curtain is more effective in some band combinations (R+G or R-G) than in others (R/G or G/R).

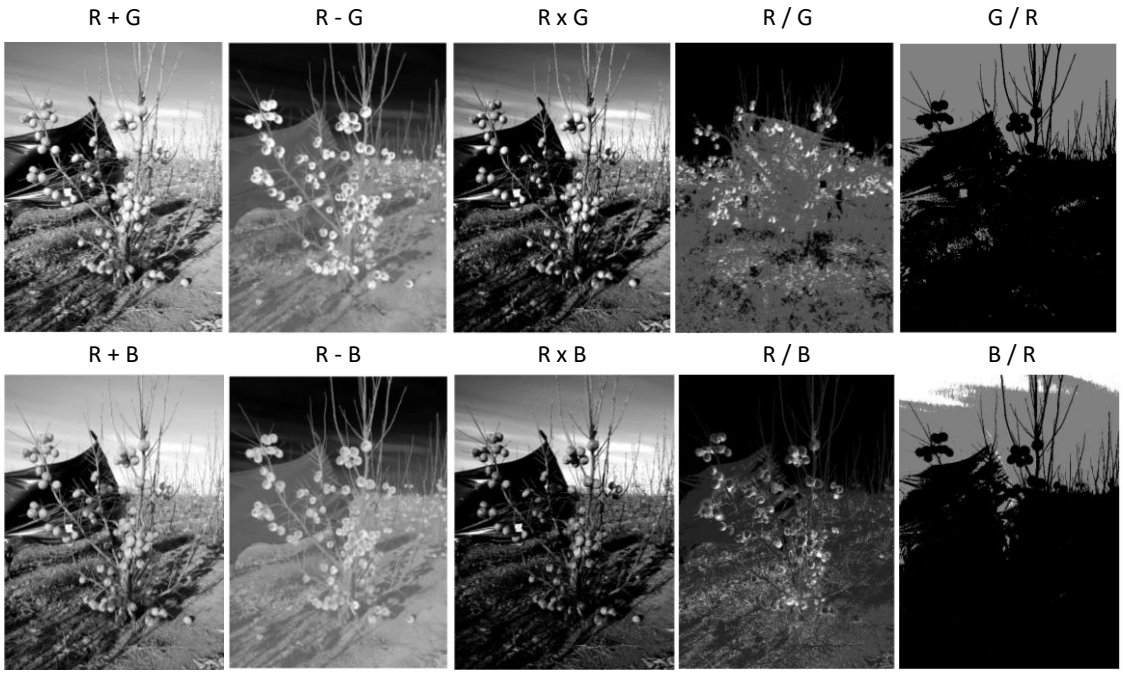

Figure 7.52. Combination for R band with G or B band to maximize the fruit detection.

7.5.2 Correction of the distance effect

Following, it is necessary to consider the effect of distance from the camera to the tree. Since our units of surface are the pixel and the distance from the camera to the object affects the relation of surface in the picture (pixel^2) to surface in reality (cm^2), the effect of different distances must be included in our method. During the picture collection, a reference was included in all the pictures. The reference was attached to the trunk of the tree.

Then, the surface of the reference object in pixels is calculated. The size of the reference in each picture is shown in Table 7.4. The value in pixels of the reference object will be used to normalize the values of the histogram. Other relevant data for future subsections, such as code of crop field and fruit weight are included. The field number is used as picture ID and the weight is used for the correlation of histograms and fruit production.

Table 7.4. Reference object in the used pictures.

Image nº	**1**	**2**	**3**	**4**	**5**
Reference surface (pixels^2)	17192	6299	8771	6299	8273
Field number	2446	2696	3230	1535	1541
Fruit weight (kg)	37	35	20	47	43

7.5.3 Analysis of histogram data

The next step is to obtain the histogram of the picture, it can be done using different options. In our case, we use the code described in [273] to obtain the data of the histogram using Matlab. Then the obtained histogram is represented, see Figure 7.53. In this graphic, the comparison of different histograms can be observed. The histogram represents the number of pixels in the image that have a certain value. In the original raster (RGB rasters) the value of pixels is between 0 and 255. Besides, in the newly generated raster, the pixels can have values from -255 to 255. In Figure 7.54, the different pictures are numbered according to the fruit weight in kg. Before analyzing the differences in the histograms of different pictures, it is necessary to normalize the data. Therefore, we are going to consider the surface of the reference object as 1UA (1 unit of area). Thus, the results of the histograms can be comparable even if the pictures have different sizes and are taken at different distances. The corrected histograms are presented in Figure 7.54. It is possible to see that the histogram shape has changed. In Figures 7.53 and 7.54, the different pixel values represent different surfaces. In our case, the persimmon, according to Figure 7.52, will be represented by the highest values. Therefore, the last part of the histograms is where the data about the fruit is contained.

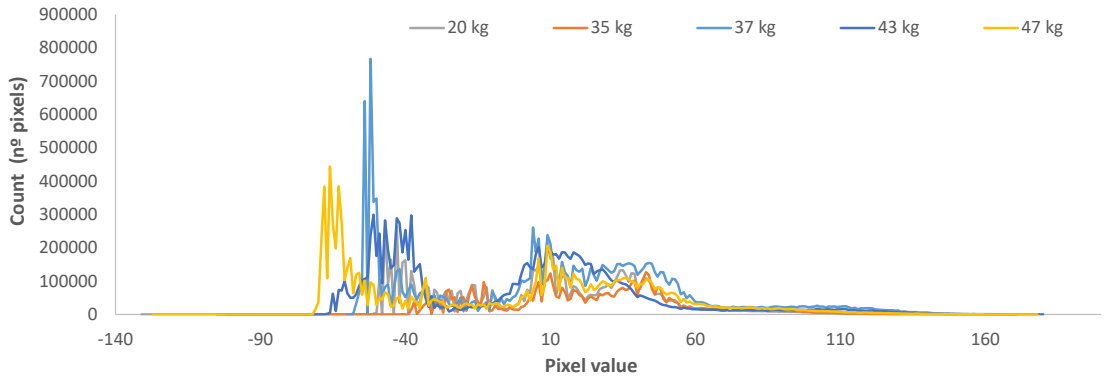

Figure 7.53. Histogram of studied images

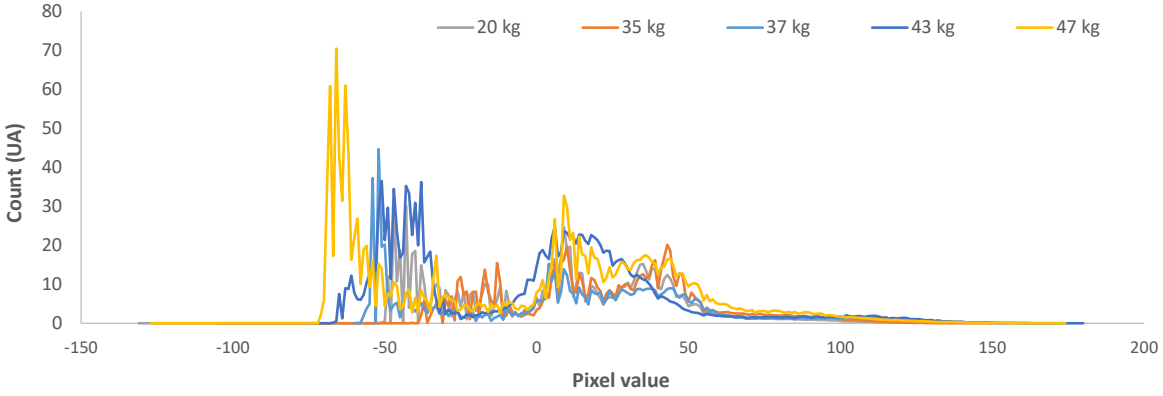

Figure 7.54. Corrected histogram of studied images considering the effect of distance.

As different parts of the fruit might have different colorations, which correspond to different pixel values, several pixel-values will be used in the correlation. First of all, we check the values of pixels in the generated rasters. The observed values of pixels in persimmon fruits go from 72to 171. The representation of histograms in this range is displayed in Figure 7.54. In this graphic, the images of trees with more fruits have higher values in the Count (UA). The distributions of values along the range (72 to 171) are related to the fruit coloration. In images 4 (47 kg), 2, (35 kg), and 3 (20 kg) the peak of pixels associated with fruit is found around 73 to 75 pixel-value. Meanwhile, in other images, this peak is found at 102 pixel-value. This is caused by differences in fruit maturity or fruit quality. The fruits of the images with a peak located at the highest pixel-value have a better coloration (uniform red color).

Finally, the correlation between the summation of pixels with pixel values between 72 and 171 and fruit production is presented in Figure 7.55. The mathematical model can be expressed as shown in equation (7.27). The correlation coefficient of the mathematical model is 0.97. The correlation coefficient offers information about the goodness of the correlation. It can take a value between 0 and 1, the closer to 1 the better the model.

$$\frac{\sum_{72}^{171} Counts\ (UA) - 19.44}{2.61} = Fruit\ weight\ (kg) \tag{7.27}$$

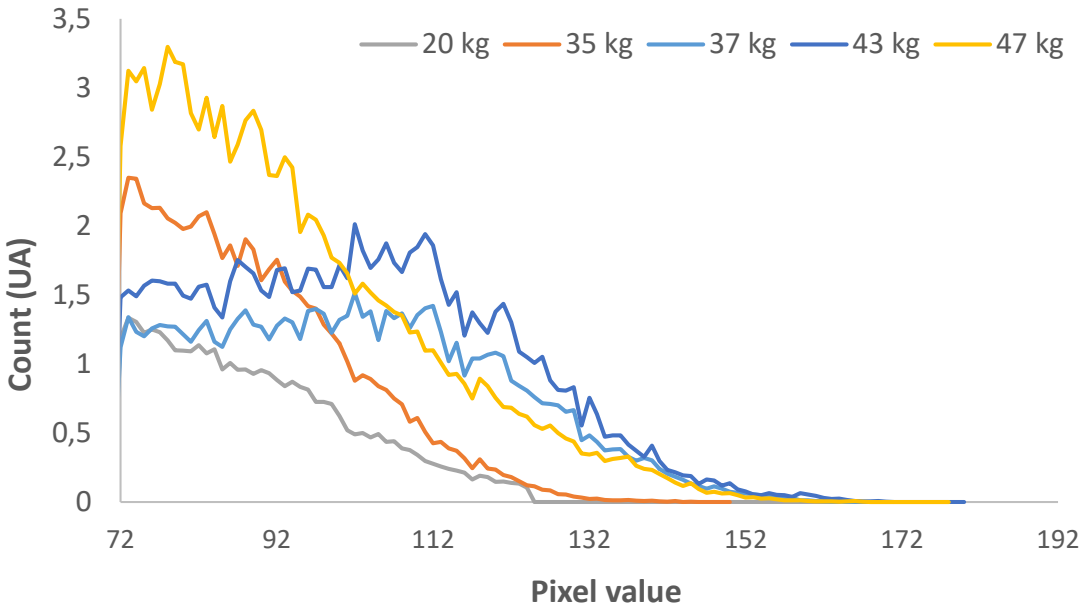

Figure 7.55. Detail of the corrected histograms.

7.6 Conclusion

In this chapter, tests have been performed in a real environment with WiFi and LoRa nodes to determine the performance of the proposed protocol. The consumed bandwidth for both 433 MHz and 868 MHz frequency bands remained within the limits for the most restrictive LoRa configurations. Therefore, the proposed protocol can be implemented considering all the deployment needs. Furthermore, high successful packet delivery rates were obtained utilizing packet transmission delays of 500 ms at the CH node.

The best location for the above-ground and underground nodes has been determined as well [45, 340, 365]. On-ground deployments had the least coverage even with vegetation where the bulk of the foliage is at higher heights. On the other hand, near-ground deployments provide the best coverage with orange trees. However, on-ground and near-ground deployment strategies in orange fields presented high variability of signal quality even with no obstacles in the line of sight between emitter and receiver. As opposed to higher emitter heights that presented a more attenuated but stable signal quality. Regarding the underground nodes, the results showed the optimal depth is 20 cm and the optimal height was 1.5 m. The connection was available up to distances of 10m. Furthermore, for the LoRa low-cost nodes and antennas, the maximum RSSI values were obtained before reaching 1 km.

The energy consumption for WiFi and LoRa transmissions was evaluated utilizing the Heltec WiFi LoRa 32 device [392]. Similar results have been obtained for both LoRa and WiFi with the default settings and 5 seconds of transmission interval. However, WiFi outperformed LoRa with a 30 second transmission interval. A similar battery life was obtained when lowering LoRa transmission power to 10 dBm.

Lastly, images of fruit trees have been utilized to determine the amount of fruit to be harvested in kg [393]. These images include a reference object to counter the effect of the distance. Normalized histograms were performed to analyze the pictures and obtain the correlation with the fruit production. For the persimmons, the red band was the best option to identify the fruits. However, it is necessary to combine the red band with a second band (green or blue), to differentiate the fruits to the color of the soil. The highest difference is observed in the R - G combination.

Chapter 8

Conclusion

8.1 Introduction

In this chapter, the conclusion on the work performed in this dissertation is presented. Then, the future lines of research are discussed. Finally, a list of the publications derived from the results presented in this thesis is provided.

8.2 Conclusion

Considering the objectives listed in Chapter 1, we can affirm that the main goals of this PhD thesis have been achieved.

The introduction of technology in agriculture allows increasing the quality of the crops, reducing resource consumption, and increasing the production. However, the remote location of the fields and its lack of access to the electric grid leads to a necessity of providing wireless solutions able to provide coverage to all the electronic devices deployed throughout the fields and irrigation canals. This work has provided a solution to this problem with the realization of the established objectives.

Firstly, an in-depth analysis on IoT and smart solutions for irrigation was performed. Over 280 papers were studied and classified to obtain an overview on the current trends of Precision Agriculture (PA) systems for irrigation. In this analysis, the main

parameters to be monitored regarding the quality and quantity of the irrigation water, the aspects of the soil and the plants, and the weather conditions that affect the calculation of the irrigation requirements and the determination of the state of the crops have been detailed. Then, the most utilized technologies for the deployment of wireless networks were presented. The most popular nodes and their characteristics have been provided, and the most utilized communication technologies and cloud platforms have been determined. Furthermore, the new trends and challenges regarding the deployment of wireless sensing nodes have been discussed.

The next objective aims at designing an architecture for a water quality monitoring system for the irrigation of crops. In order to design the architecture, the main areas to be monitored were identified in Chapter 3. One of the novelties of the proposal resides in the water treatment system that determines the water quality to decide if the biosorption process is needed. In some areas of the world, the water discharged into the water canals may be contaminated, this water treatment addition helps in improving the quality of the produce harvested from the fields. Once the need for this functionality has been established, the deployment design of the sensing nodes has been presented. Clusters of three sensing nodes have been proposed so as to avoid false positive and false negative results in contamination. This strategy has been proposed for the field area as well so as to obtain a better assessment of the moisture in the soil. The architecture considers the use of medium-range and long-range wireless technologies. The CH node is the bridge that incorporates transceivers for both the medium-range and the long-range wireless technology. This node then forwards the messages to the aggregator node, which is the node that forwards the messages to the gateway. The topology of the system has been presented as well. This topology is another novelty as allows establishing a heterogeneous network and presents a tree topology with multiple hops for the LoRa part of the network, in contrast to the usual point-to-point implementation of LoRa connections. For specific requirements, other deployment strategies and architectures have been presented. These specific requirements cover the need of monitoring numerous trees, the use of cellular communications at the gateway, underground sensor deployments with wireless communication, the use of drones for data acquisition, and the provision of security and management functionalities. After that, the proposed sensing nodes have been presented. The algorithms that indicate how the nodes operate have been presented as well. The algorithms determine how the data is gathered and if it is stored for later data transmissions. Moreover, the data can be analyzed on the node to determine if there were variations in the data and if it is necessary for the system to transmit it. This is important for variables that have slow variations such as the weather conditions. Lastly, an algorithm for the determination of the irrigation requirements of the crops has been provided.

After the requirements of the system have been determined, a heterogeneous communication protocol has been presented in Chapter 4. LoRa has been gaining popularity in the recent years as it is a good solution to provide connectivity to systems with low data transmission located in remote areas. However, in order to reduce the number of collisions, the nodes or the presented proposal that are deployed in proximity to each other use a medium-range wireless technology. It is therefore necessary to use nodes that act as a WiFi/LoRa bridge to provide between the WiFi nodes and the LoRa nodes. Considering the tree topology is comprised of devices that utilize multiple

wireless topologies according to the necessities of the area where the nodes are deployed, the developed communication protocol allows the communication of the nodes of the system with interoperability between WiFi and LoRa. The developed protocol has a reduced header of 2 Bytes which is considerably smaller than that of LoRaWAN. The configuration of all the fields in the header has been detailed and the varied messages and their payload have been defined. Several types of alarms are contemplated, as stated on the main objectives, and each of them has its own message. Furthermore, the message exchange among the elements of the network has been thoroughly explained. The implementation of the protocol has been performed in the C++ programming language and different libraries were created for each of the node types of the system.

Chapter 5 has provided varied solutions to specific needs of the proposed architecture and other possible solutions to different deployment strategies. As determined on the objectives, data aggregation algorithms have been presented to reduce the amount of data and messages that are forwarded by the nodes. The proposed topology has been updated in this chapter to add fog computing to the CH nodes and establish the aggregator nodes as edge nodes. Two algorithms have been presented, one for each of the aforementioned nodes which are situated in separated layers. Moreover, the scenario of deploying all LoRa nodes on the canal area has been contemplated as well. The main security threats of the system have been identified and the available solutions were listed. Energy-saving and fault tolerance algorithms have been provided as well. To expand on the available protocols, the use of CoAP for PA systems was introduced. The case of underground communication has been introduced as well and an algorithm that adjusts the transmission power according to the soil humidity readings has been proposed. Lastly, in this chapter, the problem of the use of drones for data acquisition was studied.

In order to meet the last objective, the results of the performance of the aforementioned proposals and the study cases that were presented have been discussed. In order to do so, simulations and practical experiments have been performed. Chapter 6 presents the results of the simulated experiments. Firstly, the results of the data aggregation algorithms are discussed. The adoption of different configurations of data acquisition allows up to 88% in data reduction and up to 85% in the reduction of the number of messages. Furthermore, a reduction in the data up to 69% and a reduction in the number of messages up to 29% at the data forwarding time was obtained compared to not performing data acquisition. Then, the results for the case of utilizing all LoRa nodes were presented. The results showed that it is possible to implement this deployment strategy, but the data transmission had to be performed twice a day in order to meet the data rate restrictions of the LoRa network. For the cases of deploying numerous WiFi nodes, the bandwidth consumption, energy consumption, and the collisions were studied. Lastly, the results for the use of remote sensing nodes for data acquisition show that the solution is difficult to achieve for high node densities, but it is possible for lower node densities utilizing several configurations of the drone flight settings if the fastest drone velocity is not employed.

Finally, the results performed in real environments have been presented in Chapter 7. Firstly, the validation of the proposed protocol is provided. The bandwidth consumption

and the successful delivery rate were presented for various configurations of frequency and forwarding delay at the CH node in a worst-case scenario. The results show that the proposed topology is applicable and the deployment of heterogeneous WiFi/LoRa networks with multiple LoRa hops is possible. Furthermore, the high successful delivery rate shows that the protocol is a good solution to implement the communication within the proposed architecture. In addition, the specifications of the protocol indicate how the lost packets can be recovered, ensuring all the data reaches the data center. After that, the coverage results of deploying WiFi nodes on vegetated and underground environments have been provided. The best location for the WiFi nodes regarding height, and depth for the underground nodes, has been obtained as well. Moreover, the coverage obtained for low-cost LoRa nodes and antennas was evaluated. Maximum RSSI values were obtained before reaching a distance of 1 km. A comparison of the energy consumption of the node LoRa/WiFi node transmitting with each of the technologies has shown that there is not a great difference. Therefore, the design for the energy-harvesting aspect of the nodes would not present many differences with the use of this type of node. Lastly, the results for a fruit quantification functionality where an image processing technique is used to determine the amount of produce in fruit trees have been provided.

The future lines of research that derive from the work presented in this dissertation are discussed in the following section.

8.3 Faced problems

In this section the problems that have arisen during the thesis are detailed. One of the problems regarded the difficulty in finding a simulator for heterogeneous networks with WiFi and LoRa devices. Furthermore, a device with both WiFi and LoRa transceivers that were able to transmit with both wireless technologies at the same time was necessary. Moreover, the variety in node types required multiple implementations of the protocol that addressed the specific aspects of each node.

As the proposed protocol is needed for a heterogeneous network, there were not simulators available to address the peculiarities of the studied scenario. Therefore, the option of developing the protocol directly for embedded boards was chosen. My stay at Korea University helped me in gaining the knowledge to implement the protocol through the work done with CoAP.

Furthermore, a device able to transmit utilizing LoRa and WiFi at the same time was necessary. After a research on the available embedded systems, a preliminary test was performed with the Heltec devices to corroborate that they were apt for the needed purpose.

Lastly, as each device type has different functions, a different library had to be created for each one of the devices. Each one was tested independently using the devices for each phase of the development of the protocol. Multiple problems arose

during the implementation of the protocol. The problems were isolated and addressed until the complete protocol was successfully implemented.

8.4 Personal contributions

During the progress in this work, I have gained a new perspective regarding how to tackle the problems that arise and how to deal with the frustrations that leading with these problems generate. I have also gained confidence in myself and my ability to design and implement protocols, which will be valuable for my future work. Lastly, I have also grown as a person through the experiences I have lived during these last years, including the time of the pandemic. The lessons I have learned will help me not only in my career but also during my lifetime.

8.5 Future research lines

There are several research lines for continuing the work presented in this dissertation.

The topology for the heterogeneous wireless network presented in this work only incorporates two wireless technologies. As a future research line, more types of technologies such as ZigBee or BLE could be added to the system in order to provide new functionalities. Furthermore, the proposed communication protocol could be extended to support these newly added technologies.

The proposed architecture includes sensing nodes and actuators. However, more elements can be added to the architecture. For example, the vehicles and machinery that are utilized on the fields could be provided of sensors to perform some monitoring actions or to act as a tracker for remote monitoring of its activity. These vehicles could also be utilized as a gateway that obtains the information from the nodes deployed on the fields. Furthermore, other devices such as cameras could be introducing to provide images that can be analyzed to detect the evolution of the crops or the presence of pests and crop diseases. Therefore, the transmission of multimedia content should be considered as well as the Quality of Service and Quality of Experience metrics.

By introducing a tree topology for a LoRa network, multiple LoRa devices need to communicate. Creating a routing protocol for multi-layer LoRa networks would allow providing more scalability to our proposal. Furthermore, it would open new possibilities for LoRa networks that could be extended to other purposes. It could be applied to monitor other remote areas such as forests or infrastructures deployed on the ocean by relaying the information through the LoRa nodes strategically deployed at the edge of the coverage area of the next hop in the network.

Lastly, the studies on IoUT are still very scarce. In this dissertation, the coverage for WiFi communications was tested. For future works, the performance of other wireless technologies such as LoRa and ZigBee for IoUT applications could be studied to

expand on the knowledge of the performance of these technologies in underground environments.

8.6 Publications derived from the PhD Thesis

The journal publications derived from the work that has been presented in this dissertation are the following ones:

Laura García, Lorena Parra, Jose Miguel Jimenez, Mar Parra, Jaime Lloret, Pedro Vicente Mauri and Pascal Lorenz, "Deployment Strategies of Soil Monitoring WSN for Precision Agriculture Irrigation Scheduling in Rural Areas", Sensors, Vol. 21, No. 5, pp. 1693, 2021, doi: https://doi.org/10.3390/s21051693. **Impact factor: 3.275, Q2**.

Laura García, Lorena Parra, Jose Miguel Jimenez, Jaime Lloret, Pedro Vicente Mauri and Pascal Lorenz, "DronAway: A Proposal on the Use of Remote Sensing Drones as Mobile Gateway for WSN in Precision Agriculture", Applied Sciences, Vol. 10, No, 19, pp. 6668, 2020, doi: https://doi.org/10.3390/app10196668. **Impact factor: 2.474, Q2**.

Laura García, Lorena Parra, Jose Miguel Jimenez, Jaime, Lloret and Pascal Lorenz, "IoT-based Smart irrigation systems: An overview on the recent trends on sensors and IoT systems for irrigation in precision agriculture", Sensors, Vol. 20, No. 4, pp. 1042, 2020, doi: https://doi.org/10.3390/s20041042. **Impact factor: 3.275, Q2**.

Laura García-García, Lorena Parra-Boronat, Jose Miguel Jimenez, Jaime Lloret, Pascal Lorenz, "Practical Design of a WSN to Monitor the Crop and its Irrigation System", Network Protocols and Algorithms, Vol. 10, No. 4, pp. 35-52, 2018, doi: 10.5296/npa.v10i4.14147.

Laura García, Jose Miguel Jiménez, Miran Taha y Jaime Lloret, "Wireless Technologies for IoT in Smart Cities", Network, Protocols and Algorithms, Vol. 10, No. 1, pp. 23-64, 2018, doi: 10.5296/npa.v10i1.12798.

Jose Miguel Jimenez, Lorena Parra, **Laura García**, Jaime Lloret, Pedro Vicente Mauri, Pascal Lorenz, "New Protocol and Architecture for a Wastewater Treatment System Intended for Irrigation", Applied Sciences, Vol. 11, No. 8, pp. 3648, 2021, doi: https://doi.org/10.3390/app11083648**. Impact factor: 2.474, Q2**.

Lorena Parra, Javier Rocher, **Laura García**, Jaime Lloret, Jesús Tomás, Óscar Romero, M Rodilla, S. Falco, M. T. Sebastiá, J. Mengual, J. A. González, B. Roig, "Design of a WSN for Smart irrigation in citrus plots with fault-tolerance and energy-saving algorithms", Network Protocols and Algorithms, Vol. 10, No. 2, pp. 95-115, 2018, doi: https://doi.org/10.5296/npa.v10i2.13205.

Furthermore, the publications in international conferences that include the work presented in this thesis are the ones listed below:

Laura García, Jose Miguel Jimenez, Lorena Parra, Jaime Lloret and Pascal Lorenz, "An overview on IoUT and the performance of WiFi low-cost nodes for IoUT Applications", 2020 IEEE Global Communications Conference (GLOBECOM 2020), Taipei, Taiwan, 7-11 December 2020, pp. 1-6, doi: 10.1109/GLOBECOM42002.2020.9348057.

Laura García, Lorena Parra, Jose Miguel Jimenez, Jaime, Lloret, Abdelhafid Abouaissa and Pascal Lorenz, "Internet of Underground Things ESP8266 WiFi Coverage Study", INNOV 2019 - The eight International Conference on Communication, Computation, Networks and Technologies, Valencia, Spain, 24-28 November 2019, pp. 1-6.

Laura García, Lorena Parra, Daniel A. Basterrechea, Jose Miguel Jimenez, Javier Rocher, Mar Parra, José Luis García-Navas, Sandra Sendra, Jaime Lloret, Pascal Lorenz, Jesús Tomás, Abdelhafid Abouaissa, Miguel Rodilla, Silvia Falco, María Teresa Sebastiá, Jesus Mengual, Juan Andrés González and Bernat Roig, "Quantifying the Poduction of Fruit-Bearing Trees Using Image Processing Techniques", INNOV 2019 - The eight International Conference on Communication, Computation, Networks and Technologies, Valencia, Spain, 24-28 November 2019, pp. 14-19.

Laura García, Jose Miguel Jimenez, Jaime, Lloret and Pascal Lorenz, "WiFi and LoRa Energy Consumption Comparison in IoT ESP 32/SX1278 Devices", SMART 2019 – The Eight International Conference on Smart Cities, Systems, Devices and Technologies, Nice, France, July 28 – August 2 2019, pp. 26-31.

Laura García, Lorena Parra, Jose Miguel Jimenez, Jaime Lloret and Pascal Lorenz, "Estimation of the Best Measuring Time for the Environmental Parameters of a Low-Cost Meteorology Monitoring System", Advanced Intelligent Systems for Sustainable Development (AI2SD'2019), Marrakech, Morroco, 8-11 July 2019, pp. 137-144.

Jose Miguel Jimenez, Lorena Parra, **Laura García**, Jaime Lloret, Miran Taha and Pascal Lorenz, "Comprehensive security framework of an Intelligent Wastewater Purification System for Irrigation", NexComm 2019, Valencia, Spain, 24-28 March 2019, pp. 10-15.

8.7 Other publications

Other related journal papers and conference publications that have been published during the thesis. The journal papers are:

Sandra Sendra, Laura García, Jaime Lloret, Ignacio Bosch and Roberto Vega-Rodríguez. LoRaWAN network for fire monitoring in rural environments. Electronics, Vol. 9, No. 3, pp. 531, 2020. doi: https://doi.org/10.3390/electronics9030531. **Impact Factor: 2.412, Q2**.

Albert Rego, Sandra Sendra, **Laura García** and Jaime Lloret. Adapting reinforcement learning for multimedia transmission on SDN. Transactions on Emerging

Telecommunications Technologies, Vol. 330, No. 9, pp. e3643., 2019. doi: https://doi.org/10.1002/ett.3643. **Impact factor: 1.594, Q2.**

Laura García, Jesús Tomás, Lorena Parra and Jaime Lloret. An m-health application for cerebral stroke detection and monitoring using cloud services. International Journal of Information Management, Vol. 45, pp. 319-327, 2019. doi: https://doi.org/10.1016/j.ijinfomgt.2018.06.004. **Impact factor: 8.210, Q1.**

Laura García, Lorena Parra, Oscar Romero and Jaime Lloret. System for monitoring the wellness state of people in domestic environments employing emoticon-based HCI. The Journal of Supercomputing, Vol. 75, No. 4, pp. 1869-1893, 2019. doi: https://doi.org/10.1007/s11227-017-2214-4. **Impact factor: 2.469, Q2.**

Laura García, Lorena Parra, Blanca Pastor Gomis, Laura Cavallé, Vanesa Pérez Guillén, Herminio Pérez Garrigues and Jaime Lloret. Valencia's Cathedral Church Bell Acoustics Impact on the Hearing Abilities of Bell Ringers. International Journal of environmental research and public health, Vol. 16, No. 9, pp. 1564, 2019. doi: https://doi.org/10.3390/ijerph16091564 **Impact factor: 2.849, Q2.**

Albert Rego, **Laura García**, Sandra Sendra and Jaime Lloret. Software Defined Network-based control system for an efficient traffic management for emergency situations in Smart cities. Future Generation Computer Systems, Vol. 88, pp. 243-253, 2018. doi: https://doi.org/10.1016/j.future.2018.05.054. **Impact factor: 6.125, Q1.**

Laura García, Lorena Parra, Jose Miguel Jimenez and Jaime Lloret. Physical Wellbeing Monitoring Employing Non-Invasive Low-Cost and Low-Energy Sensor Socks. Sensors, Vol. 18, No. 9, pp. 2822, 2018. doi: https://doi.org/10.3390/s18092822. **Impact factor: 3.275, Q2**.

Miran Taha, Jaime Lloret, Aree Ali and **Laura García**. Adaptive video streaming testbed design for performance study and assessment of QoE. International Journal of Communication Systems, Vol. 31, No. 9, pp. e3551, 2018. doi: https://doi.org/10.1002/dac.3551. **Impact factor: 1.319, Q2.**

Lorena Parra, Sandra Sendra, **Laura García** and Jaime Lloret. Design and Deployment of Low-Cost Sensors for Monitoring the Water Quality and Fish Behavior in Aquaculture Tanks during the Feeding Process. Sensors, Vol. 18, No. 3, pp. 750, 2018. doi: https://doi.org/10.3390/s18030750. **Impact factor: 3.275, Q2**.

Lorena Parra, **Laura García**, Snadra Sendra and Jaime Lloret. The use of sensors for monitoring the feeding process and adjusting the feed supply velocity in fish farms. Journal of Sensors, 2018. doi: https://doi.org/10.1155/2018/1060987. **Impact factor: 1.595, Q2**.

Touhami Achouak, Benahmed Khelifa, **Laura García-García**, Lorena Parra-Boronat, Jaime Lloret and Bounaaman Fateh. Sensor Netowork Proposal for Greenhouse Automation placed at the South of Algeria. Network Protocols and Algorithms, Bol. 10, No. 4, pp. 53-69, 2018. doi: 10.5296/npa.v10i4.14155

Raquel Lacuesta, **Laura García**, Iván García-Margariño and Jaime Lloret. System to Recommend the Best Place to Live Based on Wellness State of the User Employing the

Heart Rate Variability. IEEE Access, Vol. 5, pp. 10594-10604, Mayo 2017. Doi: 10.1109/ACCESS.2017.2702107. **Impact factor: 3.745, Q1**.

Albert Rego, Christos Gkountis, **Laura García** and Jaime Lloret. A new proposal for trust management in Wireless sensor networks based on validation. International Journal of Trust Management in Computing and Communications, Vol. 4, No. 1, pp. 1-16, 2017. doi: https://doi.org/10.1504/IJTMCC.2017.089588.

Miran Taha, Jaime Lloret, Alejandro Cánovas and **Laura García**. Survey of Transportation of Adaptive Multimedia Streaming service in Internet. Network Protocols and Algorithms, Vol. 9, No. 1-2, pp. 85-125, 2017. Doi: 10.5296/npa.v9i1-2.12412.

Albert Rego, **Laura García**, Miguel Llopis and Jaime Lloret. A New Z39.50 Protocol Client to Search in Libraries and improve Research Collaboration. Network Protocols and Algorithms, Vol. 8, no 3, pp. 29-54, 2016. doi: 10.5296/npa.v8i3.10147

Carlos Barambones, **Laura García-García**, Jose Miguel Jiménez and Jaime Lloret. A new tool to test the IP network performance. Network Protocols and Algorithms. Vol. 8, No. 2, pp. 78-106, 2016. doi: 10.5296/npa.v8i2.9673

Nikola Dobrinov, Lorena Parra-Boronat, **Laura García-García**, José Oscar Romero Martínez. Comparative Study of a Router Performance with IPv4 and IPv6 Traffic. Network Protocols and Algorithms. Vol. 8, No. 3, pp. 55-75, 2016. doi: http://dx.doi.org/10.5296/npa.v8i3.10190

The conference papers are:

Laura García, Lorena Parra, Miran Taha and Jaime Lloret. System for detection of emergency situations in smart city environments employing smartphones. 2018 International Conference on Advances in Computing, Communications and Informaticas (ICACCI 2018), Bangalore, India, 19-22 September, pp. 266-272.

Albert Rego, **Laura García**, Sandra Sendra and Jaime Lloret. Software defined networks for traffic management in emergency situations. Fifth International Conference on Software Defined Systems, Barcelona, Spain, 23-26 April, 2018, pp. 45-51.

Alejandro Veiga, **Laura García**, Sandra Sendra, Jaime Lloret and Vivian Augele. An IoT-based smart pillow for sleep quality monitoring in AAL environments. Third International Conference on Fog and Mobile Edge Computing, Barcelona, Spain, 23-26 April, 2018, pp. 175-180.

Carlos Cambra, Sandra Sendra, **Laura García** and Jaime Lloret. Low cost wireless sensor network for rodents detection. 10th IFIP Wireless and Mobile Networking Conference, Valencia, Spain, 25-27 September, 2017, pp. 1-7.

Laura García, Jose Miguel Jiménez, Miran Taha y Jaime Lloret. Video artifact evaluation based on qos and objective qoe parameters. International Conference on Advances in Computing, Communications and Informatics, Bangalore, India, 19-22 September, 2017, pp. 1048-1054.

Miran Taha, **Laura García**, Jose M. Jimenez and Jaime Lloret. SDN-based throughput allocation in Wireless networks for heterogeneous adaptive video streaming applications. 13th International Wireless Communications and Mobile Computing Conference, 26-30 June, 2017, pp. 963-968.

Carlos Cambra, Sandra Sendra, Jaime Lloret and **Laura García**. An IoT service-oriented system for agriculture monitoring. 2017 IEEE International Conference on Communications (ICC), Paris, France, 21-25 May 2017, pp. 1-6. doi: 10.1109/ICC.2017.7996640

Miran Taha, Lorena Parra, **Laura García** and Jaime Lloret,. An Intelligent handover process algorithm in 5G networks: The use case of mobile cameras for environmental surveillance. IEEE International Conference on Communications Workshops, París, Francia, 21-25 May, 2017, pp. 840-844.

The book chapters are:

Laura García, Jaime Lloret, Ángel T. Lloret, Sandra Sendra. Domestic environment monitoring and its influence on Quality of Life. Health, Wellbeing and Sustainability in the Mediterranean City: Interdisciplinary perspectives, Routledge Studies in Urbanism and the City, pp. 122-135.

References

[1] Population. United Nations. Available at: https://www.un.org/en/sections/issues-depth/population/index.html (Last access 26-04-2019)

[2] M. A. Tsiafouli et al. “Intensive agriculture reduces soil biodiversity across Europe”, Global change biology, 2014, vol. 21, no. 2, pp. 973-985.

[3] J. J. Bruinsma, “World agriculture: towards 2015/2030”, Routledge, 2017, pp. 29-36.

[4] Agriculture and rural development Agriculture and rural development. Available online: https://ec.europa.eu/agriculture/cap-post-2013/ (accessed on 03/12/2019).

[5] Cambra, C., Sendra, S., Lloret, J., García, L. An IoT service-oriented system for agriculture monitoring, 2017 IEEE International Conference on Communication (ICC), Paris, France, May 21-25, 2017, pp. 1-6.

[6] Rodrigues, J. J. P. C. Emerging An IoT service-oriented system. Network Protocols and Algorithms 5, 28-30 (2013).

[7] Kropff, M.; Wallinga, J.; Lotz, L. Modelling for Precision Weed Management. In Proceedings of Ciba Foundation Symposium 210—Precision Agriculture: Spatial and Temporal Variability of Environmental Quality, Chichester, UK, 27 September 2007, pp. 182-207. DOI: 10.1002/9780470515419.ch12

[8] Earl, R; Wheeler, P.; Blackmore, S.; Godwin, R. J. Precision Farming: The Management of Variability. AGRIS 2013, 51(4), 18-23.

[9] García, L., Parra, L., Jimenez, J. M., Lloret, J., Mauri, P. V. and Lorenz, P. DronAway: A Proposal on the Use of Remote Sensing Drones as Mobile Gateway for WSN in Precision Agriculture. Applied Sciences, 2020, 10, 6668. https://doi.org/10.3390/app10196668

[10] Rahul, D.S.; Sudarshan, S.K., Meghana, K.; Nandan, K.N.; Kirthana, R.; Sure, P. IoT based Solar Powered Agribot for Irrigation and Farm Monitoring. In Proceedings of the 2nd International Conference on Inventive Systems and Control (ICISC), Coimbatore, India, 19–20 January 2018.

[11] Millán, S.; Campillo, C.; Casadesús, J.; Pérez-Rodríquez, J. M.; Henar Prieto, M. Automatic Irrigation Schedulling on a Hedgrow Olive Orchard Using an Algorithm of Water Balance Readjusted with Soil Moisture Sensors, Sensors 2020, 20, 2526.

[12] Campos, N. G. S.; Rocha, A. R.; Gondim, R.; Coelho da Silva, T. L.; Gomes, D. G. Smart & Green: An Internet-of-Things Framework for Smart Irrigation. Sensors 2020, 20, 190.

[13] Shang, C.; Chen, W.; Stroock, A. D.; You, F. Robust Model Predictive Control of Irrigation Systems with Active Uncertainty Learning and Data Analytics. IEEE Transactions on Control Technology 2020, 28 (4), 1493-1504.

[14] Fernández-López, A.; Martín-Sánchez, D.; García-Mateors, G.; Ruiz-Canales, A.; Ferrández-Villena-García, M.; Moli-na-Martínez, J. M. A Machine Learning Model to Estimate Reference Evapotranspiration Using Soil Moisture Sensors. Applied Sciences 2020, 10, 1912.

[15] Croce, S.; Tondini, S. Urban Microclimate Monitoring and Modelling through an Open-Source Distributed Network of Wireless Low-Cost Sensors and Numerical Simulations. Engineering Proceedings 2020, 2(1), 18.

[16] M. Mekonnen and A. Hoekstra, “Four Billion People Experience Water Scarcity”, Sci. Adv., vol. 2, no. 2, 2016. DOI: https://doi.org/10.1126/sciadv.1500323

[17] OECD, “Water use in agriculture”, 2017. Avaible at http://www.oecd.org/agriculture/water-use-in-agriculture.htm (Last access may 25 to 2018).

[18] F. Pedrero, I. Kalavrouziotis, J. J. Alarcón, P. Koukoulakis, and T. Asano, “Use of treated municipal wastewater in irrigated agriculture-Review of some practices in Spain and Greece”, Agric. Water Manag., vol. 97, no. 9, pp. 1233–1241, 2010. DOI: https://doi.org/10.1016/j.agwat.2010.03.003

[19] Koutroulis, A.G.; Papadimitriou, L.V.; Grillakis, M.G.; Tsanis, I.K.; Wyser, K.; Betts, R.A. Freshwater vulnerability under high end climate change. A pan-European assessment. Sci. Total Environ. 2018, 613, 271–286.

[20] Iglesias, A.; Santillán, D.; Garrote, L. On the barriers to adaption to less water under climate change: Policy choices in mediterranean countries. Water Resour. Manag. 2018, 32, 4819–4832.

[21] L. Yi, W. Jiao, X. Chen, and W. Chen, "An overview of reclaimed water reuse in China", J. Environ. Sci., vol. 23, no. 10, pp. 1585–1593, 2011. DOI: https://doi.org/10.1016/S1001-0742(10)60627-4

[22] M. Qadir et al., "The challenges of wastewater irrigation in developing countries", Agric. Water Manag., vol. 97, no. 4, pp. 561–568, 2010. DOI: https://doi.org/10.1016/j.agwat.2008.11.004

[23] H. Tropp and A. Jägerskog, "Water Scarcity Challenges in the Middle East and North Africa", Stockholm, UNDP Human Development Report, 2006.

[24] UNESCO. Agua para todos, Agua Para la Vida: Informe de las Naciones Unidas Sobre el Desarrollo de los Recursos Hídricos en el Mundo. 2017. Available online: https://www.un.org/esa/sustdev/sdissues/water/WWDR-spanish-129556s.pdf (accessed on 5 March 2021).

[25] World Health Organization. Drinking-Water. Available online: http://www.who.int/news-room/fact-sheets/detail/drinking-water (accessed on 5 March 2021).

[26] Yadav, I.C.; Devi, N.L.; Syed, J.H.; Cheng, Z.; Li, J.; Zhang, G.; Jones, K.C. Current status of persistent organic residues in air, water, and soil, and their possible effect on neighboring countries: A comprehensive review of India. Sci. Total Environ. 2015, 511, 123–137.

[27] Andreozzi, R.; Caprio, V.; Insola, A.; Marotta, R. Advanced oxidation processes (AOP) for water purification and recovery. Catal. Today 1999, 53, 51–59.

[28] Parra, L.; Rocher, J.; García, L.; Lloret, J.; Tomás, J.; Rodilla, M.; Falco, S.; Sebastiá, M.T.; Mengual, J.; González, J.A.; Roig B. Design of a WSN for Smart Irrigation in Citrus Plots with Fault-Tolerance and Energy-Saving Algorithms. Netw. Protoc. Algorithms 2018, 10, 95–115.

[29] Kiser, M.A.; Ryu, H.; Jang, H.; Hristovki, K.; Westerhoff, P. Biosorption of nanoparticles to heterotrophic wastewater biomass. Water Res. 2010, 44, 4105–4114.

[30] Yin, P.; Yu, Q.; Jin, B.; Ling, Z. Biosorption removal of cadmium from aqueous solution by using pretreated fungal biomass cultured from starch wastewater. Water Res. 1999, 33, 1960–1963.

[31] M. Fomina and G. M. Gadd, "Biosorption: Current perspectives on concept, definition and application", Bioresour. Technol., vol. 160, pp. 3–14, 2014. DOI: https://doi.org/10.1016/j.biortech.2013.12.102

[32] V. K. Gupta and A. Rastogi, "Biosorption of lead from aqueous solutions by green algae Spirogyra species: Kinetics and equilibrium studies", J. Hazard. Mater., vol. 152, no. 1, pp. 407–414, 2008. DOI: https://doi.org/10.1016/j.jhazmat.2007.07.028

[33] R. H. S. F. Vieira and B. Volesky, "Biosorption: a solution to pollution?", Int. Microbiol., vol. 3, pp. 17–24, 2000.

[34] K. Wang, G. Colica, R. De Philippis, Y. Liu, and D. Li, "Biosorption of copper by cyanobacterial bloom-derived biomass harvested from the eutrophic Lake Dianchi in

China.", Curr. Microbiol., vol. 61, no. 4, pp. 340–345, 2010. DOI: https://doi.org/10.1007/s00284-010-9617-2

[35] V. S. Munagapati, V. Yarramuthi, S. K. Nadavala, S. R. Alla, and K. Abburi, "Biosorption of Cu(II), Cd(II) and Pb(II) by Acacia leucocephala bark powder: Kinetics, equilibrium and thermodynamics", Chem. Eng. J., vol. 157, no. 2–3, pp. 357–365, 2010. DOI: https://doi.org/10.1016/j.cej.2009.11.015

[36] Sud, D.; Mahajan, G.; Kaur, M.P. Agricultural waste material as a potential absorbent for sequestering heavy metal ions from aqueous solutions–A review. Bioresour. Technol. 2008, 99, 6017–6027.

[37] Hospido, A.; Moreira, M.T.; Martín, M.; Rigola, M.; Feijoo, G. Environmental Evaluation of Different Treatment Process for Sludge from Urban Wastewater Treatments: Anaerobic Digestion versus Thermal Processes. Int. J. Life Cycle Assess. 2005, 10, 336–345.

[38] L. García, L. Parra, J. M. Jimenez, J. Lloret and P. Lorenz, "Practical Design of a WSN to Monitor the Crop and Its Irrigation System", Network Protocols and Algorithms, Vol. 10, No. 4, pp. 35-52, 2018.

[39] Karim, L., Anpalagan, A., Nasser, N., Almhana, J: Sensor-based M2M Agriculture Monitoring Systems for Developing Countries: State and Challenges. Network Protocols and Algorithms. 5, 68-86 (2013).

[40] Rosero-Montalvo, P. D.; Erazo-Chamorro, V. C.; López-Batista, V. F.; Moreno-García, M. N.; Peluffo-Ordóñez, D. H. Environment Monitoring of Rose Crops Greenhouse Based on Autonomous Vehicles with a WSN and Data Analysis. Sensors 2020, 20, 5905.

[41] Baire, M.; Melis, A.; Lodi, M. B.; Tuveri, P.; Dachena, C.; Simone, M.; Fanti, A.; Fumera, G.; Pisanu, T.; Mazzarella, G. A Wireless Sensors Network for Monitoring the Carasau Bread Manufacturing Process. Electronics 2019, 8, 1541.

[42] Parra, L.; Ortuño, V.; Sendra, S.; Lloret, J. Low-Cost Conductivity Sensor Based on Two Coils. In Proceedings of the First International Conference on Computational Science and Engineering (CSE 2013), Valencia, Spain, 25–31 August 2013, pp. 107–112.

[43] Parra L., Rocher J., Escrivá J., Lloret J., "Design and development of low cost smart turbidity sensor for water quality monitoring in fish farms", Aquacultural Engineering, Vol. 81, Issue February, pp. 10–18, May 2018. DOI: 10.1016/j.aquaeng.2018.01.004

[44] M. Dursun and S. Ozden, "A wireless application of drip irrigation automation supported by soil moisture sensors", Sci. Res. Essays, vol. 6, no. 7, pp. 1573–1582, 2011. DOI: https://doi.org/10.5897/SRE10.949

[45] García, L.; Parra, L.; Jimenez, J.M.; Parra, M.; Lloret, J.; Mauri, P.V.; Lorenz, P. Deployment Strategies of Soil Monitoring WSN for Precision Agriculture Irrigation Scheduling in Rural Areas. Sensors 2021, 21, 1693. https://doi.org/10.3390/s21051693

[46] LoRaWAN® distance world record broken, twice. 766 km (476 miles) using 25mW transmission power. Available at: https://www.thethingsnetwork.org/article/lorawan-distance-world-record (Last accessed on 31/05/2021)

[47] D. Lundell, A. Hedberg, C. Nyberg, E. Fitzgerald. A Routing Protocol for LoRa Mesh Networks. IEEE 19th International Symposium on "A World of Wireless, Mobile and Multimedia Networks". Chania, Greece, 12-15 June 2018, pp. 14-19.

[48] Jimenez, J.M.; Parra, L.; García, L.; Lloret, J.; Mauri, P.V.; Lorenz, P. New Protocol and Architecture for a Wastewater Treatment System Intended for Irrigation. Appl. Sci. 2021, 11, 3648. https://doi.org/10.3390/ app11083648

[49] Turong, V.T., Nayyar, A. and Lone, A. System Performance of Wireless Sensor Network Using LoRa-ZigBee Hybrid Communication. Computers, Materials & Continua, Vol. 68, No. 2, pp. 1615-1635, 2021. DOI:10.32604/cmc.2021.016922

[50] Heltec WiFi LoRa 32 (v2). Available at: https://heltec.org/project/wifi-lora-32/ Last accessed on 31/05/2021.

[51] Kim D. S., Chung B. J., Son S. Y. Implementation of a Low-Cost Energy and Environment Monitoring System Based on a Hybrid Wireless Sensor Network. Journal of Sensors 2017, 1-11. DOI: 10.1155/2017/5957082

[52] RFC 7641: Observing Resources in the Constrained Application Protocol (CoAP), September 2015. Available online: https://tools.ietf.org/html/rfc7641

[53] Ababneh, A. A.; Zghoul, F. R.; Akter, L. Quantizer Design for RSSI-based Target Localization in Sensor Networks. Adhoc & Sensor Wireless Networks 2017, 35, 319-339.

[54] Oliveira, T.; Raju, M.; Agrawa, D. P. Accurate Distance Estimation Using Fuzzy based combined RSSI/LQI Values in an Indoor Scenario: Experimental Verification. Network Protocols and Algorithms 2012, 4 (4), 174-199.

[55] Baccour, N.; Koubâa, A.; Mottola, L.; Zúniga, M. A.; Youssed, H.; Boano, C. A.; Alves, M. Radio Link Quality Estimation in Wireless Sensor Networks: A Survey. ACM Transactions on Sensor Networks 2012, 8 (4), 34.

[56] Cisco Annual Internet Report (2018–2023) White Paper. Available at: https://www.cisco.com/c/en/us/solutions/collateral/executive-perspectives/annual-internet-report/white-paper-c11-741490.html , Last accesed: 15-03-2020.

[57] M. C. Vuran, A. Salam, R. Wong, and S. Irmak, "Internet of underground things in precision agriculture: Architecture and technology aspects," Ad Hoc Networks, vol. 81, pp. 160 – 173, 2018, DOI: https://doi.org/10.1016/j.adhoc.2018.07.017

[58] N. Saeed, M.-S. Alouini, T. Y. Al-Naffouri, "Toward the Internet of Underground Things: A Systematic Survey", IEEE Communications Surveys & Tutorials, Volume: 21, Issue: 4, 2019, pp. 3443-3466, DOI: 10.1109/COMST.2019.2934365

[59] D. W. Sambo, A. Förster, B. O. Yenke and I. Sarr, "A New Approach for Path Loss Prediction in Wireless Underground Sensor Networks", IEEE 44th LCN

Symposium on Emerging Topics in Networking, Osnabrük, Germany, 14-17 October 2019, pp. 50-57.

[60] T. Rault, A. Bouabdallah, and Y. Challal, "Energy efficiency in wireless sensor networks: A top-down survey", Comput. Networks, vol. 67, pp. 104–122, 2014. DOI: https://doi.org/10.1016/j.comnet.2014.03.027

[61] Bhattacharjee, B.; Bandyopadhyay, S. An Energy Efficient-Delay Aware Routing Algorithm in Multihop Wireless Sensor Networks. Adhoc & Sensor Wireless Networks 2019, 43 (1), 1-32.

[62] Yinghong, L.; Yuanming, W.; Jianyu, C. The Diffusion Clustering Scheme and Hybrid Energy Balanced Routing Protocol (DCRP) in Multi-hop Wireless Sensor Networks. Adhoc & Sensor Wireless Networks 2019, 43 (1), 33-56.

[63] M. Al Ameen, S. M. R. Islam, and K. Kwak, "Energy Saving Mechanisms for MAC Protocols in Wireless Sensor Networks", Int. J. Distrib. Sens. Networks, vol. 6, no. 1, p. 163413, 2010.

[64] Sales, N.; Remédios, O.; Arsenio, A. Wireless Sensor and Actuator System for Smart Irrigation on the Cloud. In Proceedings of the IEEE 2nd World Forum on Internet of Things, Milan, Italy, 14–16 December 2015, pp. 693–698.

[65] Fog Computing vs. Edge Computing: What's the Difference?. Available at: https://www.automationworld.com/products/data/blog/13315784/fog-computing-vs-edge-computing-whats-the-difference, Last accessed 2/11/2020.

[66] Vincent, D. R.; Deepa, N.; Elavarasan, D.; Srinivasan, K.; Chauhdary, S. H.; Iwendi, C. Sensors Driven AI-Based Agriculture Recommendation Model for Assessing Land Suitability. Sensors 2019, 19, 3667.

[67] Toth, C.; Jóźków, G. Remote sensing platforms and sensors: A survey. ISPRS Journal of Photogrammetry and Remote Sensing 2016, 115, 22-36. DOI: 10.1016/j.isprsjprs.2015.10.004

[68] Pajares, G. Overview and Current Status of Remote Sensing Applications Based on Unmanned Aerial Vehicles (UAVs). Photogrammetric Engineering & Remote Sensing 2015, 81(4), 281-330.

[69] Maes, W. H.; Steppe, K. Perspectives for Remote Sensing with Unmanned Aerial Vehicles in Precision Agriculture. Trends in Plant Science 2019, 24 (2), 152-164. DOI: 10.1016/j.tplants.2018.11.007

[70] Psirofonia, P.; Samaritakis, V.; Eliopoulos, P.; Potamitis, I. Use of Unmanned Aerial Vehicles for Agricultural Applications with Emphasis on Crop Protection: Three Novel Case-studies. International Journal of Agricultural Science and Technology 2017, 5(1), 30-39.

[71] Agriculture Drones Market by Offering (Hardware and Software & Services), Application (Precision Farming, Livestock Monitoring, Precision Fish Farming, and Smart Greenhouse), Component, and Geography - Global Forecast to 2024. Available online: https://www.marketsandmarkets.com/Market-Reports/agriculture-drones-

market-23709764.html?gclid=CjwKCAiA-P7xBRAvEiwAow-VaRPLzQ4x9YHOwUyC4e-PBfJvjpkB4Bqx9WWIt6S-lM0FsKvUcbqLdxoC_VcQAvD_BwE (accessed on 03/2/2020).

[72] Prodanović, R.; Rančić, D.; Vulić, I.; Zorić, N.; Bogićević, D.; Ostojić, G.; Sarang, S.; Stankovski, S. Wireless Sensor Network in Agriculture: Model of Cyber Security. Sensors 2020, 20, 6747.

[73] H. Liu, A. Nayak, and I. Stojmenovic, "Chapter 10: Fault-Tolerant Algorithms/Protocols in Wireless Sensor Networks Guide to Wireless Mesh Networks", in Guide to Wireless Mesh Networks, S. Misra, I. Woungang and S. Chandra Misra, 2009, p. 261-291.

[74] Google Scholar. Available online: https://scholar.google.es/ (accessed on 18 October 2019).

[75] IEEE Explore. Available online: https://ieeexplore.ieee.org/Xplore/home.jsp (accessed on 18 October 2019).

[76] Scopus. Available online: https://www.scopus.com/home.uri?zone=header&origin=searchbasic (accessed on 18 October 2019).

[77] Sensors. Available online: https://www.mdpi.com/journal/sensors (accessed on 18 October 2019).

[78] González-Amarillo, C.A.; Corrales Muñoz, J.C.; Mendoza-Moreno, M.A.; González Amarillo, A.M.; Faeq Hussein, A.; Arunkumar, N.; Ramirez-Gonzalez, G. An IoT-based traceability system for greenhouse seedling crops. IEEE Access 2018, 6, 67528–67535.

[79] Ahmed, S.; Shekhawat, A.S.; Kumar, S.G.; Nair, M.K.; Kumar, V. "Intelligation": An IOT based Framework for Smarter Irrigation. In Proceedings of the National Conference on Product Design (NCPD 2016), Banglore, India, 30 October 2016.

[80] Patokar, A.M.; Gohokar, V.V. Precision agriculture system design using wireless sensor network. In Information and Communication Technology; Springer: Singapore, 2017.

[81] Arvind, G.; Athira, V.G.; Haripriya, H.; Akshaya Rani, R.; Aravind, S. Automated Irrigation with Advanced Seed Germination and Pest Control. In Proceedings of the IEEE International Conference on Technological Innovations in ICT for Agriculture and Rural Development, Chennai, India, 7–8 April 2017.

[82] Ammour, K. Factory Automation and Irrigation Control in IoT Environments. In Proceedings of the 15th Learning and Technology Conference (L&T), Jeddah, Saudi Arabia, 25–26 February 2018.

[83] Singh, K.; Jain, S.; Andhra, V.; Sharma, S. IoT based approach for smart irrigation system suited to multiple crop cultivation. Int. J. Eng. Res. Technol. 2019, 12, 357–363.

[84] Wu, H.; Chen, F.; Hu, H.; Liu, Q.; Ji, S. A secure system framework for an agricultural IoT application. advances in computer science and ubiquitous computing. Lect. Notes Electr. Eng. 2016, 421, 332–341.

[85] Solanki, V.K.; Venkatesan, M.; Katiyar, S. Conceptual model for smart cities: Irrigation and highway lamps using IoT. Int. J. Interact. Multimed. Artif. Intell. 2017, 4, 28–33.

[86] Wasson, T.; Choudhury, T.; Sharma, S.; Kumar, P. Integration of RFID and Sensor in Agriculture Using IoT. In Proceedings of the International Conference on Smart Technologies For Smart Nation, Bangalore, India, 17–19 August 2017.

[87] Johar, R.; Bensenouci, A.; Benesenouci, M. IoT based Smart Sprinkling System. In Proceedings of the 15th Learning and Technology Conference, Jeddah, Saudi Arabia, 25–26 February 2018.

[88] Ryu, M.; Yun, J.; Ahn, I.; Choi, S.; Kim, J. Design and Implementation of a Connected Farm for Smart Farming System. In Proceedings of the 2015 IEEE Sensors, Busan, South Korea, 1–4 November 2015.

[89] Reche, A.; Sendra, S.; Díaz, J.R.; Lloret, J. A Smart M2M Deployment to Control the Agriculture Irrigation. In Proceedings of the ADHOC-NOW 2014: International Conference on Ad-Hoc Networks and Wireless, Benidorm, Spain, 22–27 June 2014.

[90] Chieochan, O.; Saokaew, A.; Boonchieng, E. Internet of Things (IoT) for Smart Solar Energy: A Case Study of the Smart Farm at Maejo University. In Proceedings of the International Conference on Control, Automation and Information Sciences, Chiang Mai, Thailand, 31 October–3 November 2017.

[91] Arumugam, S.S.; Ganeshmurthi, M.; Annadurai, R.; Ravichandran, V. Internet of things based smart agriculture. Int. J. Adv. Comput. Electron. Eng. 2018, 33, 8–17.

[92] Boonchieng, E.; Chieochan, O.; Saokaew, A. Smart farm: Applying the use of node MCU, IOT, NETPIE and LINE API for a lingzhi mushroom farm in Thailand. IEICE Trans. Commun. 2018, 101, 16–23.

[93] Rawal, S. IoT based smart irrigation system. Int. J. Comput. Appl. 2017, 159, 7–11.

[94] Guo, T.; Zhong, W. Design and Implementation of the Span Greenhouse Agriculture Internet of Things System. In Proceedings of the 2015 International Conference on Fluid Power and Mechatronics, Harbin, China, 5–7 August 2015.

[95] Khattab, A.; Abdelgawad, A.; Yelmarthi, K. Design and Implementation of a Cloud-based IoT Scheme for Precision Agriculture. In Proceedings of the 28th International Conference on Microelectronics, Giza, Egypt, 17–20 December 2016.

[96] Daskalakis, S.N.; Goussetis, G.; Assimonis, S.D.; Tenzeris, M.M.; Georgiadis, A. A uW backscatter-morse_leaf sensor for low-power agricultural wireless sensor networks. IEEE Sens. J. 2018, 18, 7889–7898.

[97] Nawandar, N.K.; Satpute, V.R. IoT based low cost and intelligent module for smart irrigation system. Comput. Electron. Agric. 2019, 162, 979–990.

[98] Barkunan, S.R.; Bhanumathi, V.; Sethuram, J. Smart sensor for automatic drip irrigation system for paddy cultivation. Comput. Electr. Eng. 2019, 73, 180–193.

[99] Parabmeswaram, G.; Sivaprasath, K. Arduino based smart drip irrigation system using internet of things. Int. J. Eng. Sci. Comput. 2016, 6, 5518–5521.

[100] Kumar, A.; Surendra, A.; Mohan, H.; Valliappan, K.M.; Kirthika, N. Internet of Things based Smart Irrigation using Regression Algorithm. In Proceedings of the 2017 International Conference on Intelligent Computing, Instrumentation and Control Technologies (ICICICT), Kannur, India, 6–7 July 2017.

[101] Kodali, R.K.; Jain, V.; Karagwal, S. IoT based Smart Greenhouse. In Proceedings of the 2016 IEEE Region 10 Humanitarian Technology Conference (R10-HTC), Agra, India, 21–23 December 2016.

[102] Abidin, S.A.H.Z.; Inrahim, S.N. Web-based Monitoring of an Automated Fertigation System: An IoT Application. In Proceedings of the IEEE 12th Malaysia International Conference on Communications, Kuching, Malaysia, 23–25 November.

[103] Banumathi, P.; Saravanan, D.; Sathiyapriya; M., Saranya, V. An android based automatic irrigation system using bayesian network with SMS and voice alert. Int. J. Sci. Res. Comput. Sci. Eng. Inf. Technol. 2017, 2, 573–578.

[104] Padalalu, P.; Mahajan, S.; Dabir, K.; Mitkar, S.; Javale, D. Smart Water Dripping System for Agriculture/Farming. In Proceedings of the 2nd International Conference for Convergence in Technology (I2CT), Mumbai, India, 7–9 April 2017.

[105] Mechsy, L.S.R.; Días, M.U.B.; Pragithmukar, W.; Lulasekera, A.L. A Mobile Robot based Watering System for Smart Lawn Maintenance. In Proceedings of the 17th International Conference on Control, Automation and Systems (ICCAS), Jeju, Korea, 18–21 October 2017.

[106] Debauche, O.; El Moulat, M.; Mahmoudi, S.; Manneback, P.; Lebau, F. Irrigation Pivot-Center Connected at Low Cost for the Reduction of Crop Water Requirements. In Proceedings of the International Conference on Advanced Communication Technologies and Networking, Marrakech, Morocco, 2–4 April 2018.

[107] Vasu, N.; Shyam; K.; V. Sri, Y. Intelligent drip irrigation system based on remote monitoring. Int. J. Ethics Eng. Manag. Educ. 2017, 4, 11–13.

[108] Agale, R.R.; Gaikwad, D.P.; Automated Irrigation and Crop Security System in Agriculture using Internet of Things. In Proceedings of the 2017 International Conference on Computing, Communication, Control and Automation (ICCUBEA), Pune, India, 17–18 August.

[109] Rau, A.J.; Sankar, J.; Mohan, A.R.; Krishna, D.D.; Mathew, J. IoT based Smart Irrigation System and Nutrient Detection with Disease Analysis. In Proceedings of the 2017 IEEE Region 10 Symposium (TENSYMP), Cochin, India, 14–16 July 2017.

[110] Sukhadeve, V.; Roy, S. Advance agro farm design with smart farming, irrigation and rain water harvesting using internet of things. Int. J. Adv. Eng. Manag. 2016, 1, 33–45, doi:10.24999/ijoaem/01010005.

[111] Roselin, A.R.; Jawahar, A. Smart Agro System using Wireless Sensor Networks. In Proceedings of the 2017 International Conference on Intelligent Computing and Control Systems (ICICCS), Madurai, India, 15–16 June 2017.

[112] Mohanraj, I.; Ashokumar, K.; Naren, J. Field monitoring and automation using IoT in agriculture domain. Procedia Comput. Sci. 2016, 93, 931–939.

[113] Keswani, B.; Mohapatra, A.G.; Mohanty, A.; Khanna, A.; Rodrigues, J.J.P.C.; Gupta, D.; De Albuquerque, V.H.C. Adapting weather conditions based IoT enabled smart irrigation technique in precision agriculture mechanisms. Neural Comput. Appl. 2019, 31, 277–292.

[114] Dasgupta, A.; Daruka, A.; Pandey, A.; Bose, A.; Mukherjee, S.; Saha, S. Smart Irrigation: IoT-based Irrigation Monitoring System. In Proceedings of the International Ethical Hacking Conference 2018, Kolkata, India, 5 October 2018.

[115] Gondchawar, N.; Kawitkar, R.S. IoT based smart agriculture. Int. J. Adv. Res. Comput. Commun. Eng. 2016, 5, 838–842.

[116] Krishna, K.L.; Silver, O.; Malende, W.F.; Amuradha, K. Internet of Things Application for Implementation of Smart Agriculture System. In Proceedings of the 2017 International Conference on I-SMAC (IoT in Social, Mobile, Analytics and Cloud) (I-SMAC), Palladam, India, 10–11 February 2017.

[117] Qi, D.; Li, G.; Dai, X. Proceedings of the 2017 9th International Conference on Intelligent Human-Machine Systems. In Proceedings of the 2017 9th International Conference on Intelligent Human-Machine Systems and Cybernetics (IHMSC), Hangzhou, China, 26–27 August 2017.

[118] Burchi, G.; Chessa, S.; Gambineri, F.; Kocian, A.; Massa, D.; Milazzo, P.; Rimediotti, L.; Ruggeri, A. Information Technology Controlled Greenhouse: A System Architecture. In Proceedings of the 2018 IoT Vertical and Topical Summit on Agriculture-Tuscany (IOT Tuscany), Tuscany, Italy, 8–9 May 2018.

[119] Crisnapati, P.N.; Wardana, I.N.K.; Aryanto, I.K.A.A.; Hermawan, A. Hommons: Hydroponic Management and Monitoring System for an IoT based NFT Farm using Web Technology. In Proceedings of the 5th International Conference on Cyber and IT Service Management (CITSM), Denpasar, Indonesia, 8–10 August 2017.

[120] Cambra, C.; Sendra, S.; Lloret, J.; Lacuesta, R. Smart system for bicarbonate control in irrigation for hydroponic precision farming. Sensors 2018, 18, 16.

[121] Fajrin, N.; Taufik, I.; Ismail, N.; Kamelia, L.; Ramdhani, M.A. On the Design of Watering and Lighting Control Systems for Chrysanthemun Cultivation in Greenhouse based on the Internet of Things. In Proceedings of the 2nd Annual Applied Science and Engineering Conference, Bandung, Indonesia, 24 August 2017.

[122] Abagissa, A.T.; Behura, A.; Pani, S.K. IoT based Smart Agricultural Device Controlling System. In Proceedings of the Second International Conference on Inventive Communication and Computational Technologies (ICICCT), Coimbatore, India, 20–21 April 2018.

[123] Mat, I.; Kassim, M.R.M.; Harum, A.N.; Yusoff, I.M. IoT in Precision Agriculture Applications using Wireless Moisture Sensor Networks. In Proceedings of the 2016 IEEE Conference on Open Systems (ICOS), Langkawi, Malaysia, 10–12 October 2016.

[124] Kassim, M.R.M.; Mat, I.; Harum, Z. Wireless Sensor Network in Precision Agriculture Application. In Proceedings of the 2014 International Conference on Computer, Information and Telecommunication Systems (CITS), Jeju, Korea, 7–9 July 2014.

[125] Zamora-Izquierdo, M.A.; Sant, J.; Martínez, J.A.; Martínez, V.; Skarmeta, A.F. Smart farming IoT platform based on edge and cloud computing. Biosyst. Eng. 2019, 177, 4–17.

[126] Rivas-Sánchez, Y.A.; Moreno-Pérez, M.F.; Roldán-Cañas, J. Environment control with low-cost microcontrollers and microprocessors: Application for green walls. Sustainability 2019, 11, 782.

[127] Purwandana, R.I.; Azmi, F.; Jati, A.N. Automatic watering plant application based on android and web using REST protocol. J. Telecommun. Electron. Comput. Eng. 2017, 9, 83–87.

[128] Zhao, W.; Lin, S.; Han, J.; Xu, R.; Hou, L. Design and Implementation of Smart Irrigation System based on LoRa. In Proceedings of the 2017 IEEE Globecom Workshops (GC Wkshps), Singapore, 4–8 December 2017.

[129] Thakur, C.; Taskeen, S.; Pavithra, S.; Monisha, S.; Namratha, K.S.; Peter, M. Internet of things (IOT) based irrigation system with and without internet and pump set control. Glob. J. Comput. Sci. Technol. H Inf. Technol. 2018, 18, 11–14.

[130] Raut, R.; Varma, H.; Mulla, C.; Pawar, V.R. Soil monitoring, fertigation, and irrigation system using IoT for agricultural application. Intell. Commun. Comput. Technol. Lect. Notes Netw. Syst. 2017, 19, 67–73.

[131] Rajkumar, M.N.; Abinaya, S.; Kumar, V.V. Intelligent Irrigation System an IoT based Approach. In Proceedings of the 2017 International Conference on Innovations in Green Energy and Healthcare Technologies (IGEHT), Coimbatore, India, 16–18 March 2017.

[132] Srivastava, P.; Bajaj, M.; Rana, A.S. Overview of ESP8266 Wi-Fi Module based Smart Irrigation System using IoT. In Proceedings of the 2018 Fourth International Conference on Advances in Electrical, Electronics, Information, Communication and Bio-Informatics (AEEICB), Chennai, India, 27–28 February 2018.

[133] Robles, T.; Alcarria, R.; Martín, D.; Navarro, M.; Calero, R.; Iglesias, S.; López, M. An IoT based reference architecture for smart water management processes. J. Wirel. Mob. Netw. Ubiquitous Comput. Dependable Appl. 2015, 6, 4–23.

[134] Kumar, V.V.; Ramasamy, R.; Janarthanan, S.; VasimBabu, M. Implementation of IoT in smart irrigation system using arduino processor. Int. J. Civ. Eng. Technol. 2017, 8, 1304–1314.

[135] Yashaswini, L.S.; Sinchana, H.N.; Vani, H.U.; Kumar, N. Smart Automated Irrigation System with Disease Prediction. In Proceedings of the 2017 IEEE International Conference on Power, Control, Signals and Instrumentation Engineering (ICPCSI), Chennai, India, 21–22 September 2017.

[136] Pernapati, K. IoT based Low Cost Smart Irrigation System. In Proceedings of the 2018 Second International Conference on Inventive Communication and Computational Technologies (ICICCT), Coimbatore, India, 20–21 April 2018.

[137] Asnawi, M.F.; Syukriasari, F. A prototype for IoT based rice field irrigation system. J. Publ. Inform. Eng. Res. 2019, 3, 260–265.

[138] Mahalakshmi, M.; Priyanka, S.; Rajaram, S.P.; Rajapriya, R. Distant Monitoring and Controlling of Solar Driven Irrigation System Through IoT. In Proceedings of the 2018 National Power Engineering Conference (NPEC), Madurai, India, 9–10 March 2018.

[139] Rukhmode, S.; Vyavhare, G.; Banot, S.; Narad, A.; Tugnayat, R.M. IoT based Agriculture Monitoring System using Wemos. In Proceedings of the International Conference on Emanations in Modern Engineering Science and Management, Nagpur Maharashtra, India, 25–26 March 2017.

[140] Sagar, S.V.; Kumar, G.R.; Xavier, L.X.T.; Sivakumar, S.; Durai, R.B. SISFAT: Smart Irrigation System with Flood Avoidance Technique. In Proceedings of the Third International Conference on Science Technology Engineering & Management (ICONSTEM), Chennai, India, 23–24 March 2017.

[141] Pandithurai, O.; Aishwarya, S.; Aparna, B.; Kavitha, K. Agro-Tech: A Digital Model for Monitoring Soil and Crops using Internet of Things (IoT). In Proceedings of the Third International Conference on Science Technology Engineering & Management (ICONSTEM), Chennai, India, 23–24 March 2017.

[142] Vijay, V.; Vishal, H.; Dhanalakshmi, S.; Vidya, P.M. Regulation of Water in Agriculture Field using Internet of Things. In Proceedings of the 2015 IEEE Technological Innovation in ICT for Agriculture and Rural Development (TIAR), Chennai, India, 10–12 July 2015.

[143] Shahzadi, R.; Tausif, M.; Ferzund. J.; Suryani, M.A. Internet of things based expert system for smart agriculture. Int. J. Adv. Comput. Sci. Appl. 2016, 7, 341–350.

[144] Visconti, P.; Primiceri, P.; Orlando, C. Solar powered wireless monitoring system of environmental conditions for early flood prediction or optimized irrigation in agriculture. ARPN J. Eng. Appl. Sci. 2016, 11, 4623–4632.

[145] Ali, T.A.A.; Choksi, V.; Potdar, M.B. Precision Agriculture Monitoring System using Green Internet of Things (G-IoT). In Proceedings of the 2nd International Conference on Trends in Electronics and Informatics, Tirunelveli, India, 11–12 May 2018.

[146] Selmani, A.; Oubehar, H.; Outanoute, M.; Ed-Dahhak, A.; Guerbaoui, M.; Lachhab, A.; Bouchikhi, B. Agricultural cyber-physical system enabled for remote management of solar-powered precision irrigation. Biosyst. Eng. 2019, 177, 18–30.

[147] Thamaraimanalan, T.; Vivekk, S.P.; Satheeshkumar, G.; Saravanan, P. Smart garden monitoring system using IoT. Asian J. Appl. Sci. Technol. 2018, 2, 186–192.

[148] Guruprasadh, J.P.; Harshananda, A.; Keerthana, I.K.; Rachana; Yadu Krishnan, K.; Rangarajan, M.; Sathyadevan, S. Intelligent Soil Quiality Monitoring System for Judicious Irrigation. In Proceedings of the 2017 International Conference on Advances in Computing, Communications and Informatics (ICACCI), Udupi, India, 13–16 September 2017.

[149] Carrasquilla-Batista, A.; Chacón-Rodríquez, A.; Solórzano-Quintana, M. Using IoT to Enhance the Accuracy of Overdrain Measurements in Greenhouse Horticulture. In Proceedings of the IEEE 36th Central American and Panama Convention (CONCAPAN XXXVI), San Jose, Costa Rica, 9–11 November 2016.

[150] Jagadesh, M.; Karthik, M.; Manikandan, A.; Nivetha, S.; Prasanth Kumar, R. IoT based aeroponics agriculture monitoring system using raspberry Pi. Int. J. Creat. Res. Thoughts 2018, 6, 601–608.

[151] Carrasquilla-Batista, A.; Chacón-Rodríguez, A. Proposal of a Fuzzy Logic Controller for the Improvement of Irrigation Scheduling Decision-Making in Greenhouse Horticulture. In Proceedings of the 1st Conference on PhD Research in Microelectronics and Electronics Latin America (PRIME-LA), Bariloche, Argentina, 20–23 February 2017.

[152] Gupta, A.; Krishna, V.; Gupta, S.; Aggarwal, J. Android based solar powered automatic irrigation system. Indian J. Sci. Technol. 2016, 9, 1–5.

[153] Suakatnto, S.; Engel, V.J.L.; Hutagalung, M.; Angela, D. Sensor Networks Data Acquisition and Task Management for Decision Support of Smart Farming. In Proceedings of the 2016 International Conference on Information Technology Systems and Innovation (ICITSI), Bandung, Bali, 24–27 October 2016.

[154] Kumar, B.D.; Srivastava, P.; Agrawal, R.; Tiwari, V. Microcontroller based automatic plant irrigation system. Int. Res. J. Eng. Technol. 2017, 4, 1436–1439.

[155] Kool, D.; Agam, N.; Lazarovitch, N.; Heitman, J.L.; Sauer, T.J.; Ben-Gal, A. A review of approaches for evapotranspiration partitioning. Agric. For. Meteorol. 2014, 184, 56–70.

[156] Pereira, L.S.; Allen, R.G.; Smith, M.; Raes, D. Crop evapotranspiration estimation with FAO56: Past and future. Agric. Water Manag. 2015, 147, 4–20.

[157] Cammalleri, C.; Anderson, M.C.; Gao, F.; Hain, C.R.; Kustas, W.P. Mapping daily evapotranspiration at field scales over rainfed and irrigated agricultural areas using remote sensing data fusion. Agric. For. Meteorol. 2014, 186, 1–11.

[158] Chirouze, J.; Boulet, G.; Jarlan, L.; Fieuzal, R.; Rodriguez, J.C.; Ezzahar, J., Raki, S.E.; Bigeard, G.; Merlin, O.; Garatuza-Payan, J.; et al. Intercomparison of four remote-sensing-based energy balance methods to retrieve surface evapotranspiration and water stress of irrigated fields in semi-arid climate. Hydrol. Earth Syst. Sci. Discuss. 2014, 18, 1165–1188.

[159] Cruz-Blanco, M.; Lorite, I.J.; Santos, C. An innovative remote sensing based reference evapotranspiration method to support irrigation water management under semi-arid conditions. Agric. Water Manag. 2014, 131, 135–145.

[160] Shin, J.H.; Son, J.E. Development of a real-time irrigation control system considering transpiration, substrate electrical conductivity, and drainage rate of nutrient Solutions in soilless culture of paprika (Capsicum annuum L.). Eur. J. Hortic. Sci 2015, 80, 271–279.

[161] Kumawat, S.; Bhamare, M.; Nagare, A.; Kapadnis, A. Sensor based automatic irrigation system and soil pH detection using image processing. Int. Res. J. Eng. Technol. 2017, 4, 3673–3675.

[162] Gulati, A.; Thakur, S. Smart Irrigation using Internet of Things. In Proceedings of the 8th International Conference on Cloud Computing, Data Science & Engineering (Confluence), Noida, India, 11–12 January 2018.

[163] Imteaj, A.; Rahman, T.; Hossain, M.K.; Zaman, S. IoT based Autonomous Percipient Irrigation System using Raspberry Pi. In Proceedings of the 19th International Conference on Computer and Information Technology (ICCIT), Dhaka, Bangladesh, 18–20 December 2016.

[164] Kodali, R.K.; Sahu, A. An IoT based Soil Moisture Monitoring on Losant Platform. In Proceedings of the 2nd International Conference on Contemporary Computing and Informatics (IC3I), Noida, India, 14–17 December 2016.

[165] Kodali, R.K.; Sarjerao, B.S. A Low Cost Smart Irrigation System using MQTT Protocol, In Proceedings of the 2017 IEEE Region 10 Symposium (TENSYMP), Cochin, India, 14–16 July 2017.

[166] Vineela, T.; NagaHarini, J.; Kiranmai, C.; Harshitha, G.; AdiLakshmi, B. IoT based agriculture monitoring and smart irrigation system using raspberry Pi. Int. Res. J. Eng. Technol. 2018, 5, 1417–1420.

[167] Kamelia, L.; Ramdhani, M.A.; Faroqi, A.; Rifadiapriyana, V. Implementation of Automation System for Humidity Monitoring and Irrigation System. In Proceedings of the 2nd Annual Applied Science and Engineering Conference, Bandung, Indonesia, 24 August 2017.

[168] Kuruva, H.; Sravani, B. Remote plant watering and monitoring system based on IoT. Int. J. Technol. Res. Eng. 2016, 4, 668–671.

[169] Salvi, S.; Jain, S.A.P.; Sanjay, H.A.; Harshita, T.K.; Farhana, M.; Jain, N.; Suhas, M.V. Cloud based Data Analysis and Monitoring of Smart Multi-level Irrigation System using IoT. In Proceedings of the 2017 International Conference on I-SMAC (IoT in Social, Mobile, Analytics and Cloud) (I-SMAC), Palladam, India, 10–11 February 2017.

[170] Kabilan, N.; Selvi, M.S. Surveillance and Steering of Irrigation System in Cloud using Wireless Sensor Network and Wi-Fi Module. In Proceedings of the 2016 International Conference on Recent Trends in Information Technology (ICRTIT), Chennai, India, 8–9 April 2016.

[171] Goap, A.; Sharma, D.; Shukla, A.K.; Krishna, C.R. An IoT based smart irrigation management system using machine learning and open source technologies. Comput. Electron. Agric. 2018, 155, 41–49.

[172] Sacvić, T.; Radonić, M. WSN Architecture for Smart Irrigation System. In Proceedings of the 23rd International Scientific-Professional Conference on Information Technology (IT), Žabljak, Montenegro, 19–24 February 2018.

[173] Zhang, X.; Zhang, J.; Li, L.; Zhang, Y.; Yang, G. Monitoring citrus soil moisture and nutrients using an IoT based system. Sensors 2017, 17, 447.

[174] Kumar, M.K.; Ravi, K.S. Automation of irrigation system based on Wi-Fi technology and IoT. Indian J. Sci. Technol. 2016, 9, 1–5.

[175] Anandkumar, V.; Kalairasan, T.R.; Balakrishnan, S. IoT based soil analysis and irrigation system. Int. J. Pure Appl. Math. 2018, 119, 1127–1134.

[176] Carrión, G.; Huerta, M.; Barzallo, B. Internet of Things (IoT) Applied to an Urban Garden. In Proceedings of the IEEE 6th International Conference on Future Internet of Things and Cloud, Barcelona, Spain, 6–8 August 2018.

[177] Carrión, G.; Huerta, M.; Barzallo, B. Monitoring and Irrigation of an Urban Garden using IoT. In Proceedings of the IEEE Colombian Conference on Communications and Computing, Medellin, Colombia, 16–18 May 2018.

[178] Malhotra, A.; Saini, S.; Kale, V.V. Automated irrigation system with weather forecast integration. Int. J. Eng. Technol. Manag. Appl. Sci. 2017, 5, 179–184.

[179] Mekala, M.S.; Viswanathan, P. A Novel Technology for Smart Agriculture based on IoT with Cloud Computing. In Proceedings of the International Conference on IoT in Social, Mobile, Analytics and Cloud, Palladam, India, 10–11 February 2017.

[180] Monica, M.; Yeshika, B.; Abhishek, G.S.; Sanjay, H.A.; Dasiga, S. IoT based Control and Automation of Smart Irrigation System: An Automated Irrigation System using Sensors, GSM, Bluetooth and Cloud Technology. In Proceedings of the International Conference on Recent Innovations in Signal Processing and Embedded Systems, Bhopal, India, 27–29 October 2017.

[181] Naik, P.; Kumbi, A.; Hiregoudar, V.; Chaitra, N.K.; Pavitra, H.K.; Sushma, B.S.; Sushmita, J.H.; Kuntanahal, P. Arduino based automatic irrigation system using IoT. Int. J. Sci. Res. Comput. Sci. Eng. Inf. Technol. 2017, 2, 881–886.

[182] Rajalakshmi, P.; Mahalakshmi, S.D. IoT based Crop-Field Monitoring and Irrigation Automation. In Proceedings of the 10th International Conference on Intelligent Systems and Control, Coimbatore, India, 7–8 January 2016.

[183] Rao, R.N.; Sridhar, B. IoT based Smart Crop-Field Monitoring and Automation Irrigation System. In Proceedings of the Second International Conference on Inventive Systems and Control, Coimbatore, India, 19–20 January 2018.

[184] Saraf, S.B.; Gawali, D.H. IoT based Smart Irrigation Monitoring and Controlling System. In Proceedings of the IEEE International Conference on Recent Trends in

Electronics Information & Communication Technology, Bangalore, India, 19–20 May 2017.

[185] Vaishali, S.; Suarj, S.; Vignesh, G.; Shivya, S.; Udhayakumar, S. Mobile Integrated Smart Irrigation Management and Monitoring System using IOT. In Proceedings of the International Conference on Communication and Signal Processing, Chennai, India, 6–8 April 2017.

[186] Venkatesan, R.; Tamilvanan, A. A Sustainable Agricultural System using IoT. In Proceedings of the International Conference on Communication and Signal Processing, Chennai, India, 6–8 April 2017.

[187] Villarubia, G.; De Paz, J.F.; De La Iglesia, D.H.; Bajo, J. Combining multi-agent systems and wireless sensor networks for monitoring crop irrigation. Sensors 2017, 17, 1–23.

[188] Zhang, P.; Zhang, Q.; Liu, F.; Song, C.; Li, J.; Cao, N. The Construction of the Integration of Water and Fertilizer Smart Water Saving Irrigation System based on Big Data. In Proceedings of the IEEE International Conference on Computational Science and Engineering and IEEE International Conference on Embedded and Ubiquitous Computing, Guangzhou, China, 21–24 July 2017.

[189] Chen, W.; Lin, Y.; Lin, Y.; Chen, R.; Liao, J.; Ng, F.; Chan, Y.; Liu, Y.; Wang, C.; Chiu, C.; et al. AgriTalk: IoT for precision soil farming of turmeric cultivation. IEEE Internet Things J. 2019, 6, 5209–5223.

[190] Chhaya, L.; Sharma, P.; Kumar, A.; Bhagwatikar, G. IoT-based implementation of field area network using smart grid communication infrastructure. Smart Cities 2018, 1, 176–189.

[191] Dabre, K.R.; Lopes, H.R.; D'monte, S.S. Intelligent Decision Support System for Smart Agriculture. In Proceedings of the International Conference on Smart City and Emerging Technology, Mumbai, India, 5 January 2018.

[192] Dagar, R.; Som, S.; Khatri, S.K. Smart Farming-IoT in Agriculture. In Proceedings of the International Conference on Inventive Research in Computing Applications, Coimbatore, India, 11–12 July 2018.

[193] Davcev, D.; Mitreski, K.; Trajkovic, S.; Nikolovski, V.; Koteli, N. IoT Agriculture System based on LoRaWAN. In Proceedings of the 14th IEEE International Workshop on Factory Communication Systems, Imperia, Italy, 13–15 June 2018.

[194] Deekshath, R.; Dharanya, P.; Dimpil Kabadia, K.R.; Deepak Dinakaran, G.; Shanthini, S. IoT based environmental monitoring system using arduino UNO and thingspeak. Int. J. Sci. Technol. Eng. 2018, 4, 68–75.

[195] Guillermo, J.C.; García-Cedeño, A.; Rivas-Lalaleo, D.; Huerta, M.; Clotet, R. IoT Architecture based on Wireless Sensor Network Applied to Agricultural Monitoring: A Case of Study of Cacao Crops in Ecuador. In Proceedings of the International Conference of Information and Communication Technologies for Adapting Agriculture to Climate Change II, Cali, Colombia, 21–23 November 2018.

[196] Heble, S.; Kumar, A.; Prasad, K.V.V.D.; Samirana, S.; Rajalakshmi, P.; Desai, U.B. A Low Power IoT Network for Smart Agriculture. In Proceedings of the IEEE 4th World Forum on Internet of Things, Singapore, 5–8 February 2018.

[197] Boobalan, J.; Jacintha, V.; Nagarajan, J.; Thangayogesh, K.; Tamilarasu, S. An IoT based Agriculture Monitoring System. In Proceedings of the International Conference on Communication and Signal Processing, Chennai, India, 3–5 April 2018.

[198] Jiang, X.; Yi, W.; Chen, Y.; He, H. Energy Efficient Smart Irrigation System based on 6LoWPAN. In Proceedings of the International Conference on Cloud Computing and Security, Haikou, China, 8–10 June 2018.

[199] Jirapure, A.B.; Pal, A.; Majumder, D.; Patil, G.; Shrivastava, S. Automatic smart irrigation using wireless sensor network and raspberry Pi. Int. J. Eng. Sci. Comput. 2018, 8, 16762–16763.

[200] Kamienski, C.; Soininen, J.; Taumberger, M.; Dantas, R.; Toscano, A.; Salmon Cinotti, T.S.; Filev Maia, R.F.; Torre Neto, A. Smart water management platform: IoT-based precision irrigation for agriculture. Sensors 2019, 19, 1–20.

[201] Kiani, F.; Seyyedabbasi, A. Wireless sensor network and internet of things in precision agriculture. Int. J. Adv. Comput. Sci. Appl. 2018, 9, 99–103.

[202] Krintz, C.; Wolski, R.; Golubovic, N.; Bakir, F. Estimating Outdoor Temperature from CPU Temperature from IoT Applications in Agriculture. In Proceedings of the 8th International Conference on the Internet of Things, Santa Barbara, California, USA, 15–18 October 2018.

[203] Maja, J.M.J.; Robbins, J. Controlling irrigation in a container nursery using IoT. AIMS Agric. Food 2018, 3, 205–215.

[204] Meeradevi, M.A.; Supreetha, M.R.; Mundada; Pooja, J.N. Design of a Smart Water-Saving Irrigation System for Agriculture based on a Wireless Sensor Network for Better Crop Yield. In Proceedings of the International Conference on Communications and Cyber Physical Engineering, Kuala Lumpur, Malaysia, 19–20 September 2018.

[205] Mehra, M.; Saxena, S.; Sankaranarayanan, S.; Tom, R.J.; Veeramanikandan, M. IoT based hydroponics system using deep neural networks. Comput. Electron. Agric. 2018, 155, 473–486.

[206] Muangprathub, J.; Boonnam, N.; Kajornkasirat, S.; Lekbangpong, N.; Wanichsombat, A.; Nillaor, P. IoT and agriculture data analysis for smart farm. Comput. Electron. Agric. 2019, 156, 467–474.

[207] Munir, M.S.; Bajwa, I.S.; Naeem, M.A.; Ramzan, B. Design and implementation of an IoT system for smart energy consumption and smart irrigation in tunnel farming. Energies 2018, 11, 3427.

[208] Prabha, R.; Sinitambirivoutin, E.; Passelaigue, F.; Ramesh, M.V. Design and Development of an IoT based Smart Irrigation and Fertilization System for Chilli Farming. In Proceedings of the International Conference on Wireless Communications, Signal Processing and Networking, Chennai, India, 22–24 March 2018.

[209] Rabelo, S.L.; Jucá, S.C.S.; Gonçalves, D.L.C.; Silva, V.F.; Pereira, R.I.S.; Almeida da Silva, S. Construction of soil moisture and irrigation IoT monitoring system using project based learning. Int. J. Innov. Educ. Res. 2018, 6, 99–111.

[210] Raikar, M.M.; Desai, P.; Kanthi, N.; Bawoor, S. Blend of Cloud and Internet of Things (IoT) in Agriculture Sector using Lightweight Protocol. In Proceedings of the International Conference on Advances in Computing, Communications and Informatics, Bangalore, India, 19–22 September 2018.

[211] Rajakumar, G.; Sankari, M.S.; Shunmugapriya, D.; Maheswari, S.P.U. IoT based smart agricultural monitoring system. Asian J. Appl. Sci. Technol. 2018, 2, 474–480.

[212] Shilpa, A.; Muneeswaran, V.; Rathinam, D.D.K. A Precise and Autonomous Irrigation System for Agriculture: IoT based Self Propelled Center Pivot Irrigation System. In Proceedings of the 5th International Conference on Advanced Computing and Communication Systems, Coimbatore, India, 15–16 March 2019.

[213] Suruthi, N.; Saranya, R.; Subashini, S.; Shanthi, P.; Umamakeswari, A. Managing irrigation in indian agriculture using fuzzy logic-A decision support system. Int. J. Eng. Technol. 2018, 7, 321–325.

[214] Das, R.K.; Panda, M.; Dash, S.S. Smart Agriculture System in India using Internet of Things. In Proceedings of the Fourth International Conference on Soft Computing in Data Science 2018 (SCDS2018), Bangkok, Thailand, 15–16 August 2018.

[215] Indira, D.N.V.S.L.S.; Harshita, M.; Pranav, D.S.; Sai, J.P.M. TILLAGE DRIP: An Efficient Seed Selection and Conservative Irrigation with Crop Defective Alert by IOT. In Proceedings of the 1st International Conference on Smart Computing and Informatics, Visakhapatnam, India, 3–4 March 2017.

[216] Ananthi, N.; Divya, J.; Divya, M.; Jonani, V. IoT based Smart Soil Monitoring System for Agricultural Production. In Proceedings of the IEEE International Conference on Technological Innovations in ICT for Agriculture and Rural Development, Chennai, India, 7–8 April 2017.

[217] Mondal, A.; Rehena, Z. IoT based Intelligent Agriculture Field Monitoring System. In Proceedings of the 8th International Conference on Cloud Computing, Data Science & Engineering, Noida, India, 11–12 January 2018.

[218] Premkumar, A.; Monishaa, P.; Thenmozhi, K.; Amirtharajan. R.; Praveenkumar, P. IoT Assisted Automatic Irrigation System using Wireless Sensor Nodes. In Proceedings of the International Conference on Computer Communication and Informatics, Coimbatore, India, 4–6 January 2018.

[219] Jariyayothin, P.; Jeravong-aram, K.; Ratanachaijaroen, N.; Tantidham, T.; Intakot, P. IoT Backyard: Smart Watering Control System. In Proceedings of the Seventh ICT International Student Project Conference, Nakhonpathom, Thailand, 11–13 July 2018.

[220] Kinjal, A.R.; Petel, S.; Chintan Bhatt, C. Smart irrigation: Towards next generation agriculture. Internet Things Big Data Anal. Towar. Next-Gener. Intell. Stud. Big Data 2018, 30, 265–282.

[221] Acharya, C.; Kuzhalvaimozhi, S. Irrigation and internet of things platform. Int. Res. J. Eng. Technol. (IRJET) 2016, 3, 1643–1646.

[222] Maskara, R.; Maskara, N.; Bandopadhaya, S. Solar system powered IoT solution for smart irrigation. Asian J. Cover. Technol. 2019, V, 1–4.

[223] Anbarasi, M.; Karthikeyan, T.; Ramanathan, L.; Ramani, S.; Nalini, N. Smart multi-crop irrigation system using IoT. Int. J. Innov. Technol. Explor. Eng. 2019, 8, 153–156.

[224] Kamaruddin, F.; Malik, N.N.A.; Murad, N.A.; Latiff, N.M.A.; Yusof, S.K.S.; Hamzah, S.A. IoT-based intelligent irrigation management and monitoring system using arduino. TELKOMNIKA 2019, 17, 2378–2388.

[225] Kwok, J.; Sun, Y. A Smart IoT-based Irrigation System with Automated Plant Recognition using Deep Learning. In Proceedings of the 10th International Conference on Computer Modeling and Simulation, Sydney, Australia, 8–10 January 2018.

[226] Fernández, D.; Sánchez, P.; Álvarez, B.; López, J.A.; Iborra, A. TRIoT: A Proposal for Deploying Teleo-Reactive Nodes for IoT Systems. In Proceedings of the International Conference on Practical Applications of Agents and Multi-Agent Systems, Porto, Portugal, 21–23 June 2017.

[227] Suciu, G.; Istrate, C.; Ditu, M. Secure Smart Agriculture Monitoring Technique Through Isolation. In Proceedings of the Global IoT Summit, Aarhus, Denmark, 17–21 June 2019.

[228] Yamini, R.; Reddy, K.V.C. Smart irrigation using IoT. Int. J. Adv. Res. Ideas Innov. Technol. 2019, 5, 467–471.

[229] Sawane, S.S.; Dixit, P.N. IOT based irrigation system. Int. J. Appl. Eng. Res. 2019, 14, 113–117.

[230] González-Briones, A.; Castellanos-Garzón, J.A.; Mezquita Martín, Y.; Prieto, J.; Corchado, J.M. A framework for knowledge discovery from wireless sensor networks in rural environments: A crop irrigation systems case study. Wirel. Commun. Mob. Comput. 2018, 1–14, 6089280.

[231] Abayomi-Alli, O.; Odusami, M.; Ojinaka, D.; Shobayo, O.; Misra, S.; Damasevicius, R.; Maskeliunas, R. Smart-Solar Irrigation System (SMIS) for Sustainable Agriculture. In Proceedings of the International Conference on Applied Informatics, Medan, Indonesia, 18–19 September 2018.

[232] Selvaraj, J.D.F.; Paul, P.M.; Jigle, I.D.J. Automatic wireless water management system (AWWMS) for smart vineyard irrigation using IoT technology. Int. J. Ocean. Oceanogr. 2019, 13, 211–218.

[233] Gartner. Agricultural IOT Will See a very Rapid Growth over the Next 10 Years. Available online: https://machinaresearch.com/news/agricultural-iot-will-see-a-very-rapid-growth-over-the-next-10-years/ (accessed on 22 December 2019).

[234] International Telecommunications Union. Radio Regulations. Available online: https://www.itu.int/pub/R-REG-RR/en (accessed on 22 December 2019).

[235] Maia, R.F.; Netto, I.; Tran, A.L.H. Precision Agriculture using Remote Monitoring Systems in Brazil. In Proceedings of the IEEE Global Humanitarian Technology Conference, San Jose, CA, USA, 19–22 October 2017.

[236] Patil, P.; Sachapara, V. Providing Smart Agricultural Solutions/Techniques by using IoT based Toolkit. In Proceedings of the International Conference on Trends in Electronics and Informatics, Tirunelveli, India, 11–12 May 2017.

[237] Balaji, G.N.; Nandhini, V.; Mithra, S.; Priya, N.; Naveena, R. IoT based smart crop monitoring in farm land. Imp. J. Interdiscip. Res. 2018, 4, 88–92.

[238] Patankar, U.S.; Koel, A.; Nitnaware, V. Smart System for Automatic AC Motor Starter based on GSM. In Proceedings of the IEEE International Conference on Consumer Electronics, Las Vegas, NV, USA, 11–13 January 2019.

[239] Pawar, M.; Chillarge, G. Soil Toxicity Prediction and Recommendation System using Data Mining In Precision Agriculture. In Proceedings of the 3rd International Conference for Convergence in Technology, Pune, India, 6–8 April 2018.

[240] Prathibha, R.; Hongal, A.; Jyothi, M. IoT based Monitoring System in Smart Agriculture. In Proceedings of the International Conference on Recent Advances in Electronics and Communication Technology, Bangalore, India, 16–17 March 2017.

[241] Payero, J.O.; Mirzakhani-Nafchi, A.; Khalilian, A.; Qiao, X.; Davis, R. Development of a low-cost internet-of-things (IoT) system for monitoring soil water potential using watermark 200SS sensors. Adv. Internet Things 2017, 7, 71–86.

[242] Suma, N.; Samson, S.R.; Saranya, S.; Shanmugapriya, G.; Subhashri, R. IOT based smart agriculture monitoring system. Int. J. Recent Innov. Trends Comput. Commun. 2017, 5, 177–181.

[243] Avotins, A.; Potapovs, A.; Apse-Apsitis, P.; Gruduls, J. Crop weight measurement sensor for IoT based industrial greenhouse systems. Agron. Res. 2018, 16, 952–957.

[244] Sarangi, S.; Naik, V.; Choudhury, S.B.; Jain, P.; Kosgi, V.; Sharma, R.; Bhatt, P.; Srinivasu, P. An Affordable IoT Edge Platform for Digital Farming in Developing Regions. In Proceedings of the 11th International Conference on Communications Systems and Networks, Bengaluru, India, 7–11 January 2019.

[245] Na, A.; Isaac, W.; Varshney, S.; Khan, E. An IoT based System for Remote Monitoring of Soil Characteristics. In Proceedings of the International Conference on Information Technology, Noida, India, 6–7 October 2016.

[246] Ali, A.H.; Chisad, R.F.; Mnati, M.J. A smart monitoring and controlling for agricultural pumps using LoRa IoT technology. Indones. J. Electr. Eng. Comput. Sci. 2019, 13, 286–292.

[247] Nurellari, E.; Srivastava, S. A Practical Implementation of an Agriculture Field Monitoring using Wireless Sensor Networks and IoT Enabled. In Proceedings of the IEEE International Symposium on Smart Electronic Systems, Hyderabad, India, 17–19 December 2018.

[248] Roopaei, M.; Rad, P.; Choo, K.R. Cloud of things in smart agriculture: Intelligent irrigation monitoring by thermal imaging. IEEE Cloud Comput. 2017, 4, 10–15.

[249] Bandyopadhyay, S.; Sengupta, M.; Mait, S.; Dutta, S. Role of middleware for internet of things: A study. Int. J. Comput. Sci. Eng. Surv. (IJCSES) 2011, 2, 94–105.

[250] Vani, P.D.; Rao, K.R. Measurement and monitoring of soil moisture using cloud IoT and android system. Indian J. Sci. Technol. 2016, 9, 1–8.

[251] S. Koduru, S.; Padala, V.G.D.P.R.; Padala, P. Smart Irrigation System using Cloud and Internet of Things. In Proceedings of the 2nd International Conference on Communication, Computing and Networking, Chandigarh, India, 30–29 March 2018.

[252] Ahad, M.A.; Tripathi, G.; Zafar, S.; Doja, F. IoT data management-security aspects of information linkage in IoT systems. Princ. Internet Things (IoT) Ecosyst. Insight Paradig. 2020, 174, 439–464.

[253] Tseng, F.; Cho, H.; Wu, H. Applying big data for intelligent agriculture-based crop selection analysis. IEEE Access 2019, 7, 116965–116974.

[254] Mohapatra, A.G.; Keswani, B.; Lenka, S.K. Optimizing farm irrigation mechanism using feedforward neural network and structural similarity index. Int. J. Comput. Appl. 2017, 7, 135–141.

[255] Goldstein, A.; Fink, L.; Meitin, A.; Bohadana, S.; Lutenberg, O.; Ravid, G. Applying machine learning on the sensor data for irrigation recommendations: Revealing the agronomist's tacit knowledge. Precis. Agric. 2018, 18, 421–444.

[256] E. D. Ayele, K. Das, N. Meratnia and P. J. M. Havinga, "Leveraging BLE and LoRa in IoT Network for Wildlife Monitoring System (WMS)", IEEE 4th World Forum on Internet of Things, Singapore, Singapore, 5-8 February 2018, pp. 342-348.

[257] M. Bor and U. Roedig, "LoRa Transmission Parameter Selection", 13th International Conference on Distributed Computing in Sensor Systems, Ottawa, ON, Canada, 5-7 June 2017, pp. 27-34.

[258] C. Pham, "Investigating and Experimenting CSMA Channel Access Mechanisms for LoRa IoT Networks", IEEE Wireless Communications and Networking Conference, Barcelona, Spain, 15-18 April 2018, pp. 1-6.

[259] A. Pötsch and F. Haslhofer, "Practical Limitations for Deployment of LoRa Gateways", IEEE International Workshop on Measurement and Networking, Naples, Italy, 27-29 September 2017, pp. 1-6.

[260] J. Mesquita, D. Guimaraes, C. Pereira, F. Santos and L. Almeida, "Assessing the ESP8266 WiFi module for the Internet of Things", IEEE 23rd International Conference on Emerging Technologies and Factory Automation, Turin, Italy, 4-7 September 2018, pp. 784-791.

[261] F. Montori, R. Contigiani and L. Bedgoni, "Is WiFi suitable for energy efficient IoT deployments? A performance study", IEEE 3rd International Forum on Research and Technologies for Society and Industry, Modena, Italy, 11-13 September 2017, pp. 1-5.

[262] G. D. Putra, A. R. Pratama, A. Lazovik and M. Aiello, “Comparison of Energy Consumption in WiFi and Bluetooth Communication in a Smart Building”, IEEE 7th Annual Computing and Communication Workshop and Conference, Las Vegas, NV, USA, 9-11 January 2017, pp. 1-6.

[263] Baker, T., Asim, M., Tawfik, H., Aldawsari, B., Buyya, R. An energy-aware service composition algorithm for multiple cloud-based IoT applications. Journal of Network and Computer Applications. 89, 96-108 (2017). doi: 10.1016/j.jnca.2017.03.008

[264] Cunliffe, A. M.; Brazier, R. E.; Anderson, K. Ultra-fine grain landscape-scale quantification of dryland vegetation structure with drone-acquired structure-from-motion photogrammetry. Remote Sensing of Environment 2016, 183, 129-143.

[265] Zhang, J.; Hu, J.; Lian, J.; Fan, Z.; Ouyang, X.; Ye, W. Seeing the forest from drones: Testing the potential of lightweight drones as a tool for long-term forest monitoring. Biological Conservation 2016, 198, 60-69. DOI: 10.1016/j.biocon.2016.03.027

[266] Urbahs, A.; Jonaite, I. Features of the use of unmanned aerial vehicles for agriculture applications. Aviation 2013, 17(4), 170-175. DOI: 10.3846/16487788.2013.861224

[267] Raeva, P. L., Šedina, J.; Dlesk, A. Monitoring of crop fields using multispectral and thermal imagery from UAV. European Journal of Remote Sensing 2019, 52(1), 192-201. DOI: 10.1080/22797254.2018.1527661

[268] Stehr, N. J.; Justen, V. Drones: The Newest Technology for Precision Agriculture. Natural Sciences Education 2015, 44(1), 89-91. DOI: 10.4195/nse2015.04.0772

[269] Kurkute, S. R.; Deore, B. D.; Kasar, P.; Bhamare, M.; Sahane, M. Drones for Smart Agriculture: A Technical Report. International Journal for Research in Applied Science and Engineering Technology 2018, 6(4), 341-346. DOI: 10.22214/ijraset.2018.4061

[270] L. Parra, V. Torices, J. Marín, P. V. Mauri, and J. Lloret, "The Use of Image Processing Techniques for Detection of Weed in Lawns", The Fourteenth International Conference on Systems (ICONS 2019), Valencia, Spain, 24 – 28 March 2019, pp. 50-55

[271] D. Ulzii-Orshikh, M. Lee, and S. Yun, “An yield estimation in citrus orchards via fruit detection and counting using image processing”, Computers and Electronics in Agriculture, August 2017, vol. 140, pp. 103-112.

[272] Marín, J.; Parra, L.; Rocher, J.; Sendra, S.; Lloret, J.; Mauri, P. V.; Masaguer, A. Urban Lawn Monitoring in Smart City Environments. Journal of Sensors 2018, 8743179. DOI: 10.1155/2018/8743179

[273] J. M. S. Hutchinson, A. Jacquin, S. L. Hutchinson and J. Verbesselt, “Monitoring vegetation change and dynamics on U.S Army training lands using satellite image time series analysis”, Journal of environmental management, vol 150, 2015, pp. 355-366.

[274] Puri, V.; Nayyar, A.; Raja, L. Agriculture drones: A modern breakthrough in precision agriculture. Journal of Statistics and Management Systems 2017, 20(4), 507-518. DOI: 10.1080/09720510.2017.1395171

[275] Valente, J.; Sanz, D.; Barrientos, A.; del Cerro, J.; Ribeiro, A.; Rossi, C. An Air-Ground Wireless Sensor Network for Crop Monitoring. Sensors 2011, 11(6), 6088-6108. DOI: 10.3390/s110606088

[276] Hunt, E. R. Jr.; Daughtry, C. S. T. What good are unmanned aircraft systems for agricultural remote sensing and precision agriculture?. International Journal of Remote Sensing 2018, 39, 15-16, 5345-5376, DOI: 10.1080/01431161.2017.1410300

[277] Tsouros, D. C.; Bibi, S.; Sarigiannidis P. G.; A Review on UAV-Based Applications for Precision Agriculture, Information 2019, 10(11), 349; https://doi.org/10.3390/info10110349

[278] Daponte, P.; De Vito, L.; Glielmo, L.; Iannelli, l.; Liuzza, D.; Picariello, F.; Silano, G.; A review on the use of drones for precision agriculture, IOP Conference Series: Earth and Environmental Science 2019, 275, pp. 012022. https://doi.org/10.1088/1755-1315/275/1/012022

[279] Boehm, F.; Schulte, A. Air to ground sensor data distribution using IEEE802.11N Wi-Fi network. 2013 IEEE/AIAA 32nd Digital Avionics Systems Conference (DASC), East Syracuse, NY, USA, 5-10 Oct. 2013, pp. 4B2-1-4B2-10. DOI: 10.1109/DASC.2013.6712581

[280] Stek, T. D. Drones over Mediterranean landscapes. The potential of small UAV's (drones) for dite detection and heritage management in archaeological survey projects: A case study from Le Pianelle in the Tappino Valley, Molise (Italy). Journal of Cultural Heritage 2016, 22, 1066-1071. DOI: 10.1016/j.culher.2016.06.006

[281] M. C. Vuran, A. Salam, R. Wong, S. Imark, "Internet of Underground Things: Sensing and Communications on the Field for Precision Agriculture", IEEE 4th World Forum on the Internet of Things, Singapore, Singapore, 5-8 February 2018, pp. 586-591.

[282] N. Saeed, M. Alouini, T. Y. Al-Naffouri, "3D Location of Internet of Underground Things in Oil and Gas Reservoirs", IEEE Access, Vol. 4, pp. 1-12, 2016.

[283] L. Li, M. C. Vuran, and I. F. Akyildiz, "Characteristics of Underground Channel for Wireless Underground Sensor Networks", The Sixth Annual Mediterranean Ad Hoc Networking WorkShop, Corfu, Greece, 12-15 June 2007, p. 13-15.

[284] A. Salam and M. C. Vuran, "Impacts of the Soil Type and Moisture on the Capacity of Multi-Carrier Modulation in Internet of Underground Things", 25th International Conference on Computer Communication and Networks, Waikoloa, HI, USA, 1-4 August 2016, pp. 1-9.

[285] A. Salam, M. C. Vuran and S. Irmak, "Di-Sense: In situ real-time permittivity estimation and soil moisture sensing using wireless underground communications", Computer Networks, Vol. 151, pp. 31-41, 2019.

[286] A. Salam and M. C. Vuran, “Wireless Underground Channel Diversity Reception With Multiple Antennas for Internet of Underground Things”, IEEE ICC 2017 Mobile and Wireless Networking, Paris, France, 21-25 May 2017, pp. 1-7.

[287] R. de C. D. Leles, J. J. P. C. Rodeigues, I. Woungang, R. A. L. Rabêlo and V. Furtado, “Railways Networks – Challenges for IoT Underground Wireless Communications”, IEEE 10th Latin-American Conference on Communications, Guadalajara, Mexico, 14-16 November 2018, pp. 1-6.

[288] State-of-the-Art and Challenges for the Internet of Things Security. Available online: https://tools.ietf.org/html/draft-irtf-t2trg-iot-seccons-16#section-5.1. (accessed on 22 December 2019).

[289] Jimenez, J.M.; Garcia, L.; Taha, M.; Parra, L.; Lloret, J.; Lorenz, P. Comprehensive Security Framework of an Intelligent Wastewater Purification System for Irrigation. In Proceedings of the Twelfth International Conference on Communication Theory, Reliability, and Quality of Service, Valencia, Spain, 24–28 March 2019.

[290] Sunmehra, D.; Kumar, B.H. WSN based Automatic Irrigation and Security System using Raspberry Pi Board. In proceedings of the International Conference on Current Trends in Computer, Electrical, Electronics and Communication, Mysore, India, 8–9 September 2017.

[291] Barreto, L.; Amaral, A. Smart Farming: Cyber Security Challenges. In Proceedings of the International Conference on Intelligent Systems, Funchal, Madeira, 25–27 September 2018.

[292] Hassija, V.; Chamola, V.; Saxena, V.; Jain, D.; Goyal, P.; Sikdar, B. A survey on IoT security: Application areas, security threats, and solution architectures. IEEE Access 2019, 7, 82721–82743.

[293] Sendra, S.; Parra, L.; Ortuño, V.; Lloret, L. A Low Cost Turbidity Sensor Development. In Proceedings of the Seventh International Conference on Sensor Technologies and Applications, Barcelona, Spain, 25–31 August 2013.

[294] H. Bagci, I. Korpeoglu, and A. Yazıcı, “A Distributed Fault-Tolerant Topology Control Algorithm for Heterogeneous Wireless Sensor Networks”, IEEE Parallel Distrib. Syst., vol. 26, no. 4, pp. 914–923, 2015. DOI: https://doi.org/10.1109/TPDS.2014.2316142

[295] M. Azharuddin, P. Kuila, P. K. Jana, and S. Thampi, “Energy efficient fault tolerant clustering and routing algorithms for wireless sensor networks”, Comput. Electr. Eng., vol. 41, pp. 177–190, 2015. DOI: https://doi.org/10.1016/j.compeleceng.2014.07.019

[296] C. Gkountis, M.Taha, J. Lloret, and G. Kambourakis. "Lightweight algorithm for protecting SDN controller against DDoS attacks." 2017 10th IFIP Wireless and Mobile Networking Conference (WMNC), Valencia, Spain, 25-27 September 2017, pp. 1-6.

[297] J. Ni, K. Zhang, X. Lin, and X. S. Shen. "Securing fog computing for internet of things applications: Challenges and solutions". IEEE Communications Surveys & Tutorials, Vol. 20, No. 1, pp. 601-628, 2017.

[298] M. Kaur and P. Garg, “Improved distributed fault tolerant clustering algorithm for fault tolerance in WSN”, Proceedings - 2016 International Conference on Micro-Electronics and Telecommunication Engineering, ICMETE 2016. pp. 197–201, 2017. DOI: https://doi.org/10.1109/ICMETE.2016.99

[299] E. Aras, G. S. Ramachandran, P. Lawrence and D. Hughes. "Exploring the security vulnerabilities of lora.", 2017 3rd IEEE International Conference on Cybernetics (CYBCONF), Exeter, UK, 21-23 June 2017, pp. 1-6.

[300] Caro, M.P.; Ali, M.S.; Vecchio, M.; Giaffreda, R. Blockchain-based Traceability in Agri-Food Supply Chain Management: A Practical Implementation. In Proceedings of the IoT Vertical and Tropical Summit on Agriculture-Tuscany, Tuscany, Italy, 8–9 May 2018.

[301] Patil, A.S.; Tama, B.A.; Park, Y.; Rhee, K. A Framework for Blockchain based Secure Smart Green House Farming. In Proceedings of the International Conference on Ubiquitous Information Technologies and Applications, Taichung, Taiwan, 18–20 December 2017.

[302] Devi, M.S.; Suguna, R.; Joshi, A.S.; Bagate, R.A. Design of IoT Blockchain based Smart Agriculture for Enlightening Safety and Security. In Proceedings of the International Conference on Emerging Technologies in Computer Engineering, Jaipur, India, 1–2 February 2019.

[303] Munir, M.S.; Bajwa, I.S., Cheema, S.M. An intelligent and secure smart watering system using fuzzy logic and blockchain. Comput. Electr. Eng. 2019, 77, 109–119.

[304] Sebastian, S.; Ray, P.P. Development of IoT invasive architecture for complying with health of home. In Proceedings of the International Conference on Computing and Communication Systems (I3CS), Shillong, India, 9–10 April 2015.

[305] Ferrández-Pastor, F.J.; García-Chamizo, J.M.; Nieto-Hidalgo, M.; Mora-Pascual, J.; Mora-Martínez, J. Developing ubiquitous sensor network platform using internet of things: Application in precision agriculture. Sensors 2016, 16, E1141.

[306] Merezeanu, D.; Vasilescu, G.; Dobrescu, R. Context-aware control platform for sensor network integration in IoT and cloud. Stud. Inform. Control 2016, 25, 489–498.

[307] Robles, T.; Alcarria, R.; Martín, D.; Morales, A.; Navarro, M.; Calero, R.; Iglesias, S.; López, M. An Internet of Things-based Model for Smart Water Management. In Proceedings of the 28th International Conference on Advanced Information Networking and Applications Workshops, Victoria, BC, Canada, 13–16 May 2014.

[308] Ojha, T.; Misra, S.; Raghuwanshi, N. S. Wireless sensor networks for agriculture: The state-of-the-art in practice and future challenges. Computers and Electronics in Agriculture 2015, 118, 66-84. DOI: 10.1016/j.compag.2015.08.011

[309] Tzounis, A.; Katsoulas, N; Bartzanas, T.; Kittas, C. Internet of Things in agriculture, recent advances and future challenges. Biosystems Engineering 2017, 164, 31-48. DOI: 10.1016/j.biosystemseng.2017.09.007

[310] Rehman, A.; Abbasi, A. Z.; Islam, N.; Shaikh, Z. A. A Review of Wireless Sensors and Networks' Applications in Agriculture. Computer Standards & Interfaces 2014, 36(2), 263-270. DOI: 10.1016/j.csi.2011.03.004

[311] Ruiz-Garcia, L; Lunadei, L.; Barreiro, P.; Robla, J. I. A Review of Wireless Sensor Technologies and Applications in Agriculture and Food Industry: State of the Art and Current Trends. Sensors 2009, 9(6), 4728-4750. DOI: 10.3390%2Fs90604728

[312] Barcelo-Ordinas, J. M.; Chanet, J. P.; Hou, K. M.; García-Vidal, J. A survey of wireless sensor technologies applied to precision agriculture. In proceedings of Precision agriculture '13, Lerida, Spain, 7-11 July 2013, pp. 801-808. DOI: 10.3920/978-90-8686-778-3_99

[313] Srbinovska, M.; Gavrovski, C.; Dimcev, V.; Krkoleva, A.; Borozan, V. Environmental parameters monitoring in precision agriculture using wireless sensor networks. Journal of Cleaner Production 2015, 88(1), 297-307. DOI: 10.1016/j.jclepro.2014.04.036

[314] Yu, X.; Wu, P.; Han, W.; Zhang, Z. A survey on wireless sensor network infrastructure for agriculture. Computer Standards & Interfaces 2013, 35(1), 59-64. DOI: 10.1016/j.csi.2012.05.001

[315] Chaudhary, D. D.; Nayse, S. P.; Waghmare, L. M. Application of Wireless Sensor Networks for Greenhouse Parameter Control In Precision Agriculture. International Journal of Wireless & Mobile Networks 2011, 3(1), 140-149. DOI:10.5121/ijwmn.2011.3113

[316] Jesús María Dominguez-Niño, Jordi Oliver-Manera, Joan Girona, Jaume Casadesús. Differential irrigation scheduling by an automated algorithm of water balance tuned by capacitance-type soil moisture sensors. Agricultural water management, Vol. 228, pp. 105880, 2020.

[317] H. Huh, J. Y. Kim. LoRa-based Mesh Network for IoT Applications. IEEE 5th World Forum on Internet of Things. Limerick, Ireland, 15-18 April 2019, pp. 524-527.

[318] Abrado, A. Pozzebon. A Multi-Hop LoRa Linear Sensor Network for the Monitoring of Underground Environments: The Case of the Medieval Aqueducts in Siena, Italy. Sensors, Vol. 19, pp. 402, 2019.

[319] H. C. Lee, K. H. Ke. Monitoring of Large-Area IoT Sensors Using a LoRa Wireless Mech Network System: Design and Evaluation. IEEE Transactions on Instrumentation and Measurement, Vol. 67, No. 9, pp. 2177-2187, 2018.

[320] Lloret, J.; Sendra, S.; Coll, H.; Garcia, M. Saving energy in wireless local area sensor networks. Comput. J. 2009, 53, 1658-1673. DOI: 10.1093/comjnl/bxp112

[321] DD-WRT. Available online: https://forum.dd-wrt.com/wiki/index.php/Main_Page (Last accessed on 2 July 2021).

[322] ESP32 Hardware Design Guidelines. Available online: https://www.espressif.com/sites/default/files/documentation/esp32_hardware_design_guidelines_en.pdf (accessed on 3 January 2021)

[323] ESP32-WROOM-32D & ESP32-WROOM-32U Datasheet. Available online: https://www.espressif.com/sites/default/files/documentation/esp32-wroom-32d_esp32-wroom-32u_datasheet_en.pdf (accessed on 3 January 2021)

[324] ITU-T Recommendations. ITU-T M.3170.3 (03/2007). Available online: http://handle.itu.int/11.1002/1000/9079 (accessed on 22 December 2019).

[325] National Research Council. Chapter 5: Monitoring and managing soil quality. In book Soil and Water Quality: An Agenda for Agriculture. National Academy of Sciences, United States of America, 1993; pp. 189-236.

[326] Onwuka, B.; Mang, B. Effects of soil temperature on some soil properties and plant growth. Advances in Plants and Agriculture Research 2018, 8, 34-37.

[327] THERM 200 soil temperature probe. Available online: https://www.alphaomega-electronics.com/en/sensors-probes/2088-therm200-sensor-de-temperatura-del-suelo-40-c-a-85-c.html (accessed on 3 January 2021).

[328] Walfront FS200-SHT10 Humidity sensor. Available online: https://www.amazon.es/fs200-sht10-suelo-temperatura-humedad-Digital-medidor/dp/B07B48ZMP1 (accessed on 3 January 2021)

[329] Nittis, K.; Tziavos, C.; Thanos, I.; Drakopoulos, P.; Cardin, V.; Gacic, M.; Petihakis, G.; Basana, R. The Mediterranean Moored Multi-sensor Array (M3A): system development and initial results. Annales Geophysicae, European Geosciences Union 2003, 21, 75-87.

[330] MS02 soil PH probe. Available online: https://www.amazon.com/Sonkir-Soil-Moisture-Tester-Gardening/dp/B07BR52P26 (accessed on 3 January 2021).

[331] Parra, L.; Sendra, S.; Lloret, J.; Bosch, I. Development of a conductivity sensor for monitoring groundwater resources to optimize water management in smart city environments. Sensors 2015, 15 (9), 20990-21015.

[332] Arduino Mega, Arduino webpage. Available online: https://www.arduino.cc/en/Main/arduinoBoardMega/ (accessed on 5 March 2021).

[333] ESP8266 module. Available at: https://www.sparkfun.com/products/13678. Last access: 27/02/2018

[334] F8L10D LoRa Module Technical Specification. Available online: https://en.four-faith.com/uploadfile/2017/1122/20171122095336388.pdf (accessed on 5 March 2021).

[335] DOIT ESP32 DevKit v1 specification. https://docs.zerynth.com/latest/official/board.zerynth.doit_esp32/docs/index.html

[336] Mesas-Carrascosa, F. J., Verdú Santano, D., Meroño, J. E., Sánchez de la Orden, M., García-Ferrer, A.: Open source hardware to monitor environmental parameters in

precision agriculture. Biosystems Engineering. 137, 73-83 (2015). doi: 10.1016/j.biosystemseng.2015.07.005

[337] Allen, R. G.; Pereira, L. S.; Raes, D.; Smith. M. FAO Irrigation and Drainage Paper No. 56. Crop Evapotranspiration (guidelines for computing crop water requirements). Food and Agriculture Organization. Available online: http://www.fao.org/3/x0490e/x0490e00.htm (accessed on 15-10-2020).

[338] SIAM IMIDA. Available online: http://siam.imida.es/apex/f?p=101:46:3728946734303878 (accessed on 3 January 2021)

[339] Valencian Institute of Agricultural Research. Available online: http://riegos.ivia.es/listado-de-estaciones/gandia (accessed on 3 January 2021)

[340] García, L.; Parra, L.; Jimenez, J.M.; Lloret, J.; Abouaissa, A.; Lorenz, P. Internet of Underground Things ESP8266 WiFi Coverage Study. In Proceedings of the Eighth International Conference on Communications, Computation, Networks and Technologies, Valencia, Spain, 24–28 November 2019.

[341] García, L.; Parra, L.; Jimenez, J. M.; Lloret, J.; Lorenz, P. Estimation of the Best Measuring Time for the Environmental Parameters of a Low-Cost Meteorology Monitoring System. Advanced Intelligent Systems for Sustainable Development (AI2SD'2019), Marrakech, Morocco, 8-11 July 2019, pp. 137-144.

[342] Liao, C.H.; Zhu, G.; Kuwabara, D.; Suzuki, M.; Morikawa, H. Multi-hop LoRa Networks Enabled by Concurrent Transmission. IEEE Access 2017, 5, 21430–21446.

[343] Cisco Cybersecurity Reports. Available at: https://www.cisco.com/c/en/us/products/security/security-reports.html (Last accessed on 26-11-2018).

[344] Cloud Security Principle 1: Data in transit protection. Available at: https://www.ncsc.gov.uk/guidance/cloud-security-principle-1-data-transit-protection (Last accessed on 26-11-2018).

[345] Gemalto, Actility and Semtech, "LoRaWAN Security: Full end-to-end encryption for IoT application providers", 2017.

[346] R. Roman, J. Lopez and M. Mambo, "Mobile edge computing, Fog et al.: A survey and analysis of security threats and challenges", Future Generation Computer Systems, Vol. 78, pp. 680-698, 2018.

[347] M. U. Farooq, M. Waseem, A. Khairi and S. Mazhar, "A Critical Analysis on the Security Concerns of Internet of Things (IoT)", International Journal of Computer Applications, Vol. 111, No. 7, pp. 1-6, 2015.

[348] L. García, L. Parra, O. Romero, J. Lloret, "System for monitoring the wellness state of people in domestic environments employing emoticon-based HCI", The Journal of Supercomputing, pp. 1-25, 2017. DOI: https://doi.org/10.1007/s11227-017-2214-4

[349] Dual-Band Wireless-N Gigabit Router with Storage Link SKU WRT600N. Available at:

http://downloads.linksys.com/downloads/userguide/1224638362365/WRT600N_ug.pdf (Last accessed on 21/11/2018).

[350] ESP-CoAP library. Available online: https://github.com/automote/ESP-CoAP (Last accessed on 21/11/2018).

[351] Asadpour, M.; Giustiniano, D.; Hummel, K. A. From Ground to Aerial Communication: Dissecting WLAN 802.11 for the Drones. In proceedings of the 8th ACM International workshop on Wireless network testbeds, ecperimental evaluation & characterization, 30 September 2013, Miami, FL, USA, pp. 25-32.

[352] Rosati, S.; Kruzelecki, K.; Traynard, L: Rimoldi, B. Speed-Aware Routing for UAV Ad-Hoc Networks. In proceedings of Globecom 2013 Workshop- Wireless Networking and Control for Unmanned Autonomous Vehicles, Atlanta, USA, 9-13 December 2013, pp. 1367-1373.

[353] Rahman, A. Enabling Drone Communications with WiMAX Technology. In proceedings of the 5th International Conference on Information, Intelligence, Systems and Applications, Chania, Greece, 7-9 July 2014, pp. 323-328.

[354] Yuam, Z.; Huang, X.; Sun, L.; Jin, J. Software defined mobile sensor network for micro UAV swarm. In proceedings of the IEEE International Conference on Control and Robotics Engineering, Singapore, Singapore, 2-4 April 2016, pp. 1-4.

[355] Popescu, D.; Stoican, F.; Stamatescu, G.; Ichim, L.; Dragana, C. Advanced UAV-WSN System for Intelligent Monitoring in Precision Agriculture. Sensors 2020, 20(3), 817. DOI: 10.3390/s20030817

[356] Specifications of the WEMOS MINI DI. Available online: https://docs.wemos.cc/en/latest/d1/d1_mini.html (accessed on 03/02/2020)

[357] Specifications of the Node MCU. Available online: https://joy-it.net/en/products/SBC-NodeMCU-ESP32 (accessed on 03/02/2020).

[358] Specifications of the Arduino Mega. Available online: https://store.arduino.cc/arduino-mega-2560-rev3 (accessed on 03/02/2020).

[359] Specifications of the Arduino UNO. Available online: https://store.arduino.cc/arduino-uno-rev3 (accessed on 03/02/2020).

[360] Specifications of the Raspberry Pi Model B+. Available online: https://www.raspberrypi-spy.co.uk/2018/03/introducing-raspberry-pi-3-b-plus-computer/ (accessed on 03/02/2020).

[361] Anguera, J.; Perez, A. In Book Teoría de Antenas 1º ed. Barcelona, Spain. Edicions UPC, 2008. ISBN: 84-8301-625-7

[362] Yoppy; Arjadi, R. H.; Candra, H. ; Prananto, H. D.; Wijanarko, T. A. W. RSSI Comparison of ESP8266 Modules. In proceedings of the 2018 Electrical Power, Electronics, Communications, Controls and Informatics Seminar, Batu, Indonesia, 9-11 October 2018, pp. 150-153.

[363] Guillen-Perez, A.; Sanchez-Iborra, R.; Cano, M; Sanchez-Aarnoutse, J. C.; Garcia-Haro, J. WiFi Networks on Drones. In proceedings of the ITU Kaleidoscope: ICTs for a Sustainable World, Bangkok, Thailand, 14-16 November 2016, pp. 1-8.

[364] García, L.; Jimenez, J.M.; Sendra, S.; Lloret, J.; Lorenz, P. Multi-layer Fog Computing Framework for Constrained LoRa Networks Intended for Water Quality Monitoring and Precision Agriculture Systems [Manuscript accepted for publication]. 18th International Conference on Wireless Networks and Mobile Systems (WINSYS 2021), online, 7-9 July 2021.

[365] García, L.; Jimenez, J. M.,; Parra, L.; Lloret, J.; Lorenz, P. An overview on IoUT and the performance of WiFi low-cost nodes for IoUT Applications. IEEE Global Communications Conference (GLOBECOM 2020), Taipei, Taiwan, 7-11 December 2020, pp. 1-6.

[366] Bouguera, T.; Diouris, J.; Chaillout, J.; Jaouadi, R.; Andrieux, G. Energy Consumption Model for Sensor Nodes Based on LoRa and LoRaWAN. Sensors 2018, 18, 2104.

[367] Blenn, N.; Kuipers, F. LoRaWAN in the Wild: Measurements from the Things Network. arXiv 2017, arXiv:1706.03086.

[368] Zorbas, D.; Di Puglia Pugliese, L.; Razafindralambo, T.; Guerreiro, F. Optimal drone placement and cost-efficient target coverage. Journal of Network and Computer Applications 2016, 75, 16-31. DOI: 10.1016/j.jnca.2016.08.009

[369] LoRaWAN 1.0.3 Regional Parameters. Available at : https://lora-alliance.org/wp-content/uploads/2020/11/lorawan_regional_parameters_v1.0.3reva_0.pdf (Last accessed on 03/06/2021)

[370] Muhammad, A.; Mazliham, M. S.; Boursier, P.; Shahrulniza, M.; Mustapha, J. C. Terrain/Clutter Based Error Calculation in Location Estimation of Wireless Nodes by using Receive Signal Strength. In proceedings of the 2nd International Conference on Computer Technology and Development, Cairo, Egypt, 2-4 November 2010, pp. 95-99.

[371] Khalifeh, A.; Darabkh, K. A.; Khasawneh, A. M.; Alqaisieh, I.; Salameh, M.; AlAbdala, A.; Alrubaye, S.; Alassaf, A.; Al-Haj Ali, S.; Al-Wardat, R.; Bartolini, N.; Bongiovannim, G.; Rajendiran, K. Wireless Sensor Networks for Smart Cities: Network Design, Implementation and Performance Evaluation. Electronics 2021, 10, 218.

[372] Bauer, J.; Aschenbruck, N. Towards a Low-cost RSSI-based Crop Monitoring. ACM Transactions on Internet of Things 2020, 1(4), 21.

[373] Azpilicueta, L.; López-Iturri, P.; Aguirre, E.; Mateo, I.; Astrain, J. J.; Villadangos, J.; Falcone, F. Analysis of Radio Wave Propagation for ISM 2.4 GHz Wireless Sensor Networks in Inhomogeneous Vegetation Environments. Sensors 2014, 14, 23650-23672.

[374] Lloret, J.; García, M.; Bri, D.; Sendra, S. A Wireless Sensor Network Deployment for Rural and Forest Fire Detection and Verification. Sensors 2009, 9, 8722-8747.

[375] Seybold, J.S. Introduction to RF propagation. John Wiley, New York, NY, USA, 2005.

[376] Recommendation UIT-R PN.837-5. Characteristics of precipitation for propagation modeling. Available online: http://www.itu.int/md/R07-WP3J-C-0014/en (accessed on 3 January 2021)

[377] Rahim., H. M.; Leow, C. Y.; Rahman, T. A.; Arsad, A.; Malek, M. A. Foliage Attenuation Measurement at Millimeter Wave Frequencies In tropical Vegetation. In proceedings of the IEEE 13th Malaysia International Conference on Communications, Johor Bahru, Malaysia, 28-30 November 2017, pp. 241-246.

[378] Ndzi, D. L.; Savage, N.; Stuart, K. Wideband Signal Propagation Through Vegetation. In proceedings of the XVII General Assembly of the International Union of Radio Science, New Dehli, India, 23-29 October 2005, pp. 23-29.

[379] Sabri, N.; Aljunid, S. A.; Ahmad, R. B.; Malek, M. F. A.; Kamaruddin, R.; Salim, M. S. Wireless Sensor Network Wave Propagation in Vegetation: Review and Simulation. In proceedings of the Loughborough Antennas & Propagation Conference, Loughborough, UK, 12-13 November 2012, pp. 1-4.

[380] Gay-Fernández, J.; Cuiñas, I. Peer to Peer Wireless Propagation Measurements and Path-Loss Modeling in Vegetated Environments. IEEE Transactions on Antennas and Propagation 2013, 61 (6), 3302-3311.

[381] Thelen, J.; Goense, D.; Langendoen, K. Radio Wave Propagation in Potato Fields, In proceedings of the First Workshop on Wireless Network Measurements, Riva del Garda, Italy, April 2005.

[382] Acuña, J.; Cuiñas, I.; Gómez, P. Wireless Networks Interference and Security Protection by Means of Vegetation Barriers. Process in Electromagnetics Research M 2011, 21, 223-236.

[383] García, L.; Parra, L.; Jiemenez, J. M.; Lloret, J.; Lorenz, P. IoT-Based Smart Irrigation Systems: An Overview on the Recent Trends on Sensors and IoT Systems for Irrigation in Precision Agriculture. Sensors 2020, 20(4), 1042. DOI: https://doi.org/10.3390/s20041042

[384] Melgy, R.; Lopez-Iturri, P.; Astrain, J. J.; Picallo, I.; Klaina, H-; Rady, M.; Paredes, F.; Montagnino, F.; Vazquez Alejos, A.; Falcone, F. Low-Cost Cloud Enabled Wireless Monitoring System for Linear Fresnel Solar Plants. Engineering Proceedings 2020, 2(1), 6.

[385] Santana Abril, j.; Santana Sosa, G.; Sosa, J.; Bautista, T.; Montiel-Nelson, J. A. A Novel Charging Method for Underwater Batteryless Sensor Node Networks. Sensors 2021, 21, 557.

[386] Klimiashvili, G.; Tapparello, C.; Heinzelman, W. LoRa vs. WiFi Ad Hoc: A Performance Analysis and Comparison. In proceedings of the 2020 International Conference on Computing, Networking and Communications: Network Algorithms and Performance Evaluation. Big Island, HI, USA, 17-20 February 2020, pp. 654-660.

[387] Specifications of the ESP8266. Available online: https://www.elecrow.com/download/ESP-12F.pdf [Last access April 12 2019]

[388] J. Lloret, I. Bosch, S. Sendra and A. Serrano, "A Wireless Sensor Network for Vineyard Monitoring That Uses Image Processing", Sensors, Vol. 11, pp. 6165-6169, 2011.

[389] J. Lloret, J. J. López, C. Turró and S. Flores, "A Fast Design Model for Indoor Radio Coverage in the 2.4 GHz Wireless LAN", 1st -international Symposium on Wireless Communication Systems, Mauritius, 20-22 September 2004, pp. 408-412.

[390] A. M. Sadeghioon, D. N. Chapman, N. Metje an C. J. Anthony, "A New Approach to Estimating the Path Loss in Underground Wireless Sensor Networks", Journal of Sensor and Actuator Networks, Vol. 6, No. 18, pp. 1-11, 2007.

[391] Herold, Bernd. 3.2 Monitoring and Mapping of Fresh Fruits and Vegetables Using Vis Spectroscopy. Optical Monitoring of Fresh and Processed Agricultural Crops, 2008, p. 157.

[392] García, L.; Jimenez, J. M., Lloret, J.; Lorenz, P. WiFi and LoRa Energy Consumption Comparison in IoT ESP 32/SX1278. The Eight International Conference on Smart Cities, Systems, Devices and Technoogies (SMART 2019), Nice, France, 28 July – 2 August 2019, pp. 26-31.

[393] García, L.; Parra, L.; Basterrechea, D. A.; Jimenez, J. M., Rocher, J.; Parra, M.; Garcia-Navas, J. L.; Sendra, S.; Lloert, J.; Lorenz, P.; Tomas, J.; Abouaissa, A.; Rodilla, M.; Falco, S.; Sebastia, M. T.; Mengual, J.; Gonzalez, J. A.; Roig, B. Quantifying the Production of Fruit-Bearing Trees Using Image Processing Techniques. The Eight International Conference on Communications, Computation, Networks and Technologies (INNOV 2019), Valencia, Spain, 24-28 November 2019, pp 14-19.